ISSN 0386-5878
Technical Memorandum
of PWRI No. 2896

PROCEEDINGS OF THE 4TH WORKSHOP ON PAVING IN COLD AREAS VOLUME 1

CANADA/JAPAN SCIENCE AND TECHNOLOGY AGREEMENT SEPTEMBER, 1990

Pavement Division
Road Department
Public Works Research Institute
Ministry of Construction

1, Asahi, Tsukuba-shi, Ibaraki-ken, 305 Japan

Copyright © (1990) by P.W.R.I.

All rights reserved. No part of this book may be reproduced by any means, nor transmitted, nor translated into a machine language without the written permission of the Director General of P.W.R.I.

この報告書は，土木研究所長の承認を得て刊行したものである。したがって、本報告書の全部又は一部の転載，複製は，土木研究所長の文書による承認を得ずしてこれを行ってはならない。

ISSN 0386-5878
Technical Memorandum
of PWRI No. 2896

PROCEEDINGS OF THE 4TH WORKSHOP ON PAVING IN COLD AREAS VOLUME 1

CANADA/JAPAN SCIENCE AND TECHNOLOGY AGREEMENT SEPTEMBER, 1990

by

Pavement Division, Road Department, PWRI

Synopsis:

This Technical Memorandum is the proceedings of the 4th workshop on "Paving in Cold Areas", held in Sapporo, September 4-6, 1990. There are 16 Japanese papers and 16 Canadian papers. The topics of the workshop are as follows;

- Paving Material for Cold Areas
- Low Temperature Cracking
- Development Testing Method for Paving Material and Performance in Cold Areas
- Deterioration of Pavement in Cold Areas and its Rrehabilitation
- Concrete Pavement
- Evaluation of Pavement Structure Using Non-Destructive Method
- Management and Maintenance of Pavement

Key Words: Canada/Japan Science and Technology Agreement, Paving in Cold Areas, Modified Asphalt, Concrete Block, Coupling Agent, Low Temperature Cracking, Rheology, Unti-Wear, Freezing Detector, Rutting, Mixture Design, Rehabilitation Surface Recyling, Roller Compacted Concrete Pavement, Continuous Reinforced Concrete Pavement, Falling Weight Deflectometer, Surface Treatment, Pavement Management System

Foreword

The workshop on "Paving in Cold Areas", which is one of the important activity of the 4th Canada/ Japan Science and Technology Agreement, will be held on September 4-6 in 1990. 16 Japanese papers and 16 Canadian papers were submitted to the Workshop. This Technical Memorandum is a proceedings, includes 15 papers which are to be presented in the top half of the Workshop. There are a lot of useful information for designing and studying not only pavement in cold areas but also pavement in other areas.

Contents

Volume 1

SESSION 1

Paving Material for Cold Areas (I)

Evaluation of Some Polymer Modified Asphalts in Alberta
K. Anderson, Univ. of Alberta, Canada
S. Hussain, EBA Engineering Consultants Ltd. ..... 1—1

An Investigation Study on Production of Modified Asphalts in Japan
K. Himeno, Hokkaido Univ.
H. Sakamoto, Y. Anzaki
PWRI, Ministry of Construction, Japan
K. Hashimoto, Ministry of Construction ..... 1—41

Cold Temperature Properties of a Polymer-Modified Asphalt Concrete
N. Ali, Technical Univ. of Nova Scotia
A. Bergan, J. Chan, Univ. of Saskatchewan
A. Papagiannakis, Memorial Univ. of Newfoundland ..... 1—69

SESSION 2

Paving Material for Cold Areas (II)

On Adhesive Layer of Thin Concrete Block Overlay
M. Inuzuka, Hokkaido Institute of Technology ..... 1—95

Silane Coupling Agents to Reduce Moisture Susceptibility of Asphalt Concrete
D. Stolle, McMaster Univ.
J. Emery, JEGEL, Canada
G. Kennepohl, Ministry of Transportation, Ontario ..... 1—113

SESSION 3

Low Temperature Cracking

Thermal Stresses Development in Pavements During Winter Time
M.A. Laforte, C.R.C.A.C. INC, Quebec ..... 1—147

Low Temperature Fracture Mechanics of Viscoelastic Pavement Structures
A. Selvadurai, M.C. Au, Carleton Univ.
P. Joseph, Ministry of Transportation, Ontario ..... 1—181

Ste. Anne Test Road Revisited Twenty Years Later
I.J. Deme, Shell Canada Products Ltd.
F.D. Young, Manitoba Department of Highways ..... 1—213

SESSION 4

Development of Testing Methods for Paving Material and Performance in Cold Areas (I)

Testing of Softening Point and Brittle Point of Asphalt Mixtures for the Evaluation of Their Rheological Properties
M. Yamada, Osaka City Univ. ..... 1—235

Test Methods to Characterize Low Temperature Cracking
V. Janoo, J. Bayer Jr., CRREL, USA
T. Vinson, Oregon State Univ.
R. Haas, Univ. of Waterloo ..... 1—255

SESSION 5

Development of Testing Methods for Paving Material and Performance in Cold Areas (II)

An Estimation of Road Wear Using Spike Ravelling Test
M. Itoh, Y. Anzaki, PWRI ..... 1—289

Snow and Ice Detection by a Dielectric Pavement Freezing Detector (DPF)
K. Takeichi, Hokkaigakuen Univ.
N. Maeno, Hokkaido Univ.
H. Kubo, former CERI, Hokkaido Development Bureau ..... 1—317

SESSION 6

Pavement Deterioration and Rehabilitation in Cold Areas (I)

Survey of Measures Against Pavement Rutting in Cold Regions
S. Sawada, K. Kawamura, T. Mizushima,
CERI, Hokkaido Development Bureau
H. Kubo, former CERI, Hokkaido Development Bureau ..... 1—339

Asphalt Pavement Rutting Experience in Canada
J. Emery, JEGEL, Canada ..... 1—371

Statistical Study of Factors Causing Rutting of Expressway Pavements in Cold Areas in Japan
K. Kaneda, T. Sakate, Y. Takayanagi, K. Kamiya,
Japan Highway Public Corporation Laboratory ..... 1—385

VOLUME 2

SESSION 7

Pavement Deterioration and Rehabilitation in Cold Areas (II)

Comparative Study on Performances of Asphalt Pavements in Cold Area
Z. Wen, Y. Takeyama, T. Fukuda, Tohoku Univ. ..... 2—1

Design of Asphalt Concrete Mixtures in Cold Climates Using Soft Asphalts
D. Palsat, Testing Services, Canada
C. McMillan, Alberta Transportation and Utilities ..... 2—17

Damage to Expressway Pavement in Hokkaido and Solutions Required
Y. Ogawa, T. Murahashi, Japan Highway Public Corporation ..... 2—51

SESSION 8

Pavement Deterioration and Rehabilitation in Cold Areas (III)

Asphalt Technology for Hot In-Place Surface Recycling
J. Emery, JEGEL, Canada
M. Terao, Taisei Road Construction Co. Ltd. ..... 2—75

Influence of Field Compaction on the Resistance
to Stripping of Asphalt Pavements in Cold Areas
A. Abd El Halim, H. El Hussein, Carleton Univ.
G. Kennepohl, Ministry of Transportation, Ontario ..... 2—105

SESSION 9

Concrete Pavement (I)

Applicability of RCCP in Cold Areas
T. Hagiwara, K. Nagasaki, M. Onojima, Ministry of Construction
E. Noda, Japan Road Contractors Association ..... 2—133

Present Status and Subject of Roller Compacted Concrete Pavement in Japan
H. Tada, Japan Road Association
H. Mori, Ministry of Construction
Y. Anzaki, Y. Sawada, PWRI ..... 2—155

SESSION 10

Concrete Pavement (II)

A Twenty Five Year Report on the Continuously Reinforced Concrete Pavement in Koriyama
H. Ohta, T. Obara, Ministry of Construction ..... 2—177

Concrete Pavement Rehabilitation and Overlay-Ontario's Experience
T. Kazmierowski, H. Sturm, Ministry of Transportation, Ontario ..... 2—203

Evaluation System of Airport Concrete Pavement
Y. Hachiya, K. Sato, S. Umeno,
Port & Harbour Research Institute, Ministry of Transport
H. Yokota, Ministry of Transport
K. Okano, New Tokyo International Airport Authority ..... 2—231

SESSION 11

Evaluation of Pavement Structure Using a Non-Destructive Method

Rapid Monitoring of Flexible Pavement Deflections, Moduli and Roughness
D. Hein, Dynatest Ltd. & Pavmatec Ltd., Canada
J. Emery, JEGEL ..... 2—259

Seasonal Variations in Bearing Capacity of Asphalt Pavements
A. Kasahara, Hokkaido Institute of Technology
K. Himeno, Hokkaido Univ.
M. Igarashi, Association of Hokkaido Pavement Constructors ..... 2—279

SESSION 12

Management and Maintenance of Pavements

Integration of Rehabilitation, Maintenance and Upgrading
in Saskatchewan's Pavement Management Information System
G.H. Heiman, N.D. Lea & Associates Ltd.
R.W. Chursinoff, M.U. Hassain,
Saskatchewan Highways and Transportation
R. Deighton, R. Deighton Associates Ltd. ..... 2—299

Evaluation of the Performance of Asphalt Pavement in
Consideration of Reliability
Y. Takeyama, T. Fukuda, Tohoku Univ.
T. Obara, Ministry of Construction ..... 2—321

A Generic Framework for Pavement Management
and Staging Modules for Implementation
R. Haas, Pavement Management System Ltd.
N. Mcleod, Univ. of Waterloo ..... 2—339

Evaluation of Some Polymer Modified Asphalts in Alberta

K. Anderson, Univ. of Alberta, Canada
S. Hussain, EBA Engineering Consultants Ltd.

EVALUATION OF SOME POLYMER MODIFIED ASPHALTS IN ALBERTA

by
K.O. Anderson, Professor of Civil Engineering
University of Alberta, Edmonton
and
S.R. Hussain, (former Graduate Student)
EBA Engineering Consultants Ltd., Edmonton

ABSTRACT

Low temperature transverse cracking and permanent deformation at high temperatures are serious and costly distress modes in asphalt pavements experiencing cold climates and relatively high traffic loadings during summer periods. In recent years there has been a great deal of interest in the use of various additives to improve the behaviour of the binder properties to increase both resistance to rutting and low temperature cracking. Several types of polymer modified asphalt cements have been used in Alberta in anticipation of such benefits.

Laboratory evaluation of conventional and polymer modified asphalt cements has been accomplished by conducting tests on compacted mixture specimens. Indirect tensile tests at low temperatures ranging from 0 C to -30 C, together with repeated load triaxial tests at 25 C to 45 C, have been the primary test methods. Observations have shown that the polymer modified mixes generally exhibit higher failure stresses, higher failure strains and lower failure stiffnesses compared with conventional asphalt cements. At higher temperatures up to 45 C the polymer modified mixes manifest considerably less permanent deformation. These characteristics indicate that pavements constructed with polymer modified binders should be more resistant to thermally induced stresses at low temperatures and permanent deformation due to traffic loading at high temperatures.

1. INTRODUCTION

1.1 Background

Low temperature transverse cracking is a very serious and costly pavement distress mode found in many locations with relatively cold climates, and has been a major topic of interest at our PICA Workshops since their inception in 1982. A review of the three PICA Proceedings would enable a state-of-the-art to be synthesized concerning this problem in Canada and Japan particularly. Since effective solutions to the low temperature cracking problem cannot be developed without consideration of the behaviour of the pavement at high summer temperatures, the thrust of our recent research effort has been to develop test methods to evaluate asphalt paving mixtures under both extremes of service temperatures. As an example, air temperature extremes for a a 20-year period in Edmonton range from 35 C to -48 C.

At low temperatures, transverse cracking of the pavement occurs when the induced tensile stresses due to thermal contraction exceed the breaking strength of the asphalt concrete mix. At the initial stage, the cracking does not have any significant effect on the pavements, but with time, these cracks open and necessitate premature rehabilitation of the pavements. For over twenty years, ongoing research has been conducted at the University of Alberta, to evaluate the characteristics of laboratory compacted and core specimens at low temperatures.

Permanent deformation is also a common mode of pavement distress; repeated load applications, causing consolidation and lateral movement to occur, result in longitudinal depressions in the wheel-paths. The occurrence of permanent deformation is the primary factor influencing the serviceability of the pavements, including riding quality and safety. Low serviceability results in premature

rehabilitation of the asphalt concrete pavements. It is therefore very important for engineers to understand the influence of different mix properties on permanent deformation and low temperature transverse cracking, to minimize premature rehabilitation needs.

In order to alleviate the problem of permanent deformation and low temperature transverse cracking, the asphalt industry has shown a great deal of interest concerning engineered or polymer modified asphalts. Recently, various types of polymers have been used as additives to alter the asphalt binder and mix properties, thus improving their performance against both permanent deformation and low temperature transverse cracking.

Because of this interest in polymer modification, a research program was initiated to evaluate various types of polymers added to conventional paving grade asphalt cements in order to provide comparative data under both high and low service temperatures common to Western Canada. In order to predict the performance of the polymer modified asphalts, emphasis was placed on the methods used for evaluation of low and high temperature characteristics of asphalt concrete. Evaluations were conducted on both polymer modified asphalts comparable conventional asphalt cements.

1.2 Objectives of the Investigation (Hussain, 1990) were:

1. To determine the rheological properties and temperature susceptibility of conventional and polymer modified asphalt cements.

2. To evaluate the low temperature performance in the laboratory of conventional and polymer modified asphalt cements.

3. To evaluate and compare the low temperature tensile characteristics of conventional and polymer modified

asphalt concrete mixtures, utilizing the indirect tensile test method.

4. To evaluate and compare the permanent deformation characteristics of conventional and polymer modified asphalt concrete mixtures, utilizing a repeated load triaxial test method.

5. To present practical recommendations for application of asphalt concrete mixtures with conventional and polymer modified asphalts, to minimize low temperature cracking and permanent deformation.

1.3 Research Approach

The research program was divided into two parts, the first being a review of literature discussing asphalt additives used to improve performance of pavements in Canada and, more specifically, Alberta. The second part consisted of laboratory testing of selected conventional and polymer modified asphalts in order to determine their low temperature tensile and permanent deformation characteristics. Portions of this study have recently been reported (Anderson and Hussain, 1989).

Samples of conventional and polymer modified asphalts were obtained from Husky Oil Ltd. and Imperial Oil Ltd respectively. Conventional physical tests were conducted on asphalt cement samples to define rheological properties and temperature susceptibility parameters of the binders. These properties were then utilized in evaluating the low temperature characteristics of these asphalt cements.

In addition, the following tests were conducted to evaluate the characteristics of conventional and polymer modified asphalt mixes at both low and high temperatures:

1.4.1 Indirect Tensile Test (Anderson and Leung, 1987)

Indirect tensile tests were utilized to evaluate the low temperature tensile characteristics of the mixes. Twenty-four specimens, having a nominal height of 64 mm and diameter of 102mm were fabricated using each asphalt cement, according to the procedure given in Asphalt Institute Manual Series MS-2. A California Kneading Compactor was used. This enabled a replication of six specimens for each test temperature of 0 C, -10 C, -20 C, and -30 C. These tensile properties obtained in these tests were utilized in evaluating the low temperature behavior of these asphalt concrete mixtures.

1.4.2 Repeated Load Triaxial Test

Repeated load triaxial tests method (Hadipour and Anderson, 1988), were performed at temperatures of 25 C, 35 C, and 45 C in order to evaluate permanent deformation characteristics of asphalt concrete mixtures at high temperatures. Eighteen cylindrical specimens having 204 mm height and 102 mm diameter, were fabricated from each asphalt cement sample, using the California Kneading Compactor. The resulting data was used in evaluating the high temperature behavior of these asphalt concrete mixtures.

2. EXPERIMENTAL PROGRAM AND MATERIALS

The primary objective of the testing program involved in this investigation was to evaluate and compare the behaviour of a conventional asphalt cement and a polymer modified asphalt under both low and high temperatures.

2.1 City of Lethbridge Project Materials

In 1987 a comprehensive program to determine the cause of premature pavement rutting and to identify measures that could be implemented to mitigate this distress was undertaken by the City of Lethbridge, in conjunction with Alberta

Transportation and Utilities (Hogeweide and MacDonald, 1988). In addition to conventional Marshall and Hveem type mix design tests, creep and repeated load triaxial tests were performed on ten mixes with various coarse and fine aggregate characteristics and different bituminous binders. The repeated load tests were performed at the University of Alberta, using a simplified procedure of only one temperature of 40 C and 60 000 repetitions of load to compare the performance of each mix.

Following this initial study and recommendations, a series of test sections were constructed in the City of Lethbridge in June of 1988 in order to verify the anticipated improved performance of mixes with respect to instability rutting. One of these sections had a polymer modified asphalt cement designated as PMA 2 for use with virgin aggregate and another had a softer material, designated PMA 4 and incorporated into a mix containing 30 percent reclaimed asphalt pavement (RAP). A paper summarizing the design and construction of these test sections together with initial findings and recommendations has been recently presented (Dawley et al.,1990).

The construction of these test sections provided an opportunity to undertake additional independent laboratory testing on materials that are representative of those used in the field. Although not a part of the previously described study, it is anticipated that future performance information will assist in assessing the usefulness of this laboratory investigation.

For this investigation the aggregate processed for test sections constructed in Lethbridge during the summer of 1988 was used. Four different plant separated fractions of aggregates were processed, namely two sizes of crushed coarse aggregate, processed fine aggregate containing natural pit fines and manufactured fines and crushed fine aggregate produced by reducing oversized rock previously screened out.

Several different gradations for the test sections were used (Dawley et al.,1990).

Mix Code C had PMA 2, with Code B a 150-200 asphalt cement as the binder type. The gradation used for specimen preparation is given in Table 1. Comparable data for the EBA mix design and average values for the constructed test section for Mix C are also given. While some minor differences are noted the gradation used for specimen preparation is considered to be reasonably close to the as-constructed section.

The supplier of the asphalt cement and polymer modified binder on the project was Husky Oil Operations Ltd. They provided the 150/200 penetration grade asphalt cement and PMA 2 sampled from their Lloydminster refinery in early 1989 for use in this investigation. Conventional physical tests were conducted to evaluate the consistency properties of these two binders. Table 2 gives the physical test properties obtained, with comparable values reported by other laboratories. With the exception of absolute viscosity at 60 C for the PMA 2 binder, the test values are within ASTM limits for multilaboratory precision for acceptable range of two results. Problems associated with the use of conventional viscosity tests on polymer modified binders, such as shear susceptibility, have been discussed by Zanzotto et al., (1987) and may have contributed to this large difference of 27 percent of the mean value.

A direct comparison of the penetration values at 25 C would indicate that the PMA 2 is slightly harder, but is softer at 4 C. The PMA 2 is considerably more viscous at 60 C and at 135 C. One could infer from this data that the PMA 2 should be more resistant to cracking at low temperatures and more resistant to permanent deformation at high service temperatures. It also can be seen that the higher viscosity at 135 C, would require mixing temperatures to be correspondingly higher for the PMA 2 binder. This is

consistent with results previously reported and experience during construction.

2.2 Alberta Secondary Highway 794 Materials

In the summer of 1989 Alberta Transportation and Utilities (AT&U) constructed a several kilometer long test site on a secondary highway northwest of Edmonton. This highway carries heavily loaded aggregate hauling trucks and provided an opportunity to observe the behaviour of another type of polymer modified asphalt cement, designated as Imperial PMA. For convenience the physical test properties were presented in Table 2.

Table 3 presents the temperature susceptibility parameters, PVN (25-60), PVN (25-135), PI (R&B), and PI (dPen/dT). These parameters have been calculated by using the data from Table 2 and conventional methods (Leung, 1986). The 150/200A is the most temperature susceptible according to the PI(dPen/dT) method. The PI (R&B) for the 150/200 appears to be erroneous despite being based on a minimum of 4 replicate R&B tests. The use of these parameters for polymer modified asphalts is questionable, however, they are reported to show how they may be affected by using conventional tests and methods.

The test sections were constructed using either 25 or 30 percent manufactured fines. Table 4 gives the design gradation using 30 percent manufactured fines and the actual test section gradation with 25 percent manufactured fines. The gradation used for the specimen fabrication is seen to be quite close to the test section gradation on SH 794, and is quite similar to the City of Lethbridge Mix C.

2.3 Specimen Preparation

2.3.1 Indirect Tensile Test Specimens

A total of 48 specimens having nominal dimensions of 64 mm thickness and 102 mm diameter were compacted in a California

kneading compactor using the procedure given in MS-2 of the Asphalt Institute. This enabled a replication of 6 specimens for each of the test temperatures of 0 C, -10 C, -20 C and -30 C, for the low temperature indirect tensile test method. Twenty-four specimens were compacted for each mix.

For the City of Lethbridge project the specimens were mixed at a binder content of 6.0% by mass of dry aggregate (5.67% by mass of mix). This slightly higher binder content than that used in the test sections (5.67% versus 4.70% for mix B and 4.90% for mix C), was selected on the basis of preliminary mix designs run in our laboratory, which may have been influenced by marginally higher amounts passing the 0.16 mm and 0.08 mm sieve sizes.

The 150/200 penetration grade samples were compacted by kneading compaction at a temperature of 135 C and achieved a mean density of 2358 kg/m^3, having a calculated air void content of 3.1%. The PMA 2 samples were compacted at 165 C to an average density of 2359 kg/m^3 and the same air void content.

For the SH 794 project the 150/200A specimens were mixed at a binder content of 5.80% by mass of dry aggregate. Compaction was at 135 C and achieved a mean density of 2339 kg/m^3, giving a calculated air void content of 3.3 percent. The Imperial PMA mixes were compacted to a mean density of 2340 kg/m^3 at the same temperature, yielding the same air void content.

2.3.2 Repeated Load Triaxial Test Specimens

A total of 36 specimens of nominal size 102 mm diameter and 204 mm height were also compacted with the kneading compactor but using split molds for fabrication. Several trials were required to determine a procedure for producing a fairly uniform density throughout the sample to the same target.

A total of 4200 g of mix for each specimen was divided into three portions and compaction was carried out at the following pressures set on the kneading compactor:

1st lift - 1.73 MPa (250 psi) - 20 tamps

2nd lift - 2.07 MPa (300 psi) - 75 tamps

3rd lift - 3.45 MPa (500 psi) - 75 tamps

As each lift was compacted the mix was slowly added in order to assist in obtaining uniform density. Six blows with a hand Marshall hammer were finally applied to the specimens.

The 150/200 samples achieved average densities of 2359 kg/m^3 and the PMA 2 specimens had slightly lower densities of 2355 kg/m3. Replicate specimens of 6 were prepared for testing at temperatures of 25 C, 35 C and 45 C under repeated triaxial loading.

2.4 Testing Conditions

The indirect tensile testing was conducted as described previously (Anderson and Leung, 1987) at the specified temperatures. The loading rate was kept constant at a nominal rate of 1.5 mm/min resulting in failure in the order of 1 to 3 minutes.

The repeated load triaxial testing was also conducted as described previously (McMillan and Anderson, 1988). A confining pressure of 35 kPa and a repeated axial compressive stress of 350 kPa was applied through pneumatic cylinders controlled by electric solenoids. The signal to the solenoids was provided as a square wave (0.5 s on/off), resulting in a build-up of stress in 0.2 s and a dwell of 0.3 s. The permanent deformation was observed and analyzed at various intervals up to 99 000 cumulative repetitions.

3. LOW TEMPERATURE TEST RESULTS

3.1. Low Temperature Tensile Characteristics- Lethbridge

Table 5 summarizes the average stresses, strains, and stiffness moduli of the test specimens at failure, for the Lethbridge series. A major problem with undertaking tests of this type is the scatter of results, particularly at very low temperatures. It has been the practice in the past to test five specimens at each temperature, and to present the results based on the average values determined for the valid tests (Leung, 1986). Generally, strain values were rejected when they exceeded the coefficient of variation of 30 percent for temperature of 0 C and -10 C, and 40 percent for -20 C and -30 C. New averages were calculated in such instances.

Figures 1 to 3 present plots of failure stress, failure strain, and failure stiffness, versus temperature for 150/200 and Husky PMA 2 asphalt cements, for direct visual comparison. Examination of these tabulated and plotted results leads to the following observation, for comparable temperatures and using 150/200 mixes as reference:

1. Husky PMA 2 exhibits higher failure stresses, observed at temperatures of -10 C and -30 C . The greatest change in the failure stress occurs when the temperature changed from -20 C to -30 C. In general, the failure stress increases as the test temperature decreases.

2. Husky PMA 2 exhibits higher failure strains, observed at temperatures of 0 C and -10 C. At temperatures of -20 C and colder the strains experienced by both mixes are nearly the same. When the temperature changes from -10 C to -20 C, the strain decreases very rapidly. In general it is observed that the strain decreases as the temperature decreases.

3. Husky PMA 2 exhibits lower failure stiffness, especially observed at temperature of -20 C and colder. There is a very rapid change in the stiffness as the temperature decreases from -10 C and colder. In general it is observed that as the temperature decreases the failure stiffness increases.

These results support the statement of Arand, as reported by King et al.(1988) that polymers provide the asphalt concretes with higher tensile strength at low temperatures, in order to resist thermal and load-related stresses, with the additional advantage of being able to withstand greater strains without cracking.

Figures 4 to 6 present the average stress-strain curves for the test specimens fabricated with 150/200 and Husky PMA 2 asphalt cements at different test temperatures. The points on the graph are average of 6 samples tested at each temperature.

Generally, for the Husky PMA 2 asphalt, the average failure stress is higher than that for 150/200 Pen grade asphalt cement, except at 0 C where the failure stress is approximately the same for both mixes. However, the average failure strain is markedly higher for Husky PMA 2 at 0 C and -10 C.

3.2 Low Temperature Tensile Characteristics for SH 794

Table 6 summarizes the average failure stresses, strains, and stiffnesses for specimens fabricated with Secondary Highway 794 aggregate two asphalts 150/200A and Imperial PMA.

Figures 7 to 9 present the failure stress, failure strain and failure stiffness versus temperature for 150/200A and Imperial PMA asphalt cement mixes for direct visual comparison.

Examination of these tabulated and plotted results leads to the following observations, for comparable temperatures and using 150/200A mix as reference:

1. Imperial PMA exhibits lower failure stresses at temperatures of 0 C and -10 C, but at -20 C and colder temperatures, this trend reverses and an opposite trend is observed.

2. Imperial PMA exhibits higher failure strains. The difference is quite significant at all testing temperatures. The greatest decrease in the strain occurs when the temperature changes from -10 C to -20 C. Thus, Imperial PMA follows the same trend as previously reported in that, with a decrease in temperature, the failure strain decreases.

3. Imperial PMA exhibits lower failure stiffness. The stiffness at -20 C and colder temperature for 150/200A asphalt cement is very high as compared to Imperial PMA; thus, Imperial PMA shows a great improvement with respect to the factors that influence resistance to low temperature cracking.

Figures 10 to 13 present the average stress-strain curves of the test specimens fabricated with 150/200A and Imperial PMA asphalts, at different test temperatures. The failure stress for 150/200A is higher at temperatures of 0 C.

3.3 Low Temperature Evaluation of Polymer Modified Asphalt Cements

The indirect tensile tests demonstrate that PMA asphalt mixtures sustain larger strains at failure; this is an important property to resist thermally induced cracking. Furthermore, the lower tensile stiffness of the polymer modified asphalt concrete mixtures implies that the induced tensile stresses, due to changing temperatures, will be

smaller for these mixtures. Thus, the chance of thermal cracking is reduced. Also the toughness of both polymer modified asphalt cement is higher than conventional asphalt cement.

On the basis of the trends observed from laboratory testing to determine the characteristics of conventional and polymer modified asphalt concrete mixes, all point to the polymer modified mixes as being more resistant to thermally induced stresses at low temperatures and should show superior performance under these conditions.

The Lethbridge and Secondary Highway 794 aggregate series cannot be compared directly, due to the difference in the base asphalt cements. One important conclusion which can be drawn from the testing is that, in mixtures with different aggregates, both of these polymer modified asphalts exhibit higher failure strains and lower failure stiffnesses and therefore are expected to perform better than conventional asphalt cements.

4. HIGH TEMPERATURE TEST RESULTS

4.1 Repeated Load Triaxial Tests

The repeated load triaxial tests measures the percent permanent strain for each sample, at various repetitions of the axial load. Results for each individual specimen were recorded, but for convenience, average strain values are reported at selected repetitions of 10, 50, 100, 1 000, 5 000, 10 000 and in increments of 10 000 up to 99 000 repetitions or failure.

As discussed previously, two different types of aggregates were used in the fabrication of specimens, so the results for both series of test specimens will be discussed separately.

4.1.1 High Temperature Permanent Deformation Characteristics Lethbridge Aggregate

Tables 7 and 8 summarize the percent permanent strain at each temperature for the two types of binder using Lethbridge aggregate. Permanent strain values for the individual specimen tested were tabulated for a selected number of repetitions, i.e 10, 50, 100, 1 000, 5 000, and increments of 10 000 to failure or 99 000 repetitions. Average values for permanent strain are reported for convenience. Specimens which exhibited unusually large strains, for no apparent reason were removed prior to calculating the average.

Figures 14 and 15 present the permanent deformation curves for 150/200 pen grade mix, and Husky PMA 2 for three temperatures. Figures 16 to 18 present the two mixes side-by-side, for comparison at each test temperature of 25 C, 35 C, and 45 C.

Examinations of the data and plots lead to the following observations, for comparable temperatures, using 150/200 mix as a reference:

1. At 25 C, the strain for Husky PMA 2 is 1 percent compared to 150/200 pen grade asphalt which has a strain of about 2.8 percent at 99 000 repetitions under the same conditions.

2. At 35 C, the strain for Husky PMA 2 was 1.3 percent compared to 150/200 mix which has strain of about 6.8 percent at 80 000 repetitions under the same conditions.

3. At 45 C the strain for Husky PMA 2 was 1.9 percent compared to 150/200 mix, which has strain of about 9.7 percent, 40 000 repetitions, under the same testing conditions.

An overview of the results for the above mixes, shows that the strain increases as the temperature increases. This is due to the fact that, as the temperature increases, the binder stiffness decreases, making the mixes to be less resistant to permanent deformation.

In addition, from Figure 18, it can be observed that the Husky PMA 2, at 45 C, had a strain of 3.2 percent after 90 000 repetitions, whereas the control mix (150/200) had a strain of about 10 percent after only 40 000 repetitions.

The data and plots incicate that the polymer modified mixes tested show improved resistance to permanent deformation under repeated loading and thus could be expected to demonstrate superior performance under traffic loadings at high temperatures.

4.1.2 High Temperature Permanent Deformation Characteristics SH 794 Aggregate

Tables 9 and 10 summarizes the percent strains at each test temperature, for the two types of binders using the SH 794 aggregate. Average values for the tested specimens at each temperature are reported, with those having unusually large strain values for no apparent reason being removed.

Figures 19 and 20 present the the permanent deformation curves for both the 150/200A and Imperial PMA, at the three test temperatures. Figures 21 to 23 compare the two mixes side-by-side, at test temperatures of 25 C, 35 C and 45 C.

Examination of the data and figures leads to the following observations, using the 150/200A mix as a reference:

1. At 25 C, the strain for Imperial PMA is 0.8 percent compared to 2.6 percent at 99 000 repetitions.

2. At 35 C, the strain for the Imperial PMA is 0.99 percent compared to 5.7 percent at 99 000 repetitions.

3. At 45 C, the strain for the Imperial PMA is 1.4 percent compared to 7.8 percent at 80 000 repetitions.

Again, the data indicates that the polymer modified mixes, as compared to conventional mixes show improved resistance to permanent deformation under repeated loading conditions, and thus could be expected to demonstrate superior performance under traffic loading, especially at high temperatures.

4.2 High Temperature Performance of Conventional and Polymer Modified Asphalt Cements

According to the observed behavior of both conventional and polymer modified asphalt cements during repeated load triaxial testing, it is noted that, in general, polymer modified asphalt cement mixes perform better than the conventional asphalt cement mixes, especially at high temperatures, where the conventional mixes were seen to undergo large strains.

Although the types of aggregate used to fabricate the test specimens were different for the Husky PMA 2 and Imperial PMA mixes, it is observed from the data and the plotted results that both polymer modified asphalt cement mixes performed better than the mixes made with the conventional type of asphalt cements. The Imperial PMA showed better performance in terms of lower percent permanent strain, as compared to the Husky PMA 2. This may be due to the presence of higher amount of manufactured fines in the Secondary Highway 794 aggregate. Figures 24 and 25 compare the permanent strain at 25 C, 35 C, and 45 C for conventional and polymer modified asphalt cements. For comparable strain of 8 percent and conventional asphalt cements the Lethbridge aggregate reached

this load at 30 000 repetitions. whereas the Secondary Highway 794 aggregate sustained 60 000 repetitions at 45 C. The effect of different types of aggregates on the characteristics of conventional and polymer modified asphalt cements is evident.

5. CONCLUSIONS

Base on the laboratory test data for the conventional 150/200 penetration grade asphalt cements and the two types of polymer modified asphalts cements, the following conclusions may be drawn:

1. The indirect tensile strength test results show the that both polymer modified mixes exhibit higher failure stresses, higher failure strains, and lower failure stiffness values in the temperature range from 0 C to -30 C. According to these results, the PMA mixes are expected to be more resistant to thermally induced stresses at low temperatures.

2. For all mixes tensile failure stresses increase, failure strains decrease and failure stiffnesses increase with a decrease in temperature.

3. The repeated load triaxial test results show that the polymer modified mixes exhibit less permanent strain than the conventional mixes, demonstrating that they are more resistant to permanent deformation at high temperatures.

4. From the trends observed at the high and low temperature ranges, the polymer modified asphalt mixes are expected to perform better in resisting permanent deformation and low temperature cracking.

ACKNOWLEDGEMENTS

This paper is based on several research and commercial testing projects carried out at the University of Alberta. The initial funding grant was from the Central Research Fund of the University. Other sources have been the Natural Sciences and Engineering Research Council of Canada (NSERC) and an industry matching grant under the Alberta Advanced Education Endowment and Incentive Program. This grant became available as a result of the support provided by Esso Petroleum Canada Limited, under Imperial Oil's Committee on Higher Education. Husky Oil Operations Ltd. has also provided samples and support for testing. Materials and information provided by Alberta Transportation and Utilities, EBA Engineering Consultants Ltd and other various sources are gratefully acknowledged.

REFERENCES

Anderson, K.O. and S.R. Hussain. 1989. **"Evaluation of Low Temperature and Permanent Deformation Characteristics of Some Engineered Asphalts"**, Proceedings, Canadian Technical Asphalt Association, Vol. 34, pp.292-310.

Anderson, K.O. and S.C. Leung. 1987. **"Applications of a Method for Evaluation of Low Temperature Tensile Properties of Asphalt Concrete"**, Proceedings Mini-Workshop 3, Paving in Cold Areas, Canada/Japan Science and Technology Consultations, Ottawa, Ontario Volume 1, pp 335-366.

Dawley, C.B., B.L. Hogeweide and K.O. Anderson. 1990. **"Mitigation of Instability Rutting of Asphalt Pavements in Lethbridge, Alberta, Canada"**, Presented at the 1990 Annual Meeting of the Association of Asphalt Paving Technologists, Albuquerque, N.M. (in press).

EBA Engineering Consultants Ltd., February 1989, "**Lethbridge Rutting Study Test Pavement Installation.**", Final report submitted to the City of Lethbridge.

Hadipour, K. and K.O. Anderson. 1988. "**An Evaluation of Permanent Deformation and Low Temperature Characteristics of Some Recycled Asphalt Concrete Mixtures**", Proceedings of the Association of Asphalt Paving Technologists, Vol. 57, pp. 615-644.

Hogeweide, B.L. and A.B. MacDonald. 1988. "**Mitigation of Instability Asphalt Pavement Rutting**", Proceedings of the Annual Conference of the Roads and Transportation Association of Canada, pp D3-D27.

Hussain, S.R. 1990. "**Evaluation of Low Temperature and Permanent Deformation Characteristics of Some Polymer Modified Asphalts**", M.Sc. Thesis, University of Alberta, Spring 1990, p 246.

King, G.N., H.W. King, O. Harder and P. Chaverot. 1988. "**Low Temperature Benefits of Polymer Modified Asphalts.**", Proceedings, Canadian Technical Asphalt Association, Vol.33, pp. 198-216.

Leung, S.C. 1986. "**Evaluation of Asphalt Cements For Low Temperature Performance.**", M.Sc. Thesis, University of Alberta, Fall 1986, p 164.

McMillan, C. and K.O. Anderson. 1988. "**An Evaluation of the Influence of the Binder on Permanent Deformation of Asphalt Concrete**", Proceedings, Canadian Technical Asphalt Association, Vol. 33, pp. 236-257.

Zanzotto, L., D. Foley, C.E. Rodier and R.D. Watson. 1987. "**Modified Asphalts-Are Your Really Coming?**", Proceedings, Canadian Technical Asphalt Association, Vol. 32, pp. 92-117.

Table 1. Lethbridge Aggregate Gradation

Sieve (mm)	16.0	12.5	10.0	5.0	2.5	1.25	0.063	0.315	0.160	0.080
	Percent Passing									
U of A Lab. Spec.	100	97.0	83.0	60.3	43.8	30.9	21.7	13.7	8.2	5.6
EBA Mix C Design	100	95.7	85.2	58.4	49.2	37.6	26.8	15.4	8.9	5.1
Test Sec C	100	94.7	81.7	57.7	45.0	32.0	22.7	13.3	7.9	4.7
EBA Mix B Design	100	94.0	80.0	59.0	47.0	34.0	26.0	16.0	10.0	6.6
Test Sec B Lethbridge	100	94.3	77.3	54.7	44.7	32.0	23.0	13.3	8.0	4.9

Table 2. Physical Properties of Asphalt Cement Samples

Properties	150/200	Husky PMA 2	150/200A	Imperial PMA
Penetration @ 25 C (dmm)	146 (153)*	136 (133)*	158	96 (95)**
Penetration @4 C (dmm)	15	23	13	24 (20)
Absolute Vis @ 60 C, Pa.s	89.0 (96.0)	259 (340)	88	449 (713.9)
Kinematic Vis @ 135 C mm2/s	270 (271)	774 (848)	261	1079 (1133)
R & B Soft Point (C)	38.0	59.5	43.0	63.0

* from Table NO. 2, EBA, 1989
** from Alberta Transportation Lab Report

Table 3. Temperature Susceptibility Parameters

Parameters	150/200	Husky PMA 2	150/200A	Imperial PMA
PI(dPen/dT)	-1.05	0.57	-1.62	2.33
PI (R&B)	-2.19	4.18	0.15	3.57
PVN(25-60)	-0.26	0.86	-0.13	1.25
PVN(25-135)	-0.39	1.24	-0.35	0.78

Table 4. Aggregate Gradations Secondary Highway 794 Project

Sieve Size (mm)	16.0	12.5	10.0	5.0	1.25	0.63	0.135	0.160	0.080
	Percent Passing								
AT & U Grad. 70% C 30% M.F.	100	90.0	80.0	55.0	30.0	25.0	19.0	11.5	5.9
Test Section 75% C 25% M.F.	100	94.0	83.0	58.0	34.0	29.0	22.0	14.2	7.2
U of A Grad. 75% C 25% M.F.	100	98.0	85.0	54.0	30.0	25.0	18.0	11.0	6.9

C = Coarse
M.F = Manufactured fines

Table 5. Average Stress, Strain, and Stiffness Values for Lethbridge Aggregate

Type of Binder	Test Temperature (C)	Failure Stress (KPa)	Failure Strain (0.0001)	Failure Stiffness (MPa)
150/200	0	1 120	96.0	210
Husky PMA 2	0	1 130	160.0	120
150/200	- 10	2 050	60.0	930
Husky PMA 2	- 10	2 790	95.0	420
150/200	- 20	3 880	18.0	4 710
Husky PMA 2	- 20	3 940	22.0	3 630
150/200	- 30	4 090	4.0	17 700
Husky PMA 2	- 30	4 650	7.0	12 000

Table 6. Average Stress, Strain and Stiffness Values for Secondary Highway 794 Aggregate

Type of Binder	Test Temperature (C)	Failure Stress (KPa)	Failure Strain (0.0001)	Failure Stiffness (MPa)
150/200A	0	1 400	110.0	210
Imperial PMA	0	1 060	127.0	140
150/200A	- 10	3 455	50.0	1 260
Imperial PMA	- 10	2 755	80.0	600
150/200A	- 20	4 200	5.0	153 50
Imperial PMA	- 20	4 415	14.0	58 35
150/200A	- 30	4 330	2.5	23 980
Imperial PMA	- 30	5 030	7.25	11 060

Table 7. Percent Permanent Strain for 150/200

No of Repet (N)	Temperature (C) 25	35	45
0	0 (0.000)	0 (0.000)	0 (0.000)
10	0.152 (0.093)	0.217 (0.027)	0.386 (0.323)
50	0.278 (0.168)	0.394 (0.039)	0.629 (0.378)
100	0.458 (0.134)	0.489 (0.042)	0.659 (0.420)
1 000	0.614 (0.308)	0.983 (0.031)	1.594 (0.676)
5 000	1.188 (0.300)	1.776 (0.144)	4.015 (1.066)
10 000	1.211 (0.263)	2.331 (0.318)	4.761 (1.494)
20 000	1.391 (0.240)	2.917 (0.544)	7.081 (1.527)
30 000	1.560 (0.222)	3.579 (0.551)	7.975 (0.476)
40 000	1.698 (0.146)	4.183 (0.439)	9.661 (0.306)
50 000	1.811 (0.165)	4.970 (0.534)	
60 000	1.914 (0.247)	5.846 (0.716)	
70 000	2.037 (0.414)	6.106 (0.484)	
80 000	2.419 (0.693)	6.782 (0.241)	
90 000	2.779 (1.119)		
99 000			

( ) are standard deviations for the average strain values

Table 8. Percent Permanent Strain for Husky PMA 2

No of Rept. (N)	Temperature (C) 25	35	45
0	0 (0.000)	0 (0.000)	0
10	0.180 (0.085)	0.203 (0.024)	0.177 (0.020)
50	0.290 (0.091)	0.249 (0.028)	0.292 (0.028)
100	0.339 (0.094)	0.292 (0.028)	0.347 (0.013)
1 000	0.480 (0.105)	0.477 (0.058)	0.576 (0.059)
5 000	0.582 (0.131)	0.653 (0.072)	0.803 (0.144)
10 000	0.634 (0.117)	0.775 (0.092)	1.039 (0.211)
20 000	0.699 (0.128)	0.923 (0.113)	1.432 (0.340)
30 000	0.745 (0.141)	1.021 (0.133)	1.674 (0.403)
40 000	0.785 (0.141)	1.093 (0.147)	1.853 (0.450)
50 000	0.820 (0.158)	1.152 (0.159)	2.045 (0.489)
60 000	0.855 (0.173)	1.194 (0.166)	2.191 (0.525)
70 000	0.888 (0.213)	1.237 (0.177)	2.510 (0.740)
80 000	0.934 (0.238)	1.272 (0.185)	2.594 (0.663)
90 000	0.971 (0.278)	1.302 (0.189)	2.865 (0.749)
99 000	1.014 (0.325)	1.325 (0.192)	3.145 (0.837)

( ) are standard deviations for the average strain values

Table 9. Percent Permanent Strain for 150/200A

No of Repet. (N)	Temperature (C) 25	35	45
0	0 (0.000)	0 (0.000)	0 (0.000)
10	0.234 (0.099)	0.445 (0.403)	0.221 (0.169)
50	0.408 (0.154)	0.572 (0.407)	0.458 (0.160)
100	0.492 (0.196)	0.634 (0.408)	0.538 (0.160)
1 000	0.825 (0.438)	0.923 (0.402)	1.075 (0.247)
5 000	1.138 (0.733)	1.332 (0.347)	2.222 (0.486)
10 000	1.322 (0.924)	1.678 (0.261)	3.185 (0.712)
20 000	1.564 (1.168)	2.315 (0.202)	4.615 (1.015)
30 000	1.748 (1.397)	2.891 (0.512)	5.688 (1.186)
40 000	1.904 (1.519)	3.539 (0.995)	6.364 (0.950)
50 000	2.044 (1.666)	4.303 (1.646)	6.744 (0.718)
60 000	2.172 (1.802)	4.894 (2.065)	6.888 (0.550)
70 000	2.292 (1.926)	5.108 (1.940)	7.144 (0.542)
80 000	2.406 (2.037)	5.325 (1.806)	7.782 (0.640)
90 000	2.533 (2.137)	5.546 (1.672)	
99 000	2.628 (2.234)	5.742 (1.559)	

( ) are standard deviations for the average strain values

Table 10. Percent Permanent Strain for Imperial PMA

No of Repet. (N)	Temperature (C) 25	35	45
0	0 (0.000)	0 (0.000)	0 (0.000)
10	0.133 (0.062)	0.307 (0.159)	0.142 (0.095)
50	0.292 (0.085)	0.408 (0.163)	0.225 (0.098)
100	0.340 (0.091)	0.449 (0.165)	0.263 (0.100)
1 000	0.357 (0.098)	0.593 (0.195)	0.425 (0.095)
5 000	0.418 (0.102)	0.728 (0.253)	0.626 (0.101)
10 000	0.452 (0.100)	0.795 (0.291)	0.750 (0.111)
20 000	0.495 (0.089)	0.862 (0.330)	0.911 (0.121)
30 000	0.575 (0.120)	0.890 (0.341)	1.023 (0.124)
40 000	0.608 (0.126)	0.912 (0.348)	1.115 (0.121)
50 000	0.647 (0.170)	0.929 (0.353)	1.194 (0.113)
60 000	0.678 (0.175)	0.944 (0.357)	1.268 (0.099)
70 000	0.707 (0.195)	0.961 (0.366)	1.346 (0.082)
80 000	0.734 (0.216)	0.970 (0.366)	1.431 (0.057)
90 000	0.760 (0.240)	0.985 (0.370)	1.534 (0.019)
99 000	0.783 (0.256)	0.996 (0.373)	1.635 (0.058)

( ) are standard deviations for the average strain values

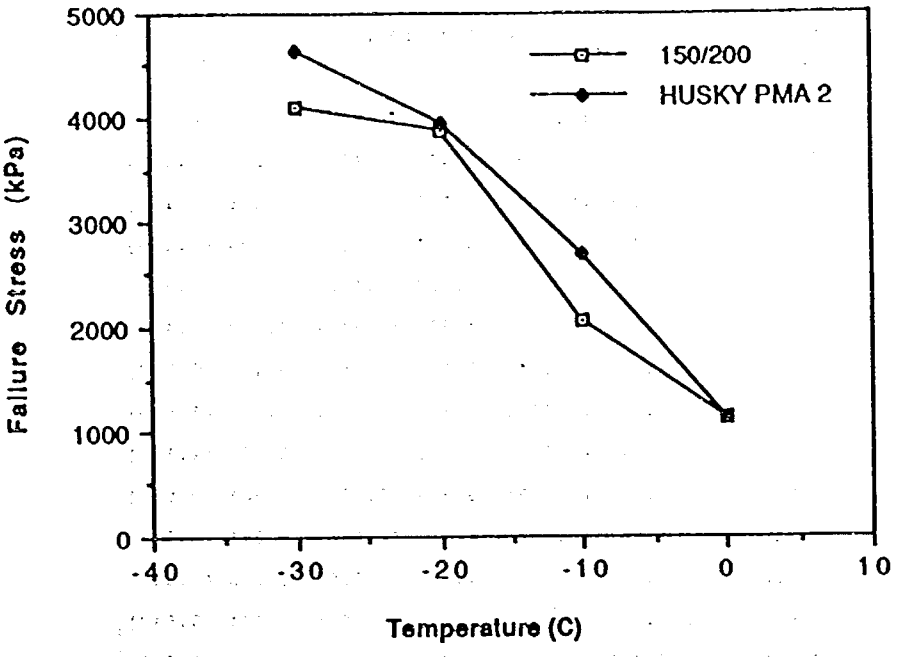


Figure 1. Average Failure Stress-Temperature Relationship for Lethbridge Aggregate

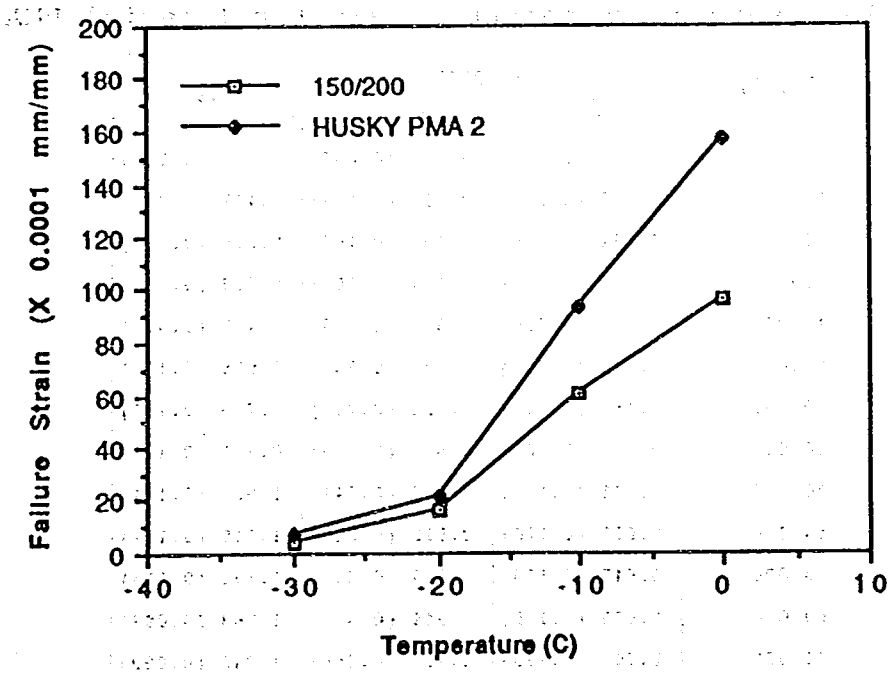


Figure 2. Average Failure Strain-Temperature Relationship for Lethbridge Aggregate

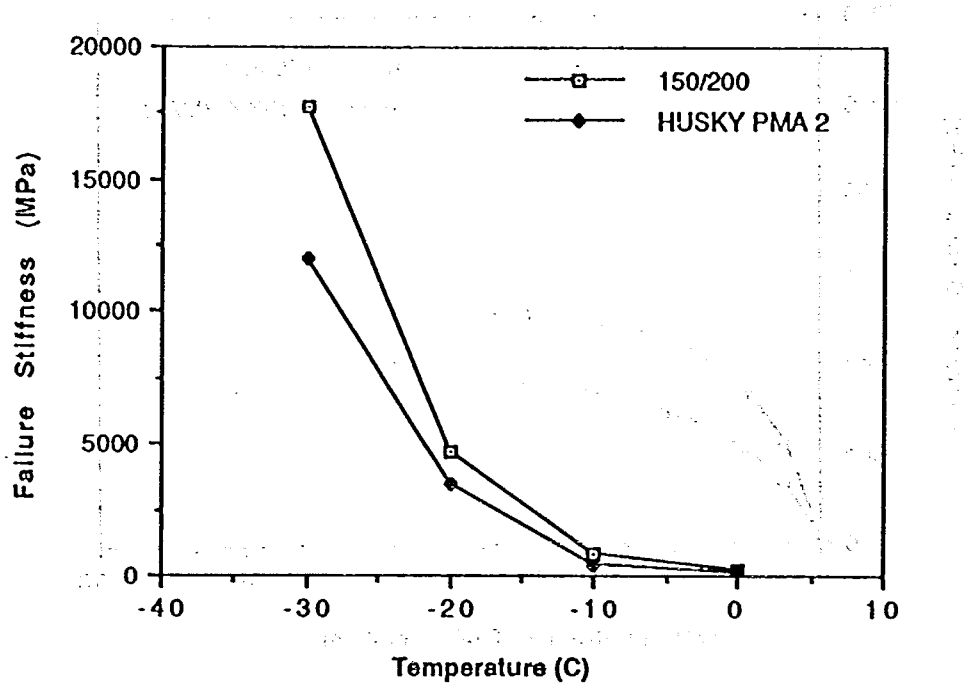


Figure 3. Average Failure Stiffness-Temperature Relationship for Lethbridge Aggregate

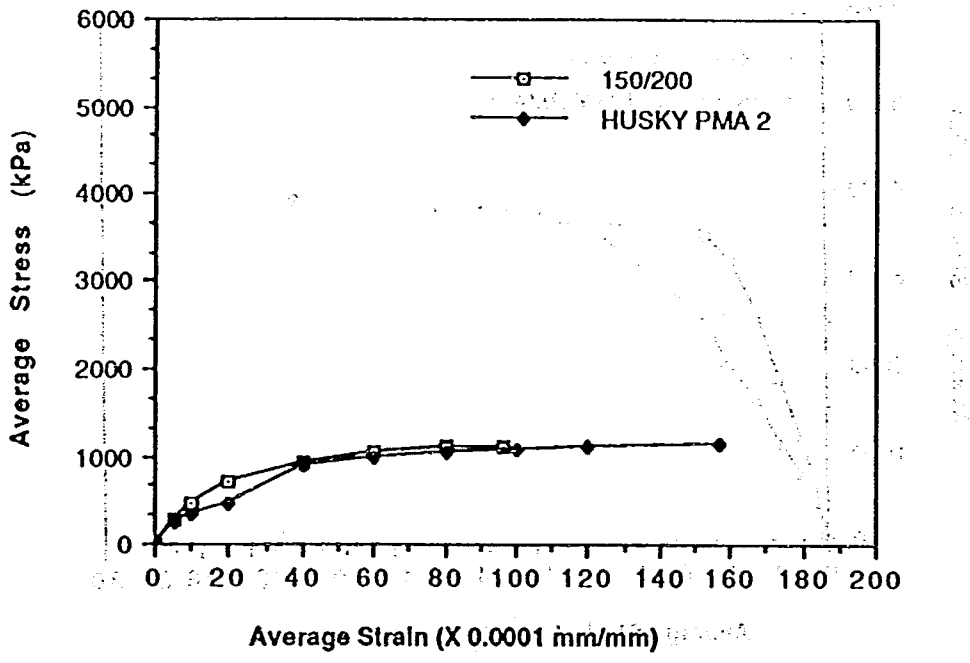


Figure 4. Average Stress-Strain Curves at 0 C for Lethbridge Aggregate

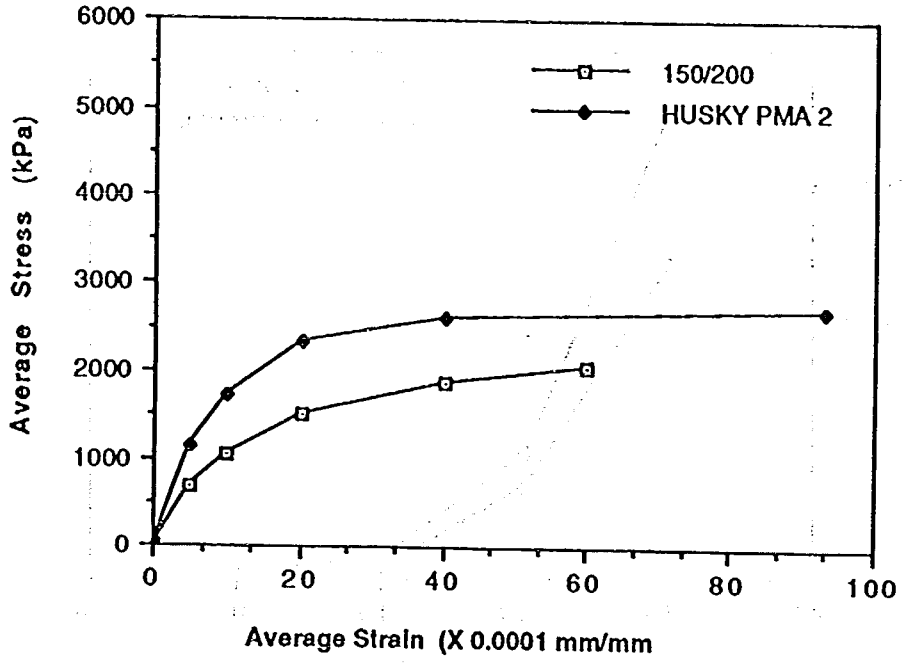


Figure 5. Average Stress-Strain Curves at -10 C for Lethbridge Aggregate

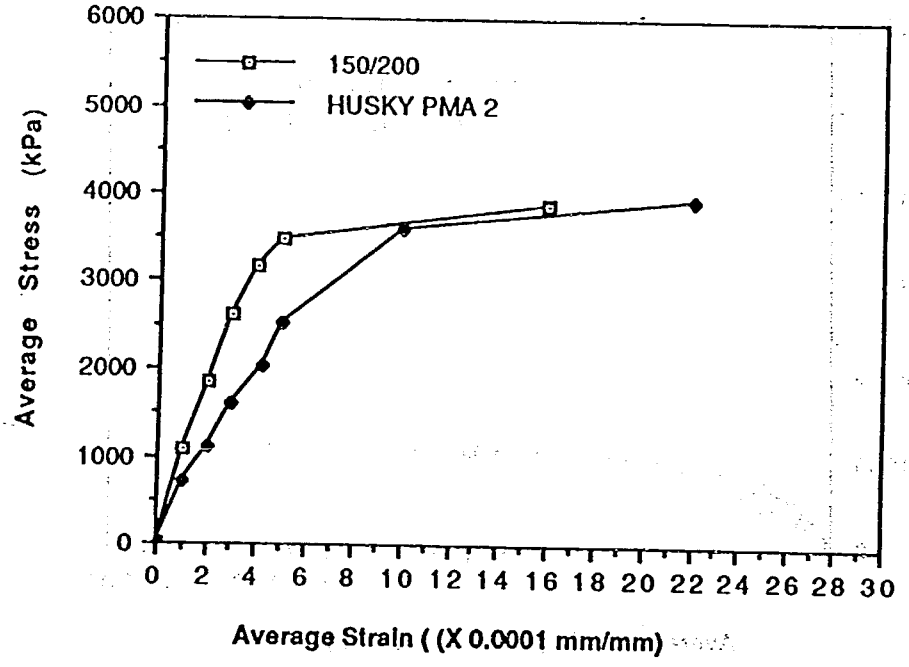


Figure 6. Average Stress-Stress-Strain Curves at -20 C for Lethbridge Aggregate

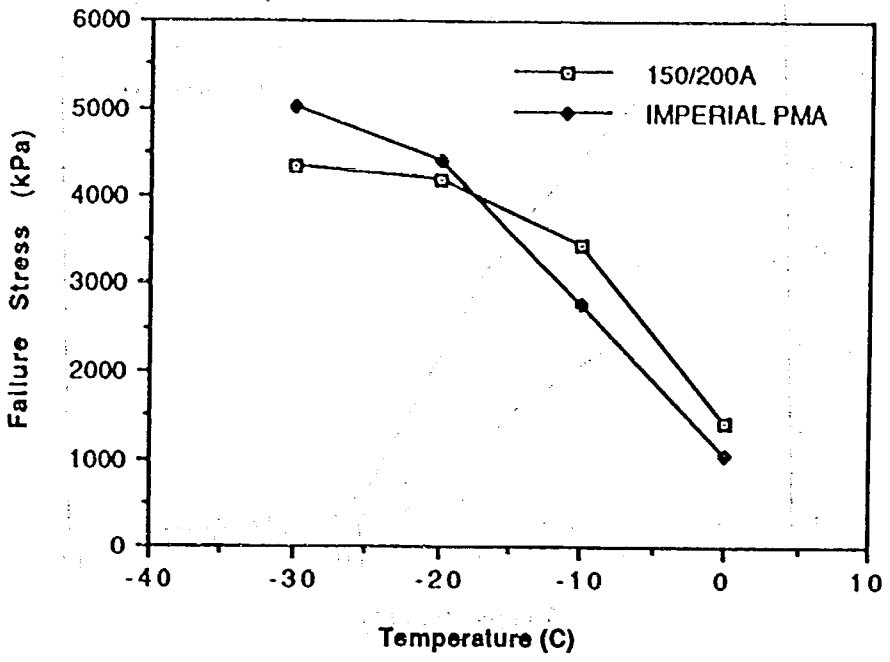


Figure 7. Failure Stress-Temperature Relationship for Secondary Highway 794 Aggregate

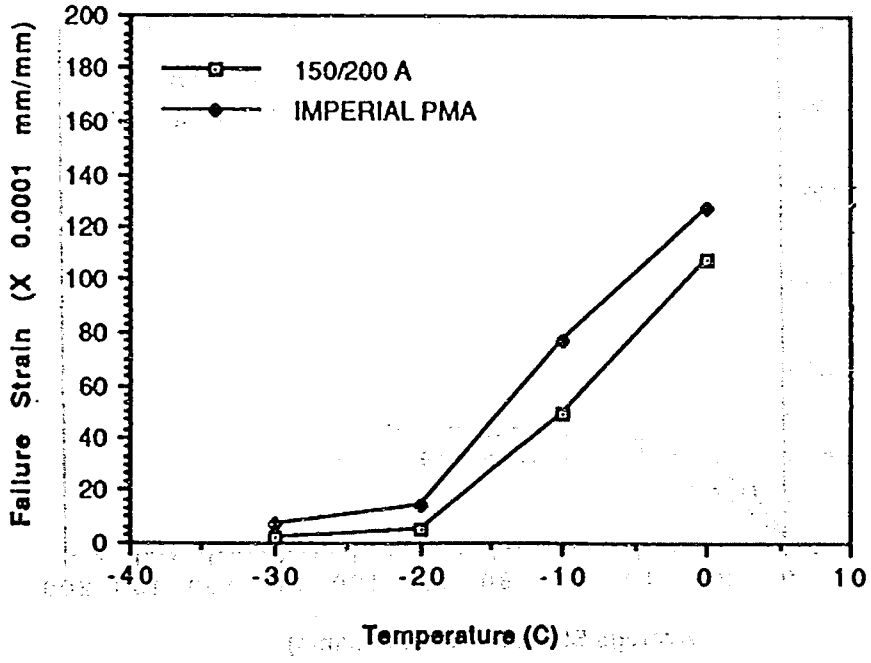


Figure 8. Failure Strain-Temperature Relationship for Secondary Highway 794 Aggregate

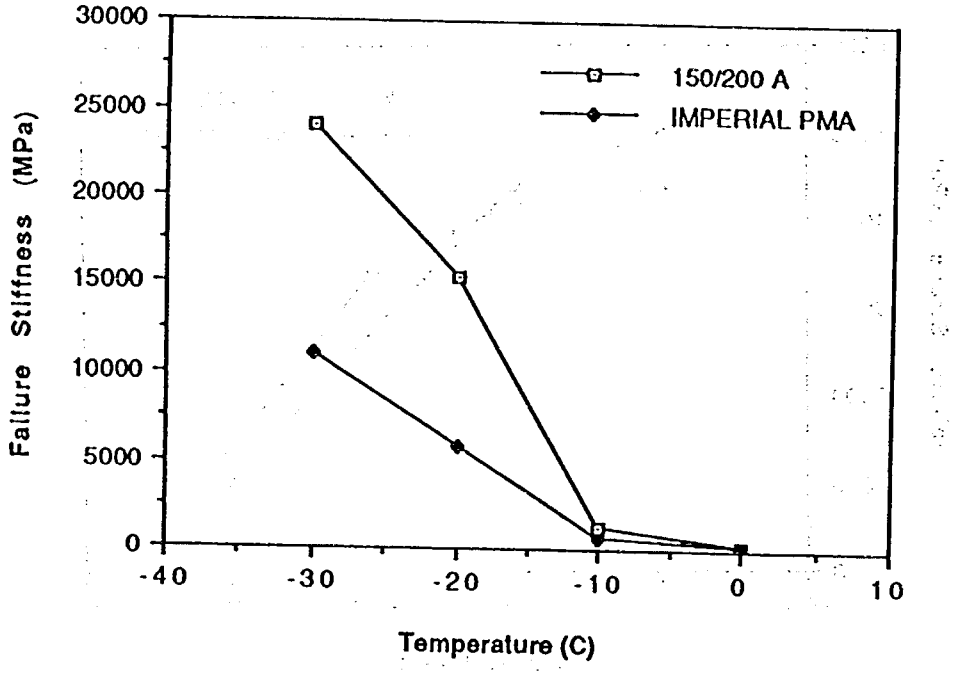


Figure 9. Failure Stiffness-Temperature Relationship for Secondary Highway 794 Aggregate

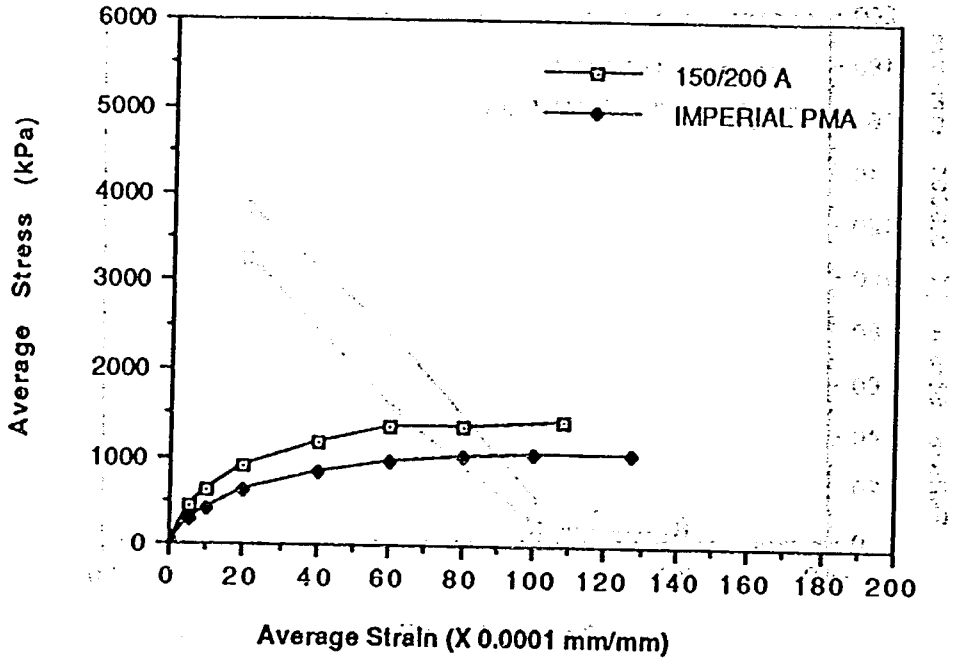


Figure 10. Average Stress-Strain Curves at 0 C for Secondary Highway 794 Aggregate

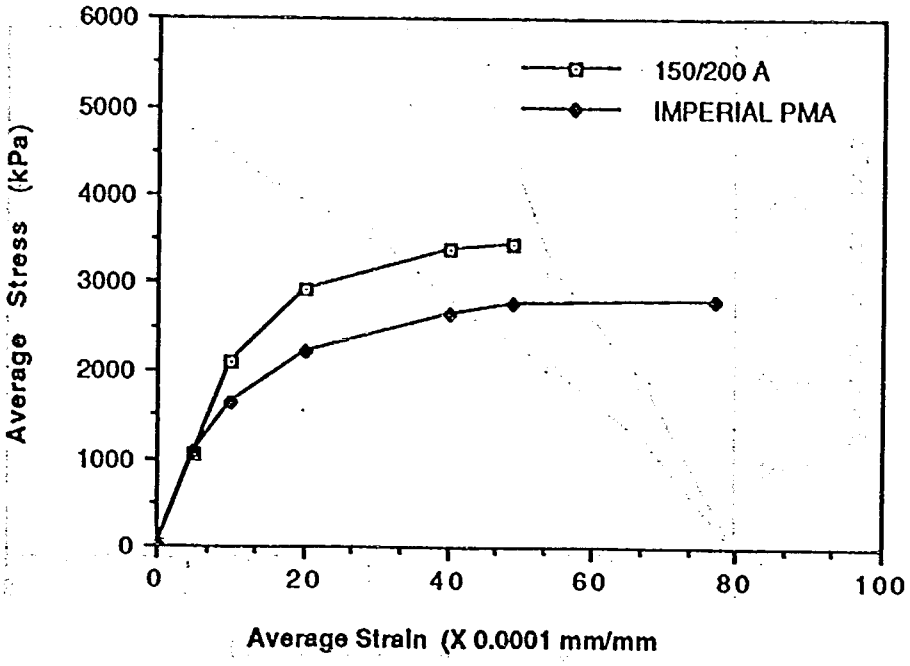


Figure 11. Average Stress-Strain Curves at -10 C for Secondary Road 794 Aggregate

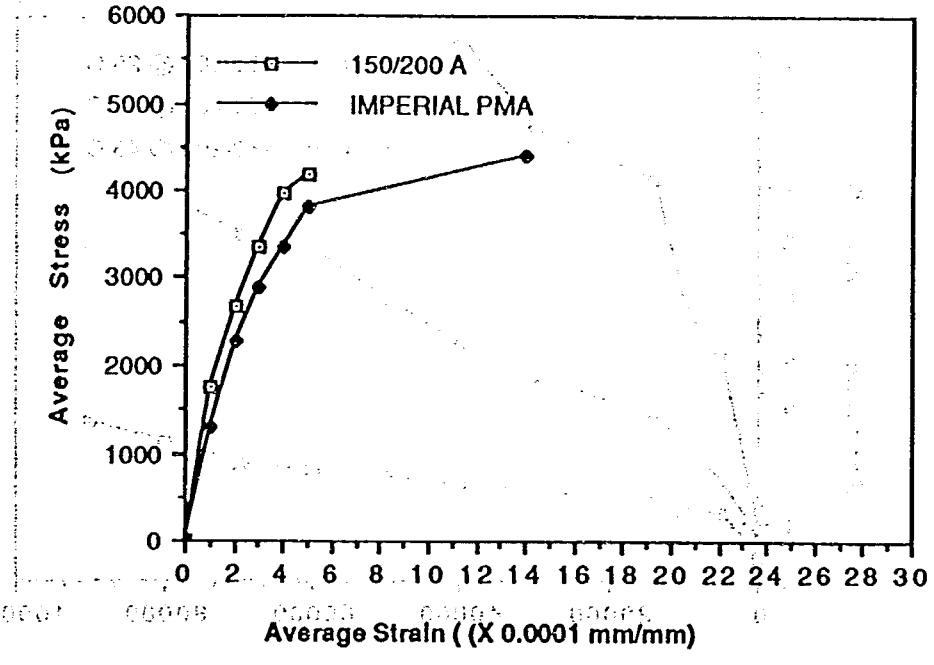


Figure 12. Average Stress-Strain Curves at -20 C for Secondary Highway 794 Aggregate

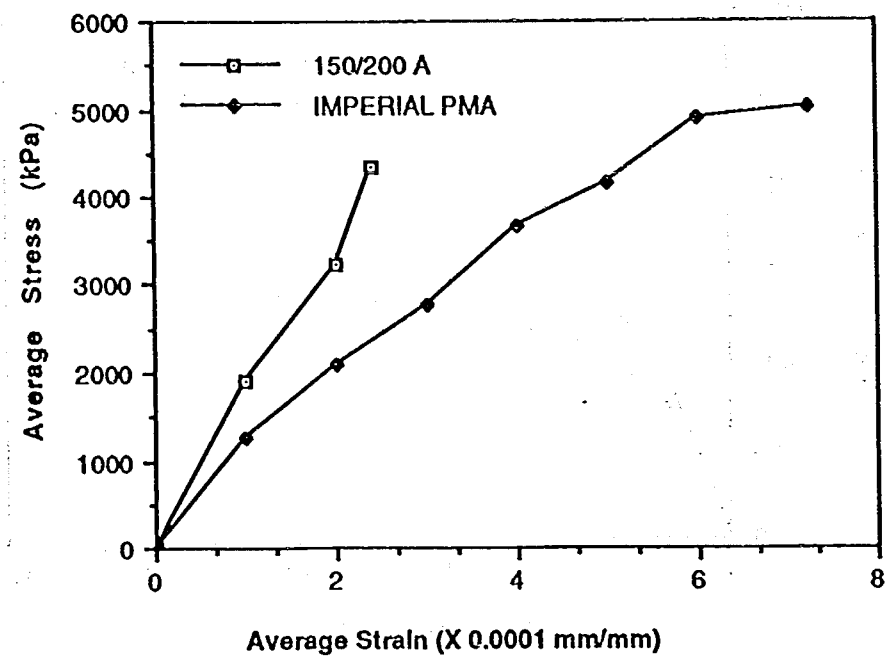


Figure 13. Average Stress-Strain Curves at -30 C for Secondary Highway 794 Aggregate

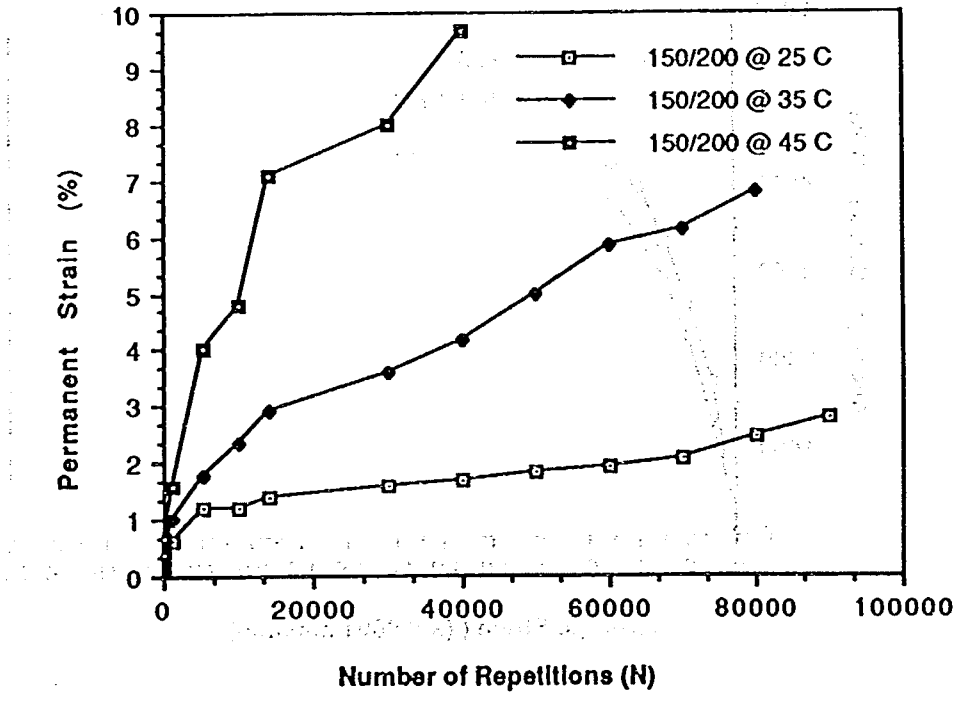


Figure 14. Permanent Deformation Curves for 150/200 Lethbridge Aggregate

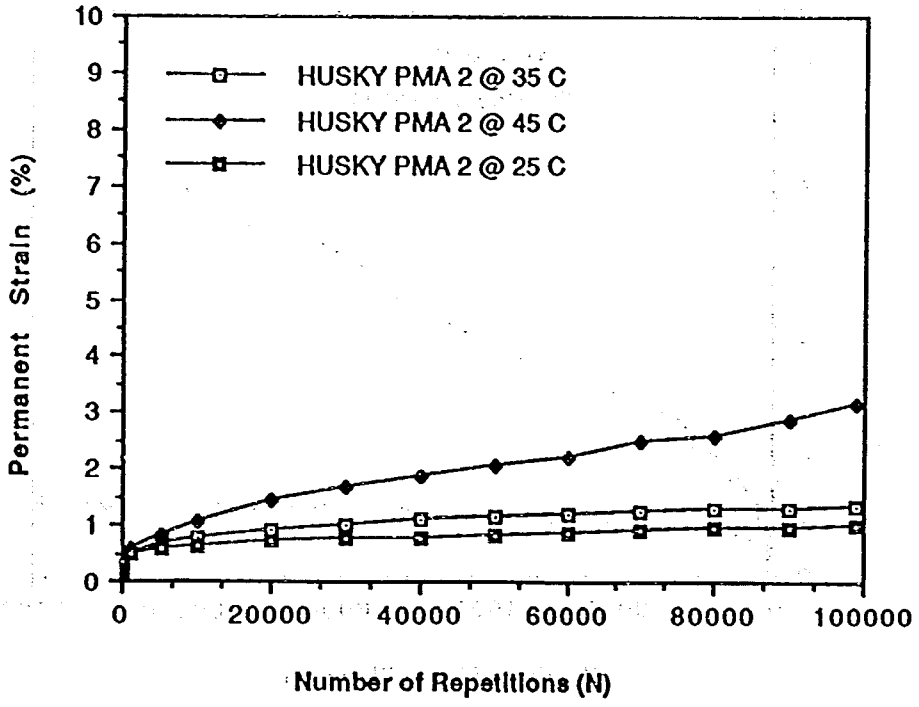


Figure 15. Permanent Deformation Curves for Husky PMA 2 Lethbridge Aggregate

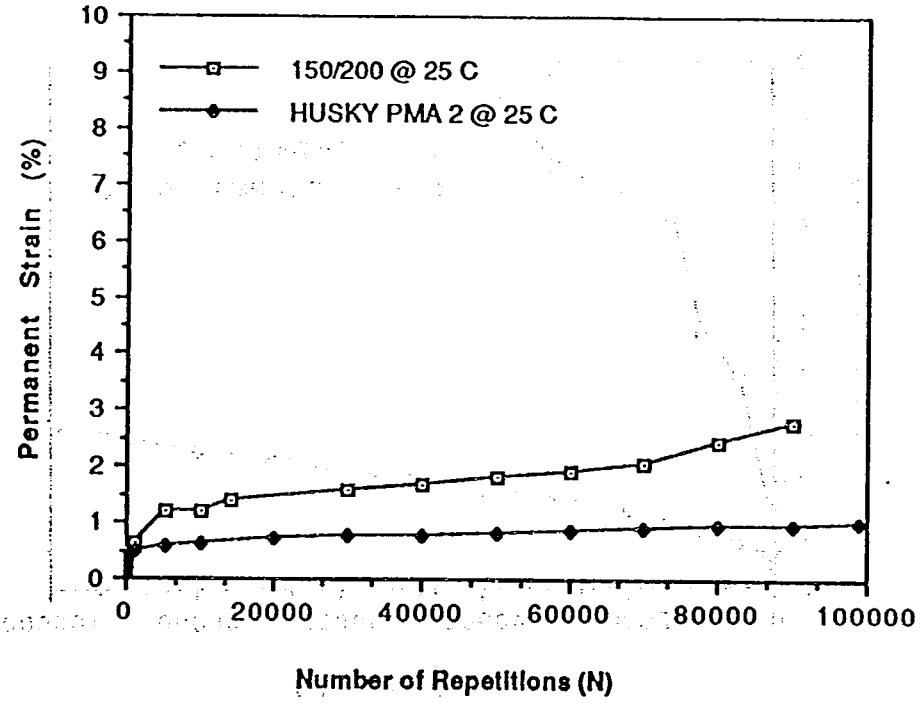


Figure 16. Permanent Deformation Curves @ 25 C Lethbridge Aggregate

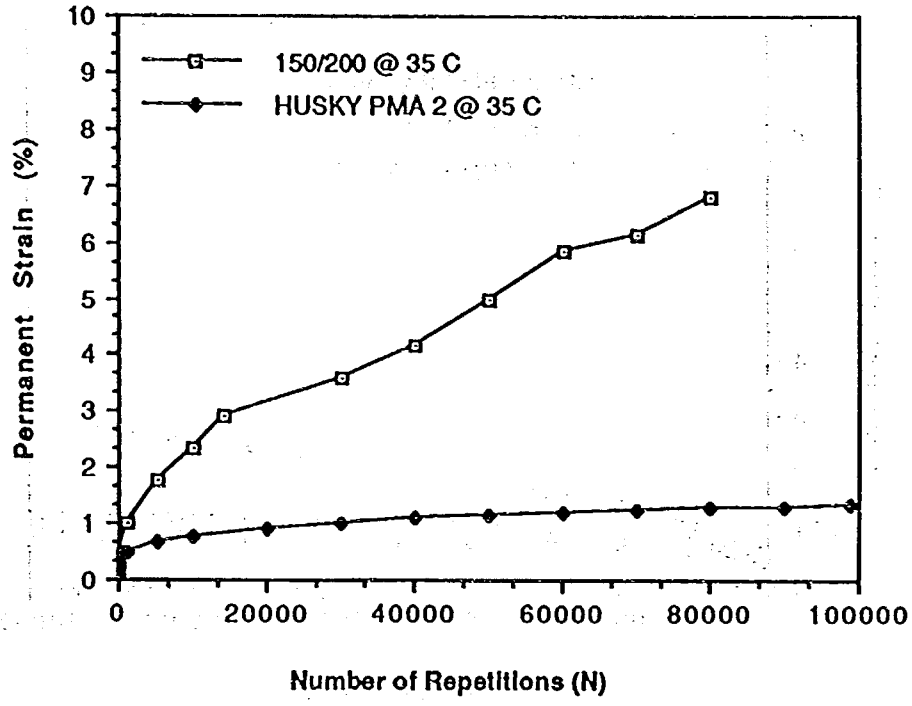


Figure 17. Permanent Deformation Curves @ 35 C Lethbridge

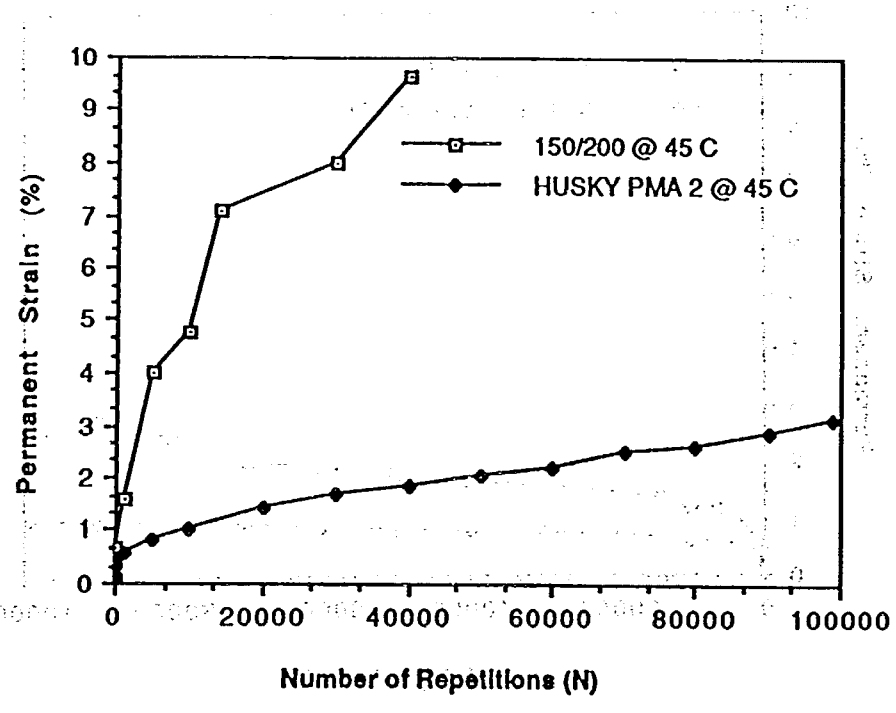


Figure 18. Permanent Deformation Curves @ 45 C Lethbridge Aggregate

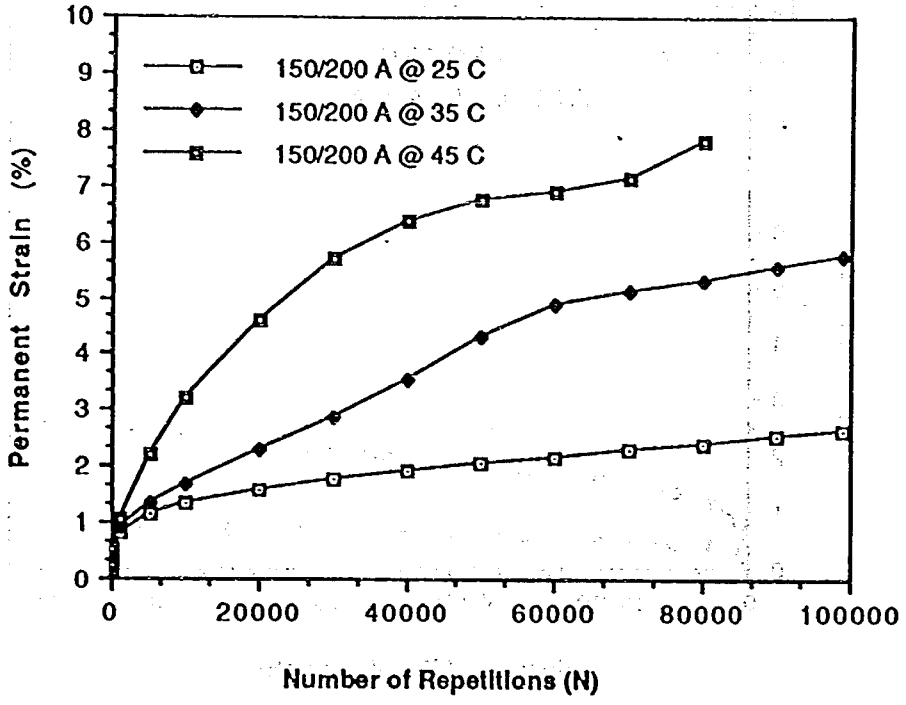


Figure 19. Permanent Deformation Curves for 150/200A and Secondary Highway 794 Aggregate

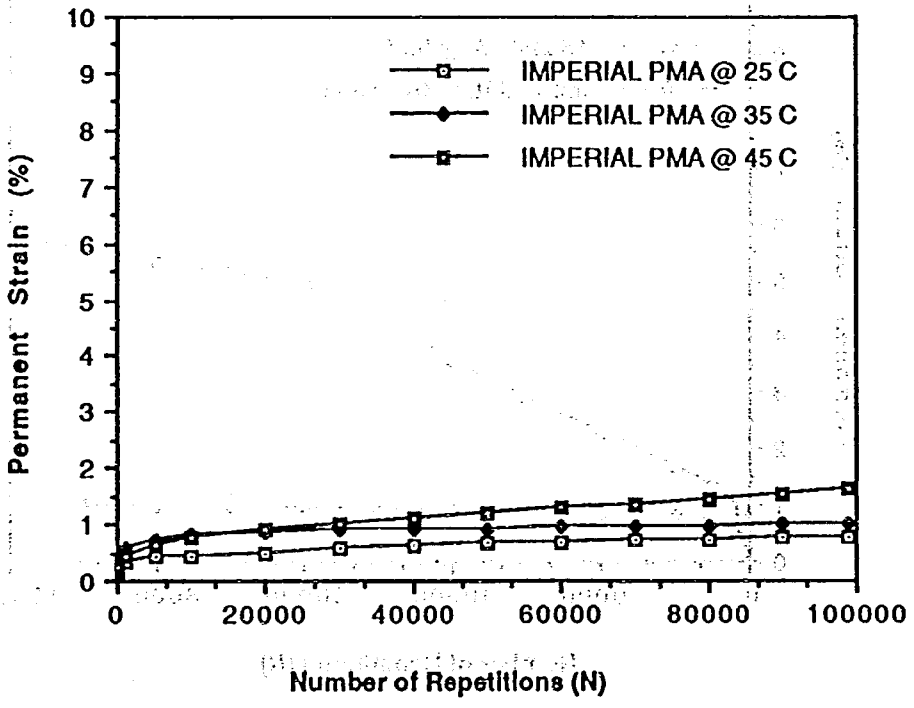


Figure 20. Permanent Deformation Curves for Imperial PMA and Secondary Highway 794 Aggregate

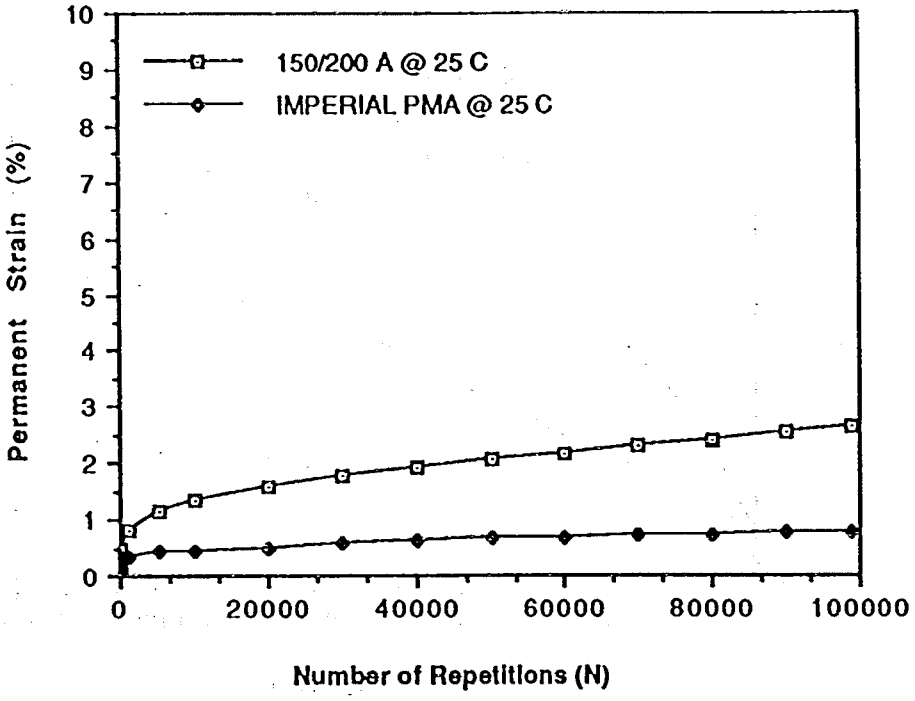


Figure 21. Permanent Deformation Curves @ 25 C Secondary Highway 794 Aggregate

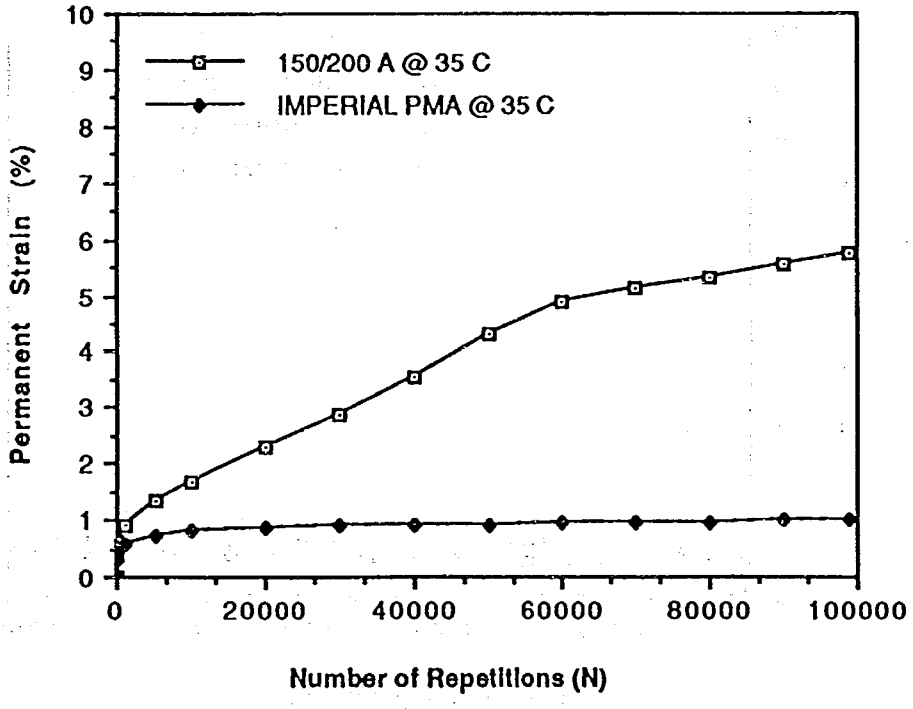


Figure 22. Permanent Deformation Curves @ 35 C Secondary Highway 794 Aggregate

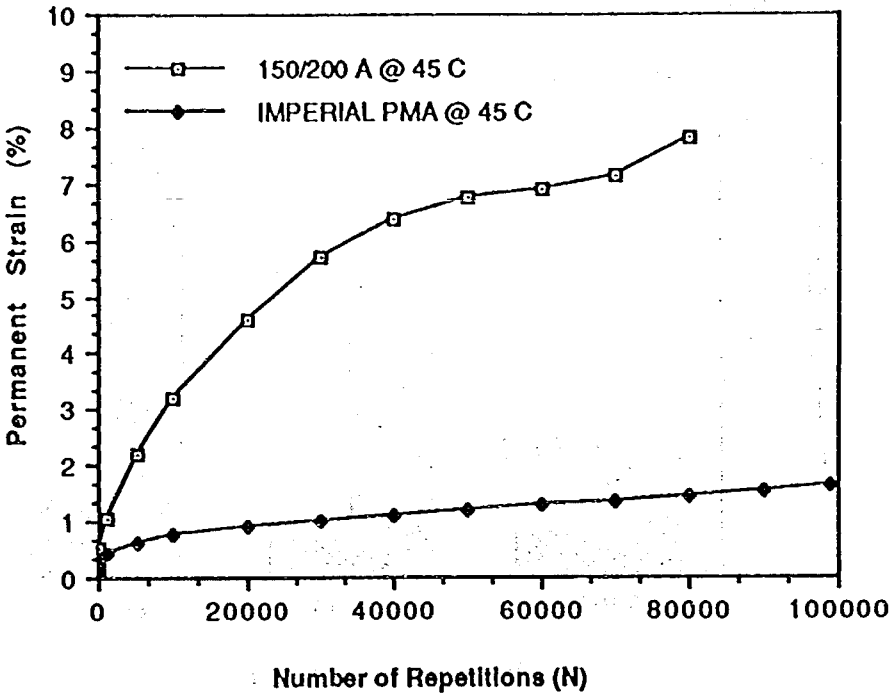


Figure 23. Permanent Deformation Curves @ 45 C Secondary Highway 794 Aggregate

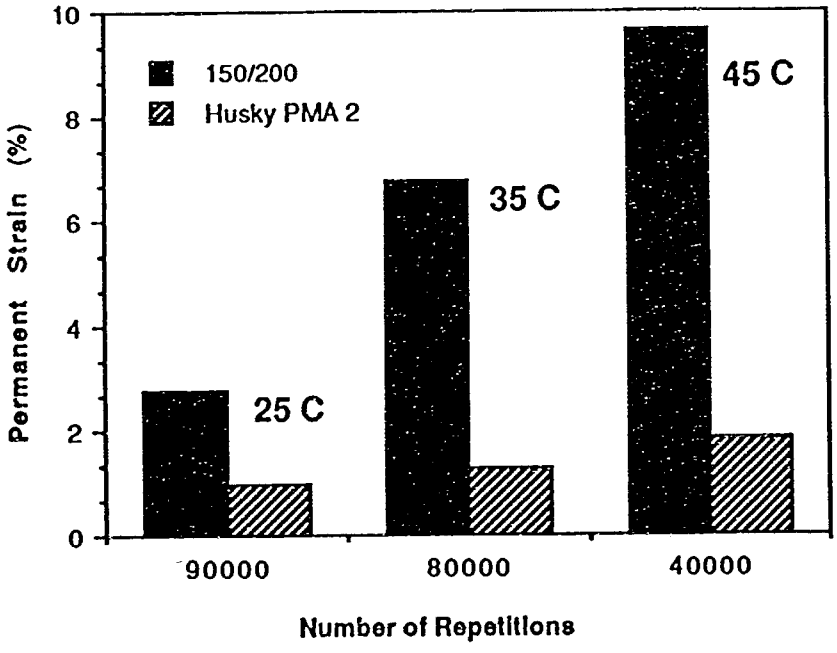


Figure 24. Permanent Strain at 25 C, 35 C, and 45 C for Lethbridge Aggregate

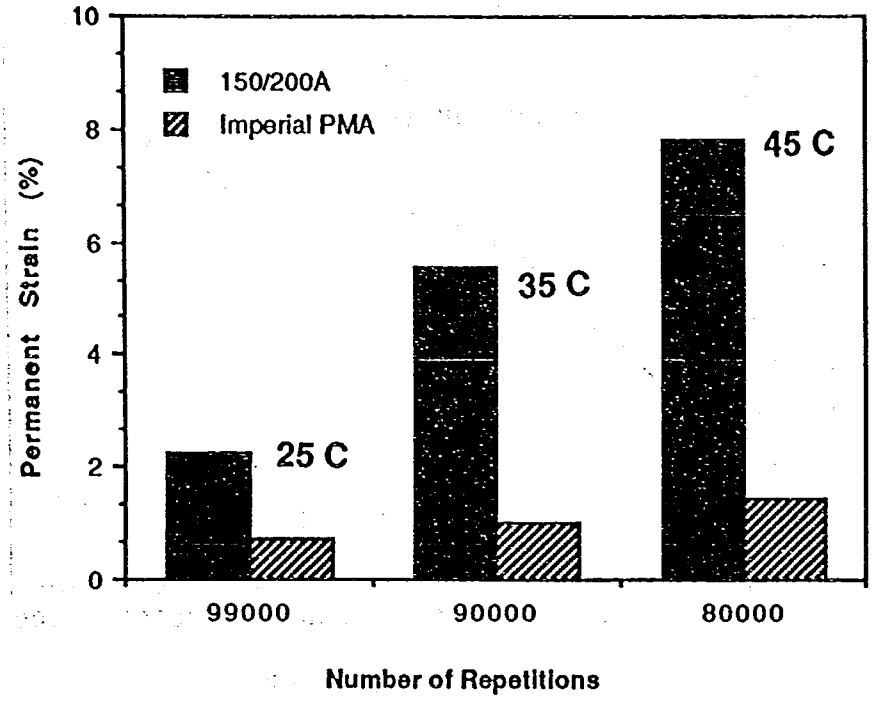


Figure 25. Permanent Strain at 25 C, 35 C and 45 C for Secondary Highway 794 Aggregate

An Investigation Study on Production of Modified Asphalts in Japan

K. Himeno, Hokkaido Univ.
H. Sakamoto, Y. Anzaki,
PWRI, Ministry of Construction, Japan
K. Hashimoto, Ministry of Construction

AN INVESTIGATIVE STUDY ON PRODUCTION OF MODIFIED ASPHALTS IN JAPAN

by

Kenji HIMENO
Associate Professor, Hokkaido University
Hiroyuki SAKAMOTO
Research Engineer, Public Works Research Institute
and
Kohtaro HASHIMOTO
Sectional Chief, Ministry of Construction

ABSTRACT

Recent years, pavement distresses as rutting caused by viscous flow of asphalt mixture or abrasion by spiked tires have become serious in Japan according to the growth of the number of the vehicle wheels and their magnitude. The national and local road administrators have been obliged to expend enormously every year for maintenance and rehabilitation programs of the road networks they manage. Various kinds of modified asphalt cements, which are considered to have higher resistance for these distresses, have been developed actively by many manufacturers, although it still remains unknown what kind of modifiers is the most effective and acceptable for these distresses.
The authors gathered information by questionnaires from the manufacturers of modified asphalt cements and their distributors in Japan to grasp the actual state of the productions and their physical properties. It was found that
a) more than 90 percent of asphalt cements contain rubber or resin,
b) Around 130,000 tons of modified asphalts are produced every year in Japan,
c) they are applied mainly against viscous flow or abrasion by spiked tires,
d) though the prices of modified asphalts are from 1.8 to 3.1 times as high as that of straight ones, those of mixes are 1.2 through 1.5 times as high,
e) the kinematic viscosities at 60°C of modified asphalt cements are 2 through 7 times as high as that of straight one,
f) the dynamic stabilities of modified asphalt mixtures obtained by the laboratory wheel tracking test are 3 through 10 times as high as that of straight one, etc.

AN INVESTIGATIVE STUDY ON PRODUCTION OF MODIFIED ASPHALTS IN JAPAN

by

Kenji HIMENO
Associate Professor, Hokkaido University
Hiroyuki SAKAMOTO
Research Engineer, Public Works Research Institute
and
Kohtaro HASHIMOTO
Sectional Chief, Ministry of Construction

1/ INTRODUCTIONS

Recent years, pavement distresses as rutting caused by viscous flow of asphalt mixture or abrasion by spiked tires have become serious in Japan according to the growth of the number of the vehicle wheels and their magnitude. The national and local road administrators have been obliged to expend enormously every year for maintenance and rehabilitation programs of the road networks they manage. Various kinds of modified asphalt cements, which are considered to have higher resistance for these distresses, have been developed actively by many manufacturers, although it still remains unknown what kind of modifiers is the most effective and acceptable for these distresses.
The authors gathered information by questionnaires from the manufacturers of modified asphalt cements their distributors in Japan to grasp the actual state of the productions and their entire physical properties.

2/ METHODS OF INVESTIGATION

The investigation was made by questionnaires for the period from July to September, 1986, to the following manufacturers of asphalts.
1) manufacturers of modified asphalts,
2) manufacturers of modified asphalt additives,
3) manufacturers of asphalts,
4) asphalt pavement contractors,
and
5) other organizations concerned.
The types of modified asphalts investigated in this study are

1) rubberized asphalts,
2) polymer-added asphalts,
3) rubberized and polymer-added asphalts,
and
4) semi-blown asphalts.

3/ RESULTS OF SURVEY

From one association and twenty five firms, forty five replies were collected for different modified asphalt products by the questionnaires. The replies have been classified by types of modified asphalts and by mixing process, as shown in Fig.1. The results of investigation are described for each item.

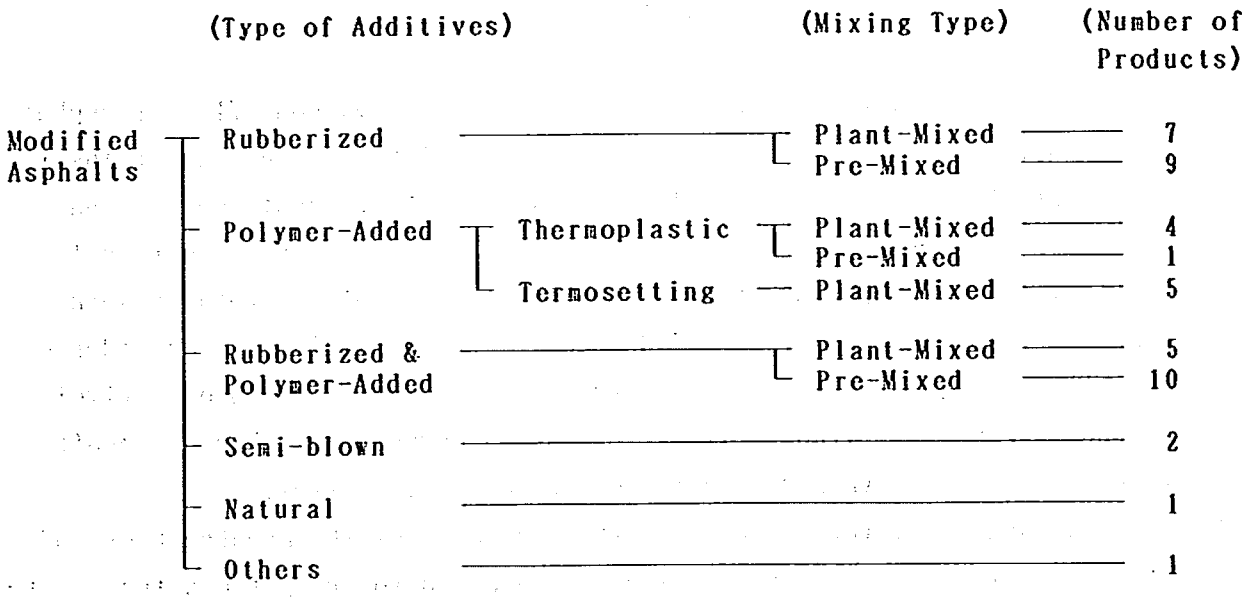


Fig.1 Classification of Modified Asphalts (45 Products)

3.1/ Production of Modified Asphalts

3.1.1/ Number of Products of Each by Type of Binder

Number of the modified asphalt products, which are almost all the products available at that time in Japan, is forty five. The percentages in the number of rubberized asphalt, polymer-added (including rubberized and polymer added) asphalts and others are thirty six percent, fifty six percent and eight percent respectively, as shown in Fig.2. The polymer-added asphalts are found to be the most popular.

3.1.2/ Amount of Productions

Around 110,000 through 130,000 metric tons of modified asphalts are being produced every year. The production index is 1.05 in FY82, 1.12 in 83, 1.16 in 84, 1.24 in 85, provided that it is 1.0 in FY81. Amount of the productions has increased by twenty five percent in the last five years. In FY85, 3.5 percent of all the asphalts used for the pavements, amounted to 3,730,000 metric tons, were modified asphalts.

Amount of rubberized asphalts produced every year ranges from 85,000 to 90,000 metric tons, whereas that of polymer-added including rubberized and polymer-added does between 23,000 and 38,000 metric tons, as shown in Fig.3. The former increased at growth rate of 1.07, and the latter at 1.6. It is found that polymer-added asphalt including rubberized and polymer-added asphalts increased remarkably. The proportion of rubberized asphalt in FY81 was eighty percent, though it was seventy percent in FY85, as shown in Fig.4. The primary purpose of the modified asphalts replied in the questionnaires was resisting viscous flow and wearing, dominating with 55.6 percent of all the replies, whereas the bridge surface pavement was listed as an additional purpose, in nearly forty percent of the replies of the questionnaires, as shown in Fig.5.

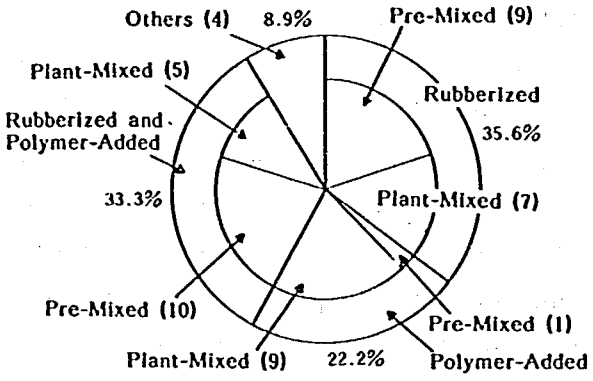


Fig.2 Numbers of Products Regarding Binder Types (N=45)

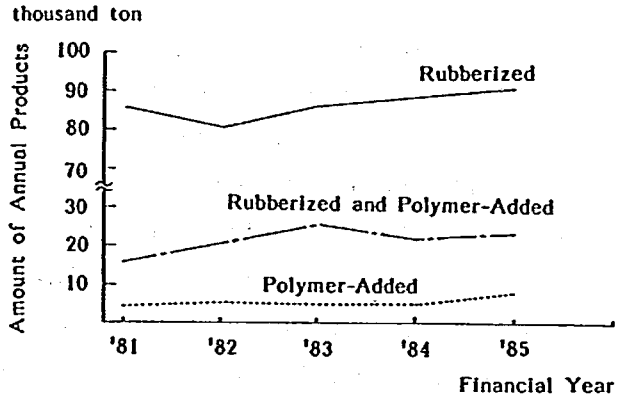


Fig.3 Change in Amount of Products Regarding Binder Types

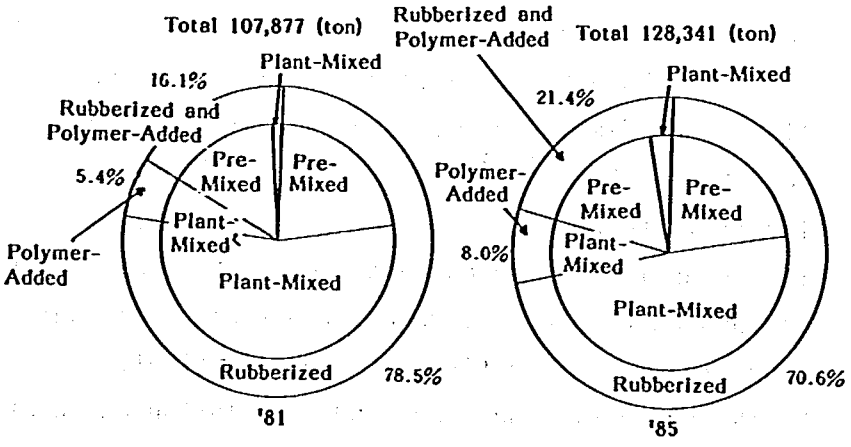


Fig.4 Rate of Amount of Products Regarding Binder Types

3.1.3/ Prices

Prices of modified asphalts vary with their quality and properties. Unit price of binder in the month of June 88 (converted price is used for plant mixed asphalts) ranged between 60,000 and 106,000 yen per metric ton, except for special quality products. The price of rubberized asphalt is 1.8 times higher than that of straight asphalt, though rubberized and polymer-added is 3.1 times higher.

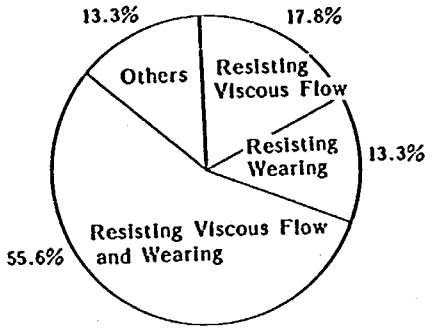


Fig.5 Numbers of Products Regarding Usages (N=45)

The price of dense graded asphalt mix using rubberized asphalt is found to range from 1.2 to 1.45 times higher than those of straight asphalt mixes and the rubberized and polymer-added mix ranges from 1.35 to 1.5 times higher, by a trial calculation based on the unit prices for the binders. On the other hand, the cost of pavement overlay with rubberized mixes ranges between 1.1 and 1.2 times higher than that of straight asphalt, and that with rubberized and polymer-added ranges between 1.2 and 1.3 times higher. The difference between the binders does not reflect largely upon the prices of the mixes or finished pavements.

3.2/ Properties of Modified Asphalts

The relationships between the various properties of modified asphalt cements and mixes have been examined, based on the replies in the questionnaires. Also, some discussion will be made with reference to the papers by formal research workers[1)-8)].

The items to be noted will be listed below.

1) The analyses were based on the test results performed independently by the various manufacturers. Hence, the types of asphalt cements and their mixture conditions with additives are not identical.

2) The regression analyses and correlation calculations were made based on the all the data available, even when some data are out of the charts. Regression lines were entered into the charts when the absolute value of coefficient of correlation exceeds 0.3.

3) Only the names of types of asphalt cements are shown in the figure, although the properties of modified asphalts vary widely depending on the intended benefits. Even when a different type of base asphalt or a different

type of aggregate gradation was used with the identical modified asphalt additives, it was considered to be a separate product made from different materials.

4) The term "rate of change" in the figures means a value of properties regarding the modified asphalt divided by that of straight asphalt.

5) The properties of binders and asphalt mixes are shown with the following symbols.

Properties of Materials	Symbols
Penetration	P
Softening point	SP
Penetration index	PI
Toughness	T_o
Tenacity	T_e
Viscosity at 60°C	η_{60}
Marshall stability	MS
Dynamic stability	DS
Chain abrasion loss	CA
Viscosity at 180°C	η_{180}
Ductility at 15°C	D_{15}
Temperature at mixing	q_M
Temperature at compaction	q_C
Fraas breaking point	Bf

Subscripts, s, m and r after a comma (,) were added after the symbols to denote the straight asphalt, the modified asphalt and the rate of change respectively. For instance, softening point of straight asphalt was expressed as $SP_{,s}$, and viscosity at 180°C of modified asphalt was as $\eta 180_{,m}$.

6) Logarithms shown in the text and the figures are all common logarithms.

3.2.1/ Binder

1) Penetrations of Straight Asphalts vs. Those of Modified Asphalts

The relationship between penetrations of straight asphalts and those of modified asphalts is shown in Fig.6. Since the penetrations of straight asphalts used as base asphalts in snowy areas are approximately 90, and those in the other areas is around 70, the dots in the figure seem to be separated into two groups. Coefficients of correlation between the penetrations of both asphalts are not high, however, it is found that the penetration of modified asphalt cements are lower than those of straight asphalts and also that the penetration of modified asphalt cements are higher than seventy percent of those of straight asphalts.

2) Softening Points of Straight Asphalts vs. those of Modified Asphalts

The relationship between softening points of straight asphalts and those of

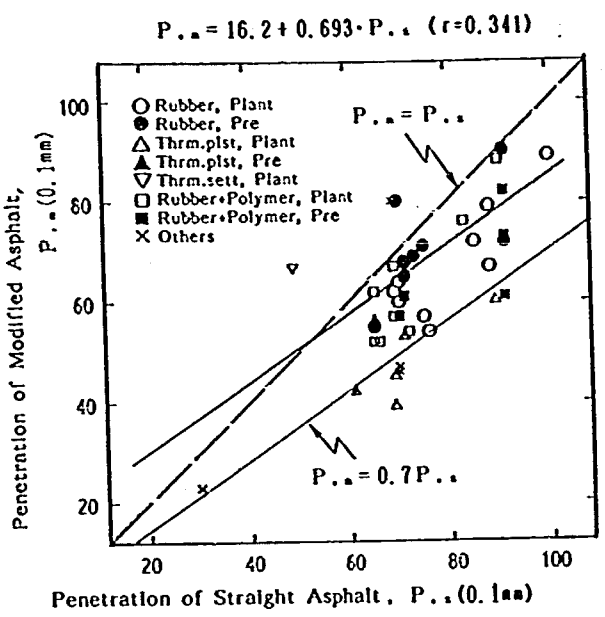


Fig.6 Penetrations of Straight Asphalts vs. those of Modified Asphalts

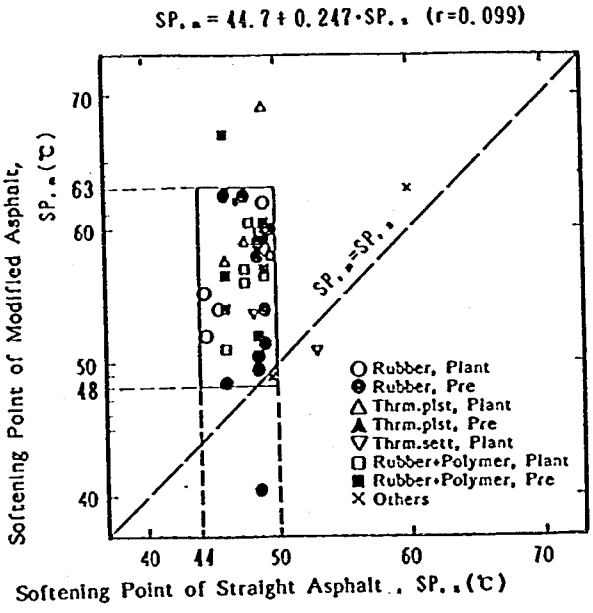


Fig.7 Softening Points of Straight Asphalts vs. those of Modified Asphalts

modified asphalts is shown in Fig.7. Correlation between both the softening points appears very weak, since those of straight asphalts are within the narrow range of 44 through 55° C, and the whole range is plotted in rectangular shape. All the softening points are located above the line of equality and plotted within a small range. The softening points of modified asphalts are higher than those of straight asphalts by 15° C at maximum, and it is seen that those of modified asphalts are within the range of 48 through 63° C.

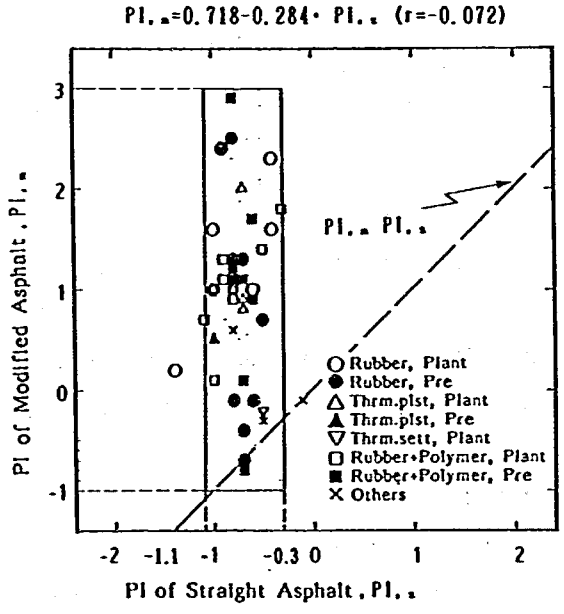


Fig.8 PIs of Straight Asphalts vs. those of Modified Asphalts

3) PIs of Straight Asphalts vs. those of Modified Asphalts

The relationship between penetration indices (PI) of straight asphalts and those of modified asphalts is shown in Fig.8. The PIs of straight asphalts range between -1.1 and - 0.3, and the those of modified asphalts are higher than these, ranging from -1.1 to +3.0. Modified asphalts have lower temperature susceptibility, and correlation of the PIs between the base asphalts and the modified asphalts is weak.

4) Kinematic Viscosities at 60°C of Straight Asphalts vs. those of Modified Asphalts

The relationship between kinematic viscosities at 60°C of straight asphalts and those of modified asphalts is shown in Fig.9. The viscosities of straight asphalts range between 1400 and 2500 Poise, and those of modified asphalts are much higher by from 2 to 7 times.

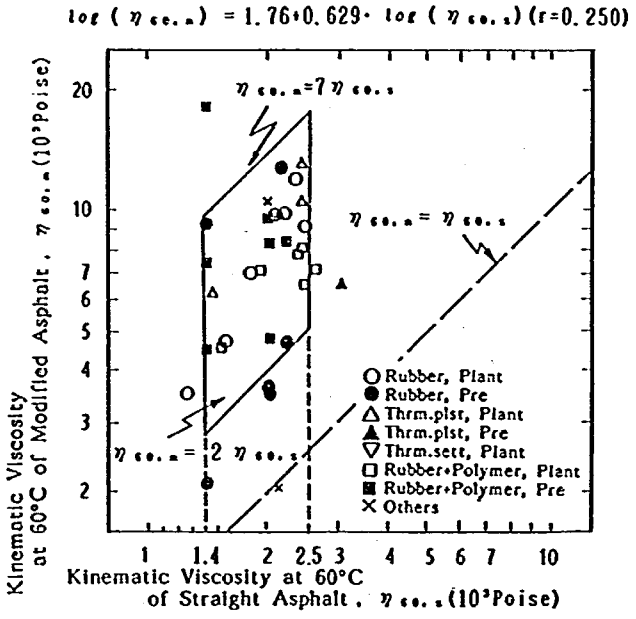


Fig.9 Kinematic Viscosities at 60°C of Straight Asphalts vs. those of Modified Asphalts

5) PIs vs. Fraas Breaking Points of Modified Asphalts

The relationship between PIs and the Fraas breaking points of modified asphalts is not much clear, although the calculated coefficient of correlation is a little high, as shown in Fig.10. This is also evident in the reference 1), where the slope in the regression line is expressed inversely.

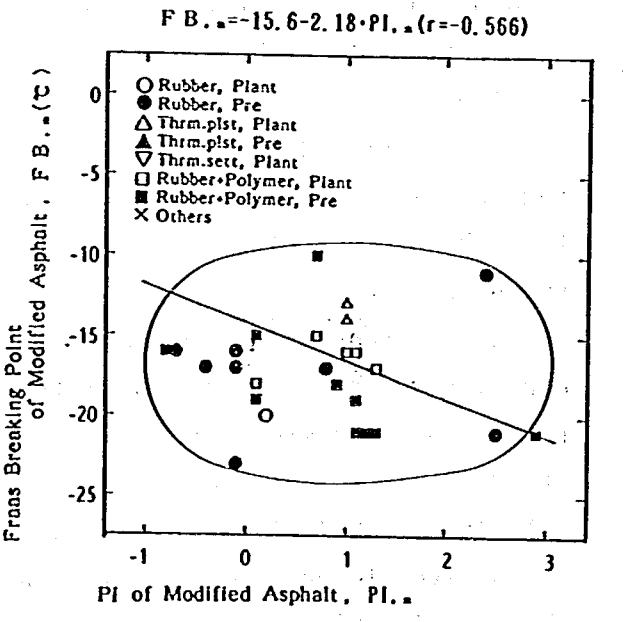


Fig.10 PIs vs. Fraas Breaking Point of Modified Asphalts

6) Relationship between Penetrations and Softening Points of Modified Asphalts

The relationship between penetrations and softening points of modified asphalts is shown in Fig.11. As shown previously in Fig.8, the PIs of modified asphalts are plotted in a wider range than those of straight asphalts, therefore, this relationship, which determines the PIs, is not so tight as in the case of straight asphalts. That is because the penetrations and the softening points of modified asphalts are plotted in a wider range. Differences in types of modified asphalt are not so clear in this relationship as shown in the reference 1).

7) Penetrations vs. Kinematic Viscosities at 60°C of Modified Asphalts

The relationship between penetrations and kinematic viscosities at 60°C of modified asphalts is not so clear as shown in Fig.12. The viscosities of modi-

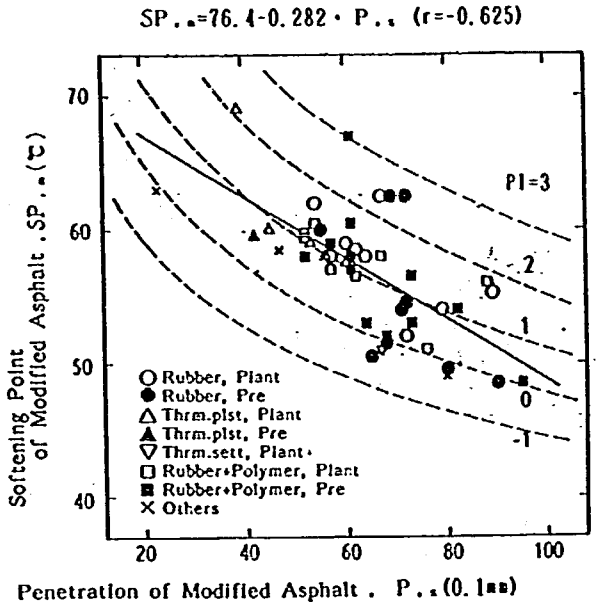


Fig.11 Penetrations vs. Softening Points of Modified Asphalts

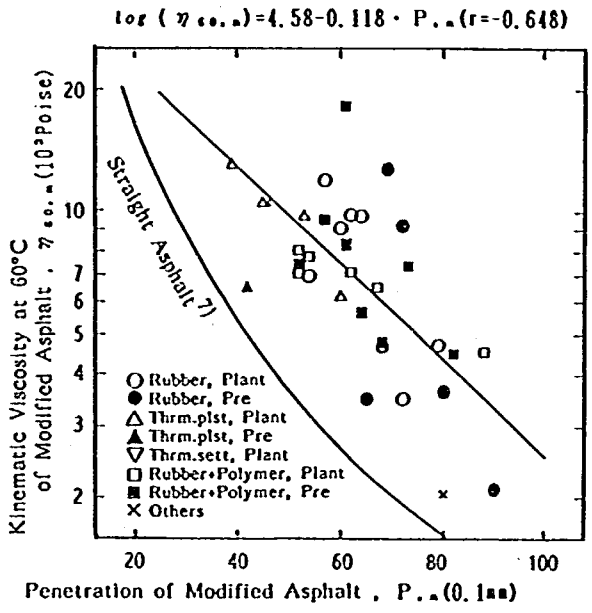


Fig.12 Penetrations vs. Kinematic Viscosities at 60°C of Modified Asphalts

fied asphalts against the identical penetrations is higher than those of straight asphalts, since the penetrations of modified asphalts are lower and the viscosity at 60°C is higher than those of straight asphalts, as shown in Figs.6 and 9.

In the reference 7), a regression equation is shown between the penetrations and the kinematic viscosities at 60°C of straight asphalts as

$$\log(\eta 60,_S)=6.49-1.73 \log (P,_S),$$

which gives lower viscosity than those obtained in this study.

8) Kinematic Viscosities at 60°C vs. Softening Points of Modified Asphalts

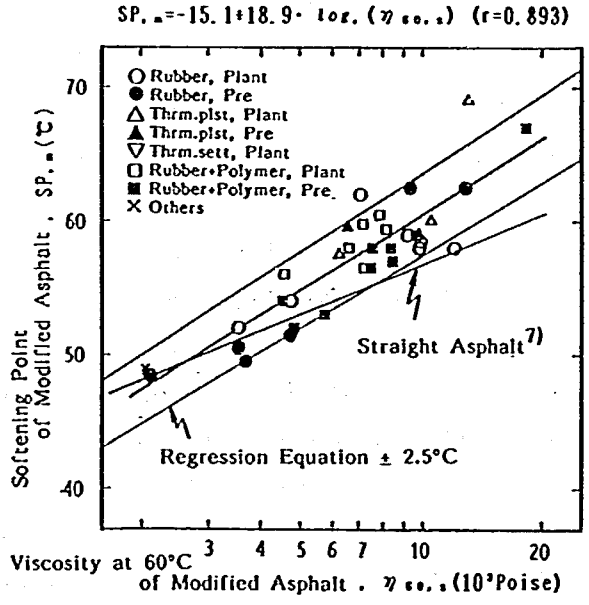


Fig.13 Kinematic Viscosities at 60°C vs. Softening Points of Modified Asphalts

The relationship between kinematic viscosities at 60°C and softening points of modified asphalts is shown in Fig.13, which gives a relatively higher correlation coefficient. This is also true in the references 2), 5), 7) and 8) as well as in the reference 6) for modified asphalts. However, the softening points at higher kinematic viscosity at 60°C of modified asphalts given by former research workers tend to be higher than those of straight asphalts, which may be because the test data at high viscosity are not available as

required, and an extreme extrapolation might be made.

In the references 7) and 8), the following regression equations are shown

$\log(\eta 60,_S) = 1.154+0.0489\ P,_S$

$\log(\eta 60,_S) = -0.229+0.074\ P,_S$

$\log(\eta 60,_S) = -0.337+0.0775\ P,_S$.

9) Kinematic Viscosities at 60°C vs. Viscosities at 180°C of Modified Asphalts

The relationship between kinematic viscosities at 60°C and viscosities at 180°C of modified asphalts is shown in Fig.14. This relationship should possess a linearlity, provided that temperature susceptibilities of all modified asphalts are equal. However, it is widely scattered, showing an variety of temperature susceptibilities.

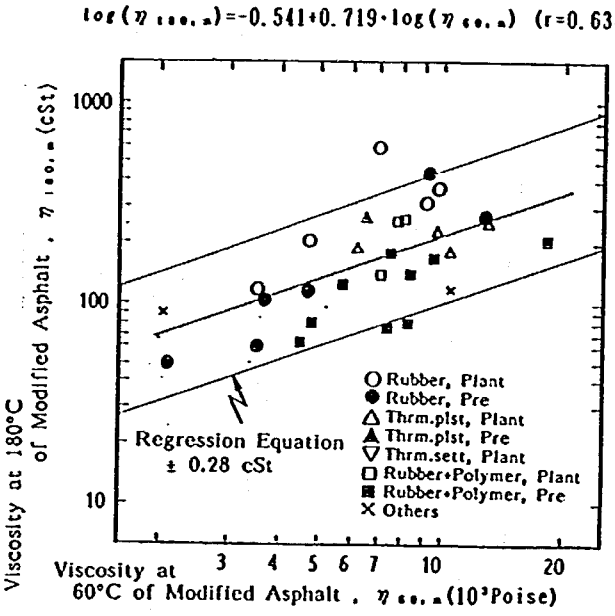


Fig.14 Kinematic Viscosities at 60°C vs. Viscosities at 180°C of Modified Asphalts

10) Toughnesses of Straight Asphalts vs. Those of Modified Asphalts

The relationship between toughnesses of straight asphalts and those of modified asphalts is shown in Fig.15. The former are concentrated between 20 and 60 (kgf.cm), although the latter are scattered between 50 and 300 (kgf.cm).

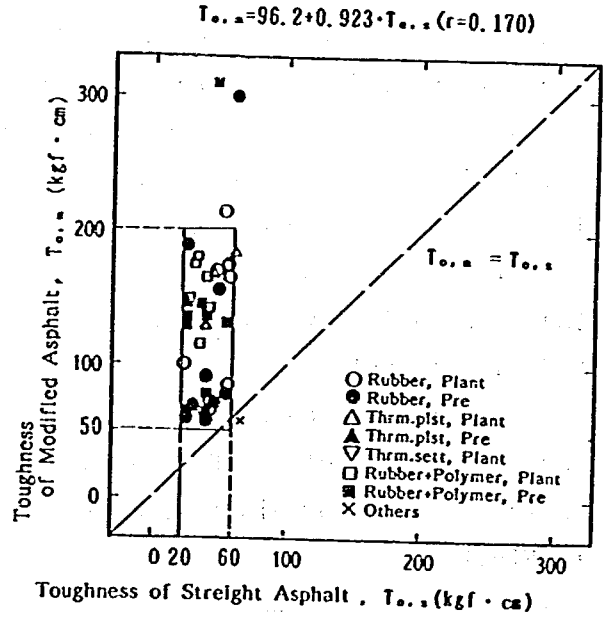


Fig.15 Toughnesses of Streight Asphalts vs. those of Modified Asphalts

11) Tenacities of Straight Asphalts vs. those of Modified Asphalts

The relationship between tenacities of straight asphalts and those of modified asphalts is shown in Fig.16. Since the former are concentrated between zero and 20, although the latter are scattered within a wider range of 20 to 250 (kgf.cm), the coefficient of correlation is very low. It is noted that the tenacity can be considerably improved by modifying the binder, however, its degree varies widely by type of the binder used.

12) Toughnesses vs. Tenacities of Modified Asphalts

The relationship between toughnesses

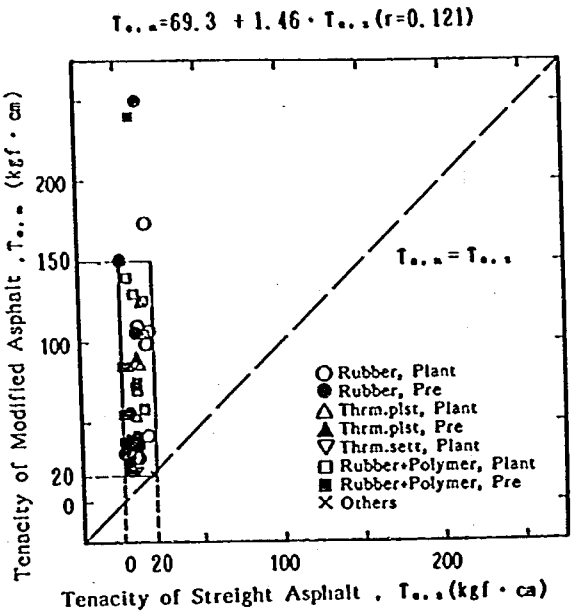


Fig.16 Tenacities of Streight Asphalts vs. those of Modified Asphalts.

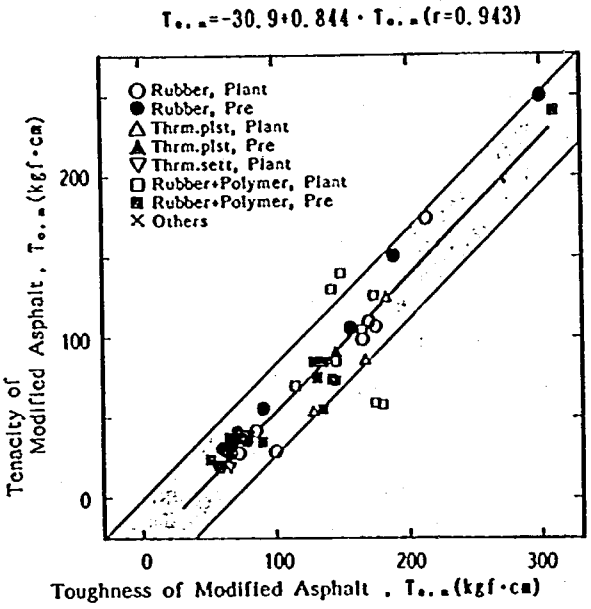


Fig.17 Toughnesses of Modified Asphalts vs. Tenacities of Modified Asphalts

and tenacities of modified asphalts is shown in Fig.17. The correlation is strong, as shown also in the reference 1). It is noted that the relationship in some plant-mixed asphalts is slightly dispersed.

13) Penetrations vs. Toughnesses of Modified Asphalts

The relationship between penetrations and toughnesses of modified asphalts is in negative correlation, as shown in Fig.18.

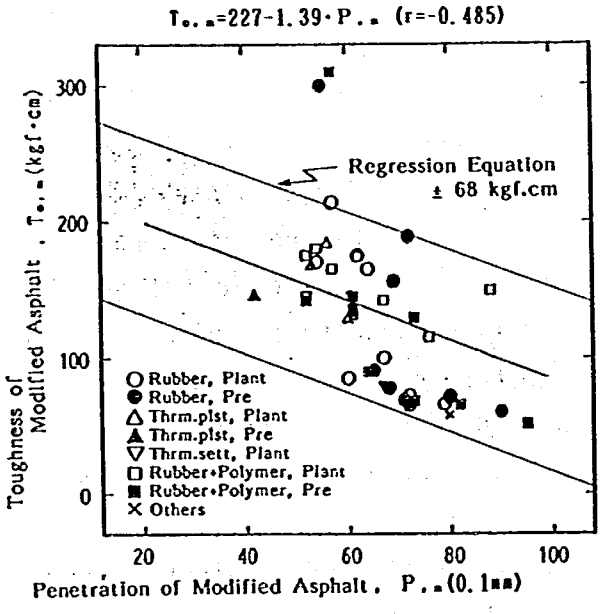


Fig.18 Penetrations of Modified Asphalts vs. Toughnesses of Modified Asphalts

14) Tenacities vs. Ductilities at 15°C of Modified Asphalts

The relationship between tenacities and ductilities at 15°C of modified asphalts is shown in Fig.19. It is not easy to make a proper evaluation of the relation, since almost all the ductilities of rubberized asphalts exceed 100 cm. It is considered that there exists no apparent relationship between the two properties even if those data are available.

3.2.2/ Asphalt Mixes

1) Marshall Stabilities of Straight Asphalts vs. those of Modified Asphalts

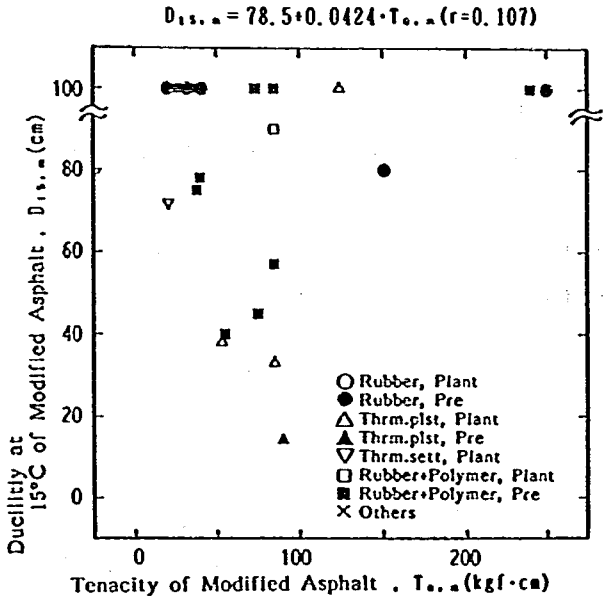


Fig.19 Tenacities of vs. Ducilities at 15°C of Modified Asphalts

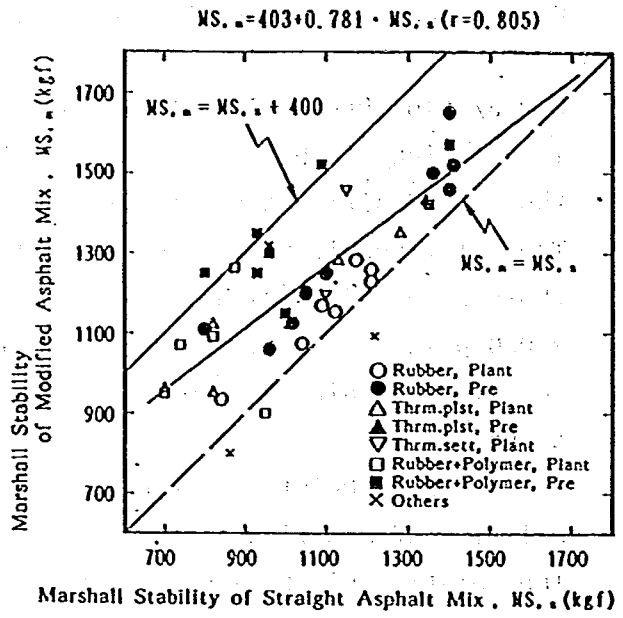


Fig.20 Marshall Stabilities of Straight Asphalt Mixes vs. those of Modified Asphalt Mixes

The relationship between Marshall stabilities of straight asphalts and those of modified asphalts is shown in Fig.20. The Marshal stabilities of modified asphalt mixes are higher than those of straight asphalt mixes with the maximum difference of only 400 kgf. The difference is smaller for rubberized asphalts and larger for rubberized and polymer-added asphalts.

2) Mixing Temperatures and Kinematic Viscosities at 60° C of Modified Asphalts

The relationship between the mixing temperatures vs. kinematic viscosities at 60° C of modified asphalts is shown in Fig.21. This implies that the mixing temperature will have to be increased provided that the viscosities are increased to have flow resistance.

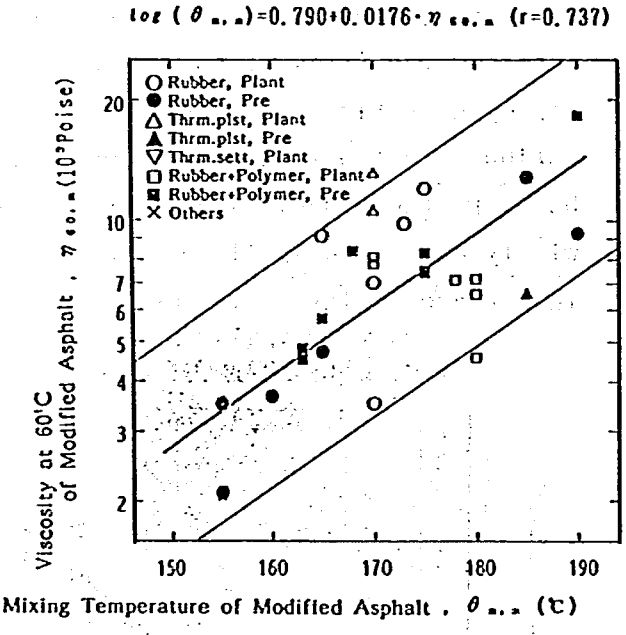


Fig.21 Mixing Temmperatures of Modified Asphalt Mixes vs. Kinematic Viscosities at 60°C of Modified Asphalts

3) Mixing Temperatures vs. Viscosities at 180° C of Modified Asphalts

The relationship between mixing temperatures and viscosities at 180° C of modified asphalts is shown in Fig.22, giving a low coefficient of correlation. This implies that the mixing temperature of modified asphalt cements are not determined based on the temperature-viscosity curves specified in Japanese

design manual of asphalt pavements.

3.2.3/ Flow Properties at High Temperature of Asphalt Mixes

1) Relationship between Dynamic Stabilities of Straight Asphalt Mixes and those of Modified Asphalt Mixes

The relationship between dynamic stabilities of straight asphalt mixes and those of modified asphalt mixes is shown in Fig.23. The latter mostly exceed 2,000 passes, which, is from three to ten times as high as those of straight asphalt mixes.

2) Softening Points vs. Dynamic Stabilities of Modified Asphalts

The relationship between softening points and dynamic stabilities of modified asphalts is shown in Figs.24, 25. Trying to eliminate the effects of personnel, equipment, and methods of testing, the rates of changes are employed in Fig.25. A positive correlation is noted to a certain degree, however, the dynamic stability varies widely even with small testing errors in a range of larger values. Some

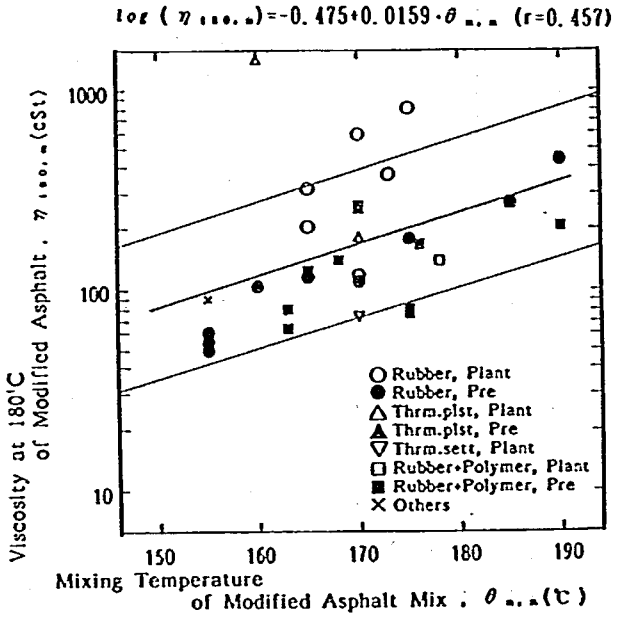


Fig.22 Mixing Temmperatures of Modified Asphalt Mixes vs. Kinematic Viscosities at 180°C of Modified Asphalts

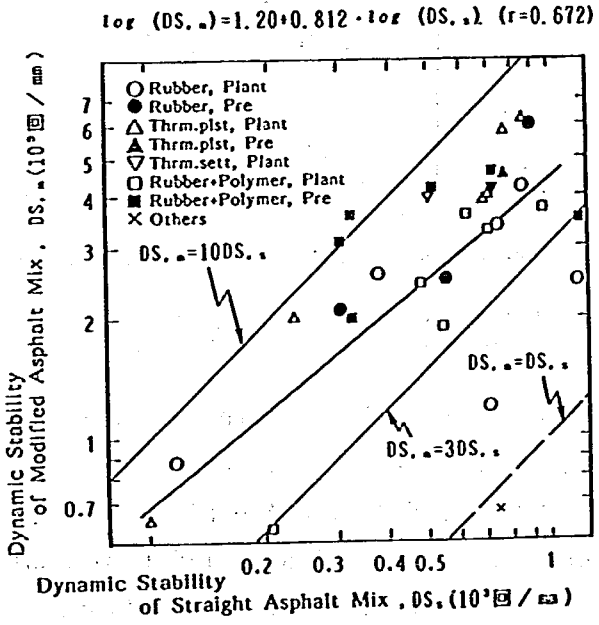


Fig.23 Dynamic Stabilities of Straight Asphalt Mixes vs. those of Modified Asphalt Mixes

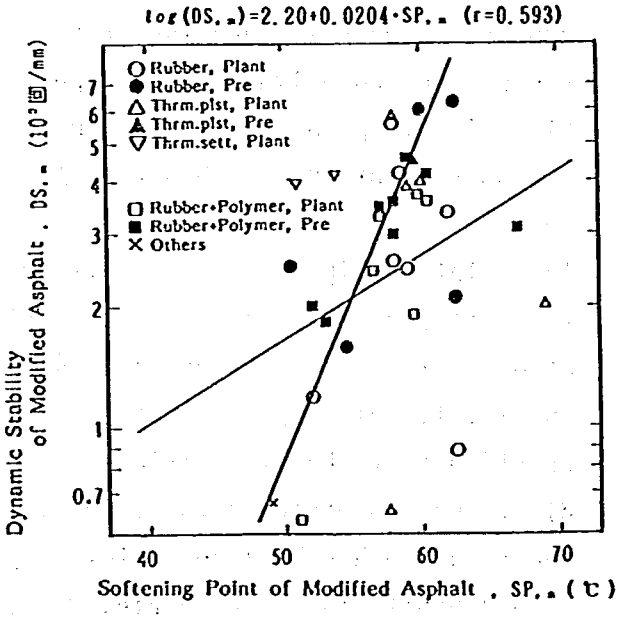


Fig.24 Softening Points vs. Dynamic Stabilities of Modified Asphalt Mixes

differences cannot be avoided because tests were performed at many different laboratories.

In the reference 2), some regression equations are shown as

$\log(DS,_S)=1.379+0.0361\ SP,_S$

$\log(DS,_S)=2.175+0.0236\ SP,_m$

3) Kinematic Viscosities at 60° C of Modified Asphalt Cements vs. Dynamic Stabilities of Modified Asphalt Mixes

The relationships between (rate of change of) viscosities at 60° C of modified asphalt and (rate of change of) dynamic stabilities of modified asphalt mixes are shown in Figs.26, 27, 28. Since wheel tracking tests were performed at 60° C as is the viscosity tests, stronger relationship was expected, although a weak positive correlation is actually noted in both the cases. In the reference 2), the relationship between straight asphalts and modified asphalts is expressed as

$\log(DS,_S)=0.803+2.290\ \log h60,_S$

$\log(DS,_S)=0.828+1.757\ \log h60,_m$.

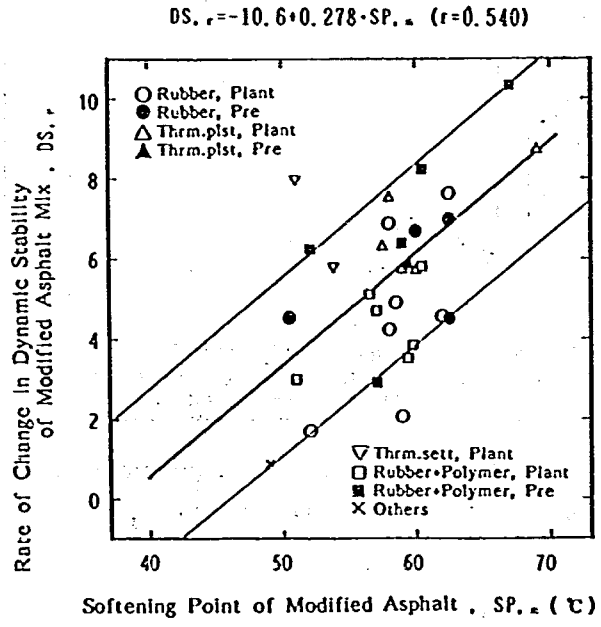


Fig.25 Softening Points of Modified Asphalts vs. Rate of Changes in Dynamic Stabilities of Modified Asphalt Mixes

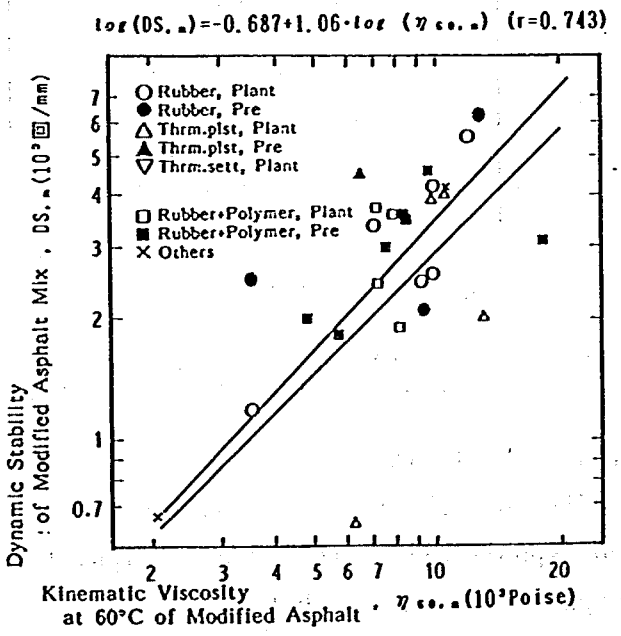


Fig.26 Kinematic Viscosities at 60°C of Midified Asphalts vs. Dynamic Stabilities of Modified Asphalt Mixes

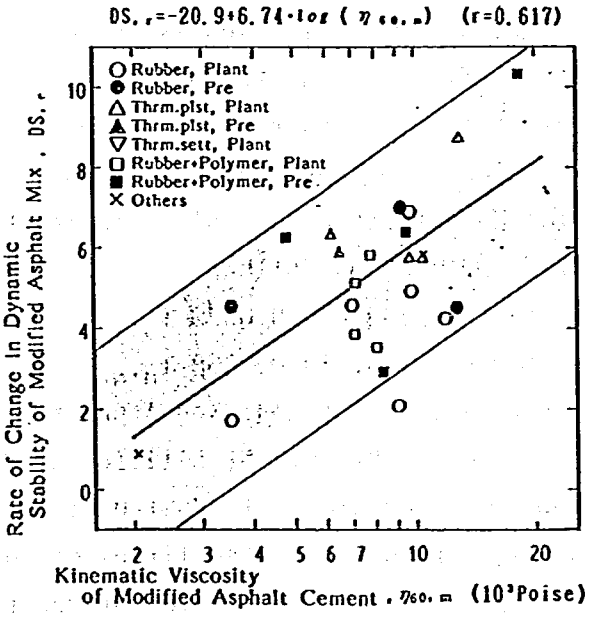


Fig.27 Kinematic Viscosities at 60°C of Midified Asphalts vs. Rate of Change in Dynamic

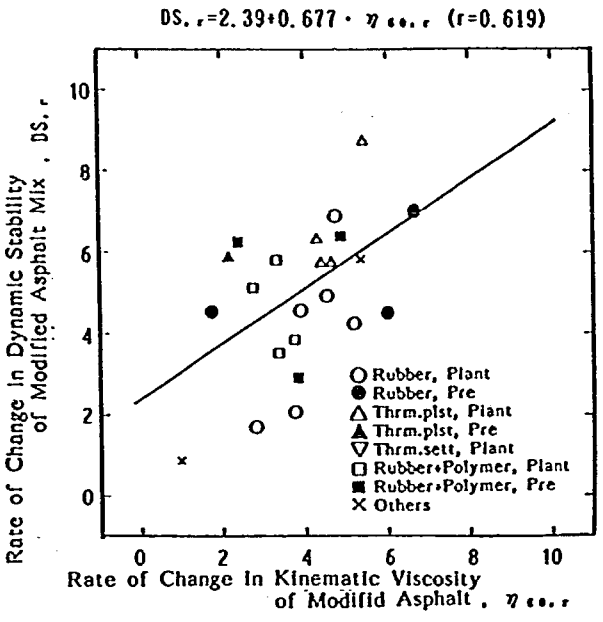


Fig.28 Rate of Change in Kinematic Viscosities at 60°C of Modified Asphalts vs. Rate of Change in Dynamic Stabilities of Modified Asphalt Mixes

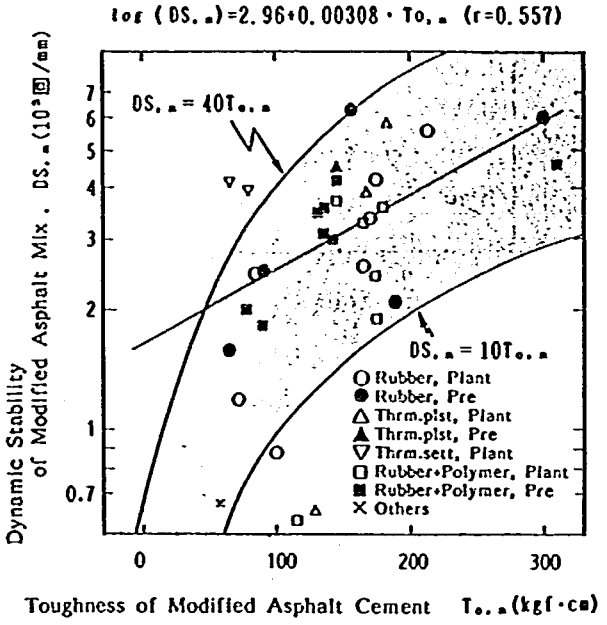


Fig.29 Toughnesses of Modified Asphalts vs. Dynamic Stabilities of Modified Asphalt Mixes

4) Toughnesses of Modified Asphalt cements vs. Dynamic Stabilities of Modified Asphalt Mixes

The relationships between toughnesses of modified asphalt cements and (rate of change of) dynamic stabilities of modified asphalt mixes are shown in Figs.29, 30. It is clearly found from these figures that the dynamic stabilities of mixes range between 10 and 40 times the toughnesses of binders. In the reference 2), this relationship is expressed as follows

$$\log(DS,_S)=3.020+0.0039\ T_{0,S}$$

$$\log(DS,_S)=3.150+0.0358\ T_{0,m}.$$

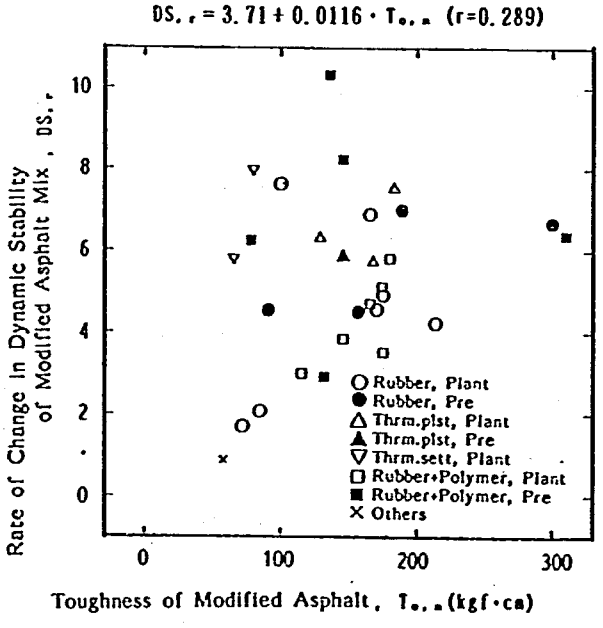


Fig.30 Toughnesses of Modified Asphalts vs. Rate of Change in Dynamic Stabilities of Modified Asphalt Mixes

5) Tenacities of Modified Asphalt Cements vs. Dynamic Stabilities of Modified Asphalt Mixes

The relationships between tenacities of modified asphalt cements and (rate of change of) dynamic stabilities of modified asphalt mixes are shown in Figs.31, 32. The dynamic stabilities of modified asphalt mixes range between 20 and 60 times as high as the tenacities of the binder, as similarly shown in Figs.29, 30, since the toughness and the tenacity have a strong relation each other as shown in Fig.17.

6) Mixing Temperatures vs. Dynamic Stabilities of Modified Asphalt Mixes

The relationship between mixing temperatures and dynamic stabilities of modified asphalt mixes is shown in Fig.33, however, no clear correlation is found, since the mixing temperatures are not determined only by viscosities of binders. Temperature susceptibility, which is different for each type of modified asphalts, also becomes one of the affecting factors.

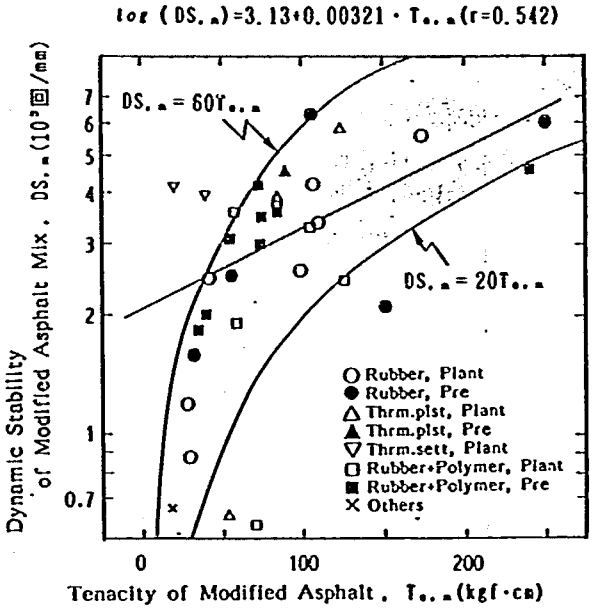


Fig.31 Tenacities of Modified Asphalt Cements vs. Dynamic Stabilities of Modified Asphalt Mixes

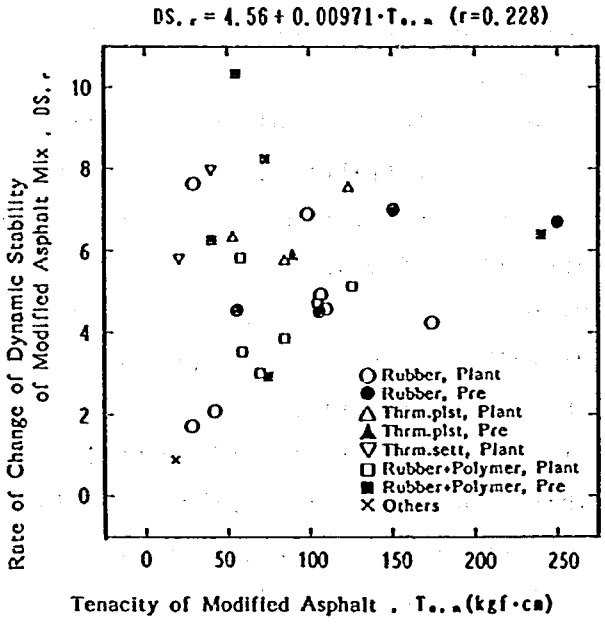


Fig.32 Tenacities of Modified Asphalts vs. Rate of Change of Dynamic Stabilities of Modified Asphalt Mixes

3.2.4/ Low Temperature Wear Properties of Asphalt Mixes

In general, different test results are obtained for the chain abrasion loss by each laboratory, because the test methods are not strictly specified. In fact, a meaningful relationship was not found during the analyses except for Fig.34, which indicates the relationship between chain abrasion losses of straight asphalt mixes and those of modified asphalt mixes. It is considered necessary to consolidate all test procedures to find low temperature wear properties. It is found that chain abrasion loss of modified asphalt is normally smaller than those

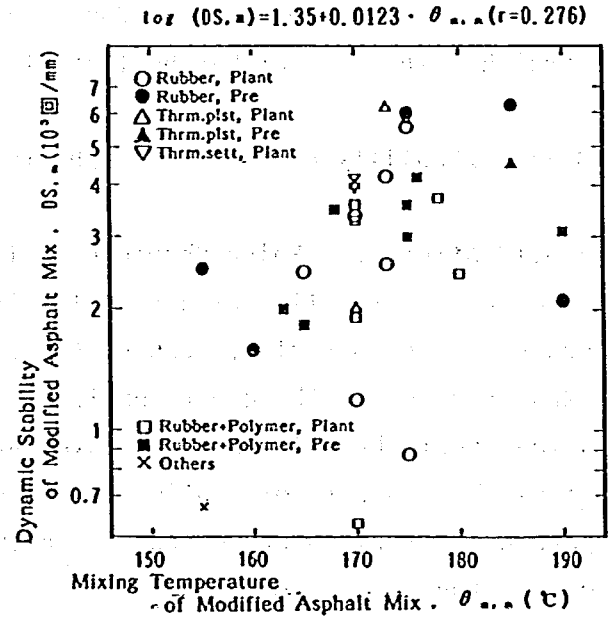


Fig.33 Mixing Temperature vs. Dynamic Stabilities of Modified Asphalt Mixes

of straight asphalts, reduced to between 33 and 70 percent of the original. In other words, modification of straight asphalts will give rise to the chain abrasion loss. However, it is not easy to compare all the different modified asphalts with each other, as test methods are not well standardized.

3.2.5/ Frequency Distributions of Properties of Modified Asphalts

Statistical frequency distributions of each property of modified asphalts are shown compared with those of straight asphalts in Figs.35 through 46. The followings are observed from these figures.

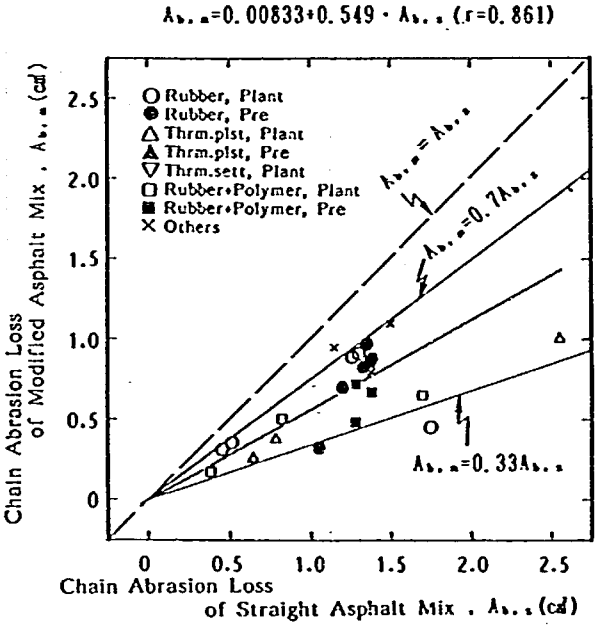


Fig.34 Chain Abrasion Losses of Straight Asphalt Mixes vs. those of Modified Asphalt Mixes

1) Properties of modified asphalts are normally distributed, except toughness and tenacity of binder, and dynamic stability of mixes.

2) Properties of modified asphalts are distributed in a wider range than those of straight asphalts, and sometimes have unexpected distributions. This tendency is remarkable especially for penetration index, kinematic viscosity at 60° C and viscosity at 180° C, toughness, tenacity, Fraas breaking point, dynamic stability, and chain abrasion loss.

3) No notable difference was found in distribution of modified asphalts and straight asphalts for Marshall stability and flow value.

3.3/ Workability of Modified Asphalts

3.3.1/ Attentions Which Should be Paid in Use of Modified Asphalts

Pavement construction with asphalt mixes is normally performed in a sequential order of manufacturing, transporting, spreading and compacting.

Many replies to the questionnaires were returned regarding the attentions which should be paid when the pavement is constructed with modified asphalt mixes. The numbers of replies for each process are shown in Fig.47. Over forty percent of replies suggested some points to be considered, especially during compaction.

Most replies pointed out of the requirement for temperature control.

The suggestions in use of modified asphalts, are also common for straight asphalts. No notable difference was pointed out by the type of asphalts. Se-

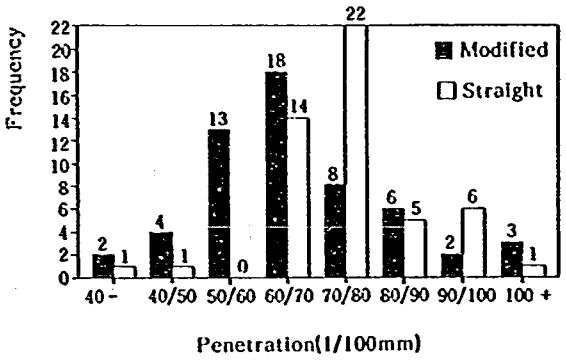


Fig.35 Distribution of Penetrations

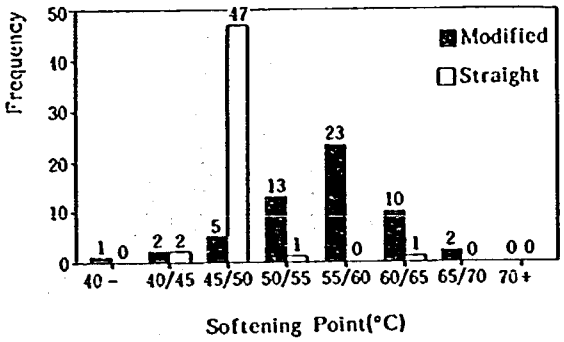


Fig.36 Distribution of Softening Points

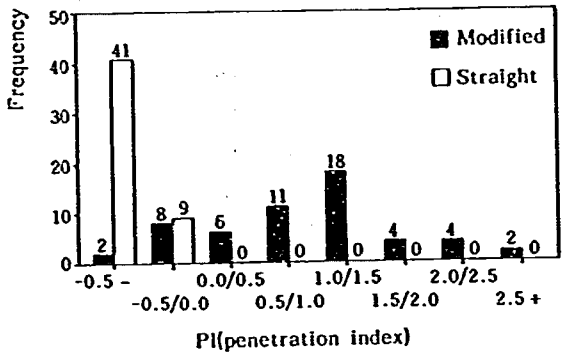


Fig.37 Distribution of PIs

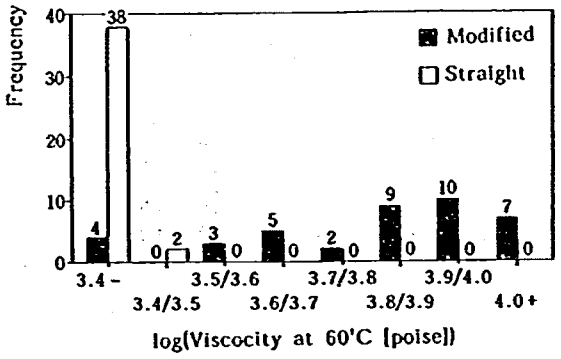


Fig.38 Distribution of Kinematic Viscosites at 60°C

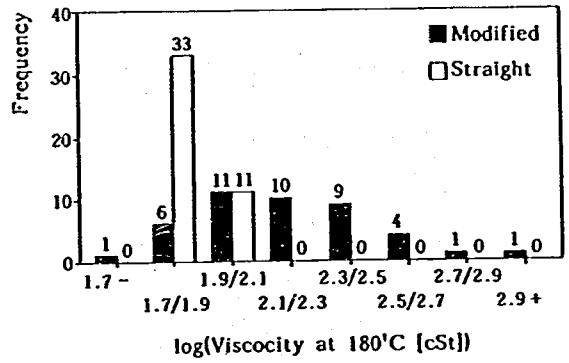


Fig.39 Distribution of Viscosities at 180°C

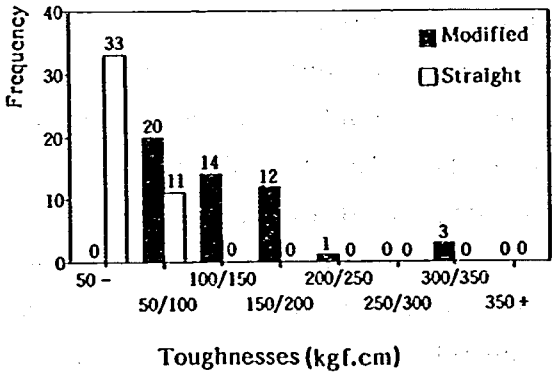


Fig.40 Distribution of Toughnesses

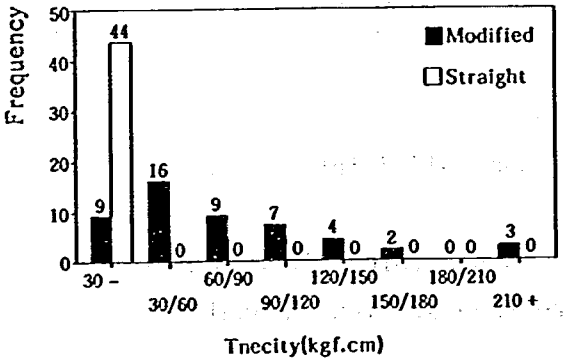


Fig.41 Distribution of Tenacities

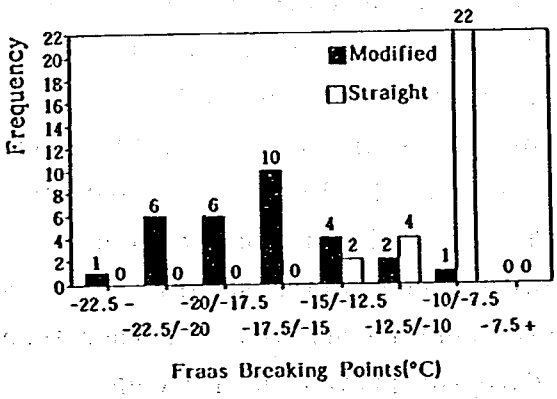


Fig.42 Distribution of Fraas Breaking Points

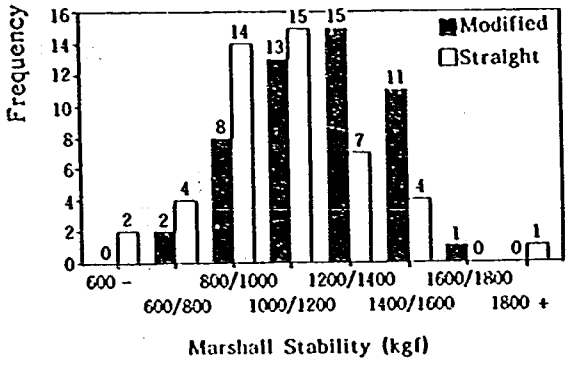


Fig.43 Distribution of Marshall Stabilities

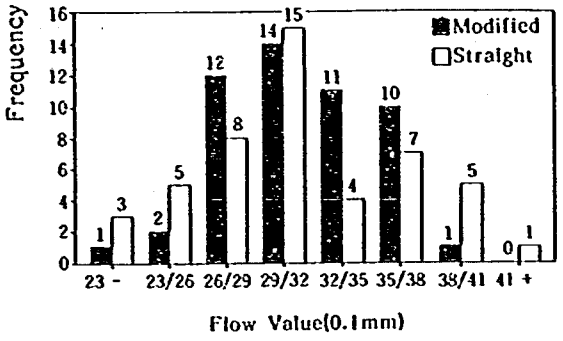


Fig.44 Distribution of Flow Values

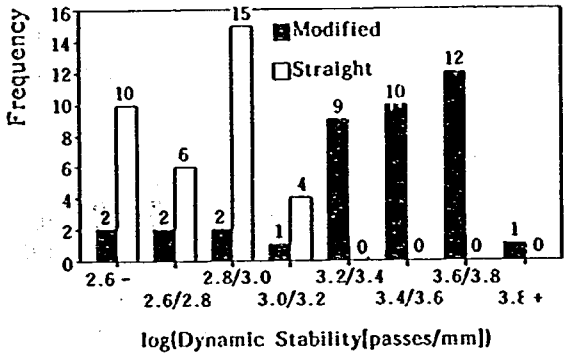


Fig.45 Distribution of Dynamic Stabilities

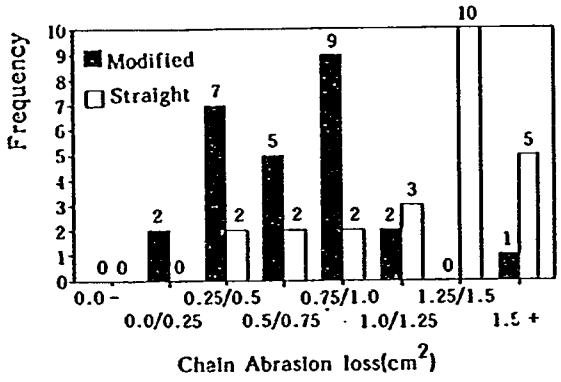


Fig.46 Distribution of Chain Abrasion losses

lected suggestions are shown below.

1) Temperature control during manufacturing, transportation and spreading

- Much attention should be paid for temperature control during the mixing.
- Much care should be taken of temperature control at transportation and its duration during low temperature seasons.
- Proper temperature should be kept during spreading and compaction.

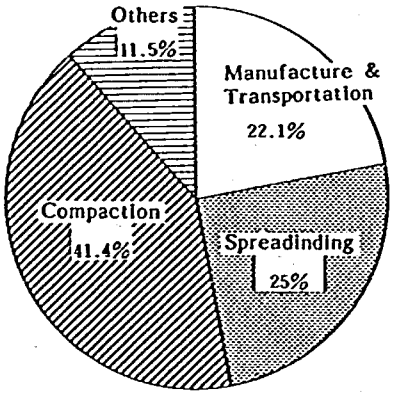


Fig.47 Construction Processes to which Attations should be paid

2) Precautions during making joints

- Hot joints are more desirable than cold ones.
- Tack coat should be spread out carefully when cold joints are to be made.

3) Timing of initial compaction

- Initial compaction should be made as soon as possible, since modified asphalts must be applied at higher temperature than straight asphalts.

4) Care for preventing pick-up

- Water should not be spread out while compacting, since it lowers the pave-

ment temperature and causes much pick-up. Rather, fuel oil should be applied over the rolling tires.

5) Compaction

- Second compaction should be made immediately after the initial compaction.
- Tire marks at pavement surface should be avoided with extreme care during the final compaction.
- Hairline cracks should be avoided with careful compaction.

6) Weather conditions

- Much attention should be paid to temperature control during the construction in winter time, and desirable air temperature is above 10° C.
- The pavement should be opened for traffic after the surface temperature is reduced under 60° C.

7) Other Notes

- Various cares to be taken of concerning aging of thermohardening resin, use of aggregates, paving techniques around to crackings and others are suggested. Most of them are common to the cases with straight asphalt mixes.

3.3.2/ Mix Temperature at Construction Recommended by Manufacturers

The ranges of mix temperatures and their averages at construction recommended by manufacturers are shown in Figs.48, 49. Fig.48 is made regarding binder types, whereas Fig.49 is drawn concerning the methods of mixing. The data for straight asphalts are also shown for reference[4]. The followings are found.

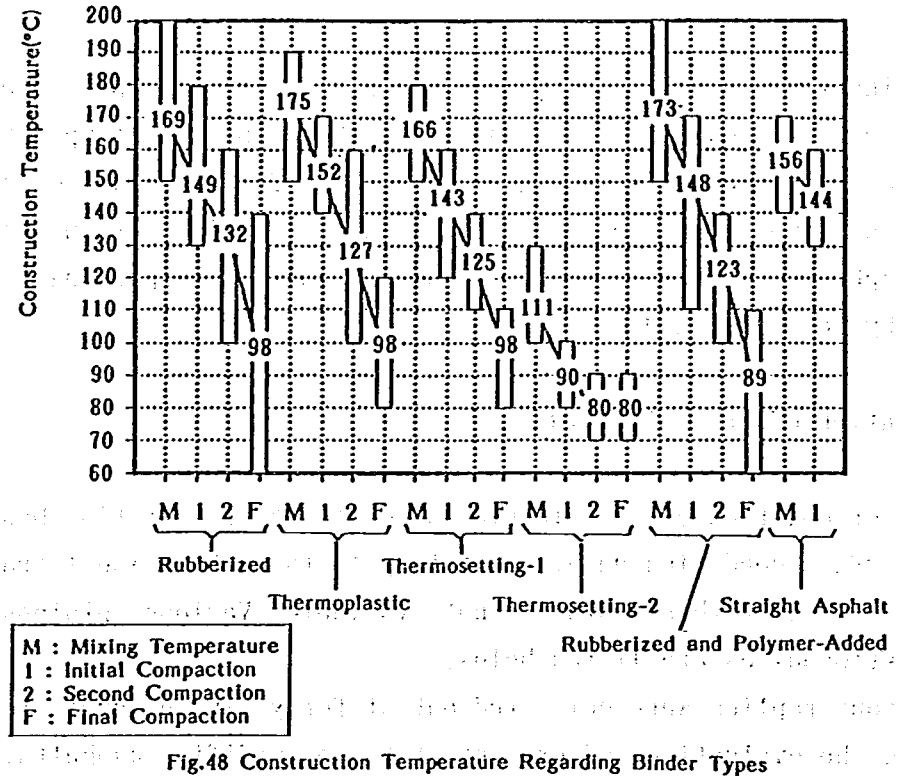


Fig.48 Construction Temperature Regarding Binder Types

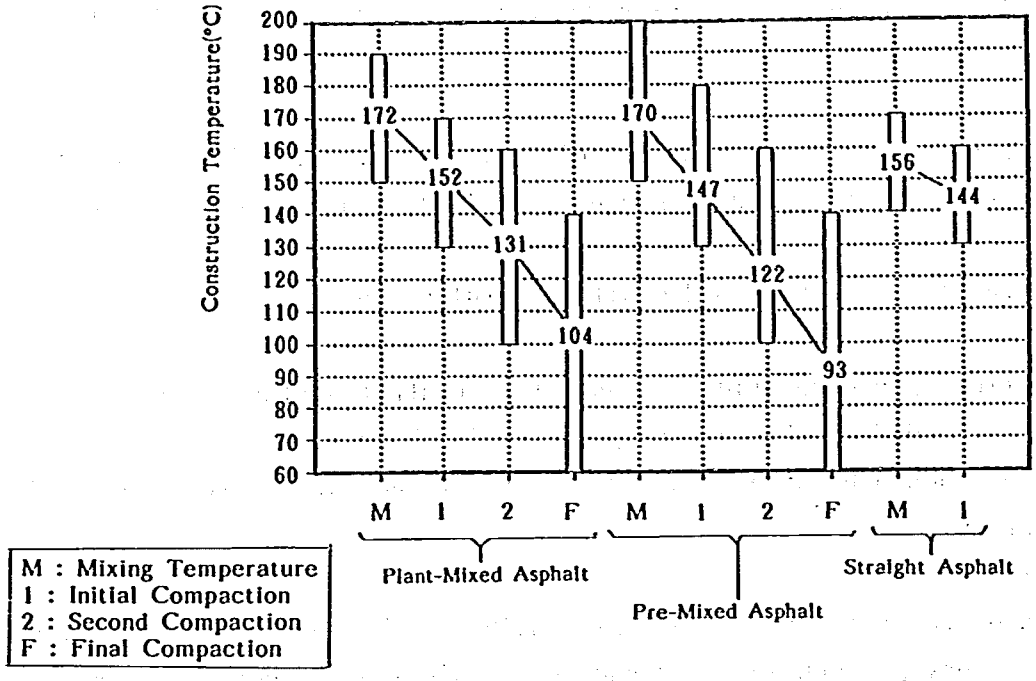


Fig.49 Construction Temperature Regarding Mixing Types

1) All the modified asphalts have similar tendencies concerning the mix temperature ranges, except for epoxy resin, shown as thermohardening 2 in Fig.48. The temperatures are higher in general than those of straight asphalts. The mixing temperatures are higher by from 13 to 19° C, and initial compaction temperatures are higher by from 4 to 8° C. The recommended temperatures for resin type are higher than those of rubberized type in almost all the processes.

2) The mixing temperatures recommended for plant-mixed and pre-mixed are almost identical as shown in Fig.49, however, the compacting temperatures for plant-mixed types are a little higher than those for pre-mixed ones.

3) The mixing temperatures of modified asphalts are higher than those of straight asphalts by from 14 to 16° C, and the initial compacting temperature is higher by between 3 and 8° C.

3.4/ Evaluation of Present Status

Efficiency of modified asphalt is evaluated at the present time based on the pavement surface condition data. Laboratory tests such as wheel tracking or labeling are used if these data are not available. Various opinions collected by the questionnaires are listed below.

1) Thirty four replies were collected out of forty five products to the question asking the evaluations of present status of modified asphalts. The num-

bers of the replies regarding each pavement distresses are

- Evaluation against viscous flow : 18
- Evaluation against crack initiation : 4
- Evaluation against abrasion by studded tires : 13
- Evaluation of improving overall efficiency : 17.

The number of replies concerning the evaluation against cracking is fewer than the others, because modified asphalts have been developed mainly to achieve higher resistance to viscous flow and abrasion by studded tires.

2) Most manufacturers acknowledged their products are effective against viscous flow and abrasion by studded tires. However, their evaluation varies much. Most replies acknowledged extended service life, although few of them had backup data.

3) Since evaluation was done by each manufacturer, data are not sufficiently available to make relative comparison among overall products. To obtain proper evaluation, a comparison should be made by a laboratory or by in-situ testing based on the same test conditions.

3.5/ Remaining Problems and Future Developments

Currently remaining problems faced to manufacturers are classified into three groups, against contractors, against contracting agencies and against manufacturers themselves.

For contractors, the manufacturers are asking for proper temperature control at mixing, especially in application of wear resistant pavement.

For contracting agencies, they should compare efficiency of plant-mixed and pre-mixed asphalts with each other before selecting the most suitable product. Though the aggregate gradations are currently specified by contracting agencies, the manufacturers should be consulted for suitability of modified asphalts instead.

For manufacturers themselves, quality assurance is required to provide proper products at adequate prices. Some replies pointed out the shortage of kettles in mixing plants.

4/ SUMMARY

It is seen through the questionnaires that various products of modified asphalt cements are being manufactured by a number of firms serving local needs. Performance of modified asphalt cements are evaluated superior to straight asphalts in properties of binders and mixes in general, leaving some problems

regarding temperature controls, although the quality and properties of products are still being evaluated independently by each manufacturer. In order to improve the effective use of modified asphalts in the future, it is considered to be necessary to take an objective view of the products, and establish quality standards and application procedures.

The replies to the questionnaires are briefly summarized below.

1) Modified asphalts are classified into rubberized, polymer-added, and rubberized and polymer-added asphalt cements. Methods of mixing are classified into plant-mixed and pre-mixed, as shown in Fig.1.

2) Modified asphalts have been consumed from 110,000 to 130,000 metric tons a year (converted to volume of binder). The consumption is being increased by twenty five percent in five years.

3) The products are sold either as modified asphalts or as modifying additives.

4) Major purposes of use of modified asphalts are to provide resistances against viscous flow and abrasion by studded tires.

5) Volume of modifying additives added on asphalts varies much, but is normally from 3 to 5 percent (dry). No deleterious substance is contained in any additives.

6) Both the binders and the mixing additives have been more improved than straight asphalt, depending on their types and applications.

7) As mixing temperatures of modified asphalts are higher than those of straight asphalts by from 15 to 20° C, the temperature must be properly controlled. The application time must be carefully coordinated for thermohardening resin.

8) In accordance with the opinions collected from manufacturers, pavement performance constructed with modified asphalts is generally higher than that with straight asphalts.

9) Prices of modified asphalts are 1.8 through 3.1 times higher than those of straight asphalts, except for thermohardening resin.

ACKNOWLEDGMENTS

The authors would like to express their sincere appreciation to the Committee of New Material Development, Japan Asphalt Institute, for kindly permitting them to make this paper presented, and its all the members who helped us processing an enormous amount of untreated replies of the questionnaires.

The authors are also indebted to Professor Teruo Sugawara of Hokkaido University for his valuable suggestions in preparing this paper.

REFERENCES

1) Arai, T.: Consideration of Use of Modified Asphalts, Road Construction, pp.81-89, Aug., 1985 (in Japanese)

2) Japan Rubberized Asphalt Institute: Research and Survey Report for Development of Rubberized Asphalts for Flow and Wear Resistances, 1982 (in Japanese)

3) Batton, J.W. et al.: Variability in Temperature Susceptibility of Asphalt Cement, NCHRP, Digest 130, 1981

4) Tatsushita, F. et al.: Trial Pavement and Initial Properties for Providing Flow Resistance, Annual Report of Tokyo Metropolitan Research Institute of Civil Engineering, 1986 (in Japanese)

5) Iwase, T. et al.: Relationship between Viscosity of Pavement Asphalt and Stability of Asphalt Mixes, Annual Report of Tokyo Metropolitan Research Institute of Civil Engineering, 1976 (in Japanese)

6) Iwase, T. et al.: Consideration for Polymer-added Asphalt Mixes, Metropolitan Tokyo, Annual Report of Tokyo Metropolitan Research Institute of Civil Engineering, 1985 (in Japanese)

7) Public Works Research Institute, Ministry of Construction: Survey Report on Physical Properties of Straight Asphalts, Vol. 2398, 1987 (in Japanese)

8) Japan Asphalt Institute: Pavement Asphalt for Heavy Traffic Roads, Development of Semi-blown Asphalt, 1984 (in Japanese)

Cold Temperature Properties of a Polymer-Modified Asphalt Concrete

N. Ali, Technical Univ. of Nova Scotia
A. Bergan, J. Chan, Univ. of Saskatchewan
A. Papagiannakis, Memorial Univ. of Newfoundland

COLD TEMPERATURE PROPERTIES OF POLYMER-MODIFIED ASPHALT MIXTURES

by

Ali, Dr. N., Assistant Professor
Department of Civil Engineering
Technical University of Nova Scotia

Chan, J. S. S., Research Engineer
Transportation Centre
University of Saskatchewan

Papagiannakis, Dr. A. T., Assistant Professor
Department of Civil Engineering
Memorial University of Newfoundland

Bergan, Dr. A. T., Professor
Department of Civil Engineering
University of Saskatchewan

ABSTRACT

Results of a laboratory testing program designed to evaluate the performance of two modified asphalt binders, LATEX and STYRELF 13, at low and high temperatures (-30°C to +44°C) are presented in this paper. The material properties evaluated were resilient modulus (M_r), permanent deformation characteristics, creep modulus, indirect tensile strength, and moisture damage.

The addition of the LATEX modifier to the conventional AC binder produced a mixture which showed significant reductions in susceptibility of the M_r to temperature and in permanent deformation, as well as having lower creep modulus at low temperatures than those of mixtures produced from the parent binder. The LATEX modified mixture did not pass the moisture damage evaluation criteria. The STYRELF 13 modified binder produced a mixture with the highest M_r for all temperatures tested, the lowest permanent deformation, and the highest creep modulus of the mixtures tested. The STYRELF 13 mixture also passed the moisture damage test and exhibited the highest tensile strength at all temperature levels.

1.0 INTRODUCTION

There has been an increased interest in the use of modified asphalt binders in the paving industry. As a result, material researchers have been asked to apply state-of-the-art material testing methods and analyses to predict the performance of such modified materials. A proper evaluation should include testing over a wide temperature range in which a pavement is expected to perform. Thus, the temperature susceptibility of these asphalts could be compared.

The primary objective of this study was to evaluate the performance of modified asphalt binders for the purpose of reducing pavement cracking, rutting, and moisture damage. The laboratory testing program was designed to examine both the stiffness and flexibility of each modified binder mixture at low and high temperatures.

2.0 MATERIALS

Asphalt binders for this study were IRVING asphalt and STYRELF 13. The IRVING asphalt (AC), a conventional binder, was sent to BASF Canada for blending with the LATEX modifier. STYRELF 13 is a premixed modified binder designed for cold temperature conditions. The physical properties of the binders are summarized in Table 1.

The same densely-graded, crushed stone was used in all mixtures in this study. The gradation of the aggregate conformed to the Nova Scotia Department of Transportation Specifications Manual (1) for Type B mix. Table 2 shows the gradation of the aggregate used.

The optimum binder content for each mixture type was determined using the Marshall Method. An effort was made to produce specimens with the same amount of air voids for all three types of mixes tested. A summary of mix properties can be found in Table 3. The stability values of the two modified binder mixtures at 60°C were higher by 10 to 40 percent than the stability values of the mixtures made with the conventional AC binder. The flow values for these binders were within acceptable limits.

3.0 SPECIMEN PREPARATION

Two types of test specimens were used in this study, namely cylindrical and briquette. The resilient modulus (M_r), permanent deformation, and creep modulus testing were performed on the cylindrical specimens. Briquette specimens were used in low-temperature indirect tensile strength and moisture-damage effect testing.

Cylindrical specimens of 101.0 mm in diameter and 203.2 mm in height were used. These were compacted in four layers and were prepared in accordance to Asphalt Institute guidelines (2).

The briquette specimens were 101.0 mm in diameter and 63.5 mm in height. These were prepared in accordance with the Marshall Method of mix design specified by the Asphalt Institute (2).

4.0 TESTING SYSTEM

An MTS Closed-loop Electro-hydraulic Testing System at the Department of Civil Engineering, University of Saskatchewan, was used in the testing program. The MTS system was interfaced with two micro-computers for load control and data acquisition purposes.

An IBM XT compatible micro-computer with a two-channel digital-to-analog conversion board was used to provide various signals to the MTS system for application of load. This allowed load functions of various types to be digitized and applied to the specimens.

High-speed data collection was achieved using a second IBM AT compatible micro-computer which was equipped with a 16-channel analog-to-digital conversion board. This was used to collect various load and response data during testing.

An environmental chamber, capable of providing air temperatures between -40°C and +50°C, was used to control test temperatures during the testing of asphalt concrete specimens. The environmental chamber can accommodate testing of both the briquette and cylindrical specimens. The experimental set up can be found in Figure 1.

5.0 TESTING PROCEDURES

5.1 Resilient Modulus

The resilient modulus (M_r) is a dynamic test response defined as the ratio of repeated axial deviator stress divided by the recoverable strain. Repeated haversine loading was used in all resilient modulus testing. Haversine loading was used to prevent impact loading to test specimens. A typical haversine load function can be found in Figure 2. Two load frequencies were used. The first frequency of 1 Hz was loaded at 0.1 seconds and unloaded at 0.9 seconds. The second frequency of 0.33 Hz was loaded at 0.25 seconds and unloaded at 2.75 seconds. Resilient modulus values were measured at the 50th and 150th cycles.

Each of the three mixtures was tested at four temperature levels: -15°C, 0°C, 20°C, and 44°C.

5.2 Creep and Permanent Deformation

Incremental static load testing at 138 kPa was conducted on cylindrical specimens to determine the permanent deformation and creep characteristics of each mixture. Each mixture was tested at -15°C, 0°C, 20°C, and 44°C. Figure 3 shows the incremental static load function used.

The permanent strain at the end of each unloading period was calculated from the measured deflection. The total permanent strains versus the corresponding incremental loading times were plotted on a log-log graph.

The creep characteristic was obtained during the 1000-second loading. Strains during various times of loading were measured.

The creep modulus at any given time, S(t), can be determined using the following equation:

$$S(t) = \frac{\sigma}{\epsilon(t)}$$

where: σ = applied stress (MPa)

$\epsilon(t)$ = axial strain at time t

5.3 Tensile Strength

The low-temperature tensile fracture strengths of briquette specimens were determined using the indirect tension. The testing procedure used has been previously reported by Anderson and Hahn (3). Due to the limited number of specimens available, testing was restricted to the rate of 1.5 mm/minute and to the temperature levels of 0°C, -10°C, -20°C, and -30°C. These test temperatures resulted in failure within 60 to 160 seconds.

Anderson and Epps (4) have documented indirect tensile testing of field core specimens at low and high temperature levels using three strain rates: 51, 5.1, and 0.51 mm/minute. The results show that there was little tensile strength dependency on the applied strain rate at low temperature levels. Therefore, using a strain rate of 1.5 mm/minute in this study was considered acceptable.

5.4 Moisture Damage Procedure

Moisture sensitivity and the effects of stripping are closely related. Stripping is primarily caused by water damage to the adhesive properties of the binder. Moisture damage evaluation can be accomplished using various methods, all of which are listed in the FHWA report (5).

According to FHWA (5), the most promising procedure for long-term testing appears to be one described in NCHRP 246. Table 4 summarizes the procedures recommended by NCHRP 246 for each moisture damage evaluation. This method evaluates either the retained ratio of resilient modulus or the indirect tensile strength of wet (moisture conditioned) and dry (unconditioned) samples.

6.0 RESULTS AND ANALYSIS

6.1 Resilient Modulus

The relationships between resilient modulus values and temperature levels for the three mixtures evaluated can be seen in Figures 4 and 5. As expected, the M_r values increased with increased loading frequency and/or decreased test temperatures. These figures clearly show the effect of the LATEX on the asphalt mixture modulus. At low temperatures, the LATEX modified binder resulted in a lower M_r; while at higher temperatures this was reversed. That is, the conventional AC binder resulted in a higher M_r than the LATEX modified mixtures. The benefit of the reduction in the temperature susceptibility of the M_r due to LATEX is obvious. It reduced the cold-temperature cracking potential, while maintaining improved resistance to rutting in the summer. In comparison, the effect of the LATEX on the temperature susceptibility of Penetration/Viscosity is not that obvious. The measured values for conventional AC binder versus LATEX modified binder were 250/150 and 260/150, respectively, yielding roughly identical Penetration Viscosity Numbers (PVN), as seen in Table 1.

The effect of STYRELF 13 on M_r is less obvious, mainly because the parent asphalt binder used was not identical to the IRVING asphalt binder tested. As mentioned earlier, the reason was that STYRELF 13 is a proprietary product that was supplied ready-mixed. For all temperatures and loading frequencies tested, the STYRELF 13 modified mixture showed higher M_r values than the conventional asphalt mixture. This was expected given that the STYRELF 13 modified binder had a considerably higher viscosity than the conventional AC binder, as referred to in Table 1. It seems, however, that the difference in the M_r of the two mixtures became lower at increased temperatures for both loading frequencies. No direct benefit in modifying M_r using STYRELF 13 can be seen from the M_r testing performed. This points out the need for testing the parent asphalt binder used for producing STYRELF 13.

Table 5 summarizes the M_r values measured for the three mixtures.

6.2 Permanent Deformation

The creep testing conducted allowed the evaluation of the permanent deformation and the creep characteristics of the three types of asphalt mixtures. Figures 6 and 7 show the permanent deformation versus the loading time curves obtained at 20°C and 44°C, as well as -15°C and 0°C, respectively. As expected, permanent deformation increased in an exponential fashion with loading time for all the temperatures tested (i.e., it appears linear in a log-strain versus log-time diagram). Comparisons of permanent strain rates between the two modified mixtures and the conventional mixture showed an increase for the relatively high temperatures (i.e., 0°C, 20°C, and 44°C), while it showed a dramatic decrease at low temperatures (i.e., -15°C). Average values of the magnitude of the reduction in permanent deformation effected by the modifiers was obtained throughout the loading time period tested (i.e., 1000 seconds). These ranged from negligible at -15°C to over one order of magnitude at 44°C. In these comparisons, the STYRELF 13 outperformed the LATEX modifier exhibiting consistently lower permanent deformation. This was expected given the lower viscosity of this binder. It is concluded that the dramatic decreases in permanent deformation were obtained by the use of modifiers for a wide range of temperatues.

Figures 8 and 9 show the creep modulus of the mixtures tested as a function of time for -15°C and 0°C, as well as 20°C and 44°C, respectively. As expected, creep moduli decreased with increased loading time and/or temperature. It can be seen that for all tempertures tested, the STYRELF 13 modified mixture exhibited a higher creep modulus than the conventional asphalt mixture. At low temperatures (i.e., -15°C and 0°C), the LATEX modified binder exhibited lower creep moduli than the conventional asphalt mixture. At higher temperatures (i.e., 20°C and 44°C), the LATEX modified binder demonstrated marginally higher creep moduli than the conventional AC mixtures. Thus the use of STYRELF 13 modified binder increased rutting resistance under low-speed driving conditions for all tempertures tested; while marginal improvement was realized by the LATEX modified binders for high tempertures only.

6.3 Moisture Damage

Moisture damage was expressed in terms of both the retained ratio of the M_r and the retained ratio of the tensile strength for wet and dry conditions, respectively. The results are shown in Table 6. It can be seen that the retained ratios ranged from 0.48 to 0.72 and 0.86 to 0.99, respectively. Both modifiers seemed to improve the weathering resistance of the mixtures compared to the conventional AC mixtures. However, when the FHWA criteria of 70 and 80 percent were used for "passing" a mixture (5), only the STYRELF 13 modified mixture passed the moisture damage test.

6.4 Tensile Strength

The results of the tensile strength test are shown in Figure 10. Tensile stress at failure was plotted versus temperature for the three mixtures tested. As was expected, tensile strength decreased with temperature, particularly for temperatures higher than -20°C. It can be seen that the LATEX modified binder reduced the tensile strength of the mixture for all but the highest test temperature. On the contrary, the STYRELF 13 modified binder demonstrated higher tensile strength than the other two mixtures.

7.0 CONCLUDING REMARKS

A series of tests were conducted on three asphalt mixtures obtained with conventional AC binder (IRVING), LATEX modified binder (IRVING + LATEX), and STYRELF 13 modified binder (proprietary mix). The tests included Resilient Modulus (M_r) (loading frequencies of 0.33 Hz and 1.0 Hz), creep, and indirect tension. A range of temperatures, -30°C to +40,C, was used for the tesing. In addition to these tests, the moisture damage resistance of these mixtures was tested using an FHWA recommended practice (5).

The LATEX modified mixture exhibited reduced susceptibility of the M_r to temperature in comparison to the conventional AC binder. It also resulted in significant reductions in permanent deformation, while its creep modulus at low temperatures was lower than that of the conventional AC binder. Also, its tensile strength was lower than that of the conventional mixture and did not pass the moisture damage test according to FHWA guidelines (5).

The STYRELF 13 modified mixture exhibited higher M_r than the other two mixtures for all temperatures tested; therefore, no improvements in the temperture susceptibility of its M_r could be demonstrated. It exhibited the lowest permanent deformation and the highest creep modulus of the mixtures tested. It passed the moisture damage test as per FHWA guidelines (5) and exhibited the highest tensile strength.

These findings should be viewed bearing in mind that the parent asphalts used for producing the two modified binders were different. Conclusive results for the performance of STYRELF 13 modified mixtures can be obtained only by testing it against its parent asphalt.

8.0 REFERENCES

1. Nova Scotia Department of Transportation & Communications (NSDOT), "NSDOT Standard Specifications, Metric Edition." NSDOT, 1988, p. 4-4-4.

2. Asphalt Institute, "Mix Design Methods for Asphalt Concrete and Other Hot-Mix Types." Asphalt Institute Manual Series No. 2 (MS-2), 1988.

3. Anderson, K.O., and Hahn, W.P., "Design and Evaluation of Asphalt Concrete with Respect to Thermal Cracking." Association of Asphalt Paving Technologists, Vol. 37, 1986, pp. 1 - 31.

4. Anderson, K.O., and Epps, J.A., "Asphalt Concrete Factors Related to Pavement Cracking." Association of Asphalt Paving Technologists, Vol. 52, 1983, pp. 151 - 197.

5. Stuart, K.D., "Evaluation of Procedures Used to Predict Moisture Damage in Asphalt Mixtures." FHWA/RD-86/090, 1986.

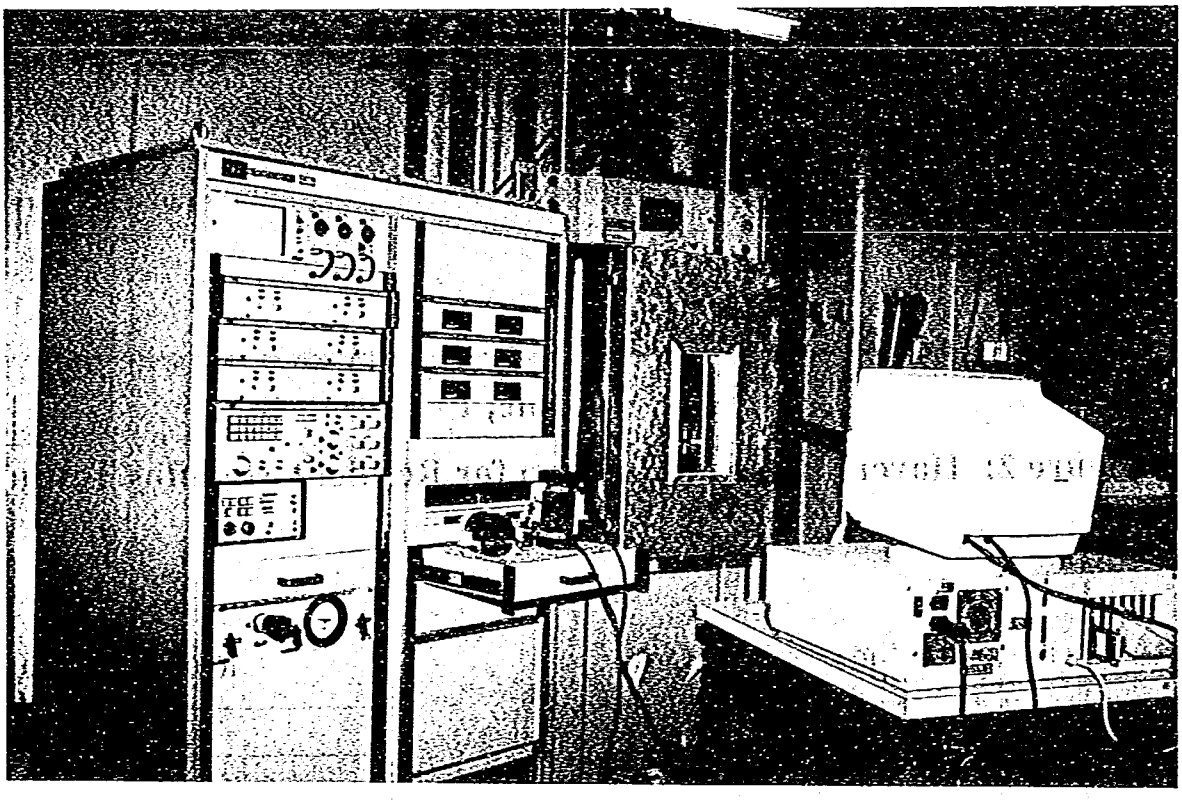


Figure 1: MTS Material Testing System

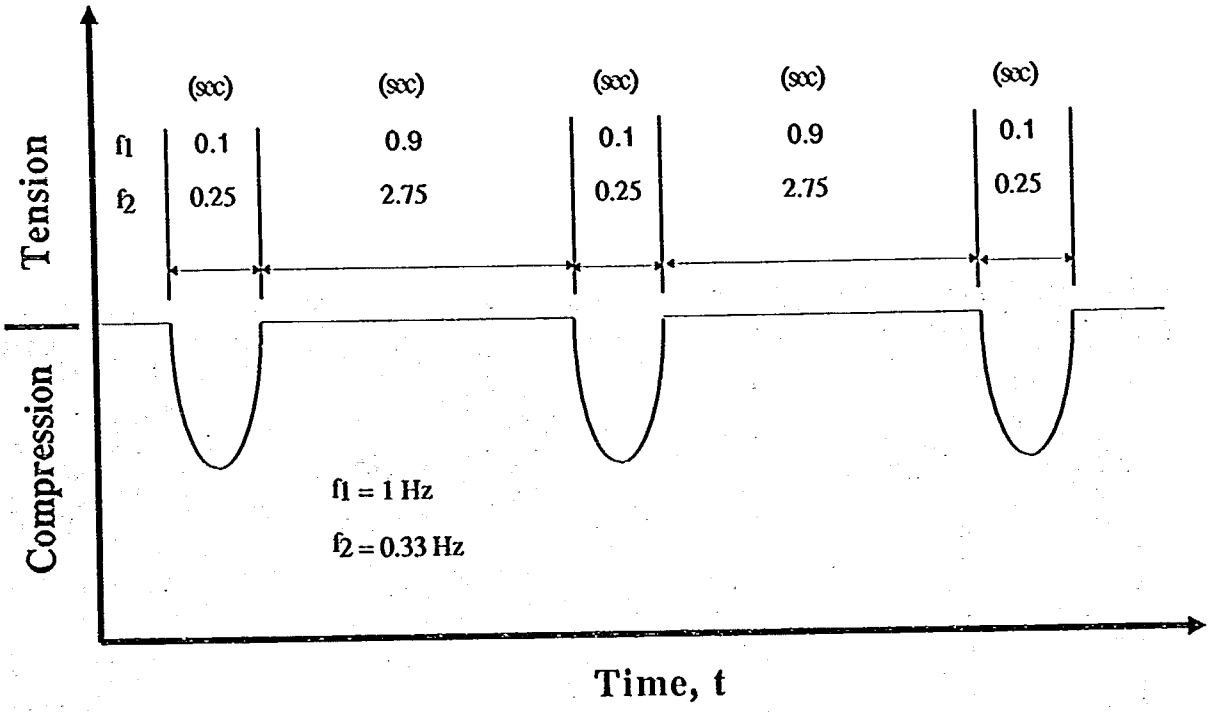


Figure 2: Haversine Load Function for Resilient Modulus Testing

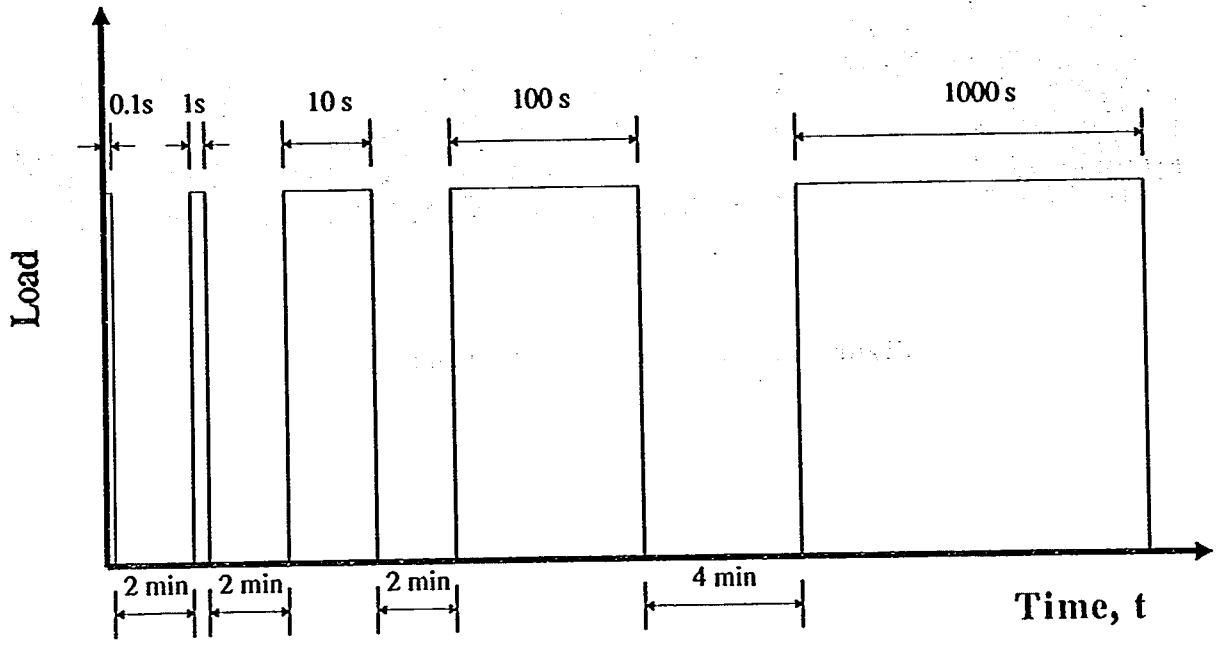


Figure 3: Incremental Static Load Function

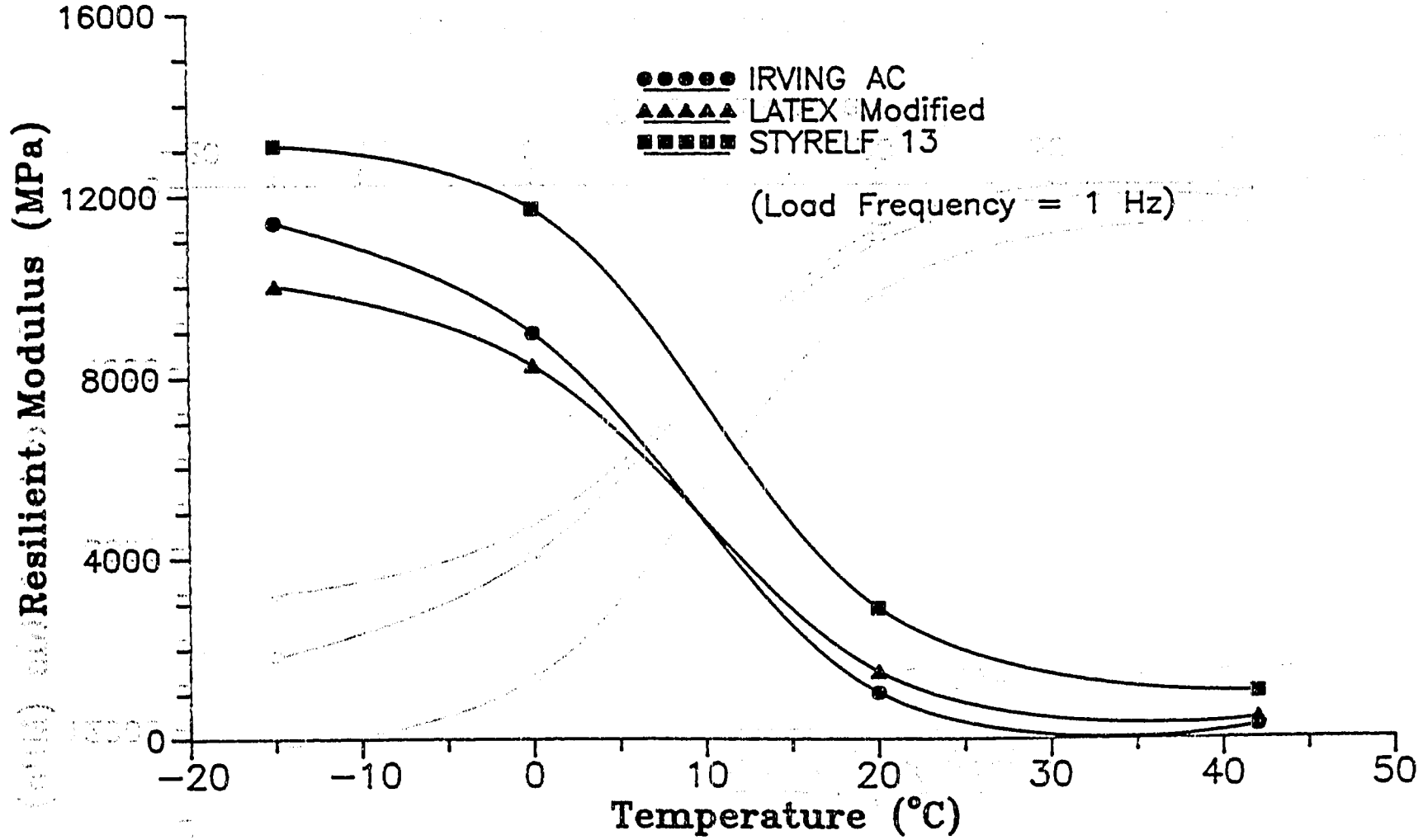


Figure 4: Resilient Modulus for 1 Hz Loading

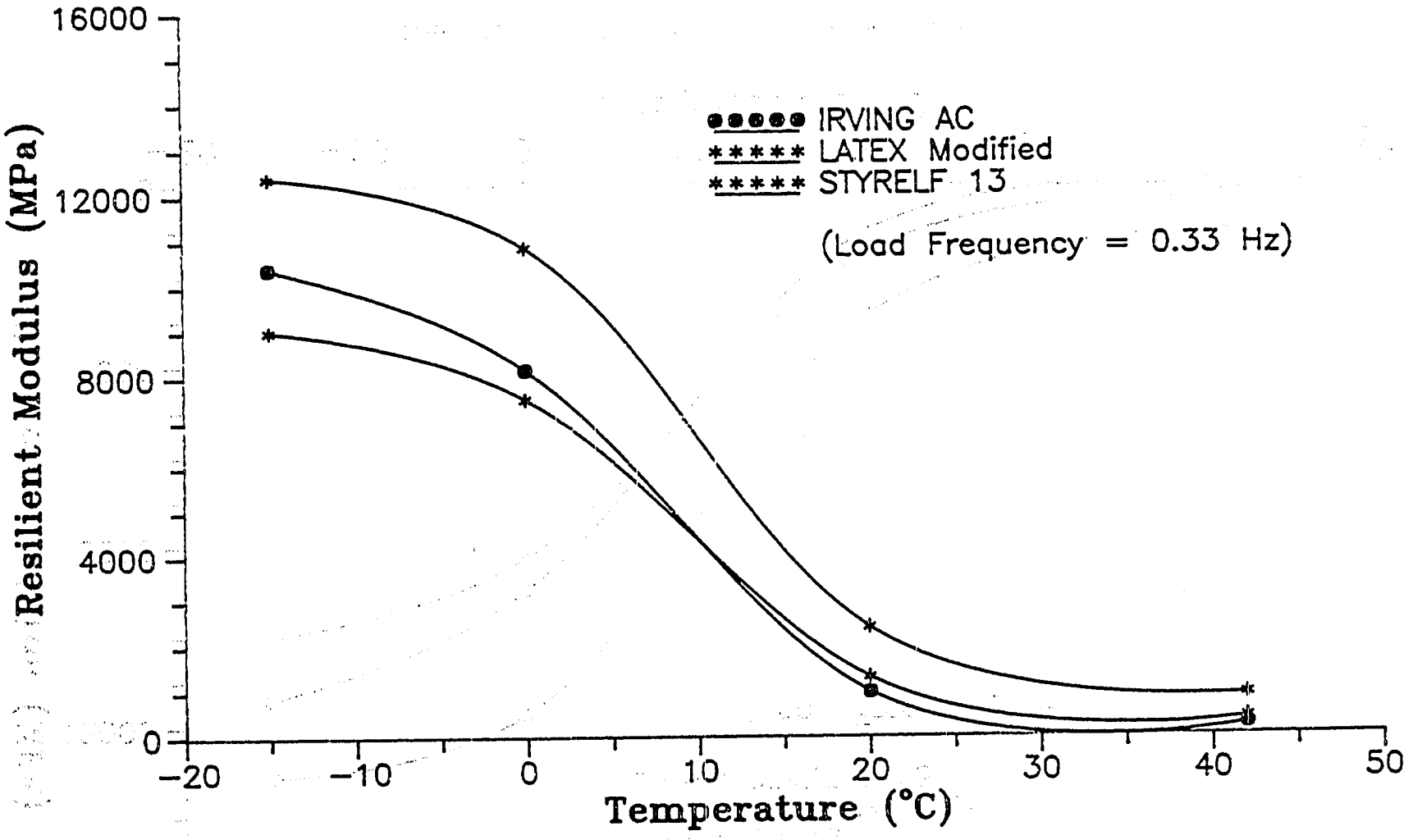


Figure 5: Resilient Modulus for 0.33 Hz Loading

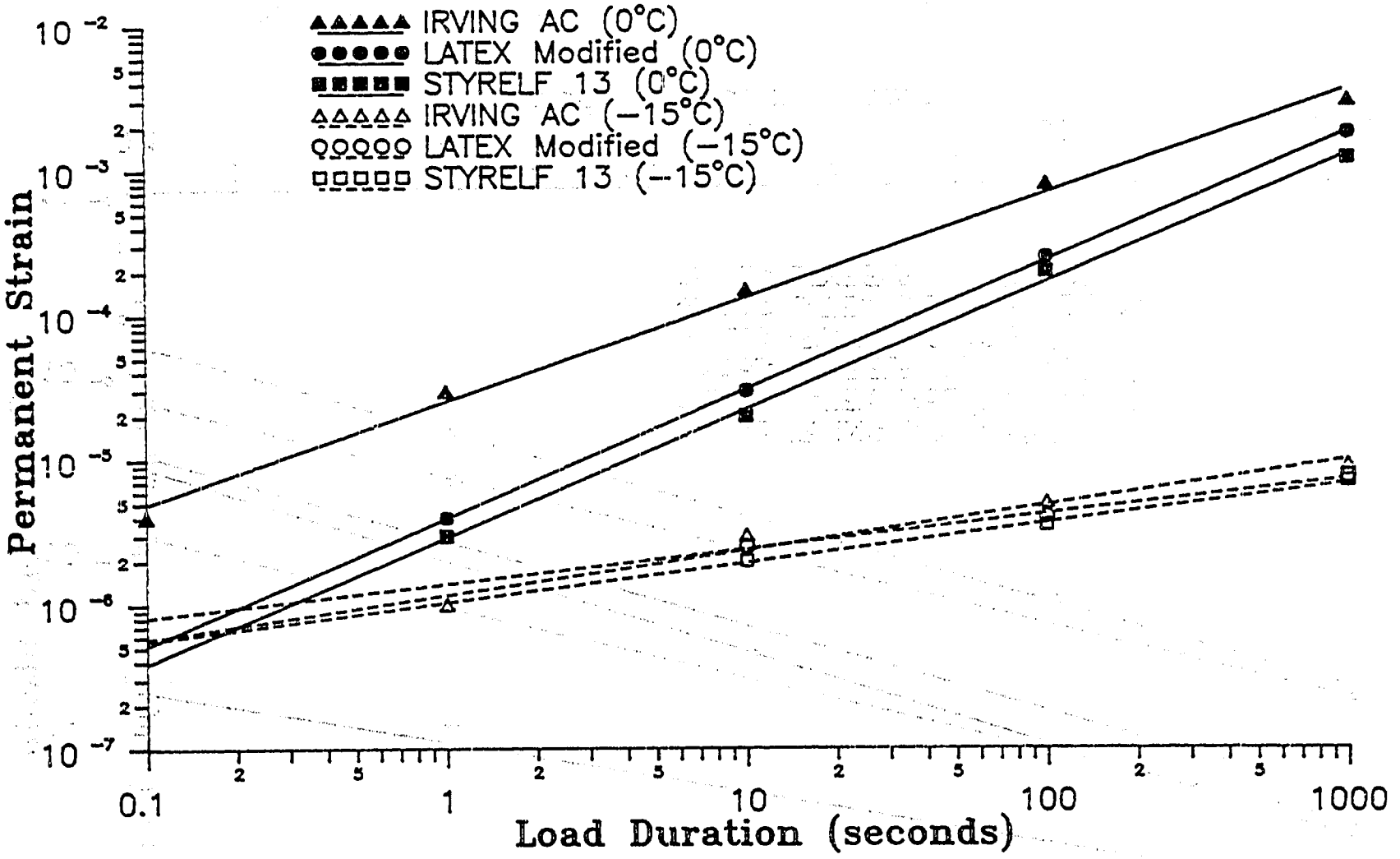


Figure 6: Permanent Deformation for Low Temperature Range

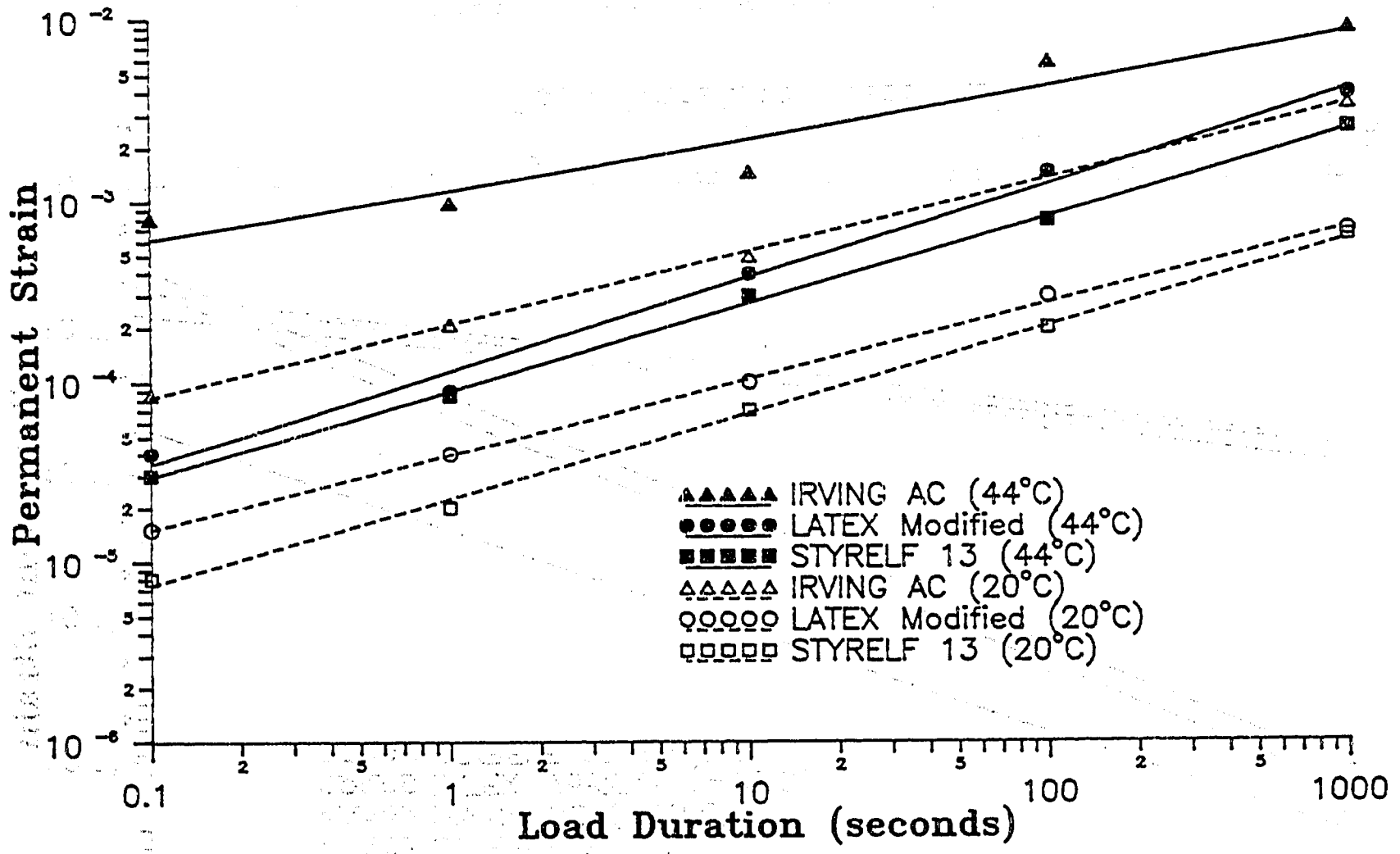


Figure 7: Permanent Deformation for High Temperature Range

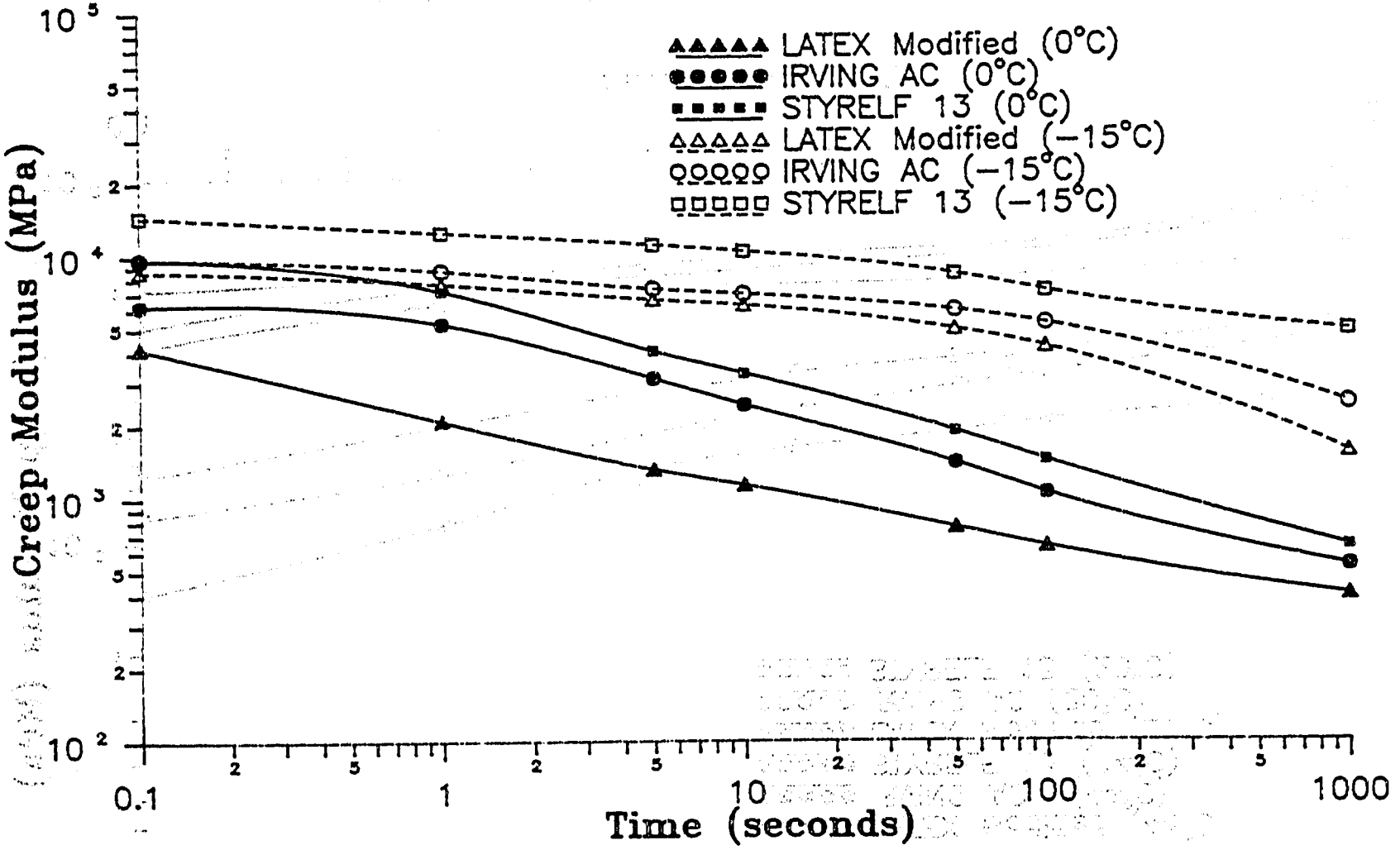


Figure 8: Creep Modulus for Low Temperature Range

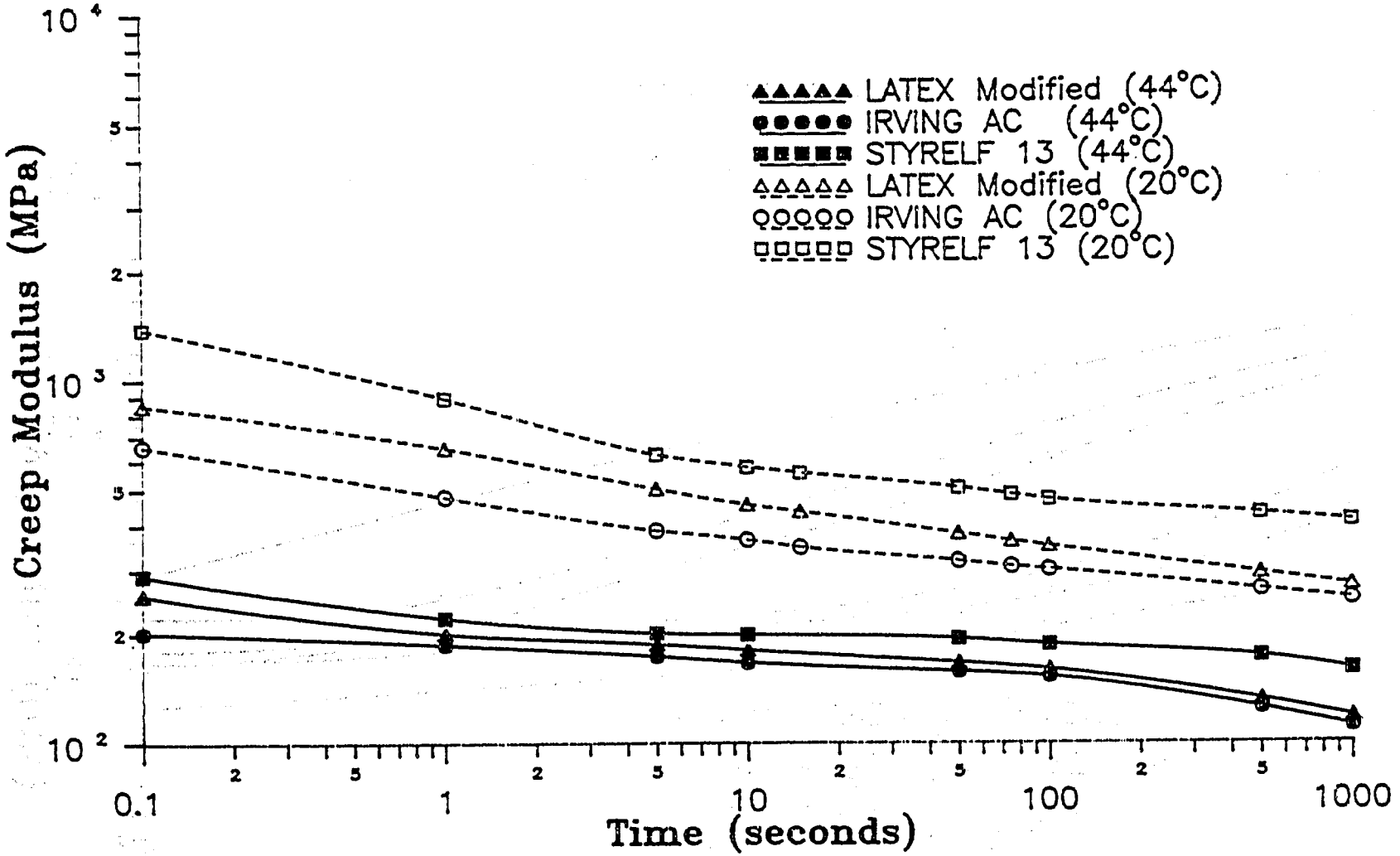


Figure 9: Creep Modulus for High Temperature Range

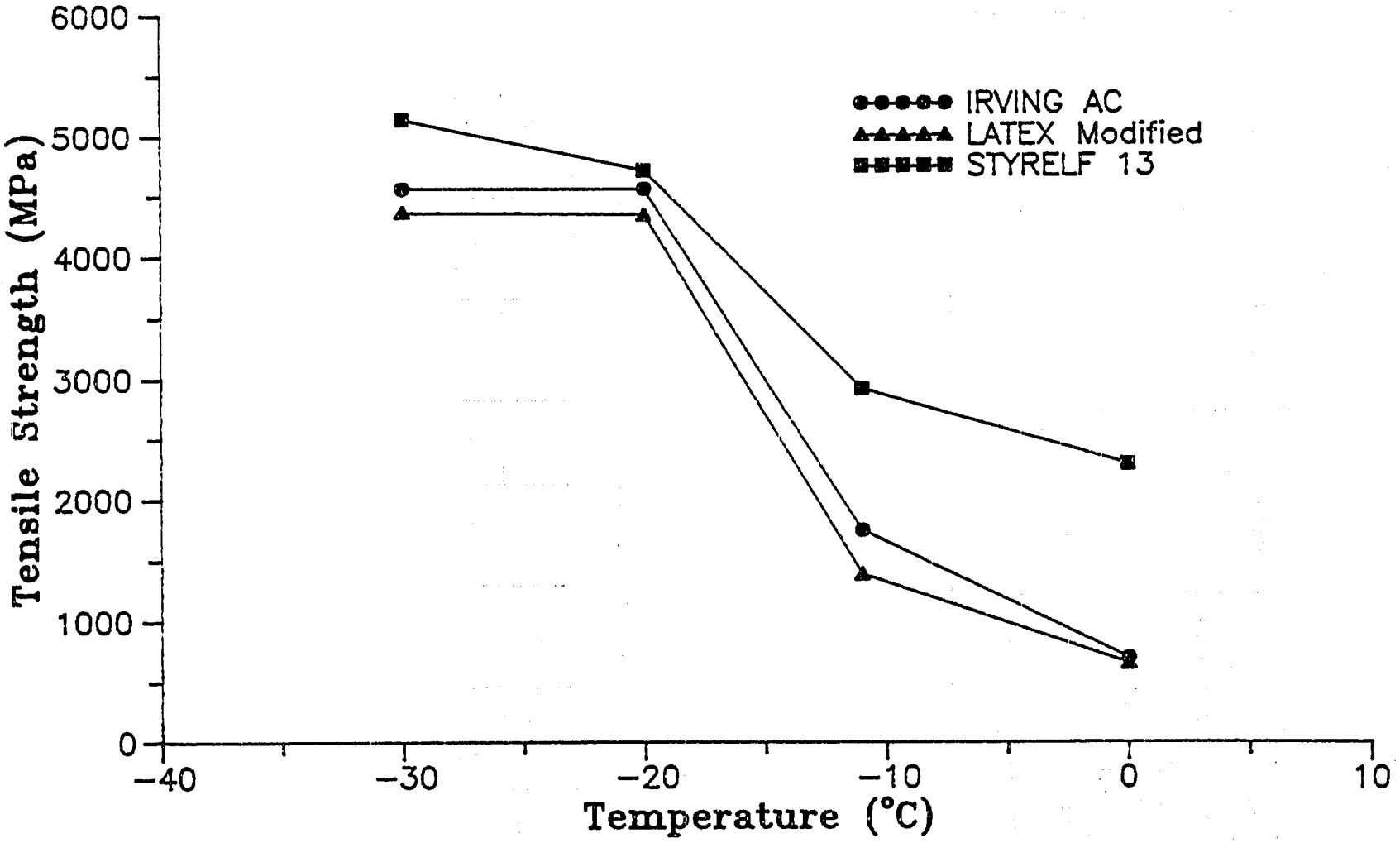


Figure 10: Indirect Tensile Strength

Table 1: Properties of Asphalt Binders

	ASPHALT BINDER		
Physical Properties	STYRLF 13	IRVING AC	LATEX Modified
Penetration (1/10 mm) at 25°C	90	250	260
Viscosity (Cst) at 135°C	888	150	150
Specific Gravity	1.029	1.025	1.02
Softening Point (°C)	49	49	52
PVN	0.60	-0.40	-0.40

Table 2: Gradation of Aggregate

Sieve Size (mm)	28	20	14	10	5	2.5	0.315	0.08
% Passing	100	97.5	70	70	50	35	11.5	5.0

Table 3: Summary of Mixture Properties

PROPERTIES	ASPHALT BINDER		
	STYRELF 13	IRVING AC	LATEX Modified
% Asphalt by wt. of mix	5.10	5.46	4.75
Bulk S.G. of Mixture	2.41	2.39	2.43
Bulk S.G. of Aggregate	2.71	2.71	2.71
VMA	15.50	16.20	14.76
% Air Void	3.5	3.6	3.5
Marshall Stability (kN)	18.06	13.23	14.30
Flow	11.0	12.0	11.5

Table 4: Summary of Moisture Damage Procedure (After NCHRP 246)

Specimen Size	Height = 63.5 mm Diameter = 102 mm
No. of Specimens	3 wet 3 dry
Air Void Range	3% to 5%
Vacuum Conditioning (Wet specimens)	- soak under vacuum of 660 mm Hg for 30 min - 30 min soaking without vacuum
Moisture Conditioning (Wet Specimens)	- 15 hrs freezing at -8°C - 24 hrs static soaking at 60°C - 3 hrs static soaking at 25°C
Damage Evaluation	- MR testing at 25°C - Tensile strength testing at 25°C and rate of 50.8 mm/min

Table 5: Results of Resilient Modulus Testing

Temperature (°C)	IRVING AC (MPa)		LATEX Modified (MPa)		STRYLF 13 (MPa)	
	1 Hz	.33 Hz	1 Hz	.33 Hz	1 Hz	.33 Hz
-15	11400	10400	10000	9000	13100	12400
0	8970	8150	8250	7500	11700	10860
20	1035	980	1500	1300	2900	2400
44	276	241	450	300	1035	900

Table 6: Results of Moisture Damage Testing

Binder Type	Mr (MPa)		Ratio	Tensile Strength (MPa)		Ratio
	Dry	Wet		Dry	Wet	
IRVING AC	1270	610	0.48	475	410	0.86
LATEX Modified	1500	800	0.53	610	500	0.82
STYRELF 13	3850	2800	0.72	1110	1100	0.99

On Adhesive Layer of Thin Concrete Block Overlay

M. Inuzuka, Hokkaido Institute of Technology

ON ADHESIVE LAYER OF THIN CONCRETE BLOCK OVERLAY

by

Masao Inuzuka, Hokkaido Institute of Technology

ABSTRACT

Various means to prevent skidding in winter are to worsen the damage and the deterioration of the asphalt pavements. Concrete blocks which are stronger than asphalt may solve the problems, covering the asphalt pavements. These blocks can enhance the aesthetic value of the pavements. These are also able to shorten the term of works at the site as well as the closing of the road, reducing the cost depending on the conditions. However, the conventional concrete blocks have faults such as the difficulty to mend the surface abrasion or the vulnerability to deformation due to the frost heave. This report centers on the overlay method with blocks which should be as thin as possible in given conditions. Blocks are to be laid on the thin adhesive layer of asphalt. The thickness of a block can be reduced with the block length shortened. The lessened blocks become unstable and vulnerable to stripping and moving, since the blocks are light and weak for restraining the adjacent ones. For stabilization, these blocks have to adhere to the asphalt road which governs the bearing capacity. The aptness of adhesive means is a key to the success of the thin block overlay. Mechanical conditions of the adhesive layer are discussed under the assumption that the blocks are rigid. The adhesion of asphalt can be obtained by heating. A good choice for a heating method can enhance the efficiency of the work and the serviceability of the pavement.

ON ADHESIVE LAYER OF THIN CONCRETE BLOCK OVERLAY

by

Masao Inuzuka, Hokkaido Institute of Technology

1/INTRODUCTION

Rapid increase in automobiles in our daily life accelerates the exacerbation of some roadproblems specific to a cold region --- roads are subjected to damages due to metal chains or other means to prevent skidding on a frozen road in winter. Roads are affected also by the frost heave or the thermal expansion. Being appropriate to bear the weight of automobiles and to distribute it underneath in such an environment, the asphalt pavements prevails mostly in a cold region. The asphalt pavements, however, have problems. Especially the rutting one is urgent to be solved. This problem has various causes. Main cause may be that the asphalt is subjected directly to wheels and exposed to the outside air. On the other hand, there are many kinds of concrete which are much stronger and more durable than asphalt. The concrete is particularly resistive to abrasion and high temperatures, although its deformation capacity is limited. Therefore it is suitable to cover asphalt for protection. The overlay with thin blocks of appropriate concrete may be a solution.

2/THIN CONCRETE BLOCKS

Each layer between the surface and the base responds to loading differently according to a combination of physical properties and geometrical conditions. When a concrete slab is subjected to wheel loading and temperature changes, the internal stresses can be given from the ratio between the maximum length and the thickness, particularly when the slab is placed on a soft

ground of lower base coefficient.Ref.1)
When the objective of surface concrete is to protect the asphalt underneath, the size of a block can be small only to reduce the internal stress and the width of a joint between slabs can be fine for thermal expansion. Ref.2) A concrete block is a concrete slab whose maximum length is made as short as possible, so far as the block functions. Blocks are normally prefabricated in a factory. Occasionally these are produced in the site, placing concrete and joint lines are notched in order to avoid the adverse cracks. The surface concrete, which has a thickness less than 60mm and is stabilized by adhesion not by the self weight, is to be analyzed as the thin concrete block. In so far as the base condition is identical, the smaller block is stronger to damage due to loading and temperature changes. The smaller the size , the stronger the block mechanically since the internal stress is reduced. On the other hand, the conventional practice has experienced the cost rise with the block size reduced. This is because the size for the mechanical unit cannot be independent from the size for the working unit. Turning over the illusion, the thin concrete blocks become practicable. Blocks , the size of which are reduced, can be connected to one another in order to enlarge the working unit. There are ways such as connecting blocks with a net and introducing notches in a block like a chocolate bar.
A mechanical problem of small sized blocks is how to stabilize these at initial positions. In the conventional concrete block practice, the sand has played the stabilizing role in joints and on the base. Subjected to pressure and the shear stress, the sand pushed into a joint can transmit the force to the adjacent block. When a block is to be raised, other blocks nearby are also raised in accordance, which can prevent each to be raised independently. The conventional concrete blocks have tendency to move because of the repetition of freeze and thaw of water absorbed in the sand underneath.
Two main functions required to concrete blocks as the protective layer are one to reduce the amplitude of temperature

variation and the other to strengthen the surface.

A. ALLEVIATION TO TEMPERATURE VARIATION The maximum amplitude of temperature variation of the naked asphalt near the surface can get to 50 degree Celsius in one day according to the record in Sapporo. It could be between 20 d. and 70 d. in summer and between -15 d. and 35 d. in winter. Ref.3) Since the highest temperatures in asphalt is found within several millimeters from the exposed surface, the concrete blocks can be protective against the thermal flow and the thermal stress , alleviating the temperature variation thanks to their reflex and high conductivity. The thicker , the more effective.

B. SURFACE STRENGTHENING Strengthened binders and appropriate aggregates in any concrete ,whether it is of cement or of asphalt, can improve the abrasive resistance and other physical properties. Prefabrication in the factories is advantageous for strengthening binders to improve the concrete. The concrete block overlay in which the joints are filled with asphalt may be taken as the asphaltic concrete of special aggregates of blocks with much less asphalt compared with the ordinary asphalt concrete mixture. Consequently the thickness of the overlay may be added to the the thickness of the asphalt pavement.

3/FRACTURE AND DEFORMATION OF ADHESIVE LAYER

The progression of fracture and deformation of blocks depends on geometric conditions of the adhesive layer, which are given by the site conditions and the construction procedures. These conditions are interwoven. Therefore several assumptions are introduced to simplify the conditions. The upper limits of stresses in the adhesive layer will be discussed with respect to the vertical and horizontal deformations.

3.1/VERTICAL DEFORMATION OF BLOCKS(PUSHING IN AND STRIPPING OFF)

The adhesive layer has to be strong enough to stabilize each block at a location. Ref.4) Blocks are by far stiffer than asphalt for the adhesive layer. Thus the blocks are assumed to behave as the rigid body on the layer. The layer is assumed to have no cavity and to be elastic at least for a period that a wheel passes by over a block in question. If there is a cavity in the layer under the block, the block is subjected to a bending moment, since the block spans the cavity. Then the block and the layer can be subjected to very high stresses to yield.

Under the assumptions above, the stresses and deformations are distributed in a linear equation. The upper limit of vertical stresses, q_1 and q_2, which are under the edges of the block, is to change as the contact stress p of a wheel passes by over the block, which has the length L and the width b. When the tread length a is longer than L, a diagram is shown in Figure 1 where the distance between the rear edge of the block and the front edge of the tread is the arbitrary x.

$$-\infty < x < \infty$$

When $x \leqq 0$, $q_1 = q_2 = 0$ (1)

When $0 < x \leqq L$ the sum of vertical forces on a block is zero.

$$\Sigma V = \frac{1}{2} b L (q_1 + q_2) - p b x = 0 \quad (2)$$

The equilibrium equation with respect to the moment at the center of the block is

$$\Sigma M = \frac{1}{2} (q_1 - q_2) b L (L/2 - L/3) - p b x (\frac{1}{2}L - \frac{1}{2}x) = 0 \quad (3)$$

Consequently the stresses at the both edges of the block are

$$q_1 = (p/L^2) \times (4L - 3x)$$
$$q_2 = -(p/L^2) \times (2L - 3x)$$

When $L < x \leqq a$, these stresses are constant.

$$q_1 = q_2 = p$$

When $a \leqq x \leqq L + a$,the stress q_1 is symmetrical to

$$q_2 \; : \; 0 < x \leqq L$$

with respect to $x = \frac{1}{2}(L + a)$

When $L + a \leqq x$, both return to zero.

$$q_1 = q_2 = 0$$

The variation is shown in Figure 2.
When the block length L is longer than the tread length a , the wheel load ap moves as the concentrated load around the block center

$$a \leqq x \leqq L$$

Thus both are in a linear equation in Figure which shows that the stress in the adhesive layer changes as a quasi-periodical equation for the maximum compressive stress to be 4/3 of the contact pressure p and for the maximum tensile stress to be 1/3 of the pressure p.

3.2/HORIZONTAL DEFORMATION OF BLOCKS

Blocks are subjected to the horizontal force of a wheel when a car stops or accelerates. When the surface of the overlay is plane, the excessive horizontal stress due to the impact of a wheel against the projection will not take place. The horizontal force can be derived from the friction coefficient and the wheel load. If the joints are fully filled up with asphalt or other materials, the force can be transmitted and dispersed to other blocks. Since the shear strength of asphaltic material is low, the distribution is the important function for the adhesive layer. The narrower the width of joints, the more effective to disperse the horizontal force, since the joints get stiffer. The most effective joints is the hair cracks caused after blocks are placed at the designed location, because these are fine. Therefore it is efficacious to arrange blocks with their sides directly contact to one another or to have the blocks properly cracked along the planned lines in order to disperse the horizontal force reducing the bending moment applied to blocks. It is also efficient to have curved joint lines for dispersing the horizontal force. The blocks , shaped as such, are called the interlocking blocks.

3.3/CHARACTERISTICS OF ASPHALTIC ADHESIVE LAYER

The stresses in the adhesive layer are governed by the wheel load and the geometrical conditions of blocks. The thinner , the less the deformation of the adhesive layer. Besides, a long term load, regardless of the weight, will give rise to a large scale of deformation to thick asphalt, since asphalt is viscositic. On the other hand, the tensile strength of asphalt which is around 85 of needle penetration index, is over 2 kg per sq.cm at 50 degree C for a period that a wheel passes over a block. The shear strength is also enough for a short period. Consequently the following conditions are required for the asphaltic adhesive layer.

(1)Space under blocks must be fully filled up leaving no cavity

(2)Thickness of adhesive layer must be as thin as possible

These two conditions seem to contradict to one another in the asphalt adhesive layer on an existing road which has a rough surface. Therefore asphalt is required to be thick enough and soft enough to get no cavity . Especially when the preheating is employed, thick adhesive layer is required. Otherwise the thin layer , spread on the road, can easily cooled by air, leaving cavity in asphalt.

4/CASE STUDIES OF ADHESIVE LAYERS

Many heating methods have been tried on the actual roads with respect to the adhesive layer construction. Three typical examples will be discussed in the followings. All these methods used specific resin concrete which has been developed by HOKKON Resin Development Engineering Co. Ltd.(Sapporo City). The concrete is strong to bending and showed abrasion less by 10 to 20 % than asphalt concrete. The overlay was applied to the roads which suffered from severe abrasion which was due to the studded tires forming two troughs on the roads. The objective of the overlay was to reduce the abrasion as well as the closing time of the roads under construction. Both of electrical heating used carbon fibres made of coal pitch and covered rather small area. The generator on a car was used for the electricity source.

4.1/HEATING BY COOKER

Hot asphalt heated by a cooker is spread on the existing road to form the layer. Thin blocks are laid before asphalt is cooled. This example is what is applied to a road in a tunnel. Several thin blocks are connected like a chocolate bar to make a working unit which is available as the ROAD PLATES of HOKKON Co. Ltd. Working procedures are shown in Plate 1 to Plate 4. Asphalt is heated by a cooker (Plate 1). Hot asphalt is

spread to form a layer which is about 30 mm thick and kept hot by a gas burner (Plate 2). The unit of blocks are placed on the plastic asphalt (Plate 3). Blocks are pressed by the tyre roller (Plate 4).

4.2/ELECTRIC HEATING

A prefabricated membrane of asphalt is spread on the existing road as shown in Plate 5. Blocks are laid on the membrane which has carbon fibers and the terminals made of aluminum foil. The electric generator is connected to the terminals for conducting electricity which flows through the terminals and carbon fibers. Heated asphalt sticks to the blocks and the existing surface. Time for arranging the blocks and pressing these is more flexible in this method than in the previous. Therefore the adhesion is more reliable. The problem is how to economically distribute carbon fibers uniformly and make reliable terminals. Blocks placed in this way have shown no mechanical troubles in service for nearly a decade.

4.3/HEATING BY MAGNETRON

The asphalt membrane, similar to the previous, is prefabricated with carbon fibers inside. Blocks are laid on the membrane. Microwave is irradiated to asphalt through blocks, as shown in Plate 6. Asphalt and carbon fibers are exclusively heated to get adhesion. The frequency is 2.4 GHz, which is only one band open to the private use in Japan. Asphalt which is heated and molten quickly under the blocks become a layer as it cools. Since there is no restriction on the terminals, the arbitrary locations can be heated for both the construction and the destruction in the same manner. The present instrument was rather cumbersome to maneuver and put a barrier to prevent a wave leakage.

5/CONCLUSION

Asphalt has been used for years from many reasons in a cold region. The surface is subjected to damages, deterioration and rutting. The temperature changes and the skid preventing means account for the adverse. Concrete blocks are to be a protective layer for the asphalt pavements. These are accompanied with not only the solution as such but also the brighter surface and the shortened construction. What is proposed may seem utterly different from the conventional pavements. However the scrutiny shows that thin blocks are on the extension of the conventional asphalt pavements. The difference is the geometrical condition of aggregates. Blocks are artificial and much bigger and more uniform than those in asphalt concrete. On the other hand, it is also possible to take it as a concrete slab which is fully processed with cracks which are uniform and of a specific shape in order to prevent the serious destruction. A larger working unit is compatible with a smaller mechanical unit, as a chocolate bar shows it.
In order to minimize the thickness of blocks under working conditions, the adhesion to blocks has to be employed. The tensile strength over 2 kg per sq.cm seems more than enough. Destruction and stripping of blocks are due to faults of the adhesive layer. Comments concerned are as follows;
(1)The destruction of blocks is due to cavities in the adhesive layer, followed by stripping, since the blocks above the cavities are subjected to the bending moment and the punching shear.
(2)The sizable undulation on the block surface will cause the impact loading against the salient of a block. Pressed asphalt will be evacuated on account of the impact, moving to other locations. When the undulation is accompanied with an adhesive layer too thick or too uneven, the undulation will be enlarged only to destruct the salient by a wheel.
(3)Block stripping takes place mostly in winter, although the tensile strength of the adhesive asphalt is higher at colder temperatures. The rate of stripped blocks seems higher at

colder temperatures. The cracks appear all the year through. The advantages of adhesive asphalt at higher temperatures are the larger ultimate strain and the recuperability.

There are many good points in making use of the thermal plasticity of asphalt for the adhesive layer. The choice of heating is closely related to the construction speed and the strength of the products. A preheating method by a cooker and two methods of electrical energy have been tried so far. The cooker method needs no special instruments except a cooker, but the skillful workers are inevitable to produce a strong overlay. The electrical methods are able to produce a reliable adhesion even by unskilled workers. The electrical heating is suitable for producing the original layer, since no complicated machines are required except a generator. The microwave method is suitable for the maintenance, since any portion of the adhesive layer can be heated easily.

REFERENCES

1) M.Inuzuka. On Precast Block Overlay.
Proc.of JCA Vol.37 (pp537-540) .1983

2) M.Inuzuka & I.Sato. Concrete Block Pavements on Asphalt Highways . Concrete Block Paving.
Proc. of 2nd Int.Conf.(pp322-329) .1984

3) M.Inuzuka. On Thin Block Overlay .
Proc.of JCA Vol.38 (pp505-508) .1984

4) M.Inuzuka & I.Sato. Adhesive Layer for Overlay with Thin Concrete Blocks. PICA Proc. of 3rd ,Canada/Japan Workshop(Vol.1). (pp525-540) .1987

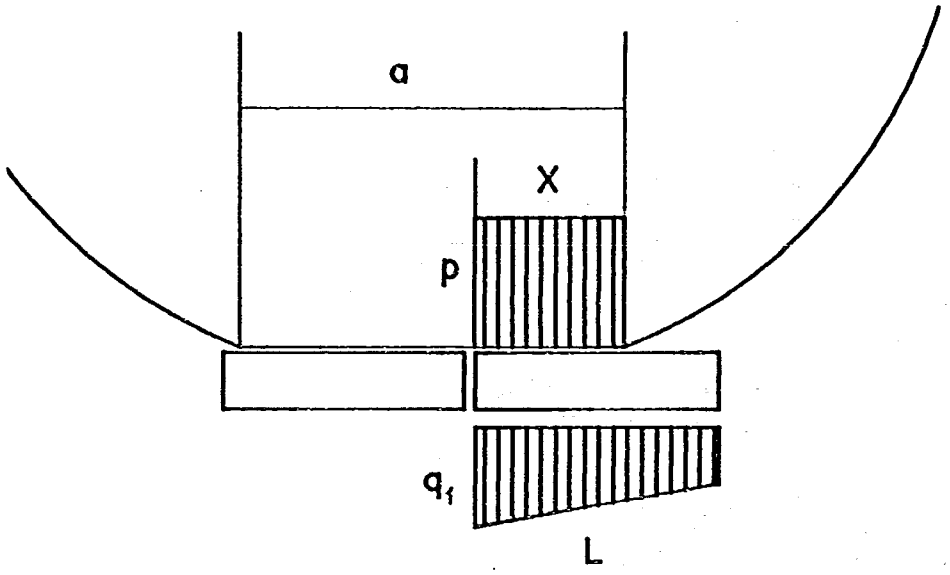


Figure 1.STRESS DISTRIBUTION UNDER THIN BLOCK AND WHEEL LOAD

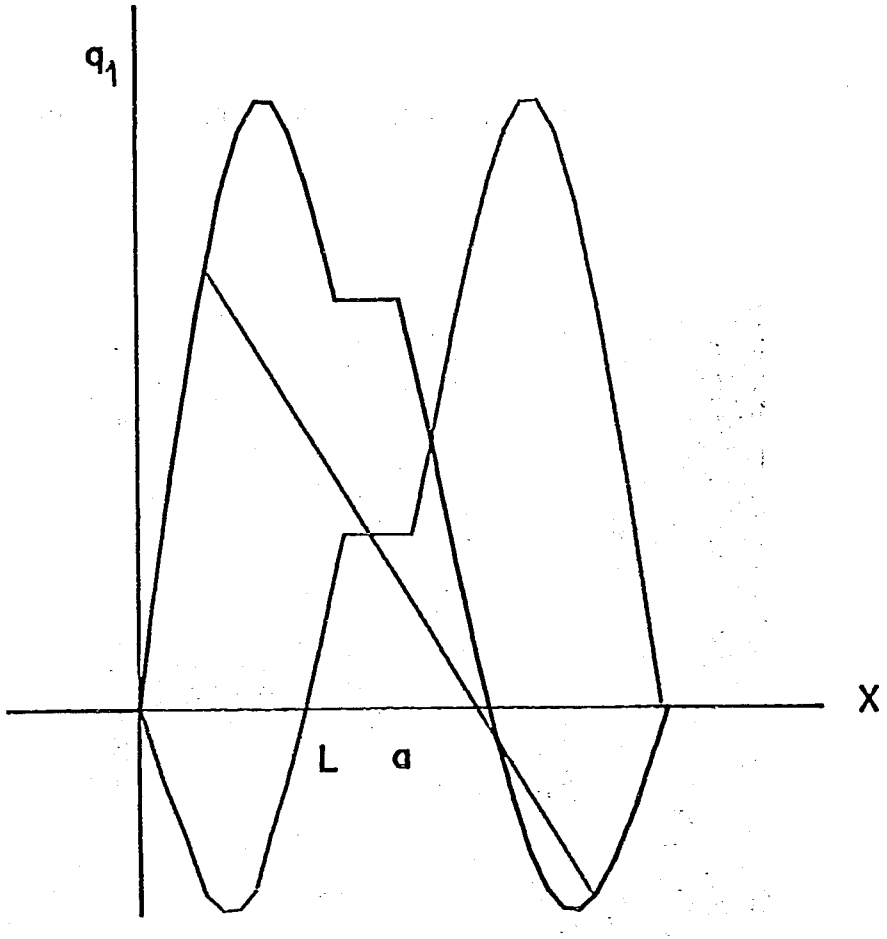


FIGURE 2.VARIATION OF END STRESS AND WHEEL LOAD

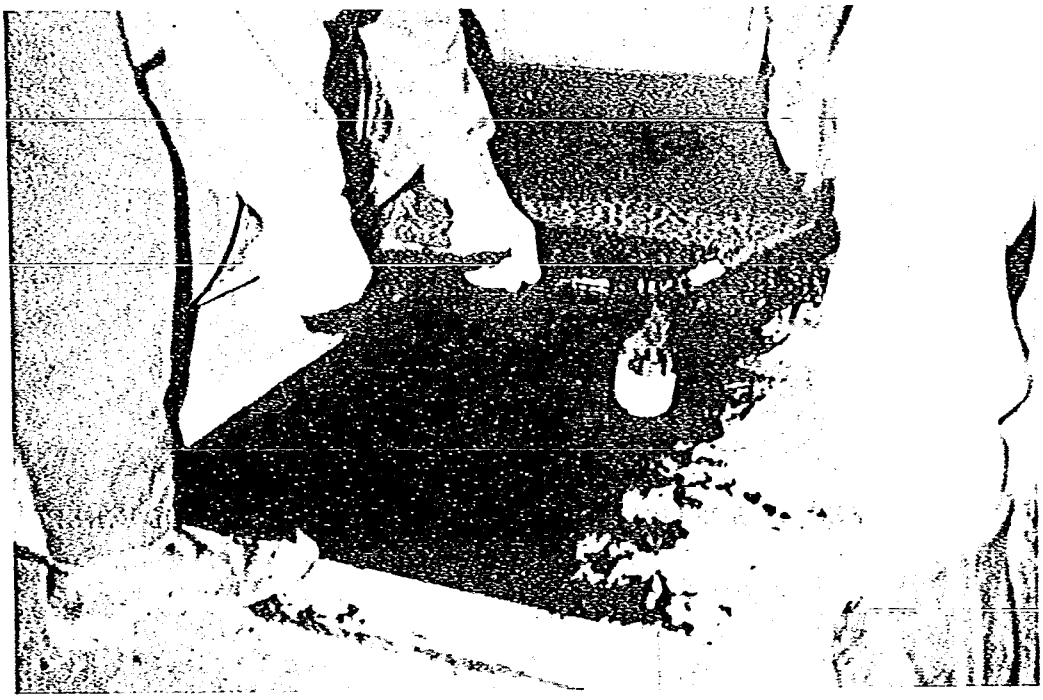


PLATE 1.SPREADING WORK OF ASPHALT

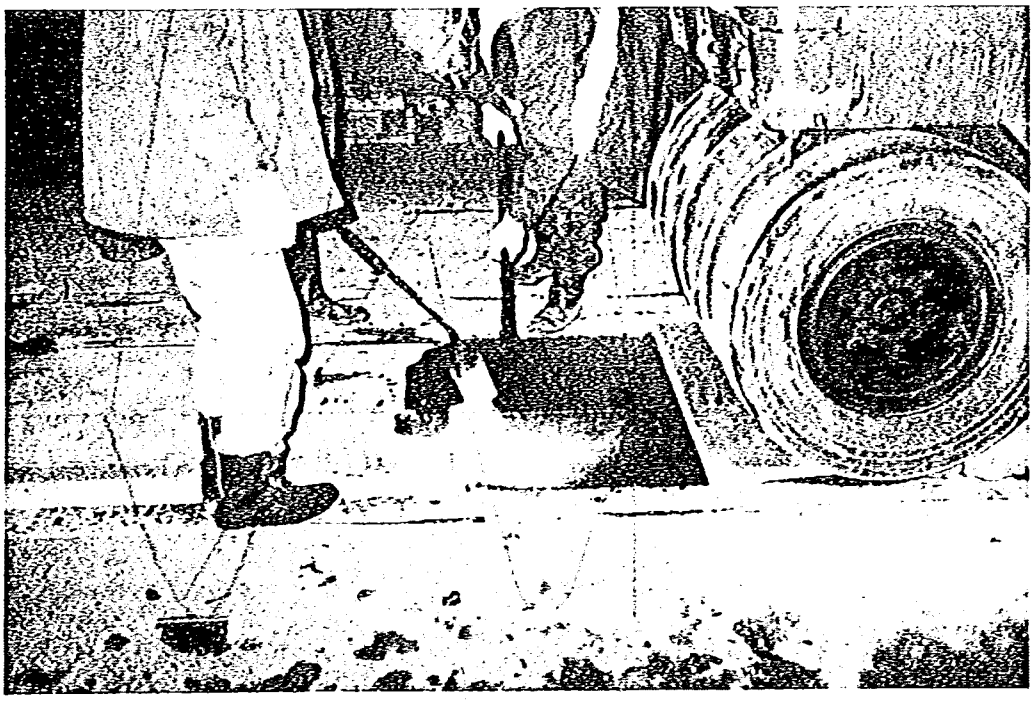


PLATE 2.BURNER HEATING OF SPREAD ASPHALT

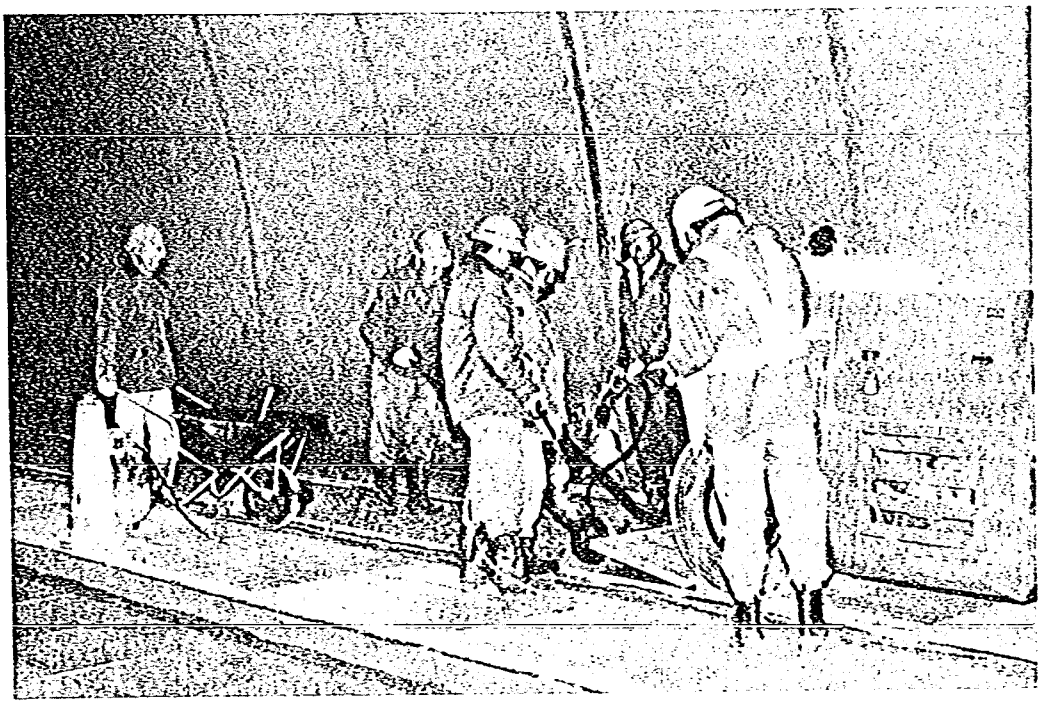


PLATE 3.LAYING WORK OF BLOCKS ON ADHESIVE LAYER

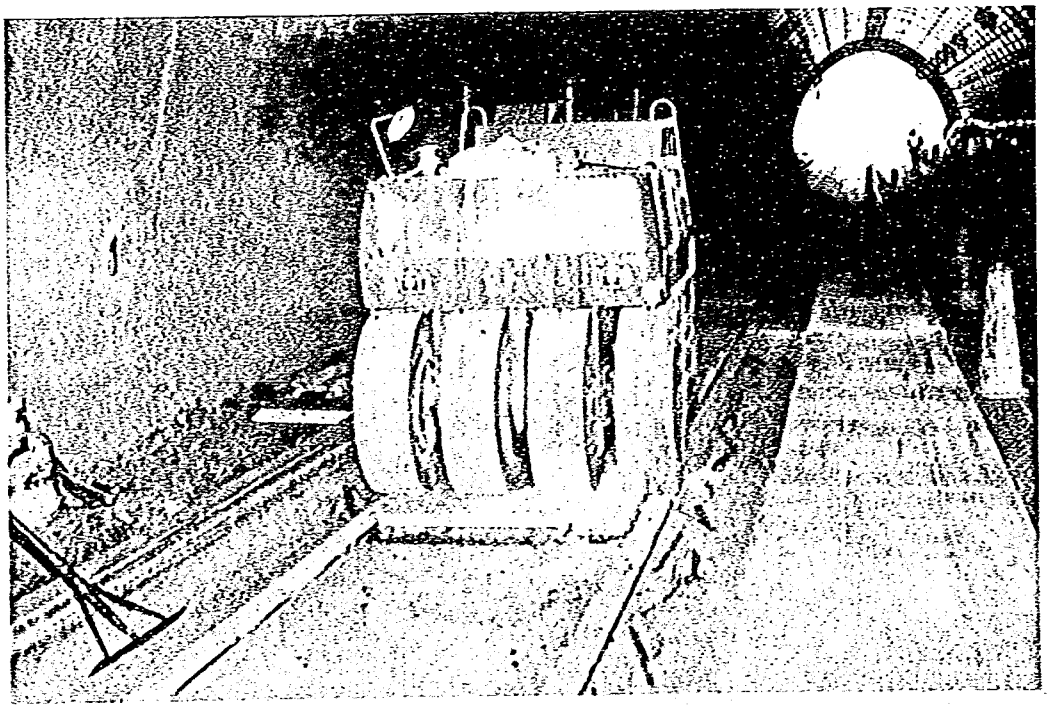


PLATE 4.BLOCK PRESSING BY TYRE ROLLER

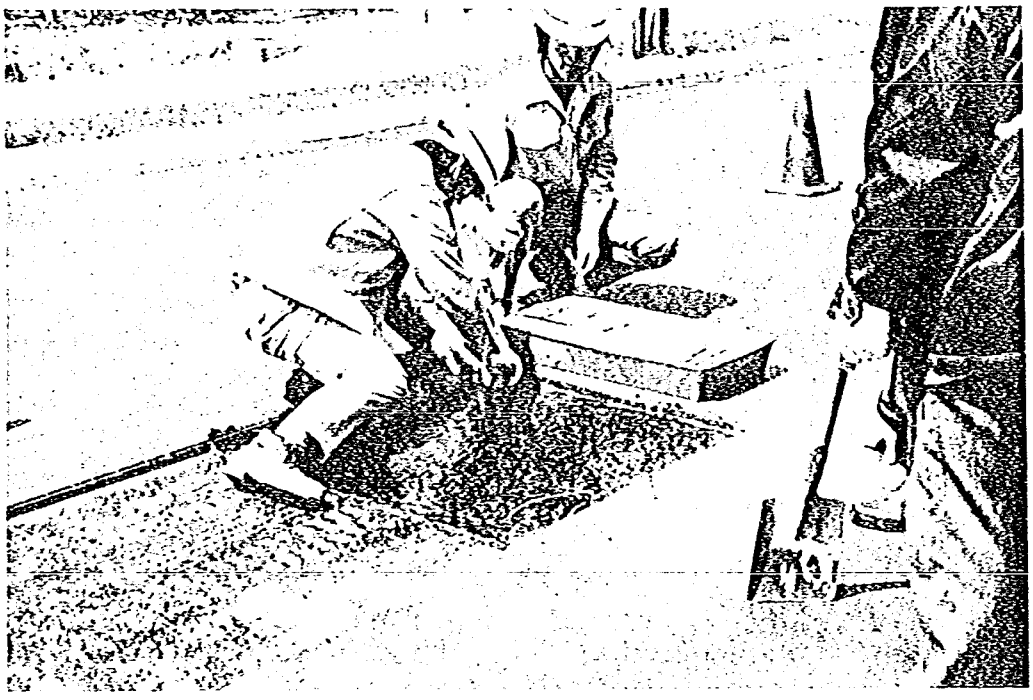


PLATE 5.SPREADING WORK OF ASPHALT MEMBRANE FOR ELECTRIC HEATING



PLATE 6.HEATING WORK OF MICROWAVE EMITTER

Silane Coupling Agents to Reduce Moisture Susceptibility of Asphalt Concrete

D. Stolle, McMaster Univ.
J. Emery, JEGEL
G. Kennepohl, Ministry of Transportation, Ontario

SILANE COUPLING AGENTS TO REDUCE MOISTURE SUSCEPTIBILITY OF ASPHALT CONCRETE

by

DIETER F.E. STOLLE
Associate Professor, Department of Civil Engineering
McMaster University, Hamilton, Ontario, Canada L8S 4L7

GERHARD KENNEPOHL
Research and Development Branch, Ministry of Transportation
Downsview, Ontario, Canada M3M 1J8

and

J.J. EMERY
President, John Emery Geotechnical Engineering Limited
Downsview, Ontario, Canada M3J 1Z5

ABSTRACT

This paper describes a study at McMaster University which addressed the effectiveness of silane coupling agents as antistripping agents and their influence on the fatigue properties of asphalt concrete.

The main conclusions of the study are:

1. based on the Japanese Petroleum Institute (JPI) test, treatment of aggregates with silanes improves the compatibility between siliceous aggregates and asphalt cement;
2. based on the JPI test, surface treatment of coarse aggregates with a silane is more effective than the use of a silane as an asphalt cement additive;
3. Pavebond A.P. and hydrated lime are more effective in improving resistance to stripping than the silane coupling agents;
4. Pavebond A.P. and silane coupling agents reduce the tensile strength of air-cured asphalt concrete - both antistripping agents 'appear' to partially inhibit the development of strong asphalt cement-aggregate bonds; and
5. owing to a reduction in tensile strength, an asphalt concrete containing Pavebond A.P. or a silane coupling agent has a shorter fatigue life than an asphalt concrete containing hydrated lime or no additive.

Since silanes appear to reduce the tensile strength of asphalt concrete, their use as an antistripping agent is not recommended.

SILANE COUPLING AGENTS TO REDUCE MOISTURE SUSCEPTIBILITY OF ASPHALT CONCRETE

1.0 INTRODUCTION

1.1 General

Moisture damage to asphalt concrete is regarded as a serious problem which is often responsible for the premature deterioration of asphalt pavements. The deterioration generally results in decreased serviceability and fatigue life, and increased maintenance and rehabilitation costs. A common procedure for improving an asphalt concrete's durability with respect to moisture damage is the addition of an antistripping agent to the mix. This paper describes a research project, completed for the Ministry of Transportation of Ontario (MTO), which evaluated the effectiveness of silane coupling agents for improving the asphalt cement-aggregate bond and reducing the moisture susceptibility of asphalt concrete [1].

There are two basic forms of moisture damage [2]: Stripping which involves a separation of the asphalt cement from the aggregate due to the presence of water; and softening of the asphalt cement which is responsible for an overall loss of asphalt concrete stability. Although emphasis in this study was on stripping, it should be kept in mind that the moisture susceptibility tests, carried out do not necessarily distinguish the damage caused by stripping from that due to softening.

1.2 Objectives and Scope

This study was motivated by the reported favourable performance of silane coupling agents as antistripping agents [3,4,5,6] and experimental results which suggest that these agents may also improve resistance to cracking [6] which is related to fatigue failure. The Highway Materials Laboratory at McMaster University coordinated the research program and implemented the experimental phase. John Emery Geotechnical Engineering Limited (JEGEL), as a sub-consultant, completed a literature review [7] and provided some technical assistance for completing the project. ORTECH International, as a subconsultant, selected suitable silanes for the experimental phase of this study [8]. The full reports prepared by JEGEL and ORTECH are provided in the full technical report submitted to the MTO [1].

The main objective of the research was to evaluate the effectiveness of silane coupling agents for improving asphalt pavement durability against stripping and for extending fatigue life. The study involved the following:

1. preparing a synthesis from the current practice and literature on stripping and the use of silane coupling agents for reducing stripping (JEGEL);
2. selecting suitable silanes which are compatible with asphalt cement (ORTECH);
3. evaluating the compatibility between asphalt cement and various Ontario aggregates in the presence of antistripping agents using an immersion test;
4. evaluating retained Marshall stability of asphalt concrete mixes where aggregate source and antistripping agent are variables;
5. evaluating fatigue performance of asphalt concrete mixes where aggregate source and antistripping agent are variables; and
6. summarizing the study findings and making recommendations regarding feasibility of silanes as antistripping agents for asphalt concrete manufactured in Ontario.

2.0 LITERATURE REVIEW

2.1 General

Stripping involves complex processes which are still not fully understood. Several factors influence the sensitivity of an asphalt concrete mix to stripping: chemical and physical properties of the asphalt cement and aggregate; compacted mix characteristics such as voids mineral aggregate (VMA) and air void content; type and volume of traffic; climatic conditions; and the nature of the base [10,11,12]. For stripping to occur, free water must be present and available internally to the asphalt mix.

Most often stripping is related to aggregate properties. Carbonate aggregates that have dust free surfaces tend to have a better resistance to moisture damage than aggregates which have a high silica content [10,13]. Although emphasis is most often placed on the stripping of coarse aggregate, the sensitivity of moisture damage to the properties of the fine aggregate must also be considered [3]. In Ontario the stripping problem tends to be regional with the most severe cases reported in the Kingston and northern areas where noncarbonate aggregates such

as granite are used [10,12]. No simple correlation between aggregate and asphalt cement chemistries have been established to date [14,15].

It is important to recognize that an asphalt mixture may still be susceptible to moisture damage even though all mix components may be chemically and electrostatically compatible [16]. In order to provide the most effective resistance to such damage, good mix designs involving compatible materials, good construction procedure and quality control, and proper drainage under the pavement structure are required [4,13]. More information on the factors influencing moisture damage are given in the References [7,10,11,13,17].

2.2 Signs of Stripping-Related Distress

Although the moisture deterioration of a pavement structure may develop from the top downward, stripping usually starts in the binder coarse [12,13]. It has been found that the damage usually progresses well into the pavement structure before excessive stripping of the coarse aggregate at the bottom, where the damage is usually the severest, is observed [12]. Since the pavement structure is weakened, further damage due to traffic loading accelerates the pavement deterioration. The damage often appears as flushing or bleeding, along with rutting and shoving of the asphalt [12,18,19]. In Ontario, stripping has also been highly correlated to random cracking [12].

2.3 Techniques for Improving Resistance to Moisture Damage

As indicated, resistance to moisture damage requires the use of good materials and appropriate mix designs, and proper construction procedures. The VMA should be high enough to provide sufficient binder coating of the aggregate and the air void content should be low enough (2-5%) to ensure a dense mix which adequately resists the penetration of moisture into the asphalt pavement. In regions where good quality aggregates are not available, it is common to use anti-stripping additives to help reduce stripping.

Antistripping agents are usually either applied directly to the aggregate surface or are introduced as an additive to the asphalt cement. Direct application to the aggregate surface has the benefit of concentrating the agent where the problem exists. On the other hand the addition of chemical additives to asphalt cement, which results in a dilution of the additive where it is required, tends to be more economical.

Many of the commercial chemical additives are based on fatty amines which are surface active compounds [20]. Although these additives improve initial aggregate coating, problems have been identified with some additives including: low heat stability; tendency to promote emulsification which can accelerate stripping at a later stage; and modification of bitumen properties yielding other adverse effects [14,20]. It has also been suggested that the additive and the asphalt cement may in some cases compete for the same adsorption sites on the aggregate surface, thereby reducing the effectiveness of the strong aggregate-attracting asphalt components [3] and, ultimately, the shear strength at the interface [17].

The effectiveness of an antistripping agent depends on the source of aggregate and asphalt cement [4,18]. The most successful antistripping agent for promoting bonding appears to be hydrated lime [4,21]. Hydrated lime performs best when applied in a slurry form as a surface treatment to the aggregate. Unfortunately this application procedure tends to be uneconomical. Although hydrated lime may also be added as a filler, it is not as effective [21]. The amount of hydrated lime required for treatment usually varies between 1-2.5% by weight of aggregate being treated. Fine aggregates, which have greater surface areas, may require more lime. Chemical additives, on the other hand are usually introduced at concentrations of 0.3-1.0% by weight of asphalt cement.

2.4 Silane Coupling Agents

Another class of antistripping agents, which appears to have performed well in research laboratories, are silane coupling agents [3,4,5,6]. JEGEL [7] reported 13 patents dealing with silane coupling agents. Although positive benefits through the use of silanes have been reported, the literature survey [7] revealed mixed results in terms of stripping resistance. In general, it has been found that silanes are not effective for all aggregate types. Sanderson's study [3], for example, demonstrated that methylchlorosilanes can have adverse effects when used with carbonate aggregates.

3.0 LABORATORY TESTING PROGRAMME

3.1 General

Owing to the apparent success of silane coupling agents, an experimental program was undertaken to determine if silane coupling agents could inhibit the stripping of asphalt concrete containing Ontario aggregates, and to confirm the claim made by Anzaki and Ikeda [6] that silanes may improve the fatigue life of asphalt concrete.

The experimental program consisted of investigating:

1. bonding of asphalt cement to aggregate in the presence of a silane coupling agent using the Japanese Petroleum Institute (JPI) stripping test;
2. retained strength of asphalt mixtures containing a silane coupling agent using the the Immersion-Marshall test; and
3. fatigue life of asphalt mixtures containing a silane coupling agent using the a repeated-load indirect tensile test.

At each stage of the experimental program the behaviour of specimens containing a silane coupling agent was compared to that of control specimens which contained no additive, hydrated lime or a commercially available amine-based antistripping agent. This approach allowed the results to be interpreted within a wider context than would have been possible if testing had been completed on the silane-treated mixtures alone.

3.2 Specimen Preparation

3.2.1 Raw Materials

(a) Aggregates

Since the effectiveness of an antistripping agent depends on aggregate surface properties and mineralogy, coarse aggregates from five separate sources were used in the testing program. This allowed taking into account the influence that coarse aggregate mineralogy could have on the results. A list of the aggregates used for this study is given in Table 1. The aggregates from Sources A to D were identified by JEGEL and MTO as aggregates with stripping problems. The aggregate from Source E, which was selected as a control aggregate, is a high quality carbonate which was assumed to have a chemistry favourable for developing a good asphalt cement aggregate bond. A standard sieve analysis (ASTM C-136) was performed on each aggregate.

During the testing program it was found that the fine aggregate component of the asphalt concrete had an important effect on the retained Immersion-Marshall stabilities. As a result, fine aggregate from two separate sources, also given in Table 1, were used for the Immersion-Marshall phase of the testing program. Both fine aggregates are used commercially in asphalt concrete mixes.

The combined gradation of the fine (FA) plus coarse aggregates (65/35 proportion) used for the tests on the compacted asphalt concrete are shown in Figure 1. Owing to the gradation of Aggregates A and D, it was not possible to meet the HL4 gradation limits at the 12.5 mm sieve. Since the experimental program was of a comparative nature, it was decided that the small deviation from specifications was acceptable. It was felt that crushing the coarse aggregate to force the combined gradation to meet specifications could have introduced an additional variable into the testing program; i.e. freshly fractured surfaces may be more susceptible to moisture damage than aged surfaces. Aggregate C was only used for the JPI test since its gradation was not suitable for preparing Marshall briquettes. This aggregate did not display any stripping during the Japanese Petroleum Institute test.

Coarse aggregates A and E together with the Campbellville fine aggregate (FA) were used for the fatigue testing program. Aggregate A was chosen since it represented an acidic aggregate for which the silanes should have been the most effective for promoting bonding. Aggregate E was used since it represented both a 'basic' aggregate and the control aggregate.

(b) Asphalt Cement

The main asphalt cement used for this study was a nonblended refinery vacuum tower bottoms asphalt cement which was obtained from Petro-Canada. During the Immersion-Marshall testing phase several specimens were also made using an asphalt cement which was obtained from the storage tank of a local asphalt batch plant. The reason for using this alternative source was to provide additional data on the influence of the stripping agents on retained Marshall stabilities.

(c) Additives

The list of the additives used for this study and their suppliers is presented in Table 2. Hydrated lime was chosen as a control additive because of the well-

documented success of this additive for improving the resistance of an asphalt mixture to stripping [7]. Pavebond A.P., an amine-based, heat-stable additive, was used in order to compare the behaviour of the silane-treated mixtures to that of asphalt mixtures containing a commercially available, MTO approved additive. Since there are hundreds of silanes which are commercially available, ORTECH was contracted to provide a short list of silanes which would be suitable as coupling agents in asphalt concrete mixtures.

Of the five silanes which were recommended, the three which were used for the experimental program include:

(a) Glymo, an epoxy silane which was also used in the Anzaki and Ikeda [6] study;

(b) Damo, a silane coupling agent containing an amine group which has been patented as an aggregate pretreatment additive [3];

(c) Octeo, a silane coupling agent which was selected for this study on the basis of solution compatibility with asphalt cement.

Since silanes are regarded as mild to severe eye, skin and inhalation irritants, protective mask, gloves and clothing were worn when working with these chemicals.

3.2.2 Proportioning and Specimen Manufacture

(a) Japanese Petroleum Institute (JPI) Test

The Japanese Petroleum Institute (JPI) test [6], was used to determine the compatibility of the Bow river asphalt cement with the various aggregates in the presence of the antistripping agents. This test was chosen since it was considered to be simple and quick to perform, yet sensitive enough to provide information on the compatibility between an asphalt cement and aggregate. All specimens for this test consisted of 10 mm nominal size coarse aggregates which were coated with 5.5 percent, by weight, asphalt cement. In addition to studying the effect of the antistripping agents on the aggregates, the JPI test was also performed using asphalt-coated glass microscope slides. The pretreated hot slides were coated with 0.05 mm of asphalt cement as described in Reference 14.

The additives were introduced as follows:

i) Hydrated Lime - one percent hydrated lime (by weight of aggregate) was applied directly to the surface of the coarse aggregates in the form of a

slurry, which consisted of 30 percent hydrated lime and 70 percent water, as recommended in Reference 21. The treated aggregate was subsequently allowed to dry in an electric oven at 43°C for 24 hours before being coated with asphalt cement.

ii) Pavebond A.P. - this additive was mixed directly into the asphalt cement (AC) at one percent (by weight of AC) as recommended by the supplier.

iii) Silanes - the silanes were used to pretreat the aggregates at room temperature via a silane-water solution. Two silane-in-water solution concentrations were used, namely 0.5 and 1.0 percent. Each aggregate was soaked in a fresh silane solution for approximately 10 minutes to ensure proper coating of the aggregate and then was placed in an electric oven set at 43°C for 24 hours to dry. It should be noted that the Glymo and Octeo required a pH adjustment of the solution to ensure solution stability [1,7]. In addition to using the silanes as an aggregate pretreatment, they were also tested as an asphalt cement additive. The silanes were added, for this group of tests, in concentrations of 0.45 and 0.9 percent (by weight of asphalt cement) directly into the hot asphalt cement.

(b) Immersion-Marshall and Fatigue Specimens

A standard mix design was used for manufacturing all specimens. Each specimen contained 5.5% (by weight of aggregate) asphalt cement. The ratio of coarse to fine aggregate was 35/65. Specimens were manufactured according to MTO LS-281 and LS-283 procedures for Immersion-Marshall and regular Marshall briquettes, respectively. When manufacturing the regular Marshall briquettes, which were used for the fatigue tests, the last three compaction blows were completed using a nonbevelled head to ensure that both faces were parallel.

When using the hydrated lime, only the coarse aggregate was pretreated. The lime and Pavebond A.P. concentrations for the asphalt briquette manufacture were one percent by weight of coarse aggregate and one percent by weight of asphalt cement, respectively. For most specimens incorporating silanes, only the coarse aggregate was pretreated with a 3 percent (by weight of coarse aggregate) silane solution which was prepared at a 1 percent silane concentration. Two sets of specimens were manufactured where the fine aggregate was also pretreated with 3 and 9 percent, by weight of fine aggregate, silane solutions. One set of specimens was manufactured with 1 percent (by weight of asphalt cement) Damo being added to the asphalt cement rather than to the aggregate surface. All

aggregates, were placed in the oven at 155°C for 24 hours before samples were manufactured.

3.3 Test Procedures

3.3.1 Japanese Petroleum Institute (JPI) Test

As indicated previously, the Japanese Petroleum Institute procedure was adopted for this study for determining the compatibility of the asphalt cement and coarse aggregate. As with other static immersion tests, the procedure involves immersing the samples of coated aggregated in hot water for a predefined period of time, and then evaluating the nature of the coating after this period. It was found that the JPI test was simple and quick to perform. The definitions of the patterns for stripping classification are shown in Figure 2. It should be noted that the JPI test was carried out in both fresh water and salt water environments.

3.3.2 Immersion-Marshall Testing

The Immersion-Marshall test was carried out following MTO LS-283 procedures. In addition to determining the retained stabilities, a visual rating of the fractured failure surface of all specimens was carried out. The Immersion-Marshall test was selected for studying resistance to stripping, rather than an advanced indirect tensile test [22,23] due to good experience with this test in Ontario; see e.g. Reference 24.

3.3.3 Fatigue Testing

After manufacturing the 100 mm diameter briquettes, they were stored overnight at room temperature in the laboratory before being tested on the following day using an indirect tensile stress loading configuration [25,26]. The indirect tensile tests were performed using a MTS closed-loop servo-controlled hydraulic ram system. Testing was completed in two stages for each mix:

1. Three samples were statically broken using the displacement control ram mode in order to establish the average tensile strength. The displacement rate of the loading ram was 50 mm/minute.
2. Samples were then failed under cyclic loading with the same support conditions as used for the static tests, see Figure 3. A load control mode, using a compressive haversine wave at a frequency of 1 Hz, was required to maintain uniform cyclic loading. Specimens were failed in fatigue using either 15 or 30 percent of static failure strength load level. These levels were chosen based on the fatigue life properties of asphalt mixtures

reported in Reference 26. According to Figure 14 of this Reference, the fatigue life should lie within the range 100 to 10,000 cycles, depending on the stress ratio.

Unlike the failure mode of Portland cement concrete, asphalt concrete failure is ductile. As a result, the number of cycles to failure is very sensitive to the definition of failure. In this study failure was defined as the point at which the rate of accumulated irrecoverable displacement appeared to accelerate; i.e. identified by Point A in Figure 4. At this stage of the loading history each specimen started to develop a well-defined crack along the vertical diameter of the specimen. It was found that the accumulated irrecoverable displacement at failure δ_f^P, was consistently between 1 and 1.5 mm. For each series of specimens, δ_f^P at failure appeared to be constant.

4.0 PRESENTATION OF RESULTS

4.1 General

Unless indicated otherwise, asphalt concrete mixtures were made using the Bow River asphalt cement and the Campbellville fine aggregate.

4.2 Japanese Petroleum Institute (JPI) Test

One objective, with the Japanese Petroleum Institute Test, was to evaluate the influence of silane addition technique on improving the asphalt cement-aggregate bond. The two procedures which were compared were the aggregate treatment and asphalt additive techniques. Since it was not clear at the beginning of this testing program how sensitive the stripping resistance would be to the silane concentration, it was decided to carry out the JPI Test using both 0.45 and 0.9% additive concentrations. Using the results of Reference 3, it was estimated that these concentrations would provide a silane concentration at the asphalt cement-aggregate interface of the same order as would be attained when treating the coarse aggregate with 3% (by weight of coarse aggregate) of 1 % silane solution. It should be noted that these levels of silane additive concentration are 10–20 times greater than that which was shown to be effective in Reference 4. Comparisons were made using only Aggregate A which was expected to undergo the severest stripping and for which the silanes were assumed to be most effective.

The results from the JPI test on the various aggregates and glass slides are summarized in Tables 3 and 4, respectively. It was clear from the results of this test that the silanes were better when used as an aggregate surface treatment than as an asphalt additive. In general, the silanes performed as well as, or better than, the other antistripping agents which are currently used. As anticipated, the tests which were completed in the salt water environment were more severe than those using fresh water. Both Glymo and Octeo were better than Damo which has been patented as an asphalt cement additive. The two worst aggregates for stripping were A and D which are highly siliceous. Since nontreated specimens containing Aggregates B and C did not strip, the reported moisture damage of asphalt concrete containing these aggregates must have been due to factors other than binder-aggregate incompatibility.

In order to study the effect of curing environment on the effectiveness of the antistripping agents, the JPI tests were completed on asphalt covered glass slides. One set of slides was cured at 25°C for 70 days whereas the other set was cured at 75°C for 24 hours. These tests indicated that only Damo appeared to be sensitive to the pre-test curing environment, thereby suggesting that Damo might display some instability due to an unfavourable curing environment. Except for Damo, the antistripping agents reduced stripping of asphalt cement from the glass surface. The results from a preliminary set of tests on slides, which were cured only for 24 hours at 25°C, were similar to those of Case A.

Since the surface treatment procedure appeared to reduce stripping more than the additive approach, it was decided to proceed with the rest of the experimental program using the silanes primarily as a surface treatment rather than as an additive.

4.3 Immersion-Marshall Test

Antistripping agent, and coarse and fine aggregate sources were variables in the Immersion-Marshall testing program. Representative results from this stage of the experimental program are summarized in Figures 5 and 6, and in Table 5. The results from this phase of the experimental program may be summarized as:

1. Specimens containing an antistripping agent had higher resistance to moisture damage than those containing no agent. In some cases the increase was very small.

2. Specimens containing silanes did not perform as well as those containing Pavebond A.P. or lime.
3. Pavebond A.P. appeared to be the most effective antistripping agent.
4. Asphalt concrete mixes made with the supposedly better control aggregate (E), did not have better resistance to stripping than those made using other aggregates.
5. Visual inspection of fractured surfaces revealed that the low retained stabilities of most asphalt concrete mixtures were due to the stripping of the fine aggregate and not the coarse aggregate which was treated.
6. An attempt to increase stripping resistance, by treating the fine aggregate with Damo or by adding the silane coupling agent as an asphalt additive rather than as an aggregate surface treatment, decreased the stability of the air-cured specimens by 30 percent (Figure 6). As a result 100% retained stability could only be achieved by a simultaneous reduction to air-cured strength and increase in water-cured specimen strength.
7. Although visual inspection of fractured surfaces revealed considerable fine aggregate stripping, the treatment of fine aggregate increased the Marshall stability of the water-cured specimens very little.

After having established that the fine aggregate was partially responsible for the low retained stabilities, a boiling test was carried out on this aggregate. The boiling test was not successful in revealing a stripping problem with the fine aggregate. During a subsequent series of tests, the Campbellville aggregate was replaced with an alternative fine aggregate, which is also used for commercial production of asphalt cement. The retained stabilities were not improved when the fine aggregate from Campellville was replaced by that from Aberfoyle. Owing to a limited supply of materials it was not possible to further investigate the sensitivity of retained stability to the nature of the fine aggregate or to the level of silane treatment of the fine aggregate. The retained stabilities appeared to be sensitive to the asphalt cement source. However, owing to the limited data for comparison, conclusions cannot be drawn with respect to the sensitivity of retained stability to asphalt cement source.

The results clearly indicated that silanes may not always be as effective as reported in some of the literature. The findings are, however, consistent with the observations reported in the literature. Sanderson [5], for example, observed that the measured improvement in resistance to stripping is sensitive to the coarse

aggregate type used in the test and the type of test performed. He showed that the treatment of limestone with methylchlorosilanes "increased" stripping in wash tests but decreased it in immersion compression tests. In a more recent study carried out in Germany [27], it was observed that, although silanes improved resistance to stripping, the asphalt mixture stability of some air-cured samples can be reduced when adding silane antistripping agents. Such a reduction in stability of air-cured samples was observed in this study; see, e.g. Figures 5 and 6. The reduction in strength for air-cured specimens, where the fine aggregate had also been treated was surprising since the fine aggregate is siliceous and silanes are supposed to be most effective with respect to promoting bonding between siliceous aggregates and asphalt cement. Although the reason for strength reduction is not clear, it is clear that Damo inhibited the development of a strong asphalt cement-aggregate bond.

Based on the results from this study and those reported elsewhere [7], it is clear that the effectiveness of silanes for decreasing sensitivity to moisture damage depends on the nature of all constituents of the asphalt concrete mixture. Furthermore, the use of an agent to increase stripping resistance may have adverse effects on other properties such as air-cured stability.

4.4 Fatigue Tests

For each set of specimens containing the same antistripping agent, three samples were first tested quasi-statically at a loading displacement rate of 50 mm/min, and then six samples were failed under cyclic loading; three samples were tested at each nominal fatigue level –15% and 30% of the static strength. These loading levels were selected after reviewing the results given by Adedimila and Kennedy [26] as indicated previously. Their results suggested that failure should occur between 100 and 10,000 cycles for the loading levels which were adopted for this study.

Figure 2 summarizes the results of the static tests. For both Aggregates A and E, it is clearly shown that Pavebond A.P. and the silane coupling agents reduced the indirect tensile strength of the asphalt concrete mixtures. An examination of the fractured faces indicated that less than 5% and from 10% to 25% coarse aggregate fracture was observed for specimens manufactured with Aggregates A and E, respectively. Since the primary failure mechanism was by debonding, this suggests that adhesion between the asphalt cement and aggregate was reduced

due to the presence of the additives. It is not clear whether the differences between Aggregates A and E in strength were due to chemical or physical differences between the two aggregates. It is clear, however, that a price must be paid for achieving an increase in stripping resistance; i.e. the chemical antistripping agents partially inhibit rather than promote bonding in air-cured specimens.

The results for the fatigue tests are shown in Figures 8 to 10. Figure 8 summarizes the data from all tests in terms of stress ratio versus the logarithm of the number of cycles to failure. There are two main observations which should be eluded to. First of all, the fatigue life of all mixes appeared to be similar when using stress ratio on the vertical axis. The scatter for each mixture was generally too large to allow for the detection of small differences in fatigue life due to the addition of an antistripping agent. The second important point is that the number of cycles to failure recorded in this study are considerably less than those reported in Reference 26. This is attributed to the difference in the definition for failure. In this study failure corresponds to a stage of loading where a well-defined crack developed whereas in Reference 26 failure corresponds to a complete fracture of the specimen. Owing to the loading configuration and failure mode of asphalt concrete, a failed sample may still be capable of supporting the applied cycle load. The authors prefers the definition adopted for this study, since it is based on the onset of failure.

Figures 9 and 10 summarize the fatigue data using applied maximum tensile stress on the vertical axis. This description of fatigue strength allows one to take into account the direct effect of the loading level on fatigue life. The main conclusion drawn from these figures is that both Pavebond A.P. and the silanes reduce fatigue life. The reduction in fatigue life is more severe for specimens containing Aggregate A. Silanes do not increase fatigue life as suggested in Reference 6. A close scrutiny of the data in Reference 6 indicates that the claim of increased fatigue life due to silane treatment of aggregates may have been premature since the reported improvement in fatigue life is quite small when taking into account the amount of scatter in the data of this reference.

For each test series, it was observed that fatigue failure occurred at a well-defined level of accumulated plastic deformation. This is significant from a theoretical point of view, since it suggests that it is possible to express asphalt concrete

damage in terms of accumulated plastic deformation and that failure occurs at some "unique damage level". Furthermore a comparison of the accumulated plastic deformation histories of the specimens indicates that the differences in the number of cycles to failure for specimens of the same series, at a given load level, were due to differences in the composition of each sample. It was found that, if two samples failed at approximately the same number of cycles then their deformation histories were the same. The primary mode of failure for the coarse aggregate was due to debonding.

5.0 CONCLUDING REMARKS AND RECOMMENDATIONS

This study provided a brief literature review on stripping and on the use of silane coupling agents for improving the resistance of an asphalt concrete mix to stripping. It also described a testing program which evaluated the effectiveness of silanes as antistripping agents for some Ontario aggregates, and investigated the notion that silanes may improve the fatigue life of asphalt concrete.

The main conclusions drawn from this study include:

1. based on the Japanese Petroleum Institute test, treatment of aggregates with silanes improves the compatibility between siliceous aggregates and asphalt cement;
2. surface treatment of aggregate with a silane is more effective than incorporating a silane as an asphalt cement additive;
3. Pavebond A.P. and hydrated lime are more effective in improving resistance to stripping than the silane coupling agents;
4. Pavebond A.P. and silane coupling agents reduce the tensile strength of air-cured asphalt concrete – both antistripping agents 'appear' to partially inhibit the development of strong asphalt cement-aggregate bonds; and
5. owing to a reduction in tensile strength, an asphalt concrete containing Pavebond A.P. or a silane coupling agent has a shorter fatigue life than an asphalt concrete containing lime or no additive.

It is clear from the results of this study that the treatment of the coarse aggregate alone will not bring about the desired improvement to the stripping resistance of an asphalt concrete mix if stripping is also due to the fine aggregate. It is

recommended that a fuller investigation of the effect of treating the fine aggregate with silanes be completed

REFERENCES

1. Stolle, D., Silane Coupling Agents to Reduce Moisture Susceptibility of Asphalt Concrete, MTO Project No. 211786, 1989, 1-80.
2. Roberts, F.L., and Kennedy, T.W., Application of Moisture Susceptibility Tests of Asphalt Mixtures to Design, Proceedings, Canadian Technical Asphalt Association, 1982, 259-288.
3. Divito, J.A. and Morris, G.R., Silane Pretreatment of Mineral Aggregate to Prevent Stripping, Transportation Research Board, TRR-843, 1982, 104-111.
4. Graf, P., Factors Affecting Moisture Susceptibility of Asphalt Concrete Mixes, Proceedings, Association of Asphalt Paving Technologists, 1986, 175-212.
5. Sanderson, F.C., Methylchorosilanes and Antistripping Agents, Proc., Highway Research Board, 1952, 288-300.
6. Anzaki, Y. and Ikeda, T, Improvement of Asphalt Pavement Durability by Surface Treatment of Coarse Aggregates, Paving in Cold Areas Mini-Workshop 3, 1987, 1-15.
7. Emery, J.J., Silane Coupling Agents to Reduce Moisture Susceptibility of Asphalt Concrete, JEGEL Report, No. 88117, 1989, 1-17.
8. Rozum, T. and Flack, J.F., Selection of Silane Adhesion Promoters as Candidates for an Asphalt Paving Study, ORTECH Report, No. A&S 352-88-69-41208, 1988, 1-16.
9. Yoon, H., and Tarrer, A., Effect of Aggregate Properties on Stripping, Paper No. 870077, 67th Annual Meeting, Transportation Research Board, Washington, D.C., Jan. 11-14, 1988.
10. Field, F., Evaluation of Anti-Stripping Additives for Asphaltic Concrete Mixes, Effectiveness and Recommended Usage, Report EM-9, MTC, July, 1977.
11. Kennedy, T., Roberts, LF., and Lee, K., Evaluation of Moisture Effects on Asphalt Concrete Mixtures, Transportation Research Board, TRR-911, 1983, 134-143.
12. Fromm, H.J., Phang, W.A., and Noga, M., The Incidence of Stripping and Cracking of Bituminous Pavements in Ontario, D.H.O. Report No. 109, 1965, 1-23.
13. The Asphalt Institute, Cause and Prevention of Stripping in Asphalt Pavements, ES-10, 1981, 1-5.

14. Fromm, H.J., The Mechanisms of Asphalt Stripping from Aggregate Surfaces, R.R.-190, M.T.C., June 1974, 1-15.
15. Peterson, J.C., Plancher, H., Ensley, E.K., and Miyaki, G., Chemistry of the Asphalt-Aggregate Interaction: Relationship with Pavement Moisture Damage Prediction Test, Transportation Research Board, TRR-843, 1982, 95-103.
16. Stuart, K.D., Evaluation of Procedures Used to Predict Moisture Damage in Asphalt Mixtures – Executive Summary, FHWA/RD-86/090, Sept., 1986, 1-28.
17. Taylor, M., and Khosla, P., Stripping of Asphalt Pavements: State-of-the-Art, Transportation Research Board, TRR-911, 1983, 150-158.
18. Busching, H., Amirkhanian, S., Burati, J., Alewine, J., and Fletcher, M., Effects of Selected Asphalts and Antistrip Additives on Tensile Strength of Laboratory Compacted Marshall Specimens - A Moisture Susceptibility Study, Proceedings, Association of Asphalt Paving Technologists, 1986, 120-148.
19. Kennedy, T., McGennis, R., and Roberts, F., Investigation of Moisture Damage to Asphalt Concrete and Its Effect on Field Performance - A Case Study, Transportation Research Board, TRR-911, 1983, 158-165.
20. ––, Anti-Stripping Agents for Bituminous Surfacings, Singapore, Oct., 1982, 1-10.
21. Kennedy. T.W., Use of Hydrated Lime in Asphalt Paving Mixtures, National Lime Association, Bulletin 325, 1984, 1-20.
22. Lottman, R., Predicting Moisture-Induced Damage to Asphaltic Concrete, Transportation Research Board, National Cooperative Highway Research Program, Report No 192, Washington, D.C., 1978, 1-46.
23. Lottman, R.P., Predicting Moisture-Induced Damage to Asphaltic Concrete: Field Evaluation, Transportation Research Board, National Cooperative Highway Research Program, Report 246, 1982, 1-50.
24. Field, R., and Phang, W.A., Stripping in Asphaltic Concrete Mixes: Observations and Test Procedures, DHO Report, 1967, 1-27.
25. Kennedy, T.W., Characterization of Asphalt Concrete Pavement Materials Using the Indirect Tensile Test, Proceedings, Association of Asphalt Paving Technologists, 1977, 132-150.
26. Adedimila, A.S., and Kennedy, T.W., Repeated-Load Indirect Tensile Fatigue Characteristics of Asphalt Mixtures, Transportation Research Board, TRR-595, 1976, 25-33.
27. Velske, S., Wirkung von Organosilanen der Firma Degussa auf die Standfestigkeit von Mischungen aus Frasasphalt and neuem Asphalt-Mischgut, Preliminary Report Part I, Wuppertal, 1987, 1-5.

TABLE 1

SUMMARY OF AGGREGATES USED FOR THE STUDY

(a) Coarse Aggregate

Designation	Source	Remarks
A	Indusmin, Midland	Badgeley Is., quartzite, 100% silica
B	Uhthoff Quarries, Barrie	upper lift, ultra fine-grained limestone
C	Rama Stone Quarry, Orillia	quartzite microcline feldspar
D	United Aggregates, Gloucester	dolomitic sandstone, 60% sandstone, 40% carbonate
E	Nelson Aggregate Co., Burlington	100% carbonate

(b) Fine Aggregate

Designation	Source	Remarks
FA	Sherman Sand and Gravel Co., Campbellville	siliceous aggregate
FB	TCG Materials Ltd., Aberfoyle	siliceous aggregate

TABLE 2

SUMMARY OF ANTISTRIPPING AGENTS USED FOR THE STUDY

Designation	Source	Remarks
Lime	Beachvilime Ltd. Ingersoll, Ontario	Hydrated Lime
Pavebond A.P.	Morton Thiokol Ltd. Carstab Division Mississauga, Ontario	Amine-based additive
Glymo Damo Octeo	Huls America Inc. Petrarch Systems Briston, PA. 19007	Silane Coupling Agents

TABLE 3

RESULTS FROM JAPANESE PETROLEUM INSTITUTE STRIPPING TEST

(a) Distilled Water Testing Environment

Antistripping Agent	Application Mode	Stripping Pattern for Aggregate A	B	C	D	E
control	– –	4-1	1	1	4-1(2)	1
Pavebond	Additive	2	1	1	1	1
Lime	ST	1	1	1	–	–
Glymo	Additive	1	–	–	–	–
	ST	1	1	1	1	1
Damo	Additive	4-1	–	–	–	–
	ST	1	1	1	1	1
Octeo	Additive	4-1	–	–	–	–
	ST	1	–	–	1	–

(b) Salt Water Testing Environment

Antistripping Agent	Application Mode	Stripping Pattern for Aggregate A	B	C	D	E
control	– –	4-2	2	2	4-1(2)	2
Pavebond	Additive	2	1	1	1	1
Lime	ST	2	1	1	1	1
Glymo	Additive	2	–	–	–	–
	ST	1	1	1	1	1
Damo	Additive	4-2	–	–	–	–
	ST	1	1	1	1	2
Octeo	Additive	4-1(3)	–	–	–	–
	ST	1	–	–	1	–

Notes:

1. Fifty percent of aggregate has rating as identified by number enclosed in brackets.
2. Additive = stripping agent added to asphalt cement
   ST = surface treatment of aggregate.

TABLE 4

RESULTS FROM JAPANESE PETROLEUM INSTITUTE TEST ON GLASS SLIDES

Antistripping Agent	Application Mode	Area Stripped (%) CASE A	CASE B
control	— —	40	100
Pavebond A.P.	Additive	0	0
Lime	ST	0	0
Glymo	ST	0	0
Damo	Additive	0	50
	ST	50	100
Octeo	ST	10	0

Notes:

1. CASE A = slide cured at 25°C for 70 days
   CASE B = slide cured at 75°C for 24 hours

2. Additive = stripping agent added to asphalt cement
   ST = Surface Treatment of aggregate

TABLE 5

SUMMARY OF RESULTS FROM IMMERSION MARSHALL TEST*

Coarse Aggregate	Stripping Agent	Visual Assessment C	F	R	Marshall Stability (kN)	Retained Stability (%)
(a)	Specimens with Bow River Asphalt Cement					
A	---	3	2	9	24.4	51
	Glymo	0	2	5	28.2	49
	Damo	0	2	5	27.4	61
	Lime	0	2	5	26.2	68
	Pavebond	0	1	5	40.0	85
B	---	3	2	9	22.8	57
	Glymo	0	2	5	26.2	50
	Damo	0	2	5	25.4	54
	Lime	0	2	5	25.1	69
D	---	3	2	9	30.7	42
	Glymo	0	2	5	29.2	50
	Damo	0	2	5	28.0	55
	Lime	0	2	5	30.1	70
E	---	3	2	7	28.2	51
(b)	Specimens with Batch Plant Asphalt Cement					
E	---	1	2	7	33.9	37
	Damo(1)	0	2	7	33.1	63
	Damo(2)		6		30.4	75
	Damo(3)	2	1	7	23.1	102
	Damo(4)	3	1	8	24.8	87
	Pavebond	0	1	5	32.2	86

Notes:
1. R = Visual Stripping Rating: No stripping, R = 3
   Worst stripping R = 9
2. Stripping level in coarse aggregate, $0 < C < 3$.
3. Stripping level in fine aggregate, $0 < F < 2$.
4. (1) = only coarse aggregate treated with 3% of 1% silane solution.
   (2) = Fine and coarse aggregate treated with 3% of 1% silane solution.
   (3) = Fine aggregate treated with 9% of 1% silane solution, coarse aggregate treated with 3% of 1% silane solution.
   (4) = 0.9 percent silane was added to asphalt cement.

* All specimens were manufactured using the Campbellville fine aggregate.

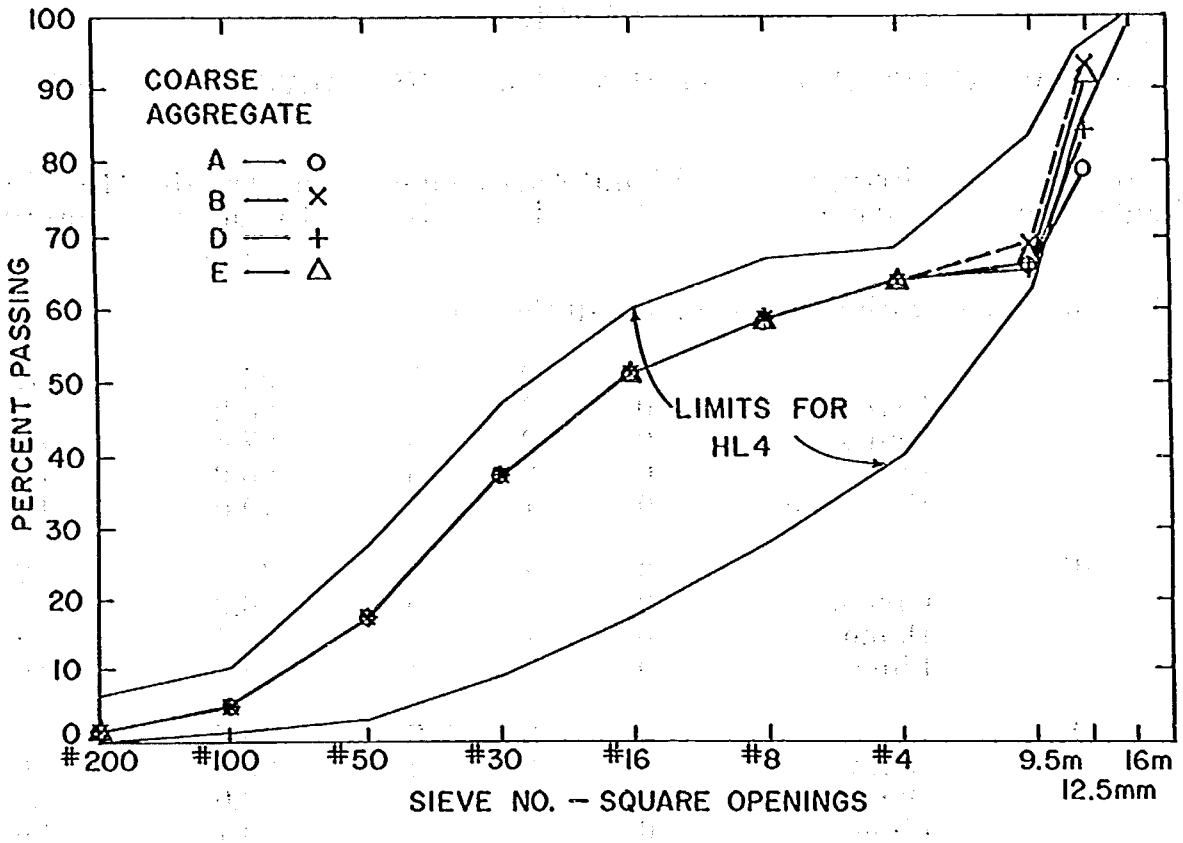


FIGURE 1. Combined gradations of fine and coarse aggregates used for manufacturing briquettes.

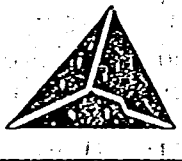
No. of Pattern	I	II	III	IV-1	IV-2
Definition	No stripping occurs. Edges can be light brown.	Stripping on edges and small dot stripping occur.	Stripping on edges widens. Dot stripping occurs.	Continuous stripping occurs.	Asphalt remains in dots.
Appearance					

FIGURE 2. Definitions of stripping patterns for JPI test [5].

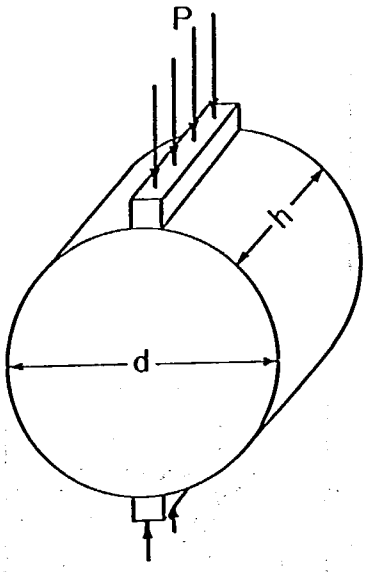


FIGURE 3. Loading configuration for split cylinder test.

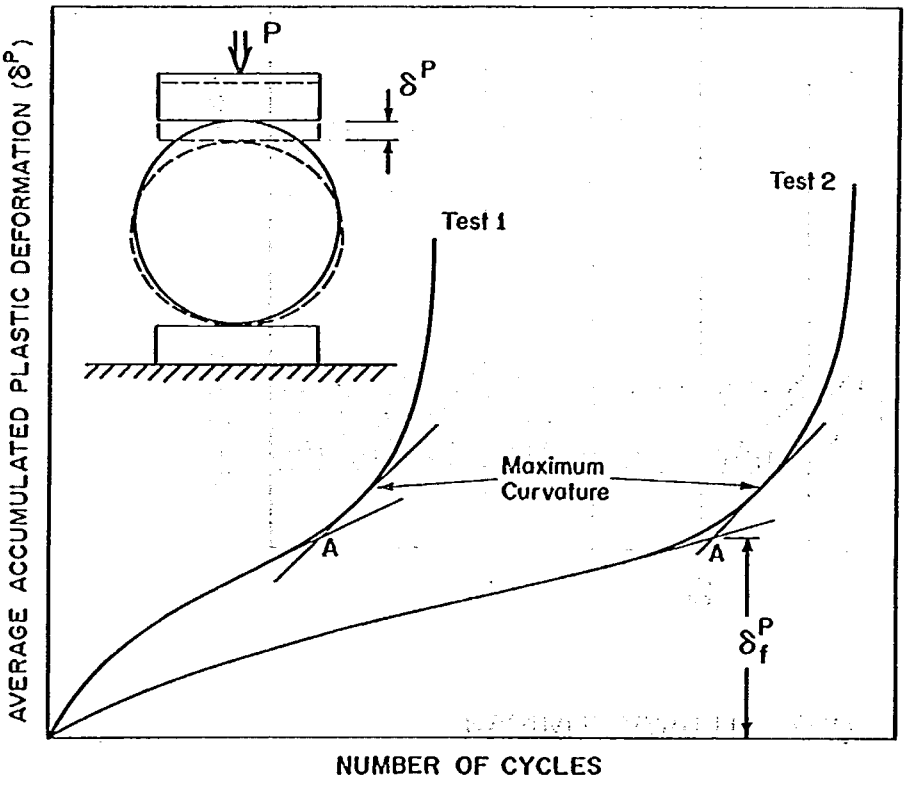


FIGURE 4. Typical deformation history results from fatigue tests (schematic).

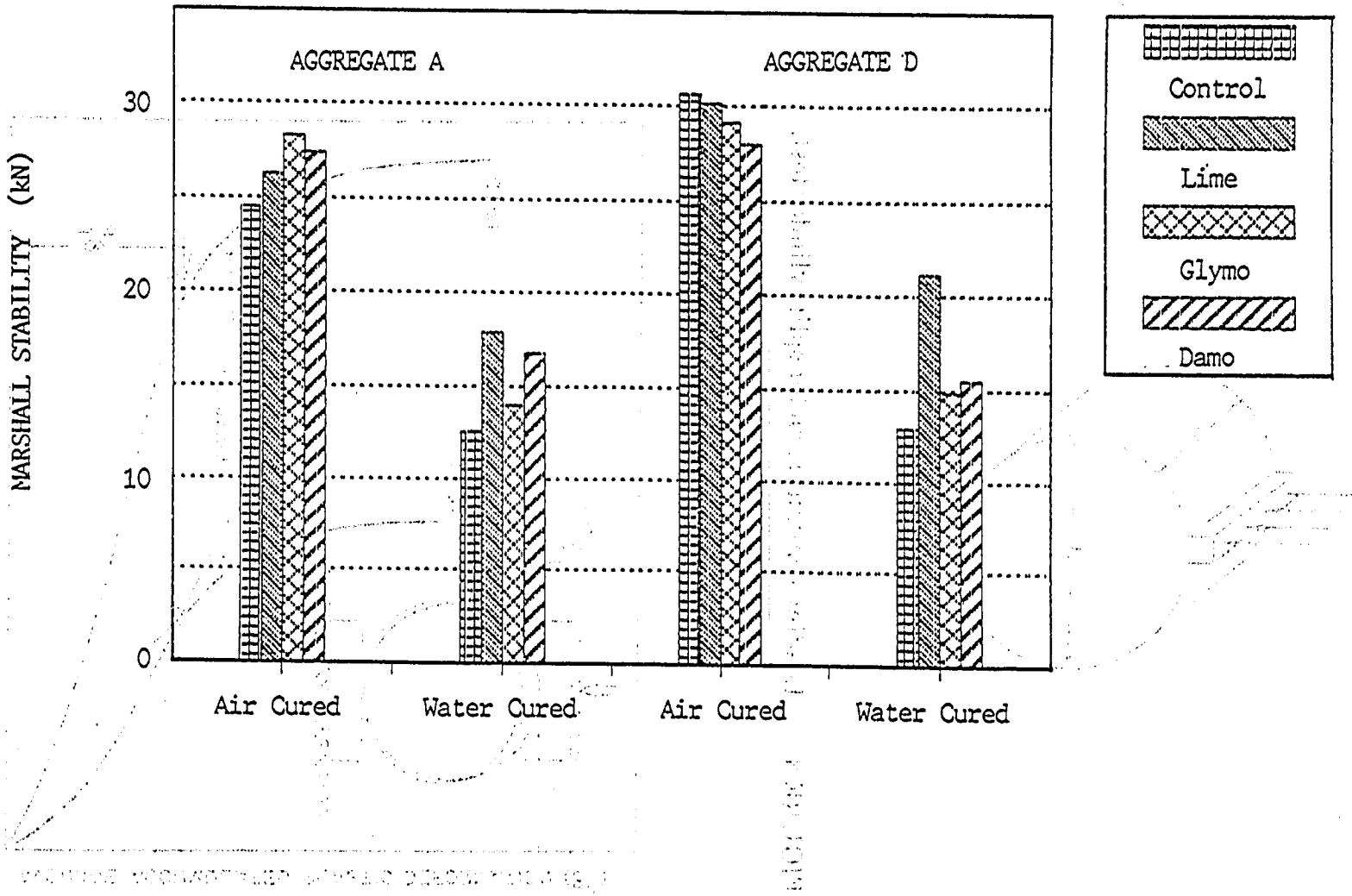


FIGURE 5. Immersion-Marshall test results of specimens manufactured using Campbellville sand and Bow River asphalt cement.

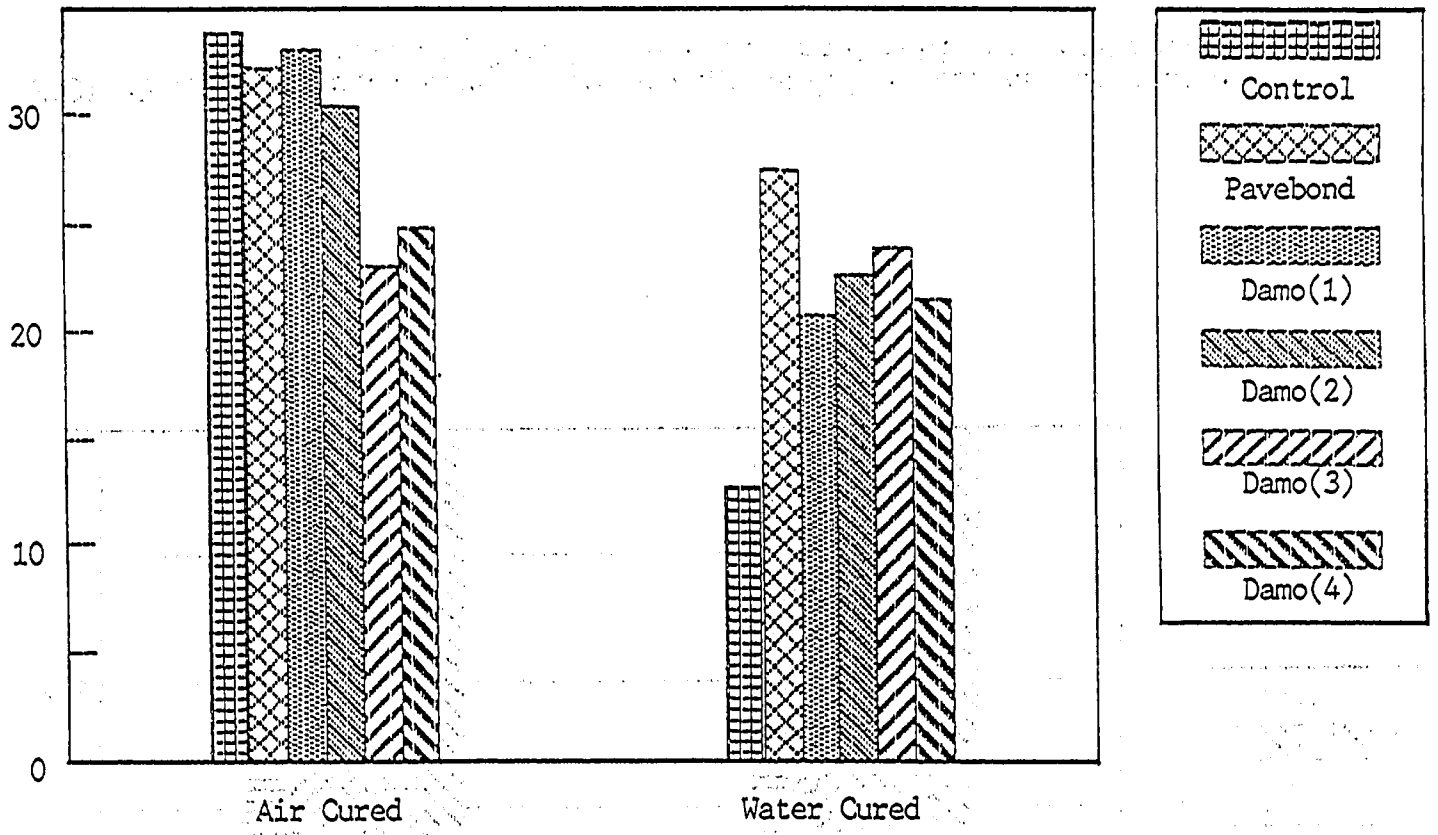


FIGURE 6. Immersion-Marshall test results of specimens manufactured using Aggregate E, Campbellville sand and batch plant asphalt cement.

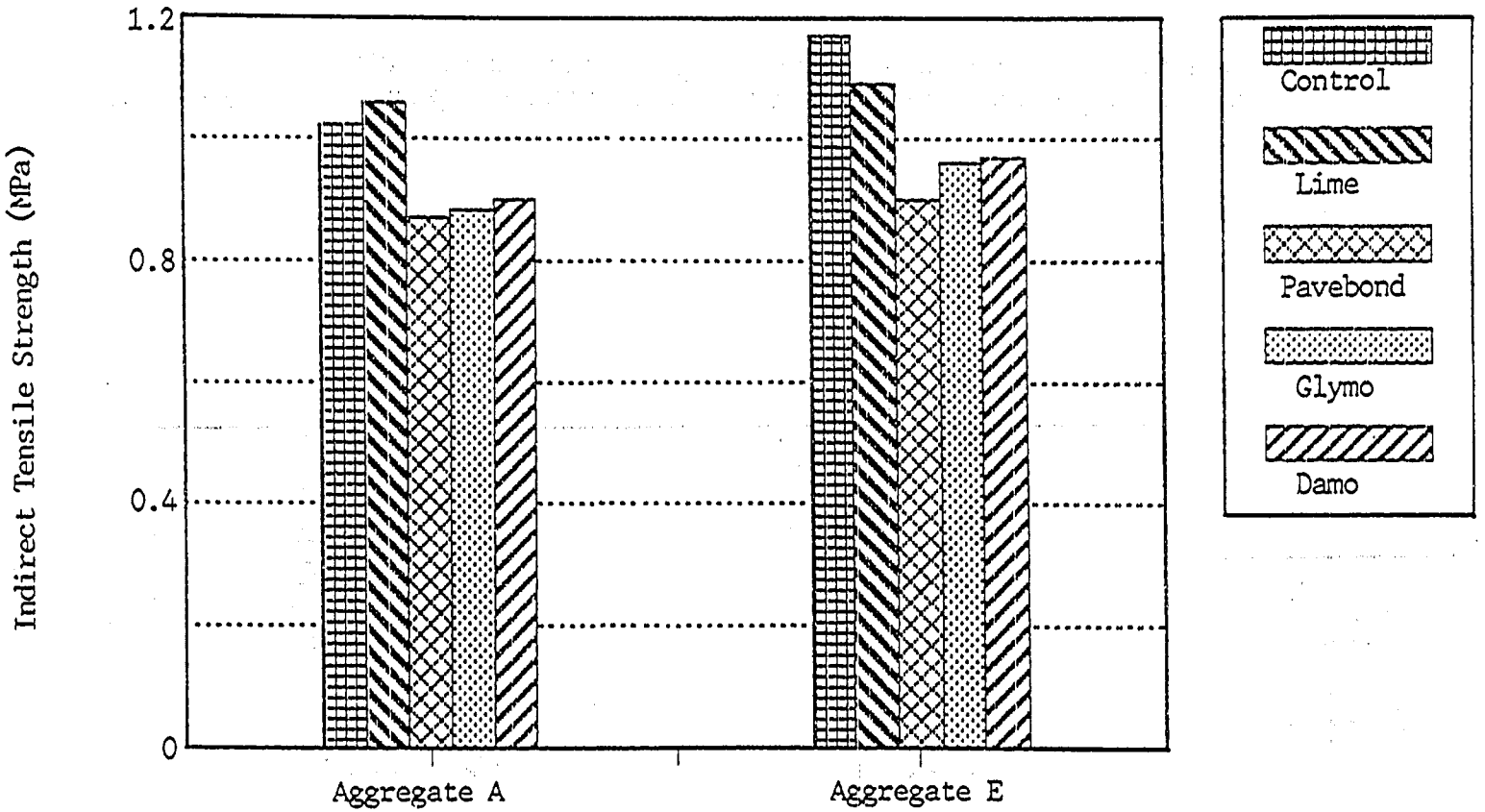


FIGURE 7. Average indirect tensile strength of fatigue test specimens manufactured using Campbellville sand and Bow River asphalt cement.

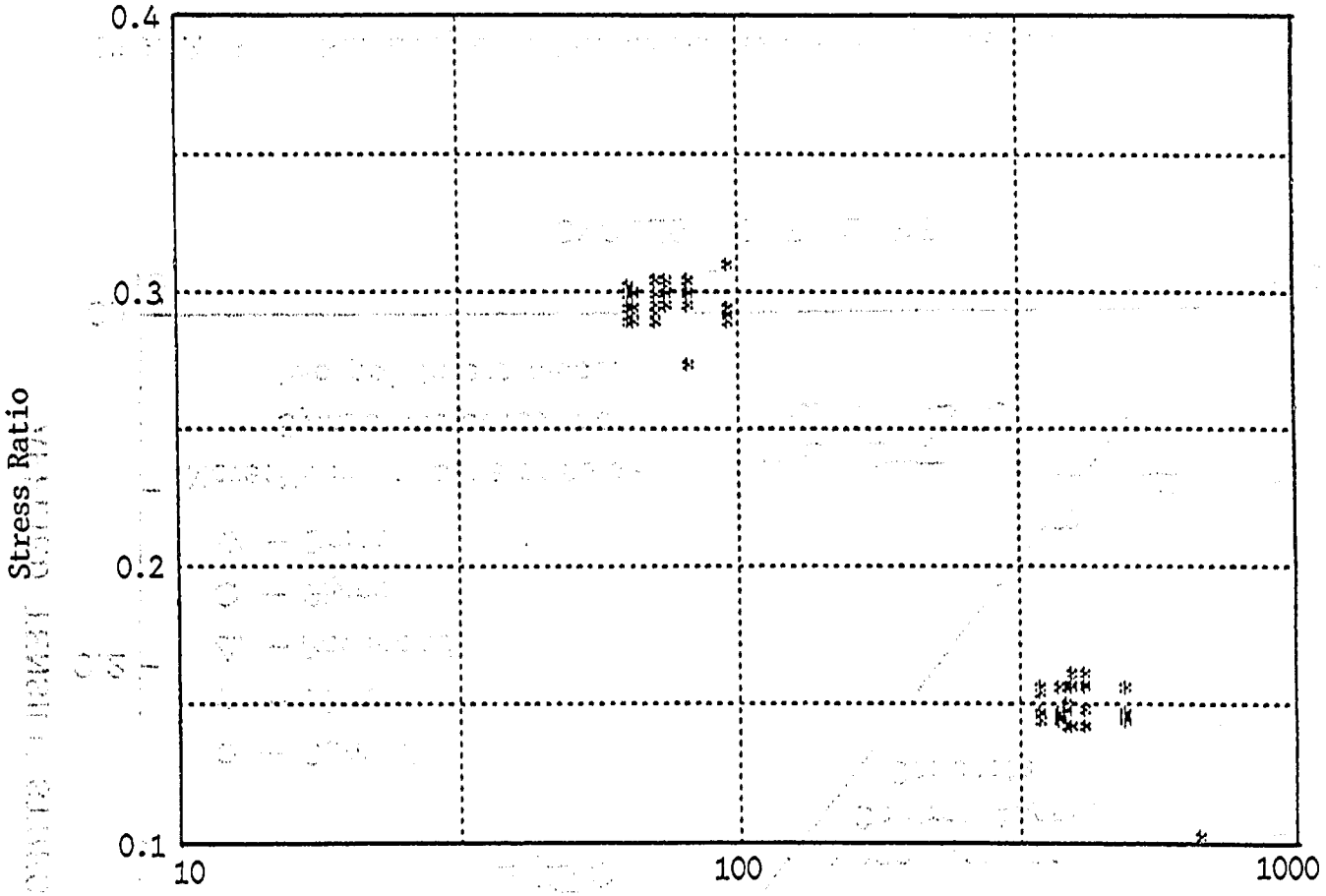


FIGURE 8. Summary of all fatigue test results in terms of stress ratio.

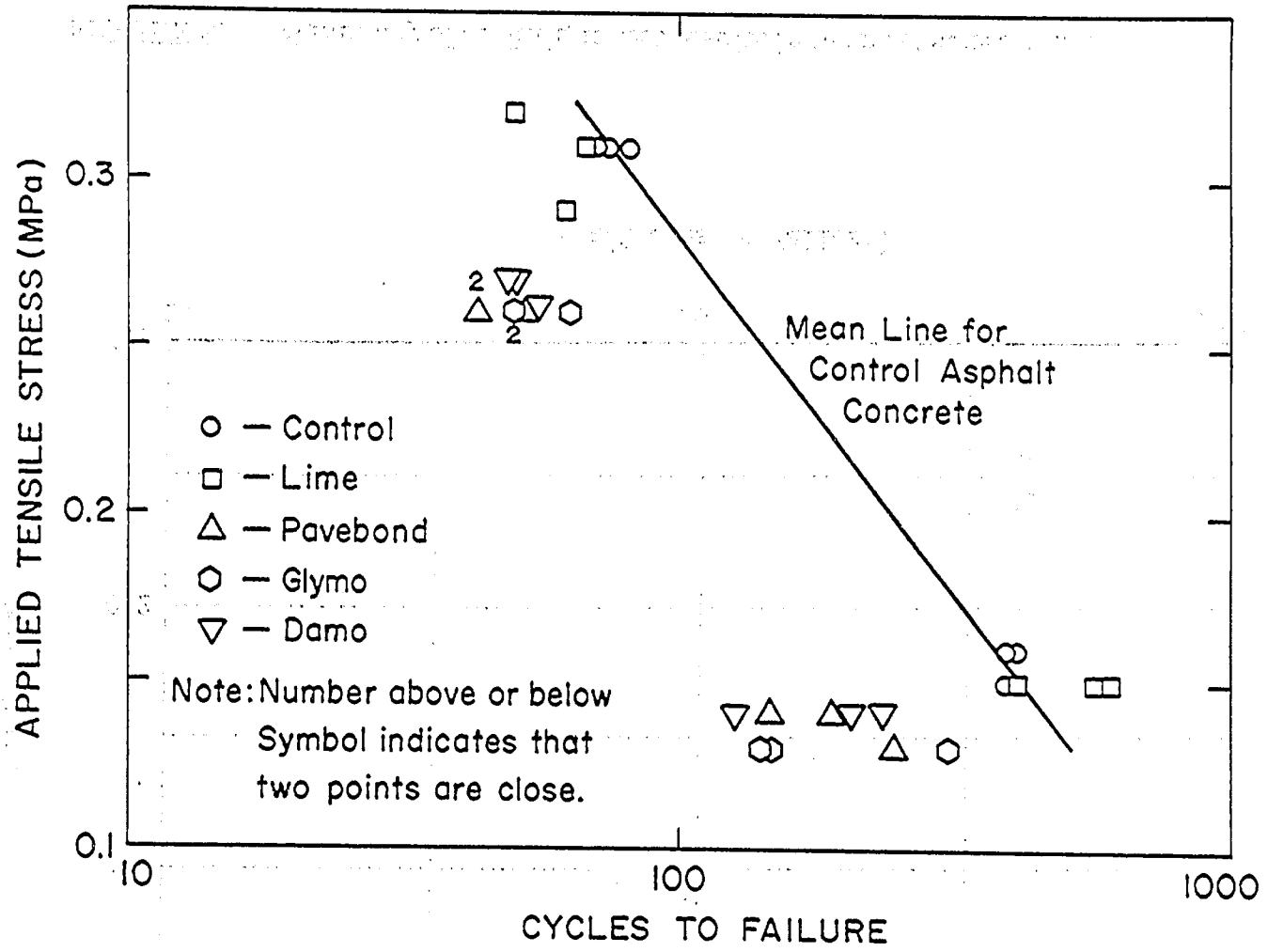


FIGURE 9. Summary of all fatigue test results for Aggregate A.

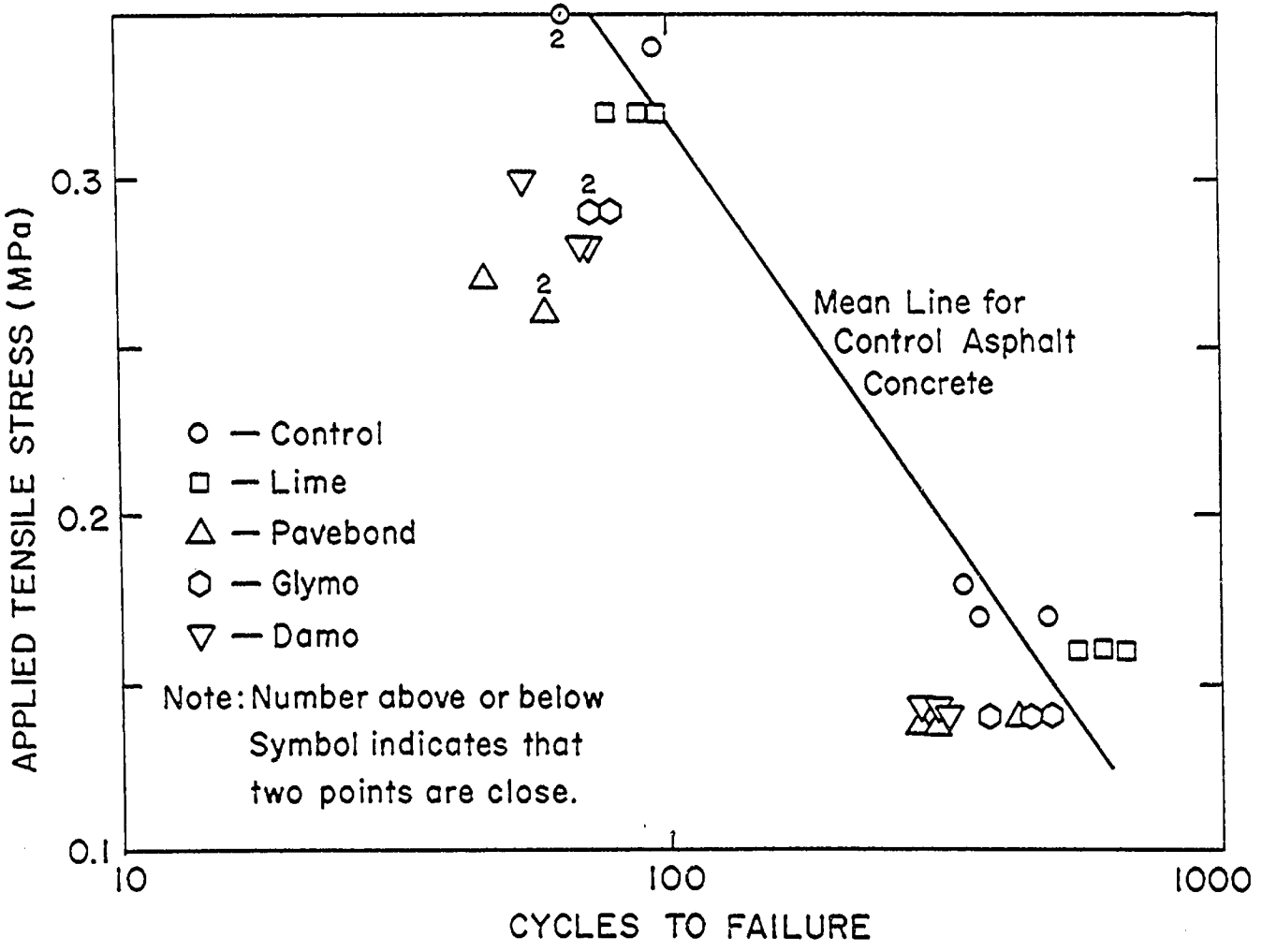


FIGURE 10. Summary of all fatigue test results for Aggregate E.

Thermal Stresses Development in Pavements During Winter Time

M.A. Laforte, C.R.C.A.C. INC

THERMAL STRESSES DEVELOPMENT IN PAVEMENTS DURING WINTER TIME

Marc-Antoine LAFORTE, Montreal, CANADA

INTRODUCTION

The effects of winter and its cold temperature on the pavement structure are both uneven frost heave of the pavement surface related to phenomena involving particularly the subgrade soils behavior and the thermal cracking of the surface asphaltic concrete layer and/or the other layers composing the pavement structure itself. Published literature discussing both problems is abondant: more than 5000 papers were written in the last 40 years addressing the first problem alone and some practical solutions exist. There are also many technical papers concerning the cracking of the pavement layers, principally the surfacing asphaltic layer.

However, the existing models consider mainly the first layer of a pavement, and very few models (COLD, in Finn et al, 1986, is an example) consider the variation of temperature and related properties occuring during a cold season. A research (Laforte, 1989), was undertaken to consider this aspect of the problem. This has permitted modelization of temperature and related thermal stresses both in the asphaltic layer and in the layers underneath, with a sinusoidal surface temperature variation and the penetration of the frost line, in the pavement, during the cold season.

This paper resumes the principal conclusions obtained from a computer

simulation using the models developped.

The conclusions given are preliminary, as it is almost impossible to characterize completely the materials laid on a road surface, both because of its high variability (both in physical and mechanical properties) and because the phenomena involved (as long term temperature or thermal regime prédiction) are not yet well understood.

DESCRIPTION OF THE MODEL

A computer program using a three-layer slab thermal model was written to modelize the effects of the base-course material typology, thickness or saturation in the thermal stress development in the pavement, and particularly in the asphaltic concrete surfacing layer.

The program uses the bending model developped in Appendix I to characterize the frozen granular base-course material behavior. It use a three-layer model (asphaltic concrete surfacing, granular base-course and subgrade soil) with varying layers' thickness and material typology or physical and mechanical characteristics.

The study does not pretend to modelize each particular case that would occur. The results are given for comparison purpose, as the aim of the original study is to determine the possible influence of the supporting frozen layers on the stress built-up in the asphaltic concrete.

The Model's hypothesis are:

i- Reference temperature (To) is set to 0°C, as this temperature

controls the freezing of the supporting layers and the beginning of a possible restrained interaction between asphaltic concrete and base course. This is a reasonnable hypothesis as above this temperature, asphalt is viscoelastic and will dissipate stresses as they are created. Also, at this temperature, the bond between asphaltic concrete and granular base is formed, changing the state of stress in the system.

ii- The thermal stress system is solve with a multilayer slab solution described in the Appendix. The choice of this kind of system is limitative, as others systems could also be used (beam or complex finite elements analysis).

iii- Freezing front is the bottom of the system, and a rigid support is considered at this front. This suppose a failure in the lower unfrozen material if conditions permit rupture.

iv- Stress is calculated with a time step varying from one to four hours, a four hour time step being the most common. This step is chosen for simplicity, so the loading time in the asphaltic concrete corresponds with the six hours (or more) loading time characteristic of many empirical models (cf. McLeod, 1968).

v- Temperature variation with depth is given by a exponantial line. This leads to a 5% stress reduction of the calculated maximum stress and up to a 10 % stress increase on the calculated minimum stress because the maximum gradient (occurring at the very top of the layer) in this layer is from 10 to 30 % higher than the mean gradient (used). This reduction (or increase) is less significant for the calculation of the stress occurring in the deeper layers (base course, or soil) as their temperature gradients are less steep and the variation of temperature becomes linear with depth.

vi- The models are models derived from the mean materials' properties. They have a coefficient of variation (mean/standard deviation) of +/- 30%

All the stresses calculated are affected by a similar coefficient of variation, the real coefficient being a complex function of the actual parameters' coefficients of variation.

PROGRAM'S PRINCIPAL ALGORITHMS

The principal algorithm of the program could be summarized as follows:

1) Air and surface temperature are first calculated for every time step, with the Barber (1957) model. The depth to freezing front is then calculated from the Painter and Aldrich model (U.S. Army 1965). The depth to freezing front is always considered as the bottom of the multilayered slab thermal model.

2) The interfaces' temperatures are calculated using a modified Lachenbruch (1959) thermal model, and the stresses are calculated using the mean mechanical properties of the material in any layer.

3) As the modulus of the frozen granular material is stress dependant, an iteration procedure calculate this modulus at each time step, guessing an initial (temperature dependant only) modulus and obtaining a final solution from this guess.

4) Stresses, and displacements, absolute or relative, are obtained at every time step, for a whole winter time, starting when the asphaltic concrete is freezing. A normal simulation goes for 4000 hours and lasts 1.5 (four hours step) to 4 hours (one hour step) on a mini-computer.

TYPICAL RESULTS

Results of the simulation are presented hereafter.

In this work, two types of bitumen (hard and soft) were modelized, as well as five asphaltic layer thicknesses (50 to 200 mm) and two types of base-course material (granitic gravel or crushed limestone) in at least five different layers thicknesses (300 to 900 mm, but up to 1800 mm) resting on two types of subgrade soil (sand or clay). Details are given in Table I.

1)CLIMATIC ENVIRONMENT:

Two environments (Temperate (MONTREAL) and Subarctic (JAMES BAY)) describe the temperature conditions. The Montreal area has a typical temperate climate with cold winter and warm summer while James Bay (La Grande) area has a subarctic climate with rigourous conditions: very cold winter and short cool summer. Table II gives the climatic conditions used in the computer program and Figure 1 gives typical temperature profiles obtained during the critical conditions as simulated in the program. It illustrates both the amplitude reduction and the phase shift occurring with depth in a typical pavement structure.

Frost depth penetration up to 2.5 meters was simulated by the Montreal climatic regime, and up to 5 meters by the Bay James climatic regime, during a typical winter conditions (from 1000 to 3000 freezing ^{o}C-days).

TABLE I

PARAMETERS USED IN THE COMPUTER PROGRAM

CLIMATIC ENVIRONMENT

Montreal	Ay = 25	Ad= 8	To= 6
James Bay	Ay = 35	Ad= 10	To= -4

BITUMEN

HARD	P.I.	1.5
	R&B	60°C
	Tc	-25°C
SOFT	P.I.	0
	R&B	40°C
	Tc	-32°C

ASPHALT CONCRETE THICKNESS

50, 75, 125, 150 et 200 mm

BASE-COURSE AGGREGATES PROPERTIES

Granitic gravel	Yd= 21.69 kN/m^3	w= 6%
Crushed Limestone	Yd= 22.32 kN/m^3	w= 6%

BASE-COURSE THICKNESS

300, 600, 900, 1200 et 1500 mm

SUBGRADE TYPES UNDER THE PAVEMENT

Sand	Yd = 17.61 kN/m^3	w= 12%
Clay	Yd = 14.62 kN/m^3	w= 33%

Notes 1) PI Penetration Index Shell
R&B Ring & Ball Temperature
Tc Critical temperature (Penetration = 1.3)
2) Ay Yearly Amplitude, °C
Ad Daily Amplitude, °C
To Mean Annual Temperature
3) Yd = Dry unit weight
w = water content, percent by weight

FIGURE 1A TEMPERATURE PROFILE, MONTREAL CLIMATE

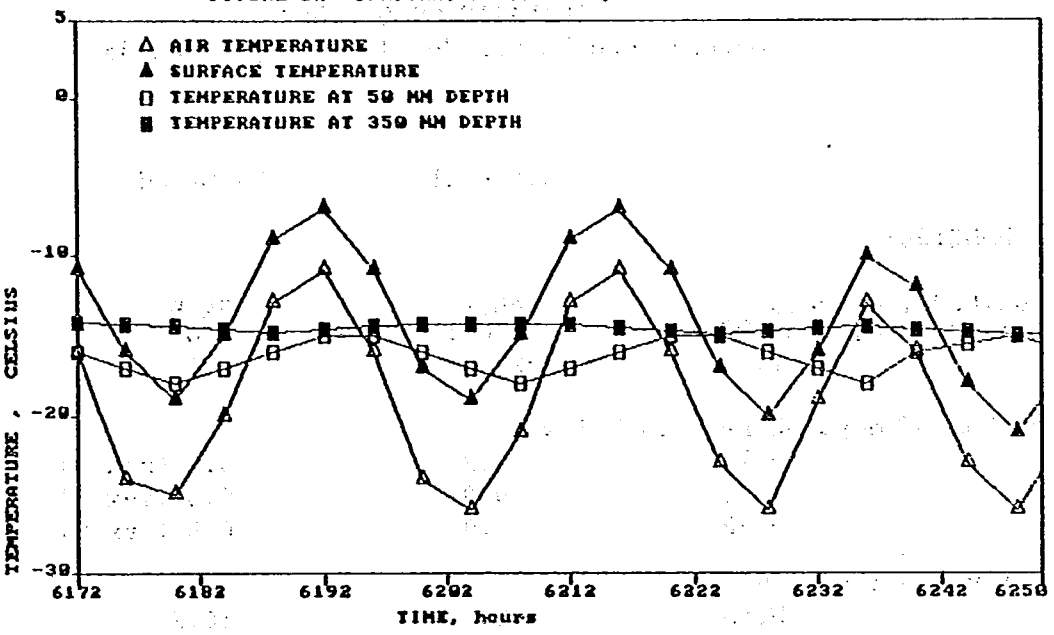


FIGURE 1B TEMPERATURE PROFILE, BAY JAMES CLIMATE

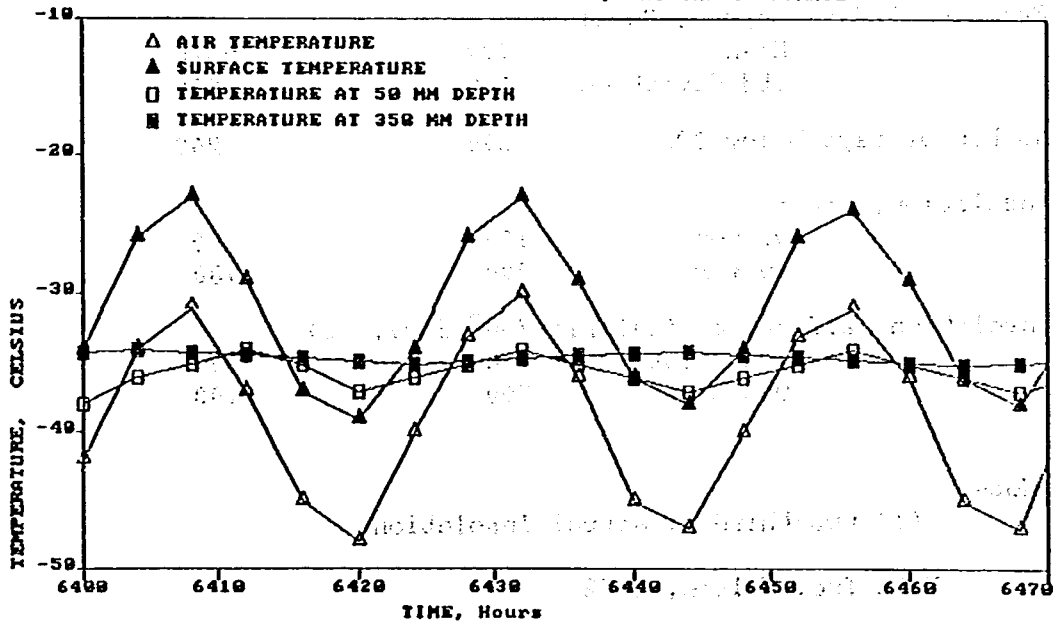


TABLE II

CLIMATIC CONDITIONS
Montreal and La Grande (James Bay), Canada

PARAMETRES	Montreal	La Grande
Latitude, degrees	45.5	52.5
Temperature, mean °C	6.1	-4
1% min	-26	-41
Number of days where T is below		
- 23	0.2	4.2 (max 9)
- 29	0.0	2.3 (max 6)
- 33	0.0	0.6 (max 3)
Daily Amplitude, °C		
Mean	8.3	10.2
std deviation	3.0	5
Annual Amplitude, °C		
Mean	26.5	35
std deviation	10	10
Freezing Index, Degrees-Days:		
Mean	777	2610
std deviation	180	390
Number of days below 0°C	208	240
Insolation, hours		
winter	125	70
summer	800	780
Insolation, effective (Calories/cm^2/day), (1)		
June 21st	670	670
Dec 21st	200	100

Notes
(1) two-third of actual Insolation

Data from Wilson, 1972

2)CONSIDERATION OF DYNAMIC LOADS AND FREEZING PRESSURES

Stresses related either to the dynamic forces acting at the surface or the freezing forces acting internally are not considered. So, the stresses dues to dynamic loads or the residual stress resulting from the freezing conditions should be added to the thermal stresses induced by temperature changes in the pavements layers giving a "gross" stress (GROSS) calculated as their sum.

3)MATERIAL PROPERTIES

Tables III and IV give the principal equations used to modelize the materials. Table III refers to the bitumen and the subgrade soils models, and Table IV, to the granular base-course models. Parameters involved are the temperature and the time since load application began. The equations presented were derived as follows:

ASPHALTIC LAYER

The modulus of the bitumen is first given by a correlation equation based on the Van Der Poel (1954) nomograph, as modified by Heukelom (1969). Modulus of the asphaltic mix was then calculated from the Heukelom (1969) equations, in which the mix modulus is dependant on the bitumen stiffness and the mix voids and physical properties. Loading rate dependant failure stress was obtained from published relationships gathered from the technical literature (e.g. Finn et al, 1986).

TABLE III

MODELS USED FOR MATERIALS' PROPERTIES

BITUMEN

RING & BALL = 40°C, P.I. = 0 (SOFT)

$$\log EBIT = 27.22055 - 0.10353\,(273+Ta) + 1.15378 \log t - 0.00746 \log t\,(273 + Ta)$$

$r^2 = .976$ (EBIT in Kg/cm^2)

RING & BALL = 60°C, P.I.=1.5 (HARD)

$$\log EBIT = 21.21552 - 0.07648(273+Ta) + 1.92105 \log t - 0.01191 \log t\,(273 + Ta)$$

$r^2 = .997$ (EBIT in Kg/cm^2)

2) SAND

CRITICAL STRENGTH = 0.5 - 0.2214 T

MODULUS , $\sigma < \sigma_{crit} = 15 - 3.4571\ T$

$\sigma > \sigma_{crit} = 0.67\ (\sigma_{crit})/0.01$

LIMIT STRENGTH ($\sigma > \sigma_{crit}$)

$= 1.1732 - 0.35224\ T - 0.02783 \log t + 0.11289\ T \log t$

3) CLAY

$$\text{CRITICAL STRENGTH} = 0.257\,|-T|^{1/2} - 0.115$$

LIMIT STRENGTH ($\sigma > \sigma_{crit}$):

$= 0.33\ (0.2919 - 0.2964\ T - (0.0673 + 0.101*T)\log t)$

MODULUS , $\sigma < \sigma_{crit}$

$T > -5 \quad 44.289\,|-T|^{1/2} - 30.07$

$T < -5 \quad 197.89\,|-T|^{1/2} - 378.94$

$\sigma > \sigma_{crit} = (0.25 + 0.05\ T)\ \sigma_{crit}/0.01$

Notes:

BITUMEN	= Data from Shell Nomograph (Heukelom, 1969)
SAND	= Vyalov, 1962; γ_d= 17.61 kN/m^3; w = 10 %
CLAY	= Akili, 1971; γ_d= 14.15 kN/m^3; w = 33 %
Ta or T	= temperature, Celsius
| -T|	= Absolute temperature, Celcius
t	= time, hours
σ	= Applied Stress
σ_{crit}	= Critical Strength

TABLE IV

GRANULAR BASE-COURSE MATERIALS MODELS

LIMESTONE CRUSHED AGGREGATE

Saturation <60 %

A1(10-3)= -0.5995 - 0.0643 T
B1(10-3)= 7.6481 + 0.1125 T
C (10-3)= 0.485222 + 0.018244 T
d = 1.26005 - 0.004175 T
So = 0.071 - 0.1605 T

Saturation >60 %

A1(10-3)= -0.009525 - 0.0406 T
B1(10-3)= 9.76985 + 0.341675 T
C (10-3)= 0.3075 + 0.0119 T
d = 0.50965 - 0.007125 T
So = 0.7225 - 0.15725 T
bf = 0.430 + 0.0174245 T
Ef = 118.35 - 25.47 T
e lim = Sf/Ef

GRANITIC GRAVEL

A1(10-3) = -0.394775 - 0.01661 T
B1(10-3) = 8.2653 - 0.3445 T
C (10-3) = 0.22375 + .013825 T
d = 0.1216 + 0.0552 T
So = 0.3622 - 0.51363 T
bf = -0.00365 - 0.108291 T

Notes (1) In all those equations, T is negative.
(2) A1, B1, C , d and So from the equation:

$$e = A1 + (B/So)\, S + C\, S^{d} \ln t$$

$$Sf(t) = So - bf \log t$$

(3) e = bending strain
S = bending stress
Sf= bending strength at time t
E = bending modulus

Data compiled from tests results given in Laforte, 1989a

FROZEN GRANULAR BASE-COURSE MATERIAL MODELIZATION

According to experimental works by Laforte (1989), the general flexure equation for the frozen material is:

$$e = A1 + (B/So)\ S + C\ S^d \ln\ t \qquad (1)$$

where A1, B1, C and d are material constants, S, the applied bending stress; So, the initial bending strength; and e, the time and temperature dependant strain.

Bending strength is time dependant, as in:

$$S = So - b \log (t) \qquad (2)$$

where A and b are temperature dependant constants. A modulus could be found from:

$$EMG = S/e = \frac{S}{A1 + (B1/So)\ S + C\ S^d \ln t} \qquad (3)$$

The initial strain (t = 0) is given by:

$$e = A1 + (B1/So)\ S \qquad (4)$$

so that the initial modulus could be given by:

$$EMG\ (t = 0) = S/(A1 + (B1/So)S) \qquad (5)$$

This modulus varies with the temperature as in (Laforte, 1989):

$$EMG(T, 0) = 118.35 - 25.45\ T \qquad (6)$$

(crushed limestone aggregate, EMG in MPa, C.V. = 35 %)

Equation like this serves as a starting point, and an iteration procedure described in Appendix I calculates the various mechanical parameters.

SUBGRADE SOIL BEHAVIOR

The behavior of the unfrozen sandy or clayed soil was modelized from the published technical literature on frozen soils. As with the frozen granular material, the failure strength and the elastic modulus are temperature, time and stress dependant if the stress is above a critical level:

i) if the applied stress σ is lower than a "critical" strength σ_{CRIT}:

$$\sigma(limit) = \sigma_{CRIT}$$

$$E = E_o\ (A_s + B_s\ T)$$

ii) if the applied stress σ is higher than σ_{CRIT}:

$$\sigma(limit) = \sigma_o - \sigma_s \log t$$

$$E = E_o - E_s \log t$$

A_s, B_s, σ_o, σ_s, E_o, E_s, and σ_{CRIT} are materials' constants: they are linearly temperature dependant, for the sandy material, but follow the square-root law, for the cohesive frozen soils.

Data base came from the papers published by Vyalov (1962), (in Johnston, 1981), in the case of the frozen sand, or by Akili (1971), for the clay model (Sault Ste-Marie Clay). Table III gives the correlation equations used in the program.

TYPICAL RESULTS FROM THE SIMULATION

CRITICAL CASES:

Three critical thermal loading conditions occur during a typical winter:

i) when the top of the base-course is freezing: very high stress could be generated. This stress is dependant mainly on the asphaltic thickness and hardness (Figure 2): it is maximum in a thin (less than 100 mm) Asphalt Concrete (A.C>) surfacing layer and for the hard bitumen surfacing, but it is significantly lower in a thicker surfacing. Climatic influence is less significant because similar temperature conditions occur in the environments considered when this critical condition happens.

The thermal stress calculated is roughly linearly proportionnal to the inverse of the thickness (ta) of the layer as in:

$$Stress = b/ta + A$$

Typical parameters values are given in table V.

The minimum stress is calculated for the thicker asphaltic concrete layer,

Table V

PARAMETERS IN THE CRITICAL STATE

(WHEN THE TOP OF THE BASE-COURSE IS FREEZING

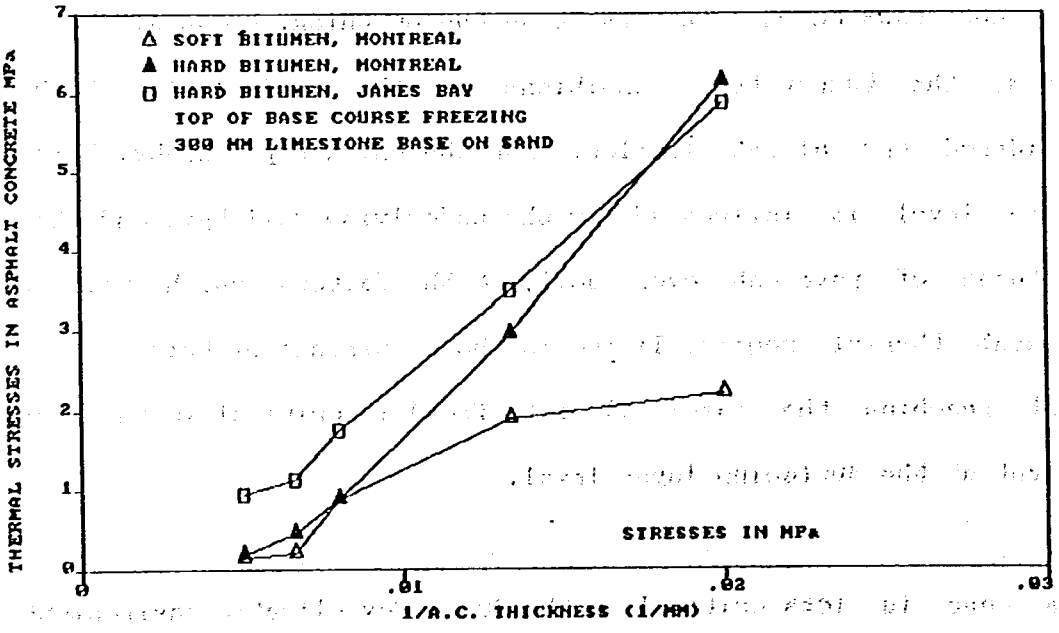
AGGREGATE TYPE	CLIMATE TYPE	A	B	BITUMEN TYPE	SOIL TYPE	r^2
Limestone,	Montreal	-2.159	385.89	Hard	Clay	0.931
	Montreal	-2.186	406.21	Hard	Sand	0.989
	Montreal	-0.485	146.66	Soft	Any	0.900
	James Bay	-1.004	241.41	Soft	Sand	0.992
Granite,	Montreal	0.378	73.12	Soft	Clay	0.982
	Montreal	-1.312	315.26	Hard	Sand	0.997
	James Bay	-1.946	393.50	Soft	any	0.983

Parameters A and B are from the equation:

$$\text{Stress} = t/B + A$$

where t = thickness of the AC surfacing, in mm
S = thermal stress while the AC-base is freezing

FIGURE 2 INFLUENCE OF A.C. THICKNESS



which also has the highest thermal and mechanical inertia. Those high stresses in the A.C. surfacing correspond to very high stress ratio (Stress in AC/Stress in Granular base) in the granular base material (up to 10). For thin surfacing (less than 100 mm), the calculated stresses in both the asphaltic concrete layer and in the granular base are higher than their respective strengths, so theoritically they fail. The actual failure will most probably occur at the frozen unfrozen material contact and the bond will be broken, resulting in a new stress state (unrestricted condition). Actual stress level will then be about 100 times lower.

For the thicker surfacings, this stress is lower than the material strength but a probable failure will occur at the freezing front where the stress in the granular base is higher then its (almost zero) tensile strength.

ii) when the top of the subgrade soil is freezing: this critical thermal stress is also almost independant of the climatic conditions considered when the base-course is less than 600 mm thick, because, when this case occurs, the temperature conditions at the surface for both climate considered are almost similar. For the thicker pavements, this critical stress level is influenced by the underlying soil type and the relative thickness of pavement over soil, both factors which also affect the pavement thermal regime. Timing in the occurrence of this event (freezing front reaching the base/soil interface) is critical in the stress development at the surfacing layer level.

This case is less critical in the James Bay climatic environment for two reasons: the thermal stresses occuring during the coldest week of the year

are most higher and this critical condition happens early in the season (time less than 5000 hours), when the relative temperature is still high, for the base-course material thickness modelized.

iii) during the coldest period of the winter, or during any cold spell that could occurs during the winter.

As illustrated in Figure 3, which compares hard or soft bitumen A.C. mix, the stress ranges calculated for this coldest period are from 1.5 to 3 times higher if the A.C. bitumen is hard (P.I.=1.5), the actual ratio depending on the thickness of the asphalt concrete and on the climatic environment.

For this particular critical case, a change in the temperature regime from the Montreal to the James Bay climate, results in an maximum increase up to about 12 times in the calculated stresses ranges; the greater increase occurs again in the thinner A.C. surfacing resting on a thin base and made with an hard bitumen. The particular effect of a climatic change is illustrated in Figure 4.

The worst conditions were given by a thin (50 mm) surfacing layer using an hard bitumen, resting on a thin (300 mm) base-course of granitic origin, on a clay material, in the James Bay environment modelized.

During the coldest time of the year, A.C. thickness, type of the aggregate used and the thickness of the base-course are all controling parameters, and this will be discussed hereafter.

FIGURE 3 INFLUENCE OF BITUMEN TYPE ON STRESSES

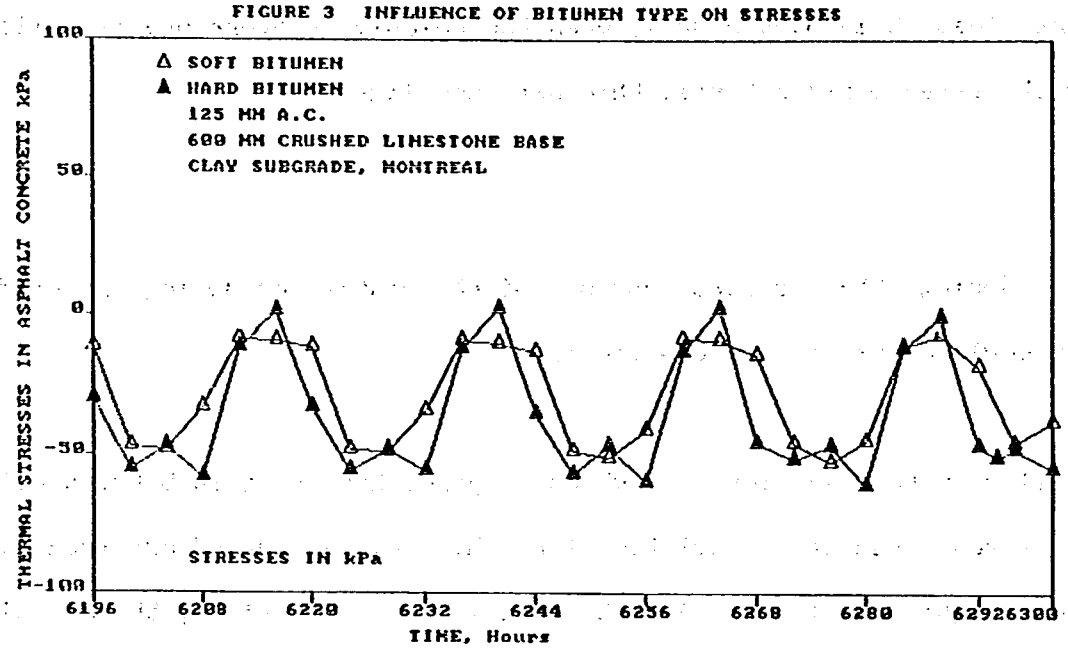
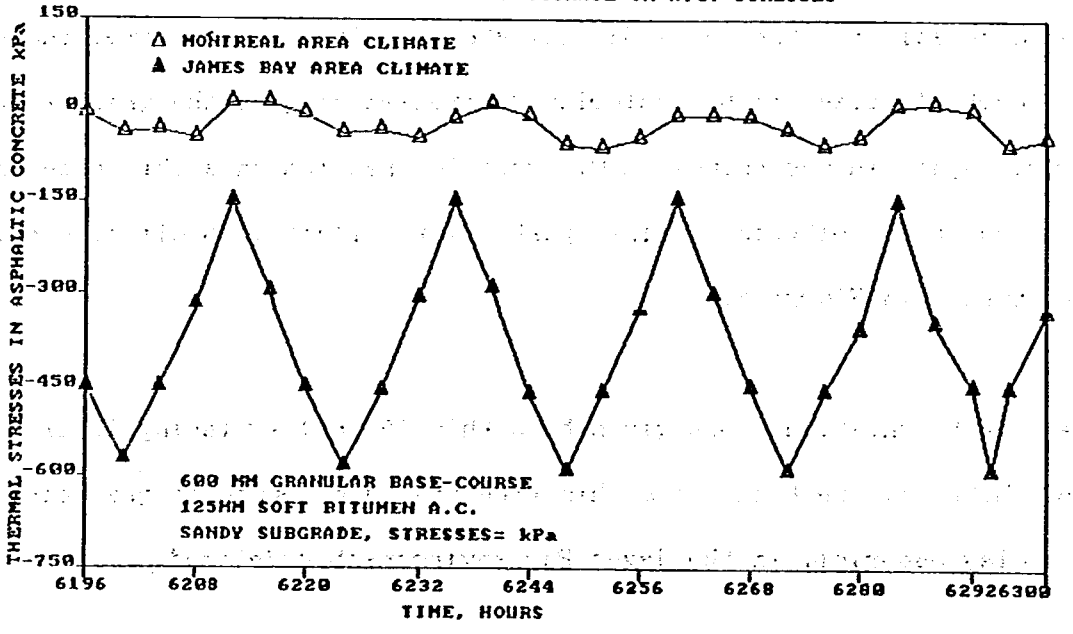


FIGURE 4 INFLUENCE OF CLIMATE ON A.C. STRESSES



INFLUENCE OF MATERIALS'DEPENDANT PARAMETERS

Hard bitumen leads to very high thermal stresses as calculated during the colder conditions. Apart climate and the asphaltic concrete thickness, the bitumen hardness was found to be the most important and this justify the amount of works done by all the searchers in this field. In fact, thermal stress was up to 100% higher than the stress calculated with a softer bitumen A.C. mix.

Typology and thickness of the base-course are important variables. In almost any case, as observed in Figure 5, slightly more thermal stresses in the surfacing layer were calculated when the base-course was a granitic gravel: (except when a hard bitumen mix in the Montreal conditions was simulated). This normally corresponds to a higher stress level in the base-course material itself.

A thinner base-course thickness always corresponds to a higher stress in the surfacing layer as well as in the base-course layer. Optimal thickness exists, as illustrated in Figure 6, which minimizes both stress in any case; this thickness is dependant on the thickness of the surfacing and slighly on the climatic environment: it is above 600 mm and varies from 600 to 1200 mm depending on the conditions. Required thickness of the surfacing layer to minimize thermal stresses is at least 100 mm.

Typology of the subgrade soil is very important. In any case, a pavement built over a clay subgrade will develop higher stresses (up to 100% higher in some cases) than a pavement built over an sand subgrade, if the conditions are the same.

FIGURE 5 INFLUENCE OF AGGREGATE TYPE ON STRESSES

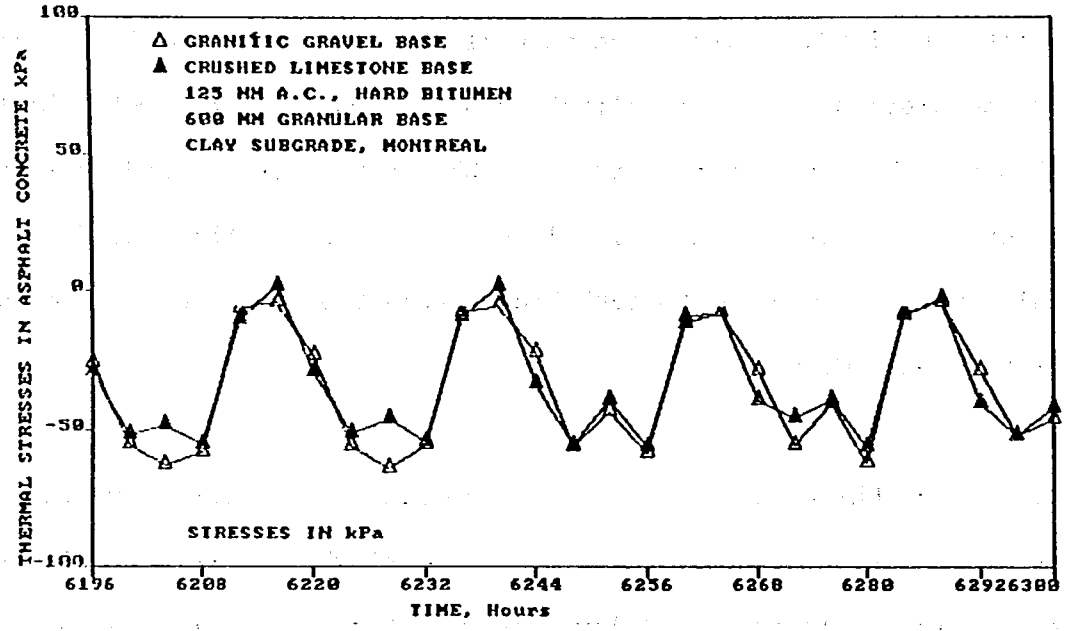
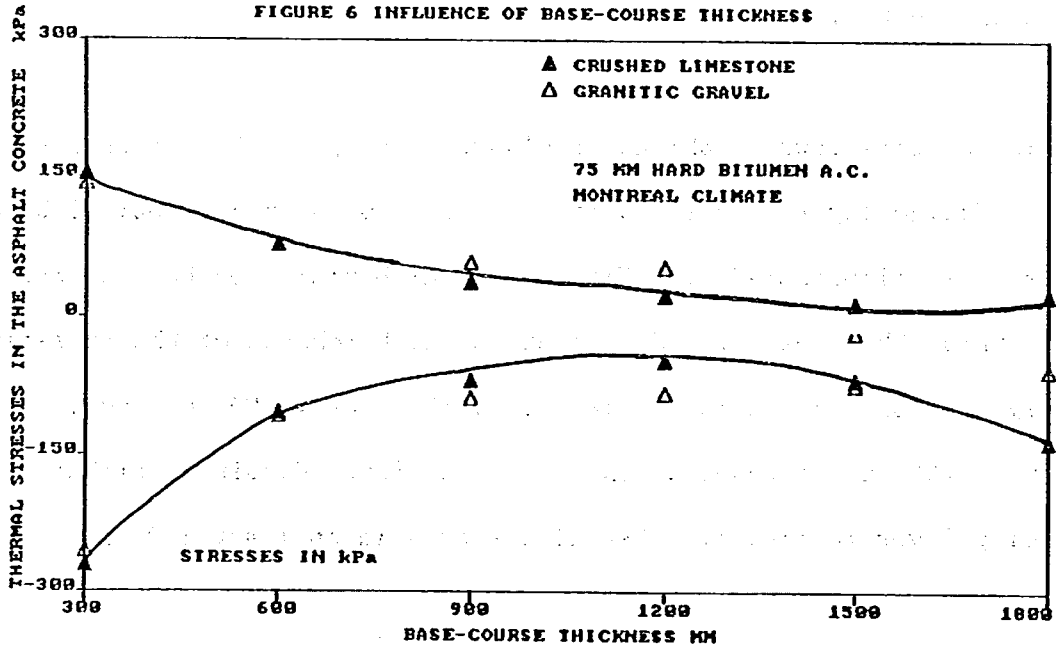


FIGURE 6 INFLUENCE OF BASE-COURSE THICKNESS



COMPARISON WITH OTHER MODELS

When compared to classical models (Christison et al, 1972; Chen et al, 1981), the calculated stresses are in the same range, if the same data are put into the program (Laforte, 1989a).

When the simulated stresses are compared to the thermal stresses calculated using a standard formula (as given in Yang, 1972, p.147), it is found that they compared to the stresses calculated with a shorter loading time (0.1 hour vs the four hours loading time from the simulation). This implies that either the calculated stresses are on the higher side, or that, if the frozen pavement acts as a slab, (the model considered), the combined effects of any layer could not be neglected, even if the mathematical model referred to is very realistic, as it considers both the thermal bending stress and the bottom layer expansion stress, in a restricted base conditions. But it neglected the possible influence of the other layers underneath, which is time and stress as well as temperature dependant. This aspect needs some more research but opens up a complete new field, as most of the works up to date were done looking only on the influence of the surfacing layer considered alone in the model. Even recently (Finn et al, 1986), both the base-course or the subgrade materials are modelized with non-time dependant values in the COLD program to calculate the critical thermal stresses in the surfacing layer.

Apart the mechanical properties of the base-course material (or the subgade soil), which are time and stress dependant, the other properties (Thermal and/or physical) are important factors in determining the thermal regime of the pavement as a whole, and the stresses occurrence both in a

frozen as well as in an unfrozen state.

In fact, both materials act as part of the pavement in the global thermal stress characterization, being either insulators or conductors, fixing the bottom limit of the frozen pavement structure and its internal thermal regime.

It is true that the asphaltic concrete surfacing, being at the top, has the higher thermal gradients, the higher hourly or daily temperature variation and so the higher thermal stress occurrence. It is also the most important insulator, a fact which is often neglected by many designers. But its bottom thermal regime and its support in any time depend on the base-course material thermal and physical properties, either frozen (time or stress dependant) and thawed (mainly dependant on the saturation and the drainage potential both fixed by its freezing, frozen or unfrozen states). Its very high strength when frozen is lost very easily when thawed, and as its saturation is high, its bearing capacity is then very low. Unsaturated material is better but, for common base-course materials, a very low saturation (less than 30 %) is needed for them to be non frost-heaving and have a low overall saturation when frozen.

This favors use of clean (no fines) material but those, if made with soft material (those with Mohs hardness < 5), create bad fines when compacted if the material is well graded. A clean uniform graded material could be an other alternative, but stabilization with bitumen will probably be needed to facilitate construction and to assure a uniform layer thickness.

CONCLUSIONS

Analysis using simulated winter conditions show that not only one, but three critical cases, are to be determined. It also shows that parameters other than the asphaltic concrete layers' properties are influencial and have to be determined. Particularly important are the thermal effects of the base and subgrade materials, as well as the critical asphaltic concrete stiffness or thickness.

This justify the numerous works to find better asphaltic materials, but this also justify pursueing research on the frozen behavior of other pavement materials as well.

APPENDIX I

WORKING HYPOTHESIS

We consider a typical flexible pavement, including an asphaltic concrete (AC) surfacing layer and a granular base-course.

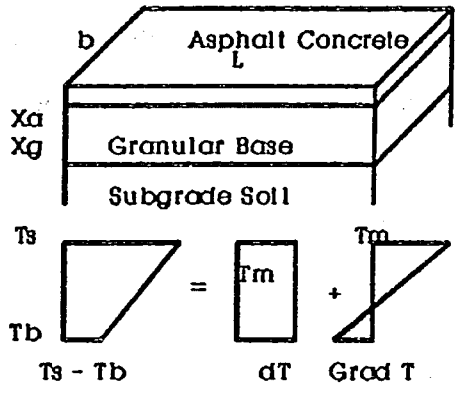
While freezing and when frozen, the pavement could be represented by a tri-layer beam or slab: the development of the equations starts from a slab model (Figure A1.1).

The first layer is the AC layer. Its modulus (EMIX) is time and temperature dependant and its thickness XA, vary from 50 to 300 mm. The second layer is the granular base-couse whose frozen behavior was modelized in Laforte (1989). The modulus of the layer (EMG) is time, stress and temperature dependant. The thickness of the layer is noted HG. The third layer is the layer formed in the subgrade soil between the base-course/ subgrade soil interface (given as XG) and the freezing front which depth HGEL is measured from the surface. The thickness of the third layer is given by the difference (HGEL - XG). Its modulus, EMS is also time, temperature and stress dependant.

The temperature is zero (T = 0°C) anytime at the freezing front and its depth (which is the model's limit) varies continually in response to the temperature changes at the surface of the pavement: nil when the winter starts; it stays in the base during early winter, and forms a two-layer pavement, the second layer being the material from the asphaltic concrete

FIGURE A1.1

Typical pavement section and stresses due to a thermal gradient



note: Sinusoidal surface Temperature
Xf = depth to freeze front
B = 6 to 10 m
L = distance between cracks

/base-course interface to the freezing front. Its thickness is the difference:

$$(HGEL - XA)$$

and also varies continually.

The model is a two-layer slab during early season, (up to the time at which HGEL = XG), and a tri-layer slab afterwards, up to the end of the winter season.

The temperature in the pavement varies and this creates thermal stresses, either bending thermal stresses or normal thermal stresses. The stress pattern in any layer is defined by the sum of a normal stress and a bending stress because any thermal differencial could be viewed as (figure A1.1):

1) a temperature change (dT) on the neutral axis
2) a temperature gradient in the layer = T1 - T2

where T1 is the temperature at the top of the layer; T2, the temperature at the bottom of the layer, and h, the thickness of the layer.

If the modulus changes with depth, the position of the neutral axis (Zo) is given by (Yang, 1972):

$$Zo = h\,(n/(n+1))$$

where n, ratio E(Top)/E(Bottom), a ratio of one giving the familiar: Zo = h/2.

The radius of curvature created by the temperature differential in between the top and the bottom of the layer is then given by:

$$1/R = Zo\ d^2w/dx^2 = 12\ M(z)/h = DIL\ (T1 - T2)/h$$

and the stress in the layer will be given by:

$$S = N/h + M\ Zo/I$$

(if we consider a constant width b) so that

$$S = E\ DIL\ (1/h)\left(\int_{-h/2}^{h/2} T(z)\,dz + Zo/I \int_{-h/2}^{h/2} T(z)\,z\,dz\right) \quad (a1.1)$$

Introducing the in-depth variation for the modulus, we have, after simplifying:

$$S = E\ DIL\ (\ dT + (n/(n+1)(T1 - T2)) \quad (a1.2)$$

which is the simplest form.

Assuming a well bounded material, restricted by the layer upon which it rests, the equations for Zo, distance to the neutral axis calculated from the bottom of the structure, and TMZ, mean temperature in the system depending on the temperatures in other layers as well, are (Swift and Heller, 1974, Burghreen, 1971):

$$Zo = \frac{\sum E_i (h_i + h_{i-1}/2)}{2 \sum E_i h_i} \qquad (a1.3)$$

$$TMZ = \frac{\sum E_i h_i DIL_i TM_i}{\sum E_i h_i} \qquad (a1.4)$$

so that the thermal stress in any layer i will be given by:

$$S_i = E_i (TMZ - DIL_i TM_i + (Zo - Z_i)/RT) \qquad (a1.5)$$

and:

$$Rt = \text{Composite radius of curvature} = \frac{E1\ h1(\ TM1 - DIL_i\ TM_i\ + \sum E_i h_i DIL_i MTM_i}{\sum E_i I_i + E1\ h1\ I1\ H/2}$$

E1, h1, TM1, DIL1, I1 refer to the first layer properties while those with indice i refer to the i layer, and where:

Tm_i = mean temperature differential in the i layer
E_i = Mean modulus/$(1-v_i)$
v_i = Poisson's ratio
I = inertia = b $h^3/12$
h = layer thickness
b = layer width
MTM = (T1 - T2)/h
T1 = temperature at the top of the layer
T2 = temperature at the bottom of the layer
TM = mean temperature measured at the neutral axis level

Measurement from the bottom of the system to the neutral axis of any layer will be always related to the actual neutral axis position in the given layer, which distance will be given using the modulus ratio (n).

MODELIZATION OF THE FROZEN GRANULAR BASE-COURSE MATERIAL

The initial temperature dependant modulus is given by (Laforte, 1989):

$$EMG\ (t = 0) = S/e = S/(A1 + (B1/So)S) \qquad (a1.6)$$

where A1, B1, So are material' constants, and the temperature dependancy is describe by linear relationship, as in :

$$EMG(T, 0) = A - B\ T \qquad (a1.6a)$$

where A and B are also material' constants. Equation a1.6a is used as a starting point, and the thermal stresses and strains are calculated in the following manner:

1) The procedure started using a mean modulus for the granular layer (EMG), which value is given as a function of temperature only (a1.6). A first approximation of the stress is then obtained using this modulus in the solution for thermal stresses in a multi-layer system (two or tri-layer slab model described before).

2) Using the stress calculated from (a1.2) and the basic stress-strain equation (a1.5), a new value for the stress is calculated from the following equations:

$$e = S/EMG \quad \text{(EMG from equation a1.6a, as a first guess)}$$

$$FZ = e - A1 - (B1/So)S - C\,S^{d} \ln t$$

$$DFZ = -(B1/So) - d\,C\,S^{d-1} \ln t$$

$$\text{new } S = \text{old } S - FZ/DFZ$$

The calculation is done with the Newton-Ralphston iteration procedure (Carnahan et al, 1969). The values of the constants are calculated from the mean temperature occuring in the layer at the time t after the starting of the loading process. This new value for the Stress (New S) defines the new modulus from equation a1.6a.

3) The calculation proceeds, holding T and t constant as long as the new modulus calculated from equation a1.6a is not equal to the modulus used in the thermal stress equation. The iteration is stopped when:

$$\text{old EMG} = \text{new EMG} +/- \text{Tol}$$

where Tol is the tolerance of about 0.5 %. The stresses in any layer can then be calculated from the mean modulus ((old EMG + new EMG)/2) of the granular layer in the multi-layer slab model.

This routine, which uses two iteration procedures, is repeated for each time step as the values for temperature and loading time are different and are needed to calculate the constants in the solution. At the end, the strain is calculated from the simple relationship:

$$e = S/EMG$$

In the procedure, EMG represents the mean value for the aggregate layer, and its value is given by:

$$EMG = (EMG\ (top) + EMG\ (bottom))/2$$

where top refers to the XA interface and bottom to the XG interface.

TEMPERATURE MODELIZATION

In first approximation, the air temperature is analysed as a sinusoidal wave, with both daily (1/24 hour) and annual (1/8760 hour) amplitude (A) and frequency of variation ($w = 2\ \pi\ f$). Air temperature then given by:

$$T(0,t) = To + A_d \sin(w_d\, t) + A_y \sin(w_y\, t)$$

where To, is the mean air temperature and the indices d and y refering to daily and yearly variations

The surface temperature (Tsurf) is calculated by the Barber (1957) model, the Depth to the freezing front is calculated from the Painter

and Aldritch (1959) equation, using the surface freezing index calculated from the surface temperature. The Surface Freezing Index is given by:

$$FI = \int_0^t |Tsurf| \, dt$$

where |Tsurf| is the absolute value of Tsurf. The depth to the freezing front (HGEL) is given by solving anytime:

$$A \, HGEL^2 + B \, HGEL + FI = 0$$

where:

A L/48 K B = L R_i/24
L latent heat in the freezing layer
K thermal conductivity at the freezing front
R_i thermal resistance in the i layers above the layer where the freezing front is located.

For the asphaltic layer, L= 0 and HGEL is calculated as:

$$HGEL = (24 \, FI \, K/Cv)$$

Cv being the heat capacity of the asphalt.

MULTI-LAYER THERMAL MODEL

The first layer is the asphaltic concrete layer. The other layers are the granular base-couse layer and the subgrade soil. When the pavement is still unfrozen, this layer is assumed to be of infinite depth, without a phreatic level. When the pavement is freezing, the bottom of the system is the depth to the freezing front, and there could be two or three layers. The temperatures at the interfaces of the layers are calculated using the Lachenbruch's (1959) two-layer model. If XA is the asphaltic concrete/base-course interface and XG, the base-course/subgrade interface, the temperature at XA is given by:

$$T(XA,t) = To + K_1 \, AD \exp(-H) \sin(w_1 t - dF_1 - a1) + K_2 \, AY \sin(w_2 t - dF_2 - a2)$$

where:

To = mean annual temperature
AD = amplitude of the daily temperature variation
AY = amplitude of the annual temperature variation
XA = Thickness of the asphaltic layer
Ka,Ca = Thermal conductivity and heat capacity of AC
Kg,Cg = Thermal conductivity and heat capacity of base course
as = Ka/Ca = thermal diffusivity of the asphaltic concrete

and:

$K_i = (1 + M)/8_i$

w_i = period of the variation

dF_i = dephasing factorgiven by:

$$ATN(dF_i) = ((1-KT)/(1+KT)) \tan(-H_1)$$

$$KT = M^2 \exp(-H_i)$$

$$M = ((Ka \, Ca)^{1/2} - (Kg \, Cg)^{1/2}) / ((Ka \, Ca)^{1/2} + (Kg \, Cg)^{1/2})$$

$$S_i^2 = 1 + 2M \exp(-2H_i)\cos(2H_i) + M^2\exp(4H_i)$$

$$H_i = XA\,(w_i/(2\,as))^{1/2}$$

(i= 1 relates to a daily variation (2 pi/24) and i= 2, to the annual variation (2 pi/8766)).

The product $(K\,C)^{1/2}$ is the thermal inertia of the layer (Symbol Q).

The equation also calculates the reduced amplitude and the shifting factor at any depth in a multi-layer system, introducing an "equivalent first layer" which thermal conductivity (Ke), specific heat (Ce) or thermal diffusivity (ae) are given by:

$$ae = Ke/Ce$$

$$Ke = \sum H_i/R_i$$

$$Ce = \sum H_i\,at_i/\,Re$$

$$R_i = H_i/K_i$$

$$Re = \sum Ri$$

the layer being a composite of i layers.

This equivalent layer model is modelized in the computer program:

a) When there are only two layers:
  First layer : asphaltic concrete
  Second layer: frozen granular material above the freezing front.

b) When there are three layers:
  First layer : asphaltic concrete
  Second Layer: base-course
  Third layer : Frozen soil above the freezing front.
  In this case, the equivalent layer is given by:
  $He = XA + HG$
where HG is the base-course thickness.

When the freezing front is at an interface, the latent heat replaces the heat capacity to evaluate the thermal inertia of the layer QF, which equals:

$$QF = (K_i\,L_i)^{1/2}$$

The indice refers to the material which is freezing.

APPENDIX II

REFERENCES

AKILI, W.; "Stress-strain Behavior of Frozen Fine-Grained Soils". Highway Research Board, Record 360, p.1-8 (1971)

BARBER, E.S.; "Calculation of Maximum Pavement Temperature from Weather Records", Highway Research Board Bulletin 168, p. 1-7, (1959)

CARNAGAN, B., LUTHER, H.A., WILKES, J.O.; "Applied Numerical Methods", John Wiley, New York, 604 pp. (1969)

CHEN, N.J., DiVito, J.A., Morris, G.R.; "Finite Elements Analysis of Arizona's Three Layers Overlay System over Rigid Pavements to Prevent Reflective Cracking". Proc. AAPT, Vol 51, p. 150-168

CHRISTISON, J.T., ANDERSON, K.O.; "The Response of Asphalt Pavements to Low Temperature Climatic Environment"; Proc. 3rd Intl Conf. Structural Design of Asphalt Pavement Structure, London (1972)

FINN, F., SARAF, C.F., KULKARNI, R., NAIR, K., SMITH, W., ABDULLAH, A.; "Development of Pavement Stuctural Subsystems". National Cooperative Highway Research Program Report 291, Dec 1986, 59 pp. (1986)

HEUKELOM, W.; "A Bitumen Test Data Chart for Showing the Effect of Temperature on the Mechanical Behavior of Asphaltic Bitumens", Journal of the Institute of Petroleum, Vol 55, No 546 (1969)

JOHNSTON, G.H., ed.; "Permafrost, Engineering Design and Construction", John Whiley and Sons, 540 pp. (1981)

LACHENBRUCH, A.H.; "Periodic Heat Flow in a Stratified Medium with Applications in Permafrost Problems", U.S. Geological Survey, Bulletin 1052, p 51-79 (1959)

LAFORTE, M.A.; "Influence du comportement des matériaux de fondations gelés sur la fissuration des pavages par temps froids," Thèse PhD, Génie Civil, Ecole Polytechnique de Montréal, 400 pp. + annexes (1989)

LAFORTE, M.A.; "Vérification du modèle présenté sur des cas simples", Technical Note presented to the Thesis Committee, Ecole Polytechnique, Sept 1989 (1989a).

MCLEOD, N.W.; "Transverse Pavement Cracking Related to the Hardness of the Asphalt Cement" , Proc. Can. Technical Asphalt Ass., Vol 13, (1968)

PAINTER, R.S., ALDRICH, P.A.; "Frost Penetration Below Highway and Airfield Pavements", Highway Research Board Bulletin 135, p. 135-144, (1959)

SWIFT, G.W., HELLER, R.A.; "Layered Beam Analysis", J.Eng.Mec. Div., A.S.C.E., EM-2, Vol 100, p. 267-282 (1974)

U.S. ARMY CORPS OF ENGINEERS; "Calculation Methods for Determination of Depths of Freeze and Thaw in Soils", U.S. Army Technical Manual TM 5-852-6 (1966)
VAN DER POEL, C.; "A General System Describing the Visco-elastic Properties of Bitumens and its Relation to Routine Tests Data", J. Applied Chemistry, Vol 4, p 221 ss. (1954)

WILSON, C.V.; "Le Climat du Québec: Notes sur les Echanges d'Energies", Climatic Studies No 23, Canada Environment, 124 pp. (1972)

YANG , N.C.; "Design of Functionnal Pavements", McGraw-Hill, (1972)

Low Temperature Fracture Mechanics of Viscoelastic Pavement Structures

A. Selvadurai, M.C. Au, Carleton Univ.
P. Joseph, Ministry of Transportation, Ontario

LOW TEMPERATURE FRACTURE MECHANICS OF VISCOELASTIC PAVEMENT STRUCTURES

A.P.S. Selvadurai and M.C. Au
Department of Civil Engineering
Carleton University
Ottawa, Ontario, Canada K1S 5B6
and
P. Joseph
Pavement and Roadway Office
Research and Development Branch
Ministry of Transportation of Ontario
Downsview, Ontario, Canada M3M 1J8

ABSTRACT

The paper presents the application of a numerical method of transient stress analysis to the study of the mechanical behaviour of a pavement structure which is subjected to heat conduction and associated thermo-viscoelastic effects. The numerical analysis is based on a finite element modelling of the governing equations. Heat conduction is induced by the sudden reduction of the surface temperature of the layered pavement structure. The single viscoelastic layer of the idealized pavement structure contains a surface crack of finite depth. The numerical analysis focusses on the evaluation of the time dependent variation of the crack opening mode I stress intensity factor at the crack tip. The paper documents the manner in which the crack opening mode stress intensity factor is influenced by the viscoelastic properties of the asphalt layer.

I. INTRODUCTION

The study of the mechanical behaviour of pavement structures which are subjected to the influences of low temperatures is recognized as an important aspect of enhancing pavement performance and design. These studies become more important in situations where defects such as cracks, delaminations, voids etc. are induced in the asphalt pavements and overlays either during its construction or during its service life. The International Conferences on Paving in Cold Areas [1,2] and recent articles and reviews [3,4] associated with low temperature properties and performance of asphalt cements have emphasized the role of low temperature on the development of short term and long term damage in asphalt pavements.

Recently, Selvadurai and Au [5] conducted a comprehensive examination of the low-temperature behaviour of a cracked pavement structure which is subjected to the combined effects of heat conduction and associated thermo-elastic effects. The objective of that study was to examine the influence of low temperatures on the behaviour of existing cracks and other flaws in the asphalt pavement. It is assumed that such flaws can be created either during construction of the pavement or during its service life. When the pavement is subjected to sudden cooling by ambient temperatures, thermal stresses can develop in the asphalt layer. Such thermal stresses will have the adverse effect of enhancing the propagation of cracks and flaws in an asphalt layer. The transient thermo-elastic modelling and the associated numerical schemes for the analysis of heat conduction, stress analysis and fracture mechanics were used extensively to examine a variety of problems of interest to low temperature performance of damaged or cracked pavements [6].

This paper extends the work in [5] to include the combined influences of heat conduction within the pavement structure and viscoelastic behaviour of the asphalt surface layer, on the mechanics of cracks and other surface defects located in an asphalt layer. Viscoelastic properties of asphalts and asphalt concrete have been studied by various researchers [4,7-13]. The results of such research [4] indicate the existence of viscoelastic or time dependent effects in aged asphalts even at temperatures of the order of -9°C. In general the influences of viscoelastic behaviour would be expected to dominate with increases in asphalt temperature beyond 0°C. Consequently it is important to establish the influences of viscoelastic asphalt behaviour on the performance of fractures

located in an asphalt layer. This paper briefly outlines the numerical treatment of the transient stress analysis of a pavement structure which is subjected to heat conduction in the presence of thermo-viscoelastic effects. The finite element technique is used to examine the heat conduction process, the viscoelastic behaviour and the modelling of surface defects or cracks located in the viscoelastic asphalt layer. The numerical treatment of the damaged pavement focusses on the evaluation of the time-dependent stress intensity factors at the crack tip. This is a measure of the energy that can be released while propagating the crack further. The numerical modelling also attempts to establish the influence of thermo-viscoelastic response of the asphalt material on the behaviour of the crack tip stress intensity factor. Specific numerical results presented in the paper illustrate the manner in which the viscoelastic behaviour of the asphalt influences the stress intensity factor at the tip of a surface crack located in a layered pavement structure, which is subjected to a sudden lowering of its surface temperature.

2. GOVERNING EQUATIONS

In this section we shall present a brief account of the fundamental equations governing the transient thermo-viscoelastic behaviour as an asphalt composite material. Detailed accounts of these developments are also given by Williams [14], Lee [15], Leitman and Fisher [16] and Christensen [17]. The state of stress in the viscoelastic medium is defined by the stress tensor $\sigma_{ij}(x_i, t)$ and the displacement field is defined by $u_i(x_i, t)$ where t is the time variable and x_i are the coordinates. In the absence of dynamic effects, the equations of equilibrium are given by

$$\sigma_{ij,j} + b_i = 0 \quad ; \quad x_i \epsilon D \tag{1}$$

where D is the region under consideration, the subscripts indicate directions x, y, z (or 1,2,3) and repeated indices are summed over the range of the subscripts. The equation governing the heat conduction in the viscoelastic body, which includes the heat source (or sink) term due to mechanical effects, can be written as

$$(kT_{,i})_{,i} - \rho c\dot{T} + T_0\beta\dot{\epsilon}_{ll} + Q = 0 \quad ; \quad x_i \epsilon D \tag{2}$$

where, k is the coefficient of thermal conductivity, c is the specific heat, ρ is the mass density, Q is the heat source term other than mechanical effect, T_0 is the initial temperature distribution when the medium is unstrained and $(\dot{})$ denotes the time derivative. The linearized strain tensor is defined by

$$\epsilon_{ij} = \frac{1}{2}(u_{i,j} + u_{j,i}) \tag{3}$$

The boundary conditions for the heat conduction process are

$$T = \overline{T} \quad \text{on} \quad x_i \epsilon S_1 \tag{4}$$

$$k\frac{\partial T}{\partial n} = \overline{q} \quad \text{on} \quad x_i \epsilon S_2 \tag{5}$$

where $\overline{T}$ is the value of the prescribed temperature on the surface S_1; $\overline{q}$ is the rate of heat loss at the boundary S_2 and the total surface is given by $S = S_1 \bigcup S_2$. The displacement and traction boundary conditions are given by

$$u_i = \overline{u}_i \quad \text{on} \quad x_i \epsilon S_3 \tag{6}$$

$$\sigma_{ij} n_j = \overline{P}_i \quad \text{on} \quad x_i \epsilon S_4 \tag{7}$$

where $\overline{u}_i$ are prescribed displacements n_j is the outward unit normal to S_4 and $\overline{P}_i$ are prescribed tractions. For the linear viscoelastic material, the stress or strain depends on the history of deformation. The appropriate constitutive relationship which takes into account such history effects can be expressed in the form of a hereditary integral of the form

$$\begin{aligned} \sigma_{ij}(x_i, t) &= R_{ijk\ell}(0)\{\epsilon_{k\ell}(x_i, t) - \alpha(0)\theta(x_i, t)\delta_{k\ell}\} \\ &\quad - \int_0^t \frac{\partial}{\partial \tau}[R_{ijk\ell}(t-\tau)]\{\epsilon_{k\ell}(x_i, \tau) - \alpha(T)\theta(x_i, t)\delta_{k\ell}\}\, d\tau \end{aligned} \tag{8}$$

where $\theta(t)$ is the "pseudo-temperature" which will be discussed later and $R_{ijk\ell}(t)$ is the relaxation modulus at time t which is given by

$$R_{ijk\ell}(t) = K(t)\delta_{ij}\delta_{k\ell} + G(t)\left\{\delta_{ik}\delta_{j\ell} + \delta_{i\ell}\delta_{jk} - \frac{2}{3}\delta_{ij}\delta_{k\ell}\right\} \tag{9}$$

where $K(t)$ and $G(t)$ are respectively the bulk and shear modulus of the material. For example, for a linear elastic material $K(t) = K(0) = K$ and $G(t) = G(0) = G$. The 4th order tensor $R_{ijk\ell}(t)$ reduces to the generalized elasticity tensor $C_{ijk\ell}$ presented in the previous study [5]. The determination of K(t) and $G(t)$ will be discussed in a later section.

The initial conditions governing the transient problem can take the forms

$$T = T_0 \quad ; \quad x_i \epsilon D \tag{10}$$

and

$$u_i = u_i(0) \quad ; \quad x_i \epsilon D \tag{11}$$

3. VISCOELASTIC CONSTITUTIVE RELATIONS

Engineering materials such as concrete, geological media, polymeric materials, asphalts and metals at elevated temperatures exhibit time dependent behaviour over certain ranges of loading and temperature. These time dependent phenomena can be characterized either by creep processes or by viscoelastic processes. In general the time dependent processes governing materials such as asphalt, concrete and other geological media are highly non-linear in character. The nonlinearities can be attributed to influence of large strains and rate dependence. The theory of linear viscoelasticity, can be conveniently employed to examine the time-dependent processes in asphaltic materials [4,7-13].

Extensive accounts of the theory of linear viscoelasticity are given in the texts by Flugge [18], Selvadurai [19], Findley and Lai [20] and Christensen [17]. The simplest forms of representation of viscoelastic behaviour utilize basic viscoelastic elements which consist of elastic and viscous responses. These basic responses can be combined to form viscoelastic models such as those described by Kelvin, Maxwell and multiparameter models [18]. These discrete viscoelastic representations are however restrictive in their general applicability. An alternative procedure employs a combination of these basic models to form a generalized viscoelastic response. In general, such a viscoelastic stress-strain relationship can be written as

$$\sum_{r=0}^{N_\sigma} p_r \frac{\partial^r(\sigma)}{\partial t^r} = \sum_{r=0}^{N_\epsilon} q_r \frac{\partial^r(\epsilon)}{\partial t^r} \tag{12}$$

where N_σ and N_ϵ are the number of operators and p_r and q_r are constant coefficients. The time derivatives of (12) can be eliminated by the application of the Laplace transform which is defined by

$$[\overline{\sigma}(s) \;;\; \overline{\epsilon}(s)] = \int_0^\infty [\sigma(t) \;;\; \epsilon(t)]\, e^{-st} dt \tag{13}$$

where s is the transform parameter and therefore (12) can be rewritten in the form

$$\left[\sum_{r=0}^{N_\sigma} p_r s^r\right] \overline{\sigma}(s) = \left[\sum_{r=0}^{N_\epsilon} q_r s^r\right] \overline{\epsilon}(s) \tag{14}$$

which is an algebraic equivalent of (12) and the transform equivalent of the stress σ is given by

$$\overline{\sigma}(s) = \sum_{r=0}^{N_\sigma} \left(\frac{c_r}{a_r s + b_r}\right) \overline{\epsilon}(s) \tag{15}$$

where a_r, b_r and c_r are constants which are derived from the representation of (14) in terms of partial fractions. Since the right-hand-side of (15) is expressed by a series summation of two Laplace transforms, the inverse transforms of the left-hand-side of (15) can be obtained by means of a convolution integral. Consequently the stress-strain relationship for the linear viscoelastic material can be expressed in an integral form as

$$\sigma(t) = R(0)\epsilon(t) - \int_0^t \frac{\partial R(t-\tau)}{\partial \tau}\epsilon(\tau)d\tau \tag{16}$$

where $R(t)$ is known as the "Relaxation Modulus" and takes the value of either $K(t)$ or $G(t)$ depending upon the "dilational" or "distortional" processes respectively, i.e.,

$$R(t) = \begin{cases} K(t) & \text{for dilational effects} \\ \\ G(t) & \text{for distortional effects} \end{cases} \tag{17}$$

Considering the right-hand-side of (15), $R(t)$ is expected to have the form

$$R(t) = \sum_{r=0}^{N_\sigma} A_r \exp(-B_r t) \tag{18}$$

where $A_r = c_r/a_r$ and $B_r = b_r/a_r$. The result (18) is known as a Dirichlet series representation of the relaxation function. Such a representation has two advantages related to the following:

(a) In relating experimental data to theoretical models, the constants A_r and B_r can be determined by a smooth curve fitting procedure [21].

(b) In the formulation of a numerical algorithm of a step-by-step time integration which accounts for the progression of viscoelastic behaviour.

The discussions related to viscoelastic constitutive behaviour presented earlier do not take into account the effect of temperature on the viscoelastic stress-strain relationships. Hence, the relaxation modulus $R(t)$ given in (18) is essentially an isothermal viscoelastic response at $T = T_0$.

In general, for a thermo-viscoelastic material such as asphalt concrete

$$R_{ijkl} = R_{ijkl}(t, T) \tag{19}$$

where the constitutive tensor has to be determined from experiments. The experimental evaluation of the thermo-viscoelasticity tensor is a complicated task. The number

of experiments will be inordinately high and the transient thermo-mechanical effect cannot be eliminated in the experimental procedure. Fortunately, both theoretical and experimental results indicate that for a certain class of material, the *effect of temperature and time on the relaxation modulus can be combined.* That is, the relaxation modulus at a certain temperature T can be obtained from the corresponding relaxation modulus at a given temperature T_0; i.e.,

$$R(T,t) = R(T_0, \zeta(t)) \tag{20}$$

where $\zeta(t)$ is the "reduced time" and the class of viscoelastic materials which satisfy a relationship of the type (20) are known as "thermo-rheologically simple materials" (see e.g., Schwarz and Staverman [22]). The reduced time $\zeta(t)$ is given by [22]

$$\zeta(t) = \int_0^t \frac{d\tau}{\psi[T(\tau)]} \tag{21}$$

where $\psi(T)$ is the temperature shift factor. The most commonly employed shift factor in thermo-viscoelastic stress analysis is the Williams, Landel and Ferry [23] result or the WLF equations

$$\log_{10}[\psi(T)] = \frac{-g_1(T - T_0)}{g_2 + (T - T_0)} \tag{22}$$

where g_1 and g_2 are material constants. Further, if the temperature effect on the expansion properties of the thermo-viscoelastic material is considered, an average effect of the expansion/contraction processes can be derived. That is, the "pseudo-temperature" defined previously (see (8)) is given by

$$\theta(t) = \frac{1}{\alpha(0)} \int_{T_0}^{T} \alpha(\tau) d\tau \tag{23}$$

Therefore, when $\alpha(T) = \alpha(0)$, $\theta(t) = T(t)$. Using these developments the integral law for the *dilational effect* can be expressed by

$$\sigma_{ii}(t) = 3K(0)\left[\epsilon_{ii}(t) - 3\alpha(0)\theta(t)\right]$$

$$- \int_0^t \frac{\partial}{\partial \tau}\left[3K(\zeta - \tau)\right]\left\{\epsilon_{ii}(\tau) - 3\alpha(T)\theta(\tau)\right\} d\tau \qquad (24)$$

and for the *distortional effect*,

$$\sigma_{ij}^D(t) = 2G(0)\epsilon_{ij}^D(t)$$

$$- \int_0^t \frac{\partial}{\partial \tau}\left[2G(\zeta - \tau)\right]\epsilon_{ij}^D(\tau) d\tau \qquad (25)$$

The complete hereditary integral given in (8) can be obtained by the combined effect of dilatation (24) and distortion (25) responses.

4. NUMERICAL MODELLING

The solution of the equations of transient thermo-viscoelasticity described in Sections 2 and 3 can be approached in a variety of ways. These include analytical methods based on integral transform techniques and numerical methods based on finite difference, finite element and boundary integral equation techniques. In this study, the finite element technique is used to solve the governing thermo-viscoelasticity problem. The finite element technique can, conveniently, take into account the constraints imposed by the pavement geometry, the crack tip behaviour and the time and temperature dependent constitutive properties. The complete details of the Galerkin finite element technique utilized in the solution of the transient thermo-viscoelasticity problem is discussed by Selvadurai and Au [24].

Finite Element Procedure

Considering the governing equations (2), (4) and (5) we have

$$\int_D \left\{k\delta T_{,i} T_{,i} + \rho c \delta T \dot{T}\right\} dD - \int_{S_2} \delta T \bar{q} dS = 0 \qquad (26)$$

where δT is a weighting function for temperature. Similarly, the global equilibrium equation (1) can be written in the form

$$\int_D \delta\epsilon_{ij} R_{ijk\ell} * d\{\epsilon_{k\ell} - \alpha\theta\delta_{k\ell}\}\, dD - \int_D \delta u_i b_i dD - \int_{S_t} \delta u_i \overline{P}_i dS = 0 \qquad (27)$$

where δu_i is a weighting function for the displacements, and $R_{ijk\ell}$ is the thermo-viscoelastic constitutive tensor and $(*)$ denotes a convolution.

Following a standard finite element procedure [24-26], equations (26) and (27) can be expressed as matrix equations

$$[K_{TT}]\{T(t)\} + [M_{TT}]\left\{\dot{T}(t)\right\} = \{P_T(t)\} \qquad (28)$$

and

$$\begin{aligned}[K_{uu}(0)]\{u(t)\} - \int_0^t [K_{uu}(\zeta-\tau)]\{u(\tau)\}\, d\tau \\ + [K_{uT}(0)]\{\theta(t)\} - \int_0^t [K_{uT}(\zeta-\tau)]\{\theta(\tau)\}\, d\tau \\ = \{P_u(t)\} \qquad (29)\end{aligned}$$

respectively, where $[K_{uu}(t)]$, $[K_{TT}]$, $[M_{TT}]$, ... etc. are volume integrals taken over the domain. Complete expressions for these matrices are given by Selvadurai and Au [24]. It is sufficient to note that the displacement equation (29) is a system of integral equations of the Volterra type. It follows that the current displacement in the viscoelastic medium has to be determined from the consideration of the complete history of deformation and temperature.

Time Integrations

Following previous studies [5,6], for the temperature unknowns, the time integration is given by

$$[[M_T] + f\Delta t\,[K_{TT}]]\,\{T(t+\Delta t)\}$$

$$= \{P_T\} - [[M_T] + (1-f)\,\Delta t\,[K_{TT}]]\,\{T(t)\} \qquad (30)$$

where Δt is the time-step and f is the scale factor ($0.5 < f < 1.0$).

For the displacement field, the governing matrix equation is a system of simultaneous Volterra integral equations of the second kind. A standard numerical method for solving this class of equations is the step-forward integration procedure, where all past solutions are required in the integration with respect to time. However, the implementation of such a procedure in the finite element scheme is virtually impossible owing to the limitations of computer storage and CPU time. In this context, the Dirchlet series representation of the relaxation moduli allows us to formulate a step-by-step time integration procedure such as the one proposed by Taylor, Pister and Goudreau [27] and Srinatha and Lewis [28].

Following these developments the system of integral equations (29) can be reduced to a recurrence relationship of the form:

$$[K_{uu}(0) + K^*_{uu}(\Delta\zeta)]\,\{u(t+\Delta t)\}$$

$$= \{P_u(t+\Delta t)\} + \{P^{me}_u(t)\} + \{P^{me}_T(t)\}$$

$$+ [K^*_{uu}(\Delta\zeta)]\,\{u(t)\} + [K^*_{uT}(\Delta\zeta)]\,\{\theta(t)\}$$

$$- [K_{uT}(0) + K^*_{uT}(\Delta\zeta)]\,\{\theta(t+\Delta t)\} \qquad (31)$$

where $\{P^{me}_u(t)\}$ and $\{P^{me}_T(t)\}$ are the memory loads due to, respectively, the deformation and the temperature up to time t.

Now, equations (30) and (31) are the time-stepping equations for both the temperature

and the displacement. The solution procedure can be started by making use of the initial conditions (10) and (11).

Crack-Tip Elements

In the available literature on viscoelastic fracture mechanics analysis (see e.g, Knauss [29], Francis, Carlton and Thompson [30] and Schapery [31]) the stress distribution near the tip of a stable crack is assumed to be of $\frac{1}{\sqrt{r}}$ type. Therefore, the quarter-point element of Henshell and Shaw [32] and Barsoum [33] is applicable in the present modelling. In the previous study (Selvadurai and Au [4]), the stress intensity factor can be evaluated by the nodal displacements along rays emanating from the crack-tip (Figure 1). For completeness, the expressions are given below as

$$K_I \quad \left\{ \begin{array}{l} (2\gamma-1)\cos\frac{\tilde{\theta}}{2} - \cos\frac{3\tilde{\theta}}{2} \\ \\ (2\gamma+1)\sin\frac{\tilde{\theta}}{2} - \sin\frac{3\tilde{\theta}}{2} \end{array} \right\}$$

$$= \frac{4G(t)}{\sqrt{\ell_i/2\pi}} \left\{ \begin{array}{l} 4u_{x2} - u_{x3} - 3u_{x1} \\ \\ 4u_{y2} - u_{y3} - 3u_{y1} \end{array} \right\} \tag{32}$$

and

$$K_{II} \quad \left\{ \begin{array}{l} (-2\gamma+3)\sin\frac{\tilde{\theta}}{2} - \sin\frac{3\tilde{\theta}}{2} \\ \\ (2\gamma-3)\cos\frac{\tilde{\theta}}{2} + \cos\frac{3\tilde{\theta}}{2} \end{array} \right\}$$

$$= \frac{4G(t)}{\sqrt{\ell_i/2\pi}} \left\{ \begin{array}{l} 4u_{x2} - u_{x3} - 3u_{x1} \\ \\ 4u_{y2} - u_{y3} - 3u_{y1} \end{array} \right\} \tag{33}$$

with $\ell_i = \ell_1$ or ℓ_2 defined in Figure 2. Also $\tilde{\theta}$ is considered to be either 0° or 180°. In (32) and (33), γ is given by

$$\gamma = \left\{ \begin{array}{ll} \frac{3K(t)+7G(t)}{3K(t)+G(t)} & (\text{plane} - \text{strain}) \\ \\ \frac{15K(t)+8G(t)}{9K(t)} & (\text{plane} - \text{stress}) \end{array} \right. \tag{34}$$

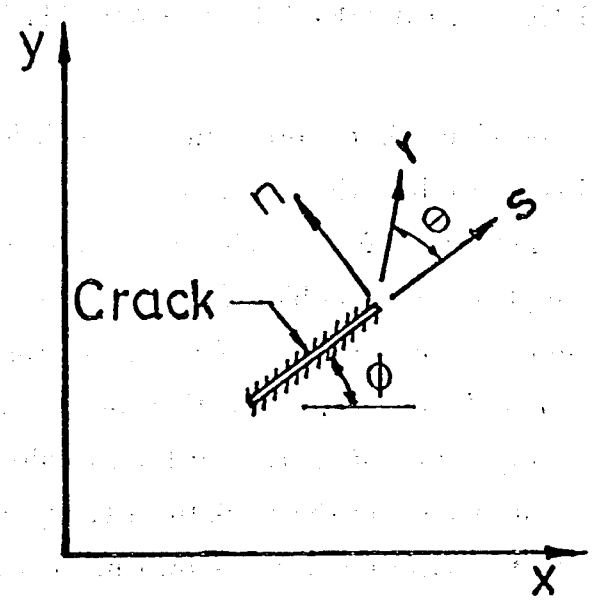


Figure 1. The geometry and coordinate system at the crack tip

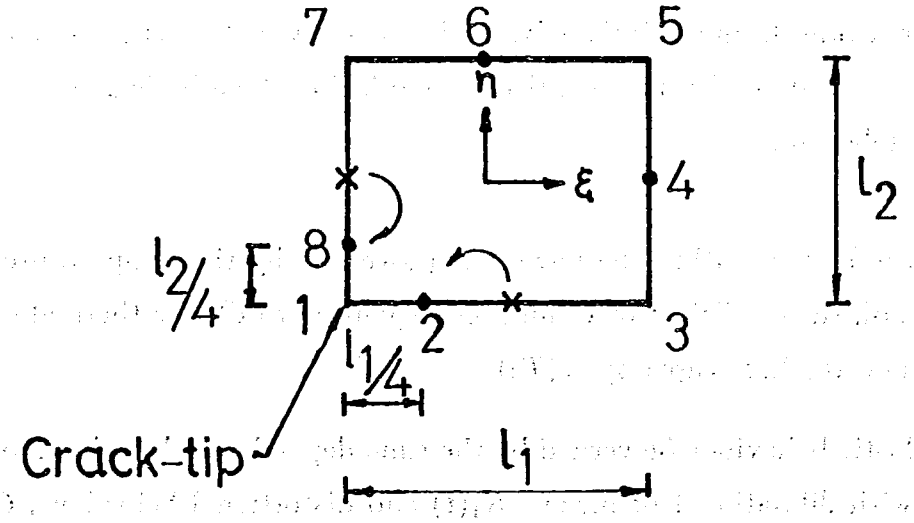


Figure 2. The quarter-point element

where $K(t)$ and $G(t)$ are the relaxation moduli given by (17).

5. CRACKS IN A VISCOELASTIC PAVEMENT LAYER

The numerical procedure developed in the preceding section is first applied to examine the transient thermo-viscoelastic behaviour of a pavement layer with a surface crack (Figure 3) underlain by an elastic halfspace. The attention is restricted to the examination of two dimensional plane strain problem in which the surface of the viscoelastic layer is subjected to a sudden decrease in the surface temperature, in the form of a step function of time. The results of previous investigations [5,6] have shown that the rapid reduction in the surface temperature of the asphalt layer results in the development of the maximum stress intensity factors at the crack tip. (The geometry of the pavement layer region in relation to the surface crack is shown in Figure 3 and the system is restrained from horizontal movement at the extreme boundaries. These are frictionless restraints.) The surface temperatures are prescribed by the following conditions

$$\begin{aligned} T(x,y) &= T_0 \quad \text{for } t = 0 \\ T(x,0) &= T_s H(t) \quad \text{for } t > 0 \end{aligned} \tag{35}$$

In order to perform the numerical analysis it is necessary to define the thermo-viscoelastic parameters associated with the constitutive modelling. The basic groups of materials parameters relate to:

(i) heat conduction within the pavement (governed by the temperature dependent values of, the coefficient of volumetric expansion $\alpha(T)$, the thermal conductivity $k(T)$ and the heat capacity $\rho c(T)$).

(ii) viscoelastic behaviour (governed by the time-dependent relaxation moduli associated with dilatational behaviour $K_1(t)$ and distortional behaviour, $G_1(t)$ of the viscoelastic medium).

For the purpose of the numerical computations we shall assume that the thermal properties $\alpha(T)$, $k(T)$ and $\rho c(T)$ are relatively uninfluenced by the temperature and are

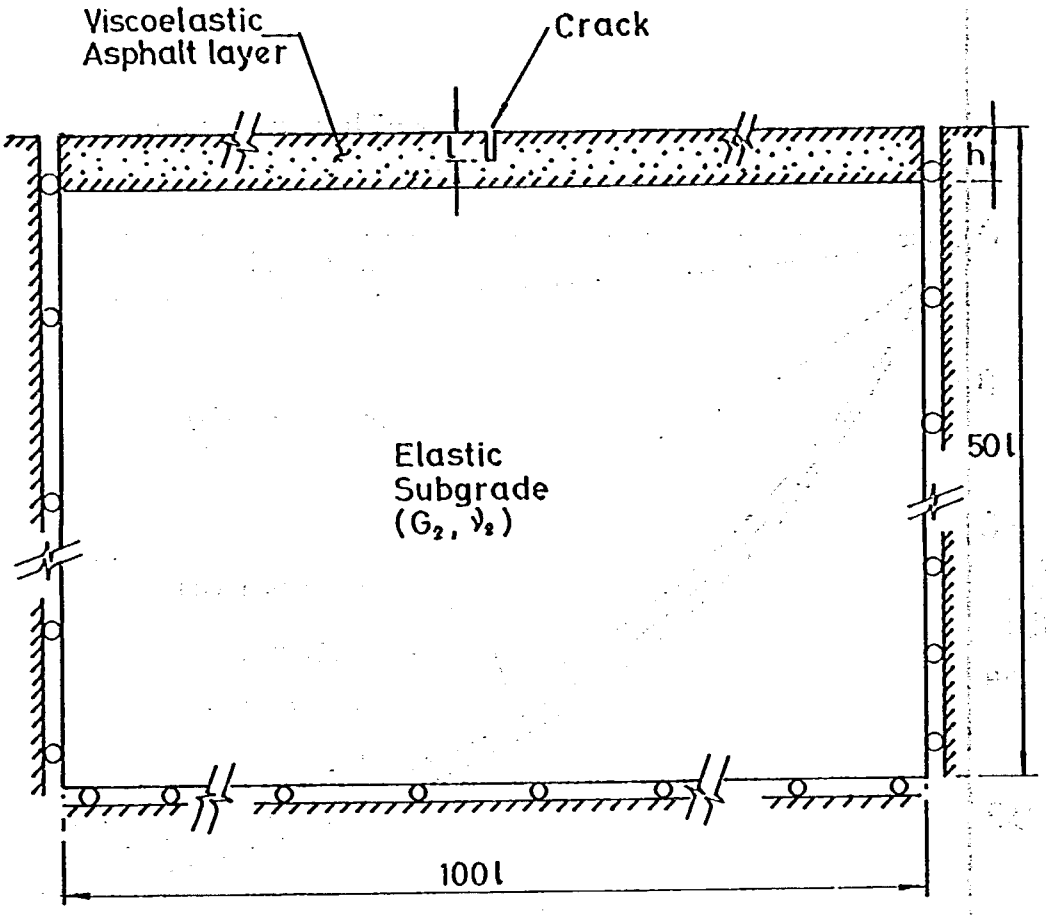


Figure 3. A surface crack in a viscoelastic layer resting on an elastic medium

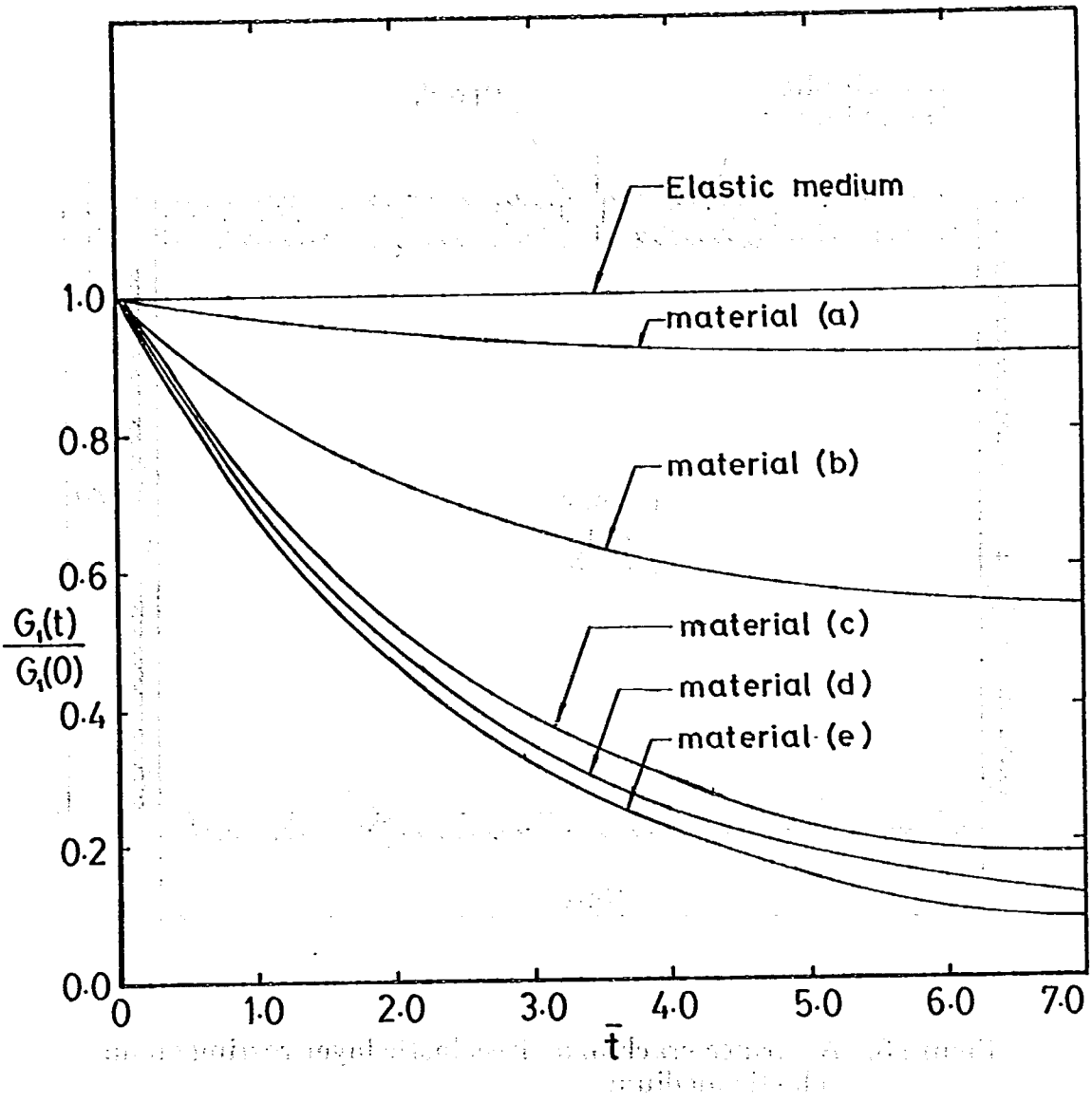


Figure 4. Relaxation functions for the viscoelastic shear modulus. Material types (a) to (e) are given in Table 1.

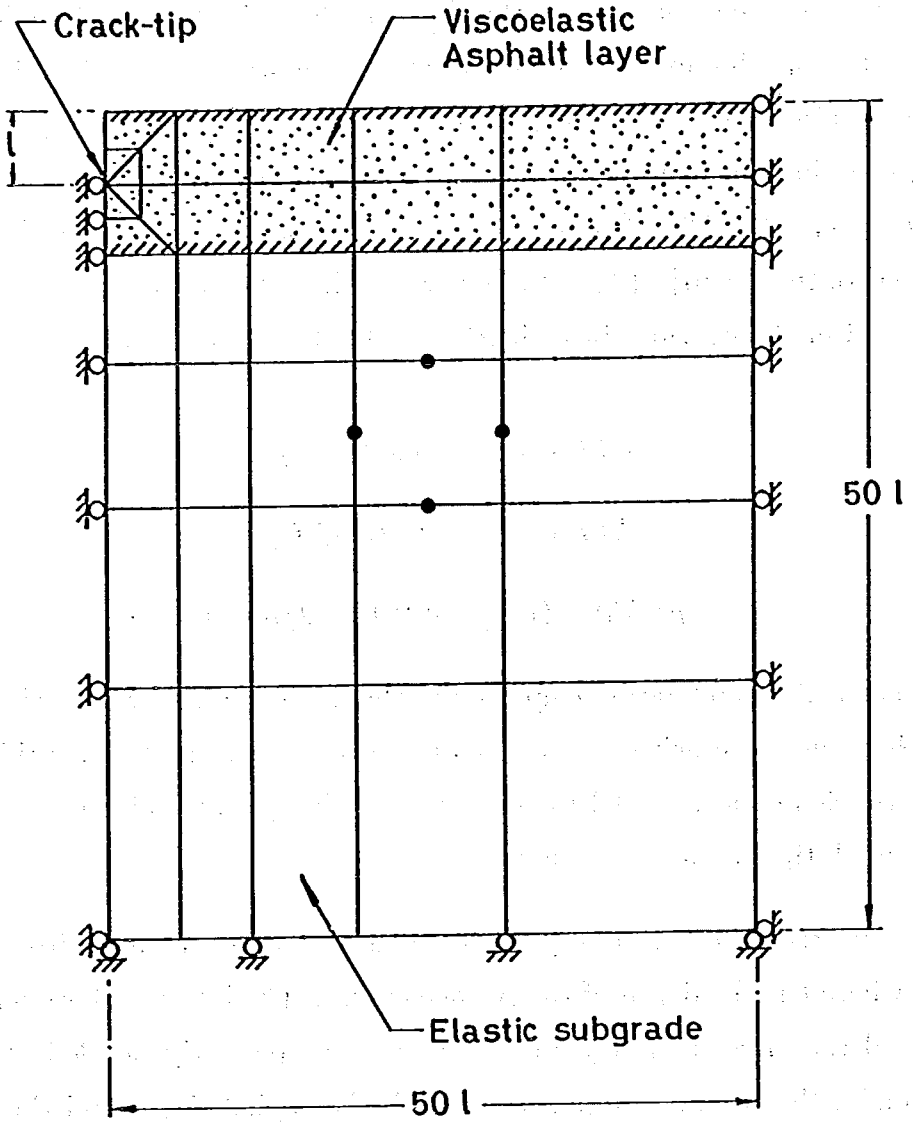


Figure 5. The finite element discretization of the viscoelastic layer and the elastic medium.

assumed to be constant. We shall further assume that the dominant mode of viscoelastic behaviour relates to the shear behaviour of the material (defined by $G_1(t)$) and that the dilatation or volumetric behaviour (defined by $K_1(t)$) of the material is non relaxing and constant in time. For the linear viscoelastic shear behaviour we consider five types of typical materials where the shear modulus $G_1(t)$ have decaying variations with time. The specific expressions for $G_1(t)$ are shown in Table 1 and the Figure 4 shows the variations of $G_1(t)/G_1(0)$ with time. The surface of the layer is subjected to the rapid reduction in the surface temperature T_s such that the thermal jump is given by $T = |T_s - T_0|$. The effect of temperature on $G_1(t)$ is accounted for by the shift function $\psi(t)$ of the $A\exp[-(T_s - T)/T_s]$ type. The values of $\alpha(T_0)$, $k(T_0)$ and $\rho c(T_0)$ are those used in the previous investigations [5,6]. For completeness we note that

$$\begin{aligned} \alpha(T_0) &= \alpha_0 = 5 \times 10^{-6} \quad /^\circ C \\ k(T_0) &= k_0 = 2 \quad J/m/^\circ C/S \\ \rho c(T_0) &= (\rho c)_0 = 4 \times 10^6 \quad J/m^3/^\circ C \end{aligned} \tag{36}$$

The finite element discretization employed in the numerical analysis of the viscoelastic region with a surface crack is shown in Figure 5. The formulation utilizes 8-noded isoparametric elements to model the domain and the quarter-point element is used to model the crack tip singular behaviour.

The pavement structure is laterally constrained at a finite distance from the surface crack 50ℓ; where ℓ is the depth of the surface crack). The interface between the elastic subgrade and the viscoelastic layer is assumed to be perfectly bonded. For purposes of the example, the thermal properties of both the asphalt layer and the elastic subgrade are assumed to be time and temperature independent. It is also assumed that the thermo-viscoelastic behaviour of the asphalt layer is characterized by a dilatation behaviour which is non-relaxing. In addition to these, two other non-dimensional parameters are important to the discussion of the thermo-viscoelastic behaviour of the composite pavement; these relate to the pavement-subgrade relative shear modular ratio defined by $G_1(t)/G_2$ where G_2 is the shear modulus of the elastic subgrade and the layer thickness-crack length aspect ratio h/ℓ. Again, for purposes of illustration we assign the following specific values for these parameters; $h/\ell = 2$ and $G_1(0)/G_2 = 0.1, 0.01$. The

finite element discretization of the asphalt layer-subgrade system is shown in Figure 5. The Figures 6 to 11 illustrate the manner in which the normalized stress intensity factor K_I^* at the crack tip located in the viscoelastic layer is influenced by the relaxation phenomena in the viscoelastic layer, the temperature shift $\psi(T)$ and the modulus mismatch between the elastic subgrade and the layer. The normalized stress intensity factor $\overline{K}_I^*$ and the normalized time t are related to the stress intensity factor K_I and time t according to the following

$$\overline{K}_I^* = \frac{K_I\sqrt{2\ell}}{G_1(0)\alpha_0 T_s} \; ; \; \bar{t} = \frac{tk_0}{\ell^2(\rho c)_0} \tag{37}$$

The equivalent results for the stress intensity factors derived for the surface crack located in viscoelastic medium and the surface crack in an elastic layer underlain by an elastic subgrade are also provided for purposes of comparison.

6. CONCLUSIONS

This report presents the theoretical basis and the associated numerical developments for the stress analysis of pavement structures which exhibit thermo-viscoelastic behaviour. Particular attention is focussed on the examination of the influence of thermo-viscoelastic behaviour of the asphalt on the behaviour of surface cracks located in a pavement structure. The basic conclusions of the research are summarized in the ensuing.

(i) Asphalt concrete materials possess complex time- and temperature-dependent stress-strain phenomena.

(ii) The theory of linear viscoelasticity serves as a useful first approximation in the study of time-dependent and temperature-dependent mechanical behaviour of asphalt materials.

(iii) The assumption of linear viscoelastic behaviour enables the description of the viscoelastic constitutive relations in terms of relaxation functions applicable to dilatational and distortional behaviour of the material.

(iv) Many viscoelastic materials which exhibit temperature dependence can be con-

veniently described as thermo-rheologically simple materials. The basic postulate of thermo-rheologically simple behaviour is that the viscoelastic relaxation functions at a series of different temperatures when plotted versus the logarithm of time can be superimposed to form a single curve simply by shifting the various curves at different temperatures along the time axis. By invoking this assumption the temperature dependence can be described by a "shift factor" which accounts for the reduction in the asphalt stiffness with increases in temperatures or vice versa.

(v) Numerical methods of stress analysis can be employed to examine transient phenomena associated with thermo-viscoelastic behaviour of pavement structures containing defects. In this study the finite element technique is used to examine the time- and temperature-dependent behaviour of the stress intensity factor at the tip of a surface crack located either in a viscoelastic medium or a viscoelastic layer underlain by an elastic subgrade. The magnitude of the stress intensity factor is an indicator of the tendency for the crack to further propagate due to low-temperature induced stresses. The particular thermal loading corresponds to a sudden reduction in the surface temperature of the medium or the layer containing the crack.

(vi) The numerical results obtained for the time-dependent variation in the stress intensity factor at the surface crack located in a viscoelastic medium indicate that, in general, the viscoelastic behaviour has the tendency of reducing the magnitude of the stress intensity factor at the crack tip. This reduction is greatly influenced by the form of the relaxation function governing, in this case, the shear behaviour of the viscoelastic medium and the shift factor.

(vii) Similar conclusions apply to the results for the time-dependent variation in the stress intensity factor at the crack tip located in a viscoelastic layer underlain by a subgrade. Additional variables in this example include the crack length to layer thickness ratio and the modulus mismatch between the viscoelastic layer and the underlying elastic medium. The results presented in the report indicate only a small degree of sensitivity of the stress intensity factor to the modulus mismatch between the viscoelastic layer and the underlying elastic medium.

TABLE 1: Viscoelastic Material Type (a) to (e)

Material Type	$G(t)/G(0)$	$K(t)/K(0)$
(a)	$0.9 + 0.1\exp(-x)$	1.0
(b)	$0.5 + 0.5\exp(-x)$	1.0
(c)	$0.1 + 0.9\exp(-x)$	1.0
(d)	$0.05 + 0.95\exp(-x)$	1.0
(e)	$0.01 + 0.99\exp(-x)$	1.0

where $x = 8t/\ell^2 \frac{\rho c}{k}$

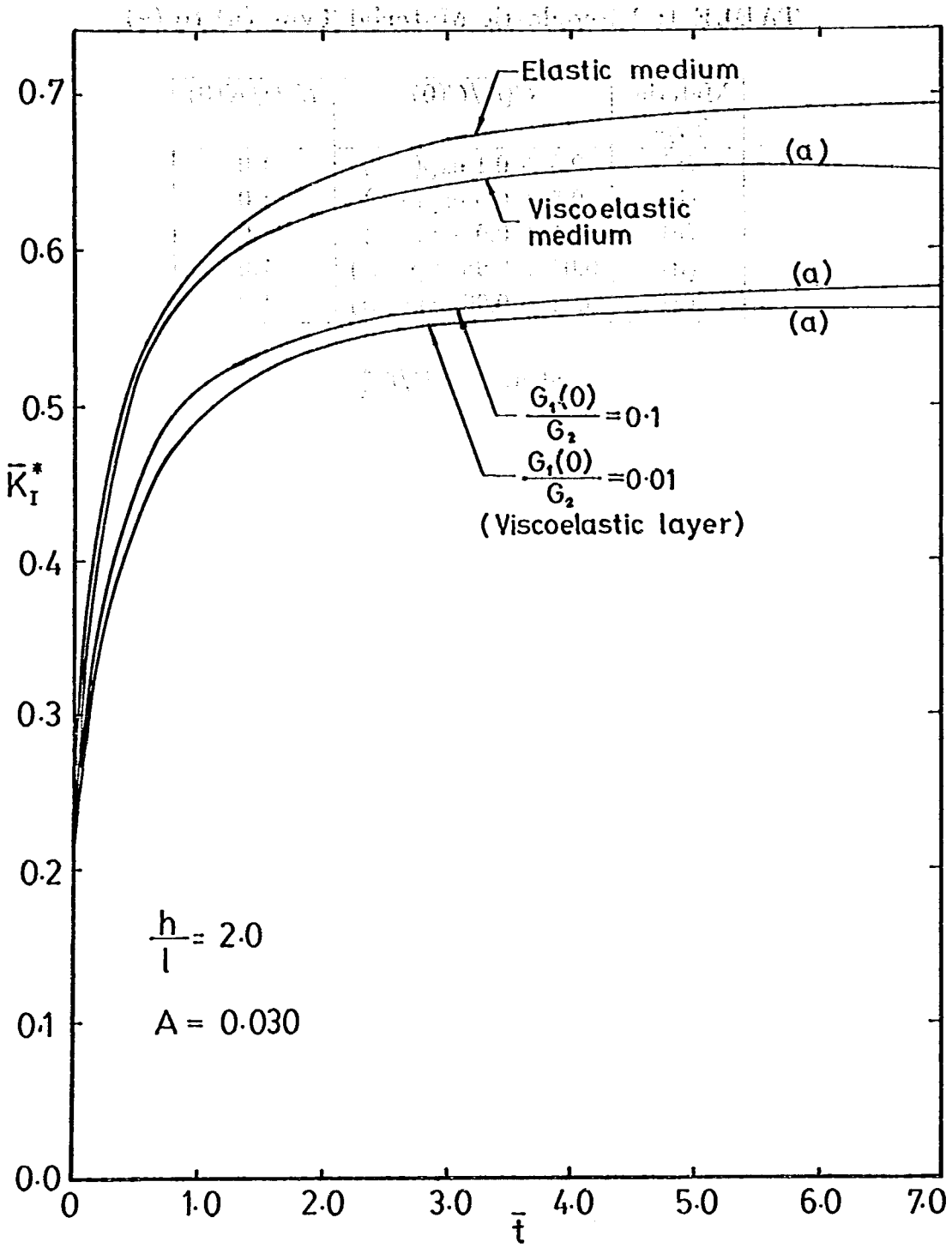


Figure 6. The influence of thermo-viscoelastic properties on the stress intensity factor at the surface crack.

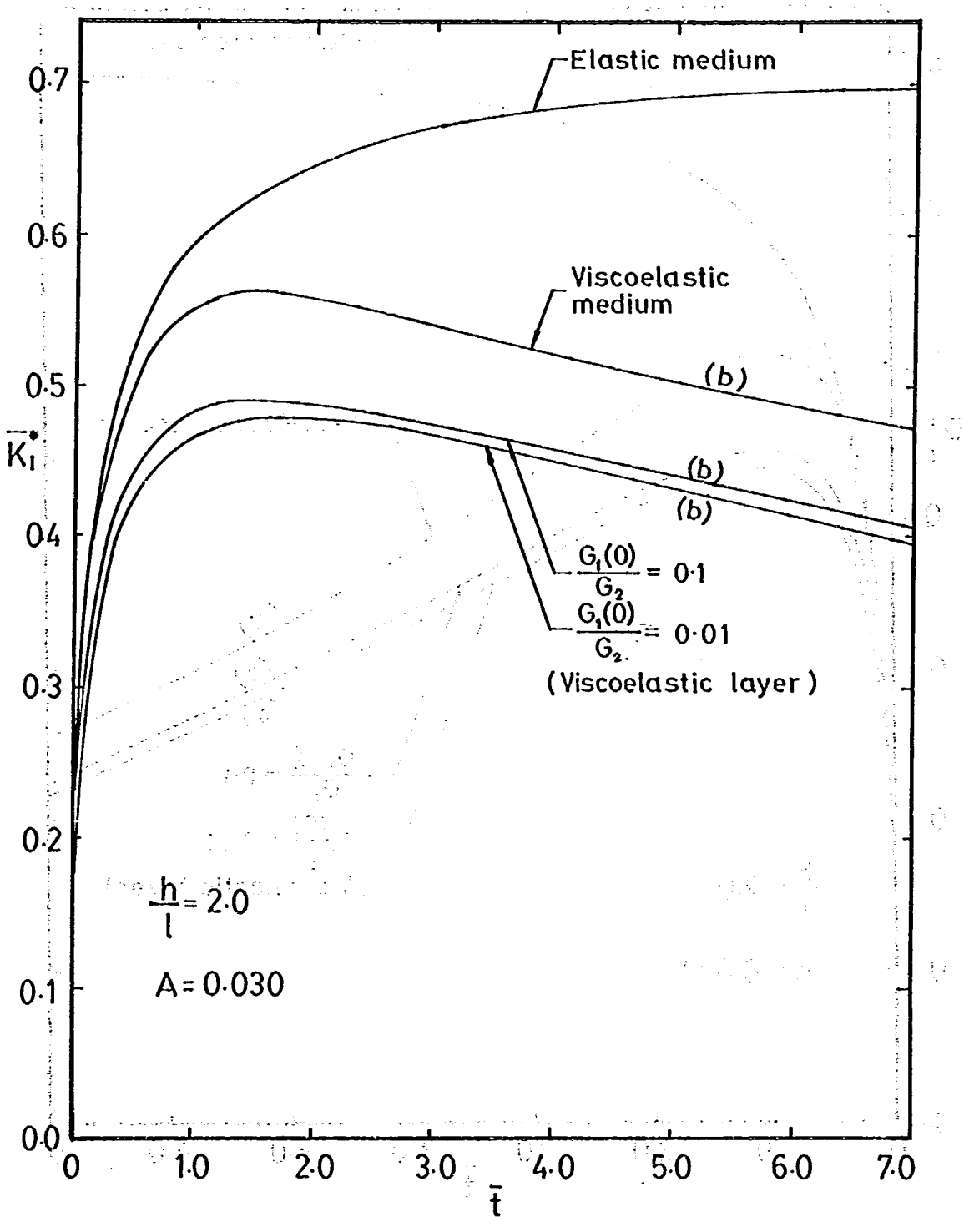


Figure 7. The influence of thermo-viscoelastic properties on the stress intensity factor at the surface crack.

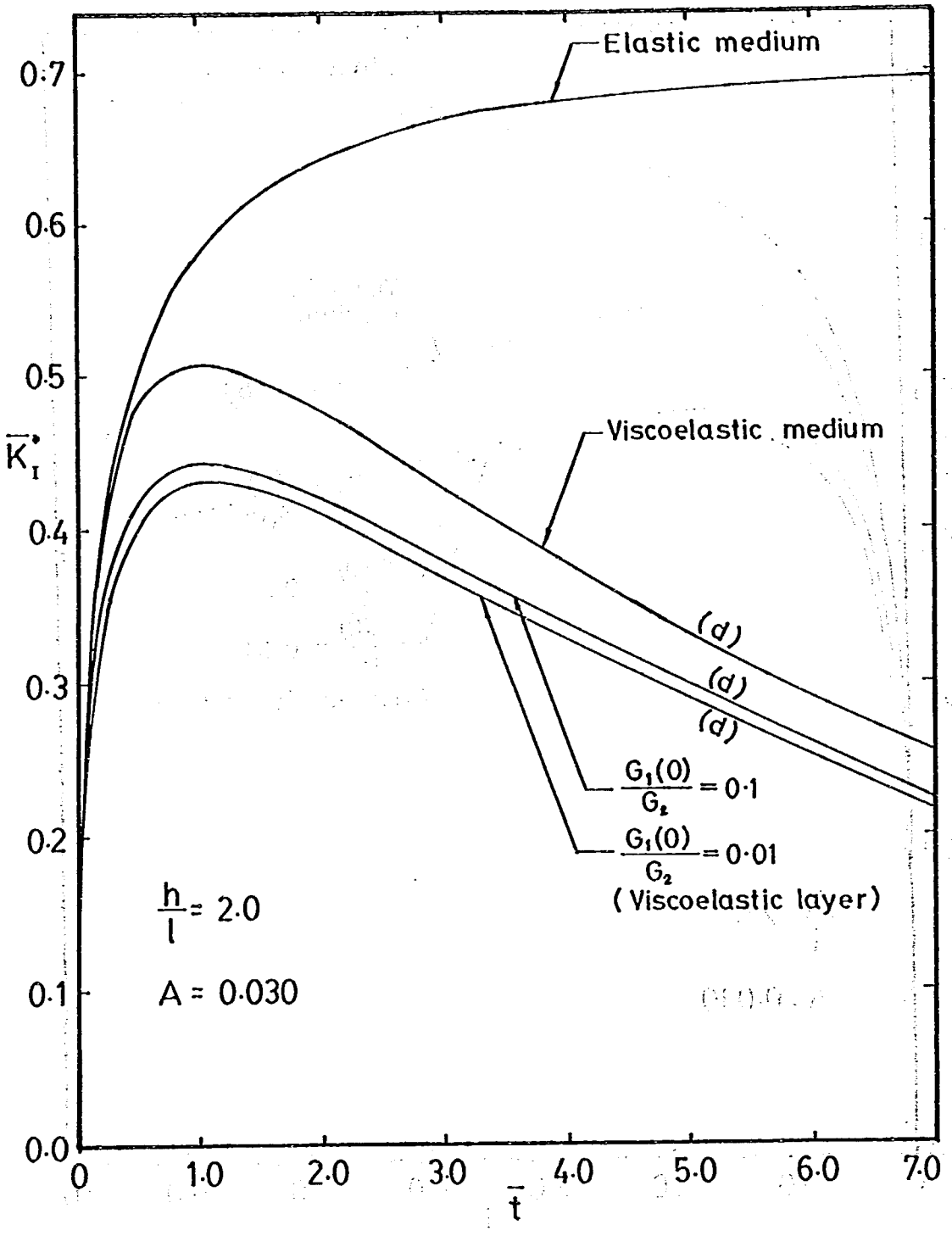


Figure 8. The influence of thermo- viscoelastic properties on the stress intensity factor at the surface crack.

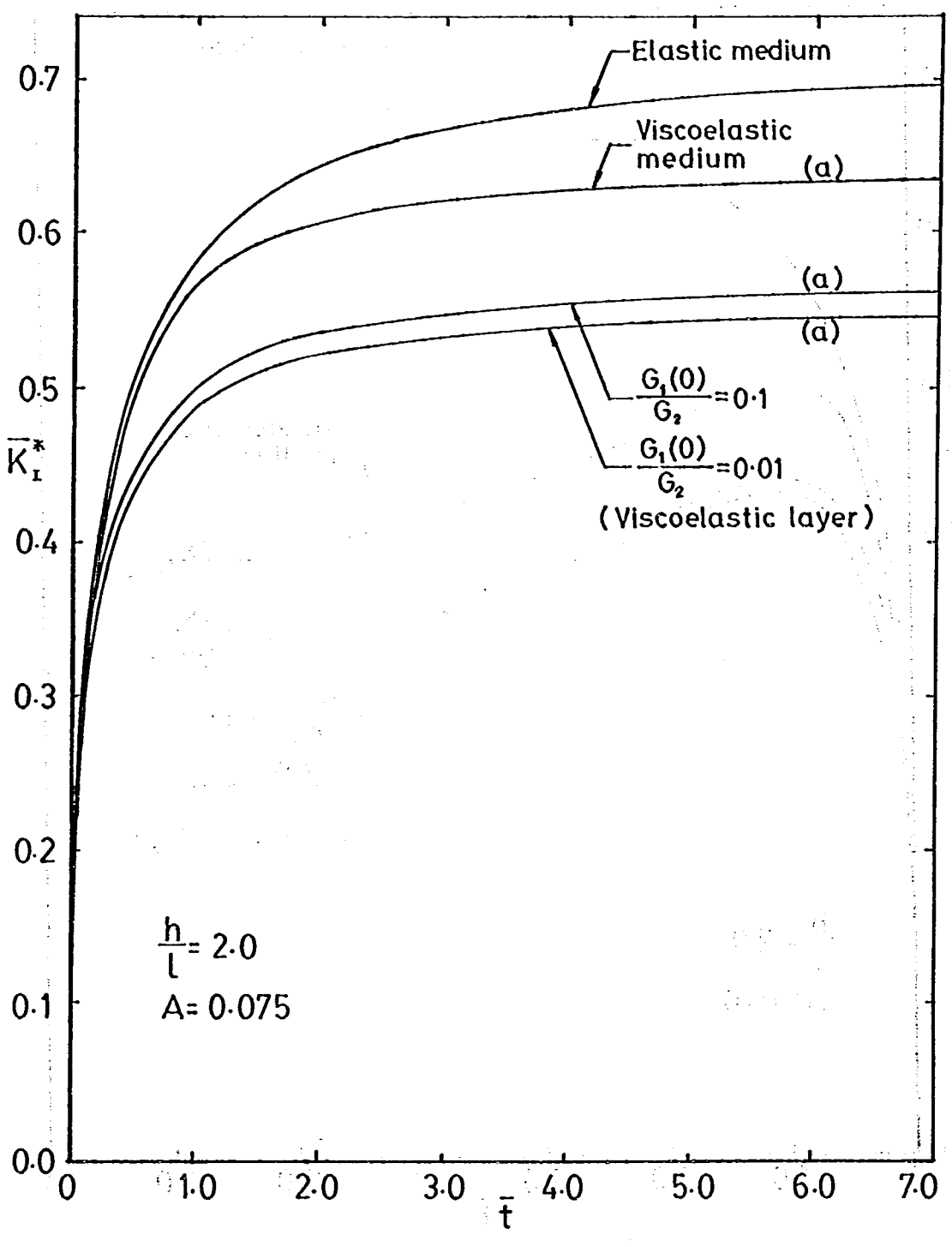


Figure 9. The influence of thermo-viscoelastic properties on the stress intensity factor at the surface crack.

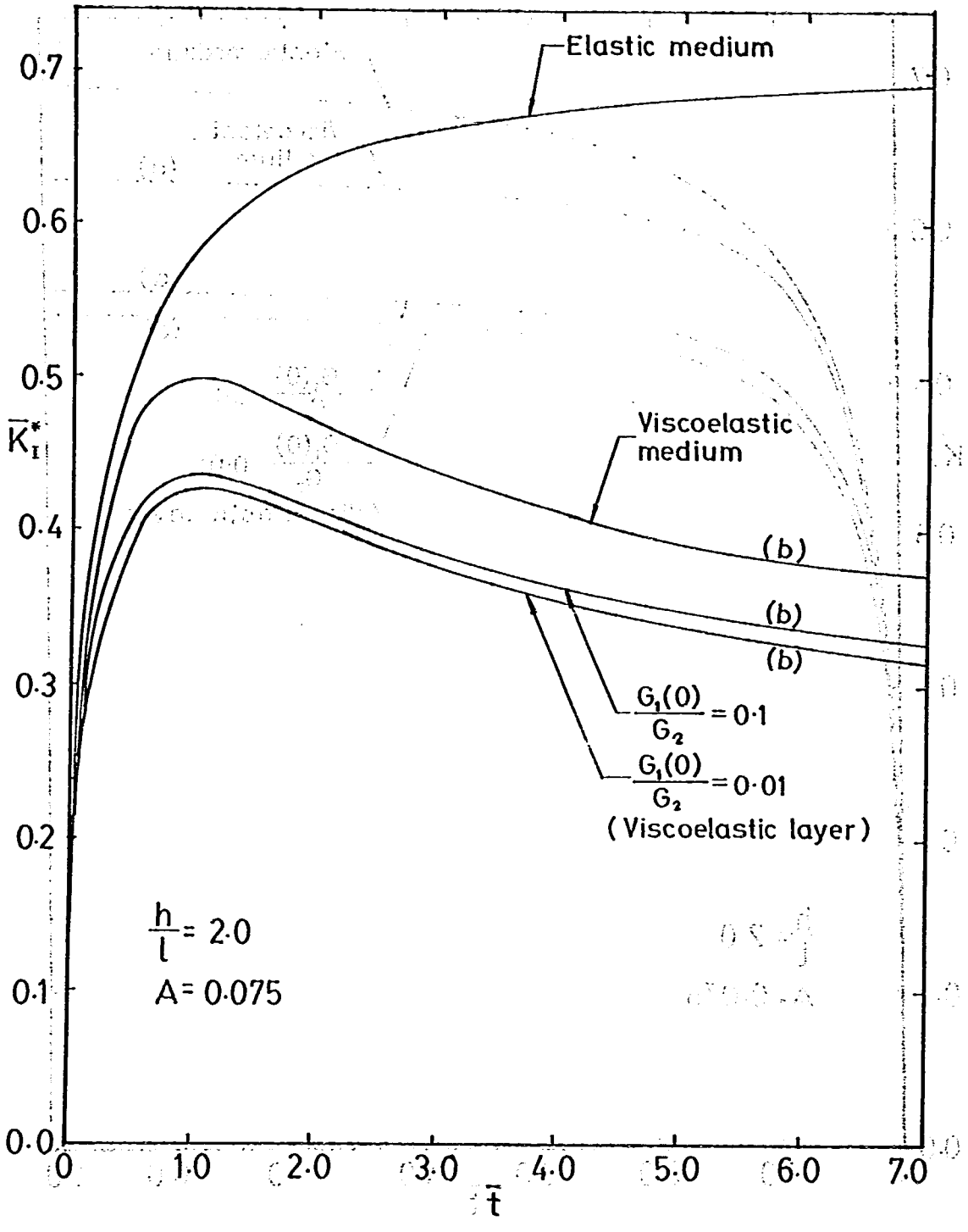


Figure 10. The influence of thermo-viscoelastic properties on the stress intensity factor at the surface crack.

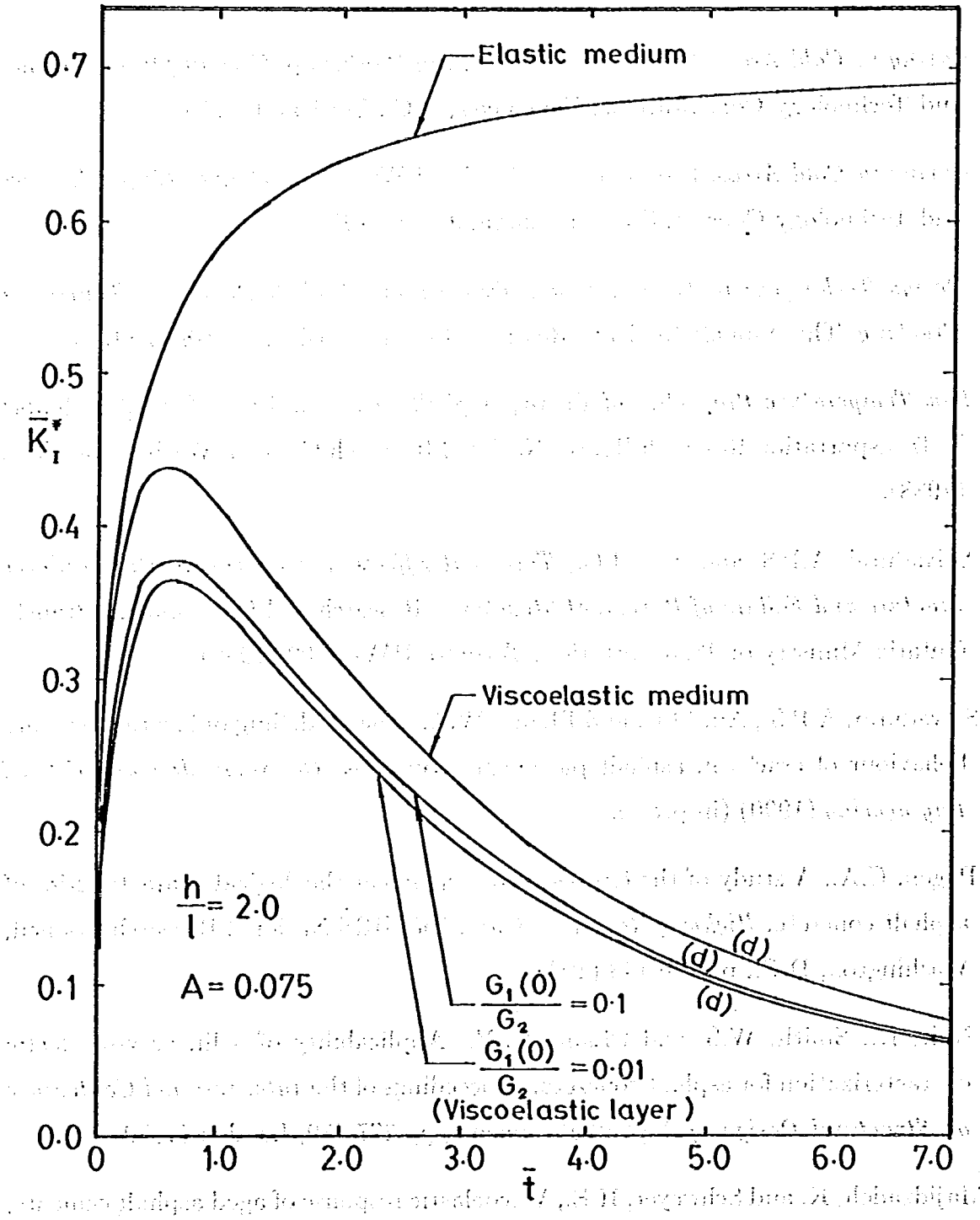


Figure 11. The influence of thermo-viscoelastic properties on the stress intensity factor at the surface crack.

7. REFERENCES

[1] *Paving in Cold Areas*, Proceedings of the Mini-Workshop, Canada/Japan Science and Technology Consultations, Vancouver, B.C., Vol.1 and 2 (1982).

[2] *Paving in Cold Areas*, Proceedings of the Mini-Workshop, Canada/Japan Science and Technology Consultations, Tsukuba, Japan (1984).

[3] *Design Techniques to Minimize Low-Temperature Asphalt Pavement Transverse Cracking*, The Asphalt Institute Research Report, No.81-1, RR-81-1 (1981).

[4] *Low-Temperature Properties of Paving Asphalt Cements*, State of the Art Report 7, Transportation Research Board, National Research Council, Washington, D.C. (1988).

[5] Selvadurai, A.P.S. and Au, M.C., *Transient Effects in Low-Temperature Induced Fracture and Failure of Pavement Structures*, Research and Development Branch, Ontario Ministry of Transportation, Toronto, PAV-88-02 (1988).

[6] Selvadurai, A.P.S., Au, M.C. and Phang, W.A., The modelling of low temperature behaviour of cracks in asphalt pavement structures, *Canadian Journal of Civil Engineering* (1990) (in press).

[7] Pagen, C.A., A study of the temperature-dependent rheological characteristics of asphalt concrete, *Highway Research Board*, 158, HRS National Research Council, Washington, D.C., pp.116-143 (1967).

[8] Nair, K., Smith, W.S. and Chang, C.-Y., Applicability of a linear viscoelastic characterization for asphalt concrete, Proceedings of the *International Conference on Structural Design of Asphalt Pavements*, pp.277-289, London (1972).

[9] Majidzadeh, K. and Schweyer, H.E., Viscoelastic response of aged asphalt cements, *Highway Research Record*, 231, HRB, National Research Council, Washington, D.C., pp.50-61 (1968).

[10] Dobson, G.R., The Dynamic Mechanical Properties of Bitumin, *Proc. Assoc. Asphalt Pav. Tech.*, 38, pp.123-139 (1969).

[11] Ashton, J.E. and Moavenzadeh, F., Analysis of three layer viscoelastic halfspace, *Jour. Eng. Mech. Div.*, Proc. ASCE, pp.117-136 (1968).

[12] Monismith, C.L. and Secor, K.E., Viscoelastic behaviour of asphalt concrete pavements, *Proc. 1st Int. Conf. Struct. Design of Asphalt Pavements*, Ann Arker, Mech., pp.476-498 (1962).

[13] Jongepier, R. and Kuilman, B., Characteristics of the rheology of bitumen, *Proc. Assoc. Asphalt Paving Tech.*, 38, pp.98-122 (1969).

[14] Williams, M.L., Structural analysis of viscoelastic materials, *AIAA J.*, 2, pp.785-808 (1964).

[15] Lee, E.H., Stress analysis in viscoelastic bodies, *Quarterly of Applied Mathematics*, 8, pp.183-188 (1955).

[16] Leitman, M.S. and Fisher, G.M.C., The linear theory of viscoelasticity, in *Handbuch der Physik*, (S. Flugge, Ed.), Vol.6a/3, pp.1-123, Springer-Verlag.

[17] Christensen, R.M., *Theory of viscoelasticity: an introduction*, Academic Press, New York (1982).

[18] Flugge, W., *Viscoelasticity*, Springer-Verlag, New York (1975).

[19] Selvadurai, A.P.S., The time dependent response of a deep rigid anchor in a viscoelastic medium, *Int. J. Rock Mech., Mining Sciences and Geomech.*, Abstr.15, pp.11-19 (1978).

[20] Findley, W.N., Lai, J.S. and Onaran, K., *Creep and relaxation of non-linear viscoelastic materials*, North-Holland Publishing, New York (1976).

[21] Bazant, Z.P. and Wu, S.T., Dirichlet series creep function for aging concrete, *J. Engineering Mechanics Div. (ASCE)*, 99(2), pp.367-387 (1973).

[22] Schwartz, F. and Staverman, A.J., Time-temperature dependence of linear viscoelastic behaviour, *Journal of Applied Physics*, 23, pp.838-843 (1953).

[23] Williams, M.L., Landel, R.F. and Ferry, J.D., The temperature dependence of relaxation mechanisms in amorphouse polymers and other glass-liquids, *J. Amer. Chem. Soc.*, 77, pp.370 (1955).

[24] Selvadurai, A.P.S. and Au, M.C., Transient Thermo-Viscoelastic Fracture Mechanics of Pavement Structures, Research and Development Branch, Ontario Ministry of Transportation, p.40 (1990).

[25] Zienkiewicz, O.C., *The Finite Element Method*, McGraw-Hill Book Company (1977).

[26] Oden, J.T., *Finite elements of non-linear continuum*, McGraw-Hill Book Company, New York (1972).

[27] Taylor, R.L., Pister, K.S. and Goudreau, G.L., Thermomechanical analysis of viscoelastic solids, *Int. J. Numerical Methods Engineering*, 2, pp.45-59 (1970).

[28] Srinatha, H.R. and Lewis, R.W., A finite element method for thermoviscoelastic analysis of plate problems, *Computational Methods in Applied Mechanics and Engineering*, 25, pp.21-33 (1981).

[29] Knauss, W.G., Delayed failure — the Griffith problem for linearly viscoelastic materials, *Int. J. Fracture* 6(1), pp.7-20 (1970).

[30] Francis, E.C., Carlton, C.H. and Thompson, R.E., Viscoelastic rocket grain fracture analysis, *Int. J. Fracture*, 10(2), pp.167-180 (1974).

[31] Schapery, R.A., A theory of crack initiation and growth in viscoelastic media - I. Theoretical development, *Int. J. Fracture*, 11(1), pp.141-159 (1975).

[32] Henshell, R.D. and Shaw, K.G., Crack tip finite elements are unnecessary, *Int. J. Numerical Methods Engineering*, 9, pp.495-507 (1975).

[33] Barsoum, R.S., On the use of isoparametric finite elements in linear fracture mechanics, *Int. J. Numerical Methods Engineering*, 10, pp.25-37 (1975).

Ste. Anne Test Road Revisited Twenty Years Later

I.J. Deme, Shell Canada Products Ltd.
F.D. Young, Manitoba Department of Highways

Ste. Anne Test Road Revisited Twenty Years Later

by I J Deme* and F D Young**

ABSTRACT

The Ste. Anne Test Road was constructed in 1967 to evaluate the factors responsible for transverse cracking of asphalt pavements. This publication provides a historical review and commentary on this study and highlights the main findings.

Some of the pavements cracked during the first winter while others resisted cracking for over eight years. All sections have now cracked after 20 years, indicating that it is possible to retard initiation of cracking and to reduce its frequency but not to prevent it in the long term under the low winter temperature conditions prevailing in the Prairie Provinces.

Transverse cracking was observed to start when the pavements cooled to temperatures at which they exceeded critical limiting values of mix and binder stiffness moduli. While asphalt stiffness was found to be the most significant variable affecting initiation of cracking, pavement thickness, subgrade type and the cumulative effects of traffic loading all affected the frequency of transverse cracking. The influence of these factors diminished with increasing asphalt softness (i.e. higher penetration) and reduction in asphalt temperature susceptibility (i.e. increase in Penetration Index). Mix binder and filler contents had no measurable influence on transverse cracking.

Two nomographs, based on initial binder properties, were developed for predicting the critical cracking temperature of pavements and for use in asphalt selection/specification.

Evaluation of specimens cut from test pavements revealed an increase in mix stiffness with time. This was attributed to 'structural hardening' of the binder. As this structure is destroyed by reheating in the binder recovery process, direct mix testing is preferred for evaluating changes in pavement resistance to cracking in the long term.

All test sections indicate the presence of transverse cracks 12 years after overlaying the test road. For the pavement sections that had cracked initially, generally between 13 and 100 per cent of the transverse cracks have reflected through the overlay.

1 INTRODUCTION

The Ste. Anne Test Road was constructed in 1967 as a joint research project by the Manitoba Highways Department and Shell Canada Limited, designed to study the transverse cracking of asphalt pavements. Different materials and pavement structures were incorporated in 29 test sections to gain insight into the mechanism of transverse cracking and to compare the performance of several variables. Asphalt properties, as it turned out later, had the most significant effect on transverse cracking.

Little was known about transverse crack initiation in 1967. Some postulated that cracking occurred in the winter, while others believed it happened in the spring; some thought it initiated at the pavement surface, while others believed that cracks migrated upward from the base. Aluminium-foil crack detectors, similar to shop-window burglar-alarm circuits, were therefore installed at various depths in the asphalt pavement to detect crack initiation. Three banks of thermocouples were installed to record temperatures at various depths in the road structure to define the temperature regime at crack initiation. The crack detector and temperature sensor circuits were monitored continuously by event recorders.

After transverse cracking was detected in some sections during the first winter, the test road was inspected daily and the occurrence of new cracks was mapped.

Extensive investigations were launched at Shell laboratories in Oakville and Amsterdam to evaluate significant properties of asphalt binders and paving mixes which could affect the initiation of transverse cracking. This publication highlights these findings and the advantages or shortcomings of techniques and test procedures used.

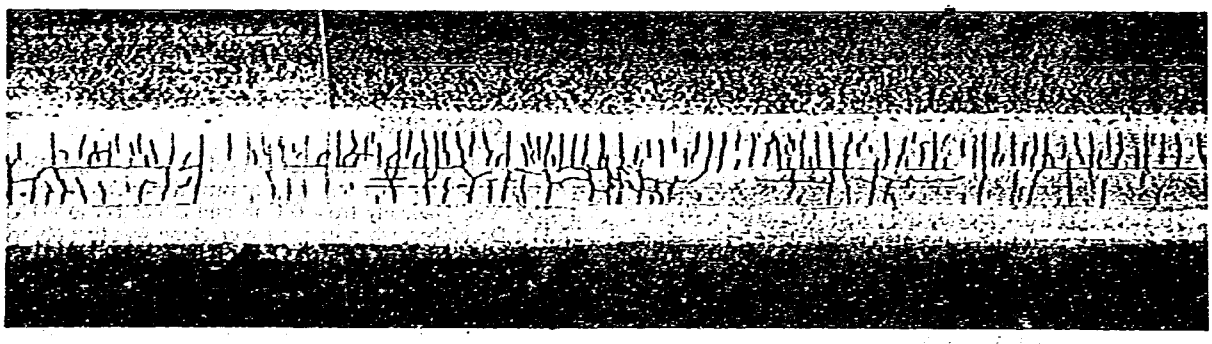
The objective is to provide a historical review and commentary on the Ste. Anne Test Road study over the last 20 years. Detailed data have been excluded for the sake of brevity and the reader is encouraged to consult the reports listed in the bibliography for project details.

2 SEVERITY OF THE PROBLEM

Transverse cracking gained prominence as a pavement distress mechanism in the early 1960s. The frequency of transverse cracks was very high in many pavements. A survey of 500 kilometres (km) of pavements in Manitoba revealed that for two-thirds of the survey mileage the spacing between transverse cracks ranged from 3 to 9 metres (m), as shown in Figure 1.

While transverse cracking did not affect the service life of some pavements, there were the exceptions where ingress of surface water into the crack caused swelling of the clay subgrade. This resulted in a ridge across the pavement. Alternatively, the water flow was responsible for washing out

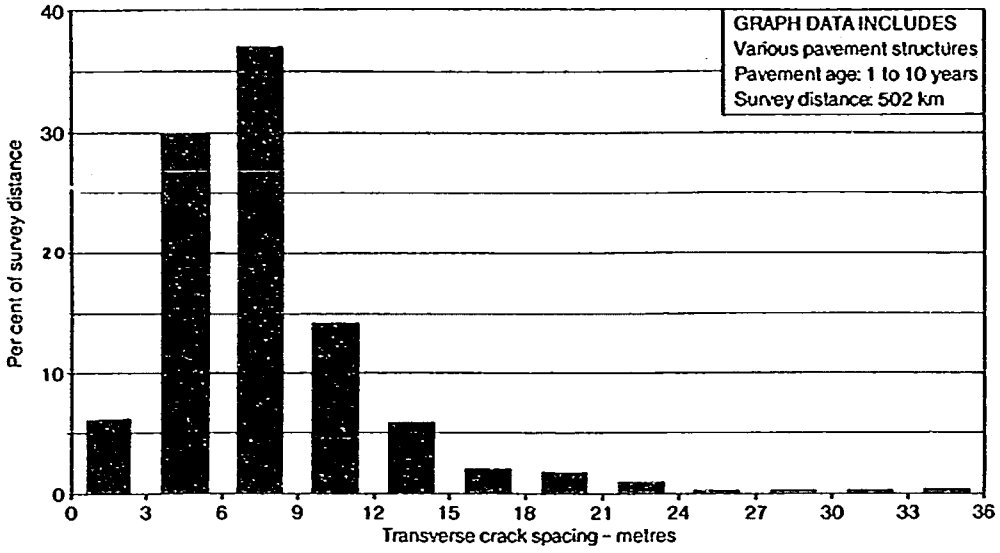
PLATE 1: AERIAL PHOTOGRAPH OF A STE. ANNE TEST ROAD SECTION EXHIBITING TRANSVERSE CRACKING



* Asphalt Manager,
Shell Canada Products Limited

** Director of Materials and Research,
Manitoba Department of Highways

FIGURE 1: SURVEY OF TRANSVERSE CRACKING OF 150 TO 200 PENETRATION ASPHALT PAVEMENTS IN MANITOBA (A-6 AND A-7-6 CLAY SUBGRADES)



silt-sized base and subgrade materials below the crack, resulting in a depression across the pavement. The service life of these pavements was shortened significantly as the transverse cracks could not be sealed properly with the liquid asphalts then in use. Adequate rubberised-asphalt sealants were not developed for asphalt pavements until the end of the 1970s.

3 TEST ROAD VARIABLES

Some asphalt practitioners believed that transverse cracking had not been a problem before the 1960s when soft cut-back asphalt such as SC-5 and SC-6 had been used, but that cracking had become more noticeable with the advent of the harder 150 to 200 penetration (pen) asphalt which had come into use to meet the requirements of higher traffic volumes. Several asphalt grades and types (i.e. differing in temperature susceptibility) were incorporated in the test road. Twenty-nine test sections, 120 m long, were constructed on clay and sand subgrades to evaluate the effects of a number of variables which could potentially influence transverse cracking.

Pavement Structures:

(1) 100 millimetre (mm) asphalt; 400 mm crushed gravel base; clay subgrade (A-7).
(2) 250 mm full-depth asphalt; clay subgrade (A-7).
(3) 100 mm asphalt; 150 mm crushed gravel base; sand subgrade (A-3).

Asphalt Mixes:

(1) Dense graded aggregate (80 per cent limestone, 20 per cent igneous) 16 mm maximum size, 2.5 per cent minus 75 μm.
(2) High filler; above aggregate with 5.5 per cent minus 75 μm.
(3) 100 per cent igneous aggregate.

Asphalt Types and Grades (Figure 2):

(1) 150 to 200 pen grade (157 pen), low viscosity (LV): 25.3 Pa.s @ 60°C, 110 mm^2/s @ 135°C.
(2) 150 to 200 pen grade (170 pen), high viscosity (HV): 59.1 Pa.s @ 60°C, 225 mm^2/s @ 135°C.
(3) 300 to 400 pen grade (283 pen), low viscosity (LV): 14.1 Pa.s @ 60°C, 86 mm^2/s @ 135°C.
(4) SC-5 (HV asphalt cut-back: 9.6 Pa.s @ 60°C, 89 mm^2/s @ 135°C.

Mix Asphalt Content:

(1) Marshall optimum (5 per cent).
(2) 1 per cent below optimum (4 per cent).
(3) 0.5 per cent above optimum (5.5 per cent).

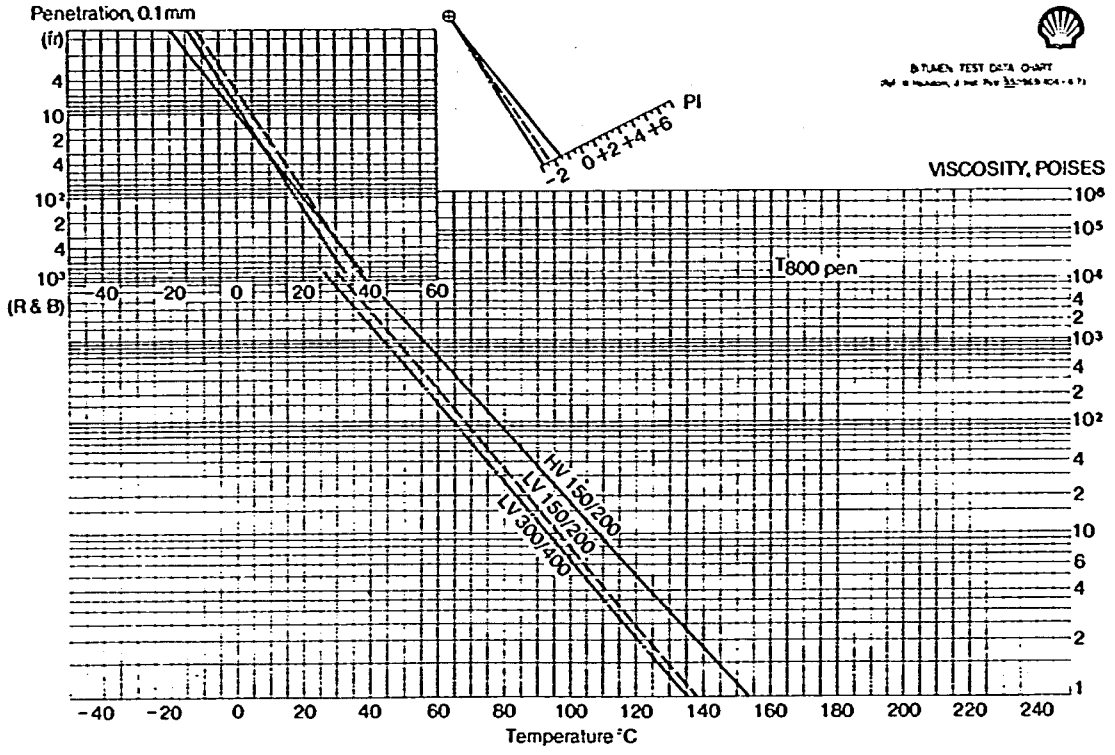
Composite Pavements:

(1) Wearing course: LV 150 to 200; binder course: HV 150 to 200.
(2) Wearing course: SC-5; binder course: LV 150 to 200.
(3) Wearing course: LV 300 to 400; binder course: HV 150 to 200.
(4) Wearing course: SC-5; binder course: HV 150 to 200.

4 TEMPERATURE CONDITIONS AT TIME OF CRACKING

A prolonged low-temperature cycle was experienced during the first winter after test road construction. The temperature decreased gradually from 0°C in mid-December to -41°C on 31st December, when transverse cracking was first observed. The asphalt pavement, acting as a heat reservoir and as an insulating material, had cooled to -32°C at mid-depth (i.e. 50 mm). The frequency of transverse cracking increased in some pavements while others showed no sign of cracking, as the temperature hovered at this low extreme for a week. Transverse cracking was most severe between 4th and 7th January, when the entire thickness of asphalt pavement was

FIGURE 2: PROPERTIES OF PENETRATION GRADE ASPHALTS



observed to have cooled to the low temperature levels shown in Figure 3. The minimum temperatures observed during this cycle were -43°C ambient temperature, -36°C at the pavement surface and -34°C at the 50 mm depth. The transverse cracking was attributed to thermal contraction of the asphalt pavement caused by low-temperature-induced stresses as the asphalt pavement gradually cooled down throughout its thickness and became stiffer (i.e. more brittle).

Thereafter, the temperature continued to cycle at slightly higher temperature levels, as shown in Figure 3, and the additional cracking observed at 'warmer' temperatures was attributed to a combination of the low temperature level and weakening of the asphalt pavement believed to result from temperature cycling.

Low-temperature intensity, duration of low-temperature cycles and their recurrence intervals were all found to be significant to transverse cracking. Analysis of the meteorological data indicated that the initial low-temperature cycle had a recurrence interval between five and ten years, as shown in Figure 4. Use of the low temperature intensity/duration concept in conjunction with pavement temperature distribution curves, such as shown in Figure 5, was later found helpful in the selection of asphalts to resist transverse cracking for various geographical locations.

5 INITIATION OF TRANSVERSE CRACKING

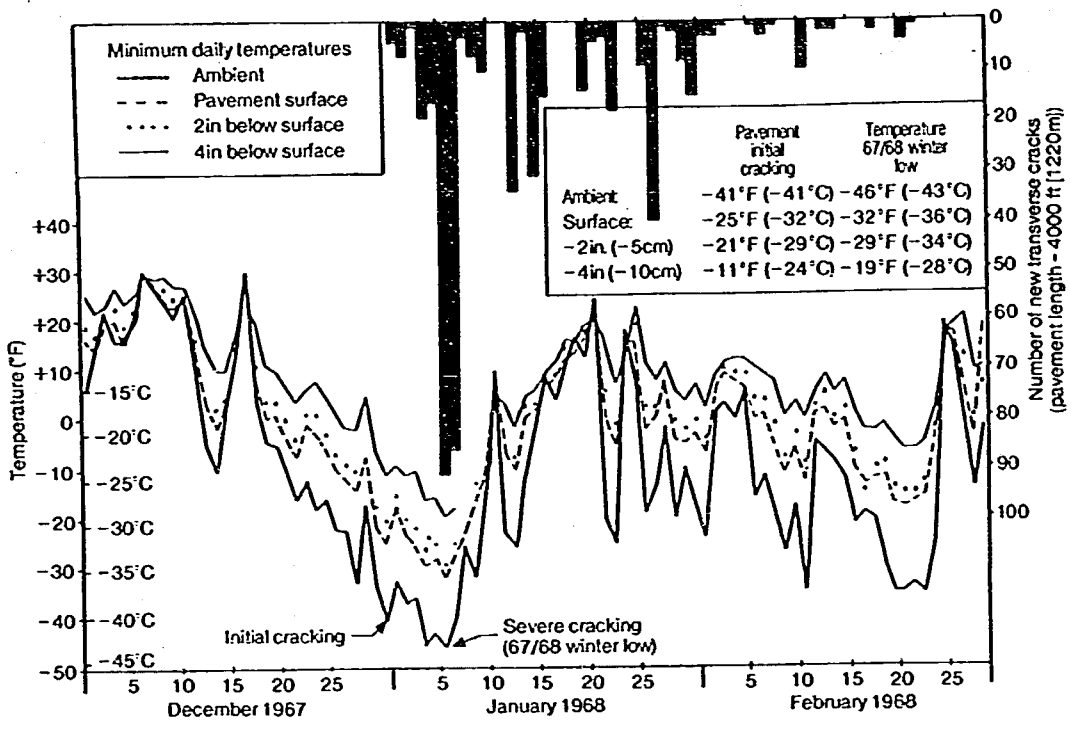
The fact that transverse cracking initiated at the pavement surface and propagated downward was verified in several different ways. The automatic recorders indicated that the crack detector tape embedded in the upper part of the pavement was broken shortly before the tape in the lower part of the pavement. Secondly, in composite pavement sections which comprised 'non-cracking' asphalt-type binder courses overlaid with 'crack-susceptible'-type wearing courses, cracking was found to occur in the 'crack-susceptible' wearing course only. Cores taken across such cracks, shown in Figure 6, and subsequent X-rays verified that the cracks penetrated through the wearing course and terminated at the top of the binder course.

Crack initiation and propagation from the most brittle (i.e. coldest) part of the pavement verified that its stiffness was the most significant variable affecting cracking, as will be shown later. It was not inferred from this that pavement contraction was the sole cause of transverse cracking. On the contrary, it will be shown later that spacing between transverse cracks was as low as one metre in some sections and that, while the 7 m-wide pavement could contract transversely without cracking, longitudinal contraction of the frozen subgrade was transmitted to the pavement surface. Based on such observations, it was concluded that less stiff or warmer asphalt pavement underlayers were capable of sustaining their own contraction and transmitted strain from the base and subgrade without cracking, but that the upper parts of asphalt pavement, which were stiffer, could not sustain tensile strains above a certain critical limit and were therefore the first to crack.

6 CRACK CHARACTERISTICS

The width of the transverse cracks in the pavements with a sand subgrade were narrower than those with a clay subgrade. The cracks in the pavements with clay subgrades ranged in width from 1 mm to 5 mm shortly after initiation. The transverse cracks in the sand subgrade sections were of hairline width and extremely difficult to trace across the pavement

FIGURE 3: LOW-TEMPERATURE CYCLE AT STE. ANNE WHEN TRANSVERSE CRACKING OCCURRED IN LV 150 TO 200 PEN. PAVEMENTS WITH SAND SUBGRADE (REF. 2)



initially. All cracks had widened a year after initiation. Laboratory tests performed to measure the linear coefficient of thermal contraction in air had demonstrated that compacted asphalt mix shrinks permanently when subjected to temperature cycling. The increase in pavement crack width was attributed to this phenomenon.

Inspection of the cracked pavement faces revealed that up to 8 per cent of the fractured face surface area passed through the limestone aggregate. No fractures were observed to pass through the stronger igneous aggregate.

7 CORRELATION OF CRACKING FREQUENCY WITH EXPERIMENTAL VARIABLES

The following pavement cracking characteristics were observed during the initial eight years of the life of the test pavements (i.e. 1967 to 1975). The pavement structures were designed for early failure and the test road was overlaid in 1975 with 125 mm of SC-5 asphalt concrete.

7.1 LV 150 to 200 Pen Asphalt Sections

(1) All of the transverse cracking occurred during the first winter and the spacing between transverse cracks was 6± 2 m for the clay subgrade sections, 2.5± 2m for the sand subgrade sections, and 15± 3 m for the full-depth 250 mm asphalt pavement on clay subgrade.

(2) Asphalt content did not affect transverse cracking frequency.

(3) Filler content, in the range studied, did not affect transverse cracking frequency.

7.2 HV 150 to 200 Pen Asphalt Sections

(1) No transverse cracks were observed in any of the pavements constructed on the clay subgrade during the initial eight years.

(2) While no transverse cracking was observed for several years in the pavements constructed on the sand subgrade, during the fifth winter severe transverse cracking developed in the traffic lane and, to a more moderate extent, in the passing lane. The pavement surface temperature reached a low of -34°C during this winter.

(3) No cracking was observed in either of the two igneous aggregate sections either on the clay or sand subgrades.

(4) Neither asphalt content nor filler content had any effect on transverse cracking frequency.

7.3. LV 300 to 400 Pen Asphalt Sections

(1) Three of the four sections on the clay subgrade cracked during the first winter with an average spacing of 20 m between cracks.

(2) While no cracking was observed to occur in any of the sections on the sand subgrade for several years, during the fifth winter severe cracking occurred in the traffic lane of three of the four sections with moderate cracking of the passing lane.

(3) Neither asphalt content nor filler content had any effect on transverse cracking frequency.

FIGURE 4: INTERVAL OF RECURRENCE AND DURATION OF THE COLDEST ANNUAL TEMPERATURE CYCLE

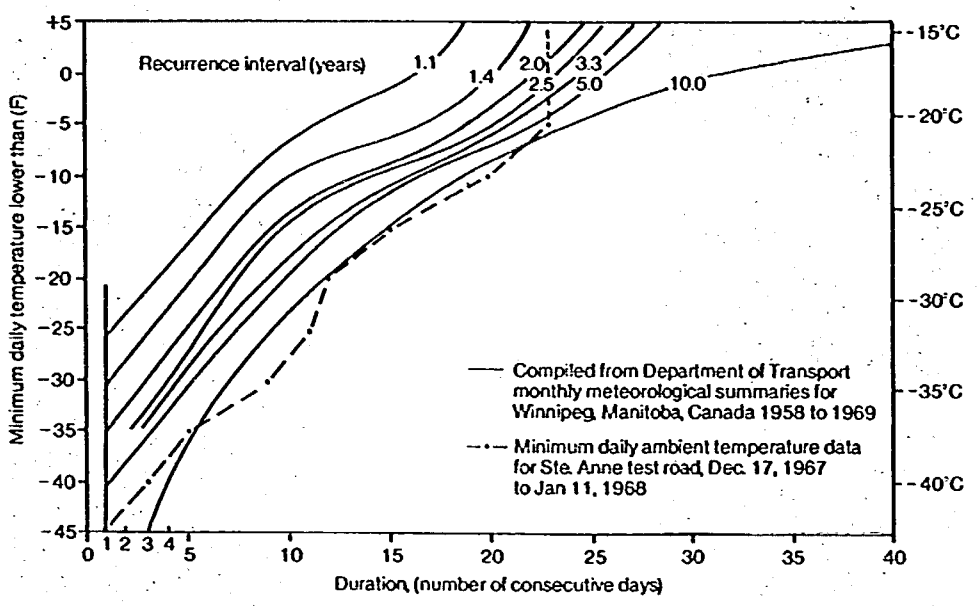


FIGURE 5: RELATION BETWEEN MINIMUM DAILY AMBIENT TEMPERATURE AND CORRESPONDING PAVEMENT TEMPERATURE DURING A LOW-TEMPERATURE CYCLE

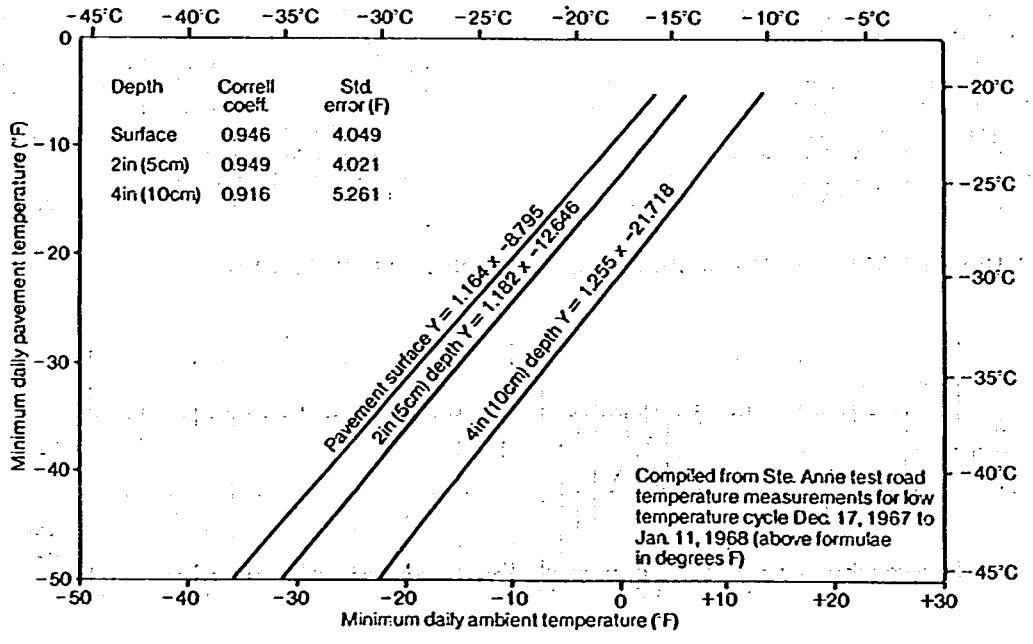
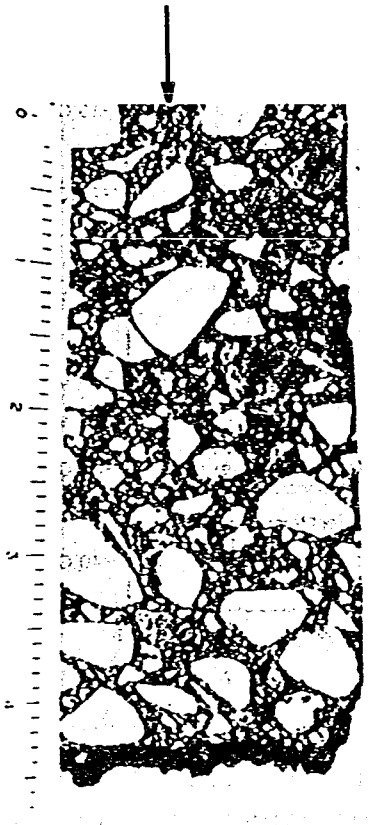


FIGURE 6: PHOTO AND X-RAY OF A PAVEMENT SLICE ACROSS A TRANSVERSE CRACK



Photograph of asphaltic concrete slice with arrow indicating location of transverse crack at surface.



X-Ray image of asphaltic concrete with white line indicating depth of crack propagation.

7.4. SC-5 Asphalt Sections

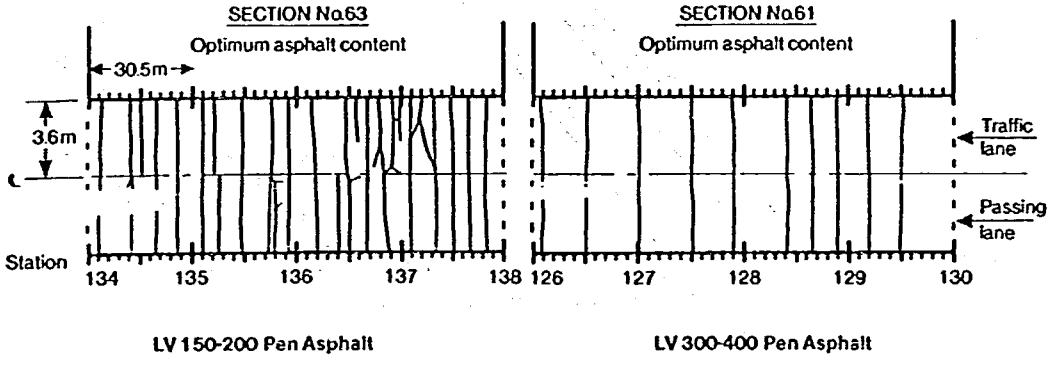
(1) No transverse cracking was observed in either of the two sections on the clay or sand subgrades during the initial eight years.

The conclusions drawn from the above observations for the initial eight years of test road performance were as follows:

(1) Asphalt grade had a significant effect on transverse cracking. The softer LV 300 to 400 pen grade asphalt pavements on the clay subgrade exhibited less transverse cracking than the harder LV 150 to 200 made from the same crude. This is illustrated in Figure 7. Use of the softer grade also delayed pavement cracking on the sand subgrade for five years.

(2) Asphalt type had a significant effect on transverse cracking. While the LV 150 to 200 pen asphalt pavements cracked severely on both clay and sand subgrades during the first winter, the less-temperature-susceptible high-viscosity type 150 to 200 pen asphalt pavements did not crack on the clay subgrade in the initial eight years. This is illustrated in Figure 8.

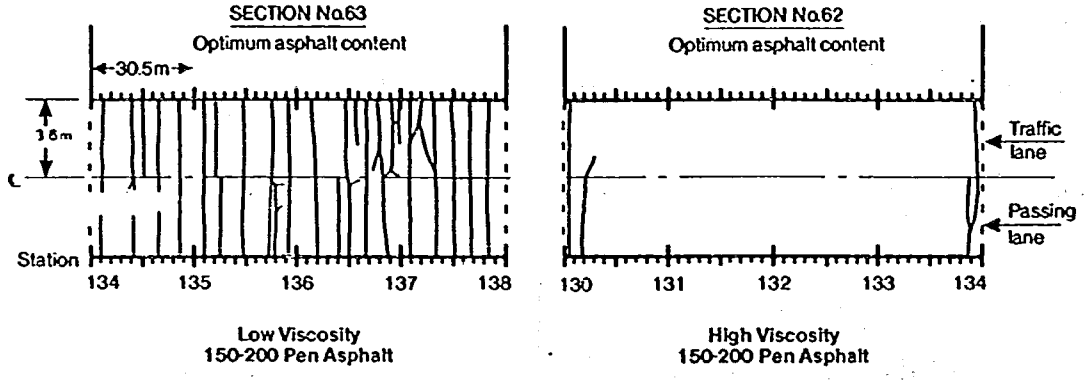
FIGURE 7: USE OF SOFT ASPHALT RESULTS IN LESS TRANSVERSE CRACKING



LV 150-200 Pen Asphalt

LV 300-400 Pen Asphalt

FIGURE 8: USE OF HIGH-VISCOSITY ASPHALT DELAYED CRACKING FOR FIVE YEARS ON SAND SUBGRADE AND FOR OVER EIGHT YEARS ON CLAY SUBGRADE PAVEMENTS



Use of the higher-viscosity asphalt also delayed pavement cracking on the sand subgrade for five years.

(3) The SC-5 asphalt, made from a high-viscosity base asphalt, incorporated features of low-temperature susceptibility and soft penetration and these pavements constructed on clay and sand subgrades exhibited no transverse cracking during the initial eight years. This is shown in Figure 9.

(4) The thickness of the asphalt pavement was found to have a significant influence on transverse cracking when using asphalts susceptible to transverse cracking. The LV 150 to 200 pen 250 mm full-depth asphalt on clay subgrade exhibited 40 per cent of the transverse cracking found in the 100 mm pavement/gravel base/clay subgrade section, shown in Figure 10.

FIGURE 9: USE OF SOFT ASPHALT MADE FROM A HIGH-VISCOSITY BASE ASPHALT DELAYED CRACKING FOR OVER EIGHT YEARS

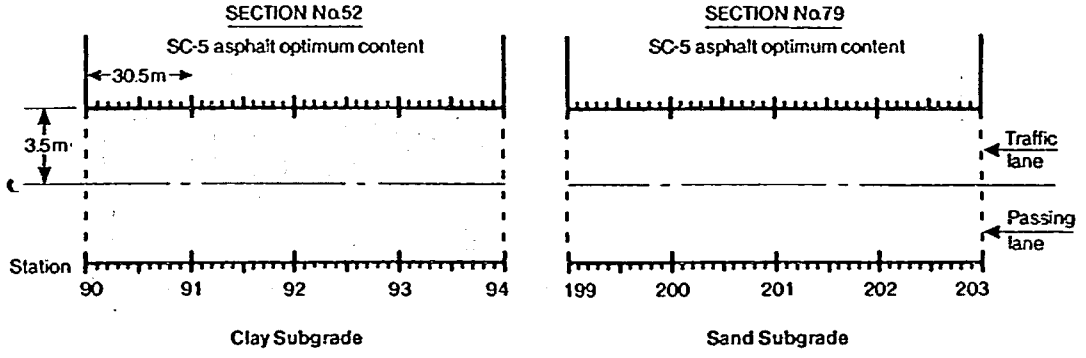
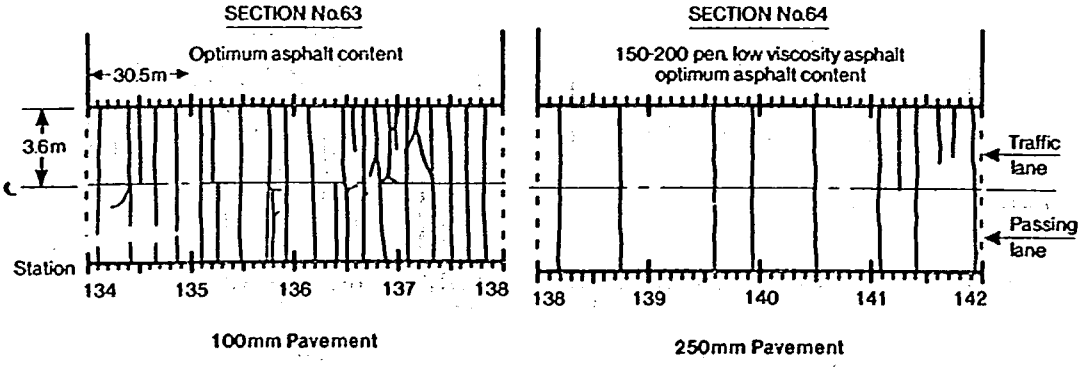


FIGURE 10: THICK ASPHALT PAVEMENTS CRACK LESS THAN THIN PAVEMENTS



(5) In the case of SC-5 asphalt pavements, the subgrade type was not a significant factor with respect to transverse cracking. For all others the subgrade/asphalt interaction affected the time of crack initiation and cracking frequency, as shown in Figure 11. After five years, a higher incidence of transverse cracking was observed in the traffic lane than in the passing lane for the LV 300 to 400 and HV 150 to 200 pavements on the sand subgrade only. This asphalt subgrade/traffic interaction is illustrated in Figure 12.

(6) Hot mix aggregate quality was found to influence transverse cracking in some instances. When 100 per cent crushed igneous aggregate (predominantly microcrystalline basalt and macrocrystalline granite) was substituted for the local 80 per cent limestone/20 per cent igneous glacial drift aggregate, neither transverse cracking nor cracking due to traffic effects was observed in the HV 150 to 200 pen asphalt section on the sand subgrade, subjected to the same traffic conditions as in item (5). This is illustrated in Figure 13.

FIGURE 11: PAVEMENT/SUBGRADE INTERACTION RESULTED IN MORE CRACKING ON SAND SUBGRADE THAN ON CLAY SUBGRADE

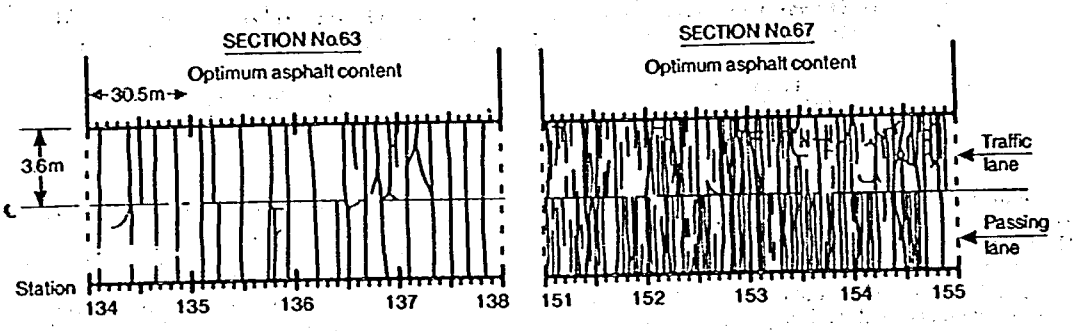


FIGURE 12: EXAMPLE OF PAVEMENT/SUBGRADE/TRAFFIC INTERACTION RESULTING IN CUMULATIVE CRACKING IN TRAFFIC LANE AFTER FIVE YEARS

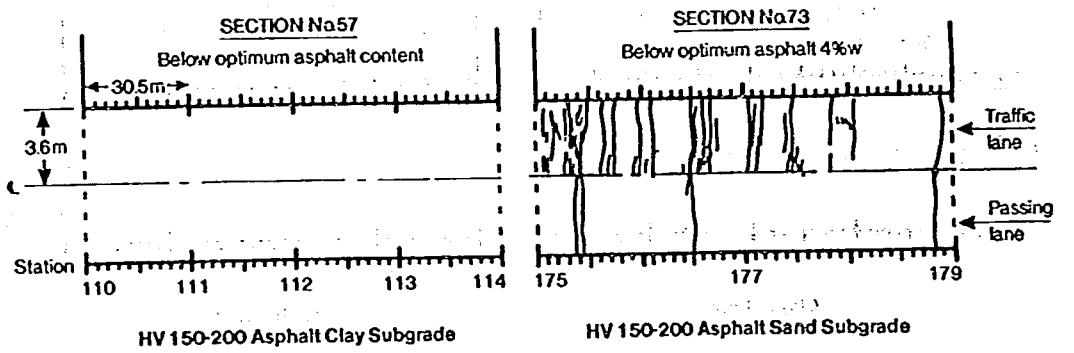
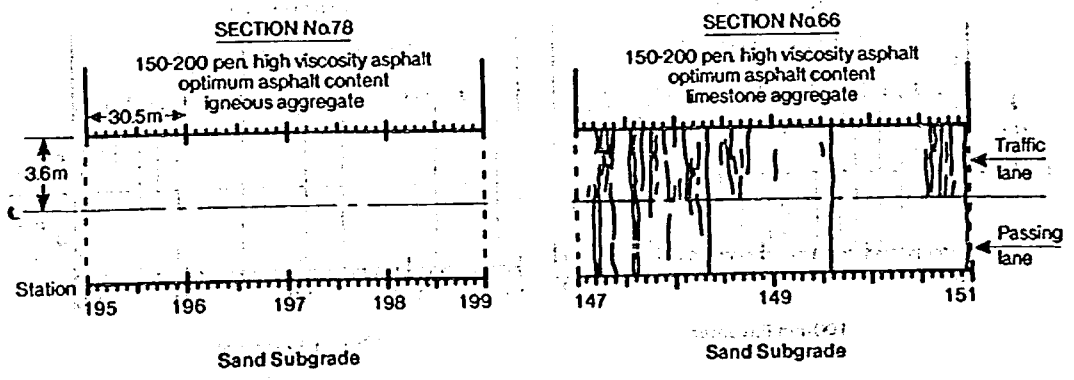


FIGURE 13: INFLUENCE OF HOT MIX AGGREGATE QUALITY ON TRANSVERSE CRACKING



(7) Asphalt content did not influence transverse cracking within the range of one per cent below Marshall optimum (4 per cent) to 0.5 per cent above Marshall optimum (5.5 per cent), as shown in Figure 14.
(8) Mix filler content did not affect transverse cracking within the range of 2 per cent to 5.5 per cent finer than the 75 μm mesh, as shown in Figure 15.

8 TRANSVERSE CRACKING OF COMPOSITE ASPHALT PAVEMENTS

As an adjunct to the main field trial, the test road mixes were also placed randomly in the sand subgrade area. This resulted in composite asphalt pavements in which the types and grades of asphalts in the wearing and binder courses differed. All of these structures comprised 100 mm of asphalt concrete and 150 mm of crushed gravel base course on a sand subgrade. This section of highway was in service for only a four-year period, from 1967 until 1971, when it was removed to permit road widening.

The performance of the composite asphalt pavements during this four-year period indicated that the type and grade of asphalt used in the wearing course was the prime factor influencing transverse cracking. No transverse cracking was observed when a non-cracking asphalt wearing course was placed over an asphalt binder course susceptible to transverse cracking. Conversely, transverse cracking was observed to progress through the wearing course and terminate at the interface when the above asphalt types were reversed in the wearing and binder courses, as shown in Figure 16. This verified that, in the short term, the temperature insulation properties of the asphalt wearing course shown in Figure 5 were sufficient to prevent transverse cracking of a composite asphalt pavement incorporating a cracking susceptible asphalt in the binder course.

From this part of the study it could only be concluded that the described composite pavement design approach was effective in delaying the onset of transverse cracking. The test did not last long enough to evaluate longer-term performance.

9 CORRELATION OF BINDER STIFFNESS WITH ROAD CRACKING OBSERVATIONS

Transverse cracking initiated during the first winter following construction. Pavement surface temperatures at the time of cracking were -34°C for the LV 150 to 200 and -37°C for the LV 300 to 400 pen asphalt pavements. Direct measurement of the asphalt stiffness modulus using the Shell sliding plate rheometer, as well as prediction using Van der Poel's nomograph (Figure 17), verified that, at the above temperatures when cracking initiated, both of the field-aged binders had a stiffness modulus of 1×10^9 N/m^2 (0.5 hour loading time), shown in Figure 18. It was concluded that the pavements with the HV 150 to 200 pen binder did not crack because its stiffness did not reach the above critical limit under the prevailing temperature extremes.

Based on this criterion, the critical cracking temperature for HV 150 to 200 pen asphalt pavements was predicted to be -44°C. This pavement surface temperature was never attained during the eight years before the test road was overlaid. The cracking of the HV 150 to 200 pavements in the sand subgrade area during the fifth winter was attributed to the pavement

FIGURE 14: ASPHALT CONTENT HAS NO INFLUENCE ON TRANSVERSE CRACKING

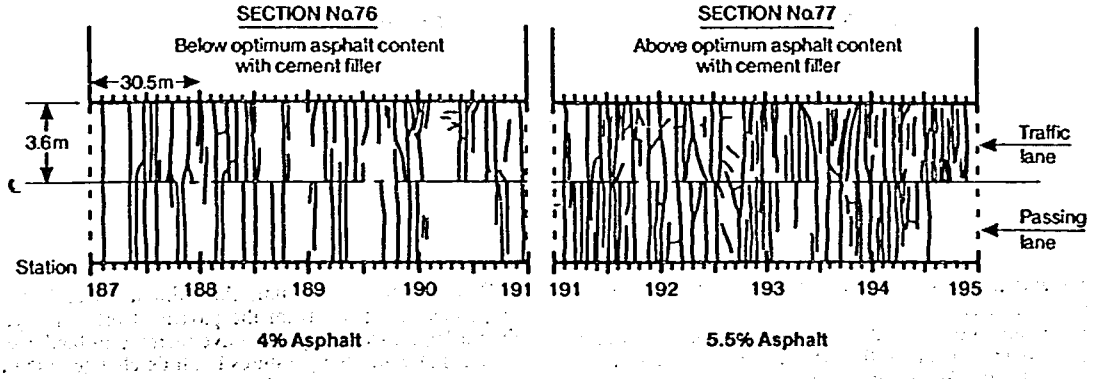


FIGURE 15: CEMENT FILLER CONTENT DID NOT AFFECT TRANSVERSE CRACKING

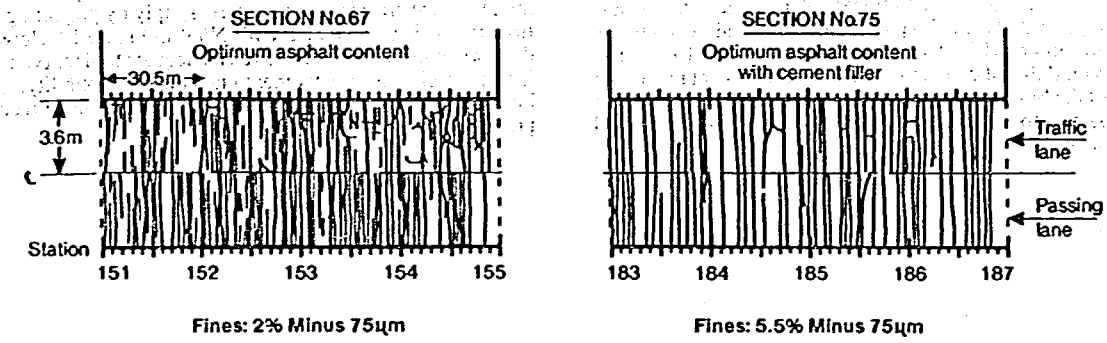
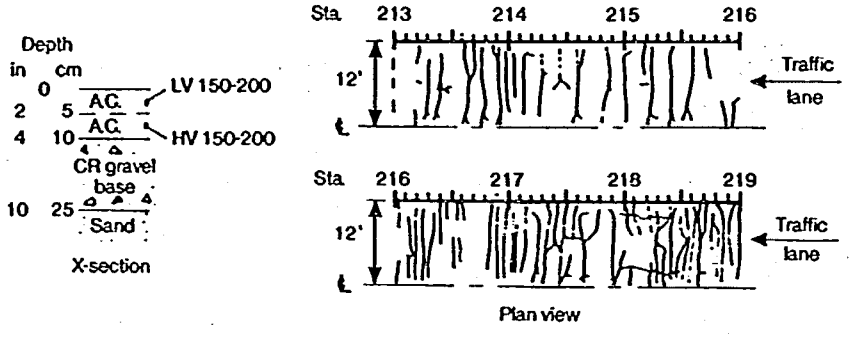
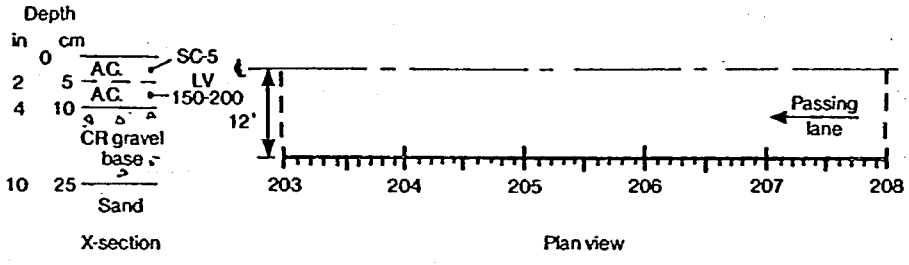


FIGURE 16: PERFORMANCE OF COMPOSITE ASPHALT PAVEMENTS SHOWING CRACKING WHEN CRACK-SUSCEPTIBLE ASPHALT USED IN WEARING COURSE AND NO CRACKING WHEN USED IN BINDER COURSE WITH NON-CRACKING ASPHALT WEARING COURSE



a) Composite LV 150-200 Pen./HV 150-200 Pen. Pavement



b) Composite SC-5/LV 150-200 Pen. Asphalt Pavement

interaction with this particular type of subgrade and cumulative damage from traffic.

The pavements constructed using SC-5 asphalt had a still lower stiffness modulus than the HV 150 to 200 pen asphalt. The reason why the SC-5 asphalt pavements neither cracked during the initial eight years before overlaying, (either on the sand or the clay subgrade), nor exhibited any susceptibility to traffic effects, was attributed to the low stiffness modulus of this binder under the lowest prevailing temperature conditions. It was concluded that this additional safety factor in stiffness modulus permitted the SC-5 pavements to override any adverse interaction imposed by the subgrade and traffic effects. The stiffness modulus of cutbacks with an oil component remaining as part of the binder could not be determined precisely as it was not possible to recover the binder without losing the oil component.

Comparison of original, thin-film aged and recovered properties of asphalt from the pavement after five years, in Figure 19, indicated a progressive increase in binder stiffness modulus at warm temperatures but little change in the regime at which transverse crack initiation was observed at low temperatures. While this was welcome news, it did not substantiate field evidence which indicated a tendency for pavement cracking to increase long term. Binder stiffness modulus appeared to be an excellent criterion for predicting the initial critical cracking temperature, simply by projecting back from the critical value of 1×10^9 N/m^2 in Figure 18. However, there was concern that this was an inadequate tool for predicting long-term change in pavement cracking susceptibility, as the binder structure was altered by reheating in the binder recovery process.

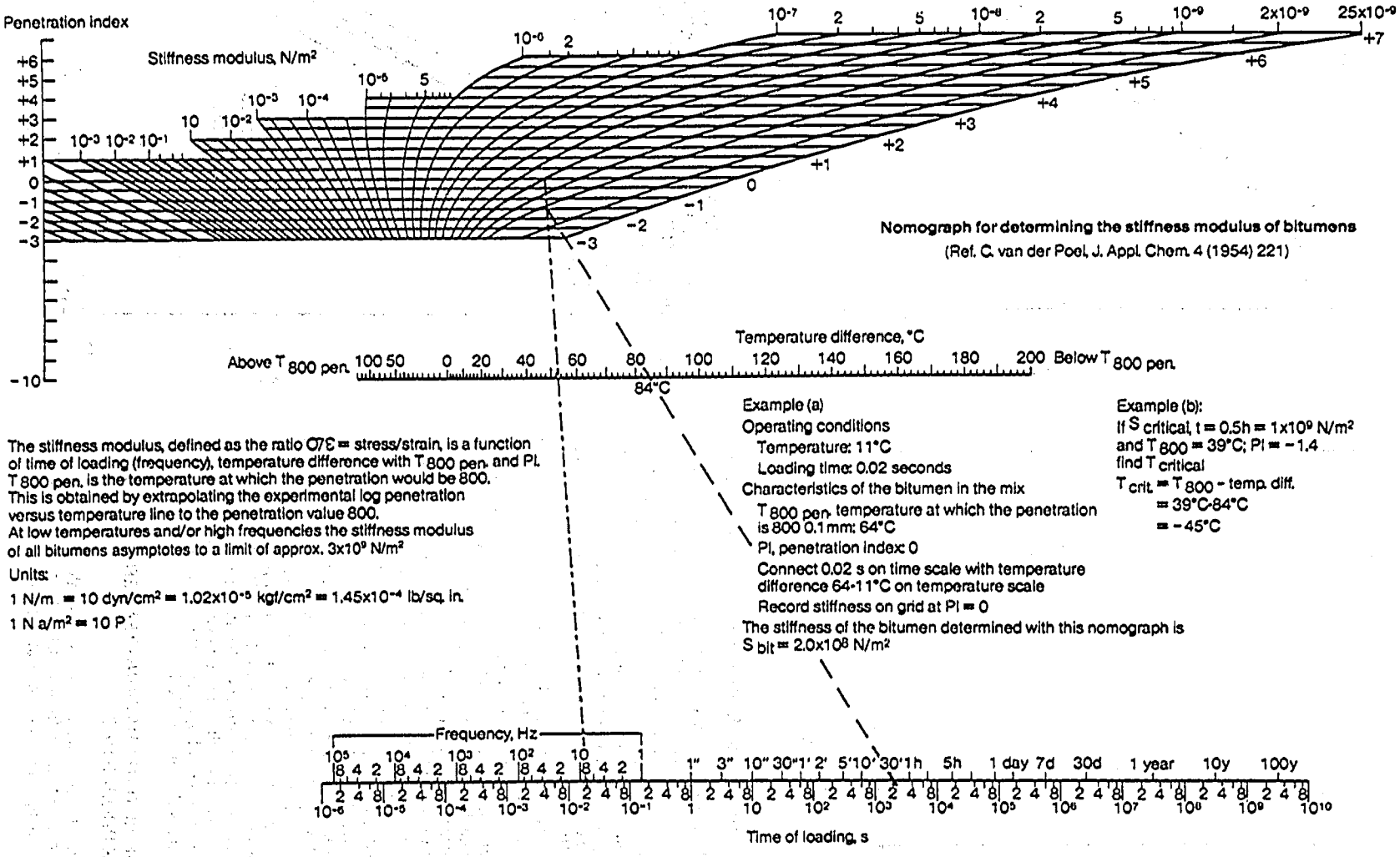


FIGURE 17: ASPHALT BINDER STIFFNESS NOMOGRAPH

FIGURE 18: CRITICAL BINDER STIFFNESS AT INITIATION OF TRANSVERSE CRACKING

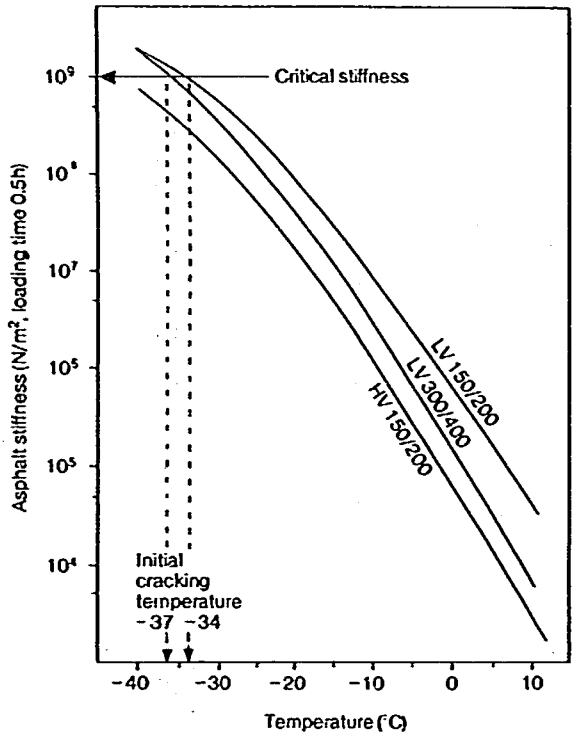
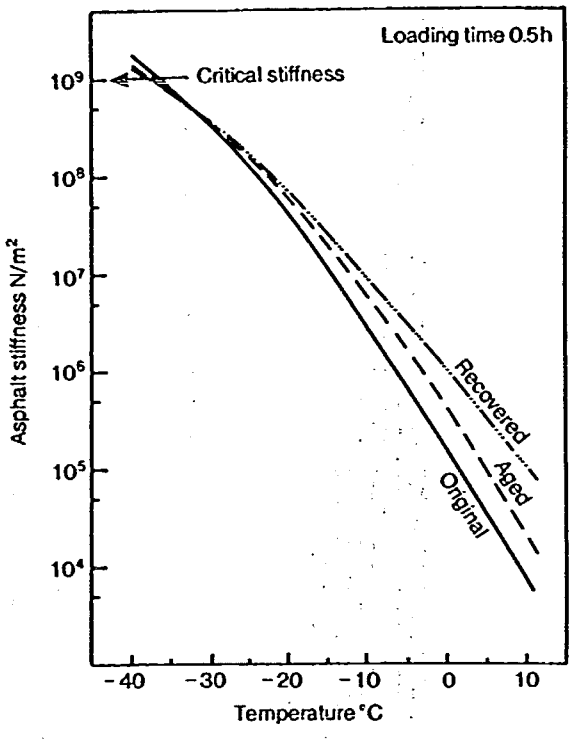


FIGURE 19: RECOVERED BINDER PROPERTIES FROM FIVE-YEAR-OLD PAVEMENT INDICATE LITTLE CHANGE IN STIFFNESS AT LOW TEMPERATURES

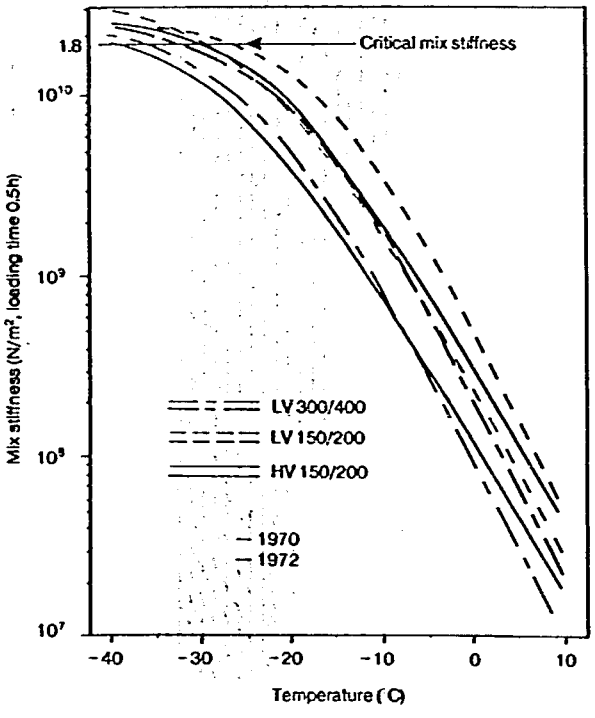


10 Influence of Mix Stiffness on Pavement Cracking

Initial mix stiffness data are not available as test techniques were only developed two years after test road construction. The relationship between temperature and mix stiffness, determined from low temperature tensile creep tests, is shown in Figure 20 for specimens cut from the test road in 1970. Based on the critical pavement temperature regime at the initiation of transverse cracking, the critical mix stiffness was estimated to be 1.8×10^{10} N/m^2.

Contrary to the recovered binder data, which indicated that binder stiffness changed little over time at low temperature extremes, the stiffness of mix specimens cut from test pavements showed an increase from 1970 to 1972 at all temperature levels, as shown in Figure 20. This has been attributed to molecular structural formation in the asphalt which is known to increase binder consistency over a period of time, commonly referred to as 'age hardening' or 'structural hardening' (as distinct from 'chemical ageing' which refers to the asphalt oxidation process). Such structure formation is readily reversible and can be destroyed on heating. The aged and recovered asphalts examined in the laboratory are free from 'age hardening' effects that presumably developed in the road mixes and therefore normal recovered asphalt properties, e.g. penetration and stiffness which do not truly represent the state of the binder at all stages of road life. On the other hand, directly-measured mix stiffness will reflect the influence of 'age hardening' in the asphalt and result in the low temperature mix stiffness increasing with age. The effect of this on mix cracking temperature is shown in Table 1.

FIGURE 20: INCREASE IN MIX STIFFNESS DUE TO PAVEMENT AGEING AND ASSOCIATED DETERIORATION OF CRITICAL CRACKING TEMPERATURE



11 PREDICTING CRACKING TEMPERATURE FROM MIX PROPERTIES

Cracking temperature for mixes was calculated from mix stiffness data, obtained from constant-load creep tests, and tensile breaking stress, obtained at a constant rate of strain.

TABLE 1: ACTUAL AND PREDICTED FRACTURE TEMPERATURES FOR STE. ANNE MIXES

Asphalt	Observed Fracture Temperature (°C) (Road Surface)		Predicted Fracture Temp. (°C) Tensile Creep Studies		Observed Fracture Temp. (°C) Quartz Frame
	Winter 1967/68	Winter 1971/72**	Spring 1970	Spring 1972	Spring 1972
HV 150/200	None*	-34	-36	-30	-31
LV 150/200	-34	-	-29	-25	-28
LV 300/400	-37	-34	-34	-30	-30

*Minimum pavement surface temperature was -38C
**Cracking occurred mainly in the sand subgrade test sections, and most extensively in the traffic lanes.

In this method the accumulated thermal stress (σ_T) is calculated from the thermal contraction coefficient (α) and mix stiffness ($S_{T,t}$) at a number of discrete temperature intervals (ΔT) using the following equation:

$$\sigma_T = \sum_{To}^{TM} (S_{T,t} \cdot \alpha \cdot \Delta T)$$

where the stiffness modulus $S_{T,t}$ = stress/strain and is a function of temperature (T) and loading time (t).

The cracking temperature is predicted by plotting both the calculated thermal stress and the breaking stress as a function of temperature and determining the cracking temperature from the intersection of the two curves, as shown in Figure 21. The stress relaxation that occurs has been taken into account automatically in the value of the stiffness modulus. Using mix stiffness at 0.5 hour loading time, Δ T of 5°C, based on an assumed cooling rate of 10°C/hour, this procedure yielded realistic differences in predicted cracking temperatures for the test road mixes which correlated with the temperatures at which the test pavements cracked initially. The predicted cracking temperatures from the two-and-a-half-year-old pavement specimens were lower than observed field cracking temperatures and still lower for the five-year-old pavement specimens. The decrease in predicted cracking temperatures was attributed to 'age hardening' or 'structural hardening' of the binder and weakening of the mix due to deterioration of mix strength resulting from cumulative fatigue effects.

The mix stiffness moduli at low temperatures and long-loading times were all determined using constant stress/load tests. Except for the condition at break, constant rate-of-strain tests lead to empirically irreconcilable differences in loading time and cannot be used in stiffness modulus determination.

The mix breaking stresses were measured under constant rate-of-strain conditions in the temperature range of 25°C to -40°C. For this type of testing only the conditions at break yield a rational test value, i.e. breaking stress, stiffness modulus and loading time pertain to the observed time to specimen failure. Except for experimental scatter, the test results for all of the different asphalts, shown in Figure 22, indicated that the mix breaking stress was a function of the mix stiffness.

The thermal coefficients of linear contraction of the mixes were measured in the two laboratories and found to be 1.8 to 1.9 x 10^{-5} κ^{-1} and 1.5 to 1.7 x 10^{-5} κ^{-1}. As coefficients of thermal contraction of asphalts are independent of source and type, differences are attributable to differences in aggregate/mix characteristics.

Consequently, when comparing the tendencies of mixes to crack at low temperatures, when the only variable is the asphalt binder, it should suffice to compare mix stiffness at temperatures close to the anticipated cracking temperature.

FIGURE 21: PREDICTION OF CRITICAL CRACKING TEMPERATURE FOR AN ASPHALT MIX

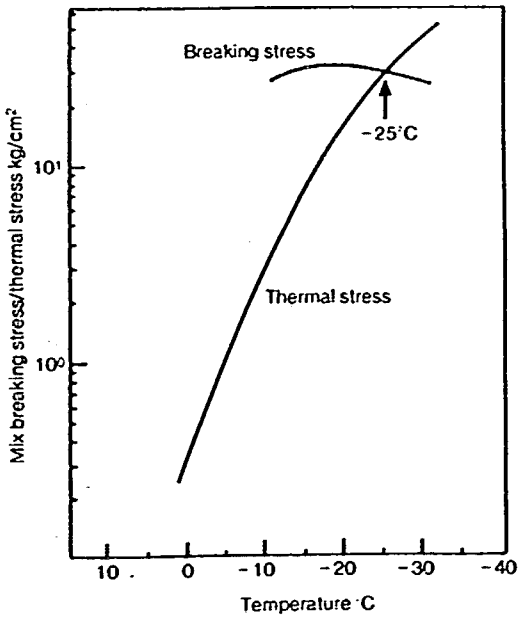


FIGURE 22: TENSILE STRENGTH OF MIX IS A FUNCTION OF MIX STIFFNESS

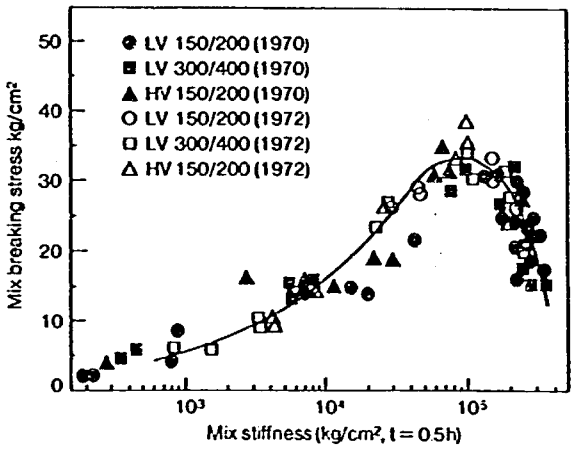
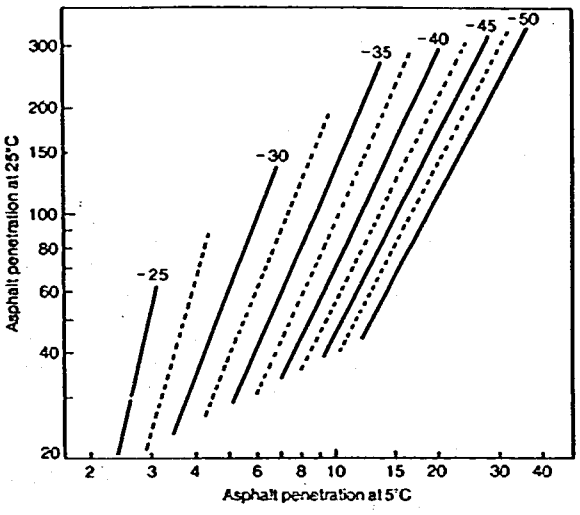


FIGURE 23: NOMOGRAPH FOR PREDICTING CRITICAL CRACKING TEMPERATURE FROM TWO PENETRATIONS



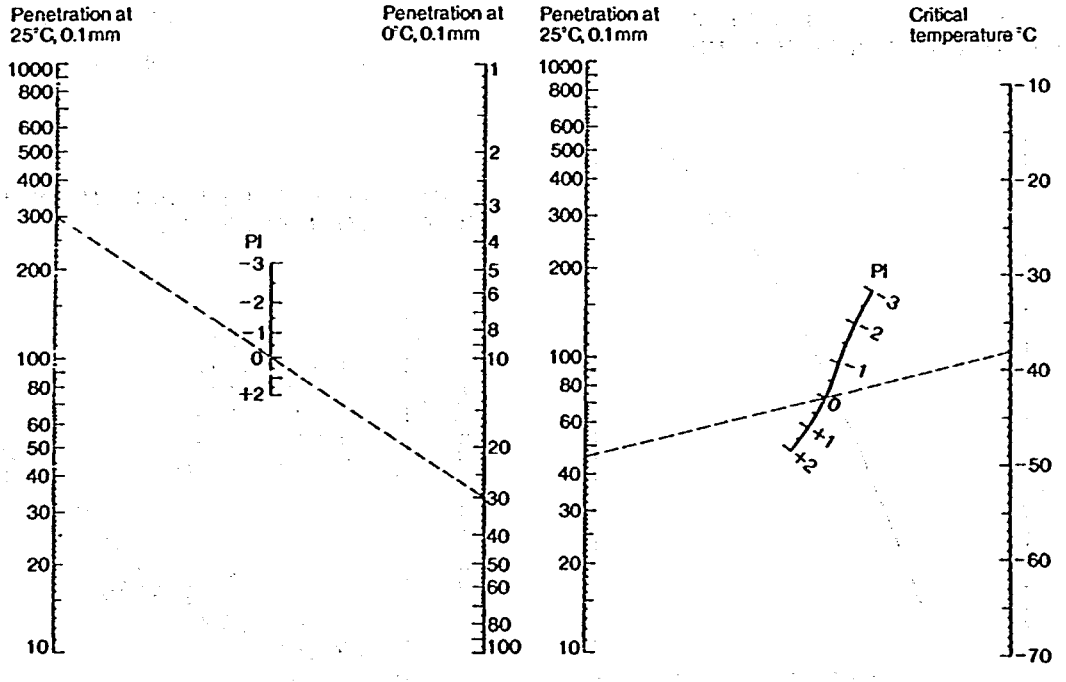
12 PREDICTION OF CRITICAL CRACKING TEMPERATURE

It was concluded from the foregoing studies that transverse cracking may be prevented, delayed or reduced for a considerable number of years by selecting for use an asphalt which has a sufficiently low stiffness modulus at the prevailing low temperature extremes. When binder stiffness is near the critical limit, then pavement thickness, mix aggregate characteristics, subgrade variables and traffic can be expected to influence the nature and frequency of transverse cracking.

Two types of nomographs have been developed for predicting the critical cracking temperature based on routine binder test data. These appear in Figures 23 and 24. As these nomographs have been based on initial cracking conditions of the Ste. Anne Test Road it is left, to the user to select a suitable safety factor. Alternatively, the designer may elect to use Van der Poel's stiffness nomograph, in Figure 17, and by selecting a binder stiffness modulus lower than $S = 1 \times 10^9$ N/m^2 (t = 0.5 h) work back to construct a transverse cracking nomograph with a built-in safety factor.

As pavements age, it becomes increasingly inaccurate to evaluate critical pavement cracking temperature from recovered binder properties due to the increase of binder consistency associated with its 'age hardening' or 'structural hardening' discussed above. The direct testing of pavement specimens to determine their stiffness or predicted cracking temperature, shown in Figures 20 and 22, is recommended for old pavements.

FIGURE 24: NOMOGRAPHS FOR PREDICTING CRITICAL CRACKING TEMPERATURE FROM PENETRATION AND PI AFTER J F HILLS

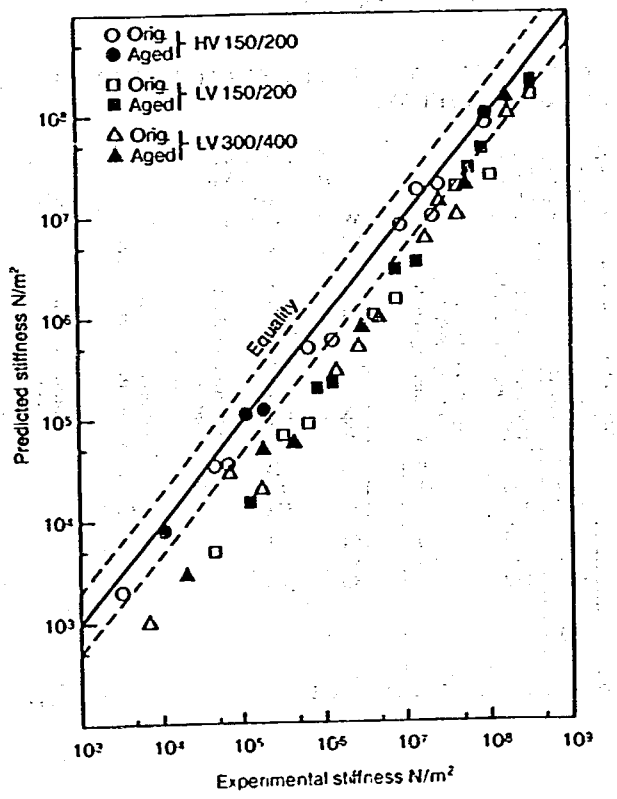


13 ASPHALT TEMPERATURE SUSCEPTIBILITY AND STIFFNESS EVALUATION

Temperature susceptibility is defined as the change in asphalt consistency with its change in temperature. The penetration index (PI) defines the slope of the penetration versus temperature line and has been found to be very useful for this purpose. Whereas there are various short-cut methods for determining PI, such as using the ring and ball softening point or viscosity, these are not applicable to all asphalts (i.e. waxy, air-blown or oxidized) and should not be used unless it has been first verified that the 'short-cut' procedures yield the same PI as determined from two penetration tests measured at different temperatures. The PI may be determined graphically with the aid of the Bitumen Test Data Chart, shown in Figure 2, by drawing a line parallel to the penetration line through the PI pivot point.

PI should not be considered as an asphalt performance criterion in its own right but rather as a useful tool in the determination of performance properties. For example, PI serves as an entry parameter in Van der Poel's nomograph, Figure 17, to permit accurate prediction of binder stiffness moduli at all temperatures in the pavement performance range. This is verified by the close agreement of the stiffness moduli between predicted values, using Van der Poel's nomograph, and directly measured values, using the Shell sliding plate rheometer. Figure 25 demonstrates close agreement for the HV 150 to 200 pen asphalt while the agreement is not quite as good for the waxy LV asphalts. This is to be expected, as Van der Poel has stated that the nomograph is not suitable for asphalts containing wax or other modifiers.

FIGURE 25: GOOD CORRELATION OF STIFFNESS BETWEEN MEASUREMENTS AND PREDICTIONS FROM VAN DER POEL'S NOMOGRAPH FOR NON-WAXY HV BINDER BUT NOT FOR WAXY LV BINDERS



In summary, the laboratory studies have verified that Van der Poel's nomograph may be used to predict asphalt stiffness very accurately over its full performance range, even down to temperature levels below -40°C. Alternatively, the Shell sliding plate rheometer has been found to be an excellent apparatus for the direct measurement of binder stiffness over the same temperature range.

14 ASPHALT SPECIFICATIONS

The Ste. Anne Test Road and observations of transverse cracking in other asphalt pavements eventually led to changes in Canadian highway department asphalt specifications to exclude the use of paraffinic asphalts such as the LV 150 to 200 pen asphalt which had been observed to be more susceptible to transverse cracking than higher viscosity asphalts. This was accomplished by raising the minimum viscosity requirement of the penetration grade asphalts.

In some Provinces the specification for the penetration range was further subdivided into two parts to separate Class A higher viscosity asphalts from Class B lower viscosity asphalts. The specifications currently used by the Western Canadian Prairies Provinces is shown in Figure 26, with PI lines superimposed. The Class A asphalt grades are generally used in the wearing course, while either Class A or Class B are acceptable for the binder course in new construction. It is believed by some that either grade may be used for thin overlays over transversely cracked pavements as the overlay from either grade will be subject to reflection cracking emanating from the old pavement.

15 PERFORMANCE OF THE OVERLAY

The Ste. Anne Test Road was designed structurally for early failure and necessitated overlaying in 1975, eight years after initial construction. The test road was overlaid with 125 mm of SC-5 asphalt concrete. Inspection of the test road overlay in 1987, twenty years after initial construction, revealed transverse cracking of the overlay to various degrees as detailed in Table 2.

FIGURE 26: WESTERN CANADIAN ASPHALT SPECIFICATION

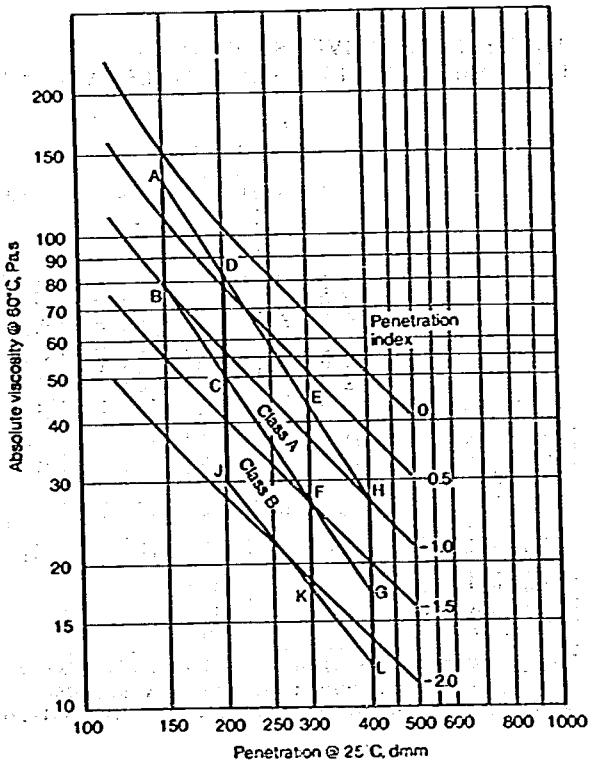
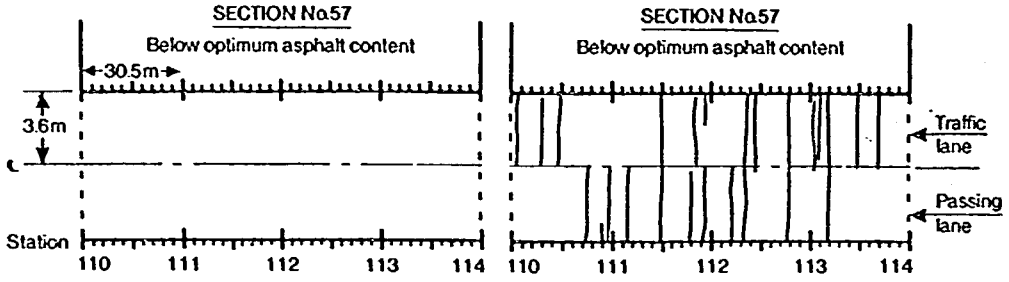


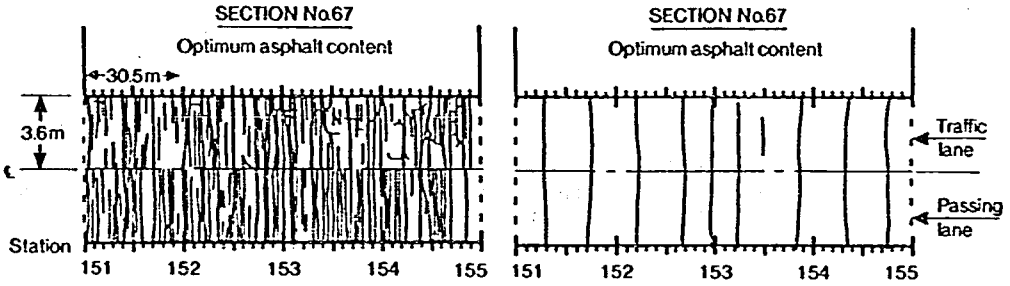
FIGURE 27: PAVEMENT WHICH HAD NOT CRACKED IN INITIAL EIGHT YEARS HAS CRACKED 12 YEARS AFTER OVERLAYING.



HV 150-200 Pavement Age: 8 Years

Same Pavement 12 Years After 125mm SC-5 Overlay

FIGURE 28: PAVEMENT WHICH HAD CRACKED IN INITIAL EIGHT YEARS SHOWS LITTLE REFLECTION RELATIVE TO ORIGINAL.



LV 150-200 Pavement Age: 8 Years

Same Pavement 12 Years After 125mm SC-5 Overlay

TABLE 2: TRANSVERSE CRACKING FREQUENCY OF TEST PAVEMENTS EIGHT YEARS AFTER CONSTRUCTION AND 12 YEARS AFTER OVERLAY (5 INCH SC-5 OVERLAY)

Road Structure	150-200 Penetration Grade Low Viscosity Asphalt (Western Canadian Crude)					150-200 Penetration Grade High Viscosity Asphalt (Western Canadian Crude)					300-400 Penetration Grade Low Viscosity Asphalt (Western Canadian Crude)				SC-5 Asph. (W.C. Crude)
	Below Optimum Asphalt Content	Below Optimum Asphalt, Cement Filler	Optimum Asphalt Content	Optimum Asphalt Content, Cement Filler	Above Optimum Asphalt Content	Below Optimum Asphalt Content	Below Optimum Asphalt, Cement Filler	Optimum Asphalt Content	Optimum Asphalt Content, Cement Filler	Optimum Asphalt Content, 100% Crush Igneous Aggregate	Below Optimum Asphalt Content	Below Optimum Asphalt, Cement Filler	Optimum Asphalt Content	Optimum Asphalt Content, Cement Filler	Optimum Asphalt Content
4 in. Pavement *	(1)156	168	177	146		0		41	8	0	66	24	89	114	0
16 in. Base Course	(2)107	50	66	66		107		49	33	41	107	82	49	57	81
Clay Subgrade	(3) 68	30	37	45				120	408		162	338	55	50	
4 in. Pavement *	437	298	656	386	386	123		16	73	0	164	33	287	107	0
6 in. Base Course	81	98	82	90	114	90		98	82	98	82	66	148	73	118
Sand Subgrade	18	33	13	23	30	73		608	112		50	200	52	69	
10 in. Full Depth *			82					50							
Asphalt Pavement			41					33							
Clay Subgrade			50					66							

* All aggregates in bituminous pavement mix processed from glacial drift deposits (20% igneous, 80% limestone, 50% crush) unless otherwise indicated.

(1) Number of transverse cracks per km after eight years (1975)

(2) Number of transverse cracks per km 12 years after overlay (1987)

In the test sections that had cracked prior to overlaying, generally 13 to 100 per cent of the cracks had reflected through the overlay with some sections developing additional cracking. The transverse cracking 'before' and 12 years 'after' overlaying of one such section is depicted in Figure 27.

All sections that had not cracked prior to overlaying exhibited transverse cracks in the overlay. One such section is shown in Figure 28. Coring across some of these cracks revealed that the transverse cracks passed through both the original pavement and the overlay. No data are available on the occurrence of these cracks.

16 ASPHALT AGEING

The progressive hardening of the test road binders over the 20-year period is shown in Table 3. The data indicates that the penetration of the recovered binders decreased between 1.5 and 2 tenths of a millimetre (dmm) per year for the 150 to 200 pen asphalts and was erratic for the softer asphalts. The properties of the SC-5 binder could not be determined precisely due to the presence of the heavy oil fraction which is prone to loss in the process of binder recovery from the mix. The rate of binder hardening observed is considered to be consistent with good

Table 3: Properties of Original Asphalts and Asphalts Recovered from Cores

Asphalt: HV 150/200

	Original Asphalt	Uncompacted Mix 1967	Cores Taken 1970	Cores Taken 1972	Cores Taken 1987
Pen. @ 25 C, dmm	159.0	71	61.0	55.0	43.0
Pen. @ 15 C, dmm	–	27	23.0	20.0	17.0
Pen. @ 5 C, dmm	–	10.2	7.5	8.4	6.3
Pen. @ 4 C, dmm	14.0	–	–	–	–
Visc. @ 135 C, mm^2/s	225.0	372	402.0	370.0	523.0
Visc. @ 60 C, Pa.s	59.1	260	299.0	259.0	525.5
Soft. Pt., R & B, C	39.0	50	49.4	53.7	53.5
Penetration Index	-1.4	-0.3	-0.8	-0.1	-0.3
Nomographic Cracking Temperature, °C (Fig. 23)	-40.0		-36.5	-39.0	-35.8

Asphalt: LV 150/200

	Original Asphalt	Uncompacted Mix 1967	Cores Taken 1970	Cores Taken 1972	Cores Taken 1987
Pen. @ 25 C, dmm	192.0	91	79.0	67.0	51.5
Pen. @ 15 C, dmm	–	28	25.0	20.0	19.7
Pen. @ 5 C, dmm	–	8.3	7.5	7.5	7.0
Pen. @ 4 C, dmm	10.0	–	–	–	–
Visc. @ 135 C, mm^2/s	110.0	158	174.0	167.0	209.7
Visc. @ 60 C, Pa.s	25.3	43.9	69.6	81.3	110.9
Soft. Pt., R & B, C	35.0	43	44.6	48.8	50.2
Penetration Index	-2.7	-1.7	-1.6	-1.0	-0.6
Nomographic Cracking Temperature, °C (Fig. 23)	-34.0		-34.0	-35.0	-36.0

Asphalt: LV 300/400

	Original Asphalt	Uncompacted Mix 1967	Cores Taken 1970	Cores Taken 1972	Cores Taken 1987
Pen. @ 25 C, dmm	313.0	177	120.0	119.0	103.0
Pen. @ 15 C, dmm	–	43	37.0	34.0	35.0
Pen. @ 5 C, dmm	–	13.7	10.5	11.4	10.5
Pen. @ 4 C, dmm	14.0	–	–	–	–
Visc. @ 135 C, mm^2/s	86.0	98	131.0	117.0	144.6
Visc. @ 60 C, Pa.s	14.1	15	34.0	33.5	36.0
Soft. Pt., R & B, C	31.2	37.2	40.7	41.7	48.0
Penetration Index	-2.9	-2.0	-1.7	-1.5	-1.4
Nomographic Cracking Temperature, °C (Fig. 23)	-37.0		-37.0	-37.5	-37.0

Table 3 (continued)

Asphalt: SC-5 – 1967 Test Pavements

	Original Asphalt	Uncompacted Mix 1967	Cores Taken 1987 1st Set Top	1st Set Bottom	2nd Set** Top	2nd Set** Bottom
Pen. @ 25 C, dmm	–	193.0	89.0	54.5	192.0	197.0
Pen. @ 15 C, dmm	–	–	36.0	27.3	67.0	68.3
Pen. @ 5 C, dmm	–	–	15.0	13.0	23.8	24.3
Pen. @ 4 C, dmm	53.0	–	–	–	–	–
Visc. @ 135 C, mm^2/s	89.0	166.0	248.0	900.2	148.1	139.3
Visc. @ 60 C, Pa.s	9.6	–	105.0	883.2	32.0	27.8
Soft. Pt., R & B, C	–	–	46.8	48.5	42.7	41.8
Penetration Index	–	–	-0.2	+1.7	-0.8	-0.8
Nomographic Cracking Temperature, 'C (Fig. 23)	–	–	-46.8	-49.0	-47.5	-47.5

** Note: Extracted asphalt had kerosine smell.

Asphalt: SC-5 – 125 mm Overlay, 1975 (1987 Core Data)

	TOP	MIDDLE	BOTTOM
Pen. @ 25 C, dmm	43.0	62.0	63.3
Pen. @ 15 C, dmm	18.5	22.0	23.2
Pen. @ 5 C, dmm	7.5	8.0	8.3
Pen. @ 4 C, dmm			
Visc. @ 135 C, mm^2/s	704.8	395.9	392.5
Visc. @ 60 C, Pa.s	475.2	239.3	221.2
Soft. Pt., R & B, C	53.5	48.8	48.7
Penetration Index	+0.03	-0.7	-0.6
Nomographic Cracking Temperature, 'C (Fig. 23)	-38.0	-37.0	-37.5

construction practice as the various asphalt mixes were designed generally for effective air void contents of 4 to 6 per cent and the pavements were compacted between 97 and 100 per cent of design density.

While of interest, the significance of the 20 year old binder data cannot be ascertained based on recovered properties only, as 'structure formation' within the binder is likely to influence its performance.

17 CONCLUSIONS

The performance of the Ste. Anne Test Road pavements over a 20-year period revealed that transverse cracking cannot be prevented in the long term under the low winter-temperature conditions prevailing in Manitoba. A number of variables were found to be significant, however, in delaying crack initiation and reducing the frequency of pavement cracking. The main findings were as follows:

(1) Transverse cracking occurred at low temperatures when the asphalt pavement was 'brittle' and when the road was subjected to longitudinal thermal contraction.

(2) The critical stiffness moduli at the time of cracking were determined to be 1.8×10^{10} N/m^2 for the asphalt mix and 1×10^9 N/m^2 for the asphalt binder, both measured at a loading time of 0.5 hour.

(3) Pavements for which the stiffness moduli exceeded the above limits (i.e. in (2) above) cracked during the first winter.

(4) Other pavements, for which the stiffness moduli were below the above limits, resisted cracking for over eight years. These were mixes incorporating soft asphalts (i.e. high penetration) or less temperature susceptible asphalts (i.e. high penetration index).

(5) Tests on pavement specimens cut from the test sections showed an increase in mix stiffness with time. This was attributed to 'age hardening' or 'structural hardening' of the binder and was judged to contribute to progressive transverse cracking with time.

(6) While recovered binder stiffness correlated with transverse cracking initially, its precision was found to diminish with time for predicting changes in susceptibility to cracking. This was attributed to the reversal of 'structural hardening' during binder recovery from the pavement.

(7) Subgrade type affected initiation and frequency of transverse cracking for mixes/binders for which the stiffness was close to the critical values (i.e. in (2) above).

(8) The 250 mm thick asphalt pavements exhibited 40 per cent of the transverse cracking found in the thin asphalt pavements.

(9) The cumulative effects of traffic increased the frequency of transverse cracking of some of the pavements on the sand subgrade.

(10) A dense mix made with 100 per cent crushed aggregate was found initially to be more resistant to transverse cracking and immune to cracking from traffic effects.

(11) Asphalt content did not influence cracking within the range of 1 per cent below to 0.5 per cent above Marshall optimum.

(12) Mix filler content did not influence cracking within the range of 2 per cent to 5.5 per cent finer than 75 μm.

(13) Composite asphalt pavements incorporating a 'non-cracking' asphalt wearing course and a 'crack-susceptible' asphalt binder course verified that the temperature insulation properties of the wearing course were adequate to prevent cracking of such a composite asphalt pavement in the short term.

(14) Twelve years after overlaying with 125 mm asphalt concrete, generally 13 to 100 per cent of the cracks had reflected through from the test pavements that had cracked initially.

(15) The penetration of the recovered binders decreased between 1.5 dmm to 2 dmm per year for the 20 year period.

(16) All of the test pavements exhibited transverse cracking 20 years after initial construction.

In restrospect, the Ste. Anne Test Road has served to define the significance of a number of variables which affect transverse crack initiation and frequency and this knowledge has contributed to the development of asphalt specifications, which have been effective in minimising transverse cracking.

18 ACKNOWLEDGEMENT

The Ste. Anne Test Road programme has been sponsored jointly by the Manitoba Highway Department and Shell Canada Limited. The findings summarised herein are a collation of the efforts of researchers from both of the above organisations.

REFERENCES

I. Deme, and D. Fisher, *Ste. Anne Test Road — Instrumentation*, Proc. Canadian Technical Asphalt Assoc., Vol XIII, Nov. 1968.

I. Deme, *A Study of Transverse Cracking of Asphalt Pavements in Manitoba*, Graduate Thesis, University of Manitoba, July 1969.

F.D. Young, I. Deme, R.A. Burgess and O. Kopvillem, *Ste. Anne Test Road - A Field Study of Transverse Crack Development in Asphalt Pavements — Construction Summary and Performance after Two Years Service*, Proc. Cdn. Tech. Asph. Assoc., Nov. 1969.

R.A. Burgess, O. Kopvillem, F.D. Young, *Ste. Anne Test Road — Relationship between Predicted Fracture Temperatures and Low Temperature Field Performance*, Proc. AAPT, Feb. 1971.

R.A. Burgess, O. Kopvillem, F.D. Young, *Ste. Anne Test Road — Flexible Pavement Design to Resist Low Temperature Cracking*, Proc. 3rd Int. Conf. on Struct. Design of Asph. Pavements, 1972.

W.J. Gaw, R.A. Burgess, F.D. Young, *Ste. Anne Test Road — Road Performance after Five Years and Laboratory Predictions of Low Temperature Performance*, Proc. Cdn. Tech. Asph. Assoc., Vol XIX, Nov. 1974.

J.T. Christison, and K.O. Anderson, *The Response of Asphalt Pavements to Low Temperature Climatic Movements*, Proc. 3rd Int. Conf. on Struct. Design of Asphalt Pavements, Vol. 1, 1972.

I. Deme, F.D. Young and R.W. Culley, *Low Temperature Performance of Composite Asphaltic Concrete Pavements*, Proc. Cdn. Tech. Asph. Assoc., Nov. 1975 and Proc. 4th Int. Conf. on Struct. Design of Asph. Pavements, Vol. 2.

F.D. Young, *Discussion*, Proc. Cdn. Tech. Asph. Assoc., Vol. XXV p. 322 — 324, 1981.



Testing of Softening Point and Brittle Point of Asphalt Mixtures for the Evaluation of Their Rheological Properties

M. Yamada, Osaka City Univ.

TESTING OF SOFENTING POINT AND BRITTLE POINT OF ASPHALT MIXTURES FOR THE EVALUATION OF THEIR RHEOLOGICAL PROPERTIES

by

Masaru Yamada, Dr. of Eng., Associate Professor
Department of Civil Engineering
Faculty of Engineering, Osaka City University

ABSTRACT

Asphalt is thermoplastic and shows stress relaxation properties. By the use of asphalt mixtures, therefore, continuously flat pavements with no joint can be constructed in a short time. Also, demolished mixtures can be reused if they are heated again. However, these are premised that the rheological properties are maintained all during the life after construction, and the properties must be sometimes examined. When an old asphalt mixture is reused, the properties of the asphalt in it are tested to recontrol them. For these purposes, asphalts are generally recovered from mixtures. However, the recovery of asphalt from mixture is difficult and also the accuracy of the recovery is not high.

In this study, two methods for testing asphalt mixtures to examine their rheological properties and also estimate those of asphalts in them without the operation of recovery are proposed. One is a method for testing softening point of mixtures which is like the ring and ball method for asphalts. The other one is a method for testing brittle point of mixtures which is like the Fraass method for asphalts. The specimens of asphalt mixtures tested by the methods are small and thin so that they are convenient for testing mixtures from existing pavements. This paper presents findings of research on applicability of the methods.

TESTING OF SOFTENING POINT AND BRITTLE POINT OF ASPHALT MIXTURES FOR THE EVALUATION OF THEIR RHEOLOGICAL PROPERTIES

by

Masaru Yamada, Dr. of Eng., Associate Professor
Department of Civil Engineering
Faculty of Engineering, Osaka City University

1/ INTRODUCTION

More than ninty percent of paved road in Japan is asphalt pavement. Asphalt used for it is a thermoplastic material which soften upon heating and again harden upon cooling. Therefore, asphalt can be easily mixed with aggregates if only they are heated to the required temperature, and the mixture becomes hard enough to resist deformation under traffic loads if it is cooled to the normal temperature. Unlike cement concretes, asphalt mixtures which contain appropriate proportions of asphalt and aggregates show remarkably stress relaxation properties at the road temperatures.

By the use of the asphalt mixtures, therefore, continuously flat pavements with no joint can be constructed in a short time. Also, demolished mixtures produced by road reconstruction can be reused if they are heated again. However, these are premised that the rheological properties above mentioned are maintained all during the life after construction, and the properties must be sometimes examined. When an old asphalt mixture is reused, the properties of the asphalt in it are tested to recontrol them. For these purposes, asphalts are generally recovered from mixtures. However, the recovery of asphalt from mixture

is difficult for road construction engineers, and also the accuracy of the recovery is not high.

In this study, two methods for testing asphalt mixtures to examine their rheological properties and also estimate those of asphalts in them without the operation of recovery are proposed. One is a method for testing softening point of asphalt mixtures, which is like the ring and ball method for asphalts. The other one is a method for testing brittle point of asphalt mixtures, which is like the Fraass method for asphalts. The specimens of asphalt mixtures tested by the methods are small and thin so that the methods are convenient for testing mixtures from existing pavements. This paper presents findings of research on applicability of the methods.

2/ OUTLINE OF THE TEST METHODS

2.1/ TEST SPECIMENS

For both tests of the softening point and the brittle point, specimens are rectangular strips cut from compacted asphalt mixture samples. Thickness, length and width of the strips are 10mm, 150mm and 50mm respectively. Test specimens from existing pavements can be cut from cylindrically cored samples of 150mm in diameter as shown in Fig-1-(a), though they are not regularly rectangular. It is advisable that the strips are cut parallel to the road surfaces, because the degree of hardening of asphalts in the pavements varies generally with the depth. For this research, test specimens were also cut from asphalt mixtures compacted with a roller compacter in the laboratory to the dimensions of 300mm×300mm×50mm as shown in Fig-1-(b).

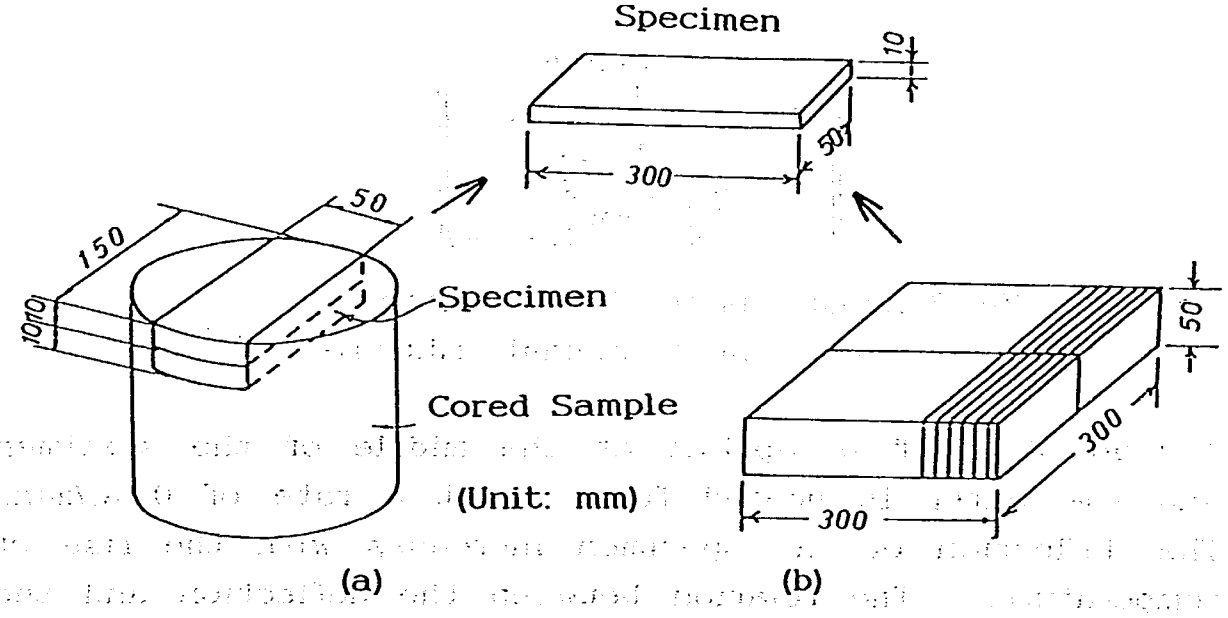


Fig-1 Preparation of specimens by cutting of asphalt mixture samples from existing pavements or compacted in the laboratory

2.2/ TEST OF SOFTENING POINT

In the ring and ball test method for the softening point of asphalt, a disc of asphalt is enclosed in a ring immersed in water at 5℃. A steel ball is placed at the top of the disc of asphalt and the water is heated at a constant rate, 5℃/min. The softening point is defined as the temperature of the water at which the asphalt softens and sags downwards a distance of 25mm under the weight of the steel ball.

In the test method for the softening point of asphalt mixture used in the research, the temperature at which the asphalt mixture softens and sags by not much more than its dead weight is similarly measured. A specimen of asphalt mixture is placed on two supports of stainless steel rod and immersed in water as shown in Fig-2. The distance between the supports is 100mm.

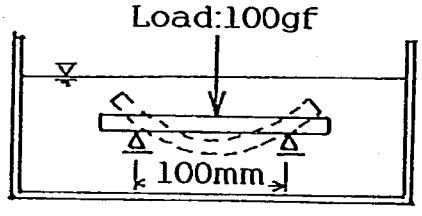


Fig-2 Apparatus for the softening point test of asphalt mixture

A load of 100gf is applied at the middle of the specimen and the water is heated from 5℃ at a rate of 0.5℃/min. The deflection of the specimen increases with the rise of temperature. The relation between the deflection and the temperture is illustrated as shown in Fig-3. The temperature at the inflection point of the curve in the figure is referred to as the softening point of the asphalt mixture. Also, the amount of deflection at the inflection point may be connected with the ductility of the asphalt mixture.

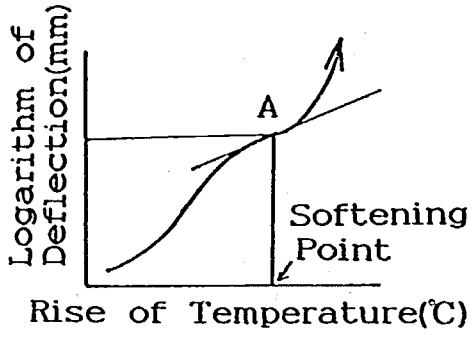


Fig-3 Definition of the softening point of asphalt mixture

2.3/ TEST OF BRITTLE POINT

In the Fraass test method for the brittle point of asphalt, a thin film of asphalt, 0.5mm thick, coated on a steel plate is cooled at a constant rate, 1℃/min, and bent repeatedly in the same direction. The brittle point, called the Fraass breaking point, is the temperature at which the film of asphalt first becomes brittle as indicated by the appearance of cracks.

In the test method for brittle point of asphalt mixture used in this research, the brittle point is also measured as the temperature at which the asphalt mixture hardens and breaks under such a small deflection as causes no damage at the normal temperature.

A specimen of asphalt mixture is set in the three-point bending apparatus as shown in Fig-4 and subjected to the very slow bending action of sinusoidal load produced by an electric vibration. The span is 120mm and the frequency is 0.01Hz. The amplitude of the deflection at the middle of the specimen is kept constant, ±0.15mm, and the load is measured. It is comfirmed that the fatigue life under this condition is more than 1000 cycles at the normal temperature. The specimen temperature during the test is

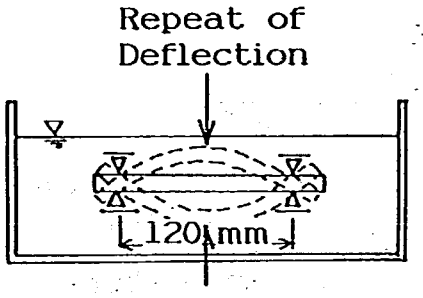


Fig-4 Apparatus of the brittle point test of asphalt mixture

controlled by a water/ethyleneglycol bath. The temperature in the bath is lowered from 15℃ at rate of 0.5℃/min.

The relation between the load and the temperature is illustrated as shown in Fig-5. The load increases with the fall of temperature till reaches at a maximum value and begins to show any sign of declining. The temperature at which the load reaches at the maximum value is referred to as the brittle point of the asphalt mixture.

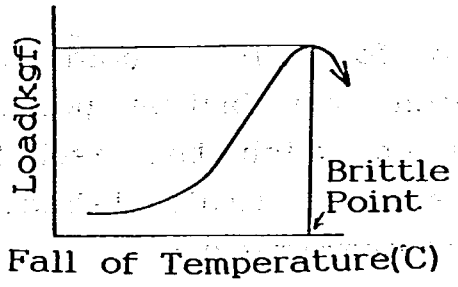


Fig-5 Definition of the brittle point of asphalt mixture

3/ RELATION BETWEEN RESULTS OF THE TESTS FOR ASPHALT MIXTURES AND PROPERTIES OF ASPHALTS RECOVERED FROM THE MIXTURES

Dense-graded asphalt mixtures containing four different types of asphalts were compacted in the laboratory and tested to investigate on the relation. Many samples of asphalt mixtures were also cored from existing pavements. To test the properties of asphalts in these mixtures, the asphalts were recovered from the mixtures by the Abson method.

Fig-6 shows the relation between the softening point of asphalt mixture and that of recovered asphalt. Although there is some scatter, a regression curve can be obtained in the figure.

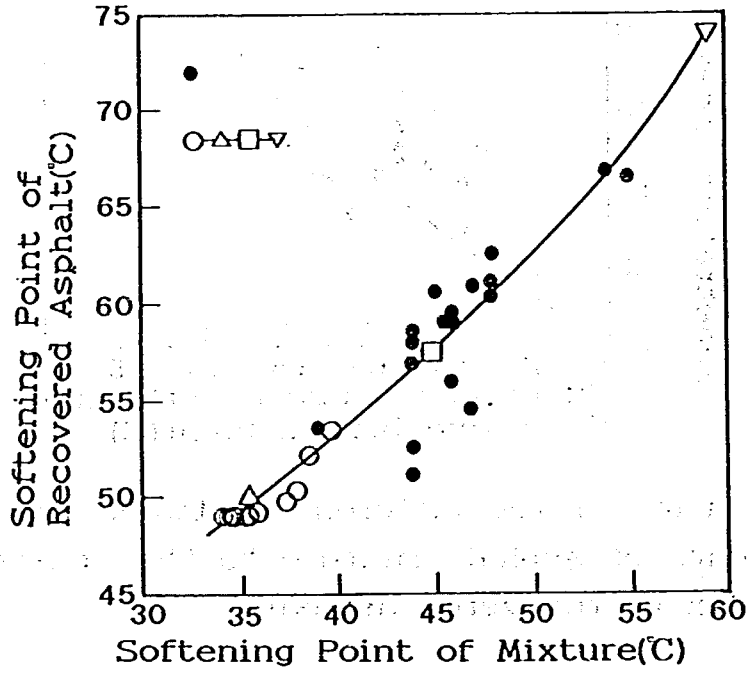


Fig-6 Relation between the softening point of asphalt mixture and that of recovered asphalt

The brittle point of asphalt mixture may be also related to the Fraass breaking point of recovered asphalt. Although the Fraass breaking point is not generally used to evaluate asphals for pavement constructions, it is known that the difference between the ring-and-ball softening point and the Fraass breaking point correlates with the penetration index.[1] The difference between softening point and brittle point of asphalt mixtures is plotted against the penetration index of their recovered asphalts in Fig-7.

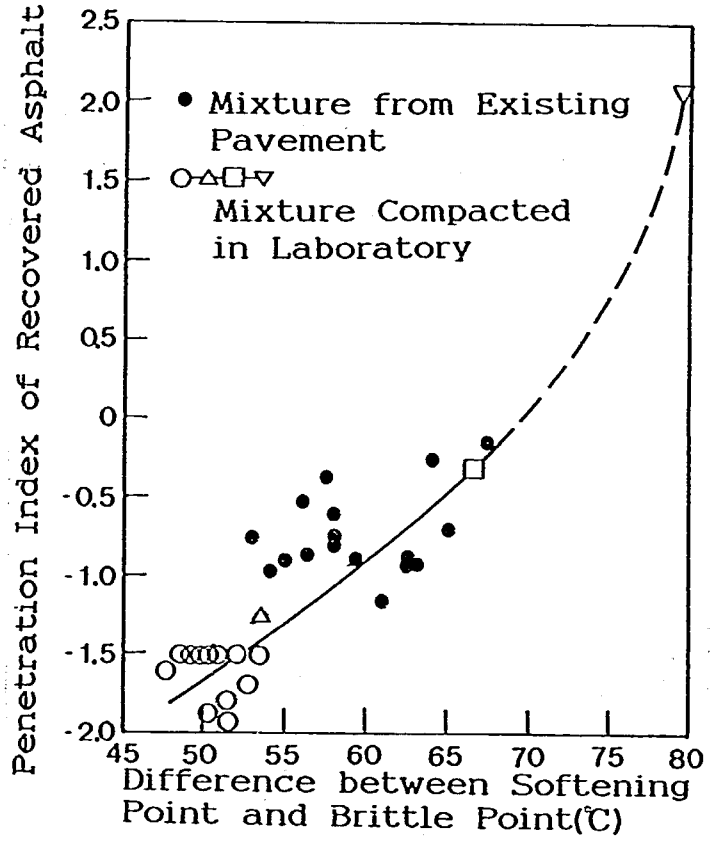


Fig-7 Relation of the difference between the two points of asphalt mixture to the penetration index of recovered asphalt

The parameter most widely used to characterize the hardness of asphalt is penetration. It is said that the penetration of an asphalt corresponds to its stiffness at 25℃ and 0.4sec.[1] In the case of asphalts used in pavement

constructions, this stiffness also corresponds to the stiffness at about 12℃ for 0.01Hz which is the test condition in the brittle point test of asphalt mixture.
Fig-8 shows the relation between the mixture stiffness at 12℃ measured in the brittle point test for asphalt mixtures and the penetration of their recovered asphalts.

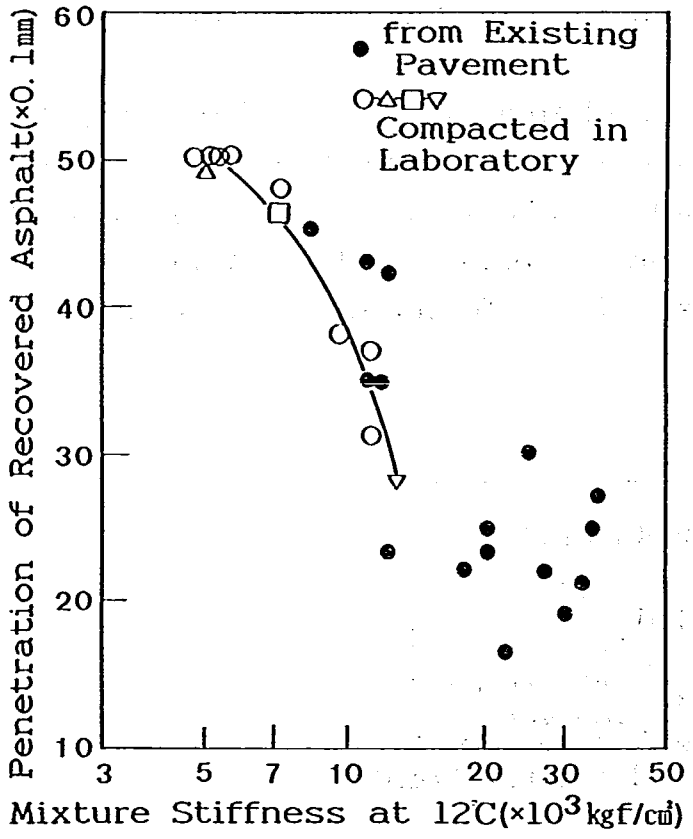


Fig-8 Relation between the mixture stiffness at 12℃ measured by the brittle point test and the penetration at 25℃ of recovered asphalt

From these results, it will be sure that the tests of softening point and brittle point of an asphalt mixture can serve to predict the rheological properties of its recovered asphalt though the prediction accuracy may be not high.

4/ INFLUENCES OF TYPE OF MIXTURE AND ASPHALT CONTENT UPON THE RESULT OF THE TESTS

It seems that the scatter of points plotted in each of Fig-6 to 8 is largely caused by errors on the recovery and the tests of asphalt. However, It cannot be overlooked that type of mixture and asphalt content may have a considerable influence on the result of the tests.

Fig-9 shows the change in the softening point, the brittle point, the between them and the mixture stiffness at 12℃ with the asphalt content in a dense-graded asphalt mixture and a fine-graded asphalt mixture which are made with the same materials. It is found in the figure that an increase

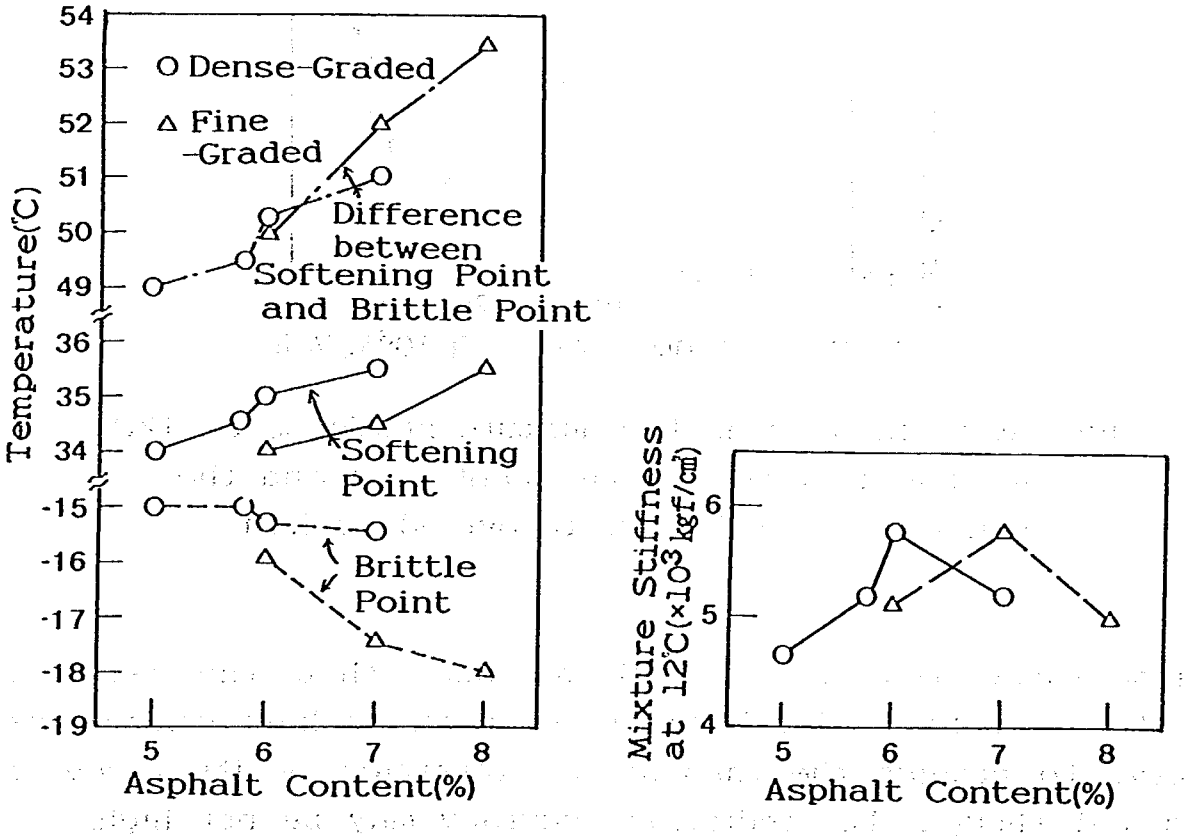


Fig-9 Results of the tests for two mixtures with different asphalt contents

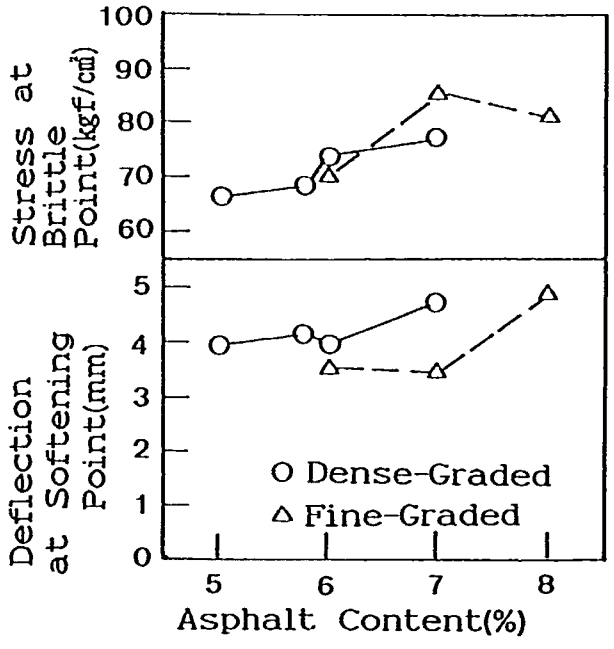
of 1% in the asphalt content effects a rise of about 1℃ in the softening point, a fall of about 1℃ in the brittle point, consequently an increase of about 2℃ in the difference between the two points and an increase of about 1000kgf/㎠ in the mixture stiffness at 12℃. Therefore, when the softening point, the penetration index and the penetration of recovered asphalt are predicted from the test results of an asphalt mixture by using the regression curves as shown in Fig-6 to 8 and if the change of asphalt content in the mixture is ±1%, errors of ±1℃, ±0.15 and 3(×0.1㎜) or so respectively seem to be unavoidable.

It is also seen in Fig-9 that the softening point and the brittle point of the fine-graded asphalt mixture are sightly lower than these of the dense-graded asphalt mixture and the differences between the two points of the two mixtures are consequently very similar. The difference between the mixture stiffnesses at 12℃ of the two mixtures is not clear.

5/ OTHER PROPERTIES MEASURED BY THE TESTS

As mentioned above, deflections and loads are measured in the tests of the softening point and the brittle point respectively. Deflections of the specimens in the brittle point test are very small. Thus, the load in the brittle test can be converted into the maximum bending stress by calculation. However, it is difficult in the softening point test to calculate the strain from the deflection, because the deflection is large.

Fig-10 shows the deflection at the softening point and the maximum bending stress at the brittle point of two mixtures with different asphalt contents. It can be seen in the figure that the deflection at the softening point and the stress at the brittle point increase with the asphalt content.



Fif-10 Relations between the deflection at the softening point or the stress at the brittle point and the asphalt content

Fig-11 and Fig-12 show test results on asphalt mixtures after heating at 60℃. The deflection at the softening of mixture decreases with the period of heating. It can be considered that this is caused by hardening of the asphalt, because the penetration of the recovered asphalt decrease with the period of heating.

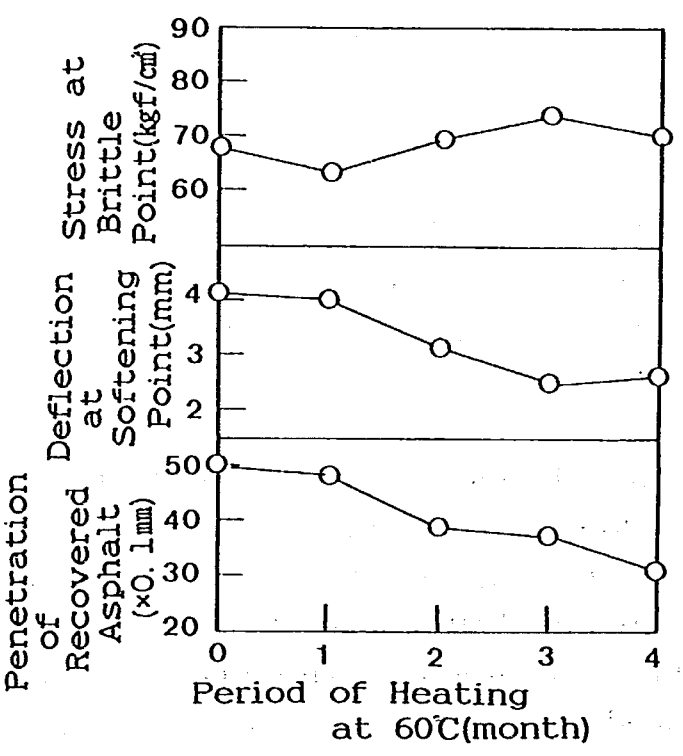


Fig-11 The deflection at the softening point and the stress at the brittle point of asphalt mixtures after heating, and the penetration of asphalts recovered from them

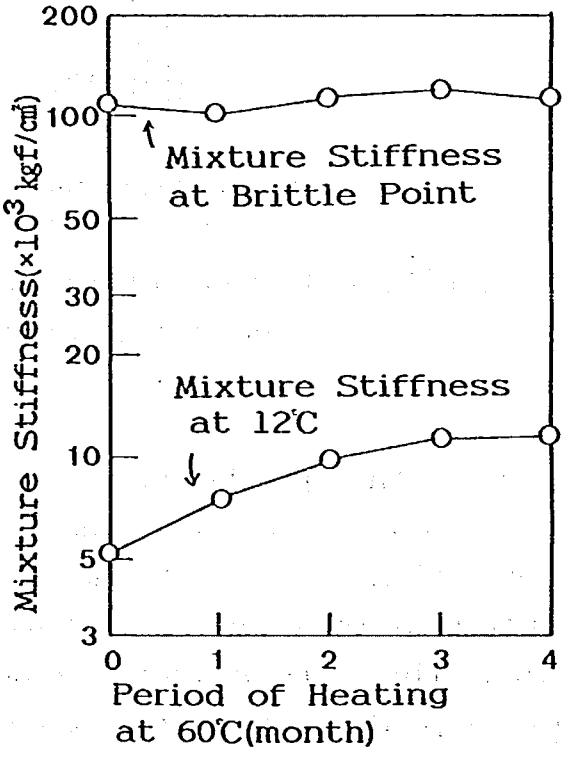


Fig-12 The stiffness at 12℃ and at the brittle point of asphalt mixtures after heating

However, the change of the stress and stiffness at the brittle point with the period of heating cannot be seen in the figures, though the increase of the stiffness at 12℃ is clear. Fig-13 shows relations of the brittle point and the stress at the point against the deflection applied for the

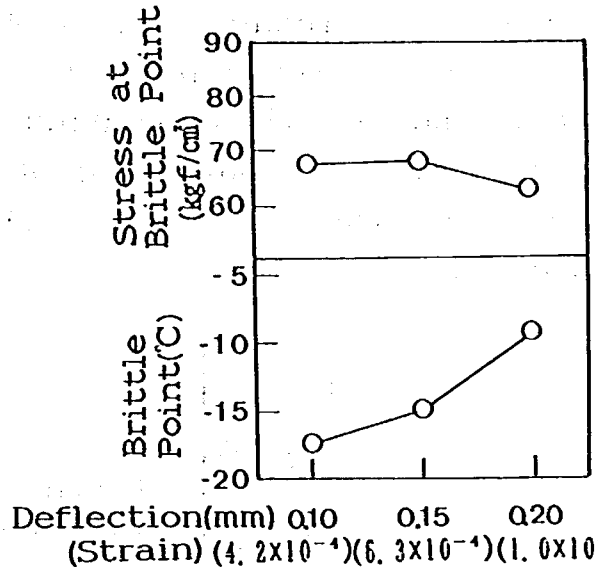


Fig-13 Relations of the brittle point and the stress at the point against the deflection applied for the test

test. Though the brittle point changes with the deflection, the stress at the point does not change unless the deflection is too large. Therefore, it is found that a specimen of asphalt mixture in the brittle point test breaks when the stress has reached at a level. The stress level of asphalt mixtures compacted in the laboratory for this research is 60kgf/cm² to 80kgf/cm².

From these results, it can be said that the deflection at the softening point and the stress at the brittle point describe the ductility at high temperatures and the strength at low temperatures respectively of the asphalt mixture.

6/ CONCLUSIONS

1) The tests of softening point and brittle point of an asphalt mixture can serve to predict the rheological properties of its recovered asphalt.
2) The deflection at the softening point and the stress at the brittle point descride the ductility and the strength respectively of the asphalt mixture.

7/ ACKNOWLEDGEMENTS

The auther would like to express the acknowledgements to the Public Bureau, Kobe City who gave their invaluable support to the research, and to Mr. M. Hashida and Mr. T. Akasaka who cooperated in the research.

REFERENCE

1) Van der Poel, C.: A general system describing the visco-elastic properties of bitumens and its relation to routine test data, J. Appl. Chem., 4, 221-236, 1954.

Test Methods to Characterize Low Temperature Cracking

V. Janoo, J. Bayer Jr., CRREL, USA
T. Vinson, Oregon State Univ.
R. Haas, Univ. of Waterloo

TEST METHODS TO CHARACTERIZE LOW TEMPERATURE CRACKING

by

Vincent Janoo, Research Civil Engineer
U.S. Army Cold Regions Research and Engineering Laboratory
Hanover, New Hampshire, USA

Ted. S. Vinson, Professor of Civil Engineering
Oregon State University, Corvallis, Oregon, USA

Ralph Haas, Professor of Civil Engineering
University of Waterloo, Waterloo, Ontario, Canada

John Bayer Jr, Research Technician
U.S. Army Cold Regions Research and Engineering Laboratory
Hanover, New Hampshire, USA

ABSTRACT

Thermal cracking of asphalt concrete pavements is a serious problem in the northern tier states of the conterminous U.S. and in Alaska, Canada, Japan and parts of Europe. One theory on the cause of thermal cracking is that the thermally induced tensile stress in the asphalt concrete exceeds its tensile strength. Cracks that result from this condition are called low temperature cracks. Another theory is that thermal cracks occur when the pavement structure is thermally fatigued by daily temperature cycles. Cracks resulting from the second mechanism are called thermal fatigue cracks. As part of a cooperative study by CRREL and U.S. Strategic Highway Research Program A003, a research project was established to investigate thermal cracking. Prior to starting the project, a literature review was conducted on current test methods for characterizing asphalt concrete behavior at low temperatures and/or under thermal cycling. The objective of the survey was to determine the types of tests and equipment currently used, the properties measured by the respective tests, and the degree to which the tests simulate actual field conditions. The purpose of this paper is to present the results of this review.

INTRODUCTION

Thermal cracking is a serious problem in the United States, Canada, Japan and parts of Europe. As shown in Figure 1, thermal cracking in the conterminous states in the U.S. has been reported at locations where the air freezing index is above 360°C days (Finn et. al. 1976). Thermal cracks usually run transversely across roads and airfield pavements (Fig.

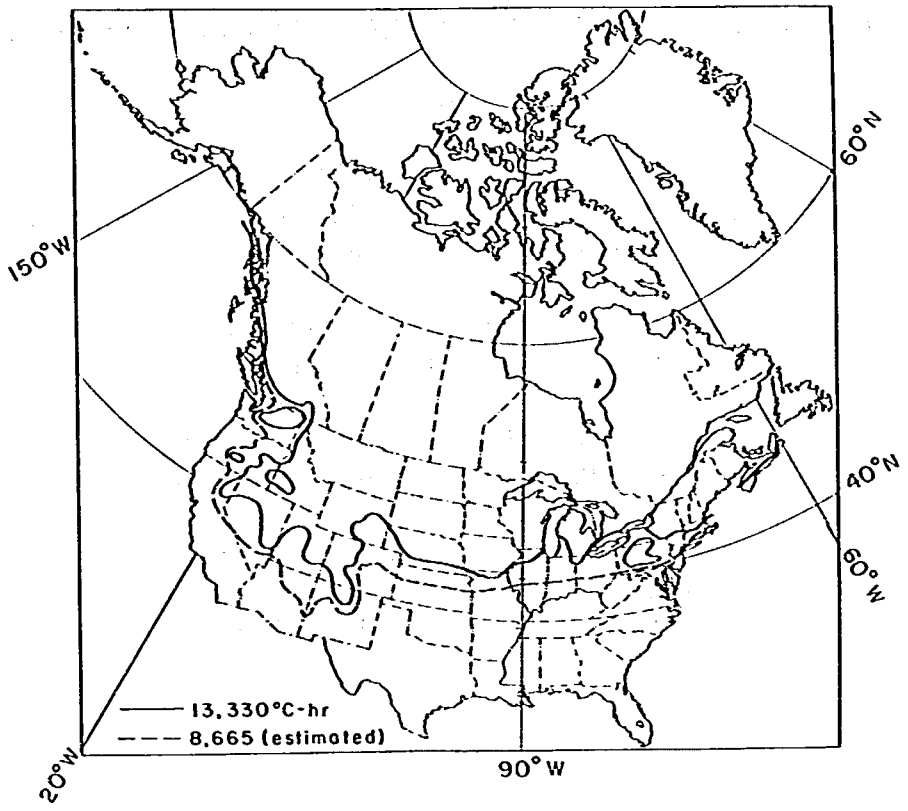
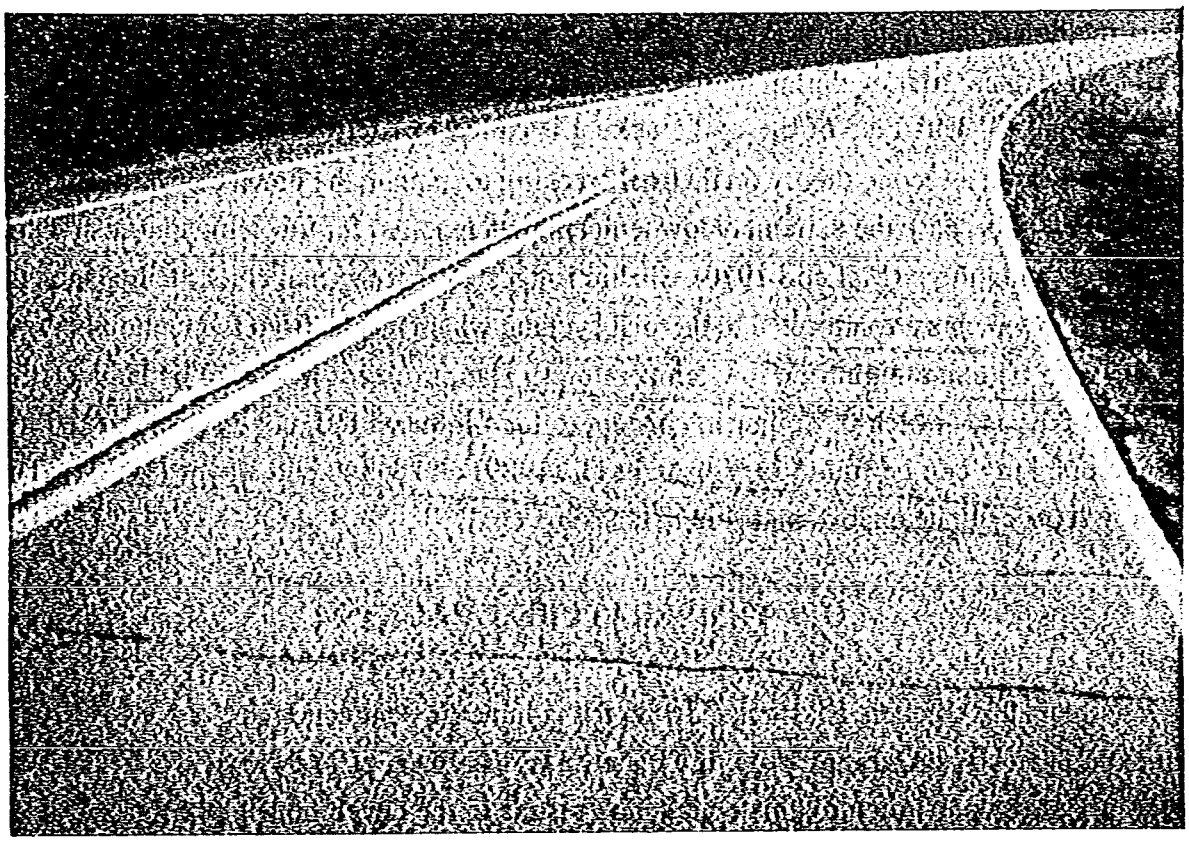


Figure 1. Areas of low temperature cracking in North America.

2a). With the propagation of the thermal cracks through the pavement structure, a conduit for the migration of water and fines into and out of the pavement is created, as shown in Figure 2b. The intrusion of water into the base/subbase and subgrade can lead to a saturated condition. When a load is applied to the saturated pavement structure, an undrained loading condition may exist, resulting in an increase in pore water pressure. This reduces the effective stress of the soil structure and, in turn, reduces the shear strength of the unbound layers. Another possible distress is pumping of fines through these cracks under traffic loading. The pumping will produce voids under the pavement and cracking around the joints will result.

The results of several studies on the economic impact of thermal cracking have been reported in the literature. For example, Haas et al. (1987) reported that the Canadian Air Transport Administration could save approximately $10 million (1985 dollars) in maintenance if thermal cracking were reduced by 50%. Linde (1988) cited a 1972 U.S. Air Force report that estimated annual damage to airplanes on the order of $130 million was directly related to pavement cracking. Another benefit of reducing thermal cracking is in the extension of time before an overlay is required.

Currently, there are two hypotheses on why thermal cracks occur. One theory states that thermal cracking results when the thermal stress in the asphalt concrete (AC) pavement ex-



a. Typical transverse cracks.



b. Crack acting as conduit for water and fines.

Figure 2. Typical low temperature cracking.

ceeds the tensile strength of the AC mixture. This form of cracking was reported on a new overlay in Galena, Alaska, during the 1988 winter where air temperatures reported were in the range of –60°C. This type of thermal cracking is called low temperature cracking. Shahin (1972) proposed a second theory on thermal cracking to explain the transverse cracking seen in west Texas, because the extremely low temperatures required for low temperature cracking are rarely found there (McLeod 1970). Shahin suggested that thermal cracks can also occur when AC pavements are subjected to thermal cycling, which results from fluctuation between the daytime high and nighttime low temperatures. The pavement is said to be subjected to "thermal fatigue," which is similar in concept to load-induced fatigue. Reviews of thermal fatigue cracking can be found in Vinson et al. (1989) and Janoo and Bayer (1990a). This paper will concentrate on low temperature cracking.

LOW TEMPERATURE CRACKING

Low temperature cracking is associated with the volumetric contraction that occurs as a material experiences a temperature drop. If a material is restrained, as in the case for asphalt concrete in a pavement structure, this contraction results in the development of a thermal stress that can produce cracking when the stress exceeds the tensile strength of the material, as shown in Figure 3. The temperature at which failure occurs is referred to as the fracture

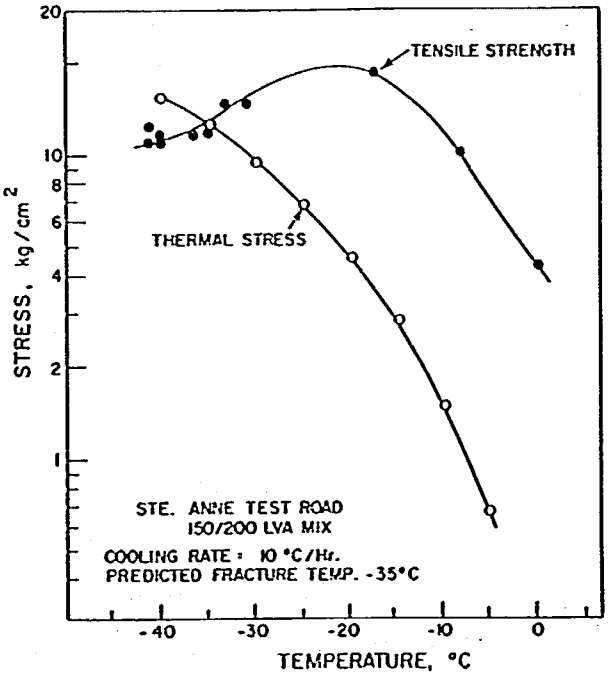


Figure 3. Prediction of fracture temperature for a restrained strip of asphalt concrete.

temperature. In new pavements, cracks generally have been observed to appear at 30-meter spacings. As the pavement ages and/or more extreme temperature drops occur, the crack spacing decreases to 3–6 m.

The parameter commonly required in design scenarios that include low temperature cracking is the *fracture temperature*. There are several methods used to determine this temperature, such as the viscous flow temperature method (Fromm and Phang 1972), penetration PI method (Sugawara et al. 1982), mix cracking temperature method, and limiting mix stiffness method. The latter two are the most commonly cited in the literature.

MIX CRACKING TEMPERATURE METHOD

The failure criterion for the mix cracking temperature method is that fracture occurs when the thermal stress exceeds the tensile strength of the asphalt concrete mixture. Computer programs such as COLD (Finn et al. 1986) and TC-1 (Shahin and McCullough 1972) use this failure criterion to predict low temperature cracking.

The thermal stress that is produced in the asphalt concrete is usually calculated using elastic analytical methods. For example Monismith et al. (1965) used the stress equations developed by Humphreys and Martin (1963) to predict the stresses in a slab composed of a linear viscoelastic material subjected to a time-dependent temperature field. Christison et al. (1972) concluded from their study that viscoelastic slab analysis tends to overestimate the thermal stresses, viscoelastic beam analysis underestimates the stresses, and a psuedo-elastic beam analysis yields intermediate values. For the sake of simplicity, the thermal stresses can be calculated using the psuedo-elastic equations put forth by Hills and Brien (1966). The equation is as follows:

$$\sigma_x(t) = \int_{t_0}^{t} S\left(\Delta t, T\right)\, \alpha(T)\, dT(t) \qquad (1)$$

where $\sigma_x(t)$ = accumulated thermal stress.
α = coefficient of thermal contraction.
$S(\Delta t,T)$ = asphalt mix stiffness modulus, function of time and temperature.

Equation 1 can be solved numerically using a finite difference scheme (Christison et al. 1972). Assuming that the coefficient of thermal contraction (α) is independent of temperature, eq 1 is approximated as

$$(\Delta \sigma_x)_i = \frac{\alpha}{2} (S_i + S_{i-1}) (T_i - T_{i-1}). \quad (2)$$

Christison et al. (1972) found that the stress calculated from the above equation was dependent on the time interval (Δt) used in the numerical evaluation. The viscoelastic methods eliminate the time dependency of the psuedo-elastic methods but require more computational effort (Christison et al. 1972). Through the evolution of high-powered personal computers, the time requirements for analysis can easily be reduced. Therefore, by better characterizing the AC, the viscoelastic methods could become a good tool for predicting thermal stresses. The material properties required in eq 1 are the coefficient of thermal contraction and the stiffness of the asphalt concrete.

Monismith et. al. (1965), Littlefield (1967), Jones et al. (1968) and Osterkamp (1986) reported measurements on the linear thermal contraction coefficients of asphalt pavement. In a survey of methods, Hooks and Goetz (1964) reported that thermal expansion of bituminous material can be measured with 127-mm and 254-mm strain gages, dual microscope apparatus, linear variable displacement transducers, and water and mercury filled dilatometers. The coefficient of thermal contraction is usually held constant in the analysis. Typical values reported are presented in Table 1.

Table 1. Coefficient of thermal contraction of AC mixtures.

Investigators	α (1/°C)	Temperature range (°C)
Monismith, et al. (1965)	$2.2 - 2.5 \times 10^{-5}$	–23 to 21
Jones et al. (1968)	2.0×10^{-5}	–37 to 16
Osterkamp et al. (1986)	$1.7 - 2.2 \times 10^{-5}$	–56 to 6.4
Burgess et al. (1971)	$1.9 - 2.2 \times 10^{-5}$	–40 to 20
Sugawara et al. (1982)	2.0×10^{-5}	?
Sato et al. (1982)	$2.1 - 3.0 \times 10^{-5}$	–20 to 10
Janoo and Bayer (1990a)	2.4×10^{-5}	–40 to 0

The stiffness of the AC mixture in eq 1 is generally determined by first estimating the asphalt cement stiffness using Van der Poel's nomograph (1954). The stiffness of the asphalt cement is then used with either the Heukelom and Klomp (1964) relationship between asphalt and mixture stiffness or the Bonnaure et al. (1977) nomograph. Hills and Brien (1966), and Christison et al. (1972) used a loading time (Δt) equal to the time step ($t_i - t_{i-1}$) to calculate

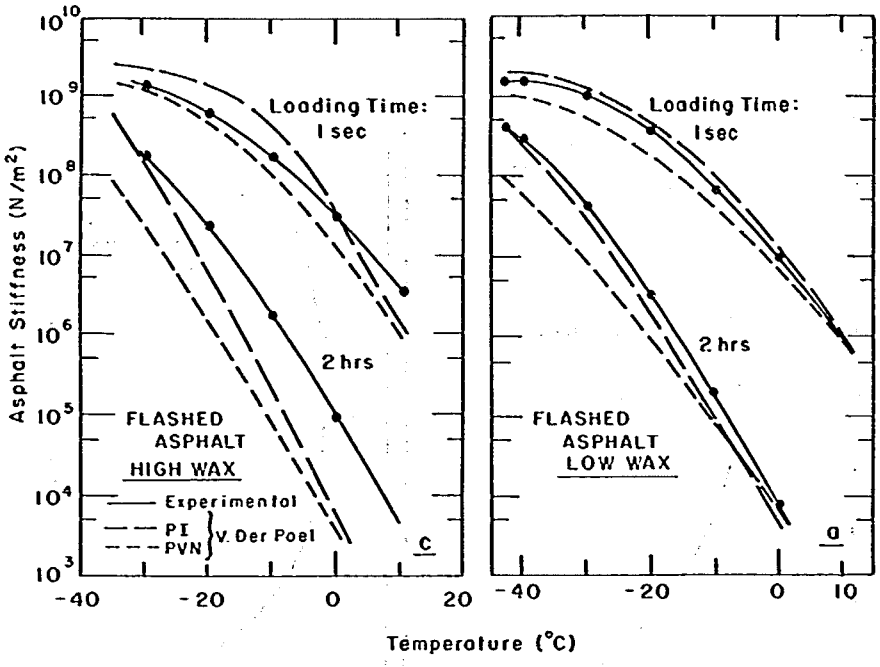


Figure 4. Comparison of calculated and measured asphalt stiffness.

the stiffness of the AC layer. Gaw (1978) compared measured and calculated asphalt cement stiffness and his results show large differences depending on whether high or low wax asphalt was used (Fig. 4). Also shown in Figure 4 is the effect of loading time on asphalt concrete stiffness. This variation in asphalt stiffness will in turn affect the stiffness of the asphalt concrete.

The tensile strength of the AC mixture is commonly determined from indirect or direct tension tests. The *indirect tension test*, or the tensile splitting test, has been used extensively to characterize the stress–strain response of asphalt concrete at low temperature (Shields 1964,Christison 1966, Anderson and Hahn 1968, Shields et al. 1970, Haas and Anderson 1969, Christianson 1970, Dempsey et al. 1980, Anderson and Epps 1983, Anderson and Leung 1987, Hadipour and Anderson 1988). The test procedure involves loading Marshall specimens (102 mm in diameter and 64 mm thick) across the diameter in a compression testing frame. As the specimen is compressed at a set temperature, a relatively uniform tensile stress develops perpendicular to and along the vertical diametrical plane of the specimen (Fig. 5). Ultimately, the specimen is subjected to a failure stress and the specimen fails by splitting along its vertical diameter. The applied load and horizontal and vertical deformations are monitored through a load cell and linear variable displacement transducers, respectively. A schematic of the tensile splitting test is shown in Figure 6.

The interpretation of the results obtained in a tensile splitting test is based on the theory of elasticity. A plane stress condition is assumed and a biaxial stress state is developed in the

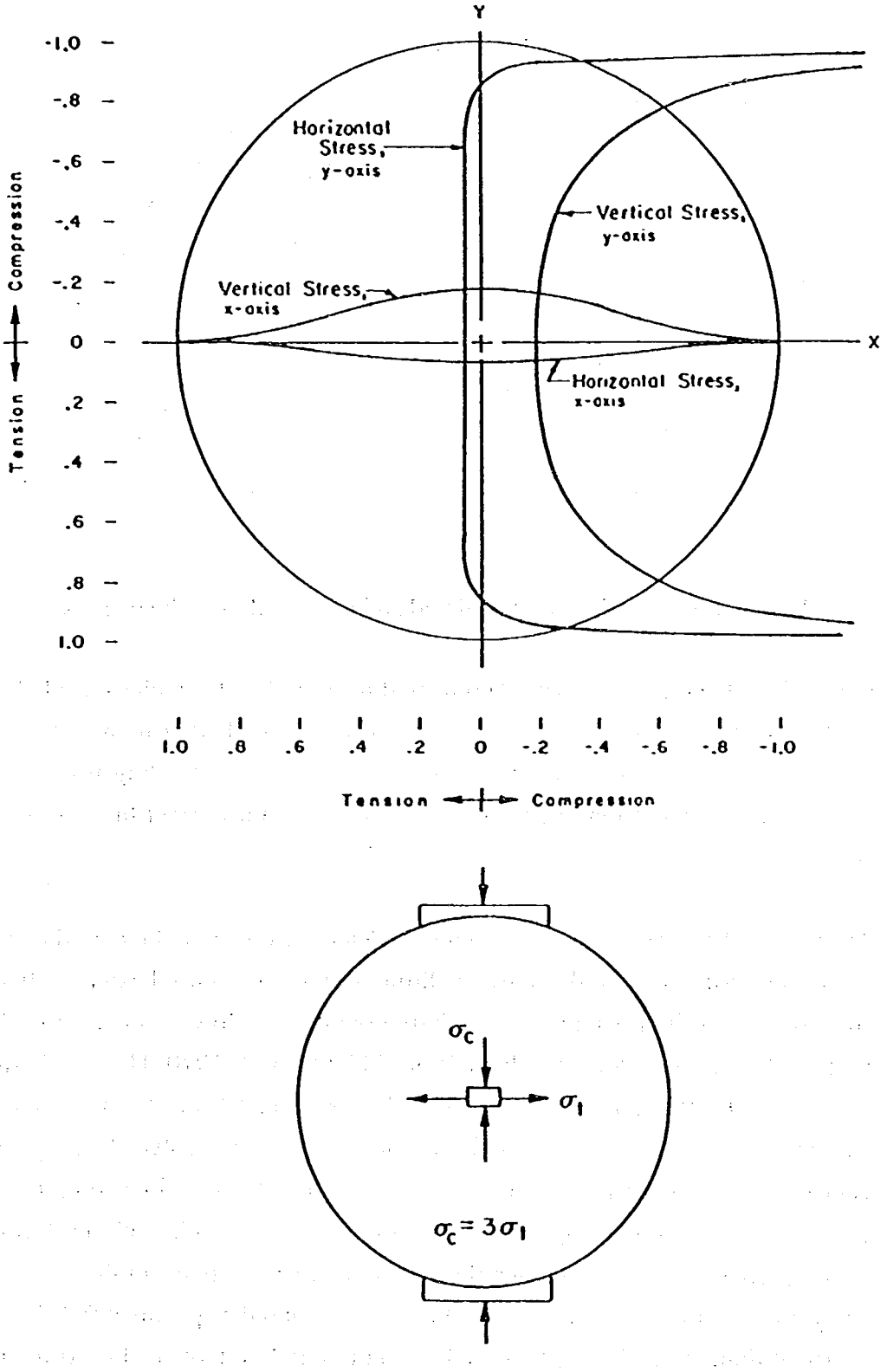


Figure 5. Relative stress distributions and element showing biaxial state of stress for the indirect tensile test (Kennedy 1977).

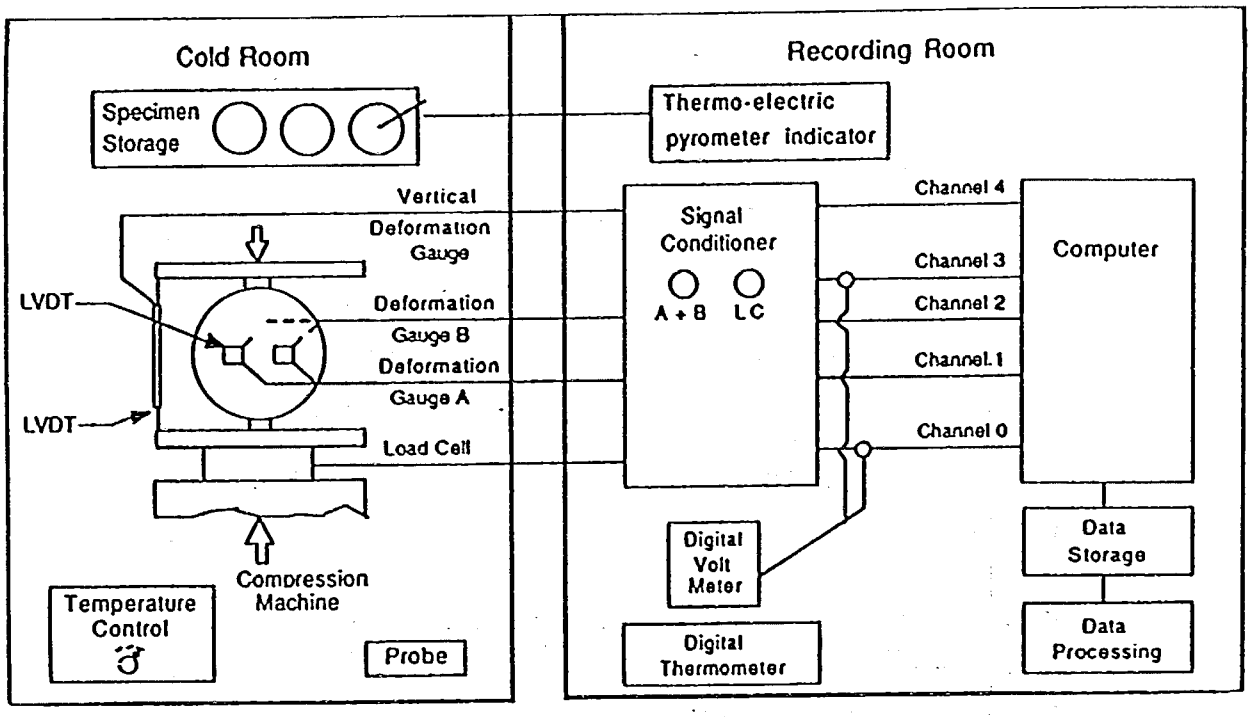


Figure 6. Schematic of diametral indirect tension test equipment (Anderson and Leung 1987).

specimen. The compressive stress in the vertical plane is greatly reduced (Fig. 5) when a distributed loading condition is applied through a loading strip. The tensile stress at the center is given by

$$\sigma = \frac{-2P}{\pi dh} \tag{3}$$

where σ = tensile stress
P = applied load
d = diameter of specimen
h = thickness of specimen

A more rigorous method for calculating the tensile strength from the indirect tension test can be found in Kennedy (1977). The tensile strength obtained from this test is dependent on the loading rate (Fig. 7). Basically, the higher the loading rate, the higher the tensile strength. Several loading rates have been cited in the literature to simulate thermal loading. Anderson et al. (1987) used a loading rate of 1.5 mm/min, Von Quintus et al. (1988) used a loading rate of 1.25 mm/min, and Dempsey et al. (1980) used a loading rate of 1.8 mm/min. Typical variation of tensile strength with temperature is shown in Figure 8.

In general, this is a popular test because it is simple to conduct, the test specimens used are the common Marshall test specimens, and extensive experience with the test method has been

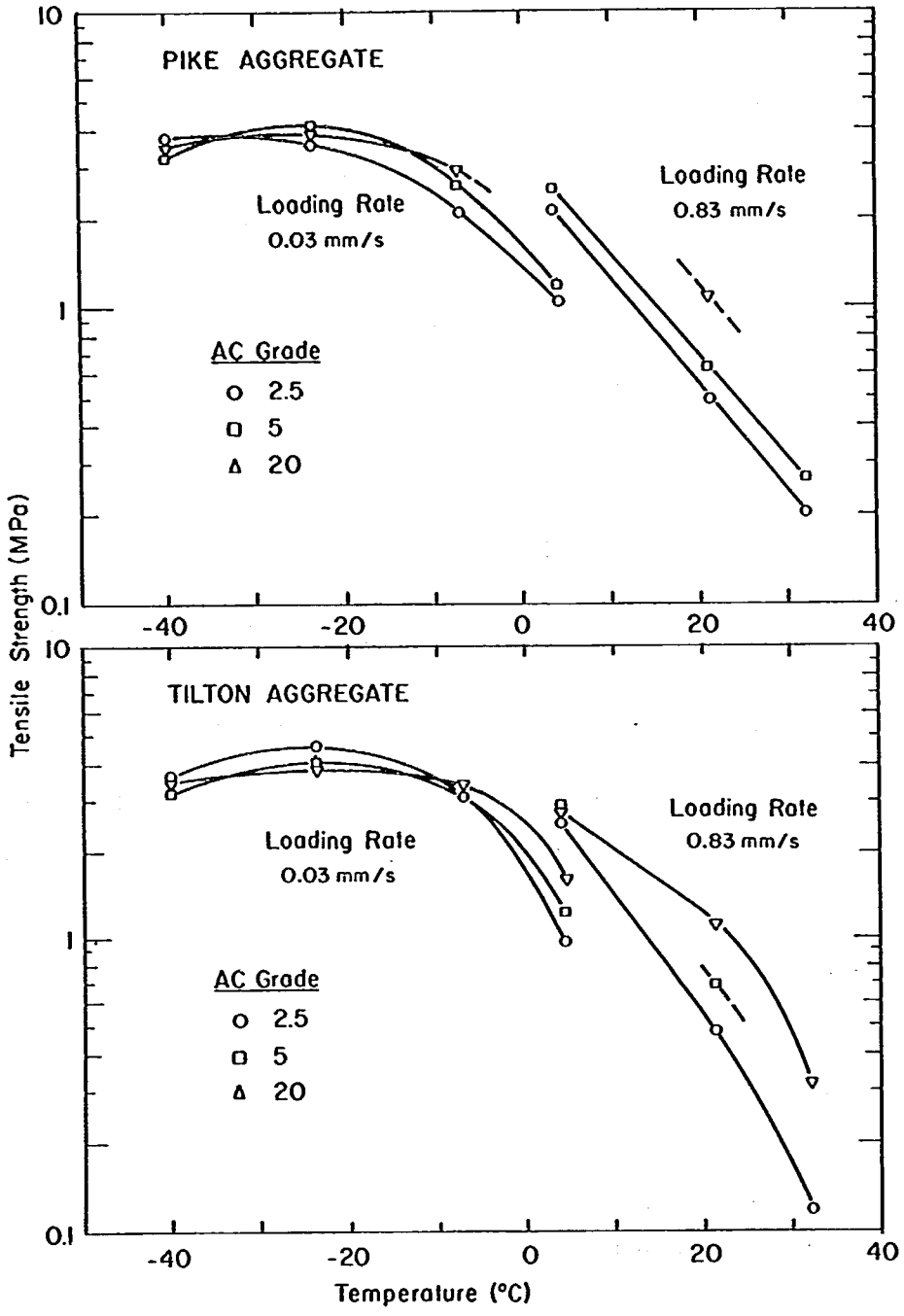
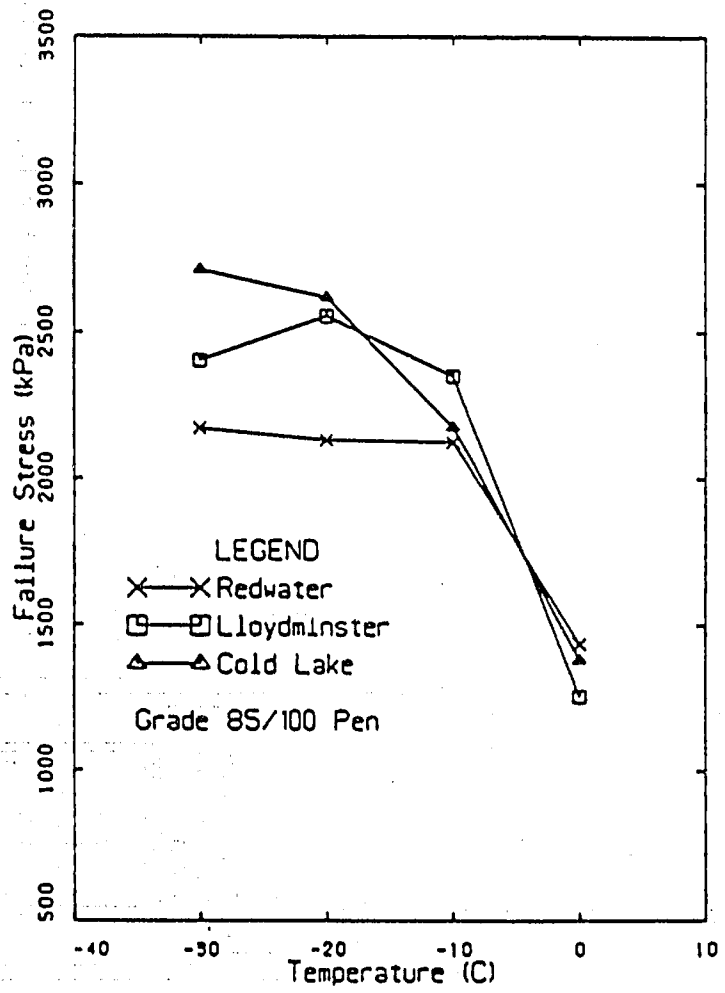
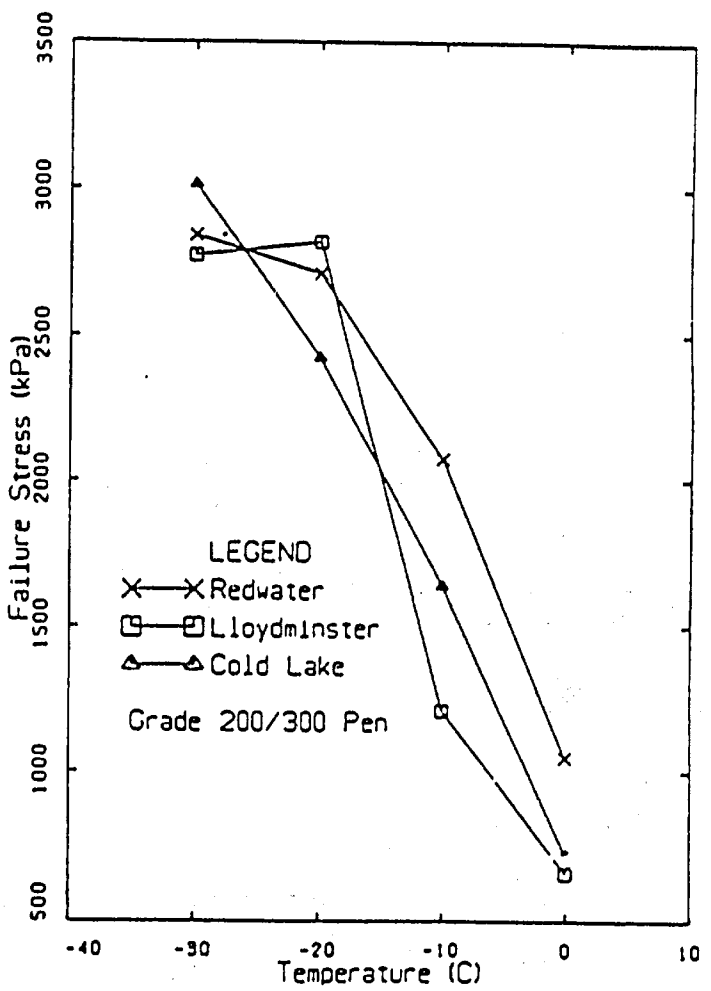


Figure 7. Effects of asphalt grade, rate of loading, and temperature on indirect tensile strength (75-blow compaction).

developed. However, the stress state is more complex than assumed. The total strain calculated is the sum of both the compression and tensile strains in the specimen. With respect to thermal cracking, the loading condition used and the mode of fracture do not simulate actual field conditions. The results of this test do not characterize the actual low temperature response of asphalt concrete but can be used as an index for characterizing the low temperature response.

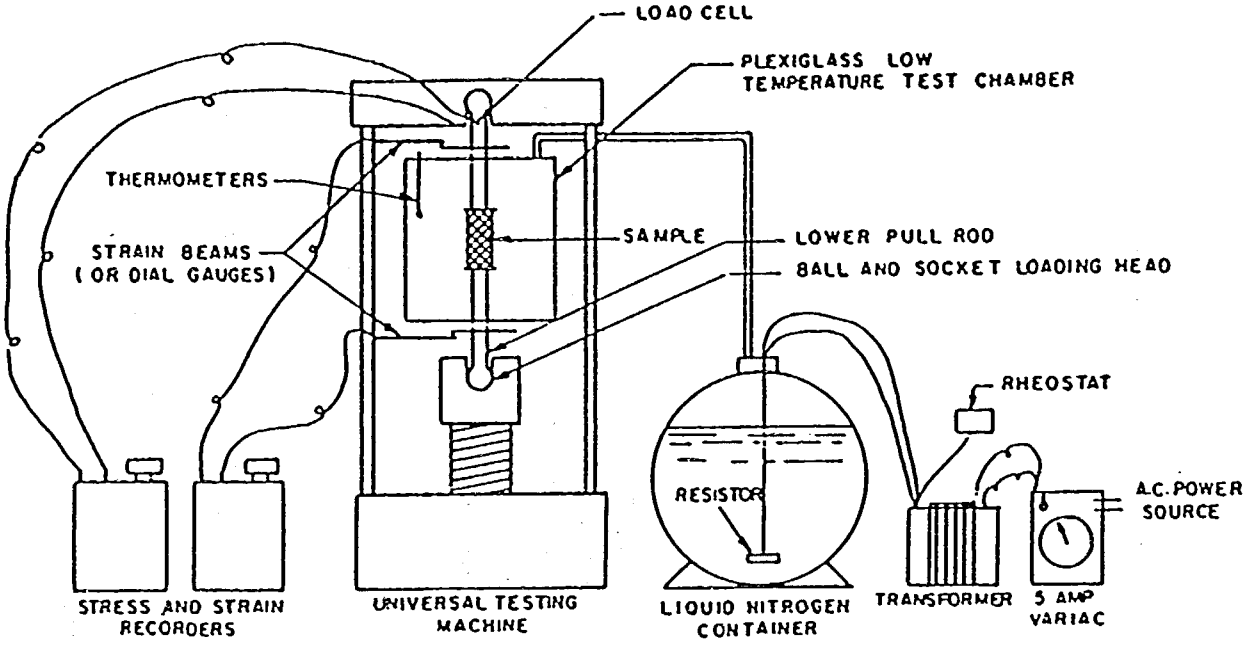


a. Pen 85/100.

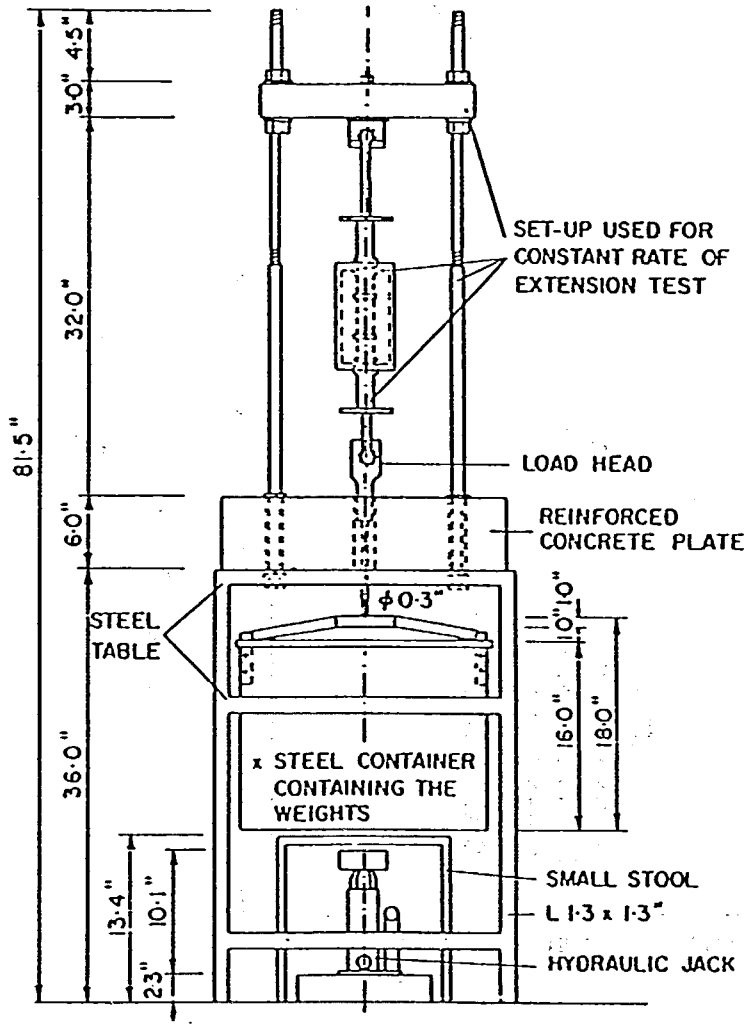


b. Pen 200/300.

Figure 8. Failure stress–temperature relationship.



a. Overall test system.



b. Constant rate of extension and creep load frame.

Figure 9. Schematic of direct tension and creep load test systems (after Haas 1973).

The *direct tension test* as used in low temperature studies of asphalt concrete was developed by Haas (1973) to overcome the problems with the indirect test. A 38- × 38- × 102-mm rectangular beam is subjected to an uniaxial tensile load at a set temperature and a constant rate of extension. A schematic of the test system is shown in Figure 9. Haas (1973) states that, with respect to low temperature behavior, this test more closely simulates the actual stress state and fracture mode that occurs in the field than do other tension tests. Since low temperature shrinkage fracture occurs under a slow buildup of tensile stresses, the rates of extension used in the test are very low. Haas (1973) gave guidelines for rates of extension to be used; Kallas (1982) used an extension rate of 0.005 mm/min. The parameters collected from the test include load, extension of the specimen, test temperature and time to failure. Typical stress–strain curves from this test method are shown in Figure 10.

The direct tension test described above is not as popular as the indirect tension test. Most of the experience with this test method comes from the University of Waterloo (Canada), the Asphalt Institute and the Ontario Ministry of Transportation. However, as noted above, this test does come closer to simulating field conditions. One drawback to this test is the specimen size. For example, for a 19-mm maximum size asphalt concrete mix, the ratio of the minimum

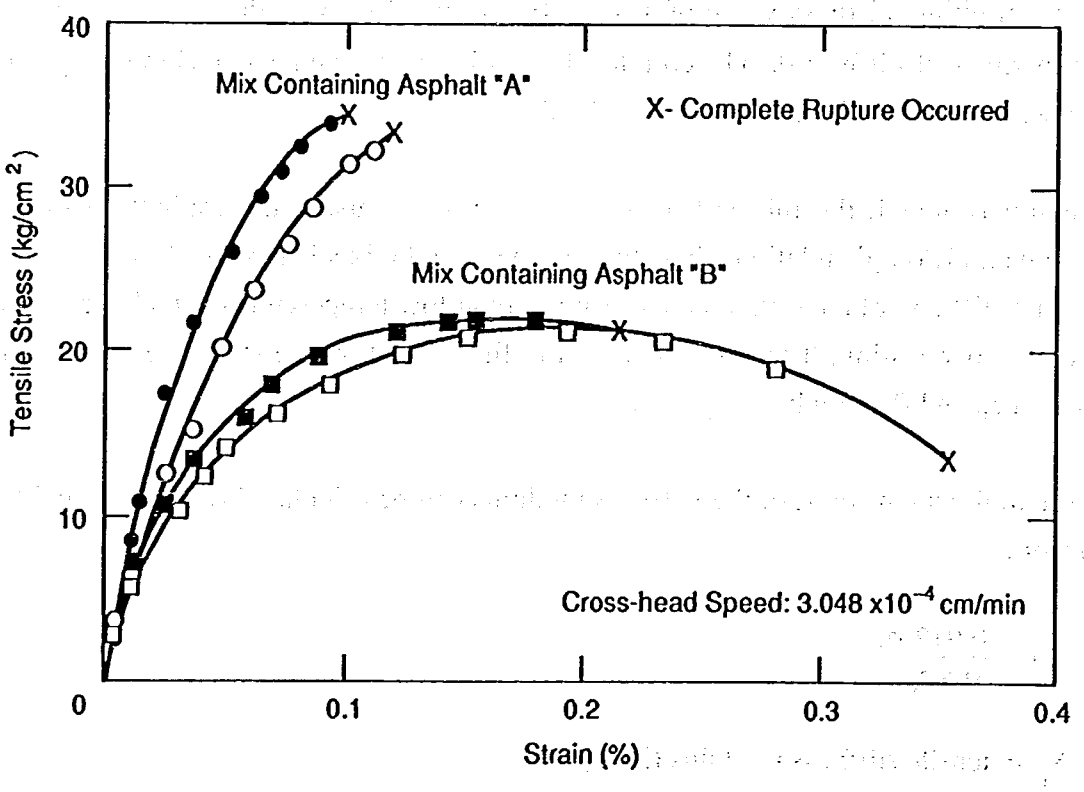


Figure 10. Stress–strain curves at temperature 0°F–constant rate extension tests (Haas 1973).

specimen to the maximum grain size is 2.0; this ratio should be in the range of 4 to 6 for a specimen to be considered homogeneous. The fracture strengths obtained from these tests may be higher than they really are, and, as in the indirect tension test, the rate of cooling is represented by an arbitrary rate of extension.

LIMITING MIX STIFFNESS METHOD

The limiting mix stiffness method is based on the criterion that thermal cracking occurs when the asphalt concrete mixture reaches a limiting stiffness value. McLeod (1970), based on his experience with pavements in Canada and the northern United States, concluded that pavements cracked when the mix stiffness was 6.9×10^9 N/m^2 at 20,000 seconds loading time. Gaw et al. (1974) based on results from the Ste. Anne Test Road, concluded that cracking occurred when the mix stiffness was 1.8×10^{10} N/m^2 at 1800 seconds loading time. Carpenter et al. (1985) suggested that cracking would occur when the stiffness of the mix was 3.5×10^9 N/m^2 at 20,000 seconds. Readshaw (1972) concluded from his study of thermal cracking in British Columbia that cracking would occur when the stiffness of the mix was 2×10^8 N/m^2 at 7200 seconds loading time. Since the mix stiffness is a function of temperature, asphalt content and air voids, it is doubtful if any one value of limiting mix stiffness could be used to control thermal cracking. The Ad Hoc Committee of the Asphalt Institute (1981) recommended a limiting stiffness value of 1.8×10^{10} N/m^2. However, they recommended that more experimental stiffness data be correlated with observed pavement cracking temperatures, such as was done with the Ste. Anne Test Road.

As previously noted, the mix stiffness can be estimated using the asphalt stiffness and Huekelom and Klomp's relationship between asphalt and mix stiffness or Bonnaure's nomograph. The stiffness of an asphalt concrete mixture at low temperatures can also be obtained from laboratory testing. The tests cited in the literature for stiffness testing are indirect tension, creep and flexural bending tests.

From the indirect tension test, the stiffness modulus can be calculated (Anderson and Leung 1987) from

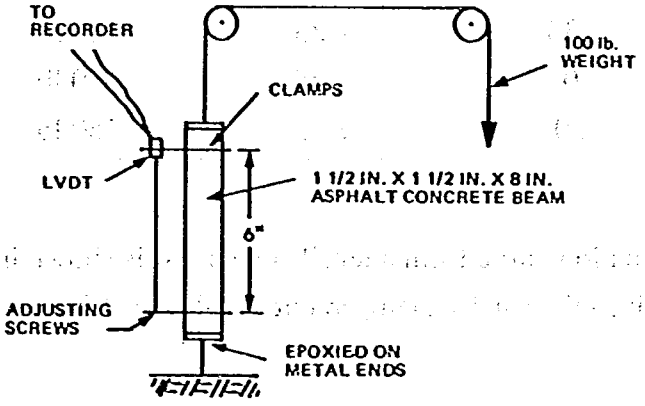
$$S_t = \frac{0.912\ \sigma_t}{0.5\ \varepsilon_{ave}} \tag{4}$$

where S_t = tensile stiffness modulus (MPa)
σ_t = tensile stress (MPa)
ε_{ave} = average strain (mm/mm)

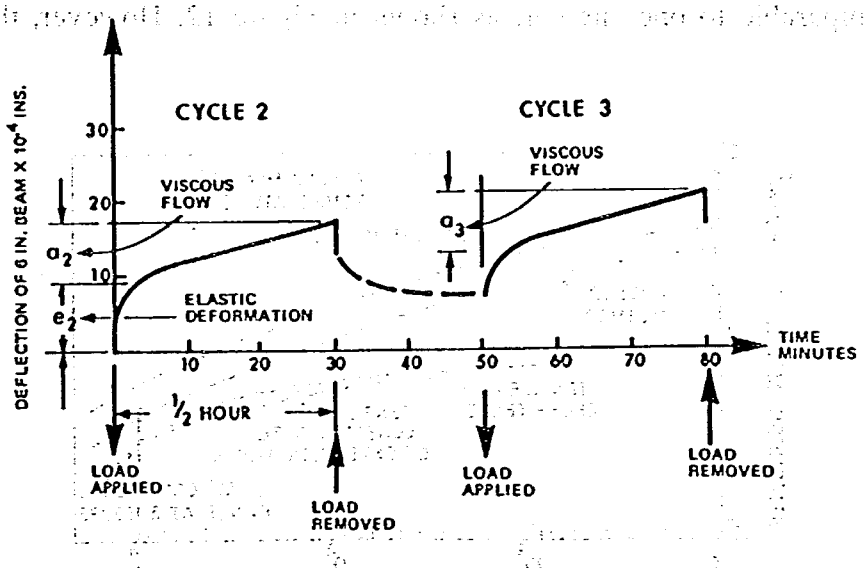
The stiffness of an asphalt concrete mix can also be obtained from the direct tension and creep tests. From the direct tension test, the stiffness at any time and at a set temperature is calculated from

$$S_{dt} = \frac{\sigma_t}{\varepsilon} \quad . \tag{5}$$

The *tensile creep test* is conducted by applying a constant load to a specimen maintained at a constant temperature and recording the resulting deformation with time as shown in Figure 11a. Haas (1973) used 38- × 38- × 102-mm specimens for his tests. The test specimen used by Fromm and Phang (1972) was similar in cross section, but 203 mm in length. Fromm and



a. Apparatus for measuring creep deformation under constant tensile stress.



b. Example of a creep test result.

Figure 11. Measurement of creep deformation under constant tensile stress (Fromm and Phang 1972).

Phang (1972) used a 30-minutes-on, 20-minutes-off load cycle for the creep tests, which were conducted at temperatures between –23°C and 4°C with an applied load of 45 kg. For a 14.4-cm^2 specimen, Haas (1973) provided some guidance for the load level that should be used in low temperature creep tests (Table 2). Parameters measured during the test are load, deformation, temperature and time.

Table 2. Some examples of creep loads (Haas 1973).

Temperature °F	Cross-sectional area $in.^2$	Load level for time of loading greater than 2 hrs
–30	2.25	500 lb
0	2.25	550 lb
30	2.25	150 lb

A typical load deformation curve from a tensile creep test is shown in Figure 11b. The stiffness of the mix at a given time and set temperature is calculated from

$$S_{ct} = \frac{\sigma_o}{\varepsilon} \quad . \tag{6}$$

Haas (1973) showed that the stiffnesses calculated from the creep test and the direct tension test were comparable to one another, as shown in Figure 12. However, the stiffnesses

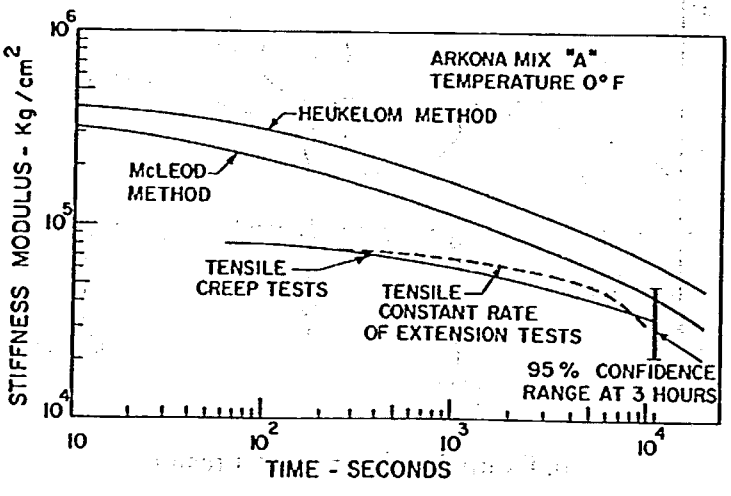


Figure 12. Relationship between stiffness modulus and time.

measured from these tests were much lower than predicted with Heukelom and Klomp's or Bonnaure's method.

As with the direct tension test, the major drawbacks to the tensile creep test are the small cross-sectional area of the specimens used and the simulation of thermal loading by mechanical means. However, both of these tests are an advancement over the indirect tension test.

The stiffness modulus of asphalt concrete can also be determined from the *flexural bending test* (Rader 1935,1937; Busby and Rader 1972; Sugawara et al. 1982). Busby and Rader (1972) used 89-mm W × 83-mm D × 381-mm L test specimens in a three point loading test. Sugawara et al. (1982) used 25 mm × 25 mm × 250 mm test specimens. To simulate thermal loading, Busby and Rader (1972) used a slow rate of loading of 0.5 mm/min. For smaller beams (51 mm W × 38 mm D x 152 mm L), Rader (1935) used a loading rate of 1.3 mm/min. Sugawara et al. (1982) used strain rates of 10^{-4} to 1.9/sec. The test temperatures ranged from –37°C to 30°C.

The stiffness modulus is determined from

$$S_f = \frac{dPL^3}{48\delta I} \tag{7}$$

where dP = change in load
L = length of beam
δ = corresponding deflection due to dP
I = moment of inertia.

The maximum stress, i.e., the tensile strength of the asphalt concrete mixture, can be calculated from

$$\sigma_t = \frac{Mc}{I} \tag{8}$$

where σ_t = tensile strength
M = moment at failure
c = one-half depth of beam.
I = moment of inertia.

DIRECT MEASUREMENT OF FAILURE STRESS AND TEMPERATURE

The direct measurement of failure stresses and temperature at low temperatures in laboratory samples has been reported by Monismith et al. (1965), Hills and Brien (1966), Tuckett et al. (1970) Chipperfield and Fabb (1971), Fabb (1974), Sugawara et al. (1982) Sugawara and Moriyoshi (1984), Sato et al. (1982), Arand (1987) and Janoo and Bayer (1990b).

The basic principle that supports the direct laboratory measurement method is that an asphalt concrete test specimen, cooled at a constant rate and restrained by a rigid frame, simulates the field conditions for low temperature cracking. Arand (1987) also used a stepping motor screw jack system in conjunction with strain gages to control the amount of movement in the asphalt concrete. He has reported being able to control movements to within 2.5×10^{-3} mm. Others have basically used small cross-section beam specimens and the rigidity of the frame to control the movement of the asphalt concrete specimens. Fabb (1974) reported that movements in excess of 0.025 mm can produce errors in load measurements up to 20%. A load cell is attached between the specimen and the rigid frame. The specimen or, in some cases, the whole experimental setup is placed in an environmental chamber. The temperature in the chamber is then lowered and the load is monitored. As the temperature decreases, the specimen will have a tendency to contract. However, since it is restrained by the rigid frame, contraction is minimized and tensile stresses develop in the specimen. As the temperature

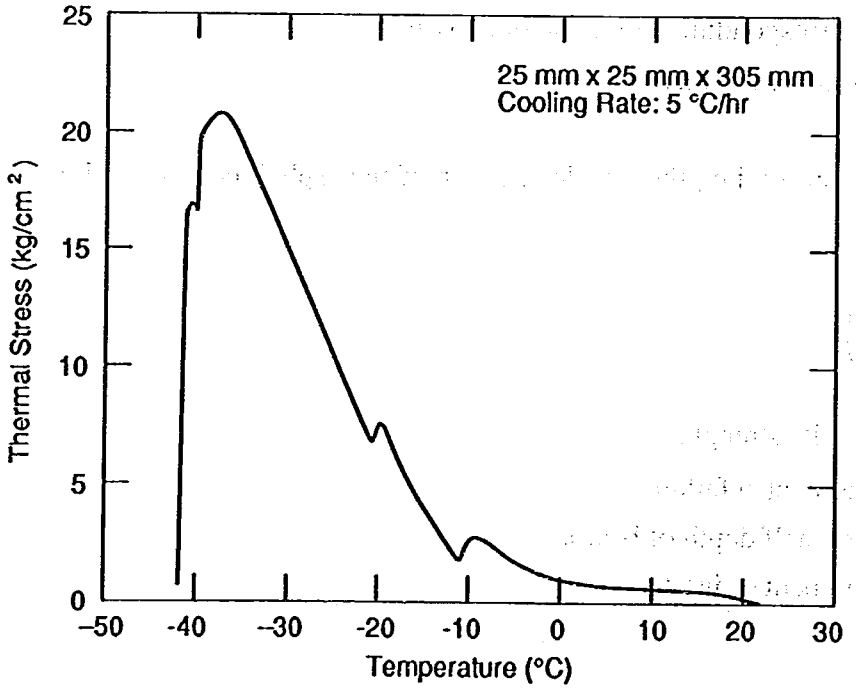


Figure 13. Typical stress–temperature curve.

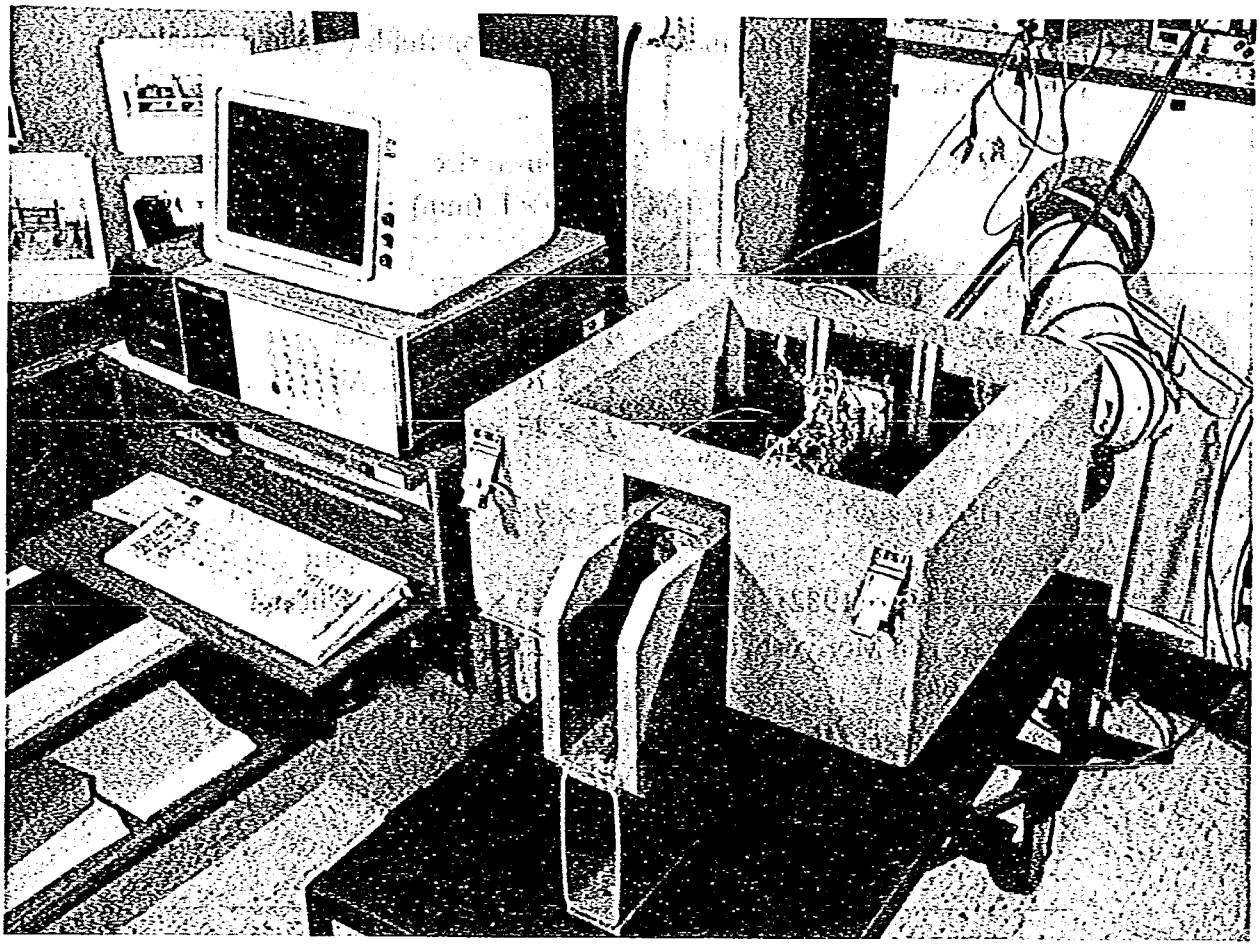


Figure 14. CRREL thermal stress test device.

drops further, the stress increases up to the tensile strength of the mix. At this time fracture occurs. A typical result from this type of test is shown in Figure 13. The thermal stress device currently used at CRREL is shown in Figure 14. A detailed description of the various thermal stress restrained specimen devices can be found in Fabb (1974), Vinson et al. (1989) and Janoo and Bayer (1990).

The specimen sizes used by the various researchers varied from 13 × 13 × 254 mm to 76 × 76 × 305 mm. The studies conducted by Chipperfield and Fabb (1971), Fabb (1974) and Sugawara and Moriyoshi (1984) and Sugawara et al. (1982) used a liquid medium to cool the specimens. All others used air as a cooling medium. The specimen size and cooling medium used are summarized in Table 3.

The cooling rates reported in the literature ranged from 3°C/hr to 30°C/hr. The majority of studies have been conducted at 10°C/hr. Fabb (1974) and Sugawara et al. (1982) established from their results that the fracture temperature and tensile strength were independent of cooling rate when it was equal to or greater than 5°C/hr. Fromm and Phang (1972) reported that in Canada the cooling rate very seldom exceeded 3°C/hr. Sugawara et al. (1982) showed that

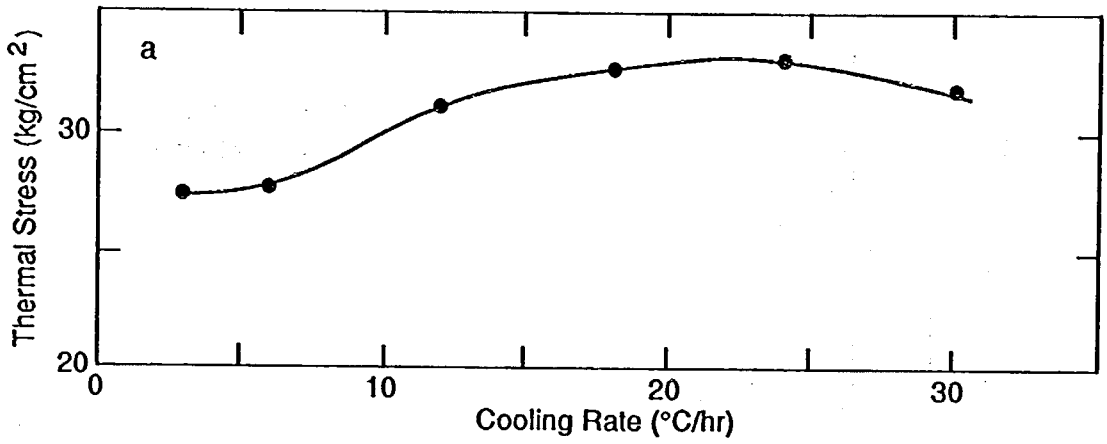
Table 3. Summary of specimen sizes and cooling fluids used in thermal stress devices.

Investigators	Specimen size W × D × L (mm)	Cooling fluid
Monismith et al. (1965)	25 × 25 × 305	Air
Hills and Brien (1966)	13 × 13 × 254	Air
Tuckett et al. (1970)	76 × 76 × 203	Air
Chipperfield and Fabb (1971)	25 × 25 × 305	50/50% water/ antifreeze
Fabb (1974)	25 × 25 × 305	Methylated spirit
Sugawara et al. (1982)	25 × 25 × 305	Methanol
Sugawara and Moriyoshi (1984)	25 × 25 × 305	Methanol
Arand (1987)	40 × 40 × 160	Air
Janoo and Bayer (1990b)	30 × 54 × 160	Air
	76 × 25 × 305	
	51 × 51 × 305	
	76 × 76 × 305	

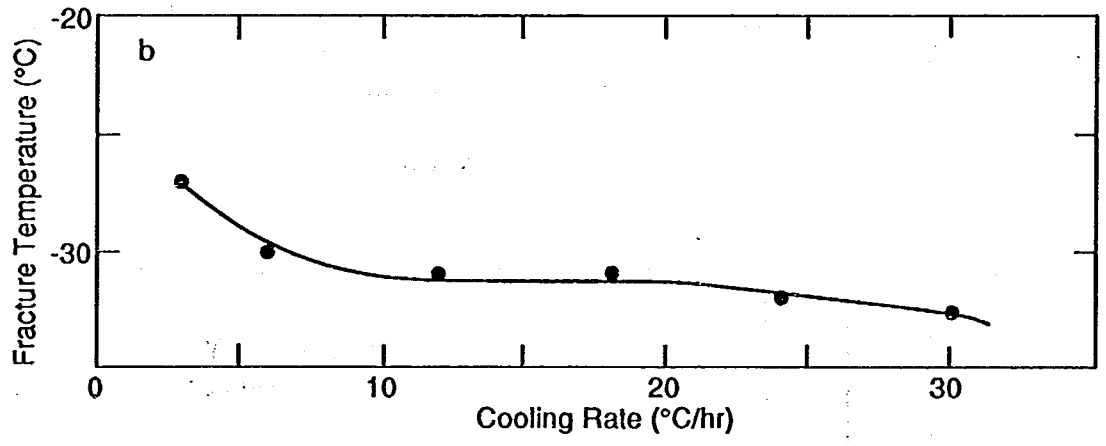
cooling rates of less than 5°C/hr affected both the fracture stress and temperature as shown in Figures 15a and b. Preliminary results (Janoo and Bayer 1990a) from a study on air cooling rates in the northern U.S. over the last 10 years indicate that the largest frequency of cooling rate is between 0.5 and 1.0°C/hr. The results for Burlington, Vermont, and Fairbanks, Alaska, for the months of November and January, from 1979 to 1989, are shown in Figures 16a and b. A summary of the cooling rates used, the minimum temperatures reached and whether cracks were visible is presented in Table 4.

The effects of specimen size on fracture strength and temperature were reported by Janoo and Bayer (1990b). As shown in Figure 17, the fracture strength decreases with increasing specimen size. Similar results have been reported in the rock mechanics literature. The failure criterion used by Janoo and Bayer (1990b) was similar to that used by Fabb (1974); i.e., failure strength was the maximum stress reached in the thermal stress test. Based on the results presented, a minimum specimen size of 51 × 51 mm should be used.

The main concerns with larger specimens are that a larger rigid frame will be required and the time for thermal equilibrium between the surface and the center of the specimen will be large.



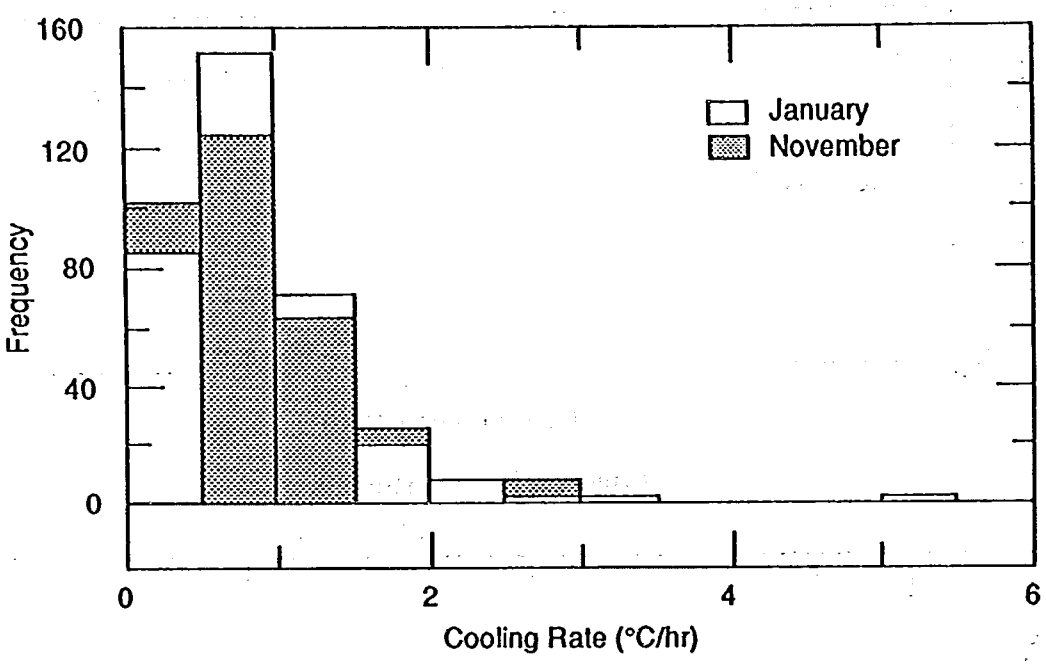
a. Effect on fracture strength .



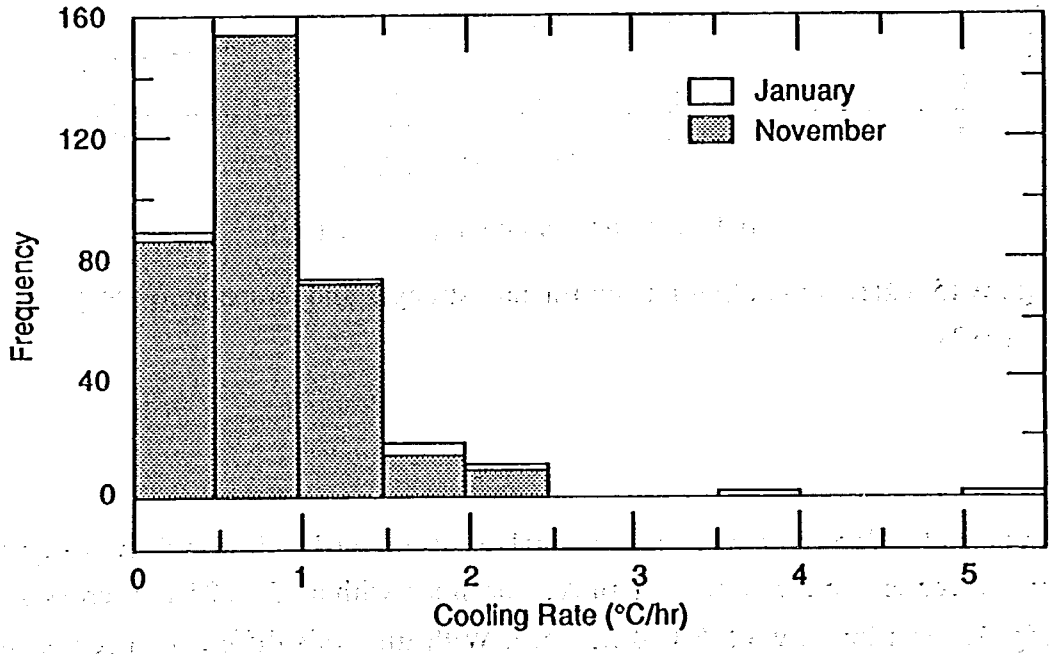
b. Effect on fracture temperature (°C).

Figure 15. Effect of cooling rate on fracture strength and temperature (Sugawara et al. 1982).

Monismith et al. (1965) presented experimental results on the lag time in thermal equilibrium between the center and the surface of an AC specimen with a 25- × 25-mm cross-sectional area (Fig. 18) and initially a 5.6°C difference. With time this difference became smaller. Similar studies were conducted with a 76- × 76-mm cross-sectional area asphalt concrete specimen by Janoo and Bayer (1990b). Typical test results for two different cooling rates are shown in Figures 19a and b. With forced air and Invar end caps, the thermal difference between the center and surface temperature was about 2°C. Thermal equilibrium was reached when the temperature was held constant for 20 minutes.



a. Burlington, Vermont.



b. Fairbanks, Alaska.

Figure 16. Cooling rates observed at Burlington, Vermont, and Fairbanks, Alaska, USA.

Table 4. Summary of cooling rates, crack observation and minimum temperatures reached in thermal stress device.

Investigators	Cooling rates (°C/hr.)	Crack observed	Minimum temp (°C)
Monismith et al. (1965)	?	No	0
Hills and Brien (1966)	10	Micro	Failure*
Tuckett et al. (1970)†	11	Yes	–9
Chipperfield and Fabb (1971)	10	No	–20
Fabb (1974)	5,10**	Yes	Failure
Sugawara et al. (1982)	3,6,12,18, 24 and 30**	Yes	Failure
Sugawara and Moriyoshi (1984)	3,6,12,18, 24 and 30	Yes	Failure
Arand (1987)	10°C/hr	Yes	Failure
Janoo and Bayer (1990a)	5,10,**20	Yes††	Failure

* The term failure is used to denote that the minimum temperature reached was sufficient to cause failure.

† The specimens were subjected to thermal cycling (–9°C/hr to 46°C/hr).

** Predominant cooling rate used in testing program.

†† Visible cracks seen in all test specimens except in 76- × 76- × 305-mm specimens. Load temperature measurements suggest that microcracks are present.

The direct measurement of failure stress and temperature in restrained specimens appears to be the best technique for simulating low temperature cracking. The test results are the fracture temperature and strength. The other test methods give the fracture strength and the mix stiffness as estimated from van der Poel's nomograph. The direct laboratory measurement test can be conducted at various cooling rates found in nature and therefore loading time does not have to be estimated in the analysis. The test has been used successfully to characterize asphalt mixture response at low temperatures.

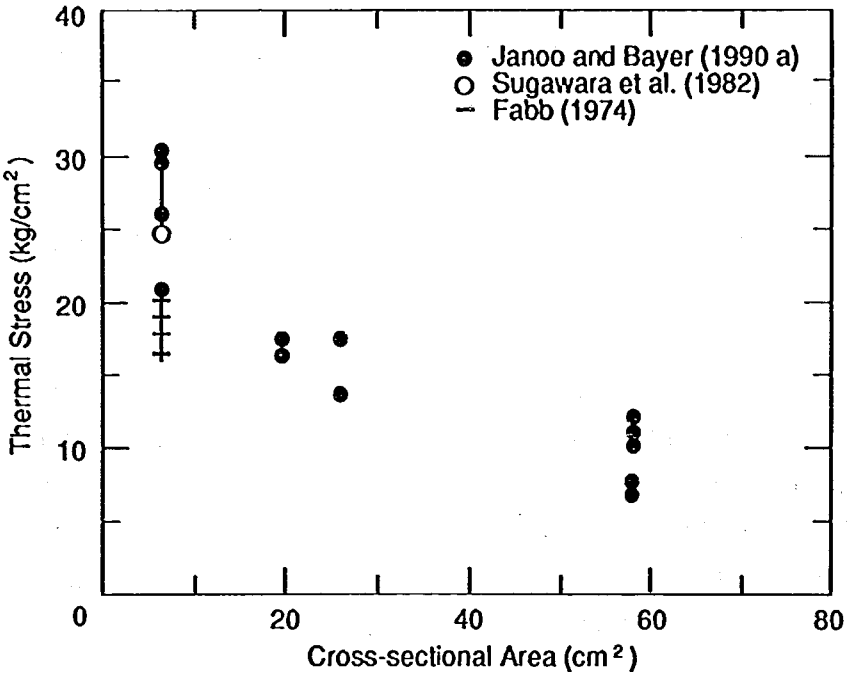


Figure 17. Effect of specimen size on peak thermal stress.

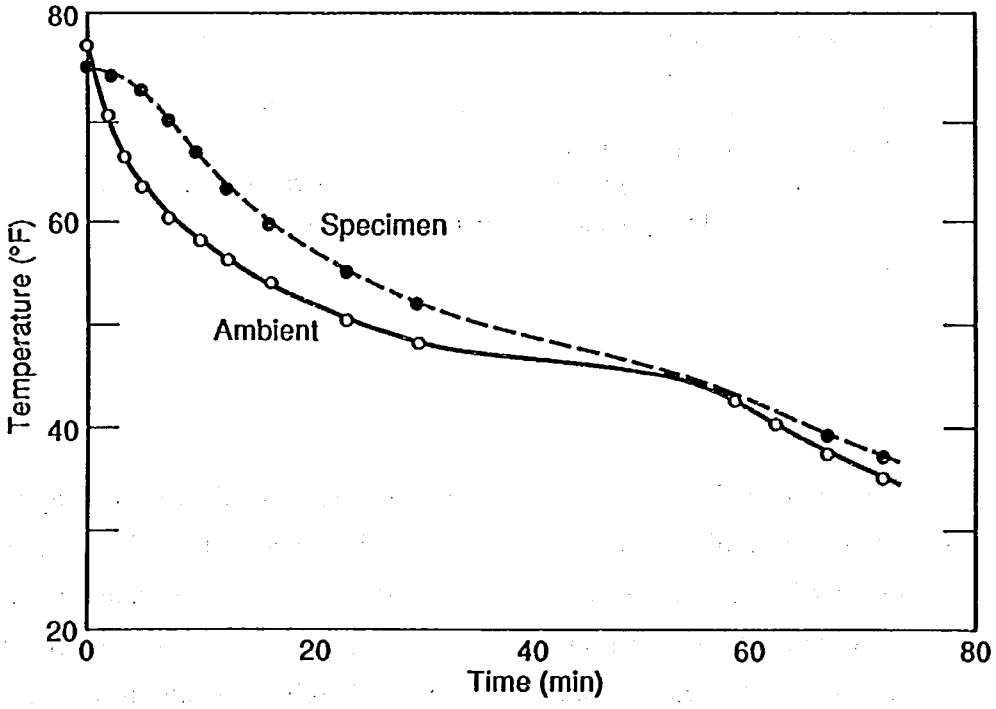
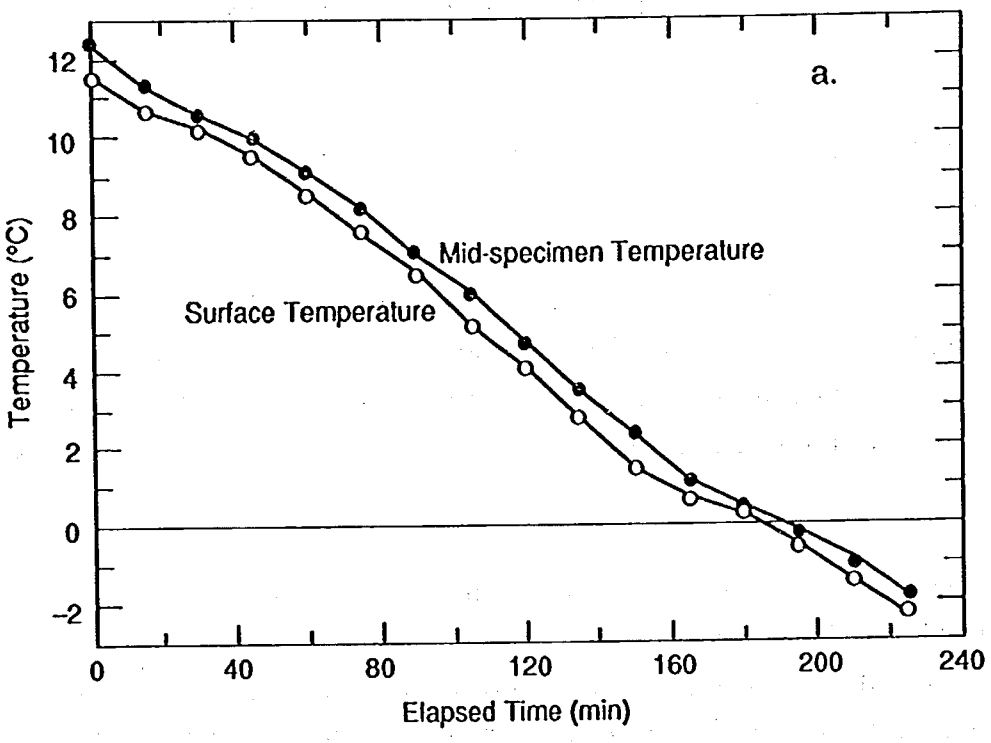


Figure 18. Comparison of ambient and specimen temperatures in restrained beam experiment (Monismith 1965).



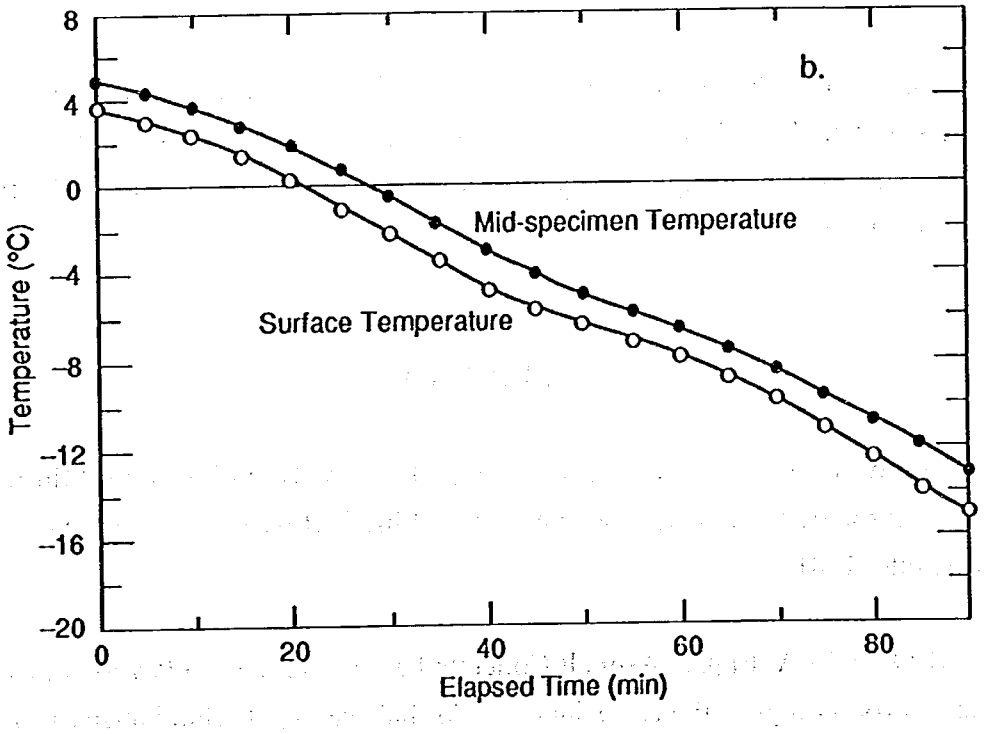


Figure 19. Comparison of surface and mid-specimen temperature at a) 5°C/hr and at b) 20°C/hr.

SUMMARY AND CONCLUSION

A summary of the various predictive methods and material characterization tests for low temperature cracking was provided. The main limitation of the predictive methods is the estimation of material stiffness.

The indirect tensile test is at best an index test for characterizing low temperature behavior because it neither simulates the field thermal loading condition nor the mode of fracture. Although the direct tensile and creep tests are better, they still lack the ability to subject the specimen to various cooling rates. The cooling rate is simulated by a slow rate of extension on these tests.

The advantage of the direct measurement of failure stress and temperature in restrained specimens is that is can simulate field conditions and the specimen can be subjected to field cooling rates. However, the cooling rates used in many of the studies are much higher than observed in the field. The tests should be conducted in the 1°C/hr range to more closely simulate actual field conditions. The fracture temperature and fracture strength were found to be lower at slower cooling rates. This may explain the observed differences between laboratory and field fracture temperatures.

The specimen size has also been found to influence the fracture strength. Large specimens presumably simulate the field conditions. The combination of low cooling rates and thicker pavement ($h > 25$ mm) may explain why low temperature cracking appears in the field when the minimum temperature never exceeds –20°C.

REFERENCES

Ad Hoc Committee of the Asphalt Institute, "Design Techniques to Minimize Low Temperature Asphalt Pavement Transverse Cracking," Research Report No. 81-1, The Asphalt Institute, 1981.

Anderson, K.O. and J.A. Epps, "Asphalt Concrete Factors Related to Pavement Cracking in West Texas," Proceedings of the Association of Asphalt Paving Technologists, 1983.

Anderson, K.O. and W.P. Hahn, "Design and Evaluation of Asphalt Concrete with Respect to Thermal Cracking," Proceedings of the Association of Asphalt Paving Technologists, pp. 1–31, 1968.

Anderson K.O. and S.C. Leung, "Applications of a Method for Evaluation of Low Temperature Tensile Properties of Asphalt Concrete," Proceedings, Paving in Cold Areas Mini-Workshop, pp. 151–197, 1987.

Arand, W., "Influence of Bitumen Hardness on the Fatigue Behavior of Asphalt Pavements of Different Thickness Due to Bearing Capacity of Subbase, Traffic Loading and Temperature," Proceedings, 6th International Conference on Structural Behavior of Asphalt Pavements, University of Michigan, 1987.

Bonnaure, F., G. Gest, A. Gravois and P. Uge, "A New Method of Predicting the Stiffness of Asphalt Paving Mixtures," Proceedings of the Association of Asphalt Paving Technologists, pp. 64–104, 1977.

Burgess, R.A., O. Kopvillem and F.D. Young, "St. Anne Test Road—Relationship Between Predicted Fracture Temperature and Low Temperature Field Performance," Proceedings of the Association of Asphalt Paving Technologists, pp. 227–246, 1971.

Busby E.O., and L.F. Rader, "Flexural Stiffness Properties of Asphalt Concrete at Low Temperatures," Proceedings of the Association of Asphalt Paving Technologists, 1972.

Carpenter, S.H. and T. VanDam, "Evaluation of Low Temperature Performance of Asphalt Cements," Final Report submitted to USA Cold Regions Research and Engineering Laboratory, March, 1985.

Chipperfield, E.H. and T.R.J. Fabb, "Development of More Durable Road Surfacing," Proceedings of the Canadian Technical Asphalt Association, 1971.

Christianson, R.H.A., "Analysis of the Tensile Splitting Testing for Low Temperature Tensile Properties of Asphalt Concrete," M.Sc. Thesis, The University of Alberta, 1970.

Christison, J.T., "The Tensile Splitting Test Applied to Thermal Cracking of Asphalt Pavements," M.Sc. Thesis, The University of Alberta, 1966.

Christison, J.T., D.W. Murray and K.O. Anderson, "Stress Prediction and Low Temperature Fracture Susceptibility of Asphaltic Concrete Pavements," Proceedings of the Association of Asphalt Paving Technologists, 1972.

Dempsey, B.J., J. Ingersoll, T.C. Johnson and M.Y. Shahin, "Asphalt Concrete in Cold Regions—A Comparative Laboratory Study and Analysis of Mixtures Containing Soft and Hard Grades of Asphalt Cement," USA Cold Regions Research and Engineering Laboratory, CRREL Report 80-5, 1980.

Fabb, T.R.J., "The Influence of Mix Composition, Binder Properties and Cooling Rates on Asphalt Cracking at Low Temperatures," Proceedings of the Association of Asphalt Paving Technologists, pp. 285–331, 1974.

Finn, F.N., K. Nair, and J. Hilliard, "Minimizing Premature Cracking of Asphalt Concrete Pavements," Proceedings of the Association of Asphalt Paving Technologists, Vol. 45, pp. 492–529, 1976.

Finn, F.N., C.L. Saraf, R. Kulkarni, K. Nair, W. Smith and A. Abdullah, "Development of Pavement Structural Subsystems, National Cooperative Highway Research Program 291, 1986.

Fromm H.J. and W.A. Phang, "A Study of Transverse Cracking of Bituminous Pavements," Proceedings of the Association of Asphalt Paving Technologists, 1972.

Gaw, W.J. "The measurement and prediction of asphalt stiffnesses at low and intermediate pavement service temperatures," Proceedings, Association of Asphalt Paving Technologists, Vol. 47, pp. 457–494, 1978.

Gaw W.J., R.A. Burgess and F.D. Young, "Ste. Anne Test Road—Road Performance After Five years and Laboratory Predictions of Low Temperature Performance," Proceedings, Canadian Technical Asphalt Association, 1974.

Haas, R.C.G., "A Method for Designing Asphalt Pavements to Minimize Low Temperature Shrinkage Cracking," Report 73-1, Asphalt Institute, 1973.

Haas, R.C.G. and K.O. Anderson, "A Design Subsystem for the Response of Flexible Pavements at Low Temperature," Proceedings of the Association of Asphalt Paving Technologists, pp. 179–223, 1969.

Haas, R., H. Lee, F. Meyer, and G. Argue, "Cold Climate Performance of Canadian Airport Pavements," Mini Workshop 3, Paving in Cold Areas, Vol.1, pp. 303–332., Ottawa, Ontario, July 20–22, 1987.

Hadipour, K., and K.O. Anderson, "An Evaluation of Permanent Deformation and Low Temperature Characteristics of Some Recycled Asphalt Concrete Mixtures," Proceedings of the Association of Asphalt Paving Technologists, pp. 615–645, 1988.

Heukelom, W. and A.J.G. Klomp, "Road Design and Dynamic Loading," Proceedings of the Association of Asphalt Paving Technologists, pp. 92–125, 1964.

Hills, J.F. and D. Brien, "The Fracture of Bitumens and Asphalt Mixes by Temperature Induced Stresses," Discussion, Proceedings of the Association of Asphalt Paving Technologists, pp. 292–309, 1966.

Hooks, CC. and W.H. Goetz, "Laboratory Thermal Expansion Measuring Techniques Applied to Bituminous Concrete," U.S. Army Engineer Waterways Experiment Station, Corps of Engineers, Report 20, August, 1964.

Humphreys, J.S. and C.J. Martin, "Determination of Transient Thermal Stresses in a Slab with Temperature-Dependent Viscoelastic Properties," Transactions, Society of Rheology, Vol. VII, 1963, pp. 155–170.

Janoo V.C. and J. Bayer, Jr., "Methodologies for Predicting and Characterizing Thermally Induced Cracking," USA Cold Regions Research and Engineering Laboratory, CRREL Report in progress, 1990a.

Janoo V.C. and J. Bayer, Jr., "Low Temperature Behavior of Asphalt Concrete Pavements, Part 1: Development of Laboratory Test Program," USA Cold Regions Research and Engineering Laboratory, CRREL Report in progress, 1990b.

Jones, G.M., M.I. Darter and G. Littlefield, "Thermal Expansion and Contraction of Asphaltic Concrete," Proceedings of the Association of Asphalt Paving Technologists, Vol. 37, pp. 56–100, 1968.

Kallas, B.F., "Low Temperature Mechanical Properties of Asphalt Concrete," Research Report 82-3, The Asphalt Institute, 1982.

Kennedy, T.W., "Characterization of Asphalt Pavement Materials Using the Indirect Tensile Test," Proceedings of the Association of Asphalt Paving Technologists, pp. 132–150, 1977.

Linde, S., "Investigations on the Cracking Behaviour of Joints in Airfields and Roads," Report 1988:23, Swedish National Testing Institute, 1988.

Littlefield G., "Thermal Expansion and Contraction Characteristics of Utah Asphaltic Concretes," Proceedings of the Association of Asphalt Paving Technologists, Vol. 36, pp, 673–702, 1967.

McLeod, N.W., Prepared Discussion in "Ste. Anne Test Road—Construction Summary and Performance After Two Years Service," Proceedings of the Canadian Technical Asphalt Association, 1969.

McLeod, N.W., "Influence of Hardness of Asphalt Cement on Low Temperature Transverse Pavement Cracking," Canadian Good Roads Association, Montreal, 1970.

Monismith C.L., G.A. Secor and K.E. Secor, "Temperature Induced Stresses and Deformation in Asphalt Concrete," Proceedings of the Association of Asphalt Paving Technologists, pp. 248–285, 1965.

Osterkamp T.E., G.C. Baker, B.T. Hamer, J.P. Gosink, J.K. Peterson and V. Groul, "Low Temperature Transverse Cracks in Asphalt Pavements in Interior Alaska," Report No. AK-RD-86-26, Alaska DOT&PF, 1986.

Rader, L.F., "Investigation of the Physical Properties of Asphalt Paving Mixtures at Low Temperatures," Proceedings of the Association of Asphalt Paving Technologists, 1935.

Rader, L.F., "Report on Further Research Work on Correlation of Low Temperature Tests With Resistance to Cracking of Sheet Asphalt Pavements," Proceedings of the Association of Asphalt Paving Technologists, 1937.

Readshaw, E.E., "Asphalt Specifications in British Columbia for Low Temperature Performance," Proceedings of the Association of Asphalt Paving Technologists, 1972.

Sato K., T. Fukute and Y. Hachiya, "Thermally Induced Cracking Due to Hardening of Asphalt Concrete in Airport Asphalt Pavements," Proceedings, Paving in Cold Areas Mini Workshop, Vancouver, B.C., 1982.

Shahin M.Y. and B.F. McCullough, "Prediction of Low Temperature and Thermal Fatigue Cracking in Flexible Pavements," Research Report 123-14, Texas Transportation Institute, 1972.

Shields, B.P., "Current Studies on Transverse Cracking of Asphalt Pavements," Conference on Recent Developments in the Design and Construction of Asphalt Pavements, The University of Alberta, February, 1964.

Shields, B.P., K.O. Anderson and J.M. Dacyszyn, "An Investigation of Low Temperature Cracking of Flexible Pavements," Proceedings, Canadian Good Roads Association, 1970.

Sugawara, T., H. Kubo and A. Moriyoshi, "Low Temperature Cracking of Asphalt Pavements," Proceedings, Paving in Cold Areas Mini-Workshop, 1982.

Sugawara, T. and A. Moriyoshi, "Thermal Fracture of Bituminous Mixtures," Proceedings, Paving in Cold Areas Mini-Workshop, 1984.

Tuckett, G.M., G.M. Jones and G. Littlefield, "The Effects of Mixture Variables on Thermally Induced Stresses in Asphaltic Concrete," Proceedings of the Association of Asphalt Paving Technologists, 1970.

Van der Poel, C., "A General System Describing the Viscoelastic Properties of Bitumens and its Relation to Routine Test Data," Journal of Applied Chemistry, Vol. 4, 1954.

Vinson, T.S., V.C. Janoo, and R.C.G. Haas, "Summary Report on Low Temperature and Thermal Fatigue Cracking," Report No. HRP-A/IR-90-001 Strategic Highway Research Program, National Research Council, June, 1989.

Von Quintus, H.L., J.A. Scherocman, C.C. Hughes and T.W. Kennedy, "Development of Asphalt Aggregate Mixture Analysis System: AAMAS. Phase II," Preliminary Draft of Final Report, 1988.

An Estimation of Road Wear Using Spike Ravelling Test

M. Itoh, Y. Anzaki, PWRI

An Estimation of Road Wear Using Spike Ravelling Test

by

Masahide Itoh, Researcher, Pavement Division,
PWRI, Ministry of Construction
and
Yutaka Anzaki, Head, Pavemnt Division, PWRI

ABSTRACT

In Japan, studded tires are still widely used in snowy and cold regions. A lot of countermeasures have been under consideration to reduce the road wear caused by studded tires. In examining these countermeasures, a testing equipment which simulates the wear using studded tires, called "Spike Ravelling Testing Machine", is generally used for laboratory evaluation of the wear resistant property of mixture.

In 1985, five research institutes which belonged to the the Japanese government had the spike ravelling testing machine, but there were no standardized testing conditions, such as wheel load and the number of tracking cycles. The five institutes then carried out a joint research to establish the standardized testing conditions of the spike ravelling test. The testing conditions were standardized through the joint resaerch and the test results obtained from different institutes came to be convertible each other in 1987.

Research was subsequently started to develop methods to estimate the rut depth of existing pavement by means of the spike ravelling test. Fourty-five test pavement sections were selected from all over the snowy and cold regions in Japan and various studies, including the spike ravelling test on the mixtures cut out from each section, survey on rut depth and traffic conditions were conducted. The results indicated that the road wear had a very high correlation with the traffic volume of vehicles which equipe studded tires, and that the gradient of the correlation equation between

them had a relation with the wear of mixture in the spike ravelling test. Finally, the road wear came to be able to estimate by means of the spike ravelling test in 1989.

An Estimation of Road Wear Using Spike Ravelling Test

by

Masahide Ito, Researcher, Pavement Division,
PWRI, Ministry of Construction
and
Yutaka Anzaki, Head, Pavemnt Division, PWRI

1. Introduction

In snowy and cold regions in Japan, there is generally heavy snowfall every year. Roads in these regions mostly run through city centers, residential areas, or agricultural fields. Thus it is generally difficult to keep the road surface exposed by means of mechanical snow removal, and there are limitations to spread deicing agents. This road conditions makes a situation that a lot of vehicles equip studded tires in the snowy and cold regions. (percentage of vehicles with studded tires in Japan is shown in Fig.-1.1) The high percentage of vehicles with studded tires in cold regions has resulted in various problems, such as wear of pavement and the generation of dust. Agencies in charge of managing of road maintenance have been taking a number of countermeasures, including the improvement of aggregate gradings, using modified asphalt and hard aggregates to improve untiwear property of mixture, in order to reduce the road wear by studded tires.

The spike ravelling test is usually used to evaluate the unti-wear properties of mixtures in a laboratory. In this test, a studded tire tracks on specimens arranged on a rotating table to simulate the wearing loss of pavement (Photo.-1.1). Since 1985 the Ministry of Construction and the Hokkaido Development Bureau have been making efforts to standardize spike ravelling test procedures and to develop a method to estimate the wear in existing roads using the results of the spike ravelling test. This paper discribes the outlines of those studies.

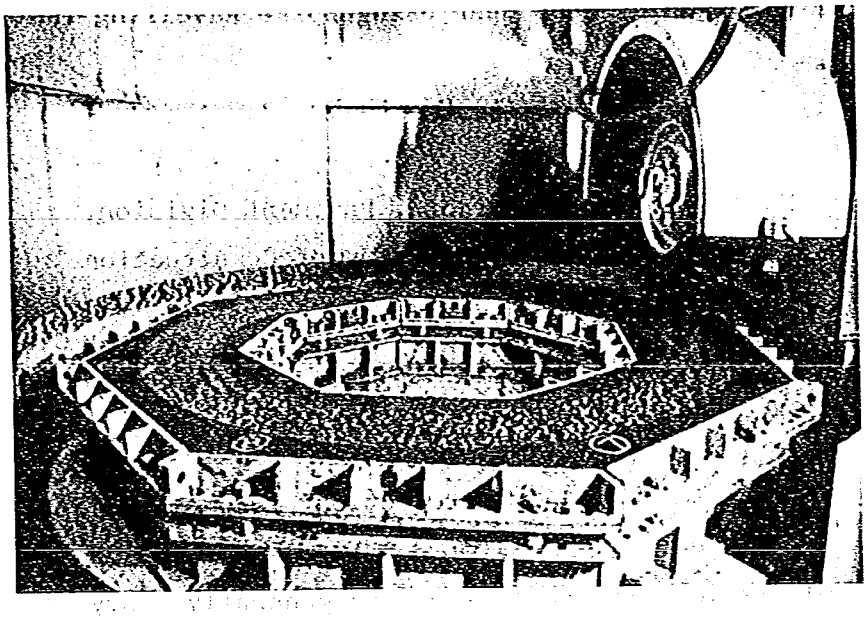


Photo.-1.1 Spike Ravelling Testing Machine

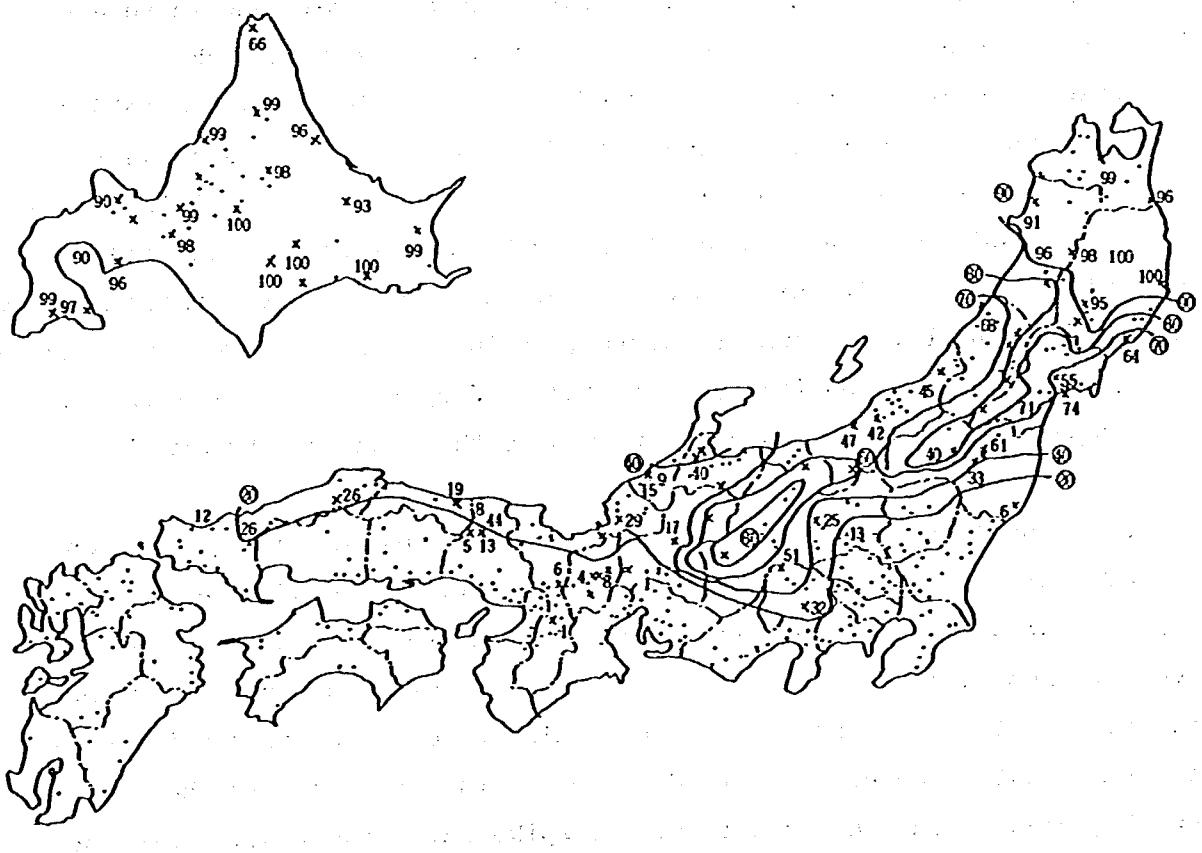


Fig.-1.1 Percentage of Vehicles with Studded Tires in Japan
(surveyed in 1982)

2. Standardizaation of Spike Ravelling Testing Procedure

2.1 Outline

In 1985, spike ravelling testing machine had been installed in the five institutes: the Construction Bureau of Tohoku, Hokuriku, and Chubu, the Public Works Research Institute (PWRI), and the Civil Engineering Research Institute (CERI) of the Hokkaido Development Bureau. However, there were no standardized testing conditions for the spike ravelling test, making it impossible to compare results obtained by different institutes. So the five institutes carried out a study to establish standard testing conditions and to provide a method for comparison of test results obtained by different institutes.

2.2 Results

The five institutes carried out spike ravelling test on several types of specimens with different aggregate gradings (Table-2.1) which were prepared at the PWRI. The ravelling test was performed under varying test conditions for wheel load, testing temperature, and tire pressure, and an analysis was made to examine the effect that variance of testing conditions has on wear of mixtures.

Fig.-2.1 shows an example of test results obtained at the five institutes for the specimens with same aggregate gradings. It can be seen that even the same grading mixture may make different wear depenading on the testing facilities.

Standard testing conditions were set up as shown in Table-2.2, based on the results of examinations on effects which varience of each testing condition has on the test results. Standard specimen of each institute were also developed in order to compare the test result by different institutes. Equation-2.1 has been developed to convert wear measurements at various institutes into those at the PWRI.

The standard testing procedures have been adopted in the five institutes since 1986. This standardization has been making it possible for the five

institute to covert the test results each other.

$$\text{Converted Wear } S_d = \alpha_i \times \frac{S_{i\theta}}{S_{ij}} \times S_j \qquad (2.1)$$

α_i : wear conversion factor of institute "i"

$$\alpha_i = \frac{S_\theta}{S_{i\theta}}$$

S_θ : wear loss of PWRI standard mixture by each institute at determining the wear conversion factor a ; (cm2)

$S_{i\theta}$: wear loss of standard mixture of each institute at determining the wear conversionfactor a ; (cm2)

S_{ij} : wear loss of standard mixture of each institute at a given time; (cm2)

S_j : wear loss in a given mixture; (cm2)

Table-2.1 Gradings of mixture

Dense Graded AC (20F)
Dense Graded Gap AC (13F)
Fine Graded Gap AC (13F)

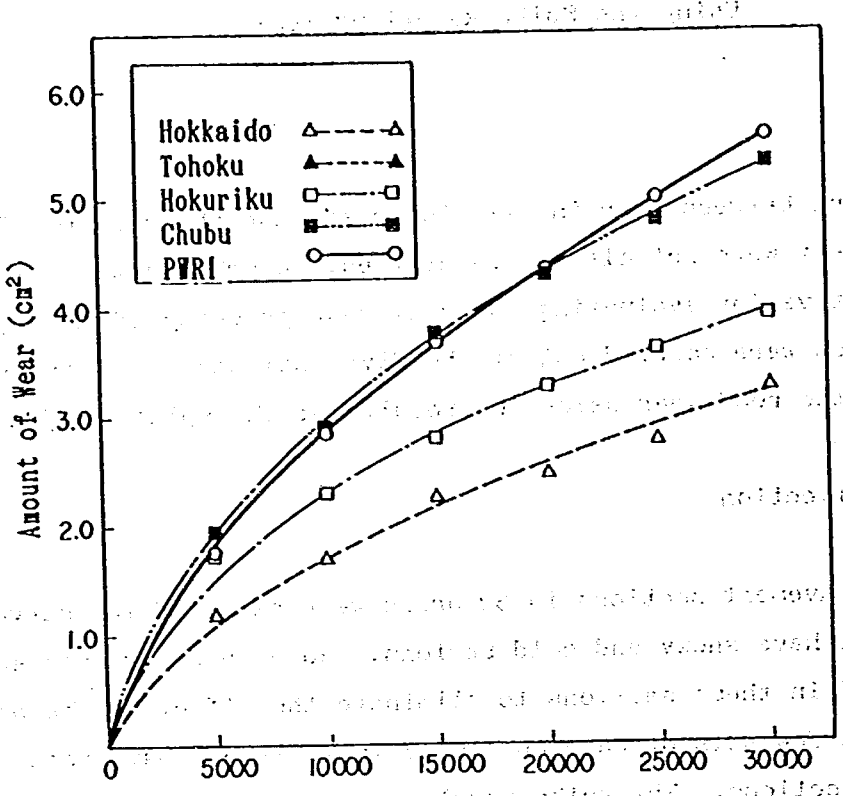


Fig.-2.1 Wear of PWRI Standard Specimens(FG(13F)) by each institutes

Table-2.2 Standard Testing Conditions of Spike Ravelling Test

Pre-Loading		Tracking by Studded Tire	
Table Speed	20km/h	Table Speed	20km/h
Tire Apeed	20km/h	Tire Speed	20km/h
Tite Type	Non-Studded	Tire Type	Studded Tire
Wheel Load	150±5kgf	Wheel Load	150±5kgf
Tire Pressure	1.6±0.1kgf/cm²	Tire Pressure	1.6±0.1kgf/cm²
Temperature	20℃	Temperature	0±2℃
Camber Angle	1.5°	Camber Angle	1.5°
Width of Traverse	±50mm	Width of Trverse	±50mm
Traverse Speed	—	Trverse Speed	—
Cureing time	4 h	Cureing Time	4 h
Tracking Cycle	5,000 round	Tracking Cycle	30,000 round
		Water Spreading	2 ℓ/min

*Pre-Loading is a procedure that give settlement to the spacimen by tracking of non-studded tire

3. Development of a Method for Estimating Road Wear Using the Spike Ravelling Test

3.1 Purpose

The relations between wear in existing roads and the results of the spike ravelling test were not clearly identified, though the test had been known to be effective for evaluating the unti-wear property of paving mixtures. Thus, studies were carried out at the five insitutes to develop a method for estimating the road wear using the results of the spike ravelling test.

3.2 Data Collection

Forty-five pavement sections in 32 areas were selected for survey from the Bureaus that have snowy and cold regions. Roads near by intersection were not included in these sections to eliminate the effect by the braking of vehicles. A few sets of data as listed in Table-3.1 have been collected from these sections. The spike ravelling test was also conducted on specimens cut out from pavements of all sections. The characteristics of the road surfaces were measured twice a year, in spring and autumn, to separate the rut caused by wear from total rut depth.

Table-3.1 Kinds of Data Collection

Data		Testing Condition, Note
Traffic Condition	Traffic Volume	All Traffic, Heavy Traffic
	Using Studded tire	Percentage of Studded-tire-equipeed vehicle
Material Properties	Aggregate Gradings	
	Loss of Aggregates	JIS A 1121
	Wear Amount of Mixture	Table-2.1
Surface Condition	Rut Depth	Measured in Spring and Autumn Each Year
	Cracking Ratio	

3.3 Results

3.3.1 Traffic Volume With Studded Tires

The proportion of vehicles with studded tires and the period of use of studded tires was surveyed to determine the total traffic volume of vehicles with studded tires in winter. To determine the period of use of studded tires, the following data were recorded: (1) when studded tires begin to be used, (2) when the proportion of vehicles with studded tires reaches a maximum, (3) when the proportion begins to decrease, and (4) when the proportion becomes nearly zero. The change in the proportion of vehicles with studded tires was assumed as a curve shown in Fig.-3.1, and total traffic volume of vehicles with studded tires was calculated by equation-3.1.

The total traffic volume were caluculated for two cases where the effect of heavy vehicles is or is not taken into account.

$$N_{SP} = (L_{12} \times SP/2 + L_{23} \times SP + L_{34} \times SP/2) \times N \qquad (3.1)$$

N_{SP} : traffic volume of vehicles with studded tire during one winter; (vehicles)

N : total traffic volume; (vehicles/day/direction)

SP : Proportion of vehicles with studded tires; (%)

L_{12}, L_{23}, L_{34} : Duration as defined in Fig.-3.1; (days)

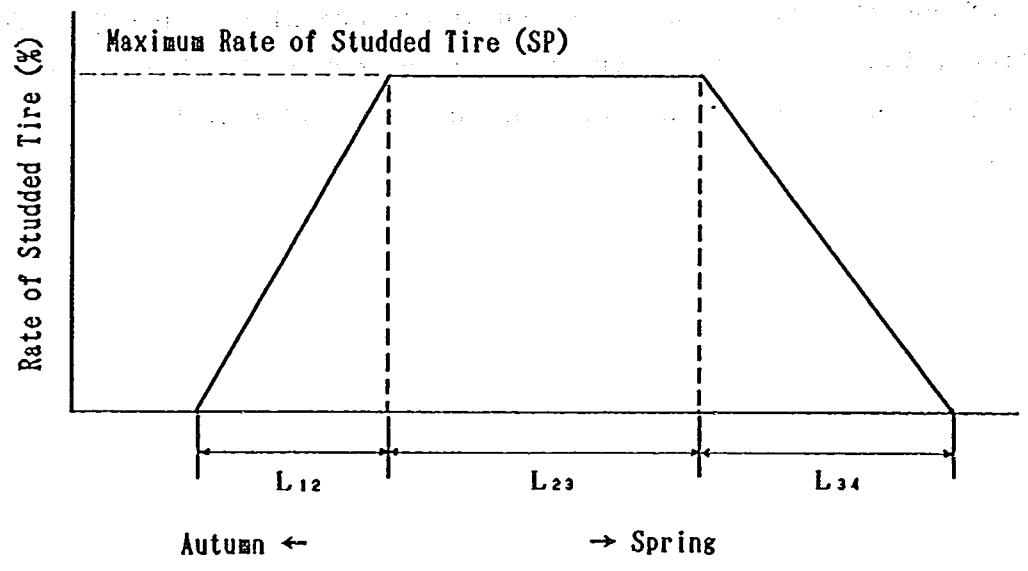


Fig.-3.1 Change in Proportion of Vehicles with Studded Tires

3.3.2 Relation between Traffic Volume and Surface Characteristics

In first, relations betweeen the traffic volume and the surface characteristics were examined.

(1) All Veehicles, Heavy Vehicles and Rut Depth

Examples of the relations in each bureau between traffic volume of all vehicles and rut depth are shown in Figs.3.2-3.5 respectively. In any sections, the rut depth rapidly increased immediately after the road had begun to be under use. This initial rut is associated with plastic flow. Except for the initial rut, the rut depth increases more in winter than in summer. Survey results suggest that the rate of increase in rut depth in summer and winter varies significantly according to each section.

The relations between the rut depth and the traffic volume of heavy vehicles have a similar tendency to those with the volume of all vehicles.

(2) Rut Depth and Traffic Volume of Vehicle with Studded Tires

In this examination, the increase in the rut depth during winter, rut depth measured in spring minus that in the previous autumn, was calculated to eliminate rut by plastic flow.

Figs.-3.6-3.9 illustrate examples of relations between rut depth in winter and the traffic volume of vehicles with studded tires. There can be recognized a high correlation between both two factors in all sections. The coefficients of correlation of regression equations are higher than 0.95 for all the sections, indicating that there is a close correlation between the increase of rut depth in winter and the traffic volume of vehicles with studded tires.

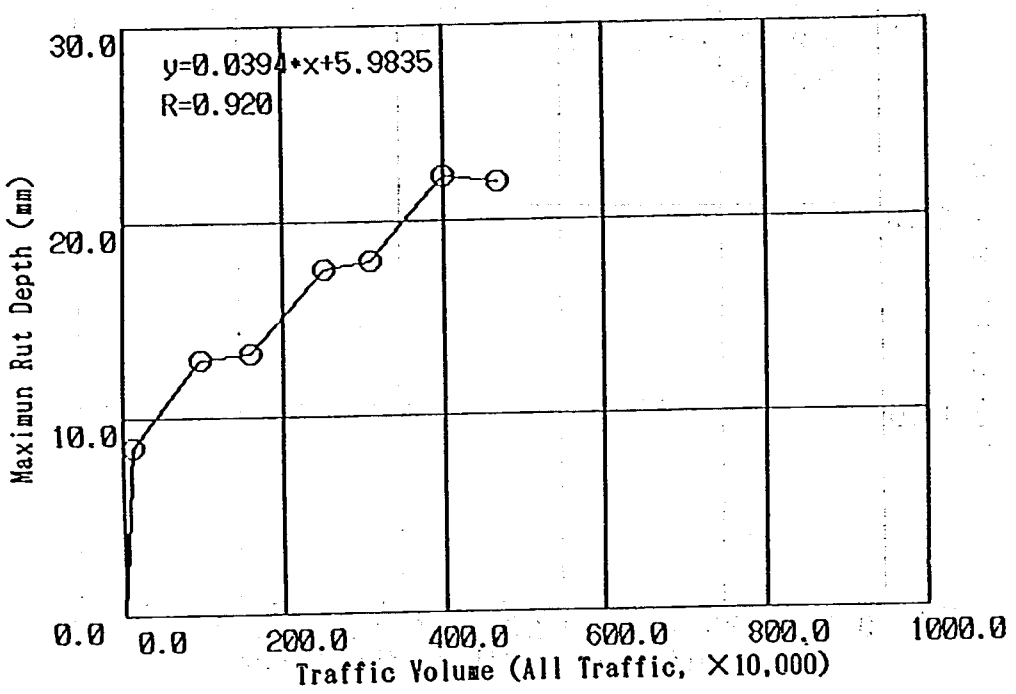


Fig.-3.2 Traffic Volume of All Vehicles and Rut Depth
(Mori-town, Hokkaido)

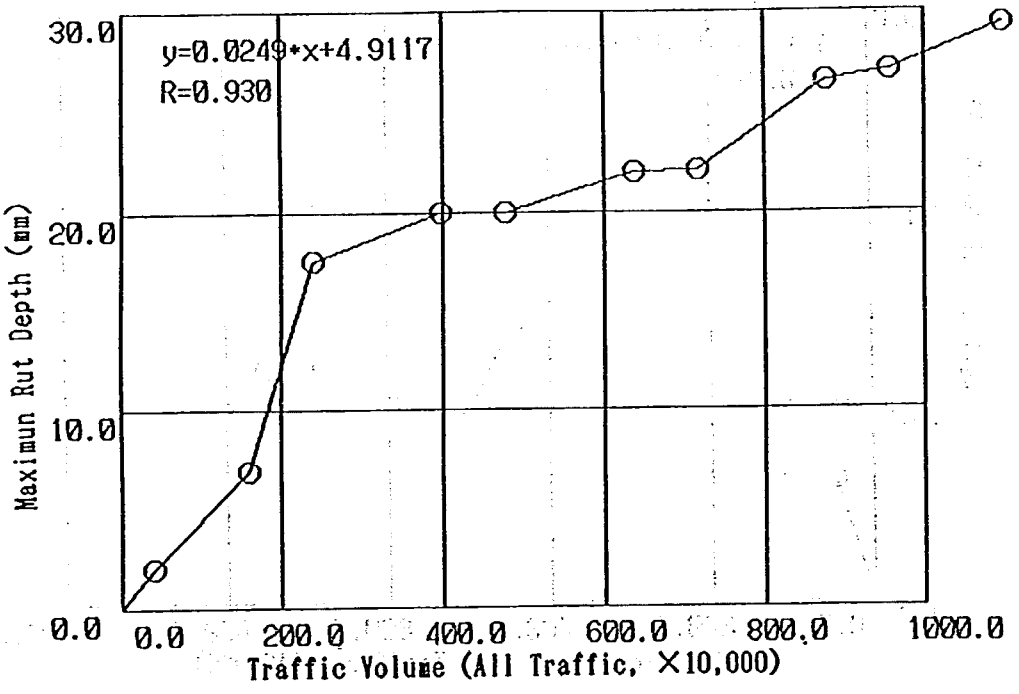


Fig.-3.3 Traffic Volume of All Vehicles and Rut Depth
(Koriyama-shi, Tohoku)

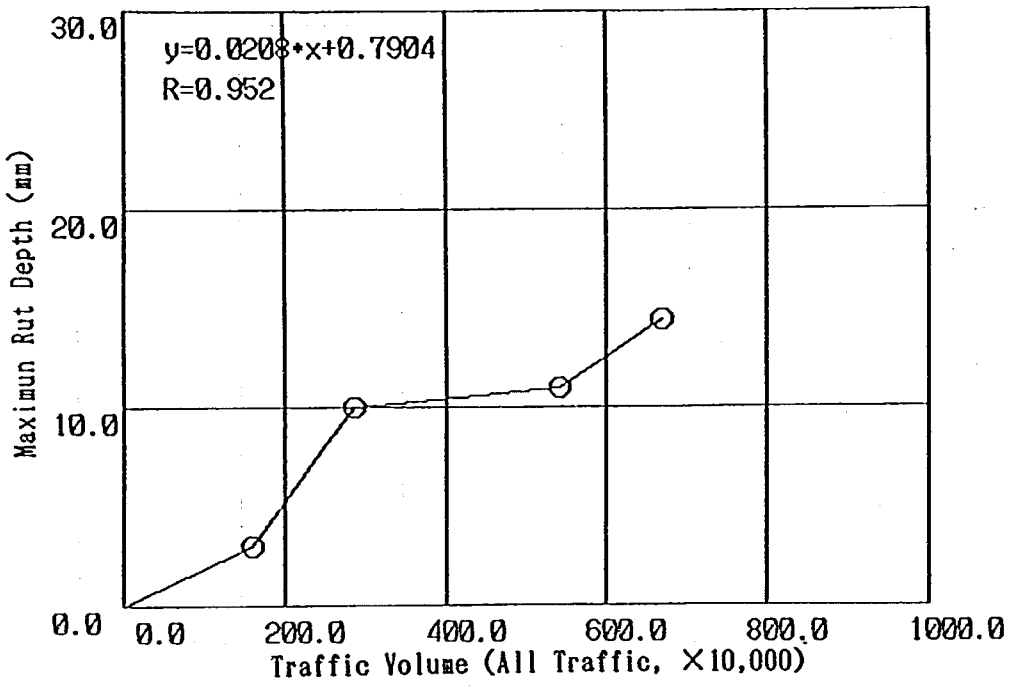


Fig.-3.4 Traffic Volume of All Vehicles and Rut Depth
(Shibata-shi, Hokuriku)

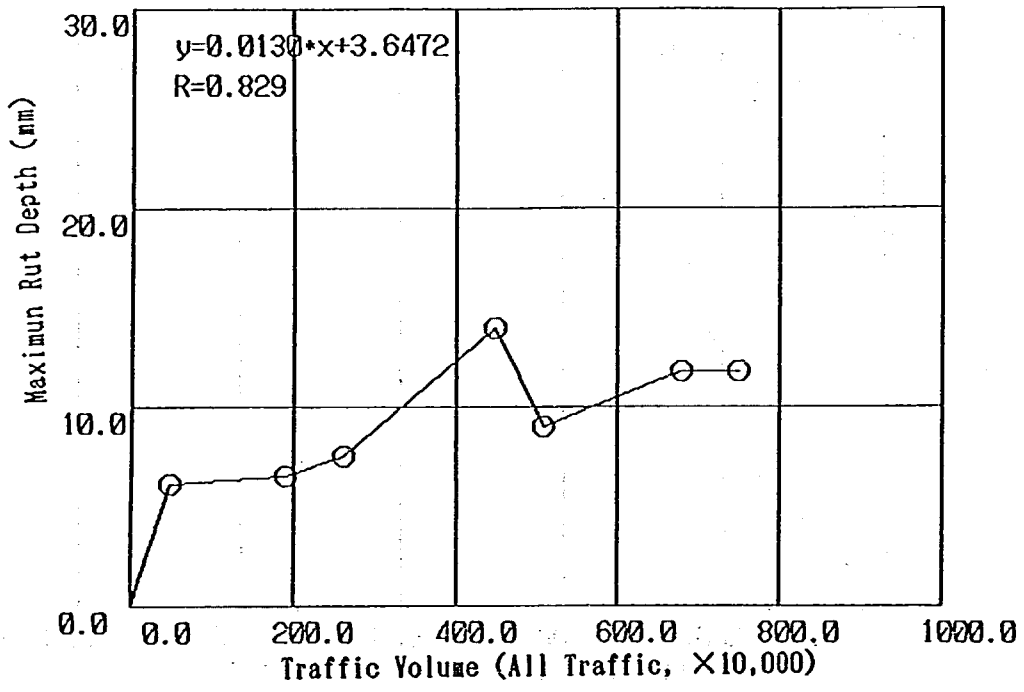


Fig.-3.5 Traffic Volume of All Vehicles and Rut Depth
(Kuguno-town, Chubu)

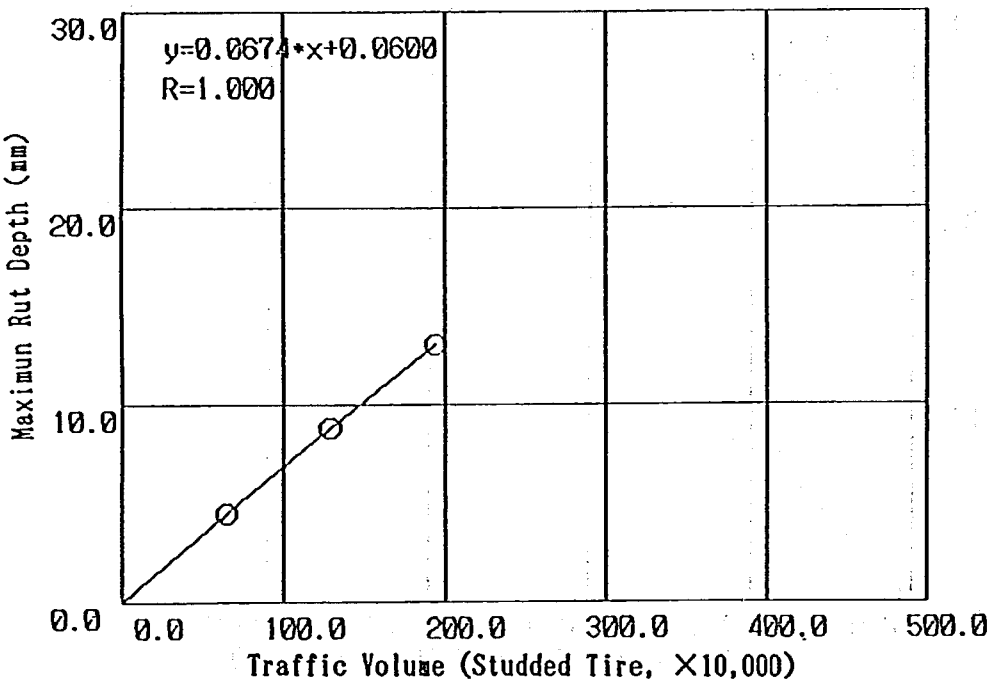


Fig.-3.6 Traffic Volume of Vehicles with Studded Tires and Rut Depth in Winter (Mori-town, Hokkaido)

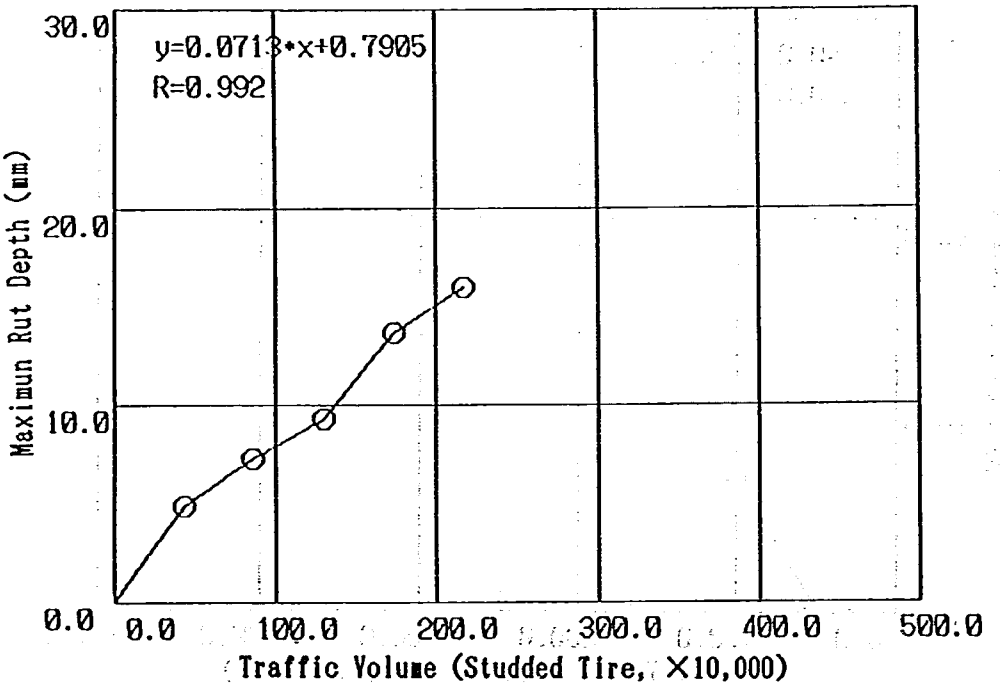


Fig.-3.7 Traffic Volume of Vehicles with Studded Tires and Rut Depth in Winter (Koriyam-shi, Tohoku)

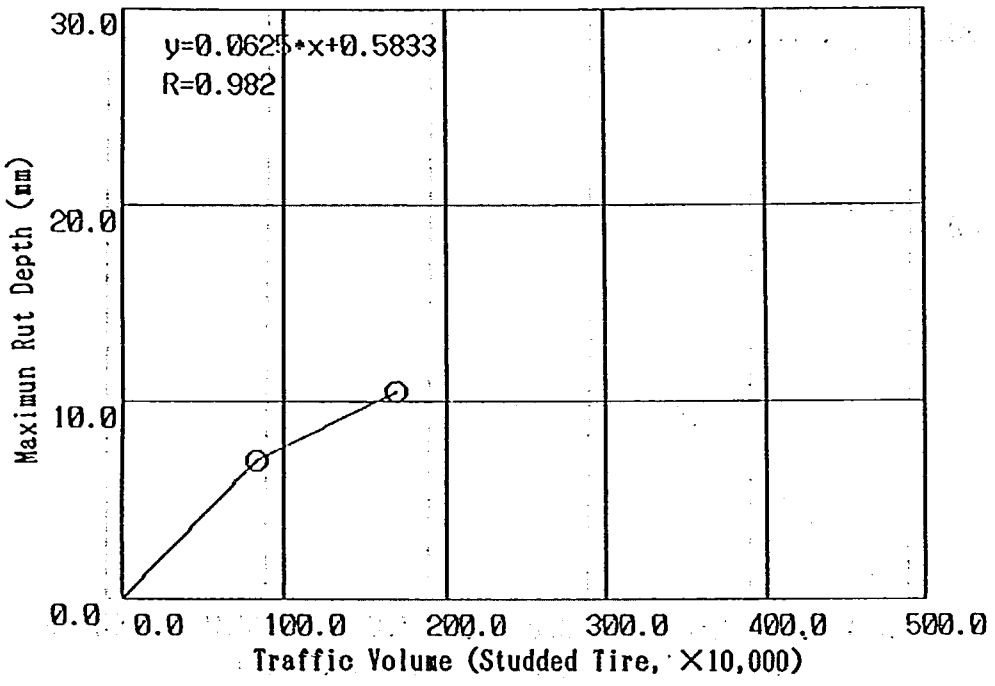


Fig.-3.8 Traffic Volume of Vehicles with Studded Tires and Rut Depth in Winter (Shibata-shi, Hokuriku)

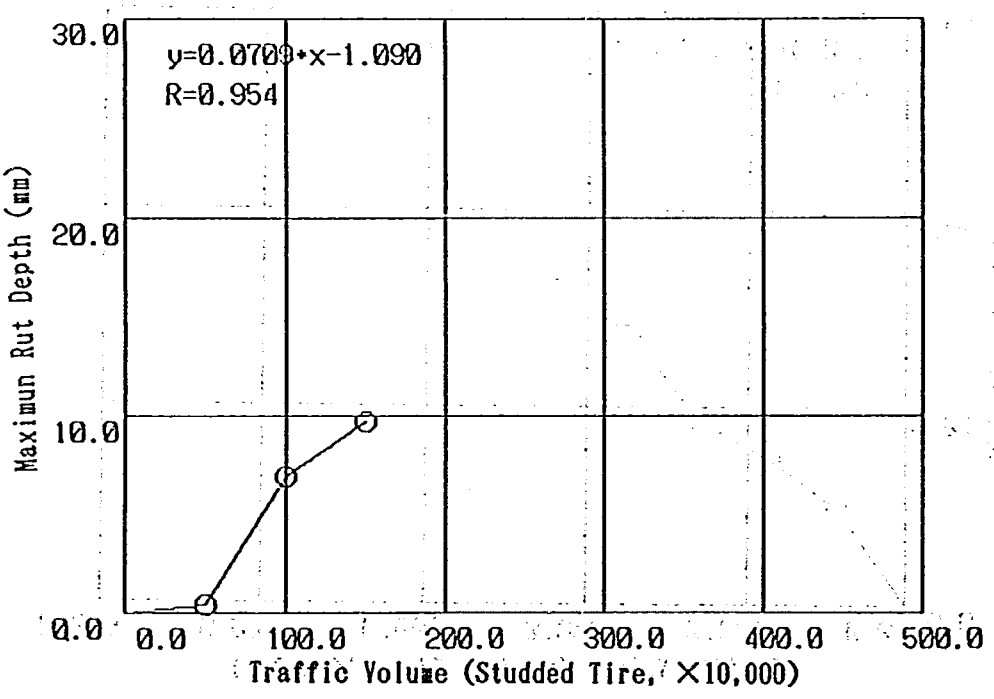


Fig.-3.9 Traffic Volume of Vehicles with Studded Tires and Rut Depth in Winter (Kuguno-town, Chubu)

3.3.3 Properties of Mixture and Increase in Rut by Wear

A regression equations for the rut by wear and traffic volume in each section were derived in the following form by means of a procedure similar to the one used in Section 3.3.2.

$$R = a \times N + b \quad (3.2)$$

R : rutting depth; (mm)
N : traffic volume: (vehicles)
a, b : constant

If the mixture used has poor resistance against wear, then the rut depth must increase rapidly, and give a large gradiant "a". The value of gradient "a" was determined for all sections, and the relations between gradient "a" and the mixture properties were examined.

Tables-3.2-3.5 show coefficients of correlation between gradient "a" and the mixture properties. There seem to be no significant relations between the mixture properties and gradient "a" in the case of all vehicles or heavy vehicles.

Even in the case of vehicles with studded tires, there are also no significant relations between the gradient "a", which is calculated from increase in rut depth in winter, and the Los Angeles abrasion loss of aggregates. On the other hand, a good correlations were seen between the gradient "a" and the ravelling wear in the case of Tohoku, while the correlation was slightly good in Hokuriku. No correlation was seen in the measurements in Hokkaido and the result calculated from the data of all bureaus. This may be attributed to the fact that roads used only for one winter period accounted for a large part of the sections in Hokkaido, as shown in Table-3.6, resulting in a dispersion among the correlations. The gradient "a" was also calculated with consideration for the following two cases:

(1) assuming that the effect of a heavy vehicle on the wear is twice that of a regular-size vehicle (to be called "heavy vehicle correction").

(2) calculating gradient "a" without using a set of measurements of first winter after paving, to eliminate the effect that degree of paving work has on the rut increase (to be called "initial correction").

However, no great difference was recognized betwwen coeffients of corre-

lation with correction and ones without correction. Thus, the follwing analysis were made without consideration for both two corrections.

Figs.3.10-3.13 show the relations without correction between the ravelling wear and the gradient "a" which is culculated from the volume of vehicles with studded tires and increase in rut in winter. In the Fig.-.3.10, ravelling wear at each institute were converted into the value at the PWRI. Specific analysis was not performed for the Chubu Construction Bureau, because the Bureau contained only one survey section, but the Chubu data were included into analysis in the case of Fig.-3.10.

Table-3.6 Number of Sections Classified by Period Under Use

Bureau	Winter Experience				
	1	2	3	4	5
Hokkaido	9	2	5		
Tohoku			8	8	2
Hokuriku		10			

Table-3.2 Coeeficient of Correlation between Gradient "a" and Mixture Properties (All Bureau)

Traffic Type	Material Property	Initial Correction	R
ALL TRAFFIC	WIGHT LOSS IN LOS ANGELS TEST (13-5mm)	YES	0.440
		NO	0.446
	WEAR IN RAVEELING TEST	YES	0.538
		NO	0.494
HEAVY TRAFFIC	WIGHT LOSS IN LOS ANGELS TEST (13-5mm)	YES	0.165
		NO	0.169
	WEAR IN RAVEELING TEST	YES	0.439
		NO	0.350
STUDDED VEHICLE without Heavy traffic Correction	WIGHT LOSS IN LOS ANGELS TEST (13-5mm)	YES	0.165
		NO	-0.163
	WEAR IN RAVEELING TEST	YES	0.066
		NO	0.082
STUDDED VEHICLE with Heavy Traffic Correction	WIGHT LOSS IN LOS ANGELS TEST (13-5mm)	YES	-0.171
		NO	-0.176
	WEAR IN RAVEELING TEST	YES	0.071
		NO	0.080

Table-3.3 Coeeficient of Correlation between Gradient "a" and Mixture Properties (Hokkaido)

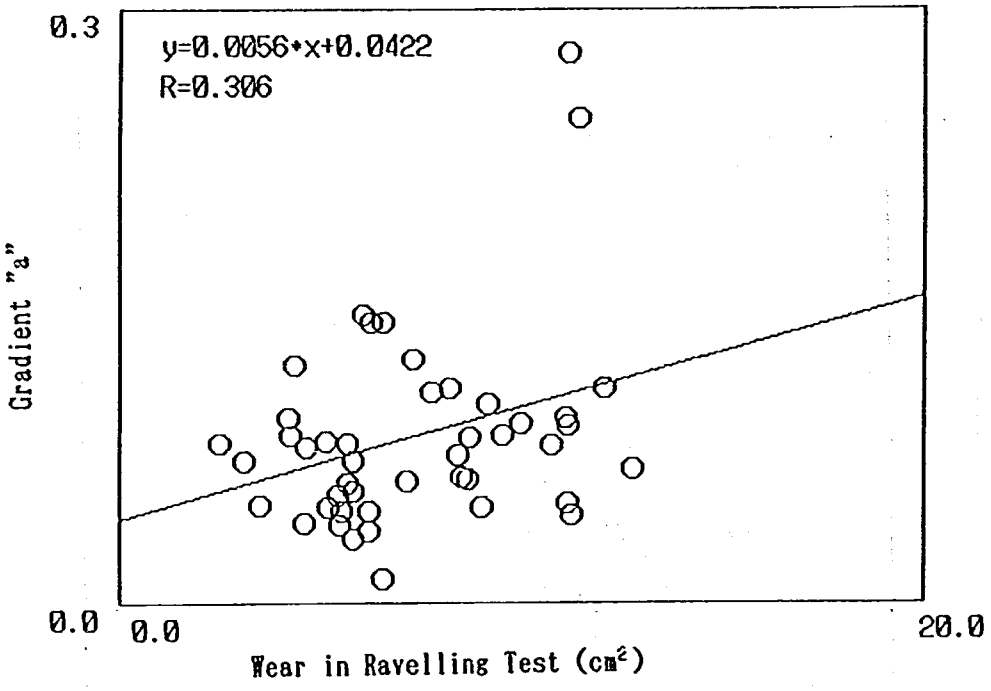
Traffic Type	Material Property	Initial Correction	R
ALL TRAFFIC	WEIGHT LOSS	YES	0.170
		NO	0.128
	RAVELING TEST	YES	-0.493
		NO	-0.391
HEAVY TRAFFIC	WEIGHT LOSS	YES	-0.512
		NO	-0.545
	RAVELING TEST	YES	0.064
		NO	0.237
STUDDED VEHICLE without Heavy traffic Correction	WEIGHT LOSS	YES	0.210
		NO	-0.106
	RAVELING TEST	YES	-0.058
		NO	-0.352
STUDDED VEHICLE with Heavy Traffic Correction	WEIGHT LOSS	YES	0.114
		NO	-0.236
	RAVELING TEST	YES	-0.307
		NO	-0.295

Table-3.4 Coeeficient of Correlation between Gradient "a" and Mixture Properties (Tohoku)

Traffic Type	Material Property	Initial Correction	R
ALL TRAFFIC	WEIGHT LOSS	YES	0.207
		NO	0.405
	RAVELING TEST	YES	0.491
		NO	0.538
HEAVY TRAFFIC	WEIGHT LOSS	YES	0.280
		NO	0.415
	RAVELING TEST	YES	0.319
		NO	0.366
STUDDED VEHICLE without Heavy traffic Correction	WEIGHT LOSS	YES	0.274
		NO	0.259
	RAVELING TEST	YES	0.854
		NO	0.864
STUDDED VEHICLE with Heavy Traffic Correction	WEIGHT LOSS	YES	0.229
		NO	0.284
	RAVELING TEST	YES	0.848
		NO	0.859

Table-3.5 Coeeficient of Correlation between Gradient "a" and Mixture Properties (Hokuriku)

Traffic Type	Material Property	Initial Correction	R
ALL TRAFFIC	WEIGHT LOSS	YES	0.260
		NO	0.068
	RAVELING TEST	YES	0.299
		NO	0.032
HEAVY TRAFFIC	WEIGHT LOSS	YES	0.184
		NO	0.002
	RAVELING TEST	YES	0.282
		NO	-0.051
STUDDED VEHICLE without Heavy traffic Correction	WEIGHT LOSS	YES	0.548
		NO	0.253
	RAVELING TEST	YES	0.591
		NO	0.573
STUDDED VEHICLE with Heavy Traffic Correction	WEIGHT LOSS	YES	0.557
		NO	0.229
	RAVELING TEST	YES	0.610
		NO	0.562



* each wear are converted into PWRI values

Fig.-3.10 Ravelling Wear and Gradient "a" (All Bureau)

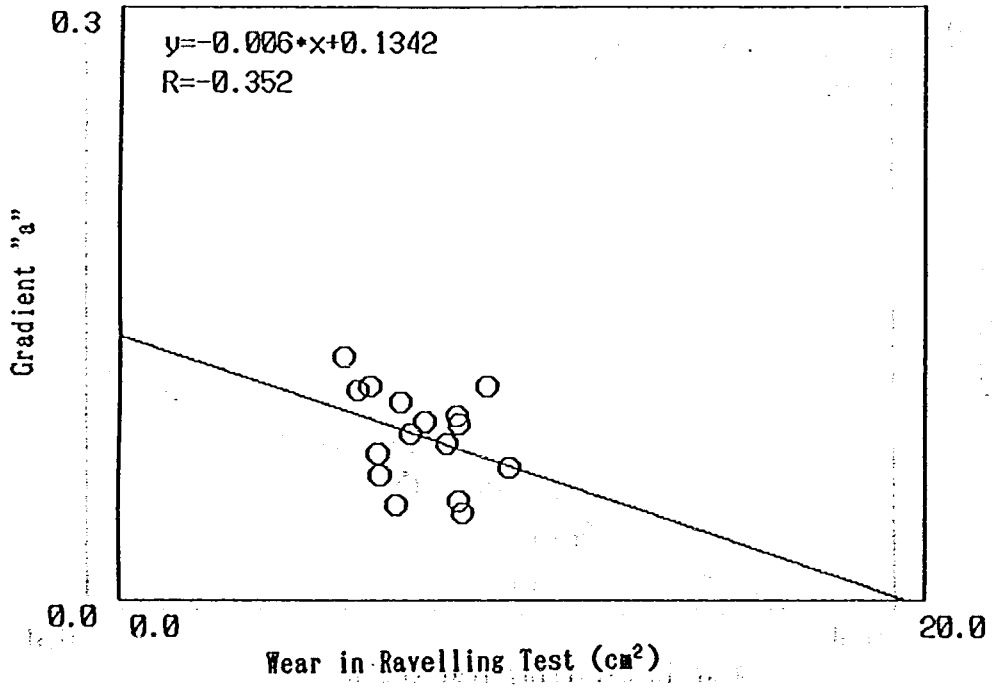


Fig.-3.11 Ravelling Wear and Gradient "a" (Hokkaido)

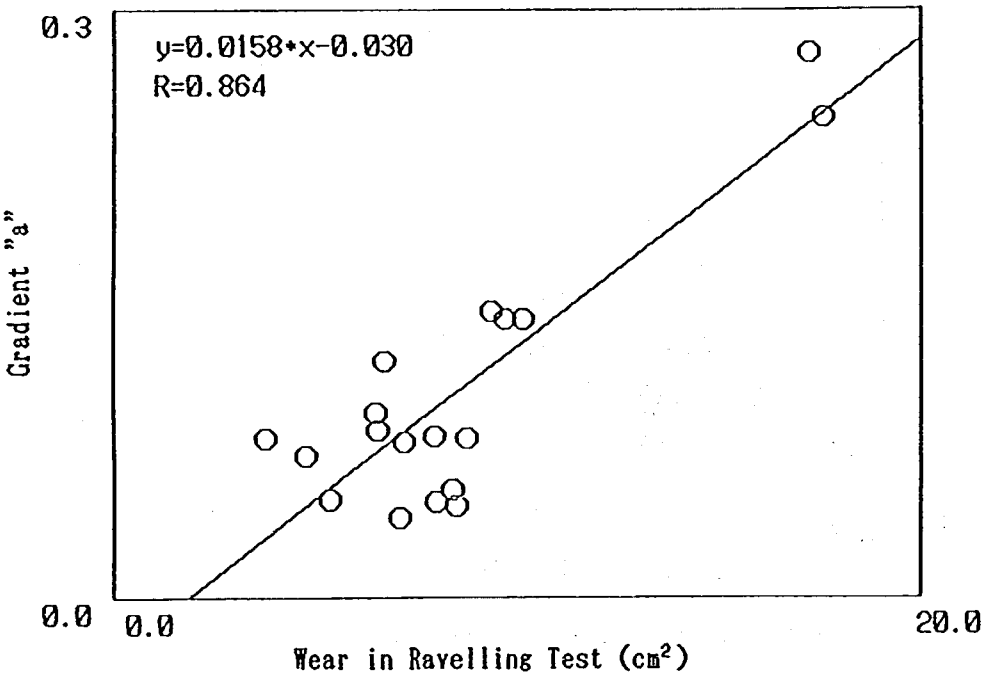


Fig.-3.12 Ravelling Wear and Gradient "a" (Tohoku)

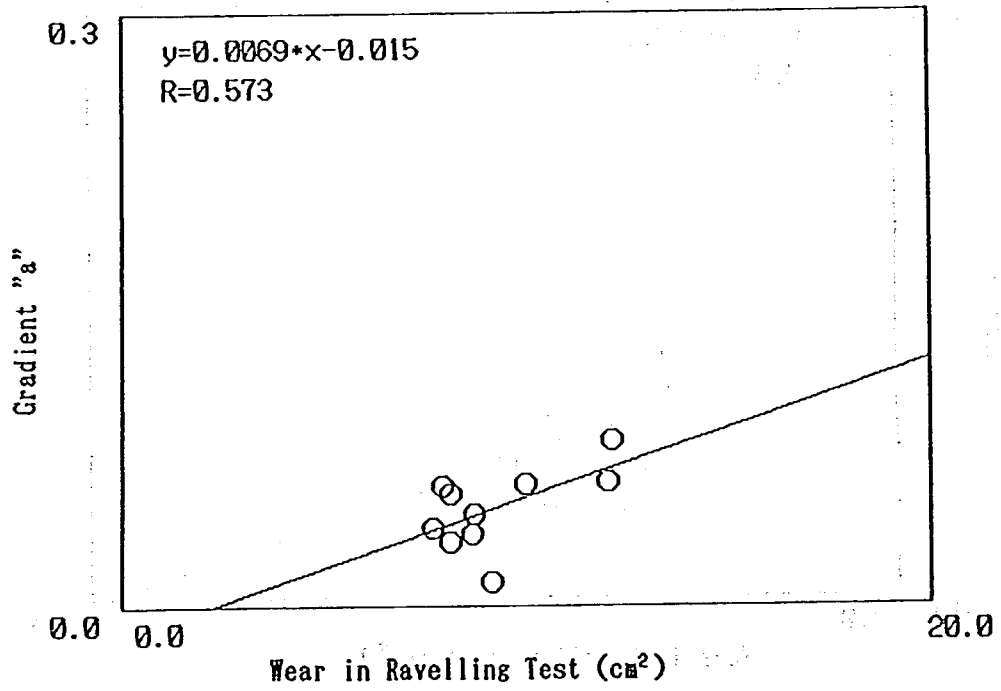


Fig.-3.13 Ravelling Wear and Gradient "a" (Hokuriku)

3.3.4 Relation between Road Wear and Ravelling Wear

From the measurements in Tohoku, where the highest correlation was recognized, the relation between the gradient "a" and ravelling wear was derived as follows:

$$a = 0.0158 \times M - 0.030 \qquad (3.3)$$

Assuming that the rut depth just after paving is 0 mm, rut depth caused by wear in Tohoku can be calculated by Equation-3.4 which is derived from Equation-3.3.

Maximum rut depth $R_{max} = (0.0158 \times M_T - 0.030) \times N_{SP}$ (3.4)

M_T : spike ravelling wear in Tohoku; (cm2)

N_{SP} : traffic volume of vehicles with studded tires (vehicles)

$$N_{SP} = (L_{12} \times SP/2 + L_{23} \times SP + L_{34} \times SP/2) \times N$$

3.3.5 Modification of Equation for Wear Estimation

Because Equation-3.4 is based on results of the ravelling test carried out by the Tohoku, and it cannot be applied to ravelling wear measurements made at other institutes. The use of studded tires in Japan have been regulated strictly year by year, and the shape and number of studs of one tire have been changing. Then, modifications have also been made each year to the specifications of tires to be used for the ravelling test. Thus, there was the possibility that Equation-3.4, which is based on the ravelling wear made at Tohoku in 1988, could become invalid even for the ravelling wear made in Tohoku, in the future.

To cope with such modifications of the tire specifications, each of the five institutes has established its own standard mixture. When conducting spike ravelling test in certain institute, the test should be also made on its standard mixture, and variation of wear due to the specification of the tire can be corrected using the wear of the standard mixture. Furthermore, as stated in Chapter-2., standard tests have been carried out every year at all five institutes using standard mixtures prepared at the PWRI, and wear obtained at each institute can be calibrated into the value at PWRI in order to compare the ravelling wear obtained at different institutes.

Thus, Equation-3.4 was modified on the basis of wear of the standard mixtures of both institutes and PWRI.

It was assumed that a given ravelling wear can be expressed in the form of a ratio to the wear of PWRI standard mixture, and that relation between this ratio and gradient "a" and can be expressed by Equation-3.5:

$$a = a' \times \frac{\overline{M_i}}{M_{dd}} + b \qquad (3.5)$$

$\overline{M_i}$: wear of a given mixture measured at a given time at institute "i" and converted into a value that might have been obtained at PWRI; (cm2),

M_{dd} : wear of PWRI standard mixture measured at PWRI at a given time; (cm2),

a : gradient for increase in rut wear

a', b : constant

Based on results of the standard test carried out each year at all these institutes using PWRI standard mixtures, the following factor was defind to convert ravelling test results at institute "i" into the value obtained at PWRI.

$$\alpha_i = \frac{{}_8M_{dd}}{{}_8M_{di}} \qquad (3.6)$$

${}_8M_{di}$: wear of PWRI standard mixture at institute "i" in a standard test; (cm2)

${}_8M_{dd}$: wear of PWRI standard mixture at PWRI in a standard test; (cm2)

The standard test also covers the ravelling test for standard mixtures of each institute. The ratio "β_i" of standard mixture's wear of institute "i" to the PWRI standard mixture's wear was defined as:

$$\beta_i = \frac{{}_8M_{dd}}{{}_8M_{ii}} \qquad (3.7)$$

${}_8M_{ii}$: wear of standard mixture of institute "i" at standard test; (cm2),

Then M_{dd} is expressed as:

$$M_{dd} = \alpha_i \times M_{di} = \alpha_i \times \beta_i \times M_{ii} \quad (3.8)$$

M_{ii} : wear of standard mixture of institute "i" at a given time; (cm2)

Equation-3.5 can be modified as:

$$a = a' \times \frac{\alpha_i \times M_i}{\beta_i \times \alpha_i \times M_{ii}} + b$$

$$= a' \times \frac{1}{\beta_i} \times \frac{M_i}{M_{ii}} + b \quad (3.9)$$

A basic equation for estimating the wear rut was obtained as:

$$R = \left[a' \times \frac{1}{\beta_i} \times \frac{M_i}{M_{ii}} + b \right] \times N_{SP} \quad (3.10)$$

On the basis of Equation-3.9, Mi/Mii were plotted on the horizontal axis and gradients "a" were plotted on the vertical axis for all data collected 45 test sections. The result is shown in Fig.-3.14.

From these results, an equation for estimating the wear rut is obtained as:

$$R_{max} = \left[0.1003 \times \frac{1}{\beta_i} \times \frac{M_i}{M_{ii}} - 0.030 \right] \times N_{SP} \quad (3.11)$$

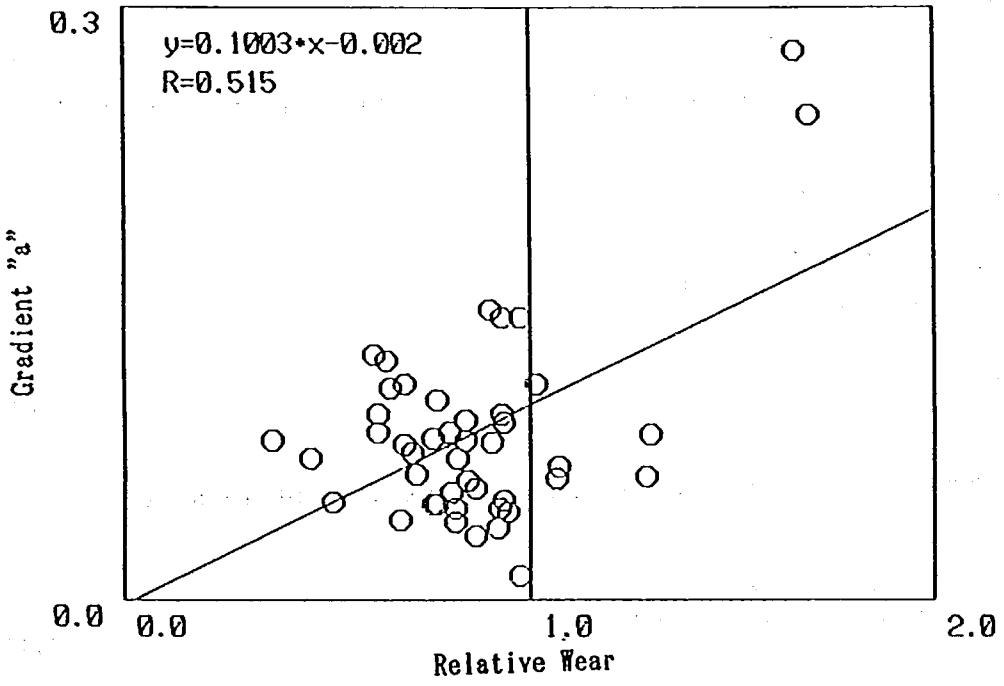
M_i : wear of a given mixture at institute "i" at a given time; (cm2)

M_{ii} : wear of standard mixture of institute "i" at a given time; (cm2)

N_{SP} : total traffic volume of vehicles with studded tires; (vehicles)

β_i : conversion factor of standard test mixture.

Table-3.7 shows ai, Bi and wear of standard mixtures of five institutes in FY1988.



* Relative wear
= (converted wear into PWRI value of any mixture)/(Standard wear)

Fig.-3.14 Mi/Mii and Gradient "a"

Table-3.7 ai, Bi, Wear of Standard Mixture

INSTITUTE	CERI	TOHOKU	HOKURIKU	CHUBU	PWRI
α_i	1.325	0.649	0.722	1.218	1.000
STANDARD WEAR(cm^2)	5.05	11.293	6.555	4.133	6.770
β_i	1.012	0.924	1.430	1.345	1.000

3.3.6 Application to Actual Pavement

Figs.-3.15, 3.16 illustrates plottings of Equation-3.11. In Fig.-3.15, rut depth by wear can be estimated for any traffic volume. In Fig.-3.16, rut depth by wear can be estimated for any mixtures. Then Fig.-3.16 is available for examining the design of mixture to keep road wear under a certain level.

When using Equation-3.11 and the curves in Figs.-3.15, 3.16, a institute should conduct the spike ravelling test on both mixture to be used in road and its standard mixture.

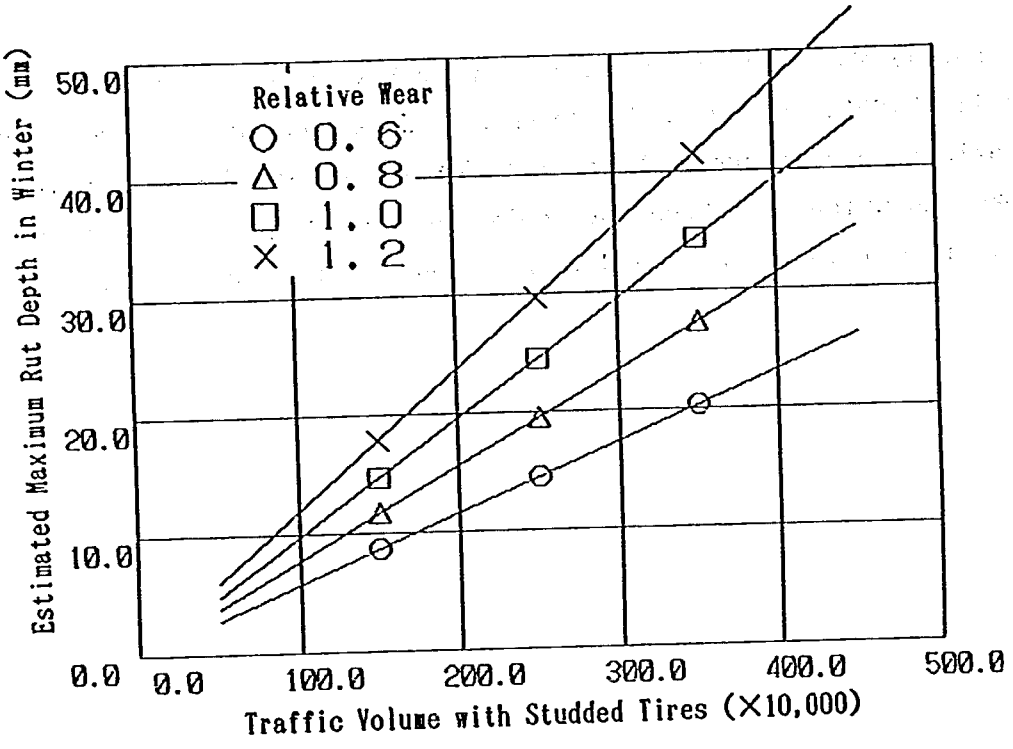


Fig.-3.15 Estimation of Road Wear at a Given Traffic Volume

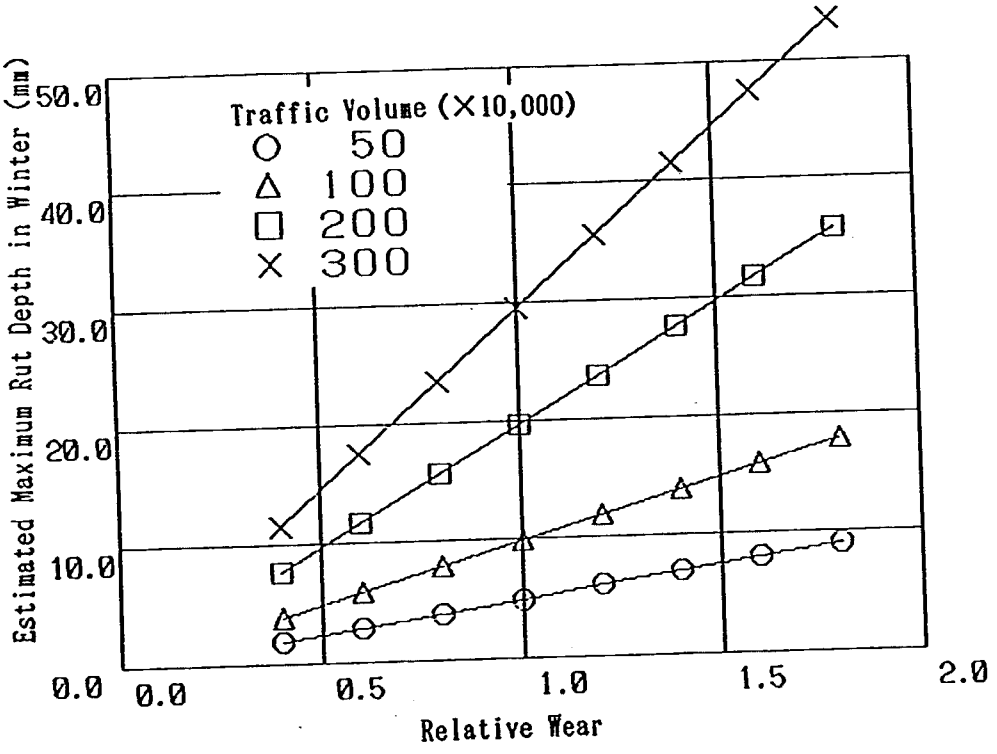


Fig.-3.16 Estimation of Road for a Given Mixture

4. Afterword

Equation-3.11 for estimating the road wear heve been derived from the studies until FY1989. However, Equation-3.11 does not estimate the road wear with satisfactory accuracy, because there are a lot of sections in Hokkaido and Hokuriku which have been used only for a short period. The surveys will continue into 1990 to provide data required to further improve Equation-3.11.

Snow and Ice Detection by a Dielectric Pavement Freezing Detector (DPF)

K. Takeichi, Hokkaigakuen Univ.
N. Maeno, Hokkaido Univ.
H. Kubo, former CERI, Hokkaido Development Bureau

SNOW AND ICE DETECTION BY A DIELECTRIC PAVEMENT FREEZING-DETECTOR (DPF)

by

Kiyoshi Takeichi, Department of Engineering, Hokkaigakuen University,
Norikazu Maeno, Institute of Low Temperature Science, Hokkaido University
and
Hiroshi Kubo, Civil Engineering Research Institute,
Hokkaido Development Bureau

ABSTRACT

The recent increasing need for the restriction on the use of studded tires in Japan has led to the requirement of a higher-level control system of roads in winter seasons, which does not imply only the quick snow removal to make minimum transport possible but also the snow and ice control of pavement surfaces to keep them safe for whole drivers. Such a system requires a reliable sensor to detect and forecast freezing of pavement surfaces most dangerous to driving. This paper presents a new detection method of freezing, Dielectric Pavement Freezing-detector(DPF), which was developed to measure and distinguish a variety of snow/ice conditions on pavements.

DPF, different from existing detectors which measure mainly temperatures and moisture on pavements, is based on the measurement of dielectric constants of snow/ice on pavements. DPF is installed on a pavement surface, which can discriminate a wide range of pavement conditions: dry, wet, compacted snow, ice film and ice crust. Thus DPF can also be used to monitor road heating systems and de-icing chemical applicaions. The dielectric constants (κ) of snow/ice on a pavement is defined as a ratio (C_x/C_a) of the electric capacitance (C_x) of snow/ice on the pavement to that of air (C_a) on the pavement without snow and ice.

The relationship between snow and ice conditions on pavements and the dielectric constans was observed throughout two winter seasons (1989 - 1991) with DPF laid on the surface in Sapporo city roads.

SNOW AND ICE DETECTION BY A DIELECTRIC PAVEMENT FREEZING-DETECTOR (DPF)

by

Kiyoshi Takeichi, Department of Engineering, Hokkaigakuen University,
Norikazu Maeno, Institute of Low Temperature Science, Hokkaido University
and
Hiroshi Kubo, Civil Engineering Research Institute,
Hokkaido Development Bureau

1/ INTRODUCTION

In North America and northern Europe roads are kept clear of snow and ice generally by spreading salt to keep pavements bare. Since around 1970 detection and warning systems of snow and ice conditions on pavements have been developed and put in use particularly in North America for minimizing salt use and providing warnings to drivers. Similar detection devices are used on some highways and trunk roads in Japan, but the use is limited due to problems with performance and installation costs.

Such sensors will play an increasingly important role in providing information on snow and ice conditions on pavements. With the increasing concern about regulations of studded tires in Japan, pavement-control policies in addition to snow removal will have to be introduced. On trunk and secondary roads, there are compacted snow, ice crusts and ice films (by consolidation of snow due to vehicles, and thawing and re-freezing of snow/ice), which easily become very slippery. The conditions on these roads change quickly, for example from wet in the daytime to frozen at night.[1)]

The development of the DPF (Dielectric Pavement Freezing-Detector) aims to provide road administrators and users with information on roads where surface conditions are likely to change. The DPF will also be very useful in identifying places where deicing chemicals should be applied, and in estimating the amounts of chemicals to apply.

The tests with this new DPF progressed as follows: Laboratory tests started in 1987, and in-situ measurements by a trial detector were made between December, 1988 and the end of March, 1989. The equipment was developed further and used in in-situ observations between January and March, 1990. This paper presents the method for detecting pavement conditions by the DPF and its use as a detection system on the basis of analyses of the laboratory tests and in-situ observations.

2/ PAVEMENT FREEZING DETECTORS AND SNOW AND ICE CONTROL IN NORTH AMERICA AND NORTHERN EUROPE

In North America and northern Europe transport of people and commodities has traditionally depended on roads to a great extent. Accordingly, there is a long history of studies of road management in winter, and adequate systems to control snow and ice are used in many areas. The following will outline such systems and the types of detectors used.

2.1/ SNOW AND ICE CONTROL SYSTEMS IN NORTH AMERICA AND NORTHERN EUROPE

North America has researched and developed sensor devices to detect mainly temperature and moisture on road surfaces for a long time, such as the Surface Condition Sensor for Bridge Decks, which was often used on bridge sections. In some states, weather and pavement condition criteria that require salt application are specified, and road management offices collect meteorological information in their areas through weather forecasing consultants. This assists in taking action to prevent road surfaces from freezing and to determine the need for snow removal [2),3)]. In some provinces in Canada, particularly Ontario and Quebec, snow and ice control on roads is managed with similar control systems.

Switzerland tries to minimize use of deicing chemicals by estimating salt content, from air and pavement temperatures and the moisture on the road surfaces, which were collected by frost warning equipments and weather radar.

The UK has adopted an original formula to forecast road-surface temperatures for road management. This formula is based on predictions of air tempera-

tures and precipitation, obtained from the weather bureau. Recently, a research team from the weather bureau and a university has worked on the development of a meteorological observation system and sensor devices to detect freezing of road surfaces.[4)]

The French road bureau adopted a forecast model (PERIDOT) and information service system (METELOTEL) of road weather conditions with meteorological radar and satellite. The bureau has also been developing a weather forecast model for use in smaller areas.

In Finland, detection system with road-surface sensor (DRS12) was developed, which grasps the current state and forecast changes in pavement conditions over several hours. The sensor is designed to detect the condition on a road surface - frost, snow, ice, salt, moisture, etc. - based on electric conductivity and pavement temperature. But conductivity does not distinguish well among dry conditions, dry snow, and black ice, so capacitance is measured to detect black ice. Furthermore, the snow and ice control is researched and traffic accidents are analyzed by classifying pavement conditions according to service levels based on the coefficient of skid resistance.[5)]

Over the last ten years Sweden has created road weather maps and a road weather information system (VVIS) and area weather models have been developed for road administration. Air and pavement temperatures and freezing conditions of road surfaces are measured by observation cars to produce the weather maps.

3/ PAVEMENT FREEZING-DETECTORS[6)]

Pavement Freezing-Detectors are generally used to monitor pavement freezing, control road heating and snow-melting sprinkler systems, and determine application of salt. Existing detectors developed in North America, North Europe, Scandinavia, and Japan are classified into five types: (a) thermometers, (b) pavement thermometers, (c) pavement moisture detectors, (d) a combination of thermometer, pavement thermometer, and pavement moisture detector, and (e) a combination of a pavement thermometer and moisture detector. These detectors have varying advantages and disadvantages depend-

ing on the measuring methods, accuracy of detection, installations, durability, influence of external disturbances, extent of observed areas, and maintenance costs. The five types may be summarized as follows:

(a) Thermometer

Air temperatures in close vicinity of the pavement are measured to estimate pavement temperatures and determine freezing.

(b) Pavement Thermometer

Infrared Radiation Method: The quantity of infrared energy radiated from a pavement is measured and converted to the temperature. The thermometer can measure a large area of pavement, without laying works as it is non-contact method, but it is easily affected by external disturbances like vehicles and dirt on the pavement.

Buried Resistance Bulb Method: Platinum resistance bulbs are buried 1cm under the surface of the pavement to measure temperatures directly. The performance is reliable, is not affected by external disturbances, but needs laying works and the exchange of resistance bulbs at pavement repair.

(c) Pavement Moisture Detector

Photoelectric Method: This detector is non-contact and requires no laying work, measures luminous energy of diffused reflection from pavement surfaces lit by lamp, and is able to distinguish among snowfall, freezing, and water. It can measure large areas of pavement, but the lamp has to be exchanged annually. It is susceptible to external disturbances such as vehicles, and not good on uneven pavements.

Buried Electrode Method: Electric resistance between electrodes buried in a pavement is measured to determine the presence of water. It detects snow and ice by melting with a built-in heater. It is not affected by external disturbances, but the observed area is small and presents the same problems as the buried resistance bulbs. Performance of this detector depends on the ability control of the built-in heater at the changing snow and ice conditions.

(d) Combination of Thermometer, Pavement Thermometer, and Pavement Moisture Detector

Air and pavement temperatures and pavement moisture are measured by shelter,

infrared radiation, and photoelectric methods. The data is electronically processed to determine pavement conditions: dry, wet, freezing, or snowfall. The accuracy is superior because of the multiple data sources, but it is susceptible to external disturbances.

(e) Combination of Pavement Thermometer and Pavement Moisture Detector

Pavement temperatures and moisture are measured by buried resistance bulb and photoelectric methods to distinguish among dry, wet, freezing and snowfall situations. This method is more accurate than single measurements despite problems with the combination of contact and non-contact methods. In Hokkaido of northernmost island of Japan, contact methods are generally used for measuring temperatures and moisture on pavements to control road heating systems.

A method of detecting ice films with ultrasonic waves has recently been developed in America for the wings of jet air planes. Measurement of ice thickness by ultrasonic waves is not new, but it is hoped that more accurate detectors will be developed. It does not seem to be very suitable for detecting a variety of conditions such as snow and ice on pavements.

The criteria for dry, wet, ice, and snow are not completely distinct for the five types of pavement freezing-detectors mentioned here. In particular, it is theoretically difficult to distinguish between snow and ice, the Dielectric Pavement Freezing-Detector, however, can distinguish among dry, wet, ice, and snow in principle.

4/ PRINCIPLE AND METHOD OF DIELECTRIC PAVEMENT FREEZING-DETECTOR (DPF)

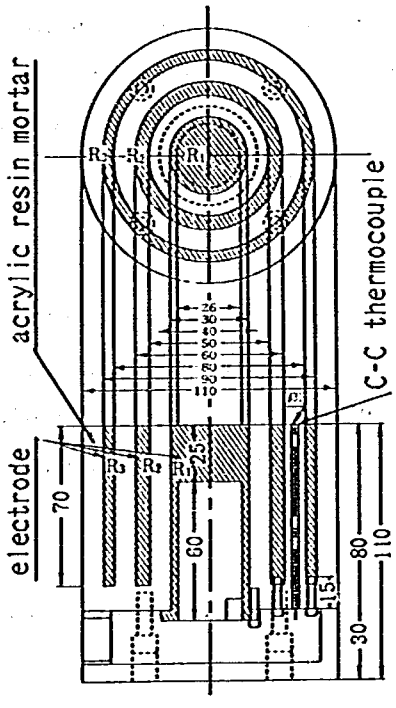
4.1/ PRINCIPLE OF DPF

Measurement of pavement temperatures and detection of moisture are necessary to evaluate pavement conditions. However, even if existing detection methods do detect moisture, it is rather difficult to distinguish among water, ice, or snow.

The Dielectric Pavement Freezing-Detector (DPF) has been developed to solve these problems by the dielectric characteristics of snow and ice based on

condenser theory. The DPF measures the electric capacitance (dielectric constant) of a pavement and pavement temperatures by a thermosensor built into the detector, to distinguish the pavement conditions (dry, wet, water film, snow, compacted snow, ice etc.). The DPF utilizes the large differences in the dielectric constants of air, ice and water, roughly 1, 3 and 80 respectively.

As shown in Figure 1 and Photo 1, the DPF uses bronze electrodes and triple rings to increase the electric capacitance, and provides a more accurate measure of the state of the snow and ice. The first detector used polyacetal resin as the insulator and there were some differences in the snow and ice condition on the surface of the detector and the pavement when it was installed.



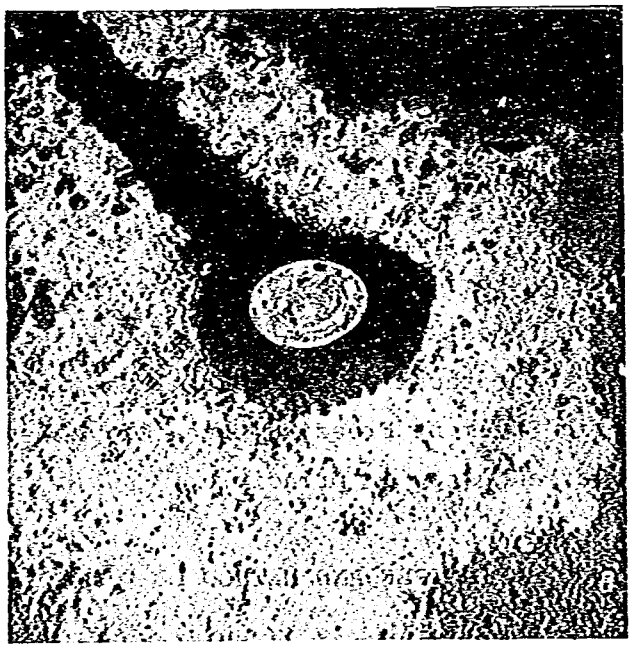


Fig. 1 Plan and cross-section of DPF Photo 1 Close-up view of DPF

The improved detector uses resin mortar (a mixture of acryl and sand) as an insulator between the cylindrical electrodes so that the surface has the same textures as the asphalt pavement. Figure 2 shows a diagram of the principle behind the DPF using a pair of parallel electrodes. Ring-type parallel electrodes are buried to expose the ends on the pavement

and the electric capacity between the electrodes is measured. The electriccapacitance of snow/ice on a pavement is detected by the electric flux penetrating in it. The electric capacitance on the pavement varies with the pavement condition (air, water, ice and snow etc.), and this makes the DPF work.

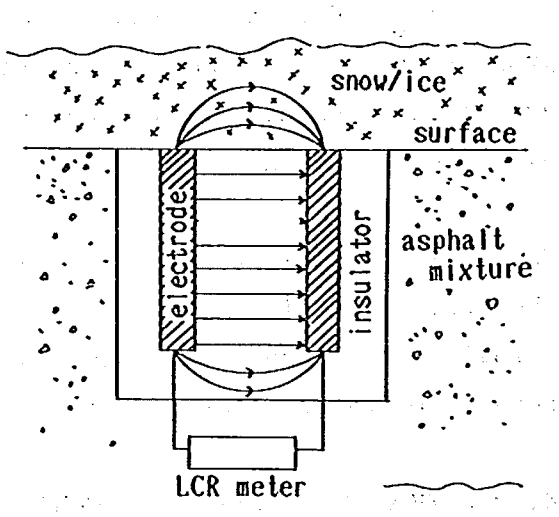


Fig. 2 Diagram illustrating the principle of measurement by DPF

4.2/ MEASUREMENT AND ANALYSIS WITH DPF

The dielectric constant of snow/ice or anything on a pavement (κ) is defined as the ratio of the measured electric capacitance (C_x) to the electric capacitance of the bare pavement in air (C_a). We hereafter call κ the DPF dielectric constant.

$$\kappa = C_x / C_a \qquad (1)$$

The electric behaviors of the pavement and electrodes are represented by an equivalent parallel circuit of electric capacitance and conductance. If the conductance is measured simultaneously, the accuracy of DPF will improve. The measured electric capacitance (C_m) is expressed by the following Equation (2), where C_x is the electric capacitance of snow/ice detected by the flux through it. C_o is the electric capacitance of the parallel electrodes, and C_s is the stray electric capacitance due to elements such as height differences of the ends of the electrodes and wiring.

$$C_m = C_x + C_0 + C_s \qquad (2)$$

The capacitance measured on a bare pavement (C_1) is given by Equation (3):

$$C_1 = C_a + C_0 + C_s \qquad (3)$$

Here C_a is the electric capacitance of air on the pavement. Consequently, the DPF dielectric constant of the pavement is determined by Equation (4) obtained from Equations (1) and (2):

$$\kappa = C_x / C_a = C_m - (C_0 + C_s) / C_a \qquad (4)$$

C_a and $(C_0 + C_s)$ are constants determined by the parallel electrodes, the properties of the insulator and the wiring which should be determined before actual measurements. An LCR meter is commercially available to measure the electric capacitance.

There are no limitations on the size and shape of the parallel electrode for the DPF. We obtained good results with both concentric circle and flat plate parallel electrodes. More distinct signals can be obtained by connecting several pairs of electrodes in parallel.

4.3/ METHOD FOR DETERMINING CONSTANTS

Two of the constants in Equation (4), C_a and $(C_0 + C_s)$ are determined before starting the measurements with DPF. Theoretically accurate values of the constants are difficult to determine but relatively accurate values are obtained from the measurement.

Two sets of measurements are necessary to determine the constants. First measurements on a bare pavement gives the electric capacitance (C_1) in Equation (3). Next, the electric capacitance (C_2) is measured with a material with a known dielectric constant (K_c) placed on the pavement. C_2 is given by Equation (5), by substituting C_a in Equation (3) for the known electric capacitance of the material $(K_c C_a)$.

$$C_2 = K_c C_a + C_0 + C_s \qquad (5)$$

The two constants of Equation (4) are given by Equations (6) and (7) from Equations (3) and (5).

$$C_a = C_1 - (C_0 + C_s) = (C_2 - C_1)/(K_c - 1) \qquad (6)$$

$$C_0 + C_s = (K_c C_1 - C_2)/(K_c - 1) \qquad (7)$$

Polymeric solutions such as methyl alcohol, ethyl alcohol, and glycerin wet completely the electrodes, are simple to handle, and so are convenient to determine the constants. In-situ experiments of the DPF using methyl alcohol (K_c = 32.6 at + 20°C) gave C_a = 2.7 (pF) from Equation (6), and $C_o + C_s$ = 147.3 (pF). C_1 and C_2 values vary with stray capacitances depending on the type and installation of DPF, but can be easily measured with the surfaces of the detector bare and wetted with methyl alcohol. Thus the characteristic

values for each detector, $C_0 + C_s$, are determined by Equation (7). Consequently the DPF dielectric constant, κ, is determined when C_m for different snow and ice conditions on the pavement are measured.

4.4/ FREQUENCY OF MEASUREMENT

Suitable DPF frequencies lie between 1kHz and 10MHz. It is rather difficult to distinguish ice from water below 1kHz, because the dielectric constant of ice approaches that of water. In the high frequency range, the microwave area, measurements become susceptible to external disturbances other than the pavement state. A lower frequency in the above range may be selected to determine snow and ice conditions of pavements in more detail. Lower frequencies give higher dielectric constants for ice, and it is easy to distinguish snow/ice from water. The frequencies 1 and 10kHz were used for our measurements, and 1kHz for the in-situ experiment.

4.5/ RELATION BETWEEN THICKNESS OF ICE, TEMPERATURE, AND DPF DIELECTRIC CONSTANT IN LABORATORY EXPERIMENTS

Figure 3 shows the experimental result at -10°C in a thermostatic chamber for the relation between the DPF dielectric constant and the thickness of ice film and ice. The relationship is nearly linear above 0.5mm.

Figure 4 shows changes in the DPF dielectric constant for the ice film (1mm thick), the ice (3mm thick), and the dry condition. The DPF dielectric constant for water films show large values, 1000 - 2000, which fall rapidly near 0°C where water and ice coexist. The DPF dielectric constant for ice film and ice decreases with the temperature, but it does not fall much below -5°C. The DPF dielectric constant for the dry condition is

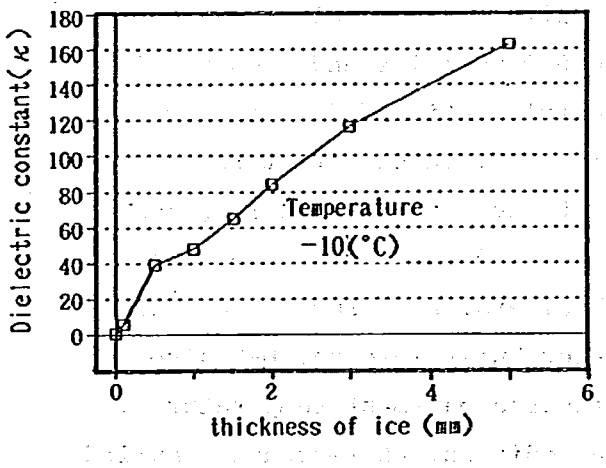


Fig. 3 Relationship between thickness of ice and dielectric constant

nearly constant independent of temperature. The relation between the DPF dielectric constants, and the surface conditions and temperatures proved very useful for the pavement freezing-detection.[6)]

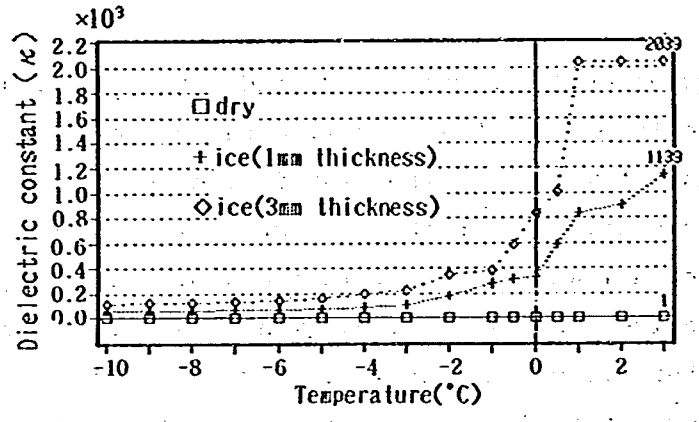


Fig. 4 Variations of dielectric constant on dry, water and ice conditions depending on temperature

5/ PAVEMENT CONDITIONS IN IN-SITU EXPERIMENTS BY DPF

5.1/ OUTLINE OF THE IN-SITU EXPERIMENTS

The in-situ experiment used the DPF buried in a trunk road in Sapporo. The observation site has a daily traffic volume of about 10,000 vehicles and a commercial vehicle ratio of 5%. As shown in Figure 5, three detectors were installed at the center of the road, and three others on the shoulders. A thermocouple thermometer built into the DPF also measured pavement temperatures. In addition, thermocouples buried under the pavement measured the temperature distribution in the depth direction.

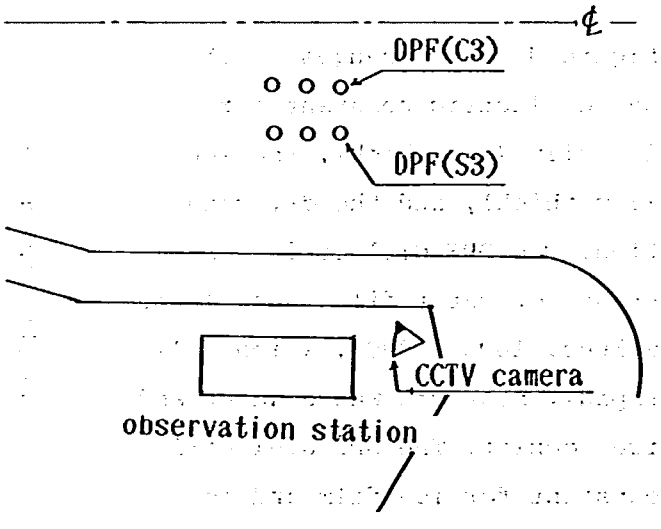


Fig. 5 Plan of field test site and locations of DPF

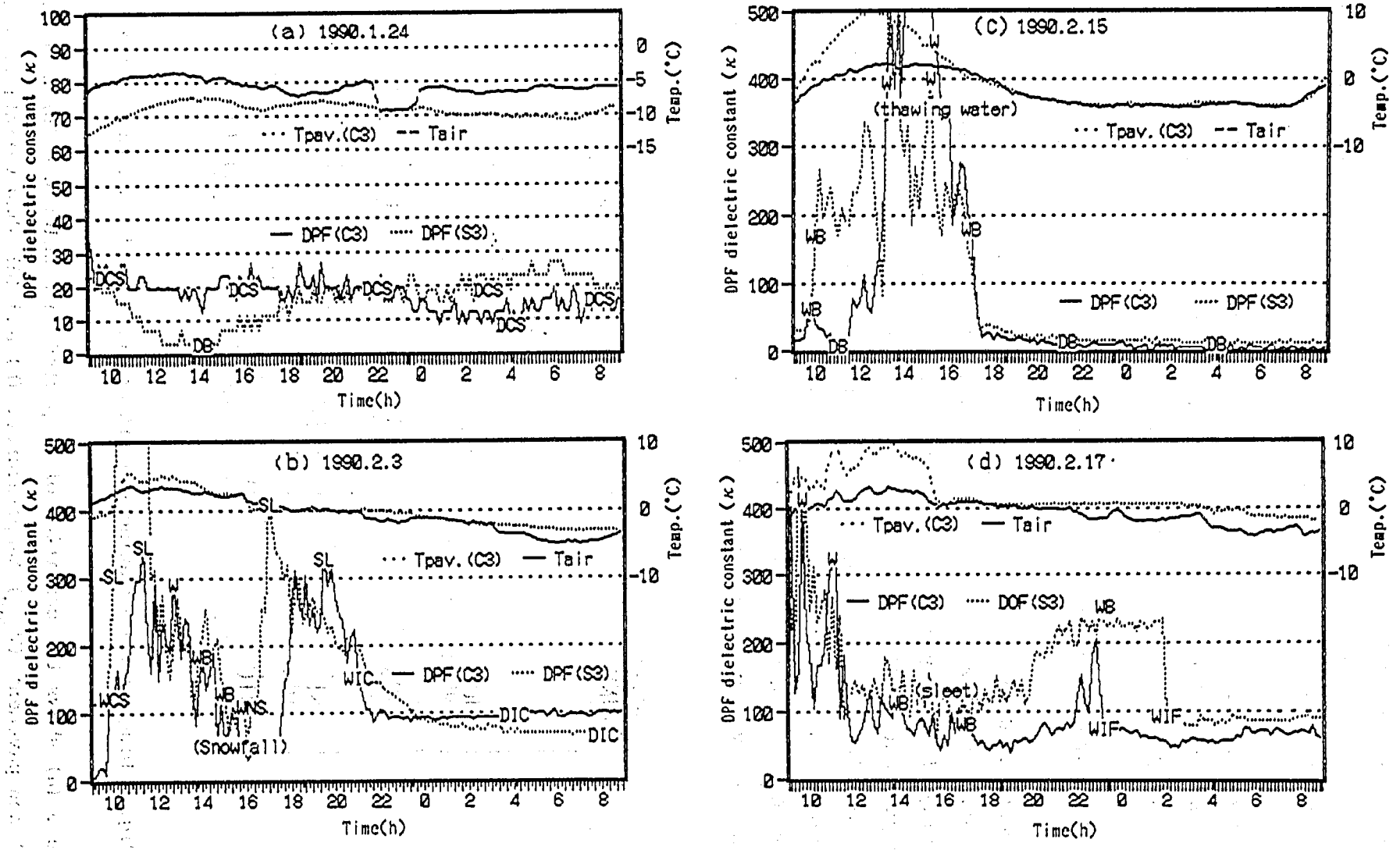


Fig. 6 (a) - (d) Relationship between DPF dielectric constants and snow/ice conditions on the pavement

Six LCR meters were installed at the observation station to measure variations in the electric capacitance of the DPF. The measuring frequency was 1kHz and the data were stored on a floppy disk at ten-minute intervals.

A video camera was installed to observe the relation between pavement conditions and DPF dielectric constants, and pavement conditions were continuously observed from January 1 to March 31, 1990.

5.2/ PAVEMENT CONDITIONS AND DIELECTRIC CONSTANTS OF PAVEMENTS

We investigated the changes in DPF dielectric constants and pavement conditions affected by weather and external disturbances (consolidation and splashing of snow by vehicles), to determine whether the DPF could distinguish pavement conditions by the dielectric constant and follow the changes in the conditions. Figure 6, (a) - (d) show the relations between the conditions and the dielectric constants of the pavement with the DPFs at the center (C_3) and on the shoulders (S_3). Figure 7 shows transitions of snow/ice on the pavement and their abbreviations used in this paper.[7)]

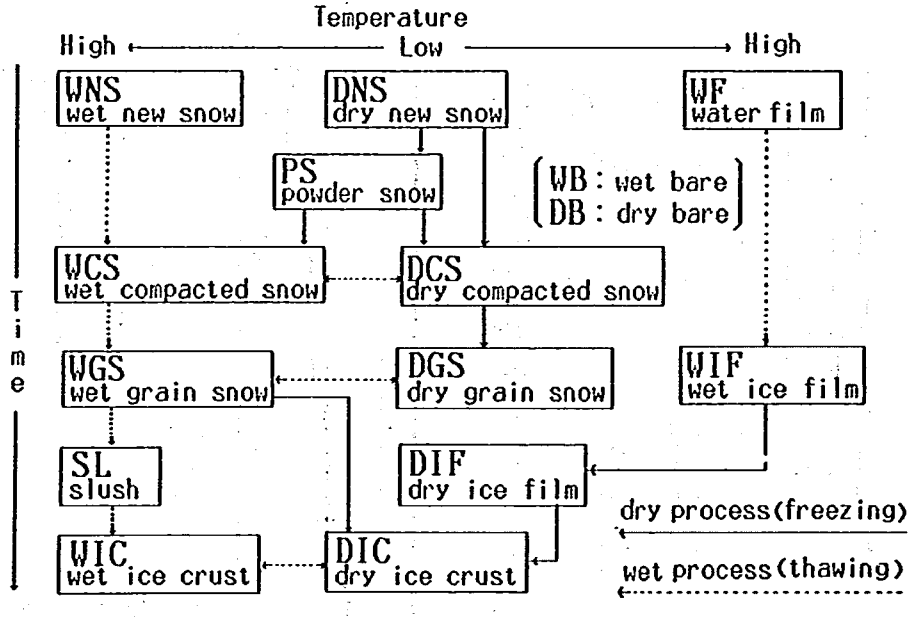


Fig. 7 Diagram illustrating transitions of snow/ice on the pavement

Figure 6 (a) shows the condition of compacted snow below 0°C for both air (T_{air}) and pavement (T_{pav}) temperatures. (b) and (d) show variations from

wet pavement to freezing, where the pavement temperature rose to 5°C during the day and fell below 0°C at night, and in (c) the pavement remained dry and bare below 0°C at night and the pavement temperature rose above 10°C during the day without snowfall.

5.3/ EVALUATION OF THE PAVEMENT CONDITIONS

As shown in Figure 6, K above 150 indicates wet or half-melted snow, not a frozen pavement. With K below 100 and a pavement temperature below 0°C, the pavement is covered with ice, ice film, and compacted snow, presenting a very slippery surface. With K between 100 - 150 and a pavement temperature between 0.5 - -0.5°C, water and ice often coexist in process of freezing on thawing. This may also be estimated from the change in pavement temperatures and pavement conditions as shown in (a) - (d) of Figure 8. In (b) and (d), the pavement temperatures in the process of changing from wet to frozen are maintained in equilibrium for some time near 0°C, and the temperature gradient is nearly zero. The pavement temperature of (c) where the change is from wet to dry are not maintained in equilibrium near 0°C. The K value of a dry pavement is often below 10, but fluctuated somewhat due to mud or water splashes. It is occasionally difficult to distinguish dry pavement from thin

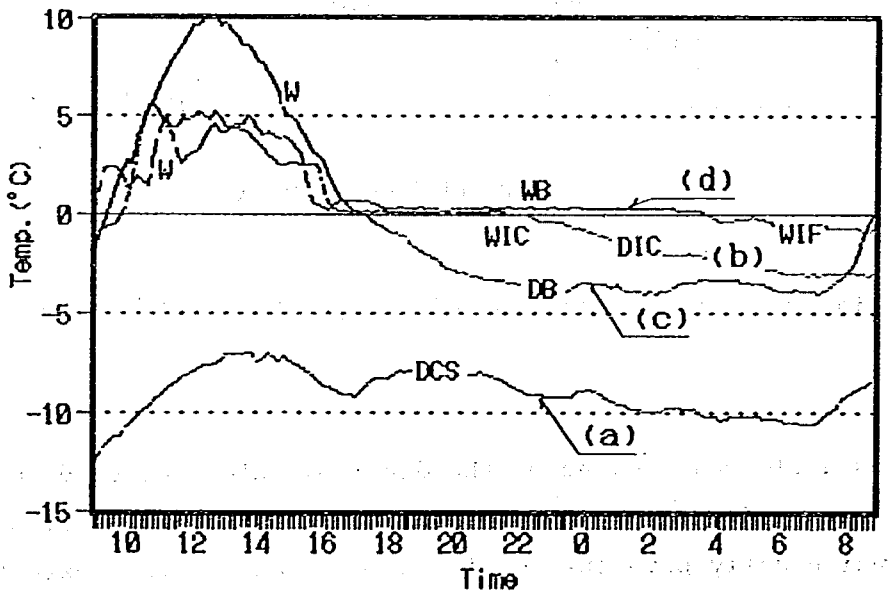


Fig. 8 Relationship between pavement temperature and snow/ice conditions on the pavement

and compacted snow or ice film with small κ. However, the algorithm integrating weather information, sequential changes of κ in snow and ice on a pavement and the pavement temperatures could improve the accuracy of the DPF.

Figure 9 shows a diagram of the relation between the pavement conditions, DPF dielectric constants of pavements, and pavement temperatures. The freezing pavement is classified as Ⓘ the change to freezing (or the inverse process) is Ⓘ, and else the pavement is wet or dry.

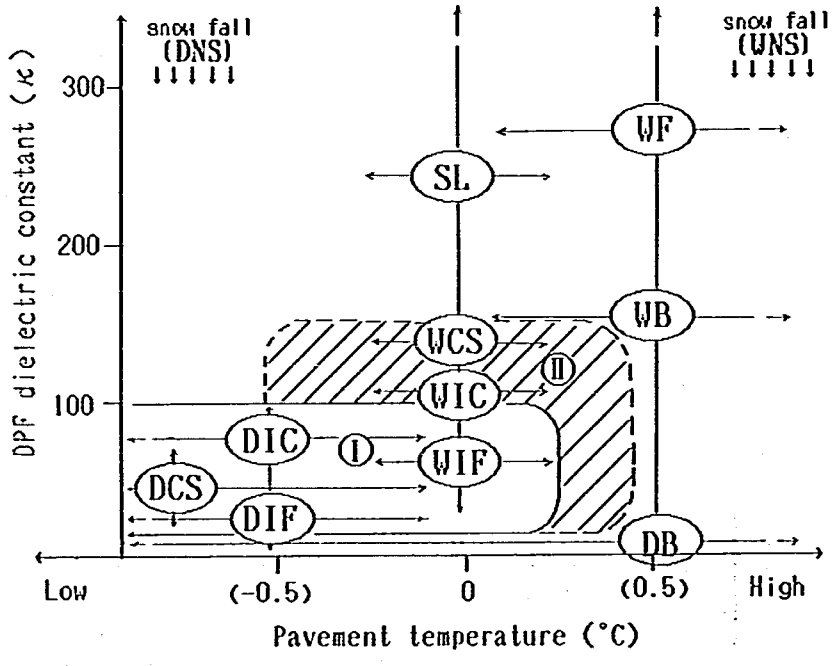
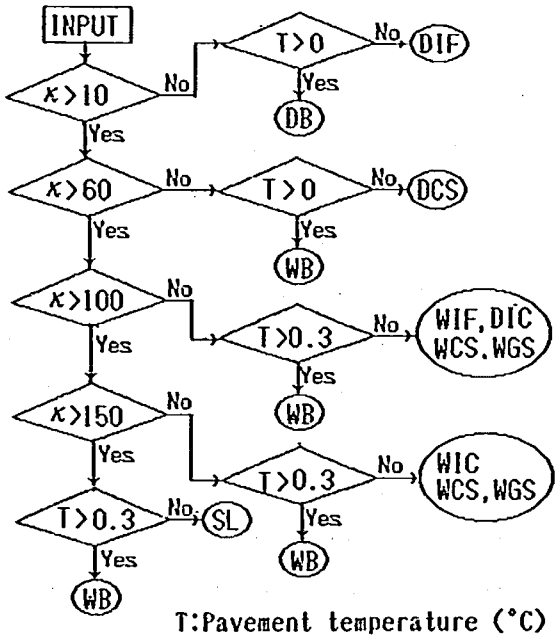


Fig. 9 Evaluation diagram of the pavement conditions by DPF

Figure 10 is a flowchart based on the diagram, which was used to verify the reliability of prediction by DPF. We sampled measurement results (402 data) in 4 days which daily pavement conditions changed to great extent, and compared them with observation results by TV camera. As results of comparisons, the coincident rate of both results was 84 percent. Most of inconsistent results lie in differences between classifications of snow/ice depending on "eyes" of DPF detection and TV camera.

5.4/ PREDICTION AND MINIMIZING OF SALT APPLICATION BY DPF

DPF can be also utilized to predict and minimize salt use, though in Japan, salt application is limited and much less is used than in other countries. We investigated the changes in DPF dielectric constants on the pavement by applying deicing chemicals to the observation site.



T:Pavement temperature (°C)
κ:DPF dielectric constants

Fig. 10 Flowchart for evaluating the pavement conditions by DPF

Figure 11 shows the relation between the pavement conditions and the DPF dielectric constants, when spreading deicing chemicals ($20g/m^2$) on 2cm thick compacted snow placed around the surface of the DPF. After the application, the DPF dielectric constant increased to more than 1000, and high values continued till the snow and water including the deicing chemical were splashed away by the traffic. Accordingly, the dielectric constant indicates not only an effective duration, but also enables a prediction to minimize salt use by the relation between κ and the salt content.

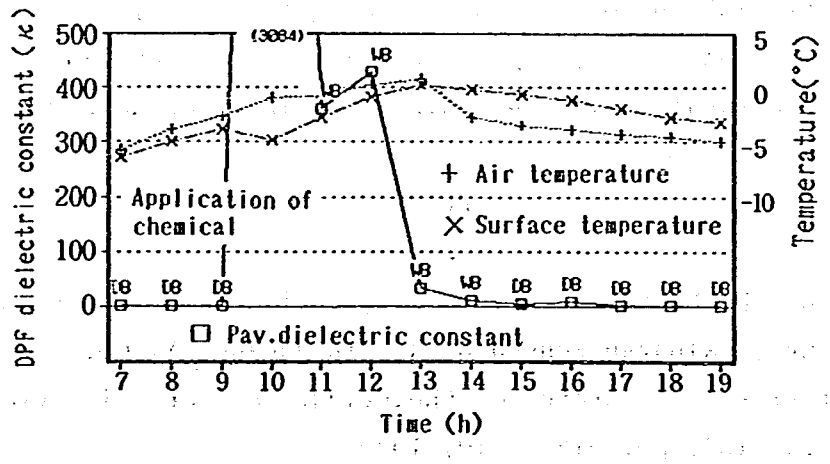


Fig. 11 Variations of DPF dielectric constants due to the application of chemicals

6/ CONCLUSIONS

(1) The DPF is a contact type detector which needs underground installation. Resin mortar with similar textures to asphalt pavements was used as an insulator between the electrodes, resulting in minimal differences in the snow and ice conditions on the surface of the DPF and on the pavement. The DPF integrated measurements of the dielectric constant and the pavement temperature, and it is not susceptible to external disturbances, and can distinguish a wide range of pavement conditions accurately.

(2) The DPF is structurally simple, easily operated and managed after installation. The cost of installing of DPF is low, making a dense network possible. It may be used to monitor local information on pavements in detail, and to control salt application and road heating.

(3) The analyses of the data show that the DPF is useful to distinguish the pavement conditions in real time. Future studies will be made to improve the accuracy of detection by establishing an algorithm for evaluation. The DPF can also be applied to pavement management systems including prediction of pavement freezing by integrating weather information.

ACKNOWLEDGEMENT

We would like to express our appreciation to Mr. Kazuo Shibuya, Civil Engineering Technical Center, Sapporo City Construction Office, Mr. Koichi Taharasako, Mr. Takeshi Osawa and Mr. Shoshichi Ishii, Sapporo Information Network, Mr. Yoichi Kimura, Japan Control Machinery and Equipment Industries Inc., and Mr. Mutsuji Kojima, Nisshin Kasei Inc. for help with the study.

REFERENCES

1) K. Takeichi, N. Maeno: Occurence Frequencies and Properties of Snow/Ice on Pavements, Kaihatsu Ronsyu No.42 (in Japanese), pp. 7 - 30, 1988.
2) J.C. Leifer: Present Status of the Bridge Ice Detection Program at FHWA, TRB, Special 185, pp. 215 - 219, 1979.
3) R.C. MacWhinney: Snow and Ice Detection Warning Systems, FHWA-RD-76-25, 1975.

4) Highways, September, pp. 37 - 39, 1988.
5) T. Wada: Countermeasures Against Freezing Pavements in Europes, Snow and Roads No.13 (in Japanese), pp. 37 - 43, 1987.
6) K. Takeichi, N. Maeno: Studies on Practical Uses of Dielectric Pavement Freezing-Detector, Kaihatsu Ronsyu No.44 (in Japanese), pp. 1 - 35, 1989.
7) N. Maeno: Names and Classifications of Snow and Ice on Pavements, Snow and Roads No.16 (in Japanese), pp. 61 - 65, 1988.

Survey of Measures Against Pavement Rutting in Cold Regions

S. Sawada, K. Kawamura, T. Mizushima
CERI, Hokkaido Development Bureau
H. Kubo, former CERI, Hokkaido Development Bureau

SURVEY OF MEASURES AGAINST PAVEMENT RUTTING IN COLD REGIONS

by

Shunsaku Sawada, Hiroshi Kubo,
Kazuyuki Kawamura, and Tatsuro Mizushima
Civil Engineering Research Institute,
Hokkaido Development Bureau

ABSTRACT

Studded tires have become widely used in Europe and North America since they were introduced in Northern Europe in 1959. They were also introduced in Japan around the same time, and by 1980 more than 90% of all cars in Hokkaido used studded tires.

The propagation of studded tires has caused an increase in pavement wear and rutting, and resulted in higher road maintenance and repair costs. Rutting of the road surface reduces traffic safety, especially at high speeds and increase in dust in and around roads has a negative effect on the environment.

The Hokkaido Development Bureau has studied asphalt mixtures for surface courses in cold districts since 1954.

This paper will describe rutting damage to cold-district pavements and its causes, as well as the problems of studded tires.

It will also discuss preventive measures against rutting; the future use of studded tires, and the selection of admixtures and mixture designs for wear-resistant asphalt pavements.

SURVEY OF MEASURES AGAINST PAVEMENT RUTTING IN COLD REGIONS

by

Shunsaku Sawada, Hiroshi Kubo,
Kazuyuki Kawamura, and Tatsuro Mizushima
Civil Engineering Research Institute,
Hokkaido Development Bureau

1/ INTRODUCTION

A growing concern in Japan today is the problems caused by wear of paved road surfaces by studded tires during the winter. The rutting produced by pavement wear places obstacles in the way of safe and enjoyable driving and generates dust that gives rise to environmental problems. The high concentrations of such traffic generated dust in the air during early winter and spring, when the paved surfaces are exposed, pose serious problems to humans.

It is necessary to establish an integrated system of countermeasures by the government and the private sector. The government acts as the manager of roads and traffic with the responsibility to improve pavements, control the use of studded tires, and impose speed limits during winter. Work to modify and improve studs in tires, and also to develop more effective studless tires will be the province of the private sector.

The Maintenance and Management Section has conducted investigations of the effects of asphalt mixtures and modified tire studs together with a series of surveys on rutting of national highways.

This paper details the status of wear of national paved roads, results with wear resistant asphalt mixtures, and the extent of studded-tire use to assist in forecasting future trends.

2/ WEAR OF NATIONAL PAVED ROADS

2.1/ OUTLINE OF SURVEY OF ROAD WEAR

The surveys were conducted on national highways at fixed points in three periods from FY 1977. The first period, 1977 to 1981, investigated the status of the wear of pavements constructed of three different materials: fine and gap-graded asphalt concrete; straight asphalt and modified asphalt (rubber added) 13F40; and dense and gap-graded asphalt concrete of modified asphalt.

During the second period, 1982 to 1985, pavements of fine and gap-graded (straight asphalt) and dense and gap-graded asphalts (modified asphalt) were surveyed. As trial pavements, fine and gap asphalt concrete (13F50 and 20F50) composed of coarse aggregate in different quantities and different maximum grain sizes, and asphalt mixtures using modified materials were also studied.

During the third period, 1986 to 1989, surveys were conducted on fine and gap graded asphalt concretes (straight asphalt) 13F40 and 13F50.

In 13F40 and 20F50, the left numerals 13 and 20 indicate the maximum size of coarse aggregate (13mm or 20mm), F stands for filler, and 40 and 50 indicate the quantities of coarse aggregate (40% or 50%).

2.2/ TRAFFIC VOLUMES AND RUTTING

2.2.1/ SURVEY METHOD

The measurement of rutting is shown in Figure 1. A tripod-mounted steel rod is erected vertically over buried pins. Then the height from the base line is measured transversely with a steel ruler to determine the differences from the previous reading. The measurements were made twice a year, in spring and autumn, and the spring to spring difference represents the annual variation, the rutting depth, and the difference from autumn to spring is the wear depth.

Unless otherwise specified, the rutting depth represents the maximum rutting

deformation depth, and the wear depth the average wear depth of a one lane wide road section.

2.2.2/ RUTTING VOLUME AND WEAR VOLUME

Figure 2 shows the relationship between annual average rutting depth and daily traffic flows for all the data, and Figure 3 shows the relationship between the wear depth and daily traffic flows. Figure 4 shows the ratio of the wear depth to the average annual rutting depth (wear depth / rutting depth), plotted against the daily traffic flow. This shows that the wear depth accounts for more than 60% of the annual average rutting depth, showing the strong effect of the studded tires. It also suggests that the somewhat low correlation coefficient, r=0.52, increases with the traffic volume.

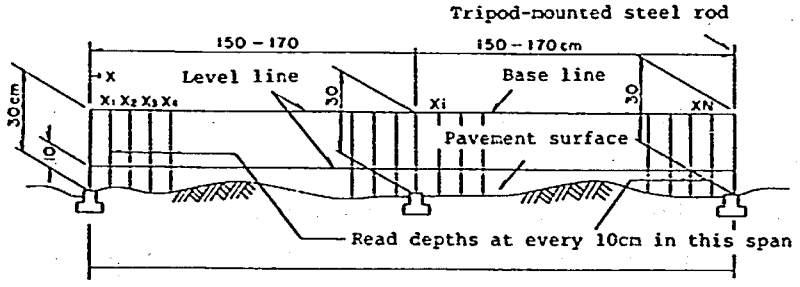


Figure 1 Measuring of the surface configuration

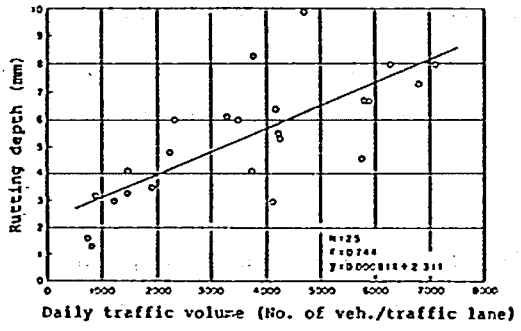


Figure 2 Annual rutting depth and daily traffic volume (1977 - 1981)

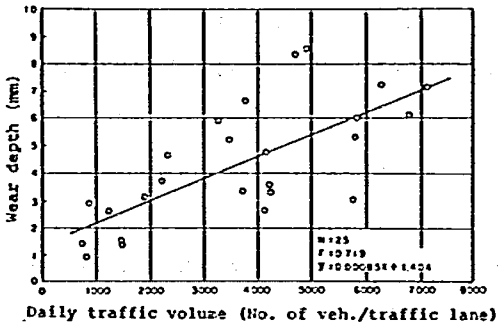


Figure 3 One winter wear depth and daily traffic volume (1977 - 1981)

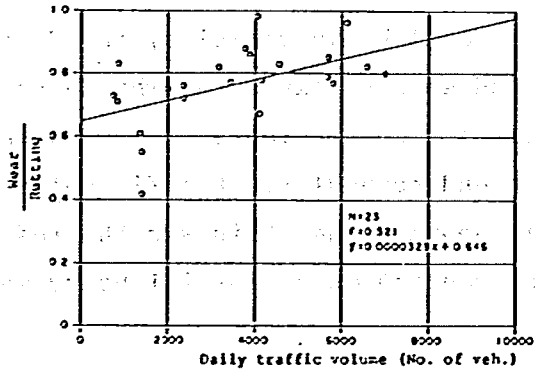


Figure 4 Wear:rutting ratio and daily traffic volume (1977-1981)

2.2.3/ CAUSES FOR THE WEAR

The causes of wear of pavements are considered to consist of elements like the number of studded tires passing over the pavement, the wheel load, the configuration of tire studs, the type of studded tires, the number of days which the paved surface is exposed, dryness, moisture, and temperature of pavements, and the wear resistance of the surface layer mixture. Figures 5 to 10 graphically displays the survey results. The graphs express accumulated wear and rutting volumes.

Figure 5 shows the relationship between wear depth and cumulative traffic volume from 1977 to 1981, and Figure 6 rutting depth versus accumulated traffic volume. The number of data sets were 83 and 75 with correlation coefficients of r=0.73 and r=0.70.

Figure 7 shows the relationship between wear depth and cumulative traffic volume, and Figure 8 rutting depth versus accumulated traffic volume, from 1982 to 1985. The number of data sets were 170 and 156 with correlation coefficients of r=0.87 and r=0.82. These graphs were drawn from the fomula: Accumulated traffic volume = daily traffic volume x days of winter road surface exposure x studded tire ratio. This is determined by relating the studded tire ratio, which is considered the most influential factor, with days of exposure. The correlation coefficients are higher than those in Figures 5 and 6.

Figures 9 and 10 show the relationship between the wear depth and the accumulated traffic volume, the rutting depth and accumulated traffic volume in the period 1985 to 1988. These graphs are the result of estimates where the accumulated traffic volume was considered 1.1 times greater, to account for the influence of commercial heavy vehicles, in addition to the studded tire ratio and days of road surface exposure. The number of data sets were 44 and 41 with the correlation coefficients of r=0.74 and r=0.87, making the correlation of wear depth and accumulated traffic volume lower than the r=0.87 in Figure 7. It is assumed that this was the result of the influence of the use of skid chains mounted on commercial heavy vehicles during the winter.

The 10% increase in the traffic volume is based on previous survey records

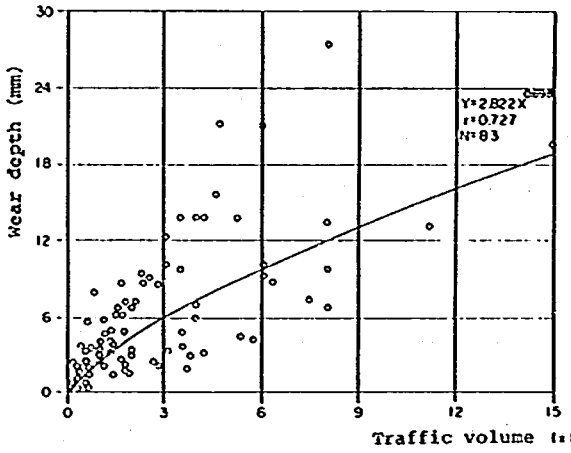


Figure 5 Wear depth and cumulative traffic volume (1977 - 1981)

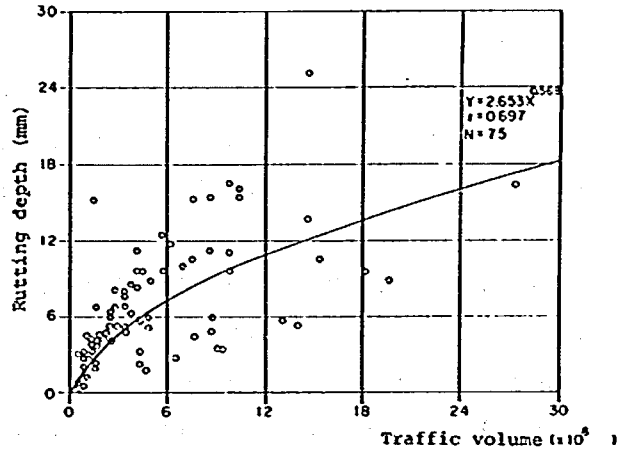


Figure 6 Rutting depth and cumulative traffic volume (1977 - 1981)

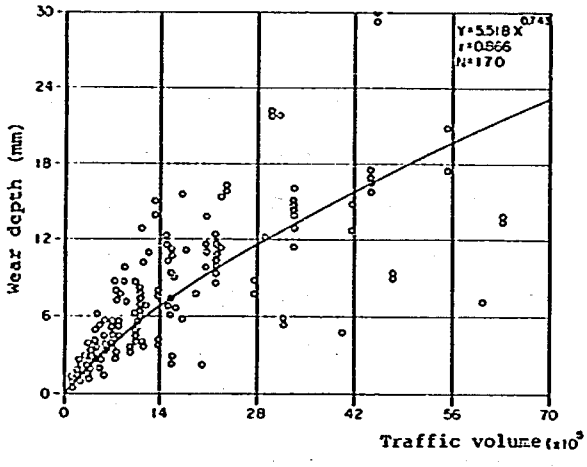


Figure 7 Wear depth and cumulative traffic volume (1982 - 1985)

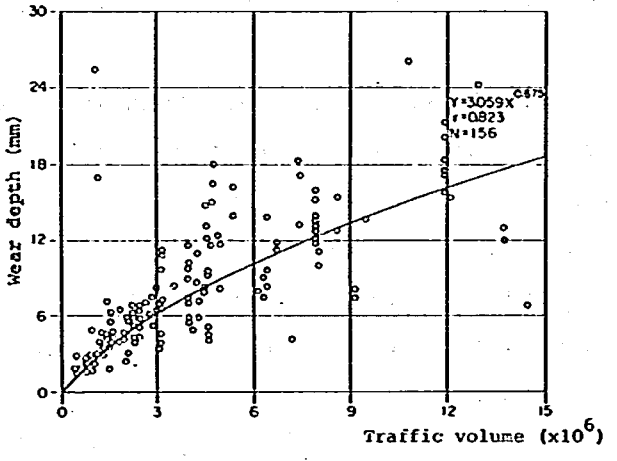


Figure 8 Wear depth and cumulative traffic volume (1982 - 1985)

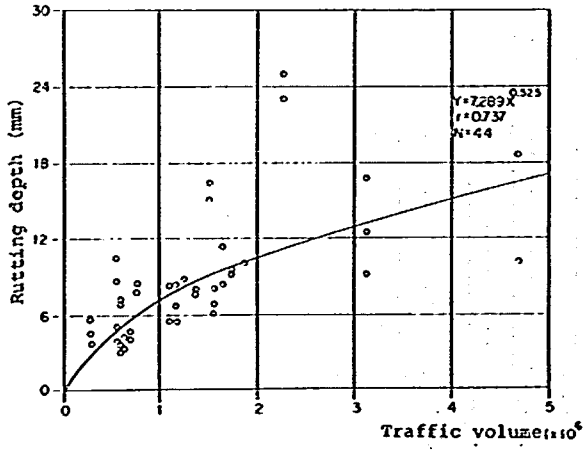


Figure 9 Wear depth and cumulative traffic volume (1985 - 1988)

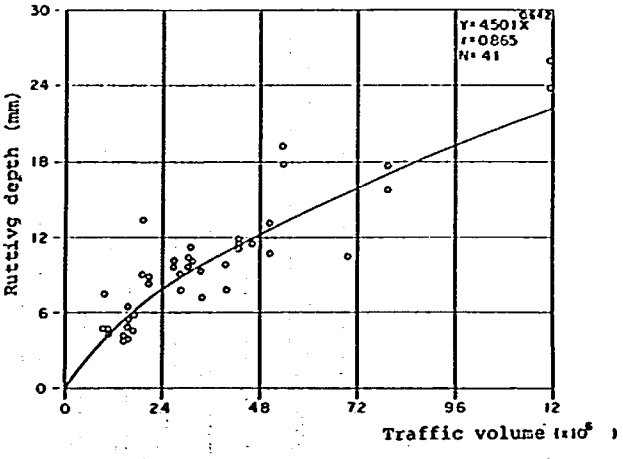


Figure 10 Rutting depth and cumulative traffic volume

which indicate that the average number of studded tires per commercial heavy vehicle is 5.6. The number of large vehicles in Hokkaido accounts for 24% of the total number of automobiles, making the wear volume per large vehicle 1.4 times that of a passenger car. Assuming all vehicles to be small translates to the equivalent of a 10% increase in the wear.[2)]

2.2.4/ WEAR VOLUME BY PAVEMENT TYPE

Figure 11 shows the differences in the rutting depth produced with different quantities of crushed stone and maximum grain sizes in the aggregate. It shows that rutting with 13F50 is less than that with 13F40 in Naie town. The 20F40 and 20F50 with the larger maximum size of aggregate produced less rutting than 13F40 and 13F50. This confirms that increasing the quantity of aggregate by 40 to 50% and using the larger maximum grain size of 20mm strengthens the resistance to rutting.[3)]

Figure 12 shows the relationship between average wear and cumulative traffic volume of a single traffic lane by type of pavement, during the period 1977 to 1985. There are very limited data on pavements with fine and gap-graded asphalt concretes and with dense and gap graded asphalt concrete (rubber added), and there are gaps in the data. However, the figure shows that the dense, and gap-graded asphalt concrete produces less rutting. This is considered due to the differences in the quantities of crushed stone.

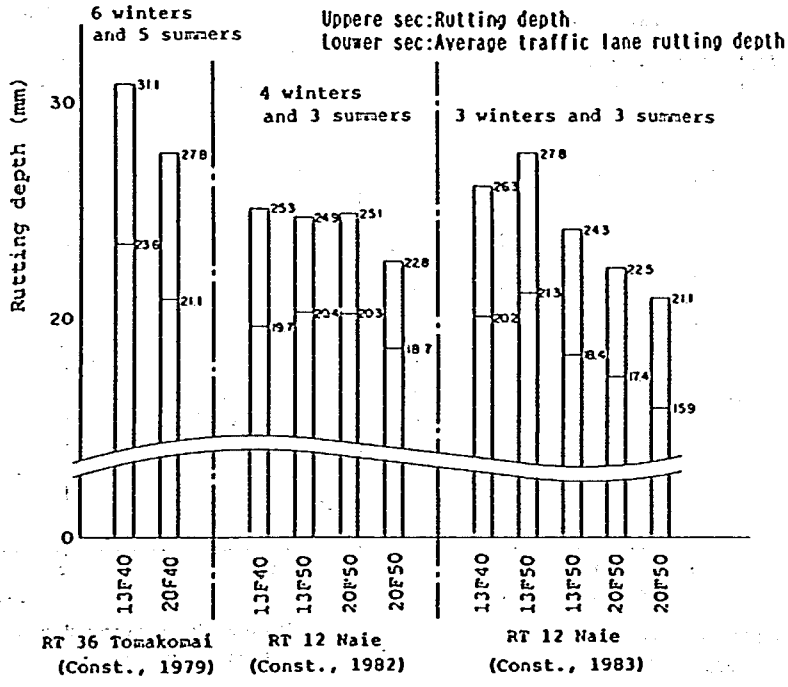


Figure 11 Rutting depth by different types of trial pavement

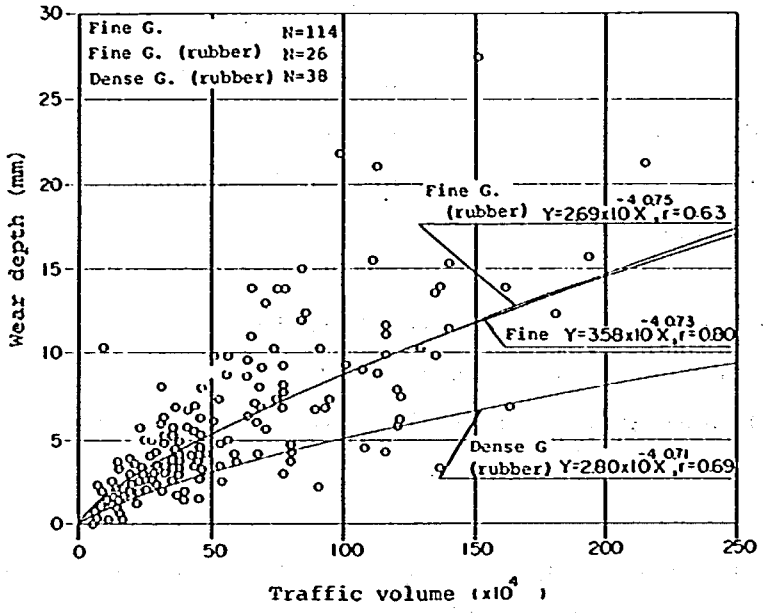


Figure 12 Rutting depth by types of pavement and cumulative traffic volume

2.3/ WEAR OF CONCRETE PAVEMENTS

Concrete pavements are generally considered to be superior to asphalt pavements in wear and plastic flow resistance. However, such pavements are expensive to construct and also to maintain and repair. Further, they take longer to construct and riding comfort is inferior to asphalt pavements. This has prevented a wider use of this kind of pavement. The following presents the results of in-situ wear surveys conducted on several types of concrete pavements.

2.3.1/ ON-SITE SURVEY ON WEAR

The surveys were conducted at two locations; a section of the Shin-Hiraiso Tunnel constructed in 1982, and the Mori By-pass of National Highway 5, repaired by an overlaying method in 1984. The survey period of the tunnel section was from November 1982 to May 1987 and for the By-pass from November 1985 to May 1988. The types of pavement were:

(a) Shin Hiraiso Tunnel:

Type of Pavement	Bending strength	Compressive strength
Normal Portland cement concrete	$b=53kgf/cm^2$	c=----
High strength concrete	$b=65kgf/cm^2$	$c=592kgf/cm^2$
Steel fiber mixed concrete	$b=67kgf/cm^2$	$c=653kgf/cm^2$
Steel fiber mixed concrete	$b=66kgf/cm^2$	$c=588kgf/cm^2$

(b) Mori By-pass

Type of Pavement	Bending Strength	Compressive Strength
Normal Portland cement concrete	b=60kgf/cm^2	c=604kgf/cm^2
Acryl resin mortar	b=190kgf/cm^2	c=801kgf/cm^2
Asphalt concrete (13F50)		

Figure 13 shows the wear depth of the Shin-Hiraiso Tunnel. The wear depth of high strength concrete, steel fiber mixed concrete (30mm), and steel fiber concrete (20mm) were about 2/3 of the normal Portland cement concrete as of June 1984.

Figure 14 is for the Mori By-pass. As of May 1988, the wear depth of normal Portland cement concrete was half and acryl resin mortar was one third of that with asphalt mixture (13F50), underlining the high wear resistance of concrete pavements.

The relationship between wear depth and cumulative traffic volume in Shin-Hiraiso Tunnel and Mori By-Pass (vehicles with studded tires, no compensation for large vehicles) by type of pavement are shown in Figure 15 and Table 1. It is generally accepted that there is a correlation between the wear depth of concrete and the compression strength. Figure 15 shows the same trend with normal strength concrete having similar compression strength, with high strength concrete, steel asphalt fiber concrete (30mm), and steel fiber concrete (20mm). The correlation coefficients for these 4 types was a high 0.98 as shown in Table 1.[4)]

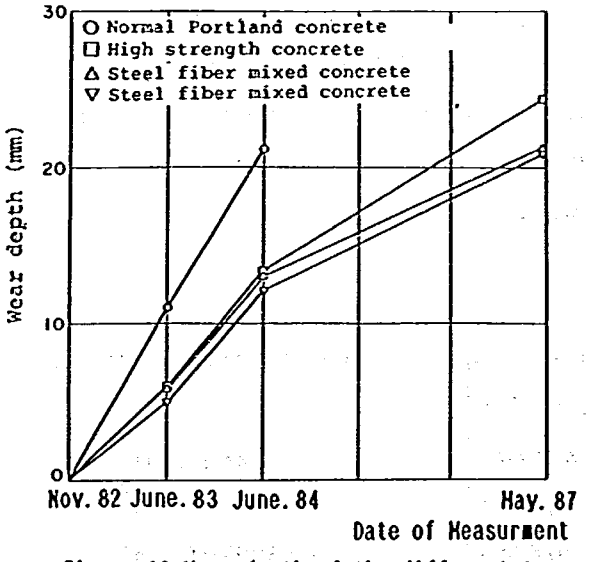


Figure 13 Wear depth of the different types of pavement

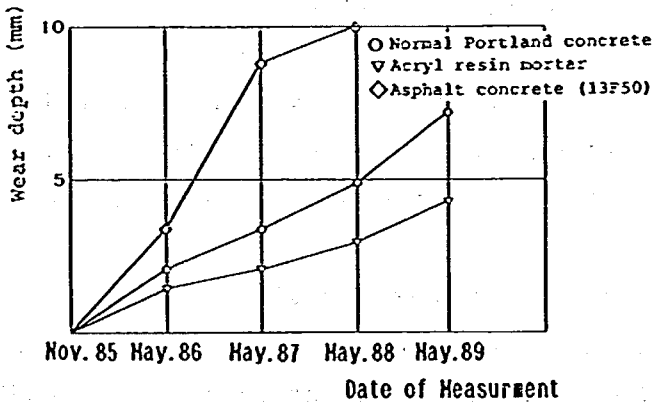


Figure 14 Wear depth of the different types of pavement

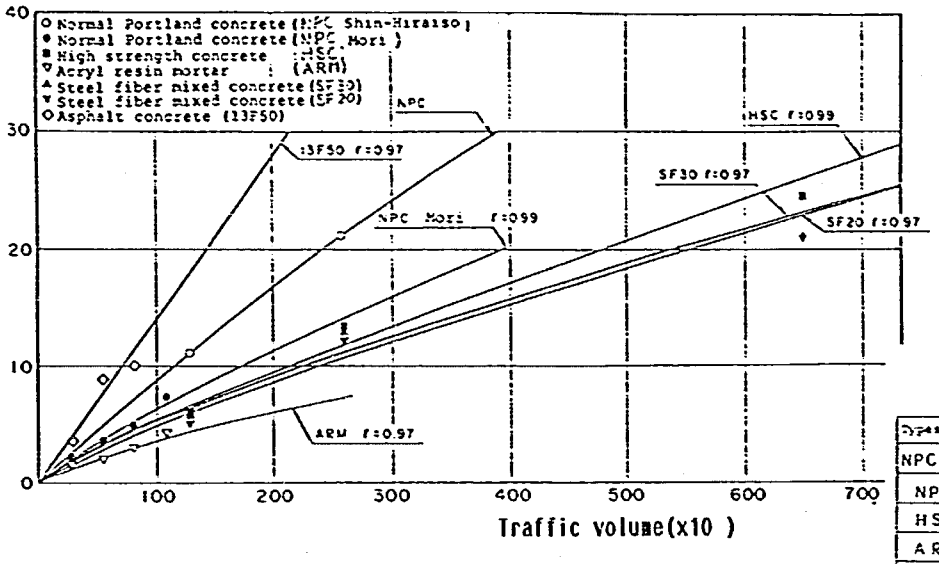


Figure 15 Wear depth by types of pavement and cumulative traffic volume

Table 1 Correlation curve by types of pavement ($Y = A \cdot X^{B}$)

Types of Pavement	A ($\times 10^{-3}$)	B	correlation
NPC Shin-Hiraiso	1.99	0.94	——
NPC(Mori)	3.98	0.87	0.99
HSC	3.22	0.87	0.99
ARM	15.46	0.73	0.97
SF30	9.55	0.79	0.97
SF20	2.04	0.89	0.97
13F50	0.99	1.03	0.97
NPC(Mori) HSC SF20 SF30	13.29	0.77	0.98

3/ DETAILS OF STUDDED TIRES AND THEIR USE

3.1/ USE OF STUDDED TIRES

Studded tires began to be used on automobiles back in 1959, when they were used as an anti-slip measure on frozen road surfaces in the Scandinavian Peninsula. [5] Before the appearance of studded tires tire chains were predominatly used. Studded tires were superior to chains in durability and riding comfort and their use quickly increased in Europe and North America. The introduction of studded tires in Japan was around 1963, in compliance with the Hokkaido Public Safty Commission (Article 12. Road Traffic Law Enactment Regulation) of 1972 that automobiles must be equipped with non-skid devices when driving on snow and ice surfaces. Since then, studded tires have rapidly spread in Hokkaido due to their simplicity and convenience. At the peak, around 1985, nearly 100% of cars and 75% of large vehicles used studded tires, an average 93% of all road vehicees.

Surveys made by the Hokkaido Prefectural Government on studded tire use of all vehicles by month and region in Hokkaido is shown in Figure 16. [6] The figure shows that the rates increase in the order, East, South and Central, and North Hokkaido.

Figure 17[7] shows the changes in the rates of studded and studless tire use in Sapporo. It shows that the rates of use of studded tires have been decreasing since 1985, with a complementary increase in the use of studless tires. The rate of studded tire use is about 80% of the peak period, still a very high rate.

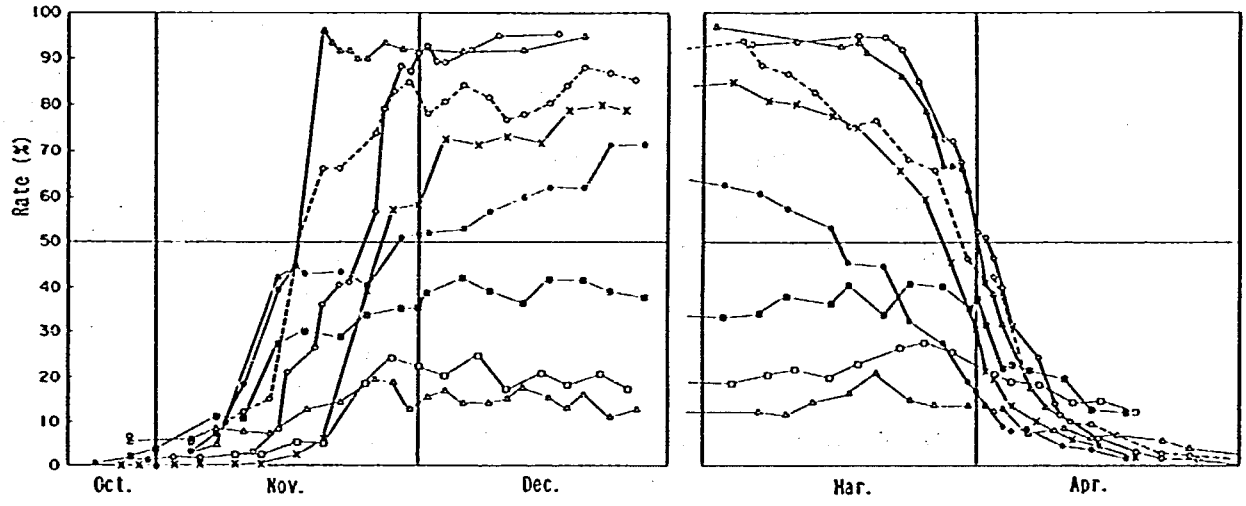
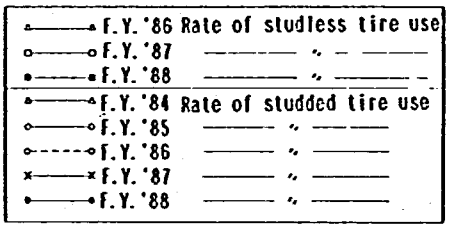


Figure 17 Rate of studded and studless tire use



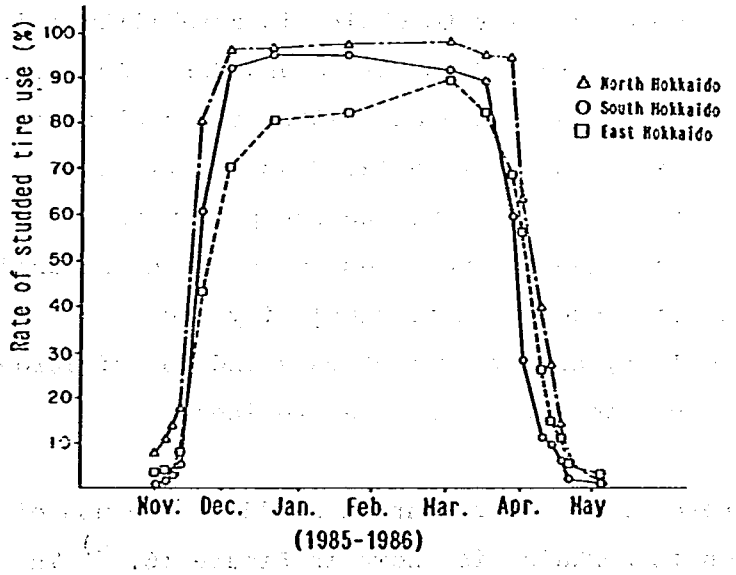


Figure 16 The rates of studded tire use by month

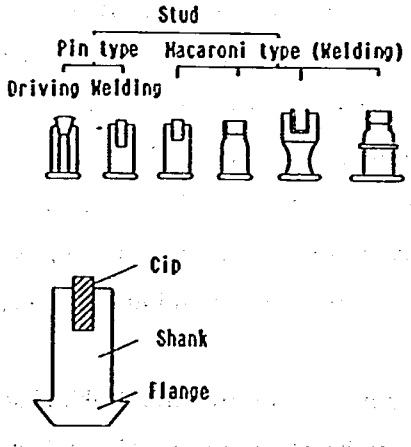


Figure 18 Configuratin of Studs

3.2/ TYPES OF STUDS AND WEAR

Two types of studs are used; one is a pin type generally used on cars, and the other is a macaroni type used on trucks, buses, and other commercial heavy vehicles, the studs are installed by welding or driving. Figure 18 illustrates the configurations of studs.

3.2.1/ WEAR TESTS

Using abrasion testing equipment as shown in 4.2, wear tests were carried out to investigate the effects of the number of studs, amount of protrusion and shape of studs on the wear. The following items were standards for the tests: drive and welded type studs with a flange diameter of 10mm, protrusion 1.5mm, and the hardness 88.5HRA. The tests were conducted by changing types and quantities of these items and the results were compared. The asphalt mixture for the tests was fine and gap-graded asphalt (13F40).

(1) Number of Studs

Figure 19 shows the relationship between the number of studs and the wear volume. A comparison was made with a protrusion of 1.5mm and 78, 65, or 52 studs. It is seen that when the numbers of studs are reduced by 20% and 30%, the wear volume is reduced by 12% and 25%.

(2) Pin and Macaroni types

Figure 20 shows the comparison of the wear volume with pin and macaroni type studs. With identical protrusion the wear volume of the macaroni type is 17% larger than with the pin type.

(3) Protrusion of pins

Figure 21 shows the relationship between the protrusion and the wear volume with pin type studs (welded and drive types). When the protrustion was reduced from 1.5mm to 1.2mm or 1.0mm, with the flange diameter 10mm, the wear volume of welded studs reduced by 23% and 22% and the wear with drive studs reduced by 10% and 29%. Drive studs with a flange diameter of 10mm and protrusions of 1.5, 1.2, or 1.0mm showed 20%, 7%, and 23% reductions in wear volume compared with welded studs.

(4) Diameter of Flange

Figure 21 also shows that changing the 10mm flange diameters to 8mm reduced the wear depth by 23% to 37%.

The results clearly show that reducing the maximum protrusion from 1.5mm to 1.2mm and the flange diameter from 10mm to 8mm in commonly used tires will result in a nearly 50% reduction in wear volume. The results of other tests conducted with different hardness and stud configurations are shown in Figure 22.

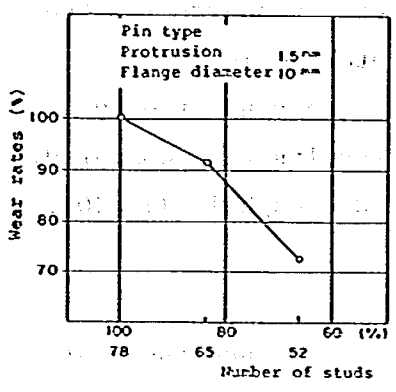


Figure 19 Wear of pavement vs stud number

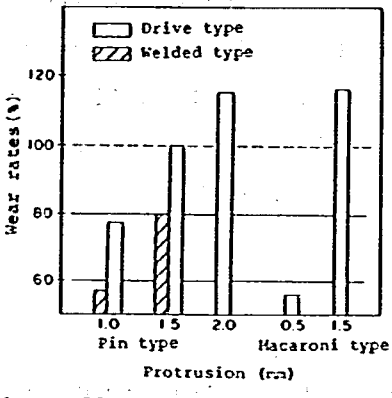


Figure 20 Protrusion of studs and wear of pavements

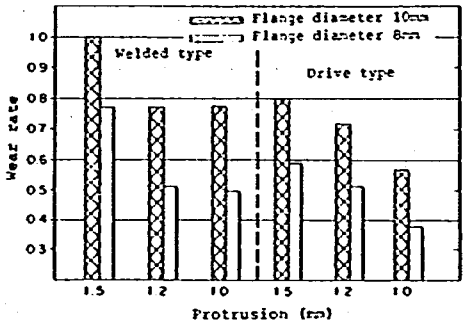


Figure 21 Wear by Different Protrusions

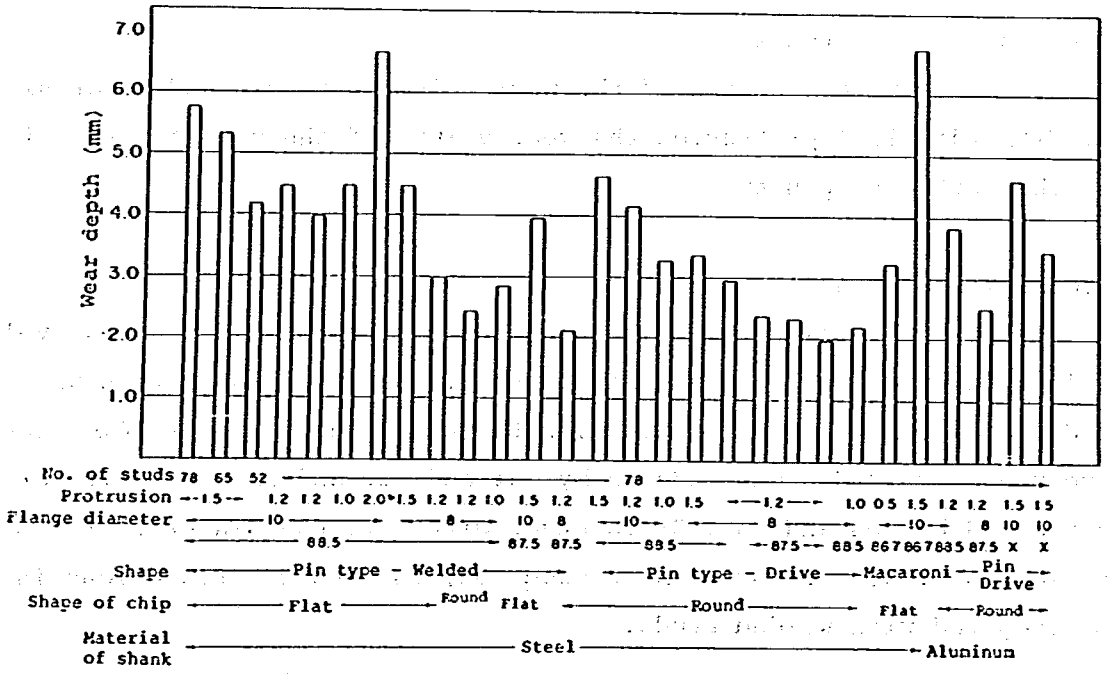


Figure 22 Wear with different types of studs

3.3/ CONTROL AND FUTURE OUTLOOK FOR STUDDED TIRES

Since the debut in 1963, studded tires have quickly become accepted due to their convenience and effectiveness as a winter-necessity in cold regions in Japan. At the same time they have created serious social problems by damaging pavement surfaces and generating harmful dust in many areas, particularly in Sendai and Sapporo.

3.3.1/ RESTRICTIONS ON STUDS

There are currently no regulations or ordinance that specify stud standards, and the manufacture is left to the discretion of the manufacturers. The first standard was issued by tire manufacturers in May 1983 as shown in Table 2. The second in May 1986 specifies different stud types for use on buses and trucks superseded by new standards announced for cars in May 1987. The main modifications of the standards were the specification of smaller flange diameters and reduced numbers.[9)]

3.3.2/ RESTRICTIONS ON STUDDED TIRES

The use of studded tires has been informally restricted in Hokkaido. Table 3 shows the changing controls specified for the use of studded tires in Hokkaido. Since 1982, domestic tire makers have started marketing studless tires, and local administration has encourage their use while tightening the controls on studded tires.

With the growing vocal criticism over the use of studded tires, the leading domestic tire manufactures are to discontinue the production of studded tires in December 1990, and sales of studded tires will be stopped at the end of March of the following year. In this environment, the Hokkaido Public Safety Commission issued new regulations with penalties to control the use of studded tires effective from April 1, 1990.

"The Hokkaido Public Safety Commission Regulations" on studded tires:
Period when use is not allowed: April 10 to October 31.
Penalties for violations: Fine of not more than 50,000 yen
Commercial heavy vehicles: 7,000 yen
Passenger cars, two wheeled vehicles: 6,000 yen
Motorcycles (50cc and less): 4,000 yen

Table 2 Stud Particulars

Tire			Shape of stud	New standard			Original standard		
				Stud			Stud		
Type	Rim diameter	Structure		Number Max	Flange diameter Max(mm)	Protrusion Max (mm)	Number Max	Flange diameter Max(mm)	Protrusion Max(mm)
Passenger cars	All	Radial	Pin	122	8	1.5	122	10	1.5
		Bias		88	10		80	12	
Small trucks	Bellow 14	Radial	Pin	104	10		122	12	
		Bias		80	10		80	12	
	Over 15	Radial	Pin	102	12		102	15	
			Macaroni	60	14		72	15	
		Bias	Pin	80	12		80	15	
			Macaroni	60	14		72	15	
Trucks and buses	All	Radial	Macaroni	60	16		72	17.5	
		Bias		60	16		72	17.5	

Table 3 Restrictions on the use of studded tires in Hokkaido

	Enforcement		
Area / Period	North	East	Central south
Apr. '84-Oct. '85	May. 1 - Oct. 15	May. 1 - Oct. 31	Apr. 15 - Oct. 31
Oct. '85-Apr. '90	Apr. 20 - Oct. 31	Apr. 20 - Nov. 10	Apr. 10 - Nov. 10
Apr. '90-	Apr. 10 - Nov. 10	Apr. 10 - Nov. 20	Apr. 1 - Nov. 20

4/ STUDY OF WEAR RESISTANT ASPHALT MIXTURES

4.1/ OUTLINE OF STUDY

4.1.1/ CHAIN-MOUNTED RAVELING TESTER

The first full-scale bituminous pavement road installed in Hokkaido was completed in 1953 between Sapporo and Chitose (35km), with a surface layer of an equal mixture of Topeka and medium graded asphalt concrete.

At this time tire chains was used for snow and ice on the road. The rutting by the chains were 5mm to 10mm, and reached maximum 50mm in one winter season in some places. To improve on this, asphalt mortar mixed with high penetration type asphalt were placed as a top or wear course. In 1954, a tire chain-mounted raveling tester was installed, and basic indoor tests were started by the Development and Civil Engineering Research Institute of the Hokkaido Development Bureau.

Since around 1967, the feasibility of asphalt mixtures containing coarse aggregate was evaluated and in 1968, the optimum coarse aggregate content of surface layer asphalt mixture, which is currently standard on the national highways, was reported.

4.1.2/ ABRASION TESTING EQUIPMENT

With increased general use of studded tires, the traffic volume increased by dramatically, causing heavy wear of pavements and environmental pollution problems due to dust. This has made a review of the design of wear resistant mixtures necessary. A series of basic research using abrasion testing equipment (stud raveling tester) were conducted from 1981. The research included studies of the effect of wear of pavements, relating stud wear to the traffic volume, and the design of asphalt mixtures including the influence of asphalt, filler, and coarse aggregate on wear resistance. This text details test results by abrasion testing equipment compared with tire chains.

4.2/ STUD RAVELING TESTER

4.2.1/ OUTLINE

This testing equipment uses test specimens of asphalt mixtures and concrete. The system works with studded tires of passenger cars, with one wheel accerelated and one wheel braked with a hydraulic motor and hydraulic pump, with 18 test specimens on the rotation board. The tire is under enough load to rotate the specimen. The rotation board rotates in a fixed direction at a set speed, and the test specimens are worn by the studs on the wheel. It is equipped with a shift mechanism to enable stabilized wear of the specimens. The tester is illustrated in Figure 23.

The equipment consists of: Primary unit, hydraulic units, control panel, and measuring board. The ambient temperatures can be varied from -20°C up to +30°C.

Specifications:

Rotation board: 200cm

Wheel load: 200 - 500kg

Traveling speed: 10 - 40km/h

Torque: 10 - 22kgm

Standard tires: 6.15 - 13 or 6.95 - 14

Test specimens: 18, each a trapezoid 288mm and 410mm wide, 350mm high, and with a thickness of 50mm.

Shift: ±50mm

Sprinkler: 10 l/min. (aprox.)

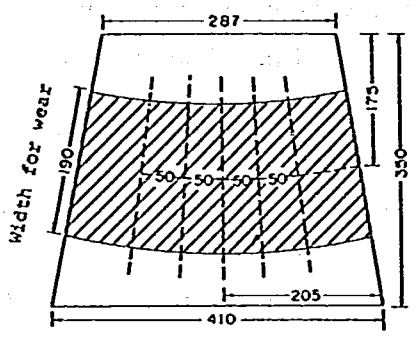
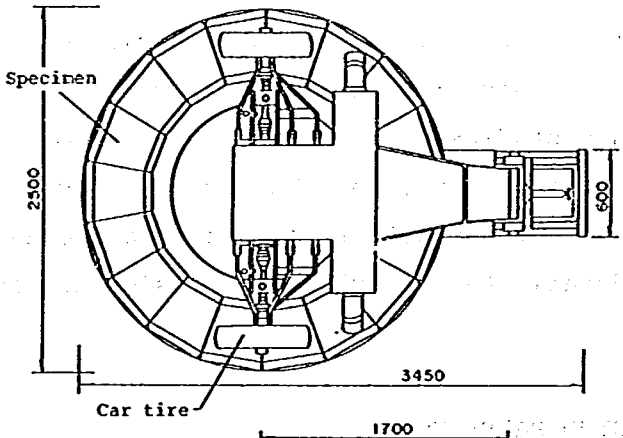


Figure 24 Sectional measuring positions of specimens (mm)



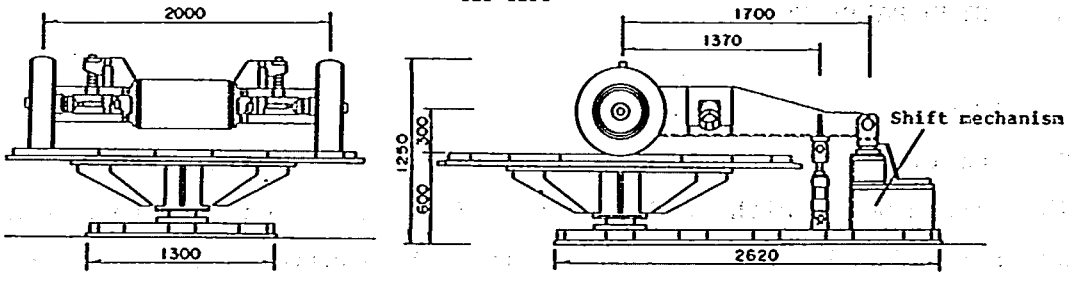


Figure 23 Stud raveling tester

4.2.2/ SPECIMEN PREPARATION

The method of manufacture is based on that of wheel tracking specimens. With a mixing temperature of Saybolt-Furol viscosity/85 sec., compaction

temperature of Saybolt-Frol viscosity of 1,000 sec., it is compacted by a roller. The compaction is done in the following sequence: with a line pressure of 20kg/cm, the surface is compacted by a steel roller in 11 passes, then 22 passes by a rubber roller, and a further 5 passes by a steel roller. The compaction is carried out to bring the compaction strength to 100±1% of the Marshall density.

4.2.3/ TESTING METHOD

The 18 specimens are arranged so that adjacent specimens have less than 1mm differences in height and are mounted on the rotation board. Prior to the raveling test, the specimen is subjected to a preload by summer tires to ensure that the specimen and the rotation board are well fixed. The test conditions were:

	Preload	Raveling
Temperature	+20°C	±0°C
Number of wheel passages	5000	30000
Tires	bias 6.15-13	bias snow 6.15-13
Air pressure	1.7kg/cm^2	1.7kg/cm^2
Load	335kg	335kg
Speed	30km/h	40km/h

The wear volume is measured with an automatic sectional area guage on five sections (see Figure 24), and then averaged.

4.3/ REVIEW OF WEAR RESISTANT ASPHALT MIXTURES

Stud raveling tests were conducted to determine the effect of various types of asphalt mixtures on the wear resistance by varying the asphalt penetration, coarse aggregate content, size of aggregate, and quantity of filler.

4.3.1/ THE PENETRATION OF ASPHALT AND F/A (D/A)

(1) The Penetration of Asphalt

Figure 25 shows the relationship between the penetration of asphalt and the wear volume. There were four types of asphalt with penetrations of 40-60, 60-80, 80-100, and 100-120. The grading of the mixtures were based on the

standard fine and gap graded asphalt concrete (13F40) specified by the Hokkaido Development Bureau. The grading of the coarse aggregate was 0-60%. The figure shows that the wear volume by studs is not related to the penetration of asphalt.[10)]

Figure 26 shows the wear volume of asphalt mortar determined by varying the penetration of asphalt, and using the two-way type chain-mounted raveling tester. The specimens of the asphalt mortar with F/A (D/A: the content of fines below 0.074mm in the filler to the asphalt) of 1.16 (1.0), 1.5 (1.3), and 1.85 (1.6), combined to obtain the maximum Marshall stability. It is seen that greater asphalt penetration causes less wear.[11)]

(2) F/A (D/A)

Figure 27 shows the relationship between differences in F/A and wear volume. The wear volume becomes smaller with increasing F/A irrespective of coarse aggregate content.[10)] Figure 26 also shows that, with chains, the wear volume decreases when the F/A becomes greater.

Figure 28 shows the relationship between F/A and the optimum asphalt content (O.A.C.). Here the O.A.C. becomes smaller with increases in F/A.[12)]

Overall, increases in F/A improves the wear resistance and is economically advantageous through smaller O.A.C.'s. However, considering workability, an F/A of 1.7 is advantageous.

4.3.2/ COARSE AGGREGATE AND MAXIMUM SIZE OF AGGREGATE

(1) Coarse Aggregate

Figure 29 shows the results of tests with the stud raveling tester, and indicates that wear becomes smaller with increases in the quantity of crushed stone for all F/A.[10)]

(2) The Maximum Size of Aggregate

Figure 30 shows the wear with different maximum grain sizes of aggregate and different quantities of crushed stone (50, 55, and 60%) for maximum grain sizes of 13mm and 20mm. The results show the 20mm crushed stone to be advantageous.[13)]

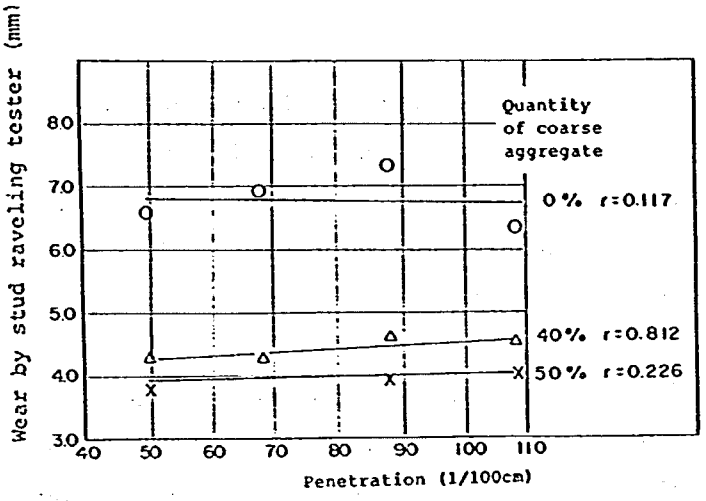


Figure 25 Asphalt penetration and wear depth

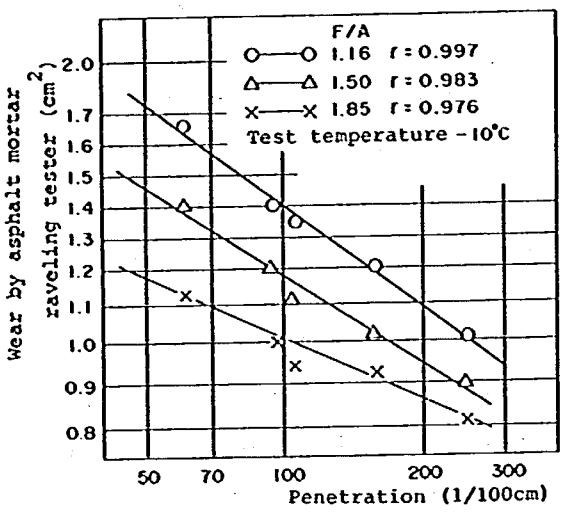


Figure 26 Asphalt penetration and wear volume

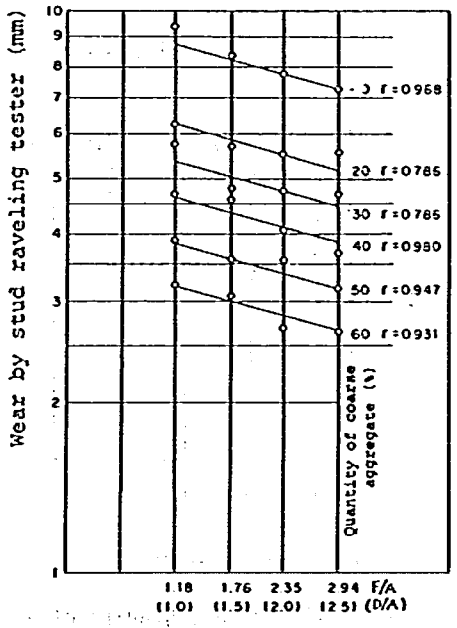


Figure 27 F/A and wear depth

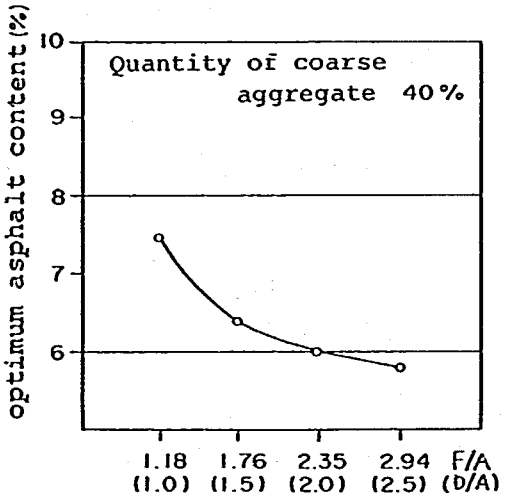


Figure 28 F/A and quantity of optimum asphalt

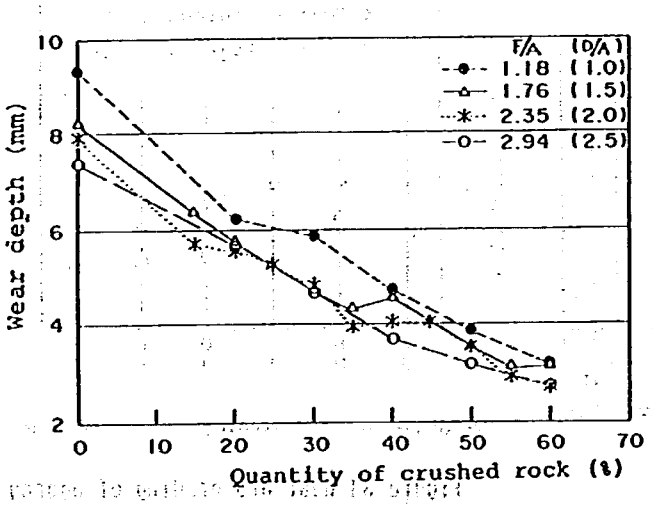


Figure 29 Crushed rock and wear volume

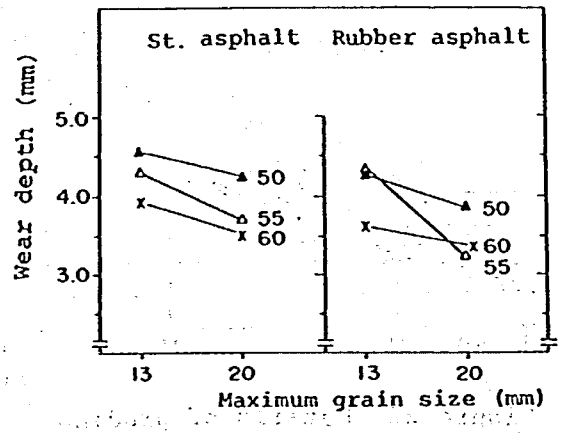


Figure 30 Maximum grain size and wear depth

4.3.3/ GRADING OF AGGREGATE

Gaps-graded mixtures are considered advantageous with tire chains, due to the higher amount of fines which cause an increase in the quantity of asphalt and results in stabilization. Wear resistance was investigated with smooth and gap-graded mixtures by chain and stud reveling testers. The grading of mixtures is shown in Figures 31 and 32.

Figure 33 and 34 show a comparison of wear with gaps and smooth grading mixture, with tires chains and stud raveling testers, with 40% or 50% coarse aggregate. The results show no appreciable differences in the wear volume by differences in grading.

With tire chains, an increase in the gap grading decreases the wear both with 40% and 50% of coarse aggregate.[14)]

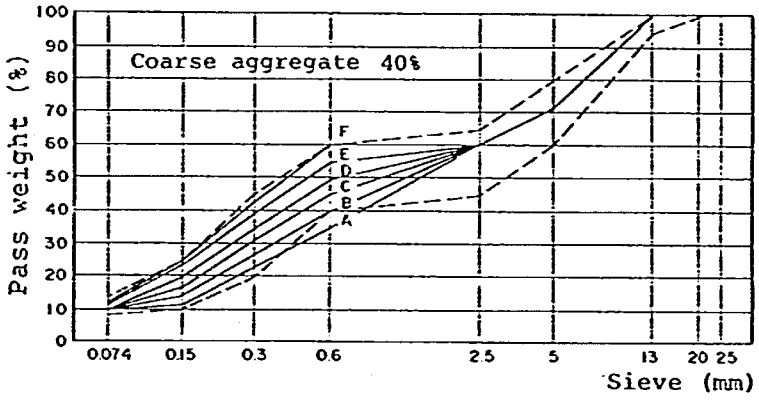


Figure 31 Details of grading

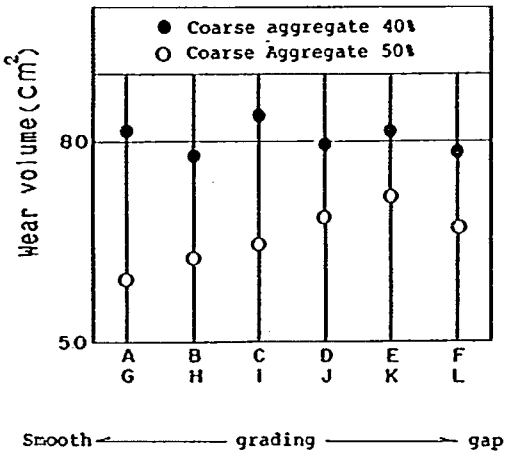


Figure 33 Wear and grading of aggregate with the stud raveling tester

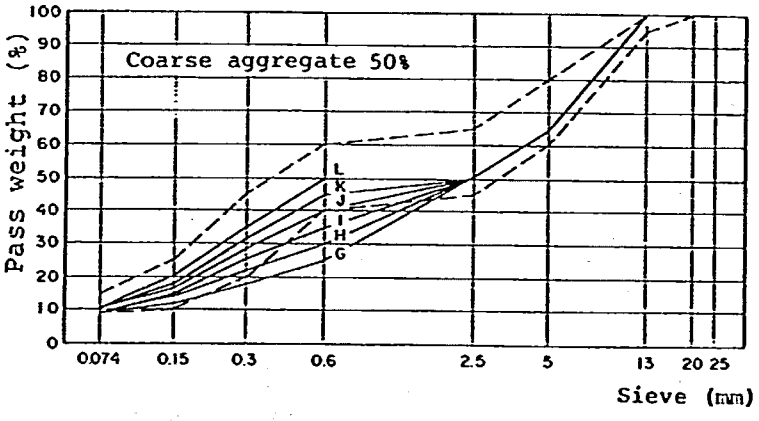


Figure 32 Details of grading

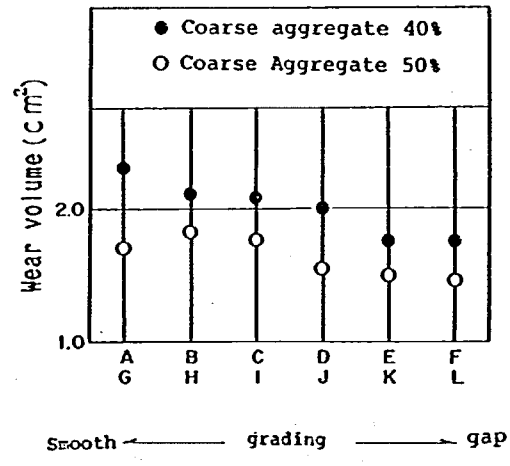


Figure 34 Wear and grading of aggregate with the chane type

4.4/ REVIEW OF FREEZING AND THAWING TESTS

In areas that are subject to snow cover, the surface layer of pavement is influenced by freezing and thawing, causing stripping and cracks, and it is necessary to consider countermeasures against this.

Tests were conducted with mixtures of different grading by repeated freezing and thawing, followed by stud and chain raveling, and wheel tracking tests. The tests used the same aggregate as in 4.3.3.

4.4.1/ GRAIN SIZE OF AGGREGATE AND WEAR VOLUME

Figures 35 and 36 show the relationship between the wear volume and the grain size of aggregate with the stud raveling tests before and after freezing and thawing. The resutls show that both with 40% and 50% aggregate the post freezing and thawing wear are irregular with no apparent trends by differences in grading. There are no significant differences in the wear after freezing-thawing. However the freezing-thawing-generated wear volume tends to be greater with 50% aggregate.

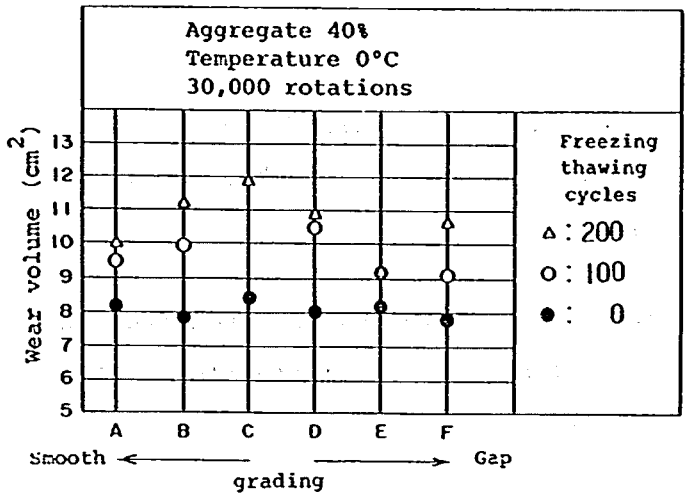
With tire chains, both the 40% and 50% aggregate asphalts show smaller wear with increasing gap grain sizes without freezing and thawing as shown in cFigures 37 and 38. The wear volume is irregular after freezing-thawing.

4.4.2/ GRAIN SIZE OF AGGREGATE AND DYNAMIC STABILITY

Figures 39 and 40 show the relationship between the dynamic stability (D.S.) after freezing-thawing and the grain size of the aggregate. Without freezing-thawing D.S. is very similar for different grain sizes with the 40% aggregate, but with 50% aggregate D.S. becomes greater with increasing gap grain sizes. The post freezing-thawing D.S. is not always smaller than that without freezing-thawing.[15)]

4.5/ MODIFIED ASPHALT

Eighteen types of wear resistance and flow resistance modified plant mixed materials and five of premixed modified asphalts, all currently used, were selected to investigate the effect of wear resistance. Details of the modified materials is shown in Table 4. The mixtures were fine and gap



Figur 35 Wear volume by stud type and aggregate

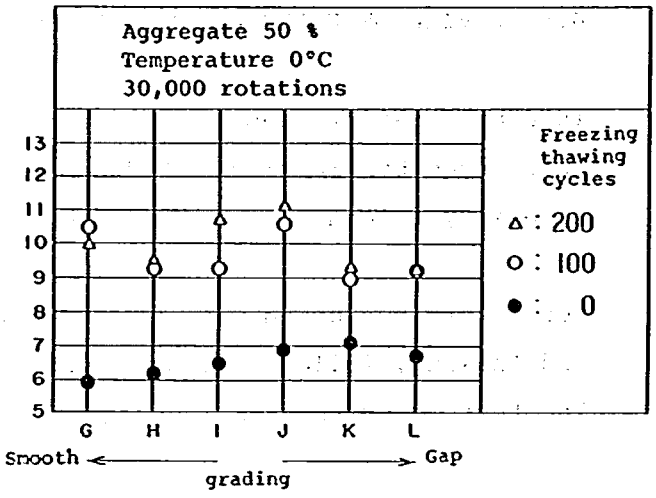


Figure 36 Wear volume by stud type and aggregate

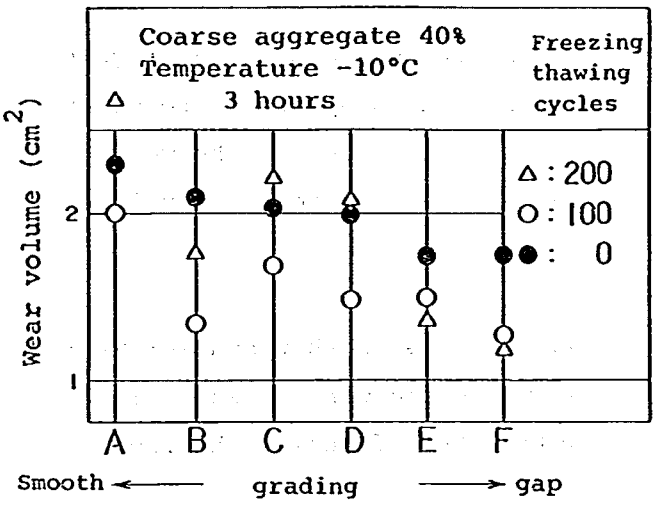


Figure 37 Wear volume by aggregate grading and chain type

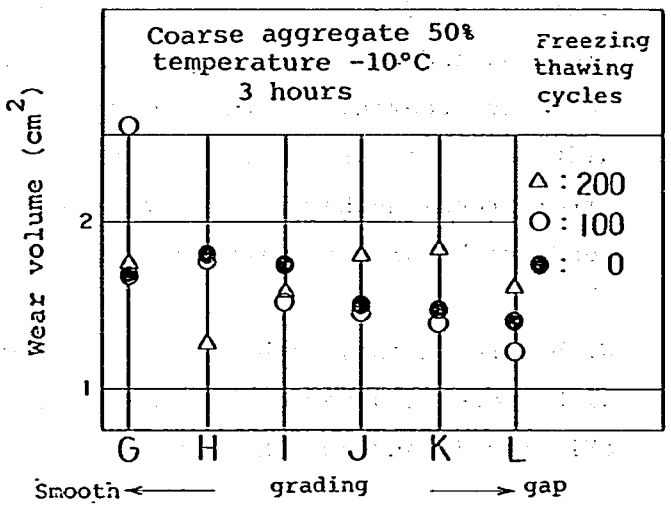


Figure 38 Wear volume by aggregate grading and chain type

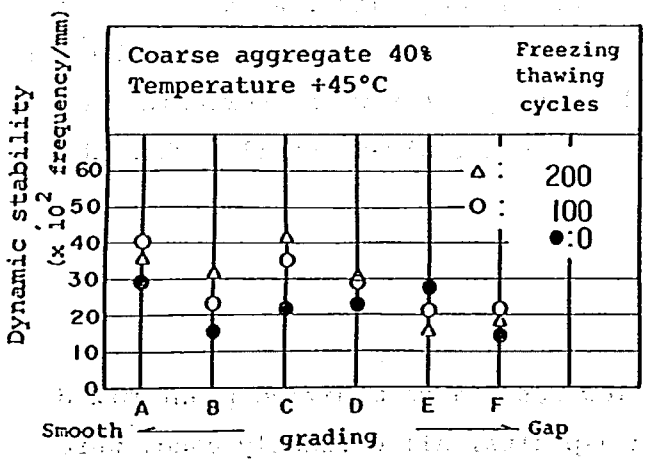


Figure 39 Aggregate grading and dynamic stability

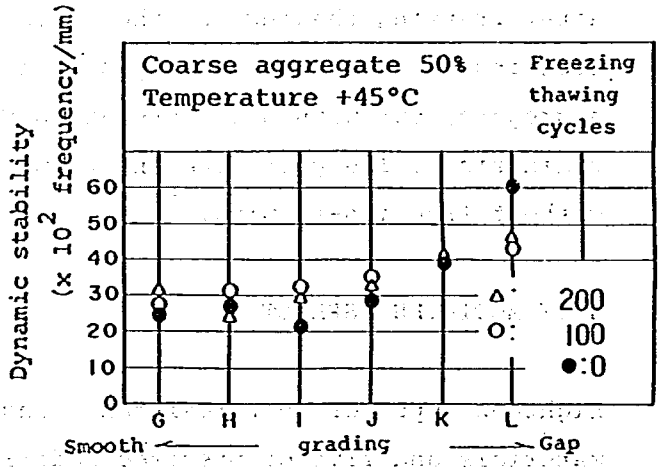


Figure 40 Aggregate grading and dynamic stability

graded asphalt concrete (13F50). The optimum quantity of asphalt was determined based on the Marshall test, and the modification for the plant mixed types was the additive to the O.A.C. in accordance with the internal and external additive specifications by the manufactures.

Figure 41 shows the results of the stud raveling tests. With the plant mix type, some mixtures have higher wear resistance than the straight asphalt. There are no clear trends among the 3 types of materials, rubber, resin, and rubber and resign, mixed. However, the premixed mixtures showed more stable values than with straight asphalt.

Wheel tracking tests were conducted with compounds which were popularly used for flow resistance and which produced good results in the stud raveling tests. Figure 42 shows the test results. There are no specific wear resistance expected with the modified asphalts, but they generally show flow resistance.[16)]

Table 4 Selected modifiers

Texture		Ingeredient	Properties	Additive		Remarks
Rubber	A	SBR	Latex	4 : 100		
ditto	B	SBR	ditto	7 : 93		
ditto	C	CR	ditto	7 : 93		
ditto	D	SBR	ditto	7 : 93		
ditto	E	SBR	ditto	7 : 93		
ditto	F	SBR	ditto	8 : 100		
ditto	G	CR	ditto	7 : 93	(modifier : asphalt ratio)	
ditto	H	CR	ditto	7 : 93		
ditto	I	CR	ditto	7 : 93		Plant mix
ditto	J	BR	Liquid	6 : 94		type
Resin	K	EEA	Powder	5 : 100		
ditto	L	Epoxide resin	Liguid	23 : 77		
ditto	M	Neopren resin	Grain	1 : 100	(modifier : asphalt ratio)	
ditto	N	Polyolefine resin	Powder	4 : 100		
Rubber/resin	O	SBR+EEA	Powder	5 : 95	(modifier : mixture ratio)	
ditto	P	IIR	Liguid	7 : 93		
ditto	Q	BR	Liguid	6 : 94		
others	R	Cement processed	Grain	6 : 100	(modifier : mixture ratio)	
Rubber	S	SBR	——			
Resin	T	EVA	——			Premixed
Rubber/resin	U	SBR+EVA	——			type
ditto	V	SBR+EVA	——			
ditto	W	SBR+EVA	——			

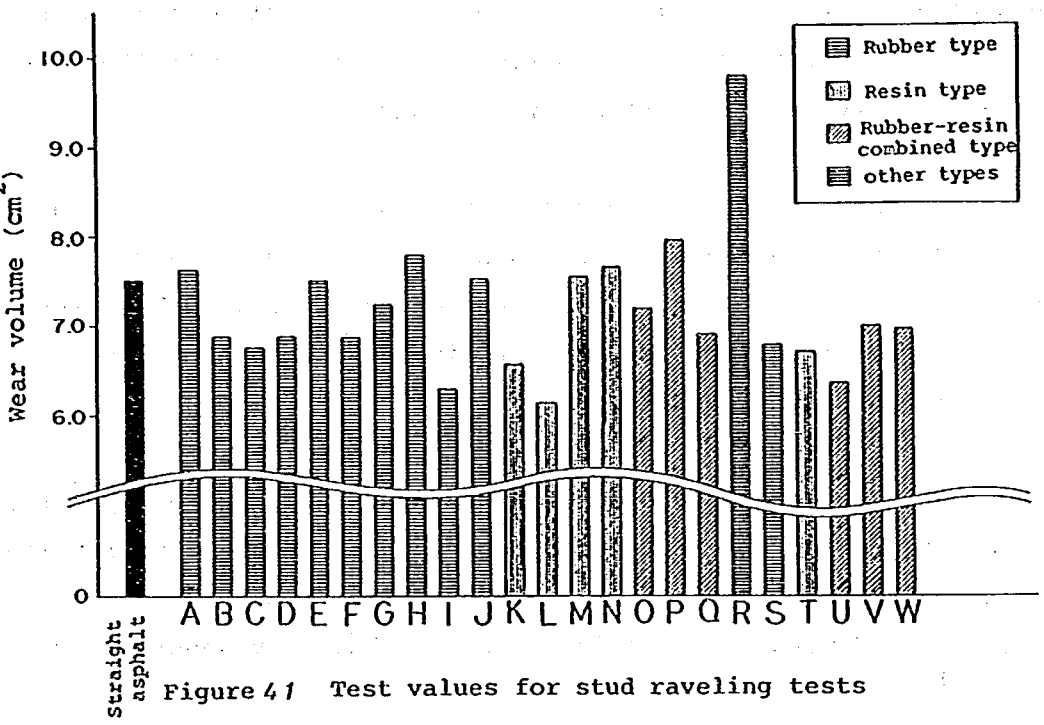


Figure 41 Test values for stud raveling tests

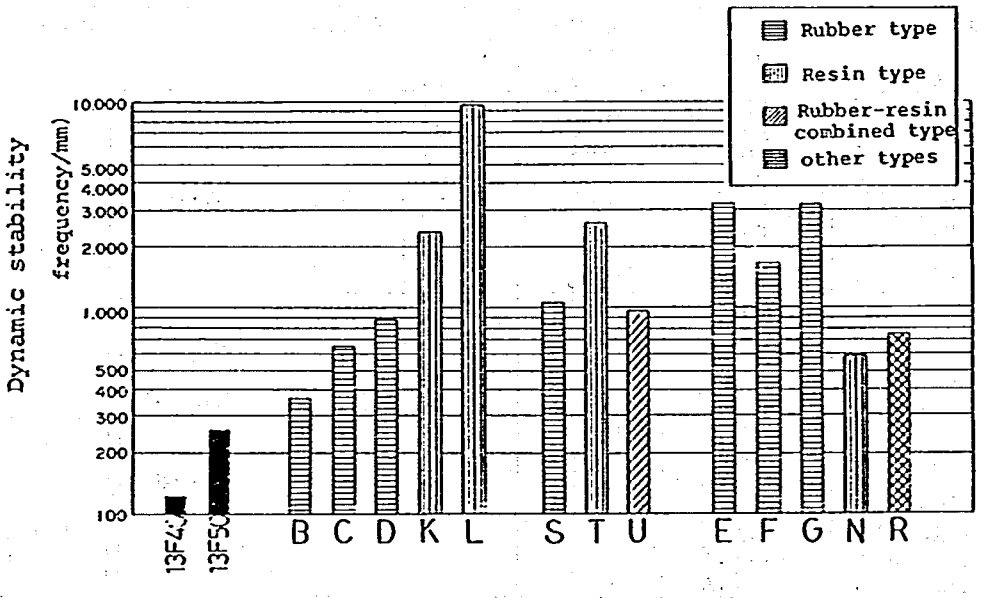


Figure 42 Results of wheel tracking test

5/ SUMMARY

The results of the research on wear resistant asphalt mixtures may be summarized as follows:

(1) The wear caused by studded tires can be significantly reduced by changing the number, protrusion, and configuration of studs.

(2) A greater penetration of asphalt produces significant advantages to counter tire chain wear, but this has no effect with studded tires.

(3) Wear resistance is improved with increased F/A, and approximately 1.7 is optimum when considering workability.

(4) Wear resistance and dynamic stability of asphalt mixture are greater with 50% coarse aggregate than with 40%.

(5) There are no differences in the effect of freezing and thawing on wear resistance with different aggregate quantities and grading.

(6) Modified asphalt shows positive flow resistance, but no appreciable increase in wear resistance.

From the results, the Hokkaido Development Bureau has embarked on trial paving projects with 13F50 and 20F50 mixtures modified from fine and gap-graded asphalt concrete (13F40), which is standard for wear resistant mixtures.

6/ POSTSCRIPT

Improvements in wear resistance of asphalt mixtures have been attained as described here. However there is limited scope in preventing rutting of pavements by research and development of asphalt mixtures. Studded tires will be subject to tighter restrictions and research and development of pavements for the post studded tire era is a pressing requirement.

We wish to express our thanks to the staff who have been engaged in the research and development activities since the time of the now defunct Pavement Section.

REFERENCES

1) Hiroshi Kubo, Shigeki Kumagai and Hyoji Sato: Monthly Report of the Civil Engineering Research Institute, No. 347 pp. 1 - 16, April, 1982.
2) Shigeki Kumagai and Masaaki Ueda: Monthly Report of the Civil Engineering Research Institute, No. 390, pp. 1 - 8, November 1985.
3) Ryoshi Yamada, Shigeki Kumagai, Shigeharu Sato, Nobuo Yamanishi, and Kazuaki Tsukahara: Thesis Collection Reading of the 30th Hokkaido Development Bureau Technological Research: pp. 135 - 140, 1986.
4) Hidehiko Ninomiya, Shunsaku Sawada, Kazuyuki Kawamura, and Tatsuro Mizushima: Monthly Report of the Civil Engineering Research Institute, No.437, pp. 2 - 8, October 1989.
5) D.R. Lamb: Studded Tires - The Thread to Road Surface, Shell Bitumen Review, 31 July 1970.
6) Hokkaido Pref. Government: Report of Actual Status of Mounting Studded Tires in Hokkaido, February 1982.
7) Sapporo city: Data Prepared by the Studded Tire Measures Section, March 1989.
8) Hiroshi Kubo, Shigeki Kumagai, Nobuo Yamanishi, Akira Ogasawara, and Kazuaki Oorui: Monthly Report of the Civil Engineering Research Institute, No. 374, pp. 1 - 9, July 1984.
9) Hiroshi Hayashi: Monthly Traffic, pp. 74, July 1986.
10) Shigeki Kumagai, Masaaki Ueda, Nobuo Yamanishi, Kazuaki Tsukahara, and Hirokatsu Iguch, Monthly Report of the Civil Engineering Research Institute, No. 382, pp. 1 - 15, March 1985.
11) Susumu Hirao, Takeshi Takahashi, Shigeki Kumagai, and Tadanobu Hokaku, Monthly Report of the Civil Engineering Research Institute; No. 160, pp. 9 - 18, September 1966.
12) Hiroshi Kubo, Shigeki Kumagai, and Nobuo Yamanishi; Road Construction, No. 444, pp. 74 - 81, January 1985.
13) Hiroshi Kubo, Shigeki Kumagai, Hyoji Sato, Nobuo Yamanishi, Akira Ogasawara, and Kazuaki Oorui: Monthly Report of the Civil Engineering Research Institute; No. 355, pp. 11 - 18, December 1982.
14) Nobuo Yamanishi, Shigeki Kumagai, Masaaki Ueda, Kazuaki Tsukahara, and Ryoshi Yamada: Monthly Report of the Civil Engineering Research Institute, No. 397, pp. 1 - 13, June 1986.

15) Kazuaki Tsukahara, Shigeki Kumagai, and Takumi Hoshi: Monthly Report of the Civil Engineering Research Institute, No. 422, pp. 24 - 31, July 1988.

16) Ikuma Umezu, Shigeki Kumagai, and Shigeharu Sato: Monthly Report of the Civil Engineering Research Institute, No. 415, pp. 1 - 12, December 1987.

Asphalt Pavement Rutting Experience in Canada

J. Emery, JEGEL

ASPHALT PAVEMENT RUTTING EXPERIENCE IN CANADA

JOHN EMERY
President
John Emery Geotechnical Engineering Limited
Dynatest Limited and Pavmatec Limited
Downsview (Toronto) Ontario

ABSTRACT

The problems, causes, 'solutions', remedial measures and action plans for mitigation of asphalt pavement rutting, in the Canadian context and focusing on plastic deformation/instability (flow) rutting, are summarized from RTAC Rutting Seminars held in Vancouver, Calgary, Edmonton, Regina, Winnipeg, Toronto, Montreal, Fredericton and Halifax. (Spring of 1989, with some 279 contractor, consultant and agency staff involved.) Rutting of asphalt concrete on highways and city roads has become a serious and expensive maintenance problem across Canada. The Seminars provided the opportunity to both determine the extent/significance of the rutting problem, and to draw from the extensive laboratory and practical experience with causes and possible solutions/implementation. While wear and structural deformation were considered, plastic deformation/instability rutting as a function of environment (hot weather), traffic (loadings, replications, tire types, tire pressures, axle configurations, buses, vehicle speed/stopping, early traffic, etc.) and asphalt mix materials and design (aggregate characteristics, asphalt cement stiffness, voids, design methodology, etc.) was the major concern. It appears that the prime 'solution' to rutting is through aggregate selection (dense grading, crushed, coarser, etc.) with engineered asphalts currently a secondary 'solution' along with, of course, improved mix design/testing procedures. Alternative approaches such as portland cement and roller compacted concrete were also discussed. It was generally agreed that rut resistant asphalt mixes can be designed and placed, but contractors will have to take care to avoid segregation and to achieve necessary compaction levels for the 'harsh' mixes involved. A number of Canadian agencies have field trials in progress incorporating engineered asphalt cements for both rutting resistance and durability enhancement. It was concluded that there is a real rutting problem across Canada, but that it can be mitigated through the use of quality aggregates and/or engineered asphalt cements, with appropriate mix designs and quality control testing.

ACKNOWLEDGEMENTS

The significant contributions to the Seminars by the Roads and Transportation Association of Canada (RTAC), Al MacDonald (EBA Engineering Consultants Ltd.), Guy Doré (Ministère des Tranports de Québec), Natalie McLean (RTAC) and the participants are gratefully acknowledged. Summary notes in French (Seminaire sur L'Orniérage Des Revetements) and the major Canadian references on rutting used for the Seminar are available from the author. The presentation of "Asphalt Pavement Rutting Experience in Canada" is supplemented by slide coverage of the theme. The opinions and findings expressed or implied in this paper are those of the author, and not necessarily the organizations involved. Comments would be most appreciated.

1. INTRODUCTION

In common with many city and highway pavement systems internationally, the significant and increasing plastic deformation/instability rutting (permanent deformation) of asphalt concrete across Canada has become a primary asphalt technology problem requiring cost effective mitigation for both existing and new pavements. The Roads and Transportation Association of Canada (RTAC) first focused group attention on the Canadian rutting problem during a 1986 Special Workshop "Rutting in Asphalt Pavement - A National Problem". This Workshop, through a series of technical papers and discussions, covered a wide range of topics related to asphalt concrete rutting as a major national pavement problem: how rutting occurs; materials considerations; traffic impact; design influences; construction methods and maintenance alternatives; future research needs; and the effectiveness of current activities. This 1986 RTAC Rutting Workshop initiative continued through the activities/presentations of both the RTAC Soils and Materials Technical Committee and Pavements Technical Committee as part of universal research and development activities to 'battle' rutting (SHRP, C-SHRP, PICA, TRB, NAPA, and AI for instance).

Given the continuing importance of implementing balanced (other pavement performance factors such as fatigue resistance, durability and frictional characteristics must be considered), technically-sound, cost-effective solutions to the rutting problem, an RTAC cross-Canada one day Pavement Rutting Seminar was developed and held during the Spring of 1989 in Vancouver (31 participants), Calgary (18), Edmonton (17), Regina (48), Winnipeg (21), Toronto (42), Montreal (46), Fredericton (28) and Halifax (28), (total attendance of some 279 contractors, consultants and agency staff involved). The organization, general references, contractor/consultant/agency/moderator interaction and general findings of the series of Rutting Seminars are given in following sections in point form to summarize the considerable technical information involved, focusing on plastic deformation/instability (flow) rutting. In addition, the technical presentation is supplemented with slides, as was the case at each Rutting Seminar, indicating both the rutting problem

across Canada, local experience in the Seminar area, and the remedial measures/action plans adopted to mitigate asphalt pavement rutting.

2. ORGANIZATION OF PAVEMENT RUTTING SEMINAR

2.1 Theme

The significant and increasing rutting (plastic deformation/instability rutting) of many city and highway asphalt pavements has become a primary asphalt technology problem requiring cost-effective, technically-sound mitigation for both existing and new pavements.

2.2 Technical Program in Each City

There were two technical moderators throughout for the Rutting Seminars (Al MacDonald and John Emery), plus local technical representatives for each presentation area in Canada to ensure that the local 'experience' with rutting and its mitigation was made available. Emphasis was placed on obtaining input from all in attendance through a workshop component, and this objective was achieved.

1. Background of the Asphalt Pavement Rutting Problem (Moderator)
2. Workshop
   Delegates worked in small groups to consider rutting in terms of local experience. Topics covered included: significance of the problem; causes; solutions; and implementation of solutions. Workshop findings were summarized at the end by Moderator.
3. Comments on Workshop Findings. (Local Chairman).
4. Local Case Study of Rutting and Its Solution (Local Representative(s)).
5. Morning Discussion and Questions.
6. Asphalt Pavement Rutting - Extent, Types and Causes (Moderator).
7. Asphalt Pavement Rutting - Solutions, Remedial Measures and Implementation (Moderator).
8. Final Discussion and Questions (Local Representatives and Moderators).
9. Summary (Moderator).

3. MAJOR REFERENCES

The major references used by the Moderators and Local Representatives to supplement the extensive technical literature on the subject were:

1. City of Lethbridge Pavement Rutting Study (Al MacDonald - RTAC, CTAA)
2. Asphalt Concrete Rutting Study - Metro Toronto Roads (John Emery - RTAC, CTAA)
3. Rutting - How Serious is the Problem? (AASHTO)
4. A Study of Permanent Deformation of Asphalt Concrete Pavement in Alberta (Alberta Transportation)
5. Natural Sand vs. Manufactured Sand (City of Calgary)
6. Asphalt Pavement Rutting Report (City of Winnipeg)
7. Pavement Rutting Study (New Brunswick Transportation/UNB)
8. Etude sur les Mélanges Bitumineux Conventionnels en Function de leur Résistance à L'Orniérage (Transports Québec)
9. L'Orniérage, un Problème Complexe (CRCAC)

4. ASPHALT PAVEMENT RUTTING BASICS

Slides and summary notes were developed covering asphalt pavement rutting basics to facilitate the Workshop and summary of the overall Seminar findings. It is of interest that there was general unanimity by contractors/consultants/agencies/moderators by the end of the nine Seminars, and that these slides covered the essence of the rutting problem and its hoped for reduction. These summary notes are given in following sections.

4.1 Types of Rutting

1. Wear in wheel paths (wear rutting).
2. Permanent deformation:
   - A. Deformation of entire pavement structure in wheel paths (structural rutting); and
   - (Focus) B. Plastic deformation/instability in the form of densification ('compaction') and/or shear of asphalt concrete in wheel paths (plastic deformation/instability rutting).
3. Combinations of above (combination rutting).

4.2 Problems Caused by Rutting
(Particularly Plastic Deformation/Instability Rutting)

1. Safety:

   A. Vehicular - hazard changing lanes, loss of control, water ponding in wheel paths (spray, 'hydroplaning'), ice forming in wheel paths and/or snow and ice removal difficult; and

   B. Pedestrian - vehicle stopping distances increased at cross walks during inclement weather.

2. Nuisance to pedestrians - splashing by vehicles.

3. Appearance - poor public perception and political reaction.

4. Cost to mitigate - improved new pavements, timely repairs, traffic flow interruptions, etc., at a time of fiscal constraints.

4.3 Causes of Rutting

1. Wear rutting:

   A. Studded tires (not permitted now by many agencies);

   B. Poor mix - low asphalt cement content, hardened asphalt cement, low durability aggregates, mix design not appropriate, etc.; and/or

   C. Inadequate compaction.

2. Structural rutting:

   A. Poor drainage;

   B. Frost action;

   C. Replication and magnitude of loadings - actual traffic (AADT) exceeds design assumptions, axle loadings greater than legal allowable (or design loadings), and/or overloads at critical periods (spring thaw 'softened' subgrade for instance);

   D. Poor and/or contaminated aggregates;

   E. Poor construction practices and/or inadequate quality control and inspection;

   F. Stripping of asphalt concrete aggregates; and/or

   G. Deterioration with time of pavement structure (wheel path alligator cracking for instance), etc.

(Focus) 3. Plastic deformation/instability rutting:

   A. Environment (hot weather);

B. Traffic (truck and bus) -

- increased axle loadings] significant
- increased tire pressures] combined
- trend in tire types] effect
  (radial replacing bias)
- growth in heavy vehicle (truck and bus) traffic
- axle configuration/loadings (high steering axle loadings)
- 'floating' axle use (abuse)
- vehicle speed (slow) and/or stopping/starting
- early traffic on new asphalt concrete;

C. Hot mix materials and design -

- aggregate physical characteristics (natural, rounded particle blend sands for instance)
- asphalt concrete too 'fine' (small coarse aggregate top size) and/or coarse aggregate content low
- aggregate gradation (pronounced 'VMA' hump for instance)
- asphalt cement stiffness too low at higher temperatures
- in-place air voids too low (less than about two percent) and/or coarse aggregate 'floating' in asphalt cement/sand matrix
- mix design methods not applicable to rutting problem (applicability of Marshall method?)
- stress/strain in asphalt concrete more severe than anticipated (composite concrete/asphalt pavements and deck waterproofing for instance).

4.4 'Solutions' to Rutting

1. Wear rutting - 'ban' studded tires, proper hot mix design, durable aggregates, good compaction, etc.

2. Structural rutting - provide drainage, control frost action, design adequate pavement structure (anticipated replications and magnitudes of loading), select durable materials, construction quality control, spring load restrictions, etc.

(Focus) 3. Plastic deformation/instability rutting:
(Little Control Over Environment and Traffic)

A. Aggregates -

- high crushed content (preferably 100 percent crushed coarse and fine aggregates)
- dense aggregate grading
- good quality aggregates
- coarse aggregate - high content and large top size

. fine aggregate - high angularity, etc.;

B. Asphalt cement -

. high stiffness at higher temperatures
. engineered (modified) asphalt cements, etc.;

C. Improved mix design/testing procedures -

. applicability of Marshall, Hveem and Gyratory methods of mix design?
. use of rational mix design procedures (role of fillers for instance)
. use of resilient modulus, creep compliance, wheel tracking and fatigue tests, etc.; and

D. Alternate approaches -

. portland cement concrete
. others?

4.5 Remedial Measures for Rutting

1. Wear rutting - spray patching, wheel path paving, thin overlay, mill/thin overlay, heat reforming, etc.

2. Structural rutting - drainage improvements, structural overlay, reconstruction, etc.

(Focus) 3. Plastic deformation/instability rutting:

A. New construction using improved hot mix (materials, design and placement) or alternate approach (concrete for instance); and

B. Repair/mitigation - mill/overlay - adequate depth and improved hot mix,
Removal/replacement - improved hot mix or alternate approach.

4.6 Action Plan for Rutting Mitigation
(Focus on Plastic Deformation/Instability Rutting)

1. Identify rutting problem (type(s), extent, magnitude).
2. Determine cause(s) of rutting.
3. Establish appropriate remedial and design measures.
4. Implement cost-effective, technically-sound measures (improved hot mix for instance) with appropriate quality control and monitoring.

4.7 Extent of Rutting Problem in North America

Rutting - How Serious is The Problem?
AASHTO, December 1988 - Plastic Deformation/Instability Rutting

1. Rutting is a significant problem for most agencies.
2. Many of the causes of rutting are well known.

3. Long lasting, high performance pavements can be built with asphalt concrete.

4. Pavement must be properly designed and built to carry the loads.

5. Quality aggregates and asphalt cement must be specified with appropriate mix designs/testing.

6. Construction must be monitored.

7. Use of marginal materials cannot continue as the long-term maintenance costs become too great ("rut-plagued road system" for instance).

4.8 Portland Cement Concrete as an Alternate
(New Construction and Whitetopping)

1. CPCA Thickness Design for Concrete Highway and Street Pavements (PCA, 1984).
Fatigue analysis (to control fatigue cracking) and erosion analysis (to control foundation and shoulder erosion, pumping and faulting).

2. PCA Guide to Concrete Resurfacing Designs and Selection Criteria (PCA, 1981).
Resurfacing of both concrete and asphalt pavements - concrete overlay of asphalt (whitetopping).

4.9 Asphalt Cement Selection

Canadian General Standards Board
Asphalt Cements for Road Purposes

Temperature Susceptibility 'Groups':

Group A - Includes asphalt cements which have a high viscosity at 60°C and at 135°C (for a given penetration at 25°C).

Group B - Includes asphalt cements which have a medium viscosity at 60°C and at 135°C (for a given penetration at 25°C).

Group C - Includes asphalt cements which have a low viscosity at 60°C and at 135°C (for a given penetration at 25°C).

(Group A has Highest Stiffness at Higher Temperatures)

4.10 'Ideal' Engineered (Modified) Asphalt Cement

1. Higher stiffness at high temperatures to resist rutting.

2. Lower stiffness at cold temperatures to resist cracking.

3. Lower stiffness at processing temperatures to expedite pumping, spraying, mixing and compaction.

4. Improved adhesion to aggregates in presence of moisture to reduce stripping.

4.11 Types of Modifiers

- rubbers (latex, SBS, reclaimed rubber, etc.)
- plastics (polyethylene, EVA, PVC, etc.)
- extenders/stiffeners (sulphur, lime, carbon, etc.)
- combinations of above.

4.12 Trends with Engineered (Modified) Asphalt Cements

- use increasing
- address specific problems
- improved performance
- monitoring of field trials in progress
- specifications and testing methods needed.

5. TYPICAL LOCAL EXPERIENCE

An example of the local experience with rutting discussed during the Seminars can be indicated by a summary of the general findings and research on the rutting problem in Metro Toronto where bus traffic is a significant factor.

5.1 Asphalt Mix Technology Contributing Factors

1. Pronounced VMA 'hump' developed by using natural, rounded, blend sands.
2. Low in-place air voids
   - Less than about two percent
   - Coarse aggregate 'floating' in matrix.

5.2 Severity

1. Composite pavements more severe than anticipated.
2. Bus bays > stop areas > turn lanes > curb lanes > rest.
3. Mainly in binder course(s).
4. 'Buckling' against curb.

5.3 Recommendations For Rutting Mitigation

Binder Course Component of Composite Pavements
High Stability HL 8 Mix

1. 100 percent crushed aggregates (natural or slag).
2. Aggregates from approved sources.
3. Reduced VMA 'hump'
   - Manufactured sand, or
   - Steel slag fine aggregate.

4. Marshall optimized for stability

   . Air voids, SSD (percent) 4
   . Flow (0.25 mm) 8 to 14
   . Minimum stability (N) 14000.

5. 'Group A' 85/100 penetration asphalt cement.

6. Minimum compaction of 97 percent.

Surface Courses

DFC, High Stability HL 1 Mix

1. Generally as for High Stability HL 8, noting specific aggregate type requirements.

2. Minimum stability of 14000 N.

3. 'Engineered' asphalt cements?

6. CAUSES OF RUTTING AND SOLUTIONS/IMPLEMENTATION

It is of interest to summarize the Workshop findings with regard to the causes of rutting and solutions/implementation. This is done in the following sections through prioritization listings with an indication of the number of delegates 'advocating' the specific cause or solution.

6.1 Causes

. Increased loads and/or tire pressures	20
. Hot mix quality (too sandy, low voids, poor aggregates, etc.)	15
. Uncrushed coarse aggregate	7
. Increased bus and truck traffic	7
. High natural sand content and/or fines (-75 µm)	6
. Pronounced VMA hump	5
. Deterioration in asphalt cement quality	5
. Lack of fine aggregate angularity	4
. Slow, stop and start heavy traffic	3
. Poor compaction	3
. Studded tires	2
. High summer temperatures	2
. Allowing traffic on new pavements too soon	2
. and many others (1 each); specifications, mix criteria, higher penetration asphalt cement, etc. (32 in all, much overlap.)	

6.2 Solutions/Implementation

. Engineered asphalt cements	11
. Manufactured sands	10
. Higher crushed content coarse aggregates	9
. Improved mix design method(s), Hveem?	7
. Larger top size aggregates	6
. Alternate materials such as portland cement concrete	6
. Control nature and amount of fines (-75 µm)	6
. Improved asphalt technology education	5
. Quality RAP	5
. Proper compaction	5
. Steel slags	4
. Higher laboratory compaction standard	3
. and many others (2 or 1 each); test for rutting resistance, higher coarse aggregate content, improved specifications, reduced VMA hump, etc. (77 in all, much overlap.)	

7. CONCLUDING COMMENTS

It is recognized that this presentation has been brief and it is hoped that any PICA 4 participant with an interest in obtaining further information on the Roads and Transportation Association of Canada 'battle' against asphalt pavement rutting will obtain the full detailed report on the Pavement Rutting Seminars from RTAC or the author. Hopefully, the technical presentation and slides developed for PICA 4 have both indicated the extent of the rutting problem in Canada and the positive action being taken with balanced, cost-effective, technically-sound solutions across Canada from Pacific to Atlantic.

Statistical Study of Factors Causing Rutting of Expressway Pavements in Cold Areas in Japan

K. Kaneda, T. Sakate, Y. Takayanagi, K. Kamiya,
Japan Highway Public Corporation Laboratory

STATISTICAL STUDY OF FACTORS CAUSING RUTTING OF EXPRESSWAY PAVEMENTS IN COLD AREAS IN JAPAN

by

Kazuo Kaneda, Head, Pavement Division,
Takashi Sakate, Deputy Head, Pavement Division,
Yoshio Takayanagi, Researcher, Pavement Division,
and
Keizo Kamiya, Researcher, Pavement Division,
Nihon Doro Kodan Laboratory
(Japan Highway Public Corporation Laboratory)

ABSTRACT

Pavement repairs on Japanese expressways are mainly concentrated on rutting and, in particular, rutting caused by abrasion in cold areas is increasingly becoming a serious problem.

The Japan Highway Public Corporation has been working on the development of a pavement management system which consists of a data base and a subsystem for evaluating repair plans in order to create efficient pavement repair procedures. The most important and difficult task involved in the development is a procedure for estimating prospective rutting depths.

It is considered that the progress of rutting on a road surface may be defined by a multiple regression analysis where the criterion variable is the increasing value of rutting depths and the explanatory variables are a number of factors possibly contributing to the progress of rutting. Results thus obtained are expected not only to help improve the reliability of the pavement management system but also to provide us with valuable information to create the type of pavement less prone to be rutted.

With this report, we intend to describe the outline of the corporation's pavement management system and also the current state of our efforts for

analyzing factors which contribute to rutting in the pavement.

In analyzing the causes for rutting, we take climatic conditions (the maximum and minimum temperatures, the numbers of summer and winter days, and the number of snow-covered days), horizontal alignment, longitudinal grade, traffic flow volume, ratio of heavy vehicles to the traffic flow, pavement data (asphalt content, penetration, softening point, Marshall test values, specific gravity of aggregate, and grading), etc. as possible factors for rutting. We have first processed qualitative data using the quantification theory of the first type, and summarized other quantitative data through principal component analysis. We have then performed multiple regression analysis with the portion of rutting depth increment which could not be defined by the quantification theory I as a criterion variable.

A STATISTICAL STUDY OF FACTORS CAUSING RUTTING OF EXPRESSWAY PAVEMENTS IN COLD AREAS IN JAPAN

by

Kazuo Kaneda, Head, Pavement Division,
Takashi Sakate, Deputy Head, Pavement Division,
Yoshio Takayanagi, Researcher, Pavement Division,
and
Keizo Kamiya, Researcher, Pavement Division,
Nihon Doro Kodan Laboratory
(Japan Highway Public Corporation Laboratory)

1. INTRODUCTION

Since its foundation in 1956, the Japan Highway Public Corporation has been engaged in the construction and maintenance of Japanese expressways on behalf of the government. The total planned length of Japanese expressways is 11,520 km of which 4,660 km is now in service as of the end of fiscal year 1989 and the extension work is continuing at the rate of 200 to 250 km per year.

The annual cost of pavement repair of 14 to 16 billion yen (US$100 million) is consumed mainly for repairing of rutting. In particular, rutting caused by abrasion on the road has become a serious problem in cold areas.

The Corporation has been in the process of developing a Pavement Management System which consists of a data base and a subsystem for the evaluation of road repair plans and, with this paper, we intend to report on the results of our statistical study we have made to date of the factors causing rutting, using the data collected in our data base.

1.1 THE OUTLINE OF THE PAVEMENT MANAGEMENT SYSTEM

The pavement management system is a concept developed in the U.S.A. around 1970 with the purpose of defining the best way for providing safe, comfortable and economical pavement for the benefit of road users. A book "Pavement

Management Systems" was written and published by Dr. Haas and Dr. Hudson in 1978 and the significance of the system was soon recognized among the engineers of Japan who are involved in road pavement. (See Fig. 1 for the basic concept of the system described in the book.)

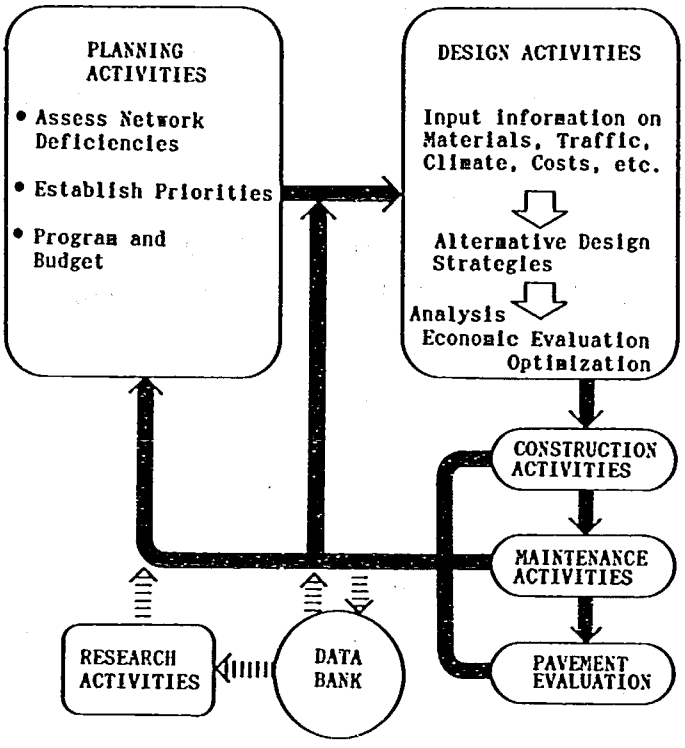


Fig. 1 Basic Concept of the Pavement Management System

The Corporation started to develop its own system in 1980 and has so far completed the initial data base and maintenance subsystem and put them into operation.

The main items of the data base are as shown in Table 1. The items related to an individual construction or repair service are prepared in writing by each contractor concerned in a prescribed form to be submitted to the Corporation which then are collected and entered into the data base by the Corporation's laboratory once a year. Data concerning rutting and cracking are collected through investigation using crack and rut surveying vehicles (see Fig. 2) performed once every 2 to 3 years on magnetic tapes and are stored by the respective operation bureaus while a copy of the tapes is sent to the Corporation's laboratory for entry into the data base.

The maintenance subsystem is to supply necessary documents for developing repair plans, and Fig. 3 shows examples of the output documents. With regard to the data collected on the rutting depth, the data obtained in the year when the regular investigation was made will have to be corrected for the difference in values added between the year investigated and the year when the repair is to be planned (or the year the repair is to be made). In this system, such correction is made by adding an estimated additional depth per year multiplied by the number of years passed to the maximum rutting depth for each 100 meter section as obtained by the regular investigation.

Table 1. Main Input Items for Pavement Data Base

<Construction outline data> Section of paving work (KP), length, construction period, date service started, geometric design, road structure (cut or embankment, tunnel, bridge), traffic direction, lane
<Structure design data> Subgrade type, subgrade materials, design CBR, design traffic flow volume, conversion equivalence thickness (T_A), pavement structure
<Mix design data> Aggregate grading (Surface & binder courses), Marshall test values, dynamic stability, optimum asphalt content, designated asphalt content
<Material data> Various test values of asphalt used, various test values of aggregates used
<Construction data> Degree of compaction at site, density at site, course thickness, flatness, skid resistance values, equipment used
<Surface condition data> Maximum rutting depth, rutting profile (at 5 points across), degree of cracking, date surveyed

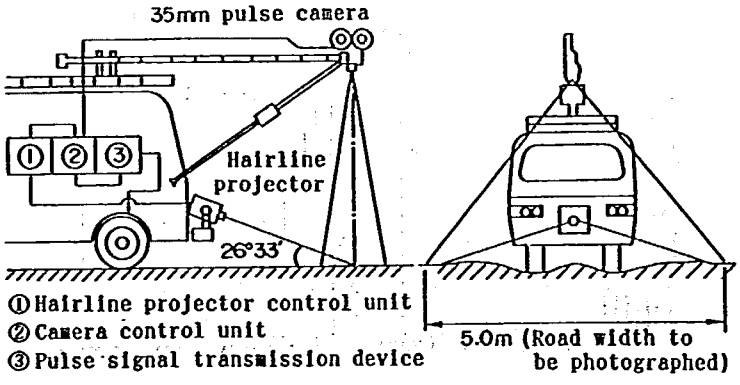


Fig. 2 Surface Condition Surveying Vehicle

<Sections requiring repair>

管理局：東京第一管理局　　予測年度：昭和61年度
事務所：横浜管理事務所　　測定年度：昭和57年度
路　線：(1010)　東名高速道路　　修繕年度：60

修繕条件：わだち掘れ＝15mm、L＝300m／500m

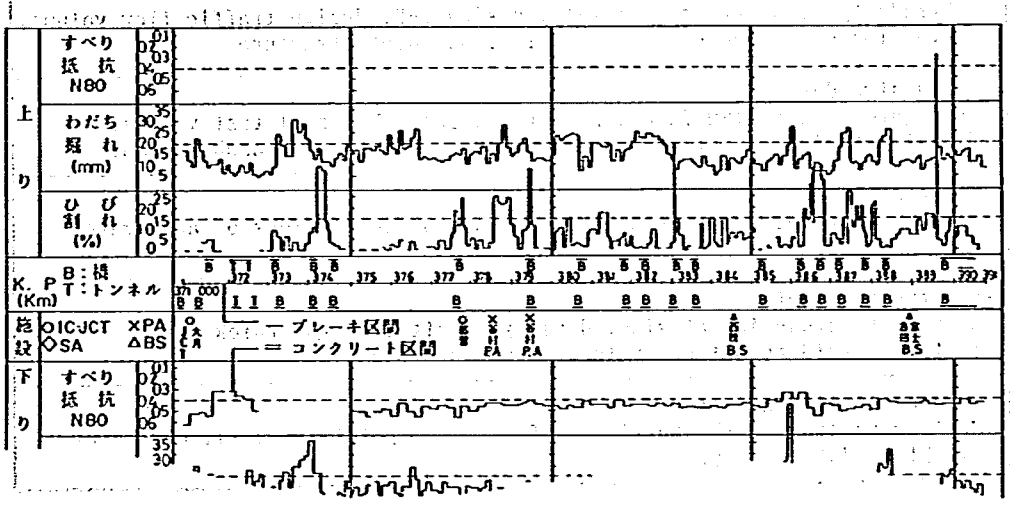
上下	車線		距離程 (自) (km)		(至) (km)	延長 (m)	わだち掘れ平均値 (mm)	わだち掘れ量					
下り	第1走行	●	3.100	-	3.600	500	16.2	B 16.2	B 16.2	B 16.2	B 15.2	B 16.2	
下り	第1走行	●	3.600	-	4.100	500	16.2	B 16.2	B 16.2	B 16.2	B 16.2	B 16.2	
下り	第1走行	●	4.100	-	4.600	500	16.2	B 16.2	B 16.2	B 16.2	B 16.2	B 16.2	
下り	第1走行	●	4.600	-	5.100	500	16.2	B 16.2	16.2	16.2	16.2	16.2	
下り	第1走行	●	5.100	-	5.600	500	16.2	16.2	16.2	16.2	B 16.2	B 16.2	
下り	第1走行	●	5.600	-	6.100	500	16.2	B 16.2	B 16.2	16.2	16.2	16.2	
下り	第1走行	●	6.100	-	6.600	500	16.2	16.2	16.2	16.2	16.2	16.2	
下り	第1走行	●	6.600	-	7.100	500	16.2	16.2	16.2	16.2	16.2	16.2	
下り	第1走行	●	7.100	-	7.600	500	16.2	16.2	16.2	B 16.2	B 15.2	B 16.2	
下り	追越		50.400	-	50.900	500	15.0	15.0	15.0	15.0	15.0	15.0	
下り	追越	●	50.900	-	51.400	500	15.0	15.0	15.0	15.0	15.0	15.0	
下り	追越	●	51.400	-	51.900	500	15.0	15.0	B 15.0	B 15.0	15.0	15.0	
下り	追越	●	51.900	-	52.400	500	15.0	15.0	15.0	15.0	15.0	15.0	
下り	追越	●						15.0	15.0	15.0	15.0	15.0	
										15.0	15.0	15.0	

B - Bridge
T - Tunnel
● Consecutive Section

<Surface Conditions>

年度：58
路線：(1101)　中央・富士吉田線
車線：追　越

調査年月　ひびわれ　：昭和58年5月
わだち掘れ：昭和58年5月
すべり抵抗：昭和58年6月



<Distribution of Rutting>

予測年度：昭和59年度　測定年度：昭和59年度　修繕年度：なし
路線：東名高速道路　　事務所：横浜管理事務所
ＩＣ：東京　　－東名川崎
上下：上り　　車線：第一走行　　路面種別：アスファルト

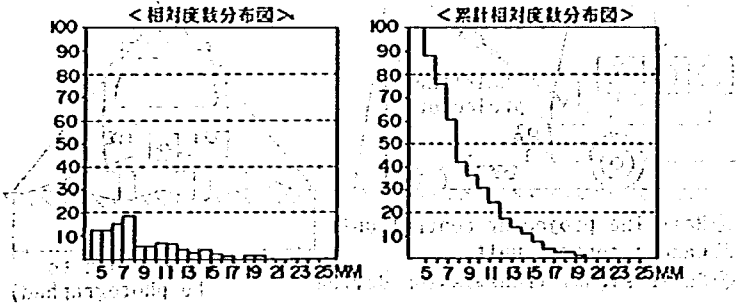


Fig. 3 Output Examples

The maximum rutting depth per 100 meter section means the average of the maximum rutting depths measured at two or more cross sections within the section. The estimated additional depths per year are given to each sector between interchanges, lane, and road structure (cut or embanked section, bridge, or tunnel) in the regular survey year and stored as yearly increased rutting depth data by the laboratory. All data required for the maintenance subsystem are prepared by the laboratory and supplied to each operation bureau as a set of a magnetic tape and a floppy disk.

The data flow is as shown in Fig. 4.

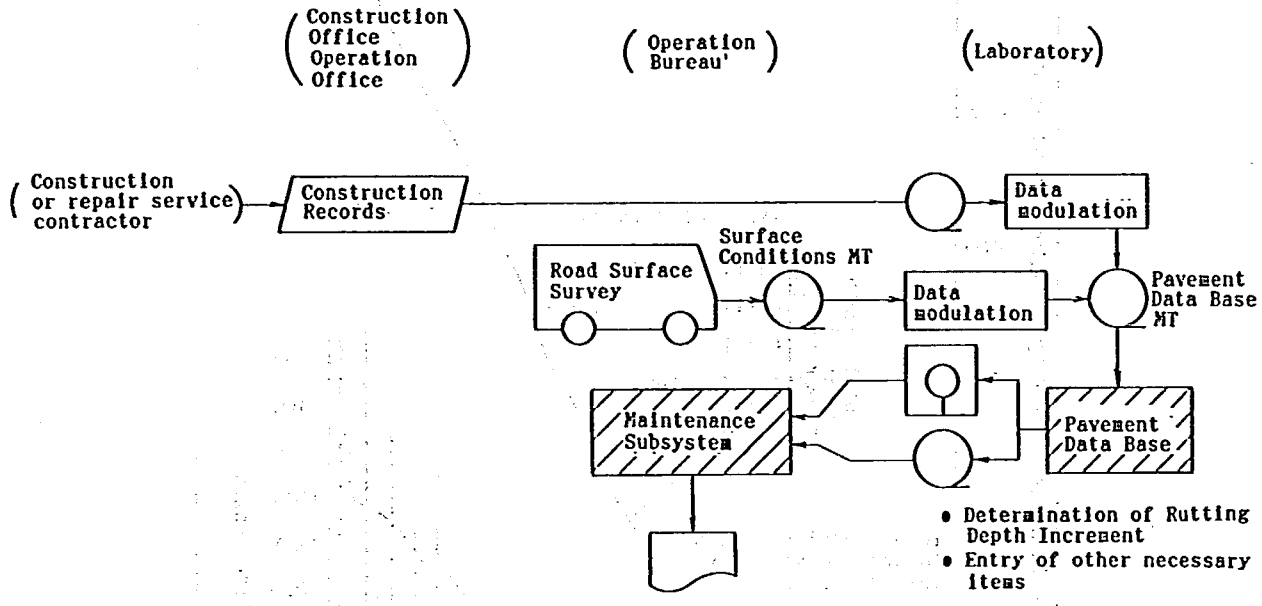


Fig.4 Data Flow

1.2 THE DESCRIPTION OF PAVEMENT DAMAGES AND REPAIRS

Figure 5 shows the changes in the length of pavement repaired by the types of repair based on data stored in the database. Although some repair service data are omitted due to delays in collection or checking processes, it is clear that the majority of damages caused to expressway pavements are by rutting and that rutting caused by abrasion has substantially increased as the length of expressway in service has increased in cold areas.

The total repaired lane length per year by types of damage and the ratio of lane length with a maximum rutting depth of 20 mm or more to the total length are shown in Figs. 6 and 7, respectively, by the respective routes. The rutting caused by abrasion progresses faster than rutting produced by flow and, consequently, pavement repairs in cold areas occur more frequently than in other areas. In spite of the more frequent repairs, the pace of repair cannot apparently keep up with the pace at which rutting progresses in cold areas.

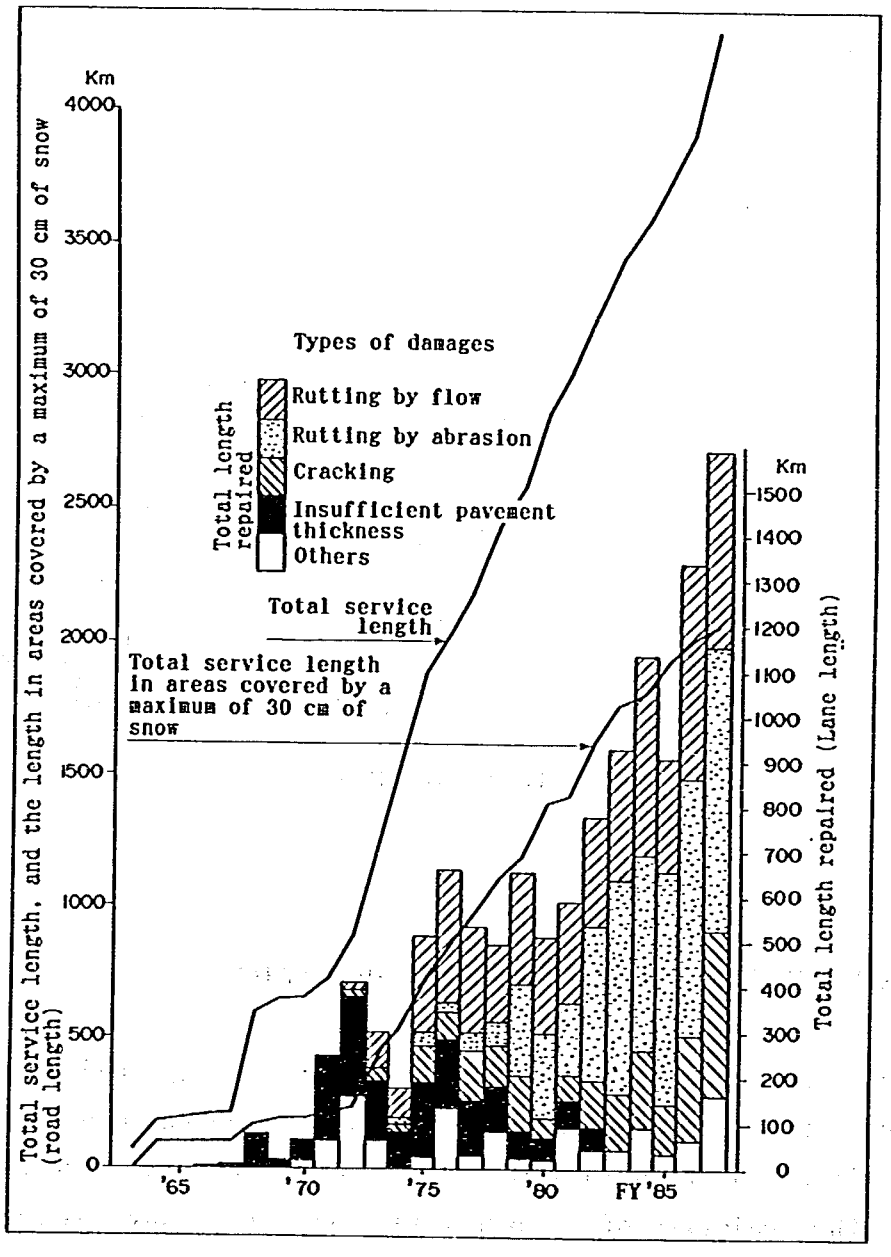


Fig. 5. Changes in the Length of Pavement Repairs on Japanese Expressways by Damage Types (Data Stored in the Data Base)

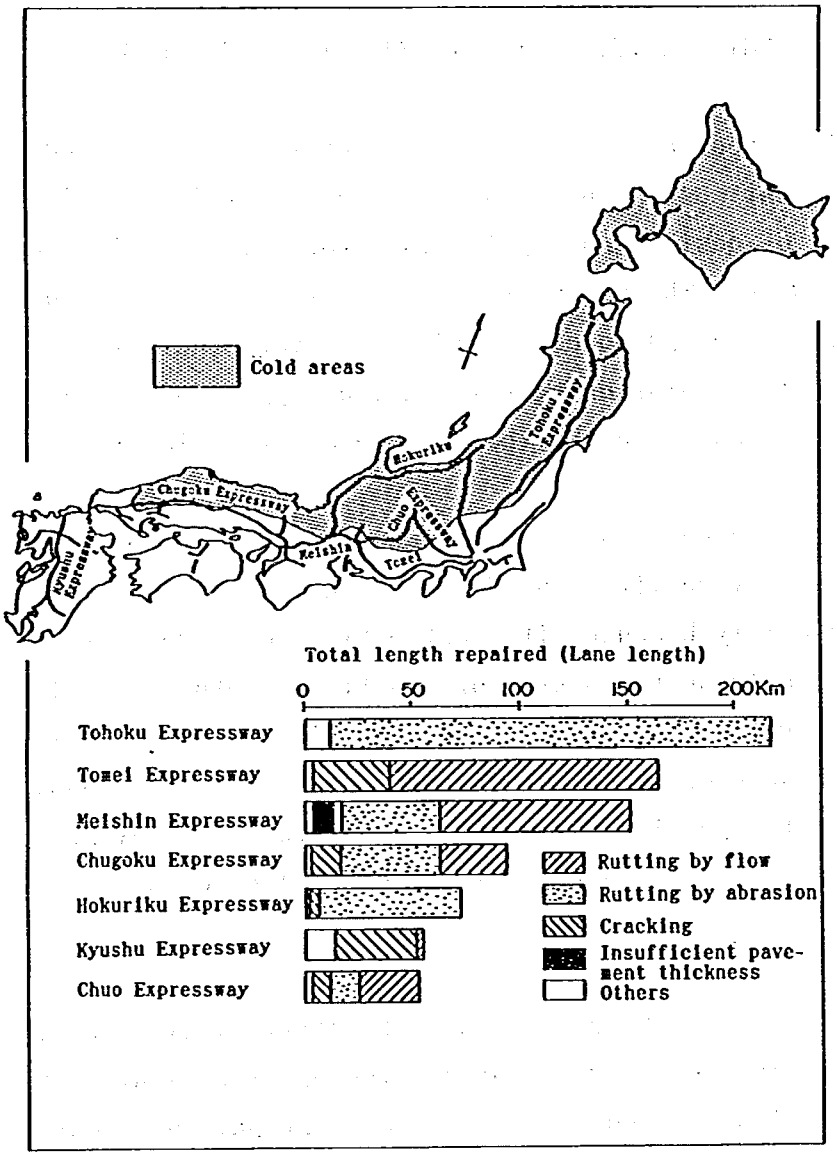


Fig. 6. The Length of Repaired Road on Major Expressways by Damage Types (The average values of 1982 - 1987)

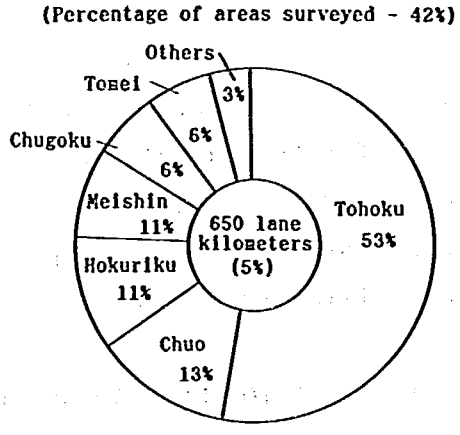


Fig. 7. The Proportion of Sections with Rutting Deeper than 20 mm to the Total Section Length (Surveyed 1980 - 1985)

2. ANALYSIS OF FACTORS CAUSING RUTTING IN PAVEMENTS IN COLD AREAS

Since pavement has to be maintained and repaired for use over a long period, necessary investments on pavement must be planned on the basis of its entire service life and, the premise of design and repair plans for pavement is to minimize the service life costs. The pavement management system may be defined as the tool for serving such purposes provided, however, that it is possible to estimate adequately secular changes in various types of damage affecting the serviceability (or change in the inclusive evaluation index).

The pavement management system has been under development by the Corporation as mentioned earlier. The service life consideration has not yet been incorporated in the system mainly because its estimation of prospective rutting depth is still made only on the basis of rutting depth actually measured in each sector. The system, therefore, is not applicable to a newly constructed sector of which such measured values are not available and, furthermore, the system cannot cope with any changes made to the pavement after a repair (such as the type of pavement or mixing design) or changes in the traffic conditions.

In this chapter, we intend to discuss the results of our statistical study, made for the purpose of formulating the progress of rutting on expressways in cold areas, using such information incorporated in the current pavement data base as rutting depth per 100 m and other pavement data together with the prevailing traffic and climatic conditions.

2.1 SELECTION OF ROAD SECTIONS FOR STATISTICAL STUDY

We have selected road sections for statistical study according to the following conditions:

1) Located to the north of Koriyama Interchange (IC) of Tohoku Expressway,

2) No repair has been made during the period between two last road surveys,

3) A part of the nearside lane of a circular curve is built on a cut or

embanked section,

4) Rutting data are obtainable at least at two sections located in a sector of the same construction between the same two interchanges,

5) If sections were repaired in the past, the repair was by milling and overlay method and made not more than once.

The reason for limiting the location to sectors on Tohoku Expressway (to the north of Koriyama IC) is partly because expanding the target area unnecessarily would render the study inefficient when we have not yet clearly defined the factors affecting the progress of rutting and, also because we anticipate some information on the relationship between climate and rutting as the route stretches over a long distance from south to north in a succession of varying climatic conditions.

Road surface inspections were performed over Tohoku Expressway recently in May, 1985 and September, 1987. We have decided to take the increase in rutting depths over the period (28 months) between the two inspections as the needed data. Sections of the road which have undergone repairs between the two inspections have been excluded as data sources from the analytical data.

With regard to different types of road structures, lanes and horizontal alignments, we have determined that it would be better to analyze one type of them separately rather than treating them as variables. Therefore, we have selected one type of each for the analysis. We have selected sections cut or embanked which comprise 70% of the entire expressway as the typical structure type, the nearside lane for the typical lane where rutting develops faster and also selected sections of circular curve rather than of clothoid curve as it is easier for numerical evaluation.

The reason why we have made it a condition to be able to obtain rutting data at least at two sections of the same construction between the same two interchanges is because we wanted to avoid evaluating the quality of pavement with data obtained from a limited part of the pavement.

We have limited the type of repair work acceptable to the milling and overlay method and also the number of repairs made to only once because we have determined that the method represents the typical type of repairs done to expressways and that the pavement which has undergone repair only once usually retains pavement characteristics similar to a newly paved surface.

The distribution of 1025 sections thus selected is as shown in Fig. 8.

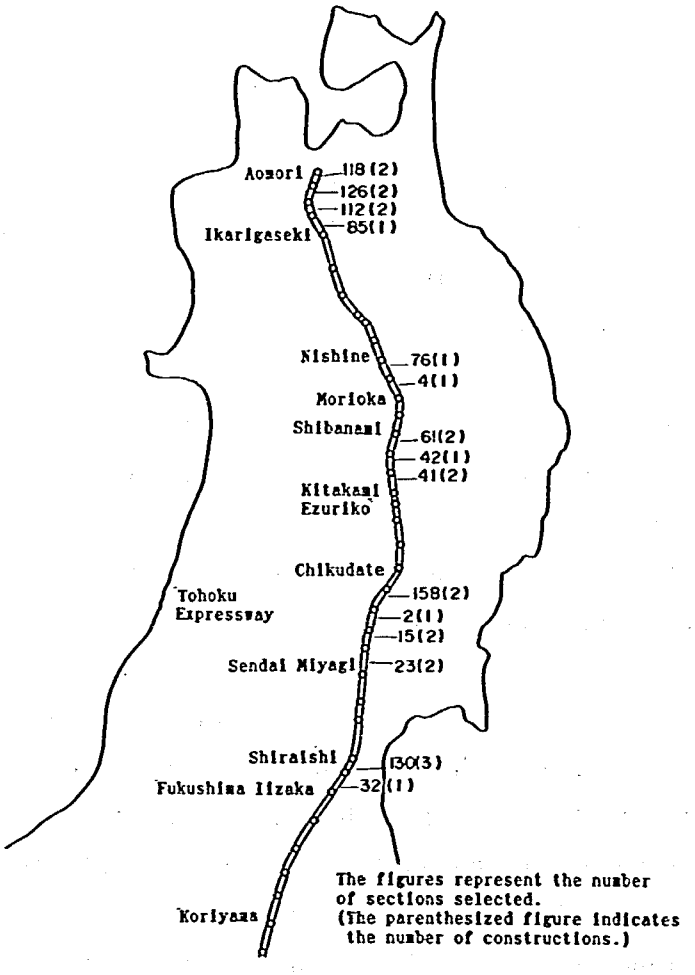


Fig. 8. Distribution of Sections Selected for Analysis

2.2 QUANTIFICATION THEORY OF THE FIRST TYPE

Factors determined as pertaining to rutting are listed in Table 2. The selection of factors, however, has been limited to those easily available with due consideration to the possibility of extending the analysis to the entire Japanese expressway system. Road characteristics, construction conditions and

the details of pavement have been limited to those actually stored in the pavement data base and also to such items commonly input at regular paving work. With regard to information related to traffic characteristics, we have adopted the cross section traffic volume by cars classified according to toll road vehicle classes. With regard to climatic conditions, we have chosen five factors; the maximum and minimum annual temperatures, the number of summer days (days of the highest temperature of 25° C or higher), the number of winter days (days of the lowest temperature of 0° or lower), the number of snow-covered days (days with snow depth 3 cm or more), from the "Annual Report of Climatological Stations" published by the Japan Meteorological Agency. We have collected average values of these factors as recorded at climatological stations nearest to the related road sections during 1979 to 1986 to be used as climatic data for the analysis.

Table 2. Items Inspected as Factors Causing Rutting

<Road characteristics> Circular curve radius, right hand or left hand curve, longitudinal grade, traffic direction
<Construction conditions> Construction month
<Climatic conditions> Annual maximum temperature, annual minimum temperature, annual number of summer days, annual number of winter days, annual number of snow-covered days
<Traffic characteristics> Cross sectional traffic volume, cross sectional traffic volume of heavy vehicles (heavy and extra heavy vehicles of 3 vehicle types according to toll classification), percentage of heavy vehicles
<Pavement characteristics> Elapsed time since pavement applied, Marshall test values, optimum asphalt content, designated asphalt content, penetration, softening point, penetration index, specific gravity of aggregates used, aggregate grading

The increase in rutting depth is obtained from the following equation:

$$Y = \text{Constant} + f(r_i) + f(c_i) + f(m_i) + f(t_i) + f(x_i) \quad \ldots\ldots (1)$$

where:

Y = increment of rutting depth

r_i = variable to represent road characteristics

c_i = variable to represent construction conditions
m_i = variable to represent climatic conditions
t_i = variable to represent traffic characteristics
x_i = variable to represent pavement characteristic

x_i remains same for all sections within a paving work, and we can also consider m_i and t_i to remain same within a paving work since a paving work does not normally extend further than 20 km. Therefore, numbering a paving work "n", it can be expressed as follows:

$$Y = \text{Constant} + f(r_i) + f(c_1) + f(n) \quad \ldots\ldots(2)$$

where:
r_1 = the radius of a circular curve
r_2 = right or left curve
r_3 = longitudinal grade
r_4 = upslope, downslope, or level
c_1 = the month of paving work
n = the paving work number

Quantification theory I is a multivariate analysis method where the criterion variable is quantitatively measurable and all explanatory variables are qualitative and, the estimation formula for the increment of rutting depth "Y" can be obtained with this method where r_1 (the radius of a circular curve) shall be expressed in a hierarchical rank and r_3 (longitudinal grade) as upslope, downslope or level.

The combinations of various items, multiple correlation coefficients and residual standard deviations in Quantification theory I are shown in Table 3. Most of these were found to be meaningless with the exception of the work number and the radius of circular curve (multiple correlation coefficients and residual standard deviations can not be largely improved) and, therefore, the desired rutting depth would be expressed as in equation (3) below, using the work number and the radius of circular curves only.

$$Y = \underbrace{9.53 + (a_1, a_2, \ldots, a_{16}) \begin{bmatrix} 1 & & & \\ & 1 & 0 & \\ & & \ddots & \\ & 0 & & 1 \end{bmatrix}}_{\text{(A) The category scores of work number; Work number 1 2 ...16}} + \underbrace{(b_1, b_2, \ldots, b_{11}) \begin{bmatrix} 1 & & & \\ & 1 & 0 & \\ & & \ddots & \\ & 0 & & 1 \end{bmatrix}}_{\text{(B) The category scores of circular curve radius ranks; Circular curve radius ranks 1 2 ...11}} \quad \ldots.(3)$$

Therefore:

$$\begin{bmatrix} a_1 \\ a_2 \\ a_3 \\ a_4 \\ a_5 \\ a_6 \\ a_7 \\ a_8 \\ a_9 \\ a_{10} \\ a_{11} \\ a_{12} \\ a_{13} \\ a_{14} \\ a_{15} \\ a_{16} \end{bmatrix} = \begin{bmatrix} -2.11 \\ -0.11 \\ -1.95 \\ -1.94 \\ -18.03 \\ -0.21 \\ 1.34 \\ 6.44 \\ 0.00 \\ 2.47 \\ 3.56 \\ 1.73 \\ 1.61 \\ 6.61 \\ 9.00 \\ 2.92 \end{bmatrix} \qquad \begin{bmatrix} b_1 \\ b_2 \\ b_3 \\ b_4 \\ b_5 \\ b_6 \\ b_7 \\ b_8 \\ b_9 \\ b_{10} \\ b_{11} \end{bmatrix} = \begin{bmatrix} -9.19 \\ -2.24 \\ -2.01 \\ -1.32 \\ -1.57 \\ -1.73 \\ -2.28 \\ -2.23 \\ 0.00 \\ 0.00 \\ 0.21 \end{bmatrix}$$

Circular curve (m)	
	~ 500
500	~ 750
750	~1000
1000	~1500
1500	~2000
2000	~3000
3000	~4000
4000	~5000
5000	~7500
7500	~10000
10000	~

Multiple correlation coefficient: 0.644

Residual standard deviation : 4.452

The equation (3) above can be divided into two parts, (A) and (B), and expressed as $Y = Y_A + Y_B$. Y_B indicates that the larger the circular curve radius (the closer it becomes to a straight line), the faster the rutting

progresses, whereas Y_A provides no information as it is, but must be expressed by m_i, t_i, and x_i instead.

Multiple regression analysis performed will be discussed in 2.4 below and, it must be noted that the residual standard deviation in the Quantification theory I is an estimation error at this stage and is not to be solved by the subsequent multiple regression analysis. The final estimation error of rutting depth should be the sum of the estimation errors derived from the Quantification theory I and the multiple regression analysis. In other words, although it is not possible to determine the residual standard deviation at an accuracy above the level of 4.45 mm, it should be considered tolerable as seen from the level of actual measurement accuracy of rutting depth (+/-3 mm tolerance is accepted as the measurement is taken from a vehicle running at a speed of up to 60 km/h) or the partial inconsistency of pavement resulted from actual paving work.

Table 3. The Combinations of Items at Quantification Theory I

Combination number	Items						Multiple correlation coefficient	Residual standard deviation
	Paving work number	Circular curve radius	Paving work month	Longitudinal grade	RH or LH curve	Traffic direction		
1	o						0.602	4.546
2	o	o					0.644	4.452
3	o	o	o				0.649	4.433
4	o	o	o	o			0.650	4.433
5	o	o	o	o	o		0.651	4.433
6	o	o	o	o	o	o	0.651	4.435

2.3 PRINCIPAL COMPONENT ANALYSIS

As mentioned, climatic conditions chosen as influential to the progress of rutting depth are the maximum and minimum annual temperatures, the numbers of summer, winter, and snow-covered days. There are strong correlations between the maximum annual temperature and the number of summer days and between the minimum annual temperature and the number of winter days (see Table 4). Therefore, a possibility exists that the problem of multicolinearity may be

generated by using all these factors as explanatory variables in a multiple regression analysis. Although the problem may be eliminated by excluding the maximum temperature (or the number of summer days) and the minimum temperature (or the number of winter days) from the explanatory variables. We were concerned that insufficient number of explanatory variables might result in an insufficient explanation and, therefore, we have decided to retain at least these five elements which are considered necessary to express climatic conditions throughout a year properly.

The principal component analysis is a method of analyzing an object as a whole instead of scrutinizing each factor separately. We can utilize this method for solving the problem of multicolinearlity as mentioned above. It derives from the fact that, for example, even if there is a strong correlation between factors x_1 and x_2, such a strong correlation may not in principle be applicable to their principal components z_1 and z_2 (See Fig. 9). Even if either of z_1 or z_2 needs to be left out of the explanatory variables, the influence of both x_1 and x_2 can still be evaluated with the remaining component.

Table 4. Correlation Coefficient Matrix of Climatic Factors

	Annual maximum temperature	Annual minimum temperature	Annual number of summer days	Annual number of winter days	Annual number of snow-covered days
Annual maximum temperature		0.721	0.952	-0.685	-0.646
Annual minimum temperature	0.721		0.747	-0.972	-0.694
Annual number of summer days	0.952	0.747		-0.708	-0.706
Annual number of winter days	-0.686	-0.972	-0.708		-0.673
Annual number of snow-covered days	-0.646	-0.694	-0.706	0.673	

: Correlation coefficient above 0.70

: Correlation coefficient above 0.90

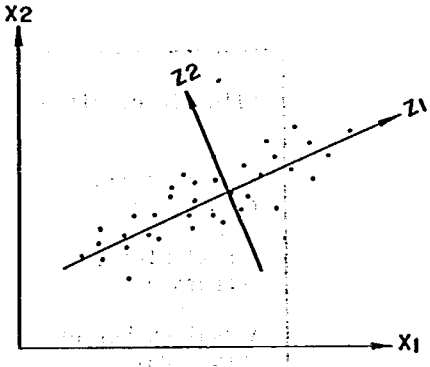


Fig. 9. Concept of Principal Component Analysis

In the analysis of principal components, a large number of variables, x_1, $x_2,\ldots,x_p$, shall be substituted by a small number of independent general indices z_1, $z_2,\ldots,$ z_m where principal component "z_i" is expressed as $z_i = a_{i1}x_1+a_{i2}x_2+\ldots+a_{ij}x_j+\ldots+a_{ip}x_p$. The vector of coefficients $\{a_{i1}, a_{i2},\ldots, a_{ip}\}$ are called i-th eigenvectors and are calculated so as to minimize the loss of information. Furthermore, the eigenvectors are orthogonal to each other. The value of each sample on the z_i axis is called the i-th principal component score of the sample and will be used as an explanatory variable in the subsequent multiple regression analysis.

The results of a principal component analysis performed on the five factors representing climatic conditions are as shown in Table 5. The scope of this analysis was extended to include seven other main expressways besides Tohoku Expressway to meet our prospective need for nationwide analyses in future. There are two different units of the temperature (°C) and the number of days to the factors and, also, the factors can not be directly compared with each other even if they take the same unit. The data, therefore, have been standardized so that each factor becomes 0 in the average value and 1 in the standard deviation ($x \rightarrow (x-x_{mean})/ s_x$).

Table 5. Results of Principal Component Analysis of Climatic Conditions

Climatic conditions	Eigenvectors				
	1st	2nd	3rd	4th	5th
Annual maximum temperature	0.448	0.530	0.256	-0.670	0.060
Annual minimum temperature	0.463	-0.456	0.213	0.095	0.724
Annual number of summer days	0.460	0.480	0.127	0.725	-0.124
Annual number of winter days	-0.452	0.529	-0.225	0.091	0.676
Annual number of snow-covered days	-0.412	0.021	0.907	0.088	-0.002
Eigenvalue	4.008	0.533	0.388	0.045	0.026
Proportion	0.802	0.107	0.078	0.009	0.005
Cumulative proportion	0.802	0.908	0.986	0.995	1.000

The next problem is how to evaluate the aggregate gradings. The influence of aggregate grading can not be evaluated simply by the volume of aggregates passing through a 2.36 mm sieve, but it needs to be more precisely analyzed by values on which the entire grading curve is reflected. Although the grading curve is usually represented by the cumulative distribution of percentages, there are inevitable correlations between the adjacent percentages of passing aggregate volumes and using all of the grading passing sieves of different sizes as explanatory variables will most probably result in generating the problem of multicolinearity like in the case of climatic conditions. This problem, however, can be solved by depicting the distribution of different particle sizes by the mixing ratio of aggregate (See Fig. 10, Table 6.)

However, it will result in the inefficiency of depicting one grading curve with 10 explanatory variables, therefore, it is more recommendable to perform the principal component analysis as in the case of climatic conditions.

The results of the principal component analysis on the mixing ratio of aggregate are listed in Table 7. The scope of analysis encompasses 7 main expressways in addition to Tohoku Expressway in the same manner as for climatic conditions where the data were collected from 379 paving works selected according to the same rule as the selection of road sections for the rutting depth increment data.

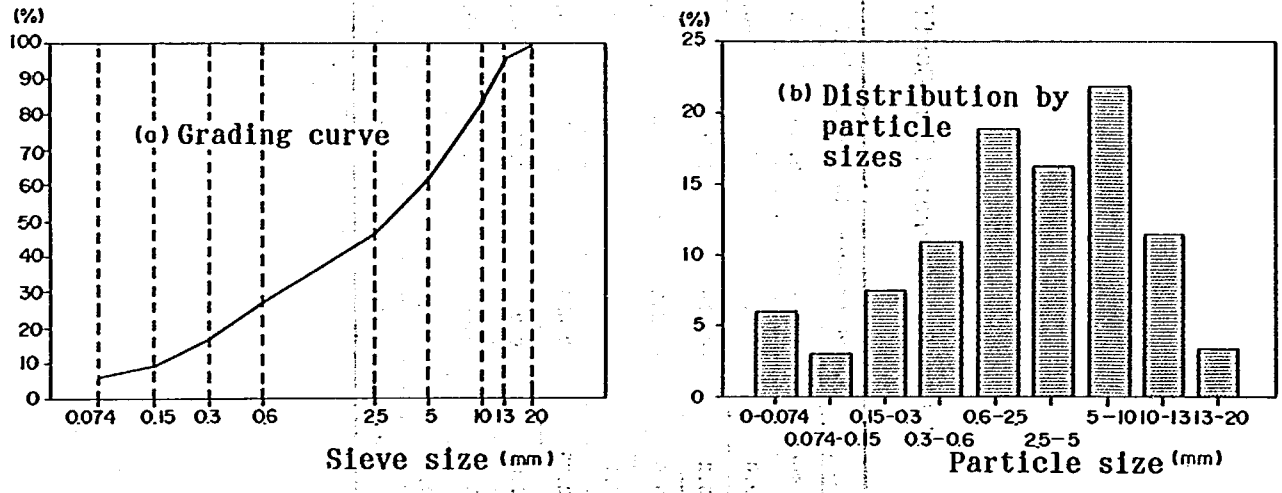


Fig. 10. Expression of Aggregate Grading

Table 6. Correlation Coefficient Matrix of Aggregate Mixing Ratios by Particle Sizes

	19.0 mm or more	13.2 - 19.0	9.5 - 13.2	4.75 - 9.5	2.36 - 4.75	0.6 - 2.36	0.6 - 0.3	0.15 - 0.3	0.075 - 0.15	0.075 mm or less
19.0 mm or more		0.831	-0.236	-0.602	-0.386	-0.005	0.040	0.085	0.003	-0.025
13.2 - 19.0	0.831		-0.267	-0.706	-0.434	-0.125	0.135	0.101	-0.069	0.011
9.5 - 13.2	-0.236	-0.267		-0.245	0.159	0.043	-0.036	-0.194	0.106	-0.213
4.75 - 9.5	-0.602	-0.706	-0.245		0.044	-0.032	-0.121	-0.014	-0.048	0.129
2.36 - 4.75	-0.386	-0.434	0.159	0.044		-0.015	-0.243	-0.227	0.105	-0.543
0.6 - 2.36	-0.055	-0.125	0.043	-0.032	-0.015		-0.421	-0.484	-0.006	-0.050
0.3 - 0.6	0.040	0.135	-0.036	-0.121	-0.243	-0.421		-0.136	-0.276	0.223
0.15 - 0.3	0.085	0.101	-0.194	-0.014	-0.227	-0.484	-0.136		-0.073	0.122
0.075 - 0.15	0.003	-0.069	0.106	-0.048	0.105	-0.006	-0.276	-0.073		-0.202
0.075 mm or less	-0.025	0.011	-0.213	0.129	-0.543	-0.050	0.223	0.122	-0.202	

: Correlation coefficient above 0.70

Table 7. Results of Principal Component Analysis of Aggregate Grading

Particle size	Eigenvectors				
	1st	2nd	3rd	4th	5th
19.0 mm or more	0.510	-0.245	0.040	-0.121	-0.097
13.2 - 19.0	0.551	-0.208	0.012	-0.035	-0.115
9.5 - 13.2	-0.154	-0.273	-0.123	0.443	0.593
4.75 - 9.5	-0.376	0.435	0.087	-0.223	-0.125
2.36 - 4.75	-0.375	-0.285	-0.312	0.076	-0.420
0.6 - 2.36	-0.146	-0.282	0.702	-0.129	-0.025
0.3 - 0.6	0.192	0.283	-0.101	0.663	-0.089
0.15 - 0.3	0.168	0.273	-0.484	-0.425	0.145
0.075 - 0.15	-0.098	-0.286	-0.165	-0.310	0.520
0.075 mm or less	0.158	0.485	0.337	0.011	0.364
Eigenvalues	2.761	1.909	1.362	1.276	0.948
Proportion	0.276	0.191	0.136	0.128	0.095
Cumulative proportion	0.276	0.467	0.603	0.731	0.826

2.4 MULTIPLE REGRESSION ANALYSIS

In this multiple regression analysis, the criterion variable is the portion (A) of the above equation (3) and the explanatory variables used are as follows:

mz_i: the "i-th" principle component score related to the climatic conditions (i = 1 - 5)

t_1: accumulated cross sectional traffic volume between two road surface inspections, t_2: accumulated cross sectional traffic volume of heavy vehicles, t_3: the percentage of heavy vehicles

x_1: the number of elapsed months since the last pavement work,
x_2: density, x_3: stability, x_4: air voids,
x_5: flow value, x_6: residual stability, x_7: the value stability/flow
X_8: the optimum asphalt content, x_9: the designated asphalt content,
x_{10}: the penetration, x_{11}: softening point, x_{12}: penetration index,
x_{13}: specific gravity of aggregate,

gz_i: the "i-th" principal component score of aggregate grading (i = 1 - 5)

Table 8. Correlation Coefficient Matrix of Explanatory Variables Applied to Multiple Regression Analysis

			az_1	az_2	az_3	az_4	az_5	t_1	t_2	t_3	x_1	x_2	x_3	x_4	x_5	x_6
1st elastic principal component score		az_1		-0.494	-0.527	0.211	0.449	0.713	0.826	0.765	-0.667	0.112	-0.285	0.050	0.451	0.431
2nd elastic principal component score		az_2	-0.494		0.279	-0.477	-0.689	-0.244	-0.251	-0.035	0.100	-0.168	-0.278	-0.042	0.126	-0.174
3rd elastic principal component score		az_3	-0.527	0.279		0.294	0.214	-0.651	-0.844	-0.455	0.769	0.003	0.579	-0.465	-0.374	-0.294
4th elastic principal component score		az_4	0.211	-0.477	0.294		0.692	-0.131	-0.098	0.030	0.169	0.001	0.356	-0.221	0.188	-0.066
5th elastic principal component score		az_5	0.449	-0.689	0.214	0.692		-0.178	-0.026	0.256	0.234	0.232	0.444	-0.225	-0.109	-0.016
Accumulated cross sectional traffic volume		t_1	0.713	-0.244	-0.651	-0.131	-0.178		0.927	0.561	-0.943	-0.095	-0.673	0.265	0.583	0.424
Accumulated cross sectional traffic volume of heavy vehicles		t_2	0.826	-0.251	-0.844	-0.098	-0.026	0.927		0.754	-0.909	0.046	-0.606	0.234	0.568	0.453
Percentage of heavy vehicles		t_3	0.765	-0.035	-0.455	0.030	0.256	0.561	0.754		-0.601	0.294	-0.420	-0.087	0.444	0.387
Number of months elapsed since pavement applied		x_1	-0.667	0.100	0.769	0.169	0.234	-0.943	-0.909	-0.601		0.031	0.652	-0.056	-0.671	-0.504
Marshall test values:	Density	x_2	0.112	-0.168	0.003	0.001	0.232	-0.095	0.046	0.294	0.031		0.503	-0.519	-0.165	0.200
	Stability	x_3	-0.285	-0.278	0.579	0.356	0.444	-0.673	-0.606	-0.420	0.652	0.503		-0.435	-0.374	-0.156
	Air voids	x_4	0.050	-0.042	-0.465	-0.221	-0.225	0.265	0.234	-0.087	-0.056	-0.519	-0.435		-0.100	-0.074
	Flow value	x_5	0.451	0.126	-0.374	0.188	-0.109	0.583	0.568	0.444	-0.671	-0.165	-0.374	-0.100		0.207
	Residual stability	x_6	0.431	-0.174	-0.294	-0.066	-0.016	0.424	0.453	0.387	-0.504	0.200	-0.156	-0.074	0.207	
	Stability/flow value	x_7	-0.495	-0.258	0.523	-0.001	0.249	-0.735	-0.708	-0.556	0.791	0.327	-0.717	-0.055	-0.906	-0.195
Optimum asphalt content		x_8	0.069	0.103	0.254	0.257	0.189	-0.147	-0.136	-0.017	0.103	-0.547	-0.214	0.261	0.184	0.047
Designated asphalt content		x_9	-0.018	0.098	0.328	0.203	0.201	-0.248	-0.234	-0.071	0.198	-0.509	-0.158	0.271	-0.017	-0.030
Penetration at 25°C		x_{10}	-0.150	-0.357	0.011	-0.308	0.033	-0.214	-0.222	-0.433	0.349	0.231	0.451	0.085	-0.611	0.034
Softening point		x_{11}	0.229	0.090	0.098	0.637	0.285	0.119	0.152	0.363	-0.150	-0.195	-0.233	-0.109	0.515	-0.221
Penetration index		x_{12}	0.237	-0.210	0.160	0.731	0.487	-0.000	0.047	0.186	0.072	-0.090	0.047	-0.097	0.257	-0.294
Specific gravity of aggregate		x_{13}	0.236	-0.201	0.174	0.195	0.610	-0.238	-0.039	0.451	0.166	0.562	0.209	-0.245	-0.262	0.062
1st grading principal component score		gz_1	-0.679	0.297	0.615	-0.317	-0.035	0.827	0.783	-0.450	0.655	0.030	0.413	-0.610	0.784	-0.384
2nd grading principal component score		gz_2	0.512	-0.203	-0.361	0.254	0.027	0.598	0.596	0.479	-0.624	0.276	-0.259	-0.251	0.381	0.293
3rd grading principal component score		gz_3	-0.285	-0.071	0.409	-0.124	0.398	-0.653	-0.532	-0.161	0.625	0.312	0.541	0.152	0.542	-0.233
4th grading principal component score		gz_4	-0.316	-0.199	0.594	0.148	0.263	-0.591	-0.583	-0.457	0.635	0.212	0.655	-0.337	-0.634	-0.175
5th grading principal component score		gz_5	0.680	-0.145	-0.661	0.051	-0.119	0.879	0.834	0.522	-0.906	-0.079	-0.483	-0.044	0.732	0.379

			x_7	x_8	x_9	x_{10}	x_{11}	x_{12}	x_{13}	gz_1	gz_2	gz_3	gz_4	gz_5
1st elastic principal component score		az_1	-0.495	0.069	-0.018	-0.150	0.229	0.237	0.236	-0.679	0.512	-0.285	-0.316	-0.680
2nd elastic principal component score		az_2	-0.208	0.103	0.098	-0.357	0.090	-0.210	-0.201	0.297	-0.203	-0.071	-0.199	-0.145
3rd elastic principal component score		az_3	0.523	0.254	0.328	0.011	0.098	0.160	0.174	0.615	-0.361	0.409	0.594	0.651
4th elastic principal component score		az_4	-0.001	0.257	0.203	-0.308	0.637	0.731	0.195	-0.317	0.254	-0.124	0.148	0.051
5th elastic principal component score		az_5	0.249	0.189	0.201	0.033	0.285	0.487	0.610	-0.035	0.027	0.358	0.263	-0.119
Accumulated cross sectional traffic volume		t_1	-0.735	-0.147	-0.248	-0.214	0.119	-0.000	-0.238	-0.827	0.598	-0.653	-0.591	0.879
Accumulated cross sectional traffic volume of heavy vehicles		t_2	-0.708	-0.136	-0.234	-0.222	0.152	0.047	-0.039	-0.783	0.596	-0.532	-0.583	0.834
Percentage of heavy vehicles		t_3	-0.556	-0.017	-0.071	-0.433	0.363	0.186	0.451	-0.450	0.479	-0.161	-0.457	0.522
Number of months elapsed since pavement applied		x_1	0.791	0.103	0.198	0.349	-0.150	0.072	0.166	0.655	-0.624	0.625	0.635	-0.906
Marshall test values:	Density	x_2	0.327	-0.547	-0.509	0.231	-0.195	-0.090	0.562	0.030	0.276	0.312	0.212	-0.079
	Stability	x_3	0.717	-0.214	-0.158	0.451	-0.233	0.047	0.209	0.413	-0.259	0.541	0.655	-0.483
	Air voids	x_4	-0.055	0.261	0.271	0.085	-0.109	-0.097	-0.245	-0.010	-0.251	-0.152	-0.337	-0.044
	Flow value	x_5	-0.906	0.184	-0.017	-0.611	0.515	0.257	-0.262	-0.785	0.381	-0.542	-0.634	0.732
	Residual stability	x_6	-0.195	0.047	-0.030	0.034	-0.221	-0.294	0.062	-0.384	0.293	-0.233	-0.175	0.379
	Stability/flow value	x_7		-0.192	-0.027	0.660	-0.504	-0.192	0.273	0.752	-0.431	0.637	0.731	-0.822
Optimum asphalt content		x_8	-0.192		0.852	-0.301	0.333	0.247	0.193	0.602	-0.171	-0.076	-0.179	-0.139
Designated asphalt content		x_9	-0.027	0.852		-0.255	0.250	0.160	0.268	0.145	-0.164	0.020	-0.082	-0.290
Penetration at 25°C		x_{10}	0.660	-0.301	-0.255		-0.797	-0.343	-0.063	0.451	-0.246	0.295	0.541	-0.336
Softening point		x_{11}	-0.504	0.333	0.250	-0.797		0.841	0.153	-0.436	0.320	-0.337	-0.342	0.256
Penetration index		x_{12}	-0.192	0.247	0.160	-0.343	0.841		0.185	-0.287	0.231	-0.264	-0.645	0.107
Specific gravity of aggregate		x_{13}	0.273	0.193	0.268	-0.063	0.153	0.185		0.174	0.074	0.505	0.029	-0.347
1st grading principal component score		gz_1	0.752	0.002	0.145	0.451	-0.436	-0.287	0.174		-0.690	0.691	0.543	-0.909
2nd grading principal component score		gz_2	-0.431	-0.171	-0.164	-0.246	0.320	0.231	0.074	-0.690		-0.701	-0.190	0.608
3rd grading principal component score		gz_3	0.637	-0.176	-0.020	0.295	-0.337	-0.264	0.505	0.691	-0.701		0.313	-0.666
4th grading principal component score		gz_4	0.731	-0.179	-0.082	0.541	-0.342	-0.645	0.029	0.540	-0.190	0.313		-0.505
5th grading principal component score		gz_5	-0.822	-0.139	-0.290	-0.336	0.256	0.107	-0.347	-0.903	0.608	-0.666	-0.505	

Correlation coefficient above 0.70

Correlation coefficient above 0.90

Table 9. Combinations of Explanatory Variables in Multiple Regression Analysis

Number of explanatory variables			4										5										6																
1st climatic principal component score		az_1		O				O							O						O	O				O				O		O							
2nd climatic principal component score		az_2															O							O	O											O			
3rd climatic principal component score		az_3																																					
4th climatic principal component score		az_4	O	O		O	O		O	O	O	O	O		O	O		O	O		O	O				O	O		O	O		O		O	O	O		O	O
5th climatic principal component score		az_5																														O							
Accumulated cross sectional traffic volume		t_1																																					
Accumulated cross sectional traffic volume of heavy vehicles		t_2							O																														
Percentage of heavy vehicles		t_3				O												O																					
Number of months elapsed since pavement applied		z_1						O									O								O														
Marshall test values	Density	z_2									O		O												O	O	O			O				O	O	O			O
	Stability	z_3												O			O											O					O				O		
	Air voids	z_4					O	O												O	O		O									O							
	Flow value	z_5																						O													O		
	Residual stability	z_6																							O									O					
	Stability/flow value	z_7																	O														O					O	
Optimum asphalt content		z_8																																					
Designated asphalt content		z_9								O												O																	
Penetration at 25°C		z_{10}			O							O		O						O			O	O				O	O				O				O		O
Softening point		z_{11}	O	O	O	O	O	O	O	O	O	O	O	O	O	O		O	O	O	O	O	O	O		O	O	O	O	O		O	O	O	O	O	O	O	O
Penetration index		z_{12}			O									O						O			O	O				O	O				O		O		O		
Specific gravity of aggregate		z_{13}														O														O									
1st grading principal component score		gz_1	O	O	O	O	O		O	O	O	O	O	O	O	O	O	O	O	O	O	O	O	O	O	O	O	O	O	O		O	O	O	O	O	O	O	O
2nd grading principal component score		gz_2																					O																
3rd grading principal component score		gz_3																																					
4th grading principal component score		gz_4																									O											O	
5th grading principal component score		gz_5	O										O		O	O	O	O	O						O	O	O	O	O					O	O	O		O	O
																										•	•				•			•		•		•	

Number of explanatory variables			6								7									
1st climatic principal component score		az_1		O					O	O										
2nd climatic principal component score		az_2	O									O	O	O	O	O		O		O
3rd climatic principal component score		az_3													O					O
4th climatic principal component score		az_4		O	O	O	O	O	O	O							O			
5th climatic principal component score		az_5													O					
Accumulated cross sectional traffic volume		t_1																		
Accumulated cross sectional traffic volume of heavy vehicles		t_2					O				O									
Percentage of heavy vehicles		t_3													O					
Number of months elapsed since pavement applied		z_1	O								O				O					
Marshall test values	Density	z_2			O		O													
	Stability	z_3		O												O	O	O		
	Air voids	z_4						O	O		O		O						O	
	Flow value	z_5				O						O	O	O			O			
	Residual stability	z_6	O																O	
	Stability/flow value	z_7									O							O		O
Optimum asphalt content		z_8								O		O								
Designated asphalt content		z_9									O			O						
Penetration at 25°C		z_{10}			O	O		O				O	O	O		O	O	O	O	O
Softening point		z_{11}		O		O	O	O	O	O		O	O	O	O	O	O	O	O	O
Penetration index		z_{12}			O	O		O				O	O	O		O	O	O	O	O
Specific gravity of aggregate		z_{13}									O									
1st grading principal component score		gz_1	O	O	O	O	O	O	O	O		O	O	O		O	O	O	O	O
2nd grading principal component score		gz_2	O																O	
3rd grading principal component score		gz_3																		
4th grading principal component score		gz_4									O									
5th grading principal component score		gz_5	O	O	O		O		O	O					O	O				
				•			•		•	•										

The correlation coefficients between the respective explanatory variables are as shown in Table 8. It is generally understood that the existence of a number of correlation coefficients above 0.90 between explanatory variables may result in generating the problem of multicolinearity. Although a strong correlation can be observed between some of the explanatory variables listed here, we have determined that the omission of such explanatory variables should not result in a vital lack of information. The reason why a significant degree of correlation exists between some of the climatic conditions or aggregate grading may be traced to the fact that, however the principal component scores were obtained from the nationwide data, the scores used here have been limited only to those obtained from the selected sections of Tohoku Expressway.

We have selected 4 to 7 explanatory variables to obtain combinations where the multiple correlation coefficients would be the maximum as shown in Table 9. There is a distinct difference observed between variables selected from 7 explanatory variables and variables selected from 4 to 6 explanatory variables (as the 4th principal component score related to climatic conditions and the 5th principal component score related to grading would then hardly be adopted). Therefore, the optimum number of explanatory variables may be determined to be 6.

We believe that the 4th principal component score related to climatic conditions, softening point and the 1st and 5th principal component scores related to aggregate grading which may be often selected for the 6 explanatory variables are quite significant. Since both the penetration and penetration index have strong correlation with the softening point and it is difficult, in practice, to make a requirement to ignore this correlation at the selection of asphalt to be used. Therefore, the penetration and penetration index are not so important that they should be selected in preference to other variables. The multiple regression analysis was performed on the combinations with asterisks as shown in Table 9 on the basis of such determination.

The results of the multiple regression analyses were obtained as shown in Table 10. There are no noticeable differences between the residual standard deviations by the ten equations as shown in the table, and the results indicate that Y_A can be deducted with standard deviation errors of not more than 1.3 mm through any of the expressions. However, as mentioned earlier, the estimated accuracy of the rutting depth increment, ($Y = Y_A + Y_B$), is the sum of the residual standard deviation obtained through Quantification theory I under the paragraph 2.1 above and the same obtained by this multiple regression analysis, and the result should then be about 5.8 mm.

With regard to climatic conditions, the analytical results indicate that the rutting depth increment becomes smaller as the 1st and 4th principal component scores get larger and, it becomes larger as the 2nd principal component score gets larger. The factor loading (the correlation coefficient of the principal component and the source variable) of the 1st, 2nd and 4th principal components is as shown in Table 11. The 1st principal components score becomes larger in a warmer climate and the 4th principal component score becomes larger as the number of summer days increases. The fact that the rutting depth increment gets smaller as these scores increase clearly indicates that the rutting depth increment becomes smaller as the prevailing climate becomes milder and, therefore, we can determine that the fact correctly represents the relationship between the rutting increment and the prevailing climate. However, the 2nd principal component score gets larger in areas of large temperature fluctuation and, it is difficult to determine the implication of the fact that the rutting increment becomes larger as this score increases. There is a certain element of negative correlation between the 2nd and 1st as well as between 2nd and 4th principal component scores and it is suspected to have certain influence on the trend.

The reason why the regression coefficient related to the traffic volume is a negative value may be due to the fact that the cross sectional traffic volume on Tohoku Highway is correlated to the changes in climatic conditions (there is greater traffic volume in warmer sections of this expressway).

Table 10. Results of Multiple Regression Analysis

			No.	1	2	3	4	5	6	7	8	9	10
Regression coefficient	Constants			-89.110	-96.351	-77.925	-70.335	-66.181	-85.103	-97.300	-88.038	-131.207	-130.802
	1st climatic principal component score		mz_1	-1.286						-1.800		-1.851	-1.911
	2nd climatic principal component score		mz_2					0.550					
	4th climatic principal component score		mz_4	-10.863	-12.572	-12.141	-11.142	-10.050	-11.148	-8.909	-11.591	-10.215	-10.804
	Accumulated cross sectional traffic volume		t_1 (10,000 vehicles)			-0.001							
	Accumulated cross sectional traffic volume of heavy vehicles		t_2 (10,000 vehicles)								-0.0036		
	Marshall test values:	Density	x_2 (g/cm^3)	-11.870	-15.247	-14.920	-12.754	-13.526			-12.7517		
		Stability	x_3 (kgf)							-0.007			
		Air voids	x_4 (%)									0.999	
		Residual stability	x_6 (%)				-0.082						
		Stability/flow value	x_7 (100 kgf/cm)						-0.302				
	Optimum asphalt content		x_8 (%)										1.808
	Softening point		x_{11} (°C)	2.728	3.081	2.701	2.561	2.364	2.276	2.445	2.787	2.920	2.744
	1st grading principal component score		gz_1	-4.325	-4.757	-4.830	-4.474	-4.484	-4.773	-3.863	-4.446	-3.819	-4.036
	4th grading principal component score		gz_4		0.426				0.693				
	5th grading principal component score		gz_5	-1.610	-2.058	-1.758	-1.867	-1.910	-2.918	-1.317	-1.729	-1.082	-1.180
Multiple correlation coefficients				0.929	0.929	0.928	0.928	0.927	0.927	0.927	0.926	0.926	0.926
Residual standard deviations				1.339	1.342	1.353	1.355	1.356	1.358	1.363	1.367	1.369	1.369

Table 11. Factor Loading on Climate Related Principal Components

Climatic conditions	Principal components		
	1st	2nd	4th
Annual maximum temperature	0.897	0.387	-0.141
Annual minimum temperature	0.926	-0.332	0.020
Annual number of summer days	0.920	0.351	0.153
Annual number of winter days	-0.905	0.386	0.019
Annual number of snow-covered days	-0.825	0.015	0.019

It can be determined from the regression coefficient related to Marshall test values that it is a more efficient measure against rutting to use asphalt mixture which is high in density, stability, residual stability and the value of stability/flow and low in air voids. The analytical results where the rutting increment proves to be smaller with a mixture with less amount of the optimum asphalt content may be explained by the fact that the optimum asphalt content is in a negative correlation to the density, stability, and stability/flow value and positively correlated to the air voids.

With regard to the softening point of asphalt, the analytical results show that the rutting increment increases with it, however, it will not allow an immediate comparison of the suitability of different grades of asphalt since the range of softening points of asphalt used in the analysis have a small spread between 44.5 and 47.5° C.

As to the aggregate grading, the rutting increment tends to become smaller as the 1st and 5th principal component scores get larger and becomes larger with the 4th score gets larger. The factor loadings of the 1st, 4th and 5th principal components are as shown in Table 12. It seems to be more efficient a measure against the rutting increment to use more of aggregates of 13.2 mm or larger and 0.3 mm or smaller and less of aggregates of sizes between 2.36 mm and 9.5 mm.

Table 12. Factor loading on Aggregate Grading Principal Components

Aggregate mixing ratios	Principal component		
	1st	2nd	4th
19.0 mm or above	0.847	-0.136	-0.094
13.2 - 19.0	0.915	-0.040	-0.112
9.5 - 13.2	-0.306	0.501	0.578
4.75 - 9.5	-0.625	-0.251	-0.122
2.36 - 4.75	-0.622	0.086	-0.409
0.6 - 2.36	-0.243	-0.146	-0.024
0.3 - 0.6	0.320	0.748	-0.087
0.15 - 0.3	0.279	-0.480	0.142
0.075 - 0.15	-0.163	-0.350	0.507
0.075 or below	0.262	0.013	0.354

The above results have been obtained from the study only of Tohoku Expressway. We must wait until other expressways are properly surveyed and the results verified before we can judge that those results may be applicable to all expressways in cold areas.

The influence of traffic volume and the grades of asphalt could not be thoroughly studied, as our study has been limited only to Tohoku Expressway. We anticipate that the future expansion of the scope of our study should help clarify these points.

3. CONCLUSION

Investments for pavement must be planned so as to grasp the pavement service life in its entirety and to minimize the general service life costs. We need to be thoroughly informed of the secular changes of damage to the pavement and, in particular, of rutting depth since the major part of repair works performed on Japanese expressways are to repair rutting.

While there are many factors affecting the rutting increment, we can safely surmise from the results we have obtained in the study performed on Tohoku Expressway that it is substantially dependent on the horizontal alignment of the road and the rutting becomes more pronounced as the radius of circular curve increases (as it gets closer to a straight line) whereas the difference between right hand or left hand curves, longitudinal grade, traffic directions, the month of paving work have little influence on rutting.

It has been verified that the rutting increment gets smaller in warmer climates according to multiple regression analyses where the portion of rutting depth increment, which could not be explained by the circular curve radii, is used as the criterion variable, while climatic conditions, traffic characteristics, the Marshall test values of asphalt mixture, the optimum asphalt content, the softening point of asphalt used, and the aggregate grading are used as the explanatory variables. With regard to rutting due to abrasion, on the other hand, it is more suitable for the prevention of rutting to use asphalt mixture where the density, stability, residual stability, stability/flow value are larger and the air voids and the optimum asphalt content are smaller. As to the aggregate grading, it is more effective to use more of grain sizes of 13.2 mm or larger and 0.3 mm or smaller and less of grain sizes between 2.36 mm and 9.5 mm.

However, it is yet to be determined whether the analytical results obtained from Tohoku Expressway are applicable to pavements on all expressways and they need to be verified by performing similar studies to all other expressways. The influences of the traffic characteristics and the grade of asphalt on the rutting depth increment could not be clarified in this analysis, but remain to be determined in the future.

REFERENCE

1) Haas, R.C.G., and W.R. Hudson : "Pavement Management Systems," McGraw-Hill, 1978.

2) Express Highway Research Foundation of Japan: "Study of Evaluation of Road Pavement," February, 1988

3) Japan Weather Association: "Annual Report of Climatological Stations," 1979 - 1986.

PROCEEDINGS OF THE 4TH WORKSHOP ON PAVING IN COLD AREAS, VOLUME1

ISSN 0386－5878
土木研究所資料第2896号
平成2年9月(1990)
建設省土木研究所

要旨　平成2年9月，札幌市で開催された日加科学技術協力協定第4回「寒冷地舗装会議」の発表論文のうち，前半の15報をとりまとめたものである。

キーワード：Canada/Japan Science and Technology Agreement, Paving in Cold Areas, Asphalt Pavement, Concreate Pavement, FWD, Pavement Management System.

郵便はがき

41円切手をはって下さい

3 0 5 - □□

茨城県つくば市大字旭一番地

建設省土木研究所

舗装研究室　御中

No.

No.

配布先氏名

配布先住所

土木研究所資料第2896号
「PROCEEDINGS OF THE 4TH WORKSHOP ON PAVING IN COLD AREAS, VOLUME1」
部

上記のとおり受領しました。

所　属（住所）

氏　名　　印